JOURNAL OF POLYMER SCIENCE: PART A VOL. 3, PP. 417–421 (1965)

Polybenzimidazoles. IV. Polybenzimidazoles Containing Aryl Ether Linkages

ROBBIE T. FOSTER* and C. S. MARVEL, *Department of Chemistry, University of Arizona, Tucson, Arizona*

Synopsis

Some polybenzimidazole polymers which have aryl ether linkages between the recurring units have been prepared in order to study their thermal stability and their film- and fiber-forming properties. All of the polymers prepared were soluble, high molecular weight materials with very good thermal stability.

In previous publications[1–3] it was shown that polymers containing the benzimidazole nucleus could be prepared by melt condensation of suitable tetraamines and the phenyl esters of aromatic dibasic acids. More recently, the mechanism of the melt polymerization has been reported,[4] and a method of solution polymerization in polyphosphoric acid to give polybenzimidazoles has been described.[5]

In continuing this series, several new polybenzimidazoles containing aryl ether linkages were prepared to study their properties.

A convenient procedure was found from the preparation of 3,3′,4,4′-tetraaminodiphenyl ether by reduction of 3,3′-dinitro-4,4′-diaminodiphenyl ether with stannous chloride and hydrochloric acid. The free tetraamine in the solid state is fairly stable to air, but some discoloration occurs on standing for long periods of time. Solutions of the amine in methanol were very sensitive to air, oxidizing rapidly to a black oil. It was found that poly[2,2′(*m*-phenylene)oxy-5,5′-bibenzimidazole] (I) was readily crosslinked by trace amounts of oxygen at high temperature to give polymers which were 100% insoluble in dimethyl sulfoxide, formic acid, and sulfuric acid. This was avoided by modifying the apparatus used for the preparation of poly[2,2′-(*m*-phenylene)-5,5′-bibenzimidazole][6] to avoid any air leaks in the apparatus. The crosslinked polymer had quite a different appearance from that of the soluble polymer. The former was a flexible, tough foam which could be broken or ground only with great difficulty, and the latter was brittle and very easily ground to a fine powder.

The polymers, poly[2,2′-(4,4′-oxydiphenylene)oxy-5,5′-bibenzimidazole] (II) and poly[2,2′-(4,4′-oxydiphenylene)-5,5′-bibenzimidazole] (III), were very hard, brittle materials which were easily ground to a fine powder.

* Postdoctoral Research Associate supported by Textile Fibers Department, E. I. du Pont de Nemours and Company, 1962–63.

Both II and III were 100% soluble in dimethylacetamide, dimethyl sulfoxide, formic acid, and sulfuric acid and showed good thermal stability.

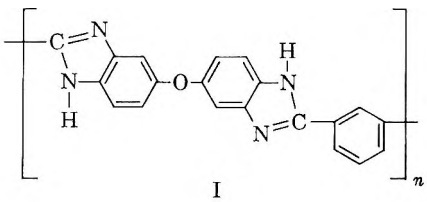

I

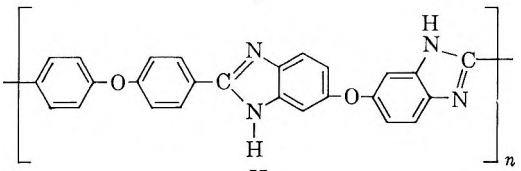

II

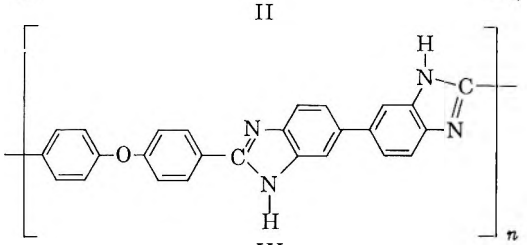

III

Polymer I, when heated in nitrogen with the temperature increased 100°C. each 1.5 hr., lost about 5% of its weight below 500°C. and then gradually lost 35% of its weight up to 900°C. Polymer II heated in nitrogen with the temperature increased 10°C./min. lost about 10% of its weight rather quickly and then underwent little change up to 550°C. The loss in weight up to 720°C. was 25.1%. Polymer III under the same conditions lost only 20.1% of its weight when heated to 720°C. For comparison, a sample of the polybenzimidazole prepared from diphenyl isophthalate and 3,5,4,4′-tetraaminodiphenyl lost only 13.6 of its weight when similarly heated to 720°C.

EXPERIMENTAL

Preparation of Reactants

4,4′-Diacetamidodiphenyl Ether. To a solution of 140 g. (0.7 mole) of 4,4′-diaminodiphenyl ether (technical oxydianiline obtained from E. I. du Pont de Nemours and Company) in 500 ml. of glacial acetic acid was added dropwise 173 g. (1.6 mole) of acetic anhydride at such a rate as to maintain a temperature of 50–60°C. The temperature was maintained at 90–100°C. for an additional hour; then the solution was allowed to stand overnight. The precipitate which formed was collected and dried in air, then in a vacuum oven at 50°C. for 12 hr. to give 153 g. of 4,4′-diacetamidodiphenyl ether, m.p. 228–229°C. (lit.[7] m.p. 228–229°C.). The filtrate from above was poured into 1 kg. of ice and the precipitate which formed was collected

and dried to give 20 g. of additional 4,4′-diacetamidodiphenyl ether. The combined yield was 87.5% of the theoretical amount.

3,3′-Dinitro-4,4′-diacetamidodiphenyl Ether. To 700 ml. of acetic anhydride was added 95 ml. of colorless 70% nitric acid, according to the procedure[8] of Bordwell and Garbish as such a rate as to maintain a temperature of less than 25°C. After the addition was complete, 75 g. (0.265 mole) of 4,4′-diacetamidodiphenyl ether was added in small portions while the temperature was maintained in the range of 15–20°C. The yellow mixture was stirred for 30 min. at room temperature, then poured into 3 liters of a 1:1 mixture of ice and water. The yellow precipitate was collected and dried in a vacuum oven at 25°C. to give a quantitative yield of 3,3′-dinitro-4,4′-diacetamido-diphenyl ether, m.p. 211–214°C.

3,3′-Dinitro-4,4′-diaminodiphenyl Ether. To a slurry of 199 g. (0.53 mole) of 3,3′-dinitro-4,4′-diacetamidodiphenyl ether in 1300 ml. of methanol was added dropwise with vigorous stirring a solution of 84 g. of potassium hydroxide in 300 ml. of methanol; then 56 g. more of potassium hydroxide was added and the mixture stirred for 3 hr. The mixture was poured into 2.5 liters of water, and the orange precipitate was collected. The filtrate was poured into 3 liters of water to give additional material. The combined precipitates, m.p. 175.5–178.5°C., were recrystallized from 95% ethanol to give 134 g. (87%) of 3,3′-dinitro-4,4′-diaminodiphenyl ether, m.p. 179–180°C. (lit.[9] m.p. 179–180°C.).

3,3′,4,4′-Tetraaminodiphenyl Ether. To a vigorously stirred solution of 240 g. of stannous chloride dihydrate in 500 ml. of concentrated hydrochloric acid was added 46.4 g. (0.16 mole) of 3,3′-dinitro-4,4′-diaminodiphenyl ether in small portions at such a rate as to maintain a temperature of 60–70°C. After the addition was complete ($1^1/_2$ hr.) the mixture was maintained at 65–70°C. for an additional 3 hr. The mixture was cooled to −10°C. and the pink precipitate collected. The tetrahydrochloride salt was dissolved in 300 ml. of hot water and 300 ml. of concentrated hydrochloric acid added. Cooling produced white needles of tetrahydrochloride salt. The material was pressed as dry as possible, then dissolved in water. The water solution was added dropwise to a vigorously stirred solution of 60 g. of sodium hydroxide in 300 ml. of water cooled in an ice bath. The grey precipitate (45 g.) was collected, washed with water, and dried in a vacuum oven overnight. The tetraamine was recrystallized from 250 ml. of methanol in an atmosphere of nitrogen to give 24.6 g. (66.7%) of light-pink 3,3′,4,4′-tetraaminodiphenyl ether, m.p. 149.5–151°C.

ANAL. Calcd. for $C_{12}H_{14}N_4O$: C, 62.59%; H, 6.13%; N, 24.34%. Found: C, 62.58%; H, 6.08%; N, 24.08%.

Polymerizations

The apparatus for the polymerizations consisted of a large Dry Ice trap with a 24-mm. side arm which was connected directly to a 70 mm. ×

200 mm. polymerization tube by a 45/50 standard taper ground glass joint to minimize any leakage into the vessel.

Poly[2,2′-(1,3-phenylene)oxy-5,5′-bibenzimidazole]. A mixture of 7.1 g. of 3,3′,4,4′-tetraaminodiphenyl ether and 10.1 g. of diphenyl isophthalate was placed in the polymerization tube, which was then evacuated and filled with nitrogen repeatedly. The mixture was then heated at 260°C. for 30 min. Water and phenol were liberated during this period. The system was slowly evacuated to 0.025 mm. and the temperature gradually raised to 340°C. over a period of 4 hr. The heating bath was removed and the system maintained at 0.025 mm. for 12 hr. The polymers obtained were 90–100% soluble in dimethyl sulfoxide and dimethylacetamide and had an inherent viscosity of 0.5–0.6 (0.5 g./100 ml. of DMSO at 30°C.). The yield was quantitative.

ANAL. Calcd. for $(C_{20}H_{12}N_4O)_n$: C, 74.06%; H, 3.73%; N, 17.28%. Found: C, 73.20%; H, 3.98%; N, 16.71%.

The insoluble portion of the polymer was removed by preparing a 15% solution of polymer in dimethylacetamide, filtering through glass wool to remove the gel, and evaporation of the solvent at reduced pressure. The dark color of the polymer could be removed by dissolving the polymer in dimethylacetamide or dimethyl sulfoxide and precipitating the polymer in benzene. The resulting polymer was a light yellow powder.

Poly[2,2′-(4,4′-oxydiphenylene)oxy-5,5′-bibenzimidazole]. This polymer was prepared by a modification of the procedure for poly[2,2′-(1,3-phenylene)oxy-5,5′-bibenzimidazole] from a mixture of 5.00 g. (0.0217 mole) of 3,3′-4,4′-tetraaminodiphenyl ether and 8.91 g. (0.0217 mole) of diphenyl oxybibenzoate* in a quantitative yield. The polymer was 100% soluble in dimethylsulfoxide and had a viscosity of 0.5 (2% solution in DMSO at 30°C.).

ANAL. Calcd. for $(C_{26}H_{16}N_4O_2)_n$: C, 74.98%; H, 3.87%; N, 13.46%. Found: C, 73.60%; H, 3.87%; N, 12.40%.

Poly[2,2′-(4,4′-oxydiphenylene)-5,5′-bibenzimidazole]. This polymer was prepared by a modification of the procedure for poly[2,2′-(1,3-phenylene)oxy-5,5′-bibenzimidazole] from a mixture of 4.64 g. (0.0217 mole) of 3,3′-diaminobenzidine and 8.91 g. (0.0217 mole) of diphenyl oxybibenzoate in a quantitative yield. The polymer was 100% soluble in dimethyl sulfoxide and had a viscosity of 0.7 (2% solution in DMSO).

ANAL. Calcd. for $C_{26}H_{16}ON_4$: C, 77.98%; H, 4.03%; N, 13.99%. Found: C, 77.30%; H, 3.86%; N, 13.92%.

We are indebted to Micro-Tech Laboratories, Skokie, Ill., for the analyses reported in this paper; to Dr. G. Ehlers, Materials Laboratory, Wright Air Development Division, Wright-Patterson Air Force Base, Ohio, for the thermogravimetric analysis of polymer

* The diphenyl 4,4′-oxydibenzoate, m.p. 185–187°C., was prepared by W. G. Jackson of Burdick and Jackson Laboratories, Inc., from 4,4′-oxydibenzoyl chloride and phenol. ANAL. Calcd. for $C_{26}H_{18}O_5$: C, 76.09%; H, 4.42%. Found: C, 76.30%, H, 4.46%.

I; and to Dr. E. L. Wittbecker, Benger Laboratory, E. I. du Pont de Nemours and Company, for the thermogravimetric data on polymers II and III. The financial support of the Textile Fibers Department of E. I. du Pont de Nemours and Company is gratefully acknowledged.

References

1. Vogel, H., and C. S. Marvel, *J. Polymer Sci.*, **50**, 511 (1961).
2. Vogel, H., and C. S. Marvel, *J. Polymer Sci.*, **A1**, 1531 (1963).
3. Plummer, L., and C. S. Marvel, *J. Polymer Sci.*, **A2**, 2559 (1964).
4. Wrasidlo, W., and H. H. Levine, paper presented at 145th American Chemical Society Meeting, New York, Sept. 1963; *Polymer Preprints*, **4**, No. 2, 15 (1963).
5. Iwakura, Y., K. Uno, and Y. Imai, *J. Polymer Sci.*, **A2**, 2605 (1964).
6. Cabaness, R., this laboratory, private communications.
7. Grather, C. F. (Dow Chemical Company), U. S. Pat. 1,900,443 (March 7, 1933).
8. Bordwell, F. G., and E. W. Garbisch, Jr., *J. Am. Chem. Soc.*, **82**, 3588 (1960).
9. Soc. Ind. Chim. Bâle, Swiss Pat. 212,641 (March 3, 1941).

Résumé

On a préparé plusieurs polybenzimidazoles possédant des liaisons aryléther entre chaque unité monomérique, en vue d'étudier leur stabilité thermique ainsi que leurs propriétés de former des films et des fibres. Tous ces polymères sont solubles, ont un poids moléculaire élevé et possèdent une grande stabilité thermique.

Zusammenfassung

Einige Polybenzimidazolpolymere mit Arylätherbrücken zwischen den Bausteinen wurden zur Untersuchung ihrer thermischen Stabilität sowie ihrer Film- und Faserbildungseigenschaften hergestellt. Alle dargestellten Polymeren waren lösliche, hochmolekulare Stoffe mit sehr guter Stabilität.

Received May 29, 1964

JOURNAL OF POLYMER SCIENCE: PART A VOL. 3, PP. 423–431 (1965)

Studies of Structure Formation in Poly(vinyl Alcohol) Solutions

P. I. ZUBOV and E. A. OSIPOV, *Institute of Physical Chemistry, Moscow, U.S.S.R.*

Synopsis

Acetalation of PVA in aqueous solution with succinaldehyde yields a gel or globular structures with strong chemical intermolecular or intramolecular bonds, depending on the solution concentration. Similar structures formed by localized physical bonds may be obtained by cooling the PVA solutions in DMF–water mixtures of certain compositions or in anhydrous DMF. Comparison of the viscosity data for the solutions with turbidity of these systems and electron microscopy leads to the conclusion that globular particles obtained by cooling the PVA solutions in anhydrous DMF are super molecular structures of colloidal size. The diameter of these particles depends not only on the solution concentration but also on the temperature to which the PVA solutions are cooled. The dimensions of the particles decrease with the temperature at which the cooled solution is kept. The globular structures are stable in anhydrous DMF and are destroyed only at 120°C. In the presence of water a redistribution of intramolecular and intermolecular bonds proceeds at room temperature and results in the formation of a thixotropic structure. The structure formation influences considerably the mechanical and adhesion properties of PVA films prepared on solid surfaces.

Structure formation in polymer solutions may be related to the formation and dissociation of local bonds between the reactive groups of chain molecules. Depending on the concentration of the solution, the increase in local bonds results either in network formation (gelation) or formation of globular structures (globulization). Globulization occurs in dilute solutions, where the probability of formation of intermolecular bonds is negligible and only intramolecular interactions take place. This phenomena was discovered in our laboratory during a study of structure formation processes in solutions of gelatin, casein, synthetic and natural rubber, poly (methacrylic acid), and methacrylic acid copolymers.[1–8]

In this paper, on the basis of viscosity, turbidity, and electron microscopic studies, it is shown that structure formation of similar nature occurs in poly(vinyl-alcohol) (PVA).

Two sets of experiments were carried out: the first, involved acetalation of PVA with dialdehyde in aqueous solution and the second, substitution of a poor solvent (dimethylformamide) for a good one (water).

The data on the changes of viscosity of aqueous PVA solutions after treatment with succinaldehyde in the presence of sulfuric acid catalyst, are shown in Figure 1. The reaction of PVA with succinaldehyde in solution

at PVA concentrations c higher than 1.5% (curves 5–7) is accompanied by an increase of viscosity. The result of this process is the formation of gel with stable network structure which is not destroyed after heating on a boiling water bath.

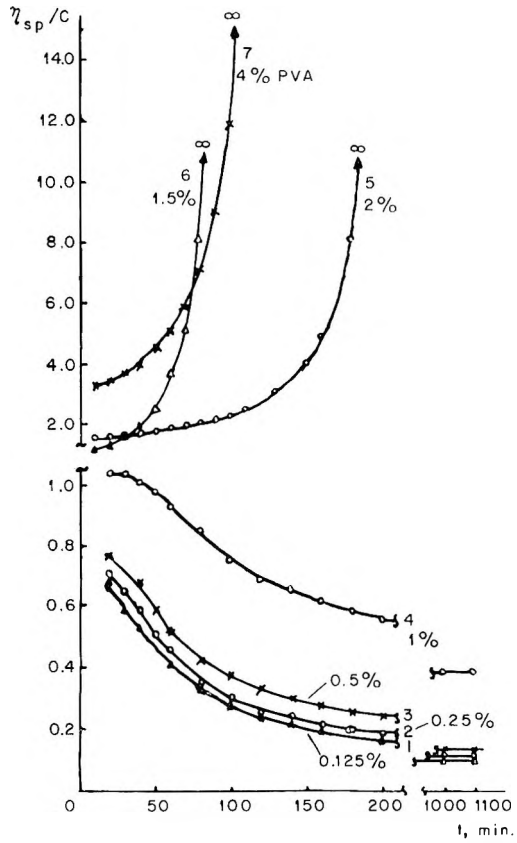

Fig. 1. Change in viscosity of aqueous PVA solutions after treatment with succinaldehyde: (*1*) 0.125% PVA; (*2*) 0.25% PVA; (*3*) 0.5% PVA; (*4*) 1.0% PVA; (*5*) 2% PVA; (*6*) 1.5% PVA; (*7*) 4% PVA.

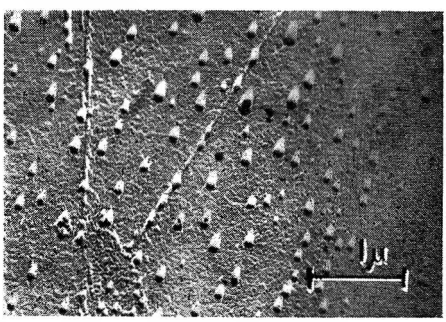

Fig. 2. Electron micrograph of globular particles formed in acetalation of a 0.5% PVA solution with succinaldehyde.

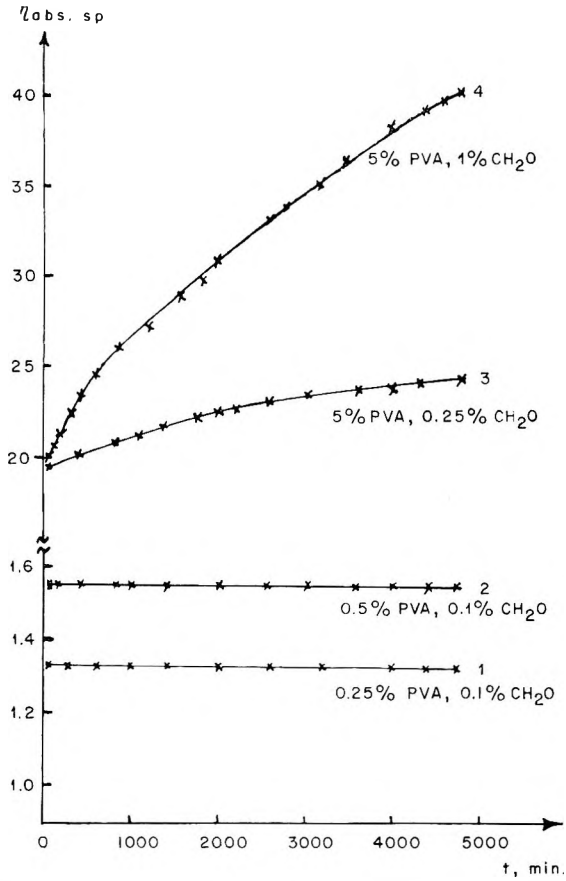

Fig. 3. Change in viscosity of aqueous PVA solutions after treatment with formaldehyde: (*1*) 0.25% PVA, 0.1% CH_2O; (*2*) 0.5% PVA, 0.1% CH_2O; (*3*) 5% PVA, 0.25% CH_2O; (*4*) 5% PVA, 1% CH_2O.

In more dilute PVA solutions (<1%) acetalation causes a decrease in viscosity with the reaction time (curves 1–4). This indicates the possibility of globulization of PVA molecules under these conditions. If the polymer concentration is lower than 0.5%, the viscosity is reduced to its limiting value quickly and does not change further. This occurs at 10–15% substitution of hydroxyl groups and indicates that globulization is completed.

The globular solutions formed are stable and transparent. The loss of solubility of globular structures and formation of precipitate occurs at more than 30% substitution of hydroxyl groups.

The data of Figure 1 enable us to propose that the formation of gel network structure and the globular particles both proceed by a single molecular mechanism which is similar to that involved in vulcanization of rubber.

The reason for the difference in behavior of concentrated and dilute solutions is that in the former a three-dimensional network of intramolecular bonds is formed, while in the latter the crosslinks are confined to the

globular particles. The diameter of the globular particles formed in the acetalation of 0.5% solution with succinaldehyde is about 1000 A., as can be seen from the electron micrograph (Fig. 2). This indicates that the globular particles are made up of many macromolecules (Fig. 2).

Both gelation and globulization occur only on treatment of the solution with bifunctional aldehydes. Acetalation of PVA molecules with mono-

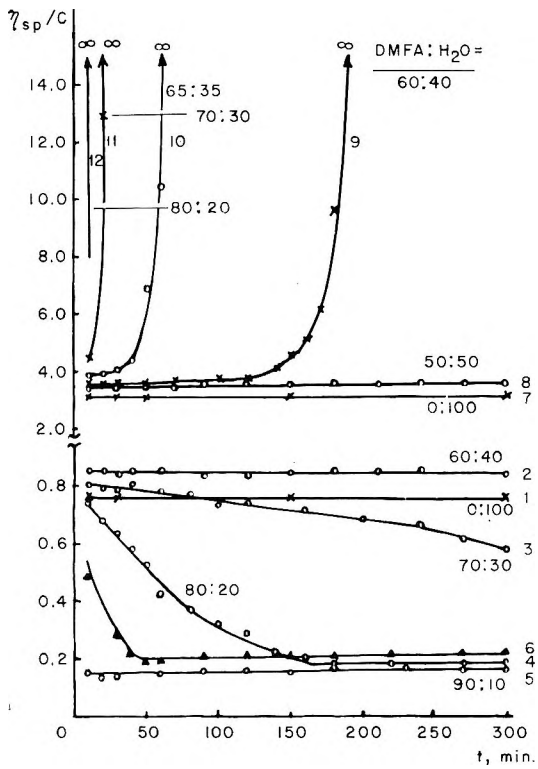

Fig. 4. Dependence of viscosity on time in various DMF–H_2O mixtures: (*1*) 0:100, 0.125% PVA; (*2*) 60:40, 0.125% PVA; (*3*) 70:30, 0.125% PVA; (*4*) 80:20, 0.125% PVA; (*5*) 90:10, 0.125% PVA; (*6*) 00:00, 0.125% PVA; (*7*) 0:100, 4% PVA; (*8*) 50:50, 4% PVA; (*9*) 60:40, 4% PVA; (*10*) 65:35, 4% PVA; (*11*) 70:30, 4% PVA; (*12*) 80:20, 4% PVA.

aldehyde (formaldehyde) does not cause these effects, as shown in Figure 3, where the viscosity changes of the PVA solutions after treatment with 0.1% formaldehyde are shown. The viscosity of 0.25–0.5% PVA solutions (curves *1* and *2*, Fig. 3) does not change. In solutions of higher PVA concentrations (curves *3* and *4*) acetalation with 0.25–1.0% formaldehyde results in an increase of the viscosity with time. The rate of the process depends on the concentration of polymer and formaldehyde. Generally, however, the rate of viscosity increase in this case is lower than that in the case of dialdehyde treatment, and gelation does not occur.

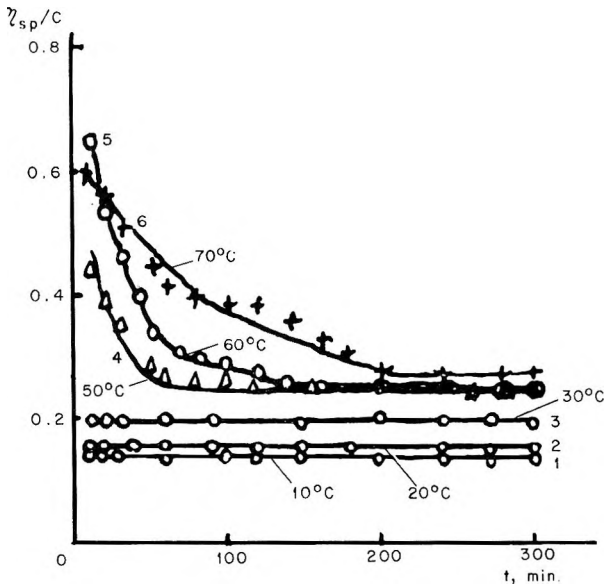

Fig. 5. Viscosity changes in 0.25% PVA solutions in anhydrous DMF heated to 145°C. and then cooled to different temperatures: (*1*) 10°C.; (*2*) 20°C.; (*3*) 30°C.; (*4*) 50°C.; (*5*) 60°C.; (*6*) 70°C.

The system remains fluid up to the point at which a precipitate forms; this is observed in concentrated and diluted solution if 45–50% of hydroxyl groups have reacted.

Globulization of dissolved PVA macromolecules may also be achieved without carrying out a chemical reaction by addition of a poor solvent such as dimethylformamide (DMF).

PVA was dissolved in a binary water–DMF mixture at an elevated temperature to form a homogeneous solution. The solution was cooled down to 20°C. over a period of 3–5 min. and the changes in viscosity with time at this temperature were followed.

Figure 4 shows the dependence of viscosity on time for PVA solutions in DMF–water mixtures of various compositions. The viscosity of aqueous 4% PVA solution as well as that in the 50:50 vol. % DMF–water mixture remain constant (curves *7* and *8*). In the case of binary mixtures with higher DMF content (60, 65, 70, and 80 vol. %, curves *9*, *10*, *11*, and *12*, respectively) the viscosity of the solutions increases sharply with time and the formation of a gel results. The gelation of the solution is associated with the formation of physical bonds between macromolecules because the gel network dissociates on heating the system. In the binary mixture, the gel melting points increase with increasing DMF content of the mixed solvent.

The behavior of dilute solutions (0.125%) is rather different. The viscosity of the aqueous solution and that of the 60% DMF mixture does not change with time. However, binary mixtures with higher DMF content

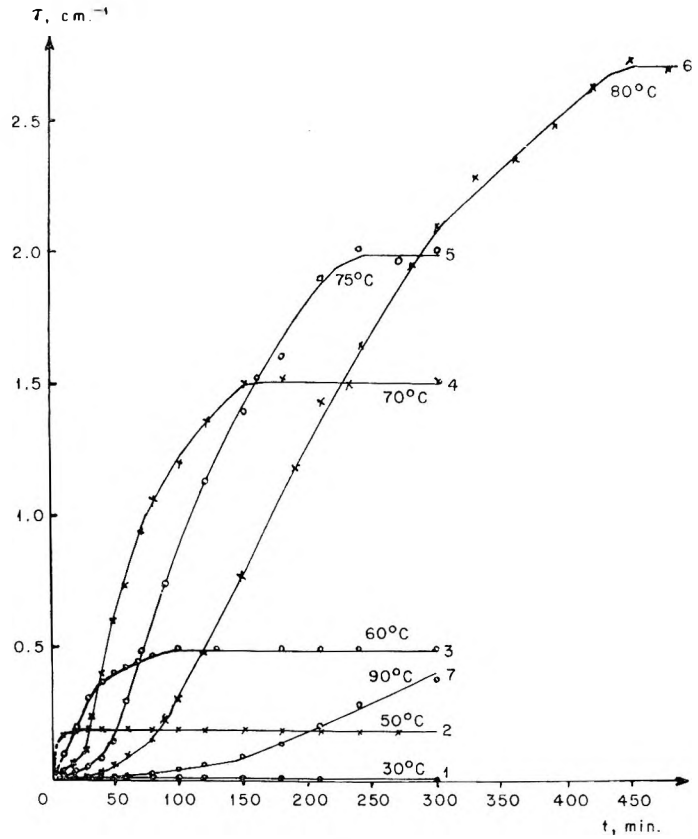

Fig. 6. Turbidity changes of PVA solutions in DMF heated to 145°C. and then cooled to various temperatures: (*1*) 30°C.; (*2*) 50°C.; (*3*) 60°C.; (*4*) 70°C.; (*5*) 75°C.; (*6*) 80°C.; (*7*) 90°C.

(curves *3–5*) the viscosity decreases when the solution is cooled, due to the formation of globular structures.

The rate of globulization depends on the composition of the binary mixture. In a mixture with 80% DMF, the viscosity approaches its limiting value in 3 hr., and in the 90% DMF mixture this value is reached in less than 10 min.

The globulization rate and the value of the equilibrium viscosity in PVA solutions strongly depends on the temperature to which the solution was cooled down.

Figure 5 shows the viscosity changes in 0.25% PVA solutions in anhydrous DMFA heated to 145°C. and then cooled down to the different temperature. Equilibrium values of viscosity were established most quickly at 30°C. and increase with the temperature. However the rate of approach to equilibrium decreases with the temperature. On the basis of these facts we propose that the number of polymer molecules making up the globular particles increases with increasing temperature. The above in-

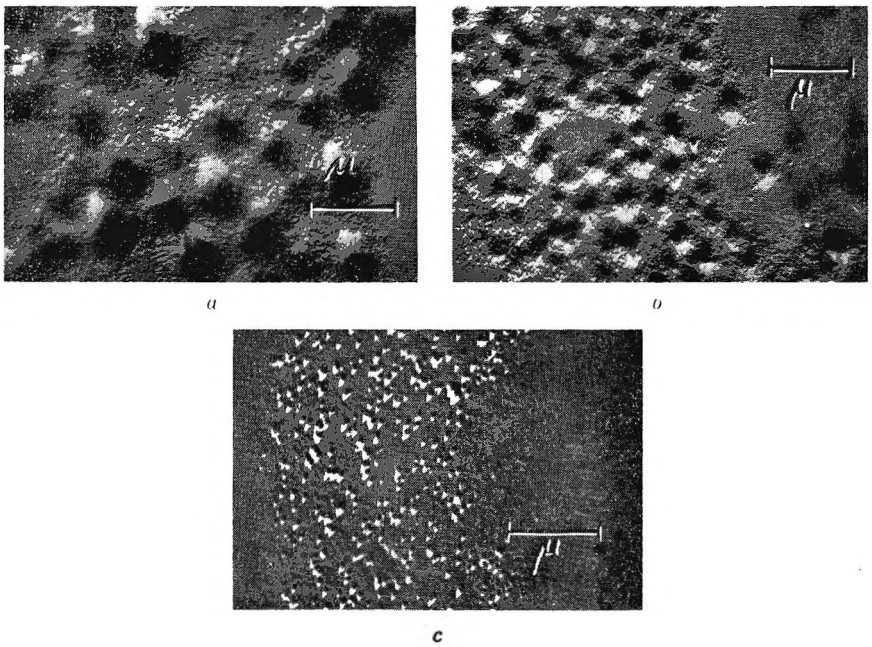

Fig. 7. Electron micrographs of globular particles of PVA in DMF formed on cooling to various temperatures: (*a*) 70°C.; (*b*) 60°C.; (*c*) 30°C.

ference was corroborated by a study of the turbidity of this system. The data obtained show (Fig. 6) that the turbidity of the solutions after their cooling changes in a similar way as the viscosity. The highest rate of the approach to equilibrium turbidity is observed at 30°C. (curve *1*, Fig. 5). An increase of the temperatures to which the solutions were cooled leads to higher values of the equilibrium turbidity and lower rates of approach to equilibrium.

The influence of the temperature at which the cooled solutions are kept on the size of the globular particles was also confirmed by electron microscopy. Cooling a 0.5% PVA solution in anhydrous DMF to 70°C. gives particles with an average size of about 5000 A. (Fig. 7*a*); cooling to 60°C. gives particles about 3000 A. in size (Fig. 7*b*); cooling to 30°C. gives particles about 700 A. (Fig. 7*c*). Thus the variation of the cooling temperature from 70 to 30°C. leads to a nearly tenfold change of globular dimensions.

The globular particles formed are quite stable. They keep their structure after complete removal of the solvent. The transparency of a globular PVA solution in anhydrous DMF does not change on prolonged storage (for more than a year). However, in the presence of even small amounts of water (less than 1%) a redistribution of intermolecular and intramolecular bonds can take place, as is shown in the gradual increase of viscosity and transformation of the solution to a transparent thixotropic gel.

A similar process of the bond redistribution takes place rapidly upon heating the solution to 120°C. At this temperature (Fig. 8) the transparent

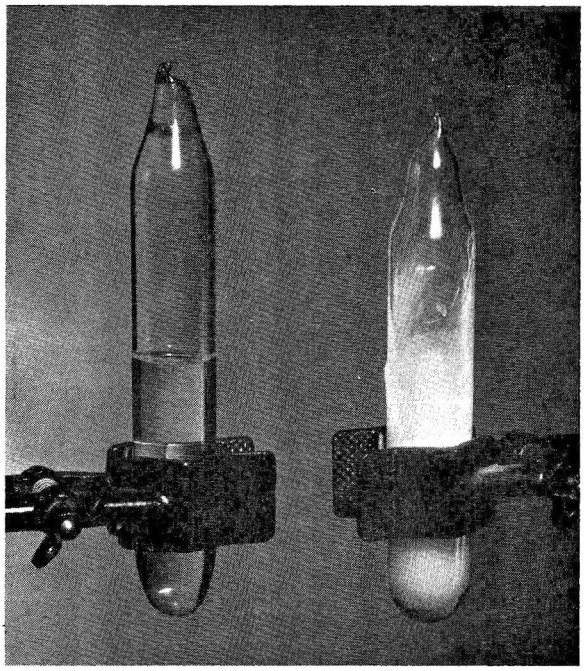

Fig. 8. 4% DMF solution of globular PVA before (left test tube) and after denaturation (right test tube).

solution is converted into an opaque gel with a network structure which can be destroyed by heating above 140°C.

The structure formation in PVA solution has a considerable influence on the mechanical and adhesion properties of films prepared from these solutions. The lowest mechanical strength is observed when the films were prepared from a solution of globular PVA in anhydrous DMF.

These films crack spontaneously and exfoliate at a stress less than 1 kg./cm.^{2}

Films prepared from solutions of globular PVA which were obtained by acetalation with succinaldehyde show somewhat better adhesion properties (maximum stress is 20 kg./cm.^{2}).

The best adhesion properties are shown by the films obtained after treatment of PVA with formaldehyde. In this case the value of adhesion to the glass surface approaches 150 kg./cm.^{2}

References

1. Zubov, P. I., D.Sci. Thesis, Moscow, 1949.

2. Zubov, P. I., Z. N. Zurkina, and V. A. Kargin, *Dokl. Akad. Nauk, SSSR*, **67**, 4, 659 (1949).

3. Zubov, P. I., Z. N. Zurkina, and V. A. Kargin, *Kolloid Zh.*, **16**, 178 (1954); *ibid.*, **19**, 420 (1957).

4. Dorokhina, T. V., and A. V. Novikov, *Vysokomol. Soedin.*, **1**, 36 (1959).

5. Novikov, A. V., T. V. Dorokhina, and P. I. Zubov, *Dokl. Akad. Nauk, SSSR*, **105**, 514 (1955).

6. Lipatov, Yu. S., and P. I. Zubov, *Vysokomol. Soedin.*, **1**, 88 (1959); *ibid.*, **3**, 432 (1959).

7. Zubov, P. I., Yu. S. Lipatov, and E. A. Kanevskaya, *Dokl. Akad. Nauk SSSR*, **141**, 2 (1962).

8. Proshlyakova, N. E., P. I. Zubov, and V. A. Kargin, *Kolloid Zh.*, **20**, 199, 202 (1958).

9. Zubov, P. I., G. A. Sheverdyaeva, and E. A. Osipov, *Kolloid Zh.*, **25**, 438 (1963).

Résumé

On peut obtenir un gel ou bien des structures sphériques en acétylant le PVA avec le dialdéhyde succinique en solution aqueuse. Ces produits possèdent de fortes liaisons inter- ou intramoléculaires selon la concentration de la solution. On peut obtenir des structures analogues, formées par des liaisons physiques localisées, en refroidissant des solutions de PVA dans des mélanges DMFA eau d'une certaine composition ou bien dans la DMFA anhydre. La comparaison des résultats de la viscosité des solutions avec la turbidité de ces systèmes et avec les images obtenues au microscope électronique nous permet de conclure que les particules sphériques, obtenues en refroidissant les solutions de PVA dans le DMFA anhydre, sont des structures supermoléculaires de la dimension des colloïdes. Le diamètre de ces particules dépend non seulement de la concentration des solutions mais aussi de la température à laquelle les solutions de PVA sont refroidies. Les dimensions de ces particules diminuent avec la température à laquelle la solution refroidie est conservée. Les structures sphériques sont stables dans le DMFA anhydre et ne sont détruites qu'à 120°C. En présence d'eau et à température ambiante il y a une redistribution des liaisons inter- et intramoléculaires et il se forme une structure thixotropique. La formation des structures influence très fort les propriétés mécaniques et l'adhésion des films de PVA préparés sur des surfaces solides.

Zusammenfassung

Durch Acetylierung von PVA mit Bernsteinsäuredialdehyd in wässriger Lösung kann man je nach der Lösungskonzentration Gel- oder Globularstrukturen mit starken chemischen inter- oder intramolekularen Bindungen erhalten. Ähnliche Strukturen mit lokalisierten physikalischen Bindungen können durch Abkühlung der PVA-Lösung in DMFA–Wassermischungen bestimmter Zusammensetzung oder in wasserfreiem DMFA erhalten werden. Ein Vergleich der Viskositätsdaten der Lösungen mit der Trübigkeit dieser Systeme und elektronenmikroskopische Aufnahmen ermöglicht den Schluss, dass die globulären, durch Abkühlung der PVA-Lösung in wasserfreiem DMFA erhaltenen Teilchen supermolekulare Strukturen von kolloider Grösse sind. Der Durchmesser dieser Teilchen hängt nicht nur von der Lösungskonzentration, sondern auch von der Temperatur ab, von welcher die PVA-Lösungen abgekühlt werden. Die Dimension der Teilchen nahm mit der Temperatur, bei welcher die gekühlte Lösung gehalten wird, ab. Die Globulärstrukturen sind in wasserfreiem DMFA beständig und werden erst bei 120°C zerstört. In Gegenwart von Wasser findet bei Raumtemperatur eine Neuverteilung der intra- und intermolekularen Bindungen statt, was zur Bildung einer thixotropen Struktur führt. Die Strukturbildung hat einen beträchtlichen Einfluss auf die mechanischen und Adhäsionseigenschaften von PVA-Filmen auf festen Oberflächen.

Received February 4, 1964

JOURNAL OF POLYMER SCIENCE: PART A VOL. 3, PP. 433–447 (1965)

Crystallization Kinetics of High Polymers: Isotactic Polystyrene

J. N. HAY, *The Department of Chemistry, The University, Old Aberdeen, Scotland*

Synopsis

The crystallization kinetics of a sample of isotactic polystyrene have been measured at various temperatures. Despite the presence of secondary crystallization sufficient accuracy can be attained to enable an Avrami relationship with a constant integral value of n to be assigned to most of the rate curves. The interpretation of the Avrami constants in terms of crystallization by growth of spherical entities, produced at fixed sites, is verified by microscope observations.

INTRODUCTION

The nature of the processes involved in crystallizing a polymer from its melt has been to some extent ascertained by analysis of the isothermal rate curves with an equation derived by Avrami for metals,[1] and by others for polymers:[2,3]

$$1 - X_c = \exp\{-k_c t^n\} \tag{1}$$

where X_c is the weight fraction of crystallized polymer at time t, k_c is a rate constant, and n a constant and an integer. The values of k_c and n depend on the mechanism of crystallization.[3]

The equation, when applied in practice, appears to have many limitations, principally because of the nature of the assumptions inherent in it,[4] and because it does not take into account the molecular environment and mechanism of bulk flow of the non-Newtonian liquid to the site of crystallization. These restrictions have been exphasized recently by the repeated discovery of nonintegral values of n[5–7] and particularly of a constant nonintegral value,[8] which could not be explained by the assumption of a complex mode of crystallization involving two or more processes each characterized by its own Avrami equation.[9]

It seems from the above there is evidence that the Avrami equation is not sufficient to explain the crystallization kinetics of certain polymers. The validity of the equation, however, could be checked by a technique which allowed direct visual evaluation of the primary processes of crystallization, i.e., nucleation and "crystal" growth. For this purpose the crystallization of isotactic polystyrene was investigated, particularly since

its spherulitic growth rate, and presumably crystallization rate, has a very small temperature dependence.[10]

EXPERIMENTAL

Materials

Isotactic polystyrene samples were prepared by the method described by Burnett and Tait,[11] a Zeigler-Natta heterogeneous catalyst system ($TiCl_3$–$AlEt_3$ in toluene as a solvent for the polymer) being used at 30°C. The polymerizations were taken to less than 10% conversion.

The crude reaction product was precipitated with a methanol–hydrochloric acid mixture to destroy the catalyst and then purified by a solvent extraction technique; treatment of the solid polymer with boiling *n*-heptane, under nitrogen, or cold methyl ethyl ketone removed the low molecular weight atactic polymer (ca. 2% by weight, limiting viscosity in bromobenzene, $\eta_{lim} = 0.08$); treatment of the residue with boiling bromobenzene, under nitrogen, removed a further 90–95% by weight of the sample. This fraction was precipitated with methanol, and purified further by redissolving and reprecipitating. The polymer sample was then vacuum dried. The above purification scheme did not cause any detectable degradation of the polymer since its viscosity before and after repeated treatments was the same. The final purified product gave no metallic (catalyst) residues on pyrolysis, and had a limiting viscosity in bromobenzene, η_{lim}, of 1.41 at 25°C. The relationship between the intrinsic viscosity $[\eta]$ and the viscosity-average molecular weight M_v, for isotactic polystyrene in bromobenzene is not known. Recently, however, Krigbaum[12] has derived relationships between M_v and η for solvents *o*-dichlorobenzene and *p*-chlorotoluene. With the use of these, a M_v value of $4—5 \times 10^5$ can be obtained.

Crystalline isotactic polystyrene samples are almost completely insoluble in cold bromobenzene, and viscosity solutions can only be made up from either quenched (noncrystalline) samples or from refluxing bromobenzene. Precautions to exclude oxygen, i.e., vacuum melting, quenching, and refluxing under nitrogen, have to be taken to prevent oxidative degradation. Repeated experiments varying experimental conditions, e.g., melt time and temperature, in no way altered this viscosity value, provided the temperature was kept below 260°C. It was thus concluded that oxidative degradation, under these conditions, was not important.

Analar grade solvents which were purified by drying and distilling under nitrogen were used throughout.

Apparatus

Dilatometers, similar in design to those used by Banks et al.,[7] were used to follow the isothermal crystallization rates. The measuring capillaries were 0.5 mm. I.D., and about 30 cm. in length. About 100–200 mg. of polymer, previously vacuum melted, out-gassed at 260°C. for several

hours, and molded into a cylindrical shape was confined over the mercury (about 2 ml.).

Isothermal crystallization rates were measured in thermostats (silicone oil) controlled accurately to within ±0.05°C. The extent of crystallization was followed by volume contraction as measured by a cathetometer reading to 0.01 mm. Each isothermal dilatometric rate determination was checked in duplicate on each dilatometer and counterchecked on one other. All rate curves quoted were reproducible.

A polarizing microscope, Leitz Dialux-Pol, was used to follow the development of the crystallizing entities in the polymer melt. The modified microscope was fitted with a hot-stage thermostatted by a thermistor bridge circuit to within ±0.1°C. for periods up to a day.[13] This degree of thermal stability could only be attained with a stabilized power supply and a draught-free thermostatted room (±2°C.).

The size, distribution, and number of entities were measured photographically and also visually with a micrometer eyepiece. To prevent oxidative degradation of the samples the thermostatted compartment of the hot-stage was flushed at intervals with air-free nitrogen. The reproducibility of the crystallization growth rates at fixed temperature was used to check for degradation of the sample.

Polymer samples were studied in thin films (0.05–1.0 mm. thick) which were placed on a thin glass microscope cover slip. Placing a sample between two cover slips had no effect on the rate of spherulite growth. No temperature gradient sufficient to cause a detectable variation in growth rate within the field of view of the sample was ever noticed.

Measurement of Crystallinity

The crystallinity of a polymer sample was calculated from its density, as measured by flotation in aqueous potassium chloride solutions at 20°C. The density of 100% crystalline isotactic polystyrene was taken as 1.125 as calculated from the crystalline unit cell.[14] The amorphous density was obtained from samples quenched rapidly from above the melting point. A linear relationship was assumed between density and degree of crystallinity.

The densities of the totally crystallized samples were found to lie in the range of 1.068–1.081 g./cm.^{3}, corresponding to 25–40% total crystallinity. These samples were allowed to crystallize and anneal well into the post-Avrami region. Variations were found between final densities and temperatures, i.e., a sample crystallized and annealed for 20 hr. at 175°C. had a density of 1.070 g./cm.^{3} (30% crystallinity) whereas a sample heated at 166°C. for only 3 hr. had a density of 1.081 g./cm.^{3} (40% crystallinity).

The relationship between density and temperature, and also extent of crystallization, as measured from the kinetic curves, in the temperature range (150–210°C.) is in the process of being studied. An approximate linear relationship has been found between density and the ratio of the

optical density of the infrared bands at 962 and 980 cm.$^{-1}$, and this can be used as a rapid check on the degree of crystallinity.

Method of Analysis

The Avrami equation, eq. (1), for the development of crystallization from a polymer melt can be rewritten in a form suitable for dilatometry, namely,

$$(h_t - h_\infty)/(h_0 - h_\infty) = \exp\{-k_c t^n\} \tag{2}$$

where h_0, h_t, and h_∞ are the dilatometric readings initially, at time t, and finally, respectively.

During the final stages of crystallization the experimental curves may deviate markedly from the symmetrical Avrami equation curve. This is due to the advent of another process, called secondary crystallization, which cannot be expressed by an Avrami equation. This makes the determination of h_∞ for the Avrami portion of the curve impossible without some assumptions being made.

Two current methods of analysis are available for the determination of k_c and n. A plot of log $[-\ln (h_t - h_\infty)/(h_0 - h_\infty)]$ against log (t) will give a straight line with a gradient of n, and an intercept when $t = 1.0$ of log k_c. This method is, however, rather insensitive to small variations in n. The second method assumes an Avrami equation with a constant n can be applied to the curves throughout the whole crystallization, in which case,

$$n = -t(dh_t/dt)\{(h_t - h_\infty) \ln [(h_0 - h_\infty)/(h_t - h_\infty)]\}^{-1} \tag{3}$$

If n is not a constant, but varies with time, a second term, $dn/dt \ln (t)$, should be added. This method normally assumes that dn/dt is very small, and neglects the term.

Difficulties arise in the two methods since dh_t/dt and h_∞ cannot be gauged with sufficient accuracy. However, they can be approximated.

If a value of h_∞ is assumed from the experimental curve an approximate value for n can be derived, and since the value of n is insensitive to small variations in h_∞ over the initial portion of the curve, the value so obtained has some significance.

Since

$$-d^2h_t/dt^2 = [(n-1)t^{n-2} - nk_c t^{2n-2}][nk_c/(h_0 - h_\infty)] \exp\{-k_c t^n\}$$

at the point of inflection, $t = t_i$, and $d^2h_t/dt^2 = 0$, for which,

$$t_i = [(n-1)/nk_c]^{1/n}$$

and so,

$$(h_i - h_\infty)/(h_0 - h_\infty) = \exp\{-(n-1)/n\} \tag{4}$$

From a plot of dh_t/dt against t, t_i and hence h_i can be found from the experimental curve, and an improved value for h_∞ can be determined. Resubstituting this value in the original eq. (3) will give a more accurate n

value. This method also assumes a constant n value throughout the primary crystallization.

dh_t/dt values were determined from the best fit of plots of $\Delta h_t/\Delta t$ against t. The statistical error was calculated and used in determining the error in n.

The rate constant k_c was determined from the values of $t_{1/2}$, the time for half of the primary crystallization to take place, and the average n value, from eq. (5):

$$k_c = \ln 2/t_{1/2}^{n} \tag{5}$$

RESULTS

Polymer Melting Behavior

A temperature–volume curve was determined dilatometrically to measure the equilibrium melting point of the sample of crystalline isotactic polystyrene. The polymer was melted at 260°C. for 1 hr. and crystallized at 210°C. for over two weeks. The temperature was then raised at the rate of 20°C./day up to 230°C., and then at the rate of 2°C./day. The point of final melting was reached at 238.5 ± 0.5°C. The sample was then recooled at the same rate, and the usual crystallization hysteresis curve obtained. The cycle was repeated at different rates of heating and melting points in the range 238.5–239.0°C. redetermined (Fig. 1). For the purpose of any calculation the higher value of 239.0°C. was taken as the equilibrium melting point.[15]

The value of 239.0°C. compares with the melting range 238–240° determined on the hot-stage microscope. On melting thin spherulitic samples,

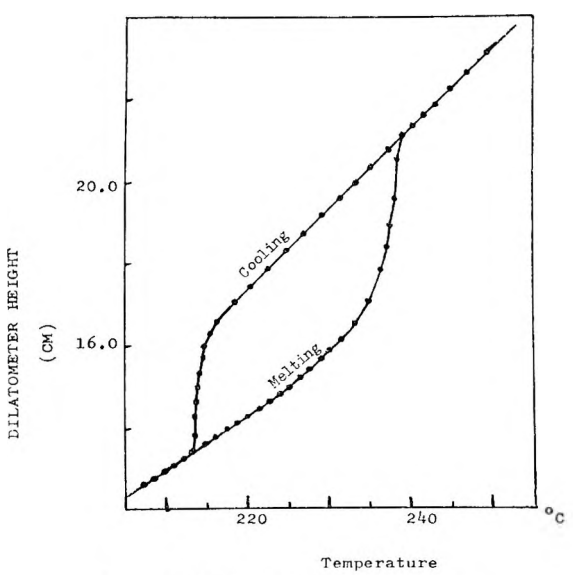

Fig. 1. Melting point determination.

on the microscope hot-stage between crossed Nicols, marked changes in birefringence occurred. At room temperature and temperatures up to 200°C. the spherulites showed no colored birefringence. Above this temperature and up to 230°C. changes in colored extinctions from dark green to light blue (with a first-order red compensator inserted) occurred. In this temperature interval, the changes in retardation could be due to refractive indices changes associated with loss of ordered structures and melting or alternatively to the thermal expansion of the sample. This latter explanation was considered to be less likely because of the reproducibility of the color changes in different samples. Above 230°C. birefringence completely disappeared, but this was not associated with complete melting of the polymer sample. On cooling, recrystallization of the sample occurred at very much faster rates and with obvious signs of the recrystallization being seeded with unmelted crystalline fragments. This seeded crystallization persisted even after long annealing in the temperature range 230–238°. Furthermore, if the sample is rapidly quenched just at the point of disappearance of the last traces of birefringence, the original spherulites are reproduced unaltered. The disappearance of birefringence would thus seem to be no criterion of total melting and certainly no measure of the equilibrium melting point.

The value of 239.0°C. taken for the equilibrium melting point for isotactic polystyrene compares with that of 240°C., as found by Natta et al.,[16] but values of 229°C.,[10] 230–235°C.,[12] and 250°C.[17] have also been found. These wide differences must either reflect differences in nonequilibrium melting conditions, as can arise when birefringence alone is used as a guide to the last traces of crystallinity or to differences in the tacticity of the polymer samples. The presence of syndiotactic or heterotactic structures in an isotactic polymer would reduce the melting point in an exactly analogous way to impurity groups.

Dilatometric Crystallization Rates

The isothermal crystallization rate curves are shown in Figure 2, where the dilatometric height h_t is plotted against log (t). It is rather apparent that the different curves are not superposable along the log t axis, over the complete range shown, nor do they fit an Avrami equation curve exactly. The h_t values do not stop abruptly at a fixed point h_∞ as required but instead continue to decrease, but at a much slower rate. This region of slow change is normally attributed to the intervention of a process of crystallization, i.e., secondary crystallization, which proceeds according to the equation:[8,18]

$$h_t' = C - D \log t' \tag{6}$$

where h_t' and t' refer to new axes, beginning at the onset of secondary crystallization, and C and D are temperature-dependent constants. An equation of this type would also seem to apply in the above example, since h_t does eventually decrease linearly with log (t). The initial portion of the

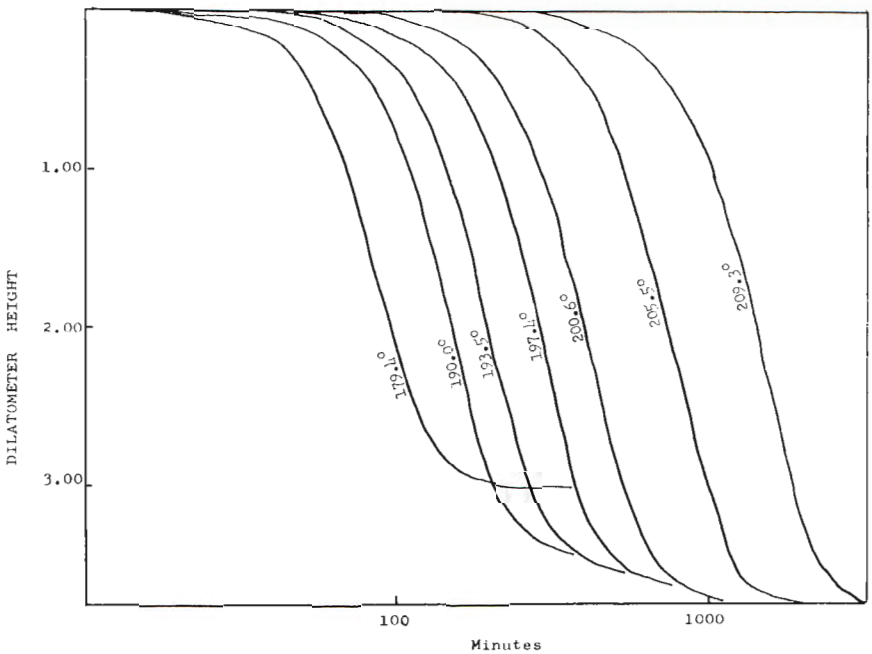

Fig. 2. Dilatometric isothermal rate curves.

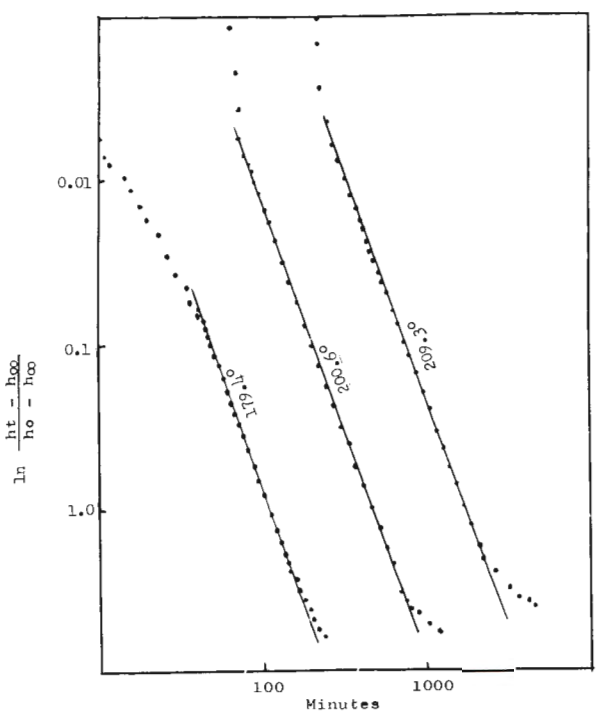

Fig. 3. Analysis of the rate curves.

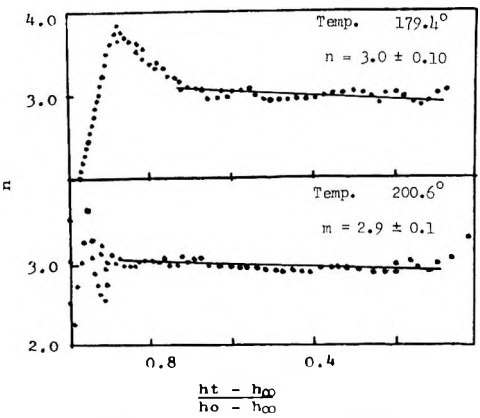

Fig. 4. Variation in n value during crystallization.

rate curves were analyzed by the methods listed above. The accuracy in determining n by both methods within the range 10–90% of the primary crystallization, is no greater than 0.1, as can be seen from Figures 3 and 4, and for most of the rate curves, n is not sufficiently different from the integer 3.0, as required by theory, to warrant using any other value. The constants for the rate curves given in Table I were calculated using $n = 3.0$.

TABLE I
Avrami Parameters

Temperature, °C.	Avrami constant n (average)	Half-life $t_{1/2}$ min.	Rate constant k_n, min.$^{-1}$ $\times 10^{10}$
179.4	3.05 ± 0.1	90	9,510
183.1	2.80	102	6,530
187.5	2.90	119	4,110
190.0	2.90	140	2,530
193.5	2.85	182	1,150
197.4	2.90	270	352
200.6	2.90	380	126
205.5	2.90	720	18.6
209.3	2.90	1380	2.95

The isothermal rate curves at the lower temperatures appeared to be anomalous. The variation in n during crystallization can be seen from Figures 3 and 4 for the run at 179.4°C. Initially n appeared to rise towards 4.0 then to fall to about 3.0, where it remained about constant till after 90% of the primary crystallization had taken place. Similar variations, but to a lesser extent were also found in the initial values of n of the other low temperature experiments, i.e., 183.1 and 187.5°C. This initial variation must be due to a change in mode of crystallization, and if n has any real significance, the crystallization must change from homogeneous nu-

cleation to heterogeneous nucleation, or from homogeneous nucleation growing in three dimensions to that in two.

Microscope Crystallization Rates

Dilatometry measures a compound crystallization rate constant, k_c, which includes constants for nucleation and growth rates (G and N, respectively). Direct observation of the crystalline sample with the aid of a microscope allows each of these to be determined separately, and so the variation in the rate constant k_c with temperature can be accounted for in terms of these more fundamental processes.

Crystallinity develops in a melt of isotactic polystyrene from spherical entities which take on the characteristic Maltese cross and radial fibrillar appearance of typical polymer spherulites.[10] There is, however, no evidence of concentric circles or zigzag birefringence patterns which have been noted in other polymers.[19] All spherulites produced in the temperature region 140–210°C. have the same general appearance, and there is no evidence of any other spherulitic modification. Growth was entirely from spherical entities.

Within the range of observation, each spherulite grew at a constant linear growth rate, until impingement with its neighboring spherulites terminated the growth abruptly. The regions of polymer melt between nontouching crystalline surfaces, however, continued to grow at the same rate. The linear radial growth rates were found to be reproducible from spherulite to

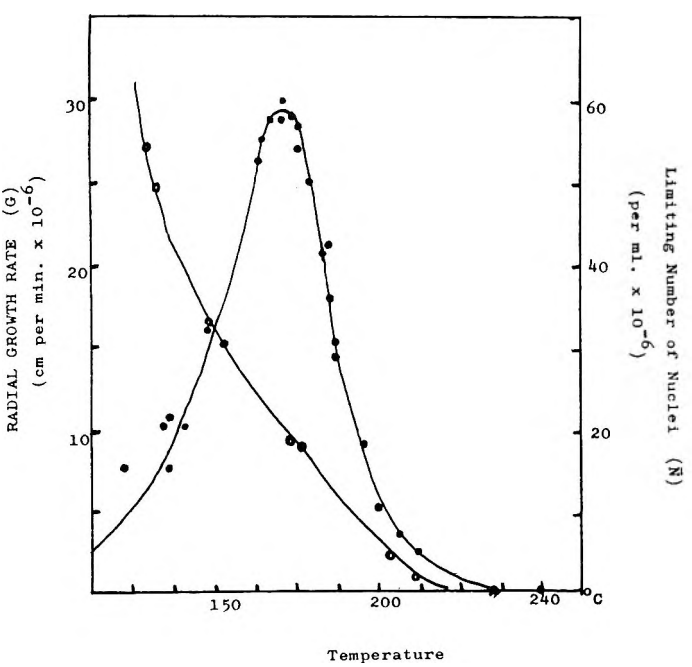

Fig. 5. Microscope observations.

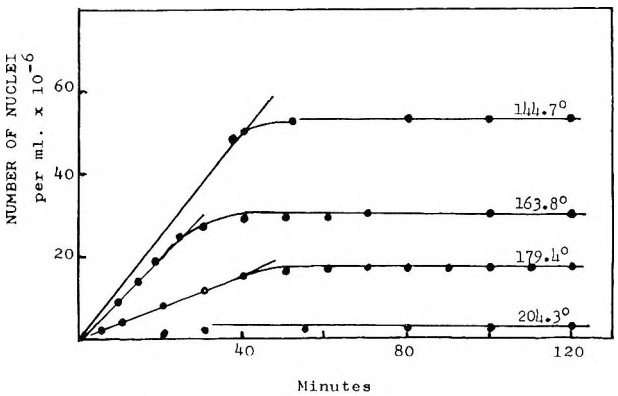

Fig. 6. Isothermal nucleation rates.

spherulite within the field of view, from sample to sample, and only dependent on the temperature of crystallization. The linear radial growth rates plotted against temperature, in Figure 5, show the normal type of distribution curve, with the maximum in radial growth rate between 170 and 180°C. (cf. Kenyon et al.[10]).

The development of nuclei with time, as measured from the total number of spherulites in the field of view, is shown in Figure 6 for various temperatures. At each temperature there is an initial region in which the number of growing centers increases linearly with time, after which the number reaches a limiting value, and then remains unchanged until the end of the

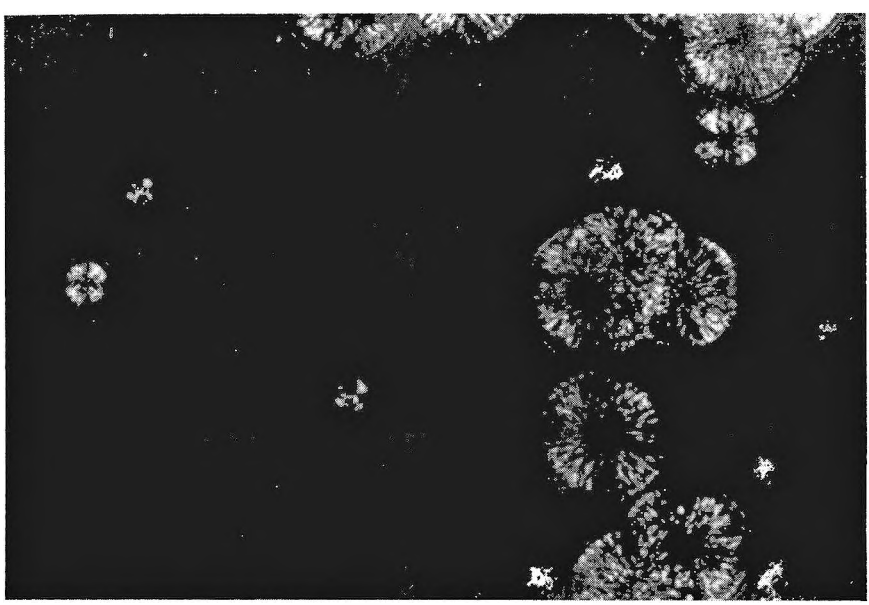

Fig. 7. Spherulites of isotactic polystyrene between crossed Nicols. Grown at a fixed temperature.

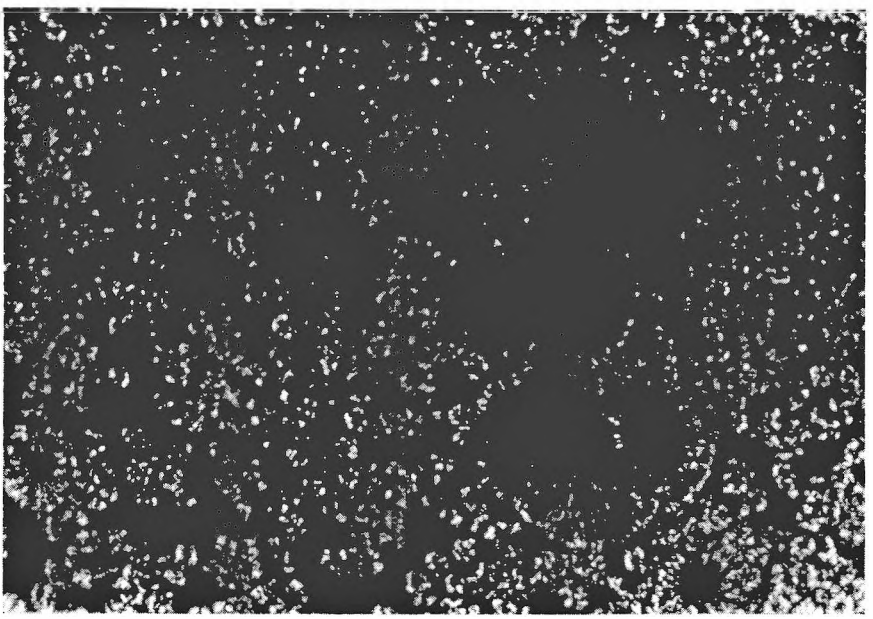

Fig. 8. Spherulites of isotactic polystyrene between crossed Nicols. Temperature of crystallization lowered then raised to the original value.

crystallization. This limiting number of nuclei changes with temperature, as can be seen from Figure 5, but unfortunately the number also varies from sample to sample. However, for any one sample the limiting number of nuclei is reproducible for each temperature, provided the sample is properly melted prior to recrystallization and given the same cooling treatment. Figures 7 and 8 show the effect of different cooling treatments on the number of nuclei in the field of view. A sample was crystallized till the limiting number of nuclei were produced (Fig. 7), cooled to a much lower temperature for a short period, and then reheated to the higher temperature again. The nuclei produced at the lower temperature continued to grow at the higher one (Fig. 8). The variation in the limiting number of nuclei with temperature shows the same general trend from sample to sample, as is shown for one sample in Figure 6. No significance other than relative can be placed on the numerical values quoted for the nucleation rate N, or the limiting nucleation number $\bar{N}$.

For a particular sample spherulites were found to be reproduced in approximately the same position for each isothermal run. The actual distribution of spherulites, however, appeared random, at least as far as can be judged from the limited number of observations. No preferential surface nucleation was noticed. Nucleation was therefore considered to be created at activated heterogeneous sites distributed at random throughout the sample, the concentration of these sites decreasing with increasing temperature. All the sites were not equivalent, since they increased linearly with time, at least initially, until saturation was reached, indicating a wide

range of activities of these heterogeneous sites. Heterogeneous nucleation in polymer crystallization has been noted in other polymers.[8]

DISCUSSION

An Avrami crystallization equation can be proposed for the model suggested by microscope observations, since the heterogeneous nucleation sites are randomly distributed throughout the sample. The crystallization growth rate constant k_c can then be related to the crystallization growth rate G and the nucleation number $\bar{N}$ by eq. (7):

$$k_c = \pi\rho_c\bar{N}G^3/3\rho_1X_w \tag{7}$$

where ρ_c and ρ_1 are the crystalline and melt densities, respectively, and X_w is the degree of crystallinity of the condensed phase. In practice, X_w is impossible to measure since it most likely varies with extent of condensation. However, an approximate value can be derived by using the final degree of crystallinity. X_w then lines between 0.3 and 0.4 but closer to 0.3. Also, since N cannot be determined exactly, direct comparison between the values of k_c determined dilatometrically and microscopically is not justified. However, since the nucleation numbers in the two systems must change with temperature in the same general way relative comparisons

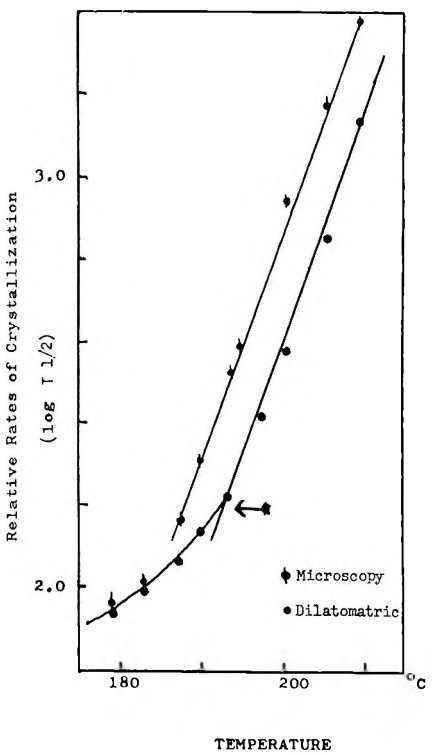

Fig. 9. Temperature dependence of log $t_{1/2}$.

are justified. For this reason the log $t_{1/2}$, as calculated for $n = 3.0$ for the two systems is plotted against temperature in Figure 9. There is clear agreement in the way in which the two sets of values for $t_{1/2}$ change with temperature above 190°C., but marked deviations occur in the dilatometric values below this temperature. These deviations arise in this region

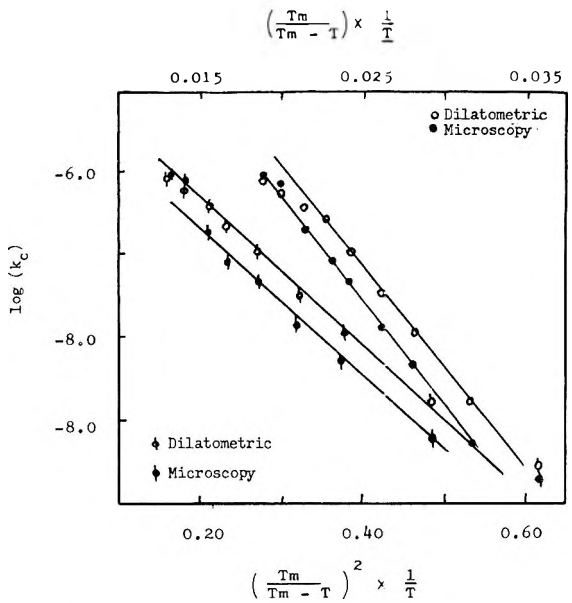

Fig. 10. Crystallization temperature dependence.

because the time required to produce all the nuclei capable of growth is a reasonable fraction of the total primary crystallization time. In this initial fraction, the number of nuclei increases linearly with time t;

$$\bar{N}_t = Nt$$

where N is the nucleation rate constant. Resubstituting this value for $\bar{N}$ in eqs. (3) and (7) makes the Avrami constant n equal to 4.0, instead of 3.0:

$$G^3\bar{N}t^3 = G^3Nt^4 \tag{8}$$

The assumption of a constant n value for these runs is not valid, so that the observed and calculated $t_{1/2}$ values do not agree. Analysis of the dilatometric rate curves for these runs did in fact show an n value decreasing initially from about 4.0 (see Figs. 3 and 4). The time scale during which this transition occurs is consistent in both cases. For the 179.4°C. run, the limiting number of nuclei is reached after about 60 min., while the value of n reaches 3.0 ± 0.1 (indicative of predetermined spherical nucleation) after 65 min., conclusive that the same phenomenon is being observed in both cases. The marked deviation in the plot of log $t_{1/2}$ against temperature below 190°C. must arise from the overlap of two Avrami processes, and the

inability to apply eq. (5) further to the system. The superposition of two Avrami processes has been dealt with before.[9]

It has been considered by Mandelkern et al.[20] that for a system crystallizing from spherical nuclei with spherical growth, the overall crystallization rate constant k_c is given by

$$\log k_c = B - [7.28\delta^3 T_m^2/(h_u)^2(T_m - T)^2 kT] \quad (9)$$

where B involves the preexponential rate factors for growth and nucleation, and a term in the activation energy for bulk flow of the polymer, T is the crystallization temperature, T_m the melting temperature, and k the Boltzmann constant. δ is the interfacial energy per unit area between the crystallizing surface and the melt, and h_u is the heat of fusion per unit volume (calculated from the x-ray unit cell of isotactic polystyrene[21] and the heat of fusion[22]). On the other hand, Burnett and McDevit[23] consider that spherulitic growth occurs by two-dimensional nucleation on the spherical surface. The rate constant k_c is then given by eq. (10):

$$\log k_c = C - C_1 T_m[T(T_m - T)]^{-1} \quad (10)$$

where C and C_1 are constants similar to those in eq. (9).

Plots of $\log k_c$ against $T_m[T(T_m - T)]^{-1}$ and $T_m^2[T(T_m - T)^2]^{-1}$ are shown in Figure 10 for k_c determined both by dilatometry and calculated from the nucleation number and growth rate. Reasonably good straight lines for both types of temperature dependence are obtained, and so, as is usually found with most polymers,[24] no discrimination can be made between the two possible mechanisms.

From the plots of $\log k_c$ against $T_m^2[T(T_m - T)^2]^{-1}$ two lines each with a slope of -6.8 were obtained, corresponding to a surface free energy δ of 4.4_4 ergs/cm.^{2}. This value must to some extent explain the low crystallization rates and small temperature dependence of these rates, since it is smaller than the range, 5.3–7.8, quoted for several polymers.[19] It may possibly reflect the stiffness of the polystyrene chain and its difficulty in crystallizing into its spiral conformation.

References

1. Avrami, M., *J. Chem. Phys.*, **7**, 1103 (1939); *ibid.*, **8**, 212 (1940); *ibid.*, **9**, 177, (1941).
2. Evans, U. R., *Trans. Faraday Soc.*, **41**, 367 (1945).
3. Morgan, L. B., *Progress in Polymer Science*, Part 1, Heywood, London, 1961, pp. 268–269.
4. Banks, W., and A. Sharples, *Makromol. Chem.*, **59**, 233 (1963).
5. Inoue, M., *J. Polymer Sci.*, **55**, 753 (1961).
6. Rohleder, J., and H. A. Stuart, *Makromol. Chem.*, **41**, 110 (1961).
7. Banks, W., M. Gordon, R.-J. Roe, and A. Sharples, *Polymer*, **4**, 61 (1963).
8. Sharples, A., and F. L. Swinton, *Polymer*, **4**, 119 (1963).
9. Banks, W., A. Sharples, and J. N. Hay, *J. Polymer Sci.*, **A2**, 4059 (1964).
10. Kenyon, A. S., R. C. Gross, and A. L. Wurstner, *J. Polymer Sci.*, **40**, 159 (1959).
11. Burnett, G. M., and P. J. T. Tait, *Polymer*, **1**, 40 (1960).

12. Krigbaum, W. R., D. K. Carpenter, and S. Newman, *J. Phys. Chem.*, **62**, 1586 (1958).
13. Hay, J. N., *J. Sci. Instruments*, **41**, 465 (1964).
14. Natta, G., *Makromol. Chem.*, **16**, 77 (1955).
15. Mandelkern, L., *Rubber Chem. Technol.*, **32**, 1392 (1959).
16. Natta, G., *SPEJ.*, **15**, 373 (1959).
17. Campbell, T. W., and A. C. Haven, *J. Appl. Polymer Sci.*, **1**, 73 (1959).
18. Majer, J., *Kunststoff Rundschay*, **10**, 9 (1963).
19. Keller, A., in *Growth and Perfection of Crystals*, R. H. Doremus, B. W. Roberts, and D. Turnbull, Eds., Wiley, New York, 1958, p. 509.
20. Mandelkern, L., F. A. Quinn, and P. J. Flory, *J. Appl. Phys.*, **25**, 830 (1954).
21. Natta, G., and P. Corradini, *Makromol. Chem.*, **16**, 77 (1955).
22. Boundy, R. H., and R. F. Boyer, *Styrene, Its Polymers, Copolymers and Derivatives*, Reinhold, New York, 1952.
23. Burnett, B. B., and W. McDevit, *J. Appl. Phys.*, **28**, 1101 (1957).
24. Mandelkern, L., in *Growth and Perfection of Crystals*, R. H. Doremus, B. W. Roberts, and D. Turnbull, Eds., Wiley, New York, 1958, p. 482.

Résumé

On a mesuré la cinétique de cristallisation d'échantillons de polystyrène isotactique à différentes températures. Malgré des phénomènes de cristallisation secondaire, on peut atteindre une précision suffisante pour pouvoir attribuer à la plupart des courbes cinétiques une relation d'Avrami présentant une valeur de n constante et entière. L'interprétation des constantes d'Avrami sur la base d'une cristallisation par croissance d'entités sphériques produites en des sites fixes est confirmée par les observations faites au microscope.

Zusammenfassung

Die Kristallisationskinetik einer Probe von isotaktischem Polystyrol wurde bei verschiedenen Temperaturen untersucht. Ungeachtet des Auftretens einer Sekundärkristallisation kann eine ausreichende Genauigkeit erreicht werden, um den meisten Geschwindigkeitskurven eine Avrami-Beziehung mit einem konstanten ganzzahligen Wert von n zuordnen zu können. Die Interpretierung der Avrami-Konstanten in Beziehung zu einer Kristallisation durch Wachstum von kugelförmigen, an festen Plätzen gebildeten Einheiten wird durch mikroskopische Beobachtungen verifiziert.

Received March 18, 1964
Revised April 27, 1964

JOURNAL OF POLYMER SCIENCE: PART A VOL. 3, PP. 449–455 (1965)

Anionic Polymerization of Butadiene and Styrene

A. F. JOHNSON* and D. J. WORSFOLD, *Applied Chemistry Division, National Research Council, Ottawa, Canada*

Synopsis

A kinetic study has been made of the polymerization of butadiene and styrene in an aliphatic hydrocarbon solvent with the use of butyllithium as an initiator. It is shown that the anomalous behavior in the initiation reaction exhibited by isoprene under these conditions is also found for these two monomers. These monomers give a sigmoidal rate curve in the initiation reaction in cyclohexane solution, and the reaction appears to be auto-catalytic. The propagation reactions were studied also, and the results compared with the rather discordant sets of data published by other authors.

It was found that the kinetics of the initiation reaction of the polymerization of isoprene with butyllithium in cyclohexane[1] differed greatly from that of the reaction of styrene and butyllithium in benzene solution.[2] The former reaction showed far more complex behavior than did the latter. It had an initial slow period with an increasing rate, giving a sigmoidal rate curve instead of an initially linear formation of active centers with time as found for styrene in benzene solution. Moreover the kinetic order in initiator was different. To find whether similar behavior occurred with other monomers in cyclohexane solution, a general kinetic investigation has been made of both butadiene and styrene polymerization initiated by butyllithium in this solvent.

Experimental

The same general techniques used before[1] were again adopted. These involve the use of high-vacuum techniques for handling the reagents, and washing the walls of the all-glass reaction vessel to cleanse them of reactive impurities. The systems used only breakseals and no greased joints or taps. For the styrene polymerization the ultraviolet absorption bands of the styrene and polystyryl anion were used to determine their concentrations for the rate measurements. The polystyryl anion has an absorption maximum at 328 mμ (ϵ = 13,500), the polybutadienyl anion at 275 mμ (ϵ = 8,330). In the case of butadiene only the initiation reaction was followed spectrophotometrically.

The propagation reaction of butadiene was followed by the drop in vapor pressure of the reaction mixture as the monomer was consumed. When

* Present address: Chemistry Department, University of Sussex, Brighton, England.

the initiation reaction was found to be complete from measurement of the optical density of the solution, a further addition of monomer was made. The apparatus was then opened, via a breakseal, to an evacuated monometer warmed above the reaction temperature. The drop in the vapor pressure of the magnetically stirred reaction mixture was measured with a cathetometer. It was found that the pressure of butadiene over its solutions was linear with concentration in the range used, normally 0.63 *M* and below.

The light-scattering measurements on the polystyrene reaction mixtures were carried out in a sealed, all-glass apparatus, in a Brice-Phoenix light-scattering photometer at 34°C. The cyclohexane solvent scattering in the sealed apparatus before the reactants were mixed was found to be as low as the best values found in more normal experiments There was a filter between the compartment where the reaction was performed and the light-scattering cell, to remove fragments of the broken glass reagent bulbs. No dissymmetry measurements were made because of the experimental difficulties, but in cyclohexane at the Θ temperature dissymmetry is not large Under these conditions polystyrenes with molecular weights of 240,000 and 500,000 have previously been found to have dissymmetries of 1.11 and 1.26, respectively, making the true molecular weights 7 and 16% respectively, higher than uncorrected values.

The treatment of the styrene has been described before. The butadiene was purified by several condensations onto butyllithium, and by bubbling through liquid sodium–potassium alloy.

Results and Discussion

It was found that when sufficiently pure monomer was used, both styrene and butadiene on reaction with butyllithium in cyclohexane showed an initial period of slow reaction, where the rate of appearance of the absorption band of the appropriate polymer anion increased with time. This same behavior was observed in the reaction of isoprene with butyllithium in this solvent.[1]

After the initial slow period, the rate of the appearance of the polymer anion absorption showed a temporary steady reaction rate before declining again as the monomer was consumed. The concentration–time curve of polymer ion concentration was in fact sigmoidal in shape. If the initiation rate is taken as the maximum rate it is found that the apparent order with respect to monomer is close to first in both cases, but the order with respect to the butyllithium is between one-half and one. The same behavior was found for isoprene.

The reaction rates were not found very readily reproducible, as is seen from Figures 1 and 2. A not quite so rigorously purified sample of butadiene was found not to have the initial slow reaction rate. The absorption of the polybutadienyl anion increased linearly with time on mixing the reagents, and the rate slowly decreased as monomer and butyllithium were depleted. Moreover, this sample of monomer showed an initial re-

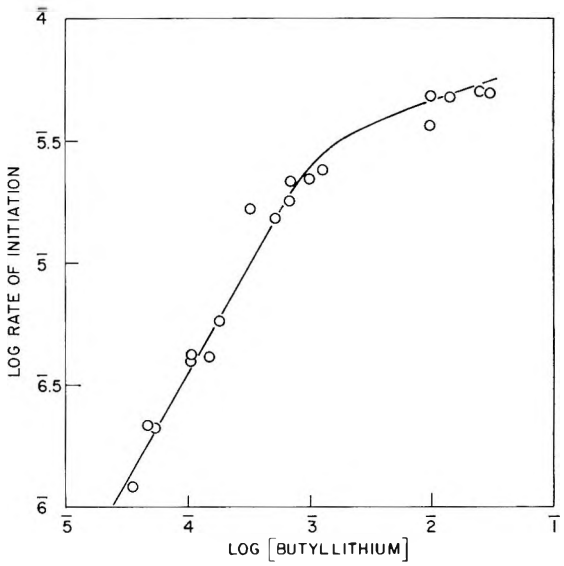

Fig. 1. Dependence of maximum rate of initiation of styrene on butyllithium concentration at 40°C.

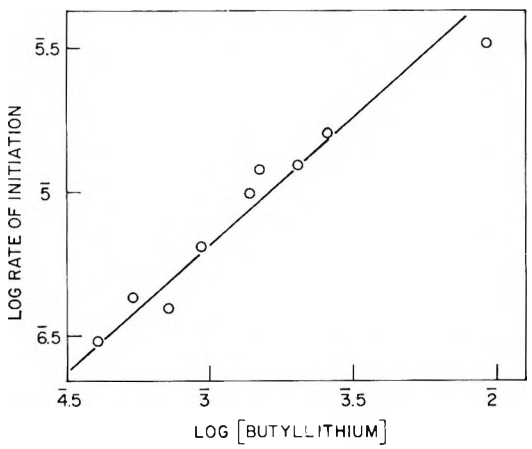

Fig. 2. Dependence of maximum rate of initiation of butadiene on butyllithium concentration at 40°C.

action rate with butyllithium about three times the maximum rate shown by the purer monomer. Evidently the impurities present acted as a catalyst. However, if, as is probable, the impurities were of a type which would destroy butyllithium, their concentration must have been very low as they had no appreciable effect on the final concentration of polybutadienyl anions as measured by their optical density.

It has been shown that the active polymer chain end has the typical spectrum of the appropriate carbanion.[3] The nature of the carbon–lithium

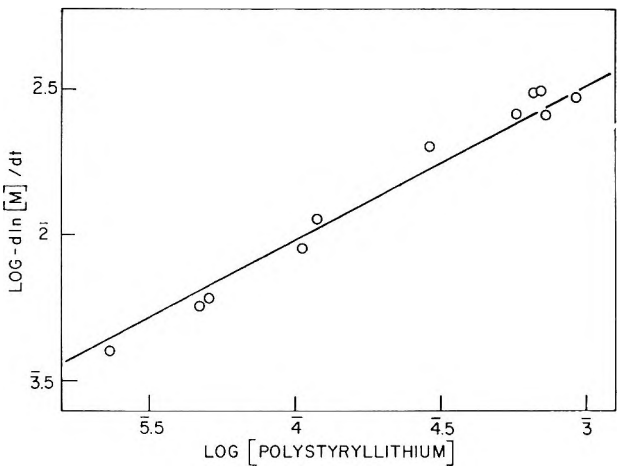

Fig. 3. Dependence of propagation rate on polystyryllithium concentration at 40°C.

bond in butyllithium is still largely in doubt, but it quite possibly has a less ionic nature than that in polybutadienyl or polystyryllithium, as there is less possibility of delocalizing the charge. The fact that it is highly associated in hydrocarbon solvents still indicates a very polar bond. In these circumstances it is not unexpected that there is a reluctance to form the highly polar polymer carbanion–lithium ion pair by a normal homogeneous bimolecular reaction in an aliphatic hydrocarbon solvent. Even the change to the more polarizable benzene as a solvent promotes the reaction rate by a factor of nearly two powers of ten in the case of styrene. Thus it is suggested that the reaction is to a certain extent autocatalytic, the presence of the already formed carbanion promoting the reaction. The presence of adventitious or deliberately added lithium salts, would also be expected to have a promoting effect as has been found. Under these circumstances the reaction kinetics would be complex, and the reaction orders arbitrarily determined from maximum rates of no simple significance. It should be noted, however, that with the highly purified monomer, for both styrene and butadiene, the initiation reaction is slow.

If it is desired to measure the propagation reaction, for both monomers care must be taken to ensure that the initiation reaction is complete. Some hundreds of monomer molecules must react for every one of butyllithium before the initiation step is complete. If sufficient monomer is present, the optical density due to the polymer anion attains a stable maximum steady value when all the butyllithium has reacted to form polymer ions. After that, the rate of the monomer disappearance is the true propagation reaction rate for that concentration of polymer anions. It was found that at this point monomer concentration–time plots were first-order over three half-lifetimes for both monomers.

The order with respect to the polystyryl carbanion in the styrene polymerization was close to one-half (Fig. 3). This is the same order as found by a

number of authors[2,4] in aromatic hydrocarbon solvents, although the actual reaction rate was only about one-third of that found in benzene solution. Thus the polystyryllithium is assumed to be dimeric in cyclohexane as well as in benzene, with a small equilibrium amount of free ion pairs which are the active agents. The lower rate in cyclohexane is probably caused by a smaller dissociation constant to free ion pairs.

Cyclohexane is a theta solvent for polystyrene at 34°C., so this should be an ideal system for determining the degree of association of the living polymer ion pairs from light-scattering measurements, as was done for polyisoprenyllithium.[1] The results are shown in Table I. The light-

TABLE I

Polystyryllithium concn., moles/l.	M. W. (calc.)	M. W. (visc.)	Light scattering	
			M. W. (killed)	M. W. (living)
8×10^{-5}	231,000	258,000	208,000	424,000
7×10^{-5}	183,000	191,000	179,000	282,000

scattering results should all be somewhat higher (10–20% depending on molecular weight), as no account was taken of the dissymmetry of the scattering. The calculated molecular weight is that found from the added butyllithium and styrene. The viscosity molecular weights were measured in toluene for the isolated polymers, and are rather higher than the calculated figure because the rather slow initiation reaction would cause the $\bar{M}_w/\bar{M}_n$ ratio to be somewhat greater than one. The ratios of the molecular weights of the "living" and "dead" polymers are 2 and 1.6 in the two cases, and indicate that even at this low concentration of polystyryllithium, it is still largely in the form of a dimer. Thus the degree of association found is the same as found by Morton et al.[4] from bulk viscosity measure-

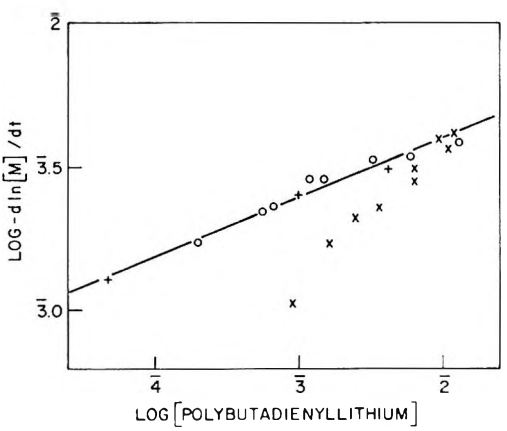

Fig. 4. Dependence of propagation rate on polybutadienyllithium concentration at 30°C. (O) this work; (+) Spirin et al.;[5] (×) Morton et al.[6]

ments in benzene solution. The association does not seem to change with hydrocarbon solvent. The same perhaps is true of other polymer carbanion–lithium ion pairs, as Spirin et al.[5] found much the same degree of association for polyisoprenyllithium in toluene and in heptane solution.

The propagation reaction for butadiene was found to have close to a one-sixth-order dependence on the concentration of butadienyllithium. The rates are in good agreement with the results of Spirin et al.,[5] and both sets of results are shown in Figure 4. There was similar agreement with this author in the case of polyisoprene, despite the different methods of rate measurement. Morton et al.[6] have found a higher order for the butadiene reaction, and their quoted figure is one-half. Their results, corrected to 30°C. by their activation energy, are also on Figure 4 and show fair agreement with the others.

It is suggested here that the degree of association is sixfold, and that this causes the one-sixth order in polybutadienyllithium in the propagation reaction. It should perhaps be mentioned that when the order is so low, the logarithmic plot is not very sensitive to the exact order.

The degree of association of these polymer lithium compounds must be a function of the carbanion. Polystyryllithium has a twofold association, polyisoprenyllithium has a fourfold, and polybutadienyllithium a sixfold, as does butyllithium. The degree of association is probably governed by the geometry of the substituents on the carbanion.

It is of little value to compare the relative rates of the propagation reactions of the various monomers in order to gauge their relative reactivities. The absolute rate constants of the free polymer ion pair would be indicative of the reactivity, but the measured rate constants are a function of the association constant too. Until a reliable method of measuring the association constants is found, the only method of comparing the activities of the monomers is by copolymerization studies, but these in turn give no indication of the activities of the polymer anions.

The authors wish to thank Dr. S. Bywater for the many helpful discussions during the course of this work.

References

1. Worsfold, D. J., and S. Bywater, *Can. J. Chem.*, **42**, 2884 (1964).
2. Worsfold, D. J., and S. Bywater, *Can. J. Chem.*, **38**, 1891 (1960).
3. Bywater, S., A. F. Johnson, and D. J. Worsfold, *Can. J. Chem.*, **42**, 1225 (1964).
4. Morton, M., L. J. Fetters, and E. E. Bostick, *J. Polymer Sci.*, **C1**, 311 (1963).
5. Spirin, Yu. L., A. R. Gantmakher, and S. S. Medvedev, *Dokl. Akad. Nauk SSSR*, **146**, 368 (1962).
6. Morton, M., E. E. Bostick, R. A. Livigni, and L. J. Fetters, *J. Polymer Sci.*, **A1**, 1735 (1963).

Résumé

On a fait une étude cinétique de la polymérisation du butadiéne et du styréne dans des hydrocarbures aliphatiques en utilisant le butyllithium comme initiateur. On a montré que le comportement anormal de la réaction d'initiation dans le cas de l'isopréne

se présente également pour ces deux monomères. Ces deux monomères donnent une courbe de vitesse sigmoide pour la réaction d'initiation en solution dans le cyclohexane et la réaction apparaît comme étant autocatalytique. On a étudié également les réactions de propagation et les résultats sont comparés aux données plutôt discordantes publiées par d'autres auteurs.

Zusammenfassung

Eine kinetische Untersuchung der Polymerisation von Butadien und Styrol in aliphatischen Kohlenwasserstoffen als Lösungsmittel unter Verwendung von Butyllithium als Starter wurde durchgeführt. Das unter diesen bei Bedingungen Isopren gefundene anomale Verhalten bei der Startreaktion tritt auch bei diesen beiden Monomeren auf. Die Monomeren liefern eine s-förmige Geschwindigkeitskurve bei der Startreaktion in Cyclohexanlösung, und die Reaktion scheint autokatalytisch zu sein. Auch die Wachstumsreaktion wurde untersucht, und die Ergebnisse werden mit den ziemlich widerspruchsvollen von anderen Autoren veroffentlichten Daten verglichen.

Recieved April 15, 1964
Revised June 8, 1964

JOURNAL OF POLYMER SCIENCE: PART A VOL. 3, PP. 457–468 (1965)

Thermal Oxidation of Deuterated Polypropylenes

H. C. BEACHELL and D. L. BECK, *Department of Chemistry, University of Delaware, Newark, Delaware*

Synopsis

This paper describes some of the aspects of the thermal oxidation of deuterated isotactic polypropylenes. Several polymers of propylene, deuterated at different sites along the polymer chain, were subjected to a kinetic treatment designed to establish the comparative rates of oxidation at different temperatures. Infrared spectroscopy was used to follow the kinetics over the temperature interval 100–130°C. These experiments have shown the existence of a deuterium isotope effect for the thermal oxidation of polypropylene.

INTRODUCTION

The deuterium isotope effect has proved to be a useful tool for investigations into the mechanisms of various chemical reactions. It has been used successfully in the study of the oxidation of 2-deuteropropanol-2 by chromic acid.[1] From this study the authors were able to conclude that the site of oxidative attack occurred at the secondary hydrogen atom, since the deuterated compound was oxidized at one-sixth the rate of ordinary isopropanol. More recently, the studies involving the deuterium isotope effect were extended to the elucidation of the mechanism of polymer oxidation reactions. Beachell and Nemphos[2] demonstrated that the reactivity of deuteropolystyrenes depends on the site of the substitution of deuterium within the molecule. It was found that on thermal oxidation the slower rates of oxidation were observed for those polymers in which deuterium was substituted for hydrogen on the tertiary carbon atom. Tryon and Wall[3] found that upon oxidation in the presence of ultraviolet radiation, the deuteropolystyrenes showed a pronounced isotope effect when a deuterium atom was substituted for hydrogen in the tertiary carbon position.

In the present work the kinetics of the thermal oxidation of various deuterated polypropylenes was investigated. The purpose of the study was to compare the oxidation behavior of the deuterated polymers with that of normal polypropylene and to determine the initial site of oxidative attack in the polymer chain. Infrared spectroscopy was used to follow the rates of the oxidation reactions.

EXPERIMENTAL

Polymerization of Monomers

The deuterated monomers were obtained from Merck Sharpe & Dohme of Canada, Ltd. in one-liter metal cylinders. A standard stereospecific catalyst,[4] diethylaluminum chloride and titanium trichloride, was used for the polymer preparations. Each deuterated propylene monomer was transferred into a pressure bottle which contained the polymerization medium (*n*-hexane) and both catalyst components. In order effectively to remove all traces of monomer during the transfer operation, the pressure bottle was cooled on a Dry Ice–acetone bath while the cylinder containing monomer was warmed with a heating lamp. In each case, the polymerization reaction was carried out at 70°C. for a period of 16 hr. After this time, the reaction was quenched with 2 ml. of methanol, filtered warm, and washed with 20 ml. of *n*-hexane. This step was followed by three successive washings with 20 ml. of methanol in order to effect catalyst removal. The resulting polymer was dried at 60°C. in a vacuum oven for a period of 24 hr. For each of the monomers, an average yield of 1.0 g. of pentane-insoluble polymer was obtained.

All deuterated polypropylenes investigated in this work were of the pentane-insoluble or predominately isotactic type.[5] The various samples studied, including a nondeuterated control sample, are listed in Table I. Also included are the polymer designations which will be used throughout the article for the reference to specific samples.

TABLE I

Polymer designations	Monomer	Repeat unit
A	Propene (control)	$-(-CH_2-CH(CH_3)-)_n-$
B	Propene-2-d_1	$-(-CH_2-CD(CH_3)-)_n-$
C	Propene-1,1-d_2	$-(-CD_2-CH(CH_3)-)_n-$
D	Propene-3,3,3-d_3	$-(-CH_2-CH(CD_3)-)_n-$
E	Propene-1-d_1	$-(-CHD-CH(CH_3)-)_n-$

Sample Preparation for the Oxidation Studies

The deuterated polypropylenes were prepared in the form of films for thermal aging studies and subsequent infrared analysis. The polymers were compression-molded by using a Carver laboratory press and under the

following conditions: temperature 200°C., pressure 6000 psi., and time 3–4 min. All films were pressed between chromium-plated, stainless steel plates and the resulting effective thickness was measured to be 7.8 ± 0.2 mils by using a modified Starret dial gauge. Cooling of the films was accomplished by immersing the plates under running tap water. This treatment served to maintain the crystallinity at moderate levels.

Rectangular pieces of uniform thickness were cut from each film and used directly for the kinetic studies. The specimens were placed into 100 ml. beakers such that maximum exposure of both sides of the film surface resulted. These were then aged in a forced-air oven set at the desired temperature. Temperature control was maintained within the limits of ±0.4°C. At frequent time intervals, the films were removed from the oven and scanned in the infrared to follow the course of the oxidation.

All infrared spectrophotometric studies were made at room temperature. The film was inserted into the sample side of the double beam instrument using a specially cut, cardboard film holder. Air was used in the reference beam. A Perkin-Elmer Model 221G infrared spectrophotometer with NaCl optics was used for the studies.

RESULTS AND DISCUSSION

The kinetics of the thermal oxidation of deuterated polypropylenes was studied with the aid of infrared spectroscopy. The infrared carbonyl absorption band was found to be particularly suitable for this purpose. Other investigators[6,7] have also found this absorption region to be of practical utility in the study of polypropylene degradation. A typical carbonyl absorption band for degraded polypropylene is shown in Figure 1, for times of 16 (lower curve) and 26 hr. (upper curve). It may be seen that the band is in general quite broad and lacks discreteness except for the absorption peak at 5.84 μ. Therefore, the infrared carbonyl peak at 5.84 μ was used to follow the course of the oxidation as a function of oven-aging time. Peak height absorbance values were used to gain a measure of carbonyl development.

From the infrared work on long-chain model compounds,[8] the 5.84 μ absorption can be attributed to the presence of acid functional groups as a major degradation product.

The relative rates of oxidation for all of the deuterated polymers, including a nondeuterated control sample, are shown in Figure 2 for an air oxidation temperature of 100°C. Polymers A, C, D, and E all show the same induction time of about 16 hr. At this point incipient degradation then becomes apparent. These polymers also show the same rate of formation of degradation product as is evidenced by the straight-line function of carbonyl development versus time. Polymer B, however, shows a longer induction time, which in this case exceeds 40 hr., and displays a considerably slower oxidation rate as determined by the slope of the line in Figure 2. Thus compared with the other polymers of the series, polymer B is the one which is highly resistant to degradation under the same experimental

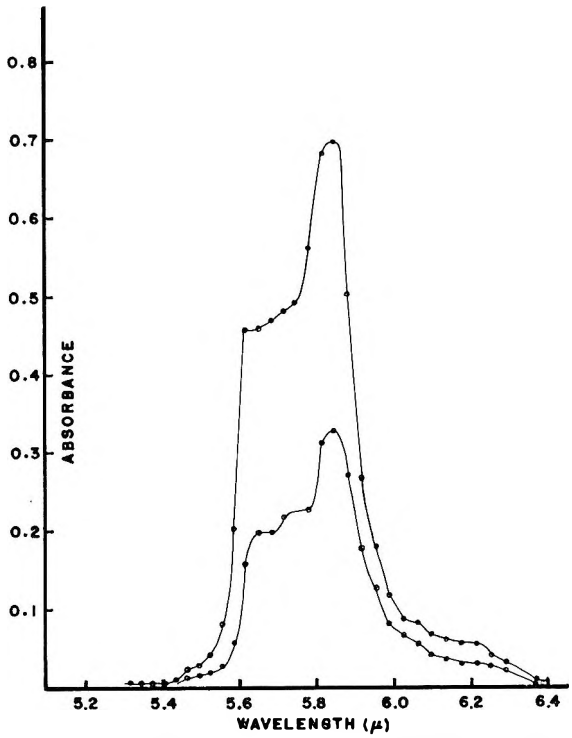

Fig. 1. Effect of thermal oxidation on carbonyl absorption.

conditions. These differences immediately suggest the existence of a deuterium isotope effect.

In order to further test this hypothesis, polymers A and B were subjected to air-oxidation studies at temperatures of 115 and 130°C. Since polymers C, D, and E showed the same behavior upon oxidation as polymer A (the nondeuterated control sample), only polymers A and B will be considered in further treatments. At both temperatures, the oxidation rate for polymer B is again much slower than that for polymer A. In both cases, polymer B also has the longer induction time. These effects are shown in Figures 3 and 4. From this evidence, there can be no doubt as to the existence of a kinetic isotope effect.

A method previously employed[9] was used to calculate the rate constants for polymers A and B at the different oxidation temperatures. On the basis of Beer's and Lambert's law:

$$\log (I/I^0) = edC \tag{1}$$

the term I/I^0 may be used as a measure of the concentration of the absorbing species, since in these experiments the thickness and extinction coefficient remain constant. Plots of log (I/I^0) versus time were made to assess the value of the rate constants for each polymer at the various temperatures studied (Figs. 5 and 6). The slopes of the lines were evaluated

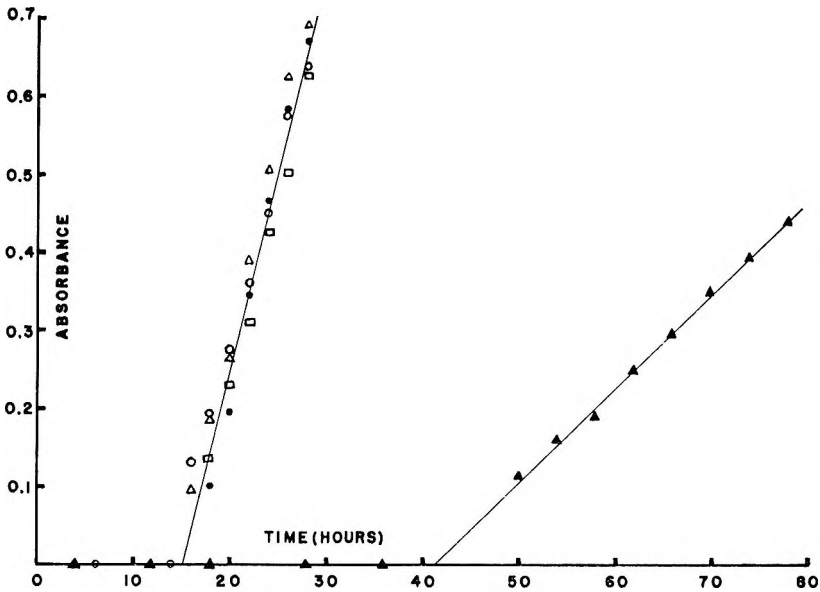

Fig. 2. Carbonyl absorption vs. time: (△) polymer A; (▲) polymer B; (○) polymer C; (●) polymer D; (□) polymer E. Oxidation temperature 100°C.

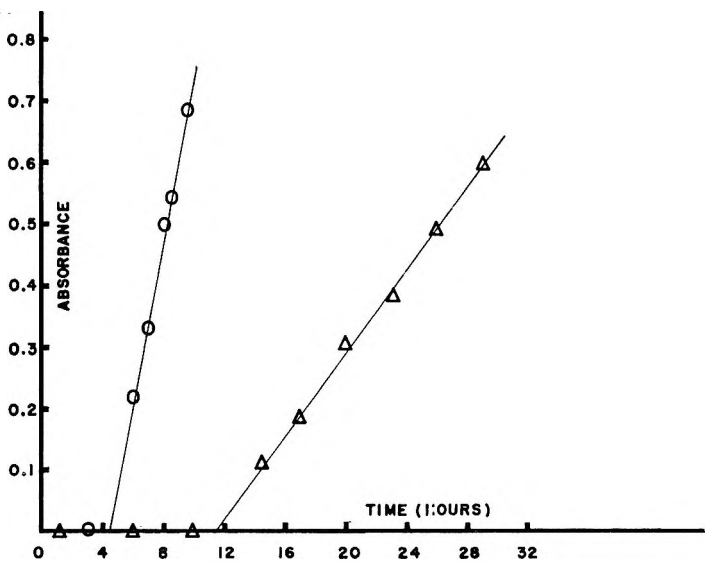

Fig. 3. Carbonyl absorption vs. time: (○) polymer A; (△) polymer B. Oxidation temperature 115°C.

from which the rate constants were obtained. From the ratio of the rate constants between polymer A and polymer B at a given temperature, the magnitude of the deuterium isotope effect is obtained. These values are shown in Table II.

It has been shown that the rate constants for polymer A (the control

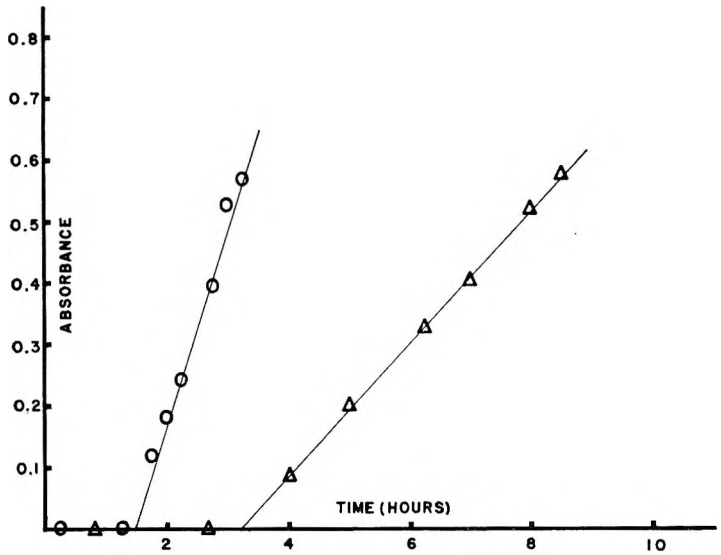

Fig. 4. Carbonyl absorption vs. time: (O) polymer A; (△) polymer B. Oxidation temperature 130°C.

TABLE II

Polymer A		Polymer B		Ratio
Temp., °C.	$k \times 10^4$	Temp., °C.	$k \times 10^4$	k_H/k_D
100	8.57	100	2.01	4.26
115	21.6	115	5.56	3.88
130	52.5	130	15.0	3.50

sample) exceed the rate constants for polymer B (the deuterated sample). Since polymer B is the polypropylene sample with a deuterium atom substituted in the tertiary carbon position, it is clear from the foregoing observations that this particular site is the point of initial oxidative attack and is responsible for the rate-controlling step in the thermal oxidation of polypropylene. Thus it has been demonstrated by means of the deuterium isotope effect that the initial step in the thermal oxidation of polypropylene involves the abstraction of hydrogen atoms form the tertiary carbon positions on the polypropylene chain.

The magnitude of the deuterium isotope effect, k_H/k_D, was found to be 4.26 for an oxidation temperature of 100°C. This experimentally determined value is in excellent agreement with the theoretical maximum value[10] of 4.3 calculated for the ratio of the rate constants in which the reactions involve the breaking of $\rangle$C—H and $\rangle$C—D bonds. In many reactions involving these bonds, however, the bond in the transition complex will not be broken, and the ratio of the rate constants may be much smaller. It may be inferred from the data in Table II that the oxidation at 100°C. involves the breaking of all C—D bonds in the rate-controlling step. The

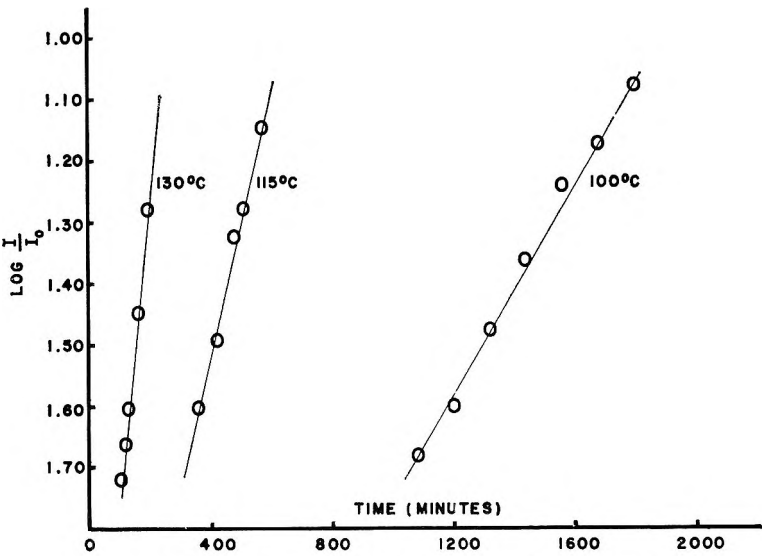

Fig. 5. Plot of log transmittance vs. time for polymer A.

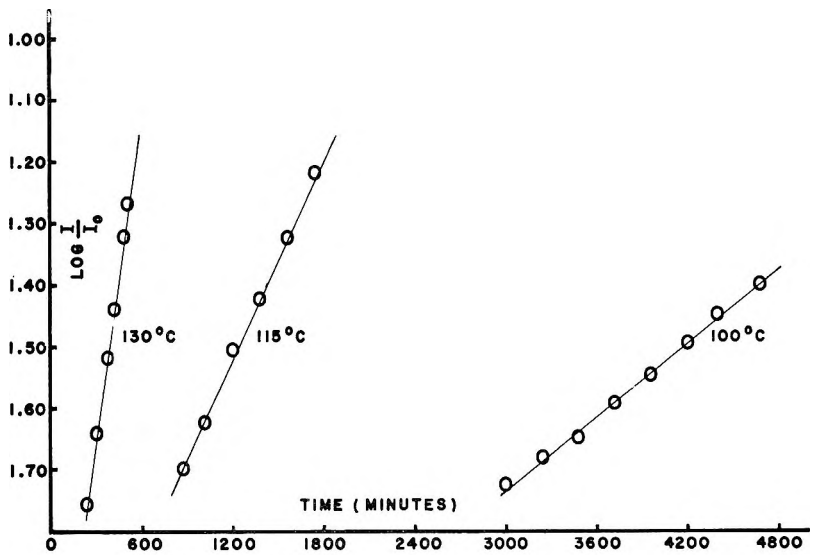

Fig. 6. Plot of log transmittance vs. time for polymer B.

experimental rate ratio equals that of the theoretical in this case. The fact that the ratio decreases at the higher oxidation temperatures indicates that a considerable number of secondary H—C—H bonds are probably broken along with the predominant number of tertiary C—D bonds. This situation becomes possible when it is considered that the tertiary C—D bond is more stable than the tertiary C—H bond. The energetics of the system are such that the breaking of a secondary H—C—H bond for the deuterated polymer B then becomes a possibility at the higher temperatures.

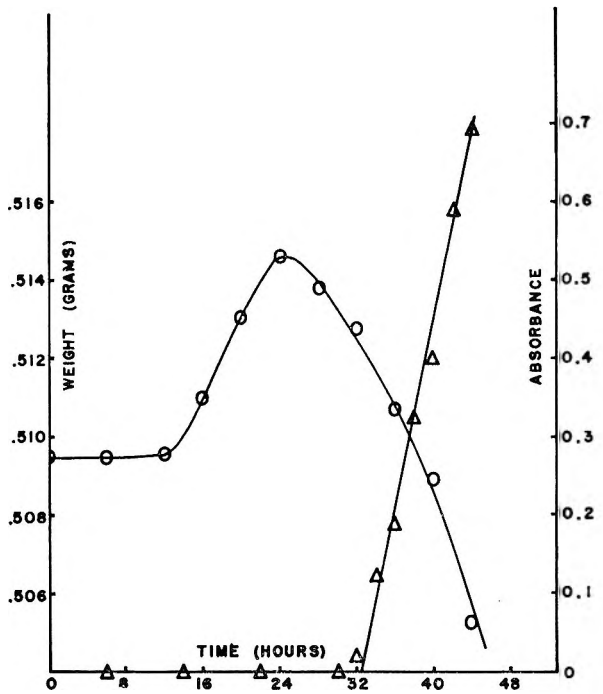

Fig. 7. Weight changes of polypropylene film vs. time, (O); and carbonyl absorption vs. time, (△). Degradation temperature 100°C.

It is not surprising to find that the weakest point in the polypropylene chain occurs at the position of the tertiary carbon atom. For example, it is well known that the order of reactivity for hydrogen atoms in saturated hydrocarbons decreases in the sequence tertiary> secondary> primary.[11] Moreover, it has been shown that the order primary> secondary> tertiary is the order of decreasing C—H bond strength. From bond dissociation energies D the pertinent results[12] have been tabulated in Table III.

Steacie and co-workers[13,14] have studied the effect of hydrogen atom abstraction on various compounds in the alkane series using deuterated ethyl radicals. Neopentane, n-butane, n-hexane, and isobutane were chosen as representatives of the basic structural features of hydrocarbons containing primary, secondary, and tertiary hydrogen atoms. The activation energies for abstraction were, respectively, 12.6 ± 0.7, 10.4 ± 0.75, 10.1 ± 0.5, and 8.9 ± 0.6 kcal. This work also demonstrates that the relative ease of abstraction is in the order tertiary> secondary> primary.

TABLE III

Bond	D, kcal.
n-C_3H_7—H (primary)	100
i-C_3H_7—H (secondary)	94
n-C_4H_9—H (primary)	101
$tert$-C_4H_9—H (tertiary)	89

From the foregoing conclusions concerning relative bond strengths in hydrocarbons, it is entirely reasonable to expect the hydrogens attached to the tertiary carbon atom to be more susceptible to attack than those at any other point in the polypropylene chain. One would further expect this point to be more vulnerable in polypropylene due to the frequency of occurrence of the tertiary carbon atoms, which is every other carbon atom along the chain. Thus we have noted by means of the deuterium isotope effect that the hydrogens on the tertiary carbon atoms are attacked quite readily by molecular oxygen.

It is now well established that hydroperoxides appear as one of the first products of oxidation reactions and that their decomposition also leads to the formation of secondary oxidation products such as ketones, aldehydes, acids, alcohols, water, carbon dioxide, etc.[15] Some insight into the nature of the induction period in polypropyl was gained by following changes in weight versus oven-aging time at 100°C. A large test piece of a 7.8 mil thick film was used for the study. The results are shown in Figure 7. It may be seen that the induction time as determined by the onset of carbonyl absorption is about 32 hr. for this particular unstabilized polymer. The weight of the film remains essentially constant at first, but then begins to increase and goes through a maximum prior to carbonyl development. The film then begins to lose weight and does so steadily as the carbonyl absorption increases. This is interpreted to mean that the initial build-up in weight is due to the formation of hydroperoxides in polypropylene. As the degradation progresses, the loss in weight may be attributed to the decomposition of the unstable hydroperoxide. Further losses in weight may be accounted for by the formation of volatile degradation products. At this point, the degradation has reached an advanced stage as indicated from the intensity of the carbonyl absorption band.

A reaction scheme consistent with the experimental data can be set forth for the thermal oxidation of polypropylene. Thus the initiation and propagation steps can be represented with a fair degree of certainty. The initial attack on the polypropylene chain is depicted as one of abstraction (without specifying the precise process involved in this step) involving the tertiary hydrogen atoms, followed by the eventual formation of hydroperoxides and other chain-propagating radicals. The decomposition of hydroperoxides presumably leads to the formation of stable secondary oxidation products such as ketones, aldehydes, alcohols, acids, etc. These products are indicated from the broad nature of the carbonyl absorption band and from the absorption corresponding to the fundamental OH stretch frequency at about 2.8–3.0 μ.

Initiation:

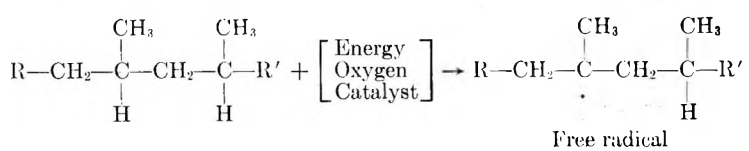

Propagation:

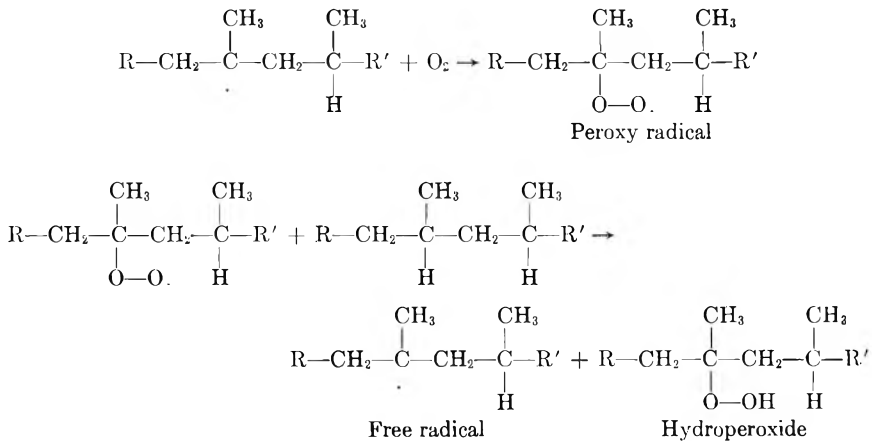

Termination:

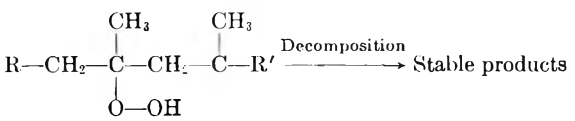

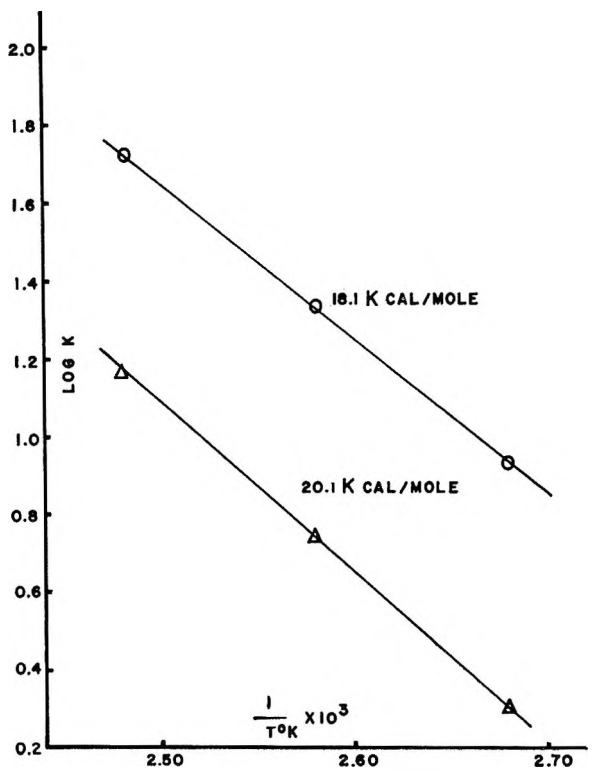

Fig. 8. Plot of log k vs. reciprocal absolute temperature to determine the activation energy for the thermal oxidation reaction of polymer A (O) and polymer B (△).

The activation energies for polymers A and B were obtained from the Arrhenius equation:

$$k = Ae^{-E/RT} \tag{2}$$

Plots of log k versus the reciprocal of the absolute temperature were made for each polymer at oxidation temperatures of 100, 115, and 130°C. The activation energies E_a were calculated from the slopes of the lines with the aid of the integrated form of the equation:

$$\log (k_2/k_1) = E_a (T_2 - T_1)/2.303RT_2T_1 \tag{3}$$

The graph is shown in Figure 8. Polymer A, the control sample, gave an activation energy of 18.1 kcal./mole, while polymer B, the tertiary deuterated sample, gave an activation energy of 20.1 kcal./mole. The difference in activation energy between polymer A and polymer B can be explained as follows. The magnitude of the difference in energy required to break bonds to deuterium as opposed to bonds to hydrogen is of the order of the difference in zero point energies between the two types of bonds. This value has been calculated from theoretical considerations to be about 1.25 kcal./mole. The experimental activation energy differences vary between 1.1 and 1.6 kcal./mole as determined by competitive abstractions of H and D atoms by radicals.[16] Therefore we may account for at least 1.6 of the 2.0 kcal./mole difference between polymer A and polymer B from a consideration of the C—H and C—D bond types present.

CONCLUSIONS

A deuterium isotope effect of $k_H/k_D = 4.26$ has been observed for the oxidation of polypropylene in which a deuterium atom is substituted for hydrogen on the tertiary carbon atom. Moreover, the induction time for this sample was found to be approximately two and one-half times as long as that of the nondeuterated control sample, demonstrating increased resistance to oxidation due to the enhanced stability of the C—D bonds present in the macromolecule. All other deuterated samples showed the same induction time and oxidation rate as the control sample. From these observations, it is clear that the rate-determining step in the thermal oxidation of polypropylene consists of the abstraction of hydrogens from the tertiary carbon atoms of the polymer chain.

Evidence from a weight change experiment is in accord with hydroperoxide being one of the first products of oxidation. It was found to appear during the induction period of the oxidation reaction, i.e., prior to carbonyl development. As the oxidation proceeds, the subsequent decomposition of the unstable hydroperoxide gives rise to both volatile products as indicated from a progressive loss in weight of the polymer and to a number of secondary oxidation products as demonstrated by the profile of the carbonyl absorption band. One of the main types of products was found to be the carboxylic acid type, which has a sharp absorption peak at 5.842 μ.

The activation energies were obtained for the tertiary substituted deuterium polymer and for the control polymer. The values found were 20.1 and 18.1 kcal./mole, respectively.

A mechanism of oxidation is postulated which is consistent with the observed kinetics and the other experimental evidence.

References

1. Westheimer, R. H., and N. Nicolaides, *J. Am. Chem. Soc.*, **71**, 25 (1949).
2. Beachell, H. C., and S. P. Nemphos, *J. Polymer Sci.*, **25**, 173 (1957).
3. Tryon, M., and L. A. Wall, *J. Phys. Chem.*, **62**, 697 (1958).
4. Natta, G., I. Pasquon, A. Zambelli, and G. Gatti, *J. Polymer Sci.*, **51**, 387 (1961).
5. Natta, G., *J. Polymer Sci.*, **16**, 143 (1955).
6. Luongo, J. P., *J. Appl. Polymer Sci.*, **3**, 302 (1960).
7. Stivala, S. S., Reich, L., and Kelleher, P. G., *Makromol. Chem.*, **59**, 28 (1963).
8. Rugg, F. M., J. J. Smith, and R. C. Bacon, *J. Polymer Sci.*, **13**, 535 (1954).
9. Beachell, H. C., and S. P. Nemphos, *J. Polymer Sci.*, **21**, 113 (1956).
10. Livingston, R., in *Investigation of Rates and Mechanisms of Reactions*, S. L. Friess and A. Weissberger, Eds. (Technique of Organic Chemistry, Vol. VIII), Interscience, New York, 1953, Chap. I.
11. Walsh, A. D., *Trans. Faraday Soc.*, **42**, 269 (1946).
12. Cottrell, T. L., *The Strengths of Chemical Bonds*, 2nd Ed., Butterworths, London, 1958.
13. Boddy, P. J., and E. W. R. Steacie, *Can. J. Chem.*, **38**, 1576 (1960).
14. Boddy, P. J., and E. W. R. Steacie, *Can. J. Chem.*, **39**, 13 (1961).
15. Myers, C. S., *Ind. Eng. Chem.*, **44**, 1095 (1952).
16. Herk, L., and M. Szwarc, *J. Am. Chem. Soc.*, **82**, 3558 (1960).

Résumé

On décrit dans cet article quelques aspects de l'oxydation thermique des polypropylénes isotactiques deutérés. Plusieurs polypropylénes, deutérés à différents endroits, le long de la chaîne polymérique, ont été soumis à un traitement cinétique, afin d'établir une comparaison entre les vitesses d'oxydation à différentes températures. On a suivi la cinétique dans un intervalle de température de 100 à 130°C par spectroscopie infrarouge. Par ces expériences on a pu montrer l'existence d'un effet isotopique dû au deutérium, pour l'oxydation thermique du polypropyléne.

Zusammenfassung

In der vorliegenden Arbeit werden einige Aspekte der thermischen Oxydation deuterierter isotaktischer Polypropylene beschrieben. Einige an verschiedenen Stellen der Polymerkette deuterierten Propylenpolymeren wurden einer kinetischen Behandlung zur Ermittlung der relativen Oxydationsgeschwindigkeit bei verschiedenen Temperaturen unterworfen. Zur Verfolgung der Kinetik im Temperaturbereich 100–130°C wurde Infrarotspektroskopie verwendet. Diese Versuche zeigten das Bestehen eines Deuteriumisotopeneffekts bei der thermischen Oxydation von Polypropylen.

Received May 15, 1964
Revised June 15, 1964

JOURNAL OF POLYMER SCIENCE: PART A VOL. 3, PP. 469–478 (1965)

Correct Determination of Staudinger's Index (Intrinsic Viscosity) and of Huggins' Constant

FADEL W. IBRAHIM, *Department of Industrial and Engineering Chemistry, Swiss Federal Institute of Technology, Zurich, Switzerland*

Synopsis

Intrinsic viscosities $[\eta]$ and Huggins' constants k are generally determined by means of one of the following equations:

$$(\ln \eta_r)/c = [\eta] + (k - 0.5)[\eta]^2 c \quad (1)$$

$$\eta_{sp}/c = [\eta] + k[\eta]^2 c \quad (2)$$

$$\eta_{sp}/c = [\eta] + k[\eta]\eta_{sp} \quad (3)$$

It was proven in an earlier paper that eq. (1) is an insufficient approximation of eq. (2) in the usual range $\eta_r = 1.2$–2.0. In this paper it is shown that eqs. (2) and (3) can lead to different Staudinger indexes (difference up to 30%). Huggins' constant k can vary from one equation to the other by as much as 300%. The experimental test of theoretical relationships between $[\eta]$, k, and other molecular constants can lead to errors of the same magnitude. Values of $[\eta]$ and k in pure and mixed theta solvents are discussed. It is moreover shown that eq. (2) is an inadequate approximation of eq. (3). Therefore eq. (3) is the only one which should be used.

INTRODUCTION

Viscosity measurement constitutes the easiest method for determining the molecular weights of high polymers. Staudinger's index $[\eta]$ (intrinsic viscosity) is related to the viscosity-average molecular weight by the modified Staudinger equation

$$[\eta] = K \bar{M}_v^a (\text{ml./g.}) \quad (1)$$

$[\eta]$ is the limiting value of $(\eta - \eta_0)/\eta_0 c$ for $c \to 0$ where η and η_0 represent the viscosity of the solution and of the solvent, respectively, and c is the concentration of the polymer in that solvent. Many equations have been put forward to enable the determination of $[\eta]$ graphically or by calculation. The best known equations today[1] are those of Kraemer,[2] eq. (2); Huggins,[3] eq. (3); and Schulz and Blaschke[4] eq. (4).

$$\ln \eta_r/c = [\eta] + (k - 0.5)[\eta]^2 c \quad (2)$$

$$\eta_{sp}/c = [\eta] + k[\eta]^2 c \quad (3)$$

$$\eta_{sp}/c = [\eta] + k[\eta]\eta_{sp} \quad (4)$$

Proceeding to the limit $c \rightarrow 0$, eqs. (2)–(4) should give equal values for $[\eta]$ and for k. Elias and Etter[5] have noticed, however, that different values for $[\eta]$ and k (Huggins' constant) were obtained through the use of these three different equations. Ibrahim and Elias[6] have shown that eqs. (2) and (3) are mathematically not equivalent for measurements at finite concentrations in the range $1.2 < \eta_r < 2.0$. They reported differences in $[\eta]$ of as much as 30%. The values of k calculated by means of eqs. (2) and (3) varied by as much as 300%. It was also proven[7] that the approximations which are generally made to calculate an expression for the viscosity-average molecular weight through the combination of eqs. (3) and (1) would lead to different averages if eq. (2) were used instead of eq. (3). The reason for these differences is that eq. (2) is an insufficient approximation of eq. (3). Concerning eqs. (3) and (4), Schulz[8,9] reported that eq. (3) seemed less linear than eq. (4) at higher concentrations. No reason was given. Weissberger et al.[10] noted that the higher terms of Huggins' equation, eq. (3), should be taken into consideration for certain systems. No comparison was attempted between eqs. (3) and (4). Huggins[11] found that both eqs. (3) and (4) were linear for values of η_{sp} smaller than 3. In this paper, eqs. (3) and (4) will be compared in the usual range of $\eta_{sp} = 0.2$–1. The lower limit is given by adsorption effects;[12,13] while the higher limit should permit both equations to be linear. It will be shown that Huggins' equation is an insufficient approximation of eq. (4).

DISCUSSION

Derivation of Equation (4)

Equations (3) and (4) shall be written in the forms

$$\eta_{sp}/c = [\eta]_H + k_H[\eta]_H^2 c \tag{5}$$

$$\eta_{sp}/c = [\eta]_S + k_S[\eta]_S\eta_{sp} \tag{6}$$

Schulz and Blaschke[4] arrived empirically at eq. (6). Huggins[3] derived eq. (7) by an extension of Kuhn's hydrodynamical treatment

$$\eta_{sp}/c = [\eta]/(1 - k[\eta]c) \tag{7}$$

Considering $k[\eta]c$ to be small yielded

$$[\eta]/(1 - k[\eta]c) = [\eta](1 - k[\eta]c + k^2[\eta]^2c^2 + \ldots) \tag{8}$$

and, neglecting the terms in c^x with $x \geqslant 2$, Huggins obtained his well known eq. (3).

Calculating c from eq. (7) we obtain

$$c = \eta_{sp}/([\eta] + \eta_{sp}k[\eta]) \tag{9}$$

Substituting for c in the right-hand side of eq. (7) yields

$$\eta_{sp}/c = \frac{[\eta]}{1 - \{k\eta_{sp}[\eta]/([\eta] + \eta_{sp}k[\eta])\}} = [\eta](1 + k\eta_{sp}) \tag{10}$$

Equation (10) is identical to the equation of Schulz and Blaschke [eq. (4)].

Thus Huggins' equation is nothing but an approximation of eq. (4) considering the theory of Huggins himself. That means that eq. (3) can be used only if it is proven that the higher terms in c [eq. (8)] can be neglected for the calculation of $[\eta]$. The importance of the error committed by neglecting these higher terms has been studied on samples of poly heptamethyleneurea,[14] nylon 66,[15] and polyisobutylene (Oppanol B 100) in pure solvents and in mixtures of solvents and precipitants.

TABLE I
Polyisobutylene in Carbon Tetrachloride–Butanone. Effect of the Approximations made by Huggins in Going from Eq. (7) to Eq. (3)

c, g./ml.	η_{sp}	$a = \frac{[\eta]_S}{1 - k_S[\eta]_S c}$	$b = [\eta]_S(1 + k_S[\eta]_S c)$	$\frac{100 \times (a - b)}{a}$ Error, %
0.002000	0.3417	169.17	164.77	2.6
0.003000	0.5550	187.32	176.26	5.9
0.003998	0.8429	209.72	187.74	10.4
0.005000	1.1974	238.22	199.23	16.4

Tables I and II show that the errors are too great to be neglected. The effect of these errors on $[\eta]$ and k shall now be discussed.

Comparison of Staudinger's Index in Equations (5) and (6)

Equation (5) will be written in the form:

$$\eta_{sp}/c = [\eta]_S + k_S[\eta]_S^2 c + k^2_S[\eta]_S^3 c^2 + \ldots \quad (11)$$

As k_S is positive, eq. (11) is a parabola with axis parallel to the η_{sp}/c axis and vertex at a negative value of c. To compare $[\eta]_S$ and $[\eta]_H$, the intercepts of the parabola (11) and of the straight line (5) with the η_{sp}/c axis must be compared (Fig. 1). The measured values are of course in the positive quadrant, i.e., on a part of the right branch of the parabola. If many points are on that branch the best straight line through the points must intercept the parabola somewhere between the two points of highest and lowest concentration, i.e., $[\eta]_S$ will be greater than $[\eta]_H$. The contrary can occur only if the measured values are at a great distance from the parabola which is generally not the case. These conclusions have been shown to be true (Table II).

Comparison of the Constants k_H and k_S

The tangent to the parabola (11) at $c = 0$ is given by $k_S[\eta]_S^2$ and the slope of eq. (5) is $k_H[\eta]_H^2$, so that

$$k_S[\eta]^2_S = k_H[\eta]_H^2 \quad (12)$$

But as $[\eta]_S > [\eta]_H$ (see above), k_S will be smaller than k_H. Experiments have shown that this conclusion is also true. The smaller value of k_S

TABLE II
Comparison of the Values of $[\eta]$ and k in eqs. (5) and (6)

Polymer	Solvent	Temp., °C.	$[\eta]$, ml./g. $[\eta]_S$ [eq. (6)]	$[\eta]_H$ [eq. (5)]	Huggins' constant k_S [eq. (6)]	k_H [eq. (5)]	$\Delta[\eta]$	$[\eta]_H k_H$	$\Delta[\eta]/[\eta]_H \times 100$	$\Delta k/k_S \times 100$
Polyisobutylene	Benzene	24.4	127.8 ± 0.65	120.1 ± 0.80	0.49 ± 0.013	0.94 ± 0.028	7.8	113	6.5	92
Polyisobutylene	Cyclohexane	25.0	478 ± 1.5	457 ± 0.87	0.236 ± 0.0030	0.405 ± 0.0022	21	185	4.6	72
Polyisobutylene	Methylcyclohexane	25.0	414 ± 3.4	380 ± 0.60	0.25 ± 0.012	0.548 ± 0.036	34	209	8.8	119
Polyisobutylene	Cyclohexanol–toluene	25.0	141.3 ± 0.61	131 ± 1.08	0.424 ± 0.0073	0.84 ± 0.014	10.3	110	7.9	98
Polyisobutylene	*n*-Octanol–methylcyclohexane	25.0	157 ± 1.7	129.4 ± 0.49	0.39 ± 0.013	1.217 ± 0.0096	27.6	157.5	21.3	212
Polyisobutylene	*n*-Heptanol–*n*-hexane	25.0	135.1 ± 0.17	126.7 ± 0.20	0.499 ± 0.0027	0.903 ± 0.0044	8.4	114	6.6	81
Polyisobutylene	Dioxane–cyclohexane	2.50	170.0 ± 0.71	154.5 ± 0.99	0.430 ± 0.0047	0.85 ± 0.015	15.5	131	10	113
Polyisobutylene	Dioxane–methylcyclohexane	25.0	225 ± 2.4	192.4 ± 0.92	0.35 ± 0.017	0.98 ± 0.010	32.6	188	17	180
Polyisobutylene	Cyclohexane–chloroform	25.0	135.1 ± 0.94	128.2 ± 0.64	0.42 ± 0.011	0.72 ± 0.010	6.9	92	5.4	72
Polyisobutylene	*n*-Heptanol–methylcyclohexane	25.0	170 ± 3.6	148 ± 3.4	0.46 ± 0.038	1.17 ± 0.058	22	173	14.9	154
Polyisobutylene	Dioxane–*n*-hexane	25.0	208 ± 1.1	189 ± 1.9	0.329 ± 0.0065	0.70 ± 0.021	19	132	10	113
Polyisobutylene	*n*-Hexanol–methylcyclohexane	25.0	156 ± 2.0	149 ± 3.1	0.41 ± 0.017	0.70 ± 0.039	7	104	4.7	71
Polyisobutylene	Butanone–CCl_4	25.0	141.8 ± 0.68	120 ± 2.16	0.57 ± 0.010	1.598 ± 0.055	21.8	192	18.2	181
Polyisobutylene	Butanone–cyclohexane	25.0	151 ± 1.3	116 ± 1.6	0.63 ± 0.010	2.44 ± 0.0044	35	283	30.2	290
Polyisobutylene	*n*-Amyl alcohol–methylcyclohexane	25.0	177 ± 1.4	164 ± 1.6	0.42 ± 0.014	0.86 ± 0.034	13	141	7.9	105

Polyisobutylene	*n*-Hexanol–*n*-hexane	25.0	152	± 1.2	140	± 2.0	0.51	± 0.016	1.05	± 0.058	12	147	8.6	106
Polyisobutylene	Butanone–*n*-hexane	25.0	156.1	± 0.62	150	± 1.4	0.47	± 0.015	0.78	± 0.041	6.1	117	4	66
Polyisobutylene	*n*-Propanol–methylcyclohexane	25.0	188	± 1.5	170.6	± 0.75	0.44	± 0.020	0.96	± 0.018	18.6	164	10.9	120
Polyisobutylene	*n*-Propanol–*n*-hexane	25.0	181.1	± 0.62	170	± 1.3	0.382	± 0.0069	0.72	± 0.030	11.1	123	6.5	89
Polysiobutylene	*n*-Butanol–*n*-hexane	25.0	167	± 1.6	156	± 1.2	0.44	± 0.034	0.86	± 0.015	11	134	7	95
Polyisobutylene	*n*-Butanol–methylcyclohexane	25.0	188	± 1.1	181	± 1.1	0.385	± 0.0087	0.63	± 0.018	7	114	3.9	64
Polyisobutylene	*n*-Propanol–chloroform	49.0	140.8	± 0.32	137.0	± 0.37	0.502	± 0.0089	0.73	± 0.011	3.8	100	2.1	45
Polyisobutylene	*n*-Butanol–methylcyclohexane	14.0	203.7	± 0.53	196.8	± 0.64	0.392	± 0.0043	0.597	± 0.0080	6.9	118	3.5	52
Polyureas														
PH 10	Dichloroacetic acid	25.0	36.5	± 0.24	33.0	± 0.11	0.57	± 0.020	1.25	± 0.012	3.5	41.2	10.6	119
PH 7	Dichloroacetic acid	25.0	22.6	± 0.38	19.2	± 0.37	0.67	± 0.014	1.85	± 0.068	3.4	55.5	17.8	26.8
PH 16	Dichloroacetic acid	25.0	16.19	± 0.020	15.69	± 0.010	0.417	± 0.0039	0.627	± 0.0013	0.5	9.9	32	50
PH 15	Dichloroacetic acid	25.0	34.9	± 0.28	32.23	± 0.076	0.49	± 0.026	0.991	± 0.0093	2.7	31.9	8.35	102
PH 16	Sulfuric acid (90%)	25.0	8.24	± 0.054	8.06	± 0.057	0.53	± 0.024	0.75	± 0.030	0.18	6.05	2.2	41.5
PH 20	Sulfuric acid (90%)	25.0	17.51	± 0.035	17.49	± 0.037	0.132	± 0.0077	0.143	± 0.0082	0.02	2.3	0	6.8
Polyamides														
K 3	*m*-Cresol	25.0	52	± 1.1	43.4	± 0.84	1.0	± 0.71	3.05	± 0.097	8.6	133	19.7	205
508 3/III	*m*-Cresol	25.0	173.9	± 0.15	173.8	± 0.16	0.047	± 0.0022	0.0489	± 0.0023	0.1	8.5	0	4
KI A	*m*-Cresol	25.0	60	± 1.05	56	± 1.3	0.79	± 0.075	1.48	± 0.095	4	82.9	7.2	69
KI B	*m*-Cresol	25.0	65.98	± 0.047	65.26	± 0.081	0.304	± 0.0020	0.383	± 0.0042	0.7	25	1.1	26
K 2	*m*-Cresol	25.0	84.8	± 0.78	82.4	± 0.84	0.51	± 0.027	0.75	± 0.036	2.4	61.8	2.9	47
G 2	*m*-Cresol	25.0	95.5	± 0.29	94.9	± 0.32	0.210	± 0.064	0.250	± 0.0080	0.6	23.7	0.6	19
K 4	*m*-Cresol	25.0	25.18	± 0.095	24.9	± 0.12	0.48	± 0.019	0.61	± 0.026	0.3	15.2	1.2	27
K 3	Formic acid	25.0	42.9	± 0.23	42.3	± 0.29	0.44	± 0.019	0.57	± 0.019	0.6	24.2	1.4	31

is more in keeping with the theories made about the value of k.[10,17–33] The importance of the differences of both constants is emphasized by Figures 2 and 3. In Figure 2 the second virial coefficient B (light scattering) has been plotted against k_S. It is seen that B is zero for $k_S = 0.5$. This is in accordance with the theory often expressed in the literature.[21,24,25,32,33] This relation does not hold if k_H is used instead of k_S (Fig. 3). It might be added here that this relation ($k_S = 0.5$ for $B = 0$) does not seem to hold

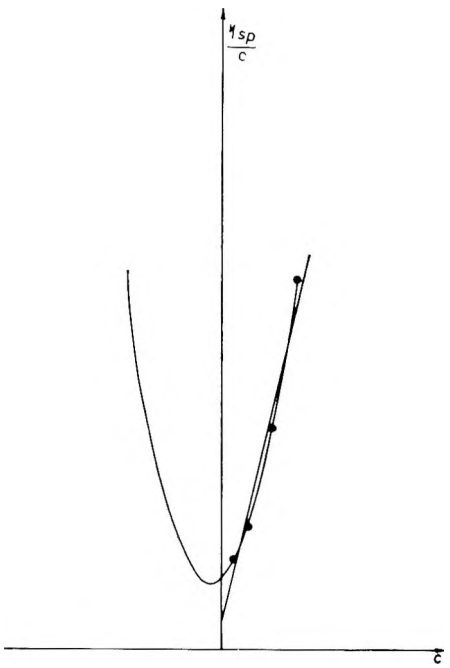

Fig. 1. Approximation of the parabola [eq. (11)] by the straight line [eq. (5)].

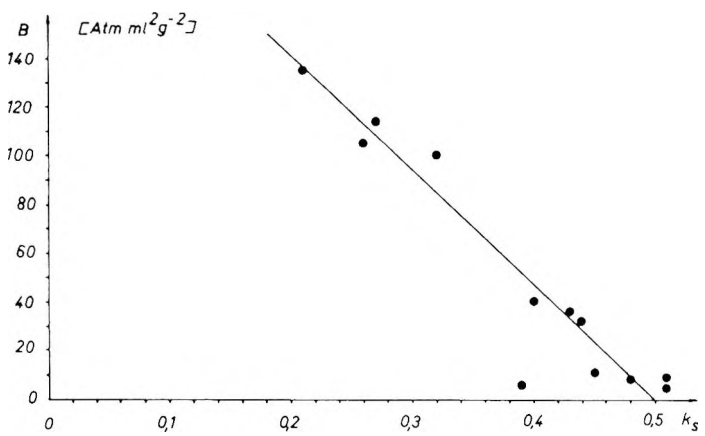

Fig. 2. Different samples of polyurea[14] in different solvents. B = second virial coefficient obtained by light scattering, k_S = Huggins' constant in eq. (6).

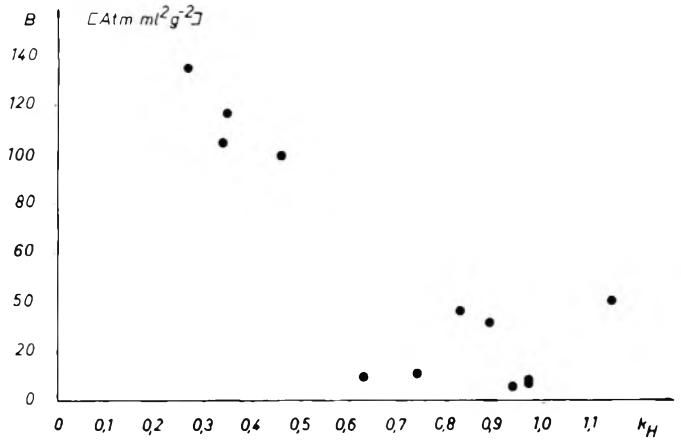

Fig. 3. Same plot as in Fig. 2 but instead of k_S [eq. (6)] k_H [eq. (5)] was used.

for solvent–precipitant mixtures: many of the mixtures in which polyisobutylene was studied were theta solvents ($B = 0$) but the value of k_S were generally smaller than 0.5. This can be explained by assuming the solvent/nonsolvent ratio inside the coil to be greater than the overall composition of the solution. The coil is thus more expanded than in a single theta solvent, and k_S is therefore smaller than 0.5. That would also explain the fact that $[\eta]_\Theta$ in a mixture of solvent and precipitant at the theta point is greater than that in a single theta solvent. This would not be true if $[\eta]_H$ were considered instead of $[\eta]_S$. If association takes place, k_S can be greater than 0.5 as shown by polyureas in different solvents exhibiting negative second virial coefficients.[14] Benzene is a pure theta solvent for polyisobutylene,[35] and its $k_S = 0.49 \pm 0.013$ fits the theory ($k_H = 0.94$). If these facts are taken into consideration, Rao's equation[33]

$$[\eta]_\Theta = [\eta][1 - (1 - 2k)^{0.5}] \tag{13}$$

might be true as long as no solvent–nonsolvent mixtures are used. In the case of the two pure solvents cyclohexane and methylcyclohexane $[\eta]_\Theta$ [eq. (13)] would be 131 ml./g. and 122, respectively, if k_S is used. (Benzene, a pure theta solvent shows $[\eta]_\Theta = 127.8$.) Considering k_H in Huggins' eq. (5), $[\eta]_\Theta$ would be imaginary in cyclohexane and 258 in methylcyclohexane. Thus the use of k_S instead of k_H might give new importance to eq. (13).

Comparison of Equations (5) and (6)

Equations (5) and (6) will differ most when the curvature of the parabola (11) is greatest and when its vertex is closest to the η_{sp}/c axis (Figs. 1 and 4). The curvature of the parabola is given by $2[\eta]_S^3 k_S^2$; the abscissa of its vertex is

$$-k_S[\eta]_S^2/(2k_S^2[\eta]_S^3) = -1/(2k_S[\eta]_S) \tag{14}$$

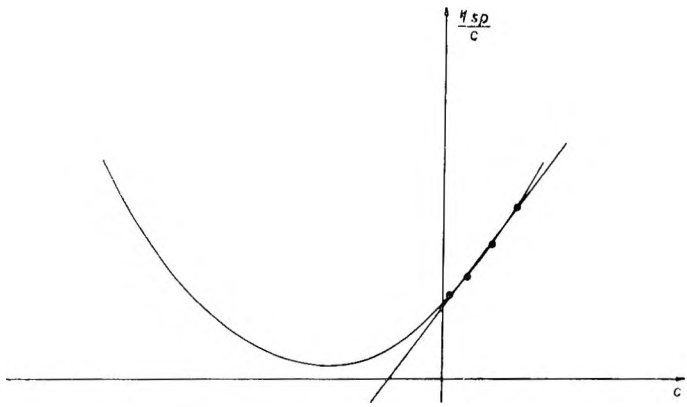

Fig. 4. Same plot as in Fig. 1. The parabola has a smaller curvature and its vertex is at a greater distance from the η_{sp}/c axis.

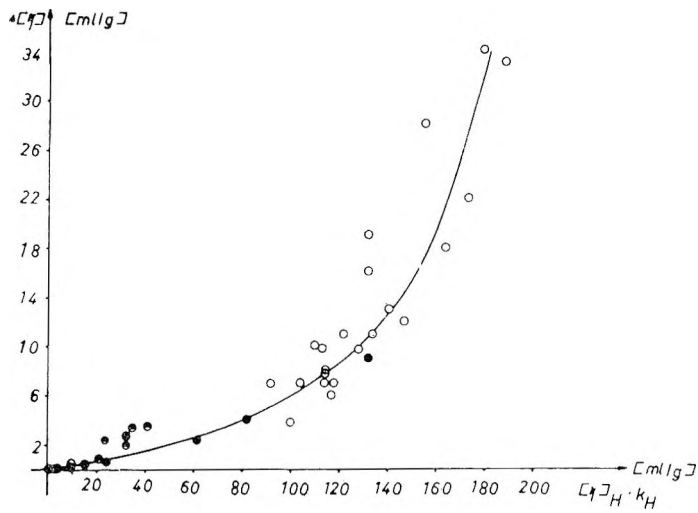

Fig. 5. ($[\eta]_S - [\eta]_H$) plotted against the product $[\eta]_H k_H$: (O) polyisobutylene; (◓) polyureas; (●) polyamide.

Noting these facts, the value of $[\eta]_S k_S$ or of $[\eta]_H k_H$ should be a good criterion for the difference between $[\eta]_S$ and $[\eta]_H$.

In Figure 5 $[\eta]_S - [\eta]_H$ is plotted against $k_H[\eta]_H$. This curve underlines the fact that the difference between eqs. (5) and (6) is of mathematical origin; this relationship is valid for different polymers, solvents, and temperatures. This curve can be used to obtain an approximate value of $[\eta]_S$ from known $[\eta]_H$ and k_H.

CONCLUSION AND SUMMARY

Table II shows that the simultaneous use of eqs. (3) and (4) for the determination of molecular weights through eq. (1) can lead to errors of as

much as 30% in $[\eta]$ and of 300% in k. An error of 20% in $[\eta]$ can lead to one of 40% in the molecular weight M_v if the value of a in Staudinger's eq. (1) is 0.5. These differences are of a mathematical nature and are far greater than errors of measurement. Values given by different authors can be compared only if they have been obtained by means of the same equation. The experimental proof of theories relating virial coefficient B, molecular weight M, Staudinger's index $[\eta]$, radius of gyration $\langle r \rangle$, and Huggins' constant k will lead to false results if Huggins' eq. (3) is used. The theoretical meaning of Huggins' constant can only be obtained by the values of that constant obtained from the equation of Schulz and Blaschke.[4] Huggins' equation is an insufficient approximation of that of Schulz and Blaschke considering the theory of Huggins himself, even in the range where both plots seem linear. Therefore only eq. (4) should be used to determine $[\eta]$ and k.

The author thanks Prof. Dr. H.-G. Elias for valuable discussions and for permission to publish this work.

References

1. Peterlin, A., in *Die Physik der Hochpolymeren*, Vol. II, H. A. Stuart, Ed., Springer Verlag, Berlin-Göttingen-Heidelberg, 1953, p. 316 ff.
2. Kraemer, E. O., *Ind. Eng. Chem.*, **30,** 1200 (1938).
3. Huggins, M. L., *J. Am. Chem. Soc.*, **64,** 2716 (1942).
4. Schulz, G. V., and F. Blaschke, *J. Prakt. Chem.*, **158,** 130 (1941).
5. Elias, H. G., and O. Etter, *Makromol. Chem.*, **54,** 78 (1962).
6. Ibrahim, F. W., and H.-G. Elias, *Makromol. Chem.*, **76,** 1 (1964).
7. Ibrahim, F. W., *J. Polymer Sci.*, **B2,** 441 (1964).
8. Schulz, G. V., *Kolloid-Z.*, **115,** 90 (1949).
9. Marx, M., and G. V. Schulz, *Makromol. Chem.*, **31,** 140 (1959).
10. Weissberger, S. G., R. Simha, and S. Rothman, *J. Res. Natl. Bur. Std.*, **47,** 298 (1951).
11. Huggins, M. L., *Physical Chemistry of High Polymers*, Wiley, New York, 1958, p. 88.
12. Streeter, D. J., and R. F. Boyer, *J. Polymer Sci.*, **14,** 5 (1954); H. Giesekus, *Kolloid-Z.*, **138,** 38 (1954); H. Umstätter, *Makromol. Chem.*, **12,** 94 (1954).
13. Oehrn, O. E., *J. Polymer Sci.*, **17,** 137 (1955); *Arkiv Kemi*, **12,** 397 (1958); S. Claesson, *Makromol. Chem.*, **35,** 75 (1960).
14. Feisst, J., Ph.D. Thesis, Swiss Federal Institute of Technology, Zurich.
15. Schumacher, R., Ph.D. Thesis Swiss Federal Institute of Technology, Zurich.
16. Weissberger, A., E. S. Proskauer, J. A. Riddick, and E. E. Toops, Jr., *Organic Solvents* (*Technique of Organic Chemistry*, Vol. VII), Interscience, New York–London, 1955.
17. Eirich, F., and J. Riseman, *J. Polymer Sci.*, **4,** 417 (1949).
18. Streeter, D. J., and R. J. Boyer, *Ind. Eng. Chem.*, **43,** 1790 (1951).
19. Bawn, C. H. E., *Trans. Faraday Soc.*, **47,** 97 (1951).
20. Palit, S. R., G. Colombo, and H. Mark, *J. Polymer Sci.*, **6,** 295 (1951).
21. Cleverdon, D., and P. G. Smith, *J. Polymer Sci.*, **14,** 375 (1954).
22. Heller, W., *J. Colloid Sci.*, **9,** 547 (1954).
23. Bhatnagar, H. L., A. B. Biswas, and M. K. Charpurey, *J. Chem. Phys.*, **28,** 88 (1958).
24. Kapur, S. L., and S. Gundiah, *Makromol. Chem.*, **26,** 119 (1958).

25. Gundiah, S., N. V. Viswanthan, and S. L. Kapur, *J. Sci. Res. (India)*, **19B**, 191 (1960).
26. Varadiah, V. V., and V. S. R. Rao, *Current Sci.*, **28**, 60 (1959).
27. Guth, E., and R. Simha, *Kolloid-Z.*, **74**, 266 (1936).
28. Simha, R., *J. Res. Natl. Bur. Std.*, **42**, 409 (1949).
29. Saito, N., *J. Phys. Soc. Japan*, **5**, 4 (1950).
30. Saito, N., *J. Phys. Soc. Japan*, **7**, 447 (1952).
31. Riseman, J., and R. Ullmann, *J. Chem. Phys.*, **19**, 578 (1951).
32. Yamakawa, H., *J. Chem. Phys.*, **34**, 1360 (1961).
33. Rao, V. S. R., *J. Polymer Sci.*, **62**, S157 (1962).
34. Gillespie, T., *J. Polymer Sci.*, **C3**, 31 (1963).
35. Flory, P. J., *Principles of Polymer Chemistry*, Cornell Univ. Press, Ithaca, N. Y., 1953, p. 615.

Résumé

On détermine généralement l'indice de Staudinger (viscosité intrinsèque) à l'aide de l'une des trois équations suivantes

$$(\ln \eta_r)/c = [\eta] + (k - 0{,}5)[\eta]^2 c \tag{1}$$

$$\eta_{sp}/c = = [\eta] + k[\eta]^2 c \tag{2}$$

$$\eta_{sp}/c = [\eta] + k[\eta]\eta_{sp} \tag{3}$$

Il a été prouvé dans une publication précédente que (1) n'est qu'une approximation de (2). Il est démontré cette fois que (2) et (3) donnent des indices de Staudinger qui peuvent différer de 30%. Les constantes de Huggins k peuvent varier de 300% selon l'équation employée. La confirmation expérimentale des relations théoriques entre $[\eta]$, k et d'autres constantes moléculaires peut mener à des erreurs du même ordre de grandeur. Les valeurs de $[\eta]$ et de k dans des solvants théta (composés d'un liquide ou d'un mélange de solvant et de précipitant) sont discutées. Il est aussi prouvé que (2) n'est qu'une approximation insuffisante de (3).

Zusammenfassung

Staudinger-Indizes $[\eta]$ und Huggins-Konstanten k werden meistens über eine der drei Gliechungen

$$(\ln \eta_r)/c = [\eta] + (k - 0{,}5)\,[\eta]^2 c \tag{1}$$

$$\eta_{sp}/c = [\eta] + k[\eta]^2 c \tag{2}$$

$$\eta_{sp}/c = [\eta] + k[\eta]\eta_{sp} \tag{3}$$

graphisch oder rechnerisch erhalten. In einer früheren Arbeit wurde gezeigt, dass (1) eine ungenügende Näherung von (2) im üblichen Messbereich von $\eta_r = 1{,}2-2{,}0$ darstellt. In dieser Arbeit wird bewiesen, dass (2) und (3) verschiedene Staudinger-Indizes (Abweichungen bis zu 30%) und verschiedene Huggins-Konstanten (Abweichungen bis zu 300%) liefern. Die experimentelle Prüfung von Theorien, die $[\eta]$ oder k mit anderen Grössen verknüpfen, kann entsprechend zu Fehlern gleicher Grössenordnung führen. Die Werte von $[\eta]$ und k in gemischten und reinen θ-Lösungen werden diskutiert. Ferner wird betont, dass Gl. (2) nichts anderes darstellt als eine grobe Näherung von Gl. (3). Es sollte folglich in Zukunft nur mit Gl. (3) gerechnet werden.

Received April 28, 1964

JOURNAL OF POLYMER SCIENCE: PART A VOL. 3, PP. 479-486 (1965)

Crystallization and Dissolution Temperatures of Polyacrylonitrile

R. CHIANG, J. H. RHODES, and V. F. HOLLAND, *The Chemstrand Research Center, Inc., Durham, North Carolina*

Synopsis

The dissolution temperature of the crystalline platelets of polyacrylonitrile in propylene carbonate bears a linear relationship with the crystallization temperature T_c. The step heights ζ of the crystalline platelets measured by electron microscopy increase with increase in crystallization temperature, in accordance with the current theory of high polymer crystallization in dilute solution. The step heights were found to be 100, 130, and 150 A. for T_c of 95, 116, and 125°C., respectively. By extrapolating the experimental values of T_s to the value at $\zeta = \infty$, a characteristic constant $(T_m)_\infty$ is obtained. The $(T_m)_\infty$ was 175°C. for the sample studied in propylene carbonate. The interfacial free energy, σ_e, calculated from the melting point and the step height is of the order of 1950 cal./mole of emerging chain repeat unit, or 45 ergs/cm.^{2} as compared to 1900 cal./mole or 70 ergs/cm.^{2} for polyethylene. It appears that the surface free energies of various organic polymers are remarkably similar. Although the degree of crystalline perfection of polyacrylonitrile is inferior to that of organic crystals with three-dimensional order, polyacrylonitrile displays a crystallization behavior similar to other semicrystalline polymers; this conclusion is supported by the linear relationship between T_s and T_c, the variation of the step height with the crystallization temperature, and the sigmoid relationship of the fractional change in specific volume as a function of time during crystallization.

INTRODUCTION

Polyacrylonitrile may be crystallized from dilute propylene carbonate solution in the form of crystalline platelets with thickness of approximately 100–150 A.[1] The crystals redissolve in the same solvent at higher temperatures. The temperature at which the crystal dissolves or loses its opacity or crystallinity is referred to as dissolution temperature.

Crystals with large surface areas melt at temperatures lower than those with small surface areas. Current theory[2–5] states that the thickness of the platelets, or the step height, is related to the depression of the melting point, ΔT, by the equation

$$\Delta T = (T_m)_\infty - (T_m)_\zeta = (T_m)_\infty - T_s = 2\sigma_e(T_m)_\infty/\zeta\Delta H_u \qquad (1)$$

where $(T_m)_\zeta$ or T_s is the dissolution temperature of the platelets of step height ζ, $(T_m)_\infty$ is the dissolution temperature of the platelets of infinite step height, σ_e is the interfacial surface energy per unit area of the platelets, and ΔH_u is the enthalpy of fusion. The effect of the crystallization tem-

perature on the step height has been studied with the electron microscope; for example, isothermal crystallization of polyethylene in xylene produces single crystals which vary in step height directly with the crystallization temperatures. In fact, eq. (1) has been used to estimate the surface free energy for the formation of polyethylene crystals; thus Jackson, Flory, and Chiang[6] arrived at a value of 1900 cal./mole of emerging chain repeat unit, or of 70 ergs/cm.^{2}, and Holland,[7] using a similar method arrived at a value of 58 ergs/cm.^{2}. The latter value results from using a low value of $(T_m)_\infty$, 106°C., in the calculation. In view of the fact that the value of σ_e is subject to the mechanism of crystal growth and crystalline order near the interfacial zone of each sample (see Jackson et al.[6] for detailed discussion), the agreement is excellent.

This investigation extends the study of the effect of the crystallization temperature on dissolution temperature of polymers to polyacrylonitrile. Polyacrylonitrile was chosen to obtain the interfacial free energy, calculated from the dissolution temperature and the thickness of the crystalline platelets, for comparison with that of other semicrystalline polymers.

EXPERIMENTAL

Materials

The polymer used in this investigation was prepared with a coordination-type catalyst. Chemical analysis of the polymer indicated no detectable amount of impurities (found: C, 67.64%; H, 5.60%; N, 26.54%; calc'd.: C, 67.88%; H, 5.70%; C, 26.41%). This polymer crystallizes over a wide range of temperatures, enabling the change in step height and in dissolution temperature with change in crystallization temperature to be easily measured.

For electron microscopic investigation, the whole polymer was fractionated by elution through a chromatographic column packed with Celite at 82.5°C. with the use of ethylene carbonate as solvent and propylene carbonate as nonsolvent. The viscosity-average molecular weight of the fraction was approximately 112,000. The dissolution and crystallization temperature measurements were carried out on the whole polymer.

Eastman Kodak reagent grade propylene carbonate was used for determining the dissolution and crystallization temperature. It was purified by a procedure developed by J. Ray Kirby of this laboratory, in which the propylene carbonate was stirred with active charcoal for 20 hr. and then passed through a column containing about 10 in. of an anion-exchange resin (Mallinckrodt Amberlite IRA-410) at bottom and about 5 in. of a cation-exchange resin (IR-120) on top, the two layers being separated by glass wool. Moisture in the resin was removed by running anhydrous isopropanol through the column prior to use. Propylene carbonate so treated was neutral to methyl red. This purification procedure is essential because discoloration of polyacrylonitrile is initiated more rapidly by impurities in the solvent than by impurities within the polymer itself. By

careful purification of the solvent, discoloration of the polymer under the severe conditions of crystallization was avoided.

Isothermal Crystallization

Isothermal crystallization was carried out by the following procedure. A concentrated solution, approximately 0.4 g. of polyacrylonitrile in 20 cc. of propylene carbonate, was prepared at 180°C. under nitrogen to minimize oxidative decomposition. Prolonged heating normally produces colored solutions. However, this polymer did not undergo discoloration even when heated for $^1/_2$ hr. at temperatures as high as 180°C.

About 0.2 cc. of the hot concentrated solution was introduced into 10 cc. of propylene carbonate which had been brought to the desired temperature. By so doing, a rapid temperature adjustment was achieved before the crystallization began. The solution was allowed to crystallize at constant temperature; the time of crystallization varied, of course, with the degree of supercooling. At the highest practical crystallization temperature, crystallization was usually carried out overnight, but sometimes several days were required. The solution was still colorless at the end of crystallization.

Determination of Dissolution Temperature

The dissolution temperature was determined by introducing the crystallized sample, without drying, directly into a large excess of propylene carbonate, the temperature of which had been so set that a well-defined final temperature can be obtained by rapid mixing. By several trials, a precise dissolution temperature was located above which the crystals started dissolving and below which the crystals remained undissolved indefinitely.

Electron Microscope Determination

The thickness of the crystalline platelets of PAN grown from dilute propylene carbonate solution was determined with a Philips EM 200 electron microscope by the following procedure.

Drops were removed from the crystallized suspensions and deposited onto carbon coated electron microscope grids. After evaporation of solvent, the grids were shadowed with platinum at an angle of 12°. Grids from the three different runs (at 95, 116, and 125°C.) were shadowed simultaneously to permit direct comparison. From the length of the shadows on the electron micrographs and the shadow angle, the step heights were determined for each preparation. The values which are given represent averages of many individual measurements.

RESULTS

Dissolution Temperature

Values of T_s and T_c are given in Table I. The rate of crystallization decreases drastically with an increase in crystallization temperature. The

TABLE I
Dissolution Temperature (T_s) as a Function of Crystallization Temperature in Propylene Carbonate of a Polymer of Acrylonitrile

T_s, °C.	T_c, °C.
121.2	61.5
133.5	87.4
138.0	98.0
143.5	108.5
148.0	118.0
152.0	125.0[a]
(175)[b]	(175)[b]

[a] The highest practical crystallization temperature.
[b] Extrapolated values as described in text.

temperature beyond which the rate of crystallization becomes prohibitively slow is referred to as the highest practical crystallization temperature. The highest practical temperature for this polymer is 125°C.

The dissolution temperature changes linearly with the crystallization temperature. When the values of T_s are plotted against T_c, a straight line is obtained (Fig. 1), which intersects with the line $T_s = T_c$ at the melting point of the crystallite of infinite step height, $(T_m)_\infty$; the value of $(T_m)_\infty$ for this polymer is 175°C.

Step Heights

Electron micrographs obtained at two different temperatures are given in Figure 2. The platelet thickness difference resulting from a difference

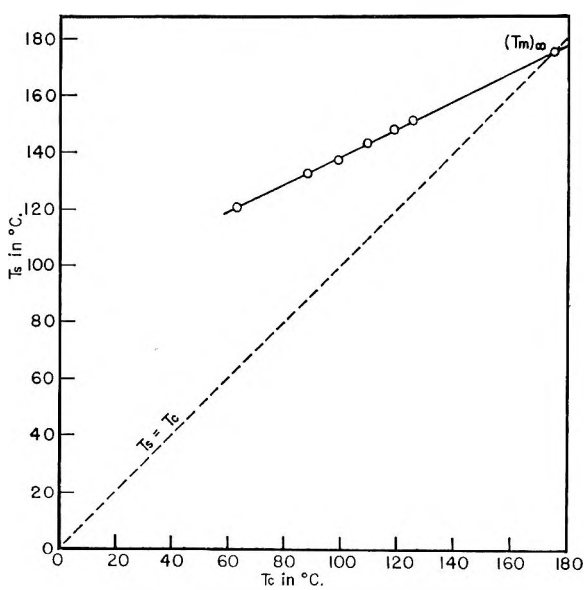

Fig. 1. Dissolution temperature T_s as a function of crystallization temperature T_c for a polymer of acrylonitrile. Solvent: propylene carbonate.

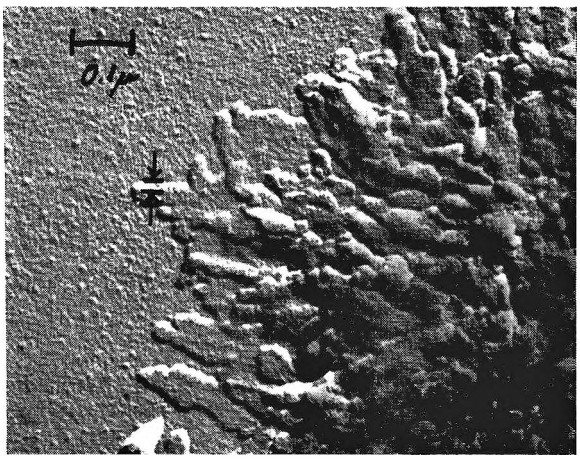

Fig. 2 (a)

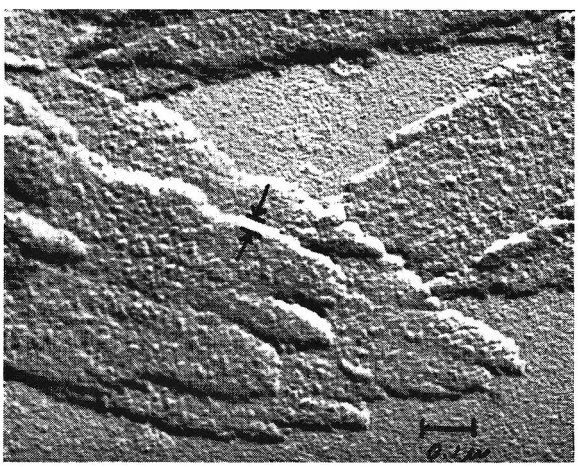

Fig. 2 (b)

Fig. 2. Isothermally crystallized polyacrylonitrile from 0.1% propylene carbonate solution (*a*) at 95°C.; (*b*) at 125°C.

TABLE II
ζ as a Function of Crystallization Temperature of a PAN Sample for which $(T_m)_\infty = 175$°C.

			σ_e (calc'd.)	
T_c, °C.	ζ, A.		cals./mole	ergs/cm.^{2}
95	100 ± 15		1950	45
116	130 ± 15		1980	45
125	150 ± 15		1890	43
		Avg.	1950	44

in crystallization temperature of 30°C. is clearly demonstrated. Values of ζ estimated from the micrographs are given in Table II together with the crystallization temperatures. The step height changes from 100 to 150 A. when the crystallization temperature changes from 95 to 125°C. Thus an increase in step height at a rate of 17% for an increase of 10°C. in crystallization temperature is observed.

Value of σ_e

Substituting into eq. (1) the measured values of ζ, together with the corresponding value of ΔT and taking $\Delta H_u = 1.16$ kcal./mole of repeating unit[8] give calculated surface energies, σ_e, of 1950, 1980, and 1950 cal./mole at a T_c of 95, and 125°C., respectively (Table II). Significantly, the value of σ_e calculated from the experimental data remains constant over a wide range of temperatures. If the cross-sectional area of the chain is taken[1,9] as 30.54 A.,[2] this 1950 cal./mole of emerging chain repeat unit corresponds to 45 ergs/cm.[2], as compared with 1900 cal./mole or 70 ergs/cm.[2] for polyethylene. It appears that the surface energies of the crystals of organic polymers are remarkably similar.

DISCUSSION

The rate of heating during the determination of the dissolution temperature affects the results. In principle, the heating rate should be very slow so that true equilibrium can be realized. On the other hand, the heating rate must be fast as compared to the rate of recrystallization so that a true dissolution temperature can be obtained before recrystallization takes place. It is difficult to compromise between these two requirements. However, a true dissolution temperature can be obtained with high precision if the size of the crystal is already large enough to minimize recrystallization and/or the rate of crystallization is very slow compared to the rate of heating. The dissolution temperature, for example, of polyethylene crystallized from the melt is 110.0°C. in tetralin determined by slow heating.[6] The crystal remains undissolved indefinitely at 109.5°C. With a high degree of supercooling, polyethylene crystallizes so fast that it is impossible to determine the dissolution temperature with the desired precision. On the other hand, polyacrylonitrile crystallizes slowly, and it is possible to determine the dissolution temperature with certainty even with a high degree of supercooling. This conclusion is substantiated by the fact that the dissolution temperatures obtained by both fast and slow heating methods are within 1°C. Thus, the dissolution temperatures reported here should be valid.

Because of the low rate of crystallization of polyacrylonitrile, the dissolution temperature and crystallization temperature can be determined accurately. Consequently, $(T_m)_\infty$ can be obtained with good precision by extrapolating the experimental value of T_s to intersection with the $T_s = T_c$ line. The validity of this extrapolation cannot be tested in this case because polyacrylonitrile with unlimited step height cannot be prepared. However, indirect evidence from other polymers studied serves to support the extrapolation procedure and the resulting values of $(T_m)_\infty$.

Determination of the relationship between the crystallization and dissolution temperature yields useful information concerning the crystallization behavior of polyacrylonitrile. Although the degree of crystalline perfection of polyacrylonitrile is inferior to that of polyethylene as evidenced by the absence of three-dimensional order as revealed by x-ray diffraction,[10] polyacrylonitrile displays a crystallization behavior in common with other semicrystalline polymers. The linear relationship between T_s and T_c, the sigmoid relationship of the fractional change in specific volume as a function of time during crystallization,[11] and the variation of the step height with the temperature of crystallization demonstrate clearly that polyacrylonitrile crystallizes in the same manner as other semicrystalline polymers.

The authors are indebted to Dr. R. Buchdahl and Dr. H. N. Friedlander for valuable discussions and suggestions.

References

1. Holland, V. F., S. B. Mitchell, W. L. Hunter, and P. H. Lindenmeyer, *J. Polymer Sci.*, **62**, 145 (1962).
2. Hoffman, J. D., and J. I. Lauritzen, *J. Res. Natl. Bur. Std.*, **64A**, 73 (1960).
3. Price, F. P., *J. Polymer Sci.*, **42**, 49 (1960); *J. Chem. Phys.*, **35**, 1884 (1961).
4. Frank, F. C., and M. Tosi, *Proc. Roy. Soc. (London)*, **A236**, 323 (1961).
5. Flory, P. J., *J. Am. Chem. Soc.*, **84**, 2857 (1962).
6. Jackson, J. B., P. J. Flory, and R. Chiang, *Trans. Faraday Soc.*, **59**, 1906 (1963).
7. Holland, V. F., *J. Appl. Phys.*, **35**, 59 (1964).
8. Krigbaum, W. R., and N. Tokita, *J. Polymer Sci.*, **43**, 467 (1960).
9. Stefani, R., M. Chevreton, M. Garnier, and C. Eyaud, *Compt. Rend.*, **251**, 2174 (1960).
10. Bohn, C. R., J. R. Schaefgen, and W. O. Statton, *J. Polymer Sci.*, **55**, 531 (1961).
11. Chiang, R., *J. Polymer Sci.*, **A1**, 2765 (1963).

Résumé

La température de dissolution des cristallites lamellaires de polyacrylonitrile dans le carbonate de propyléne est liée par une relation linéaire à la temperature de cristallisation T_c. Il ressort d'une étude par microscopie électronique que l'épaisseur des lamelles cristallines augmente avec la température de cristallisation suivant les théories communément admises pour la recristallisation des polyméres en milieu dilué. On a trouvé une épaisseur de 100, 130, et 150 A. pour des températures de cristallisation respectivement égales à 95, 116, et 125°C. L'extrapolateur des valeurs expérimentaux de T_s à $\zeta = \infty$ permet d'obtenir une constante caractéristique à savoir $(T_m)\infty$. Cette constante caractéristique $(T_m)\infty$ était de 175°C dans le cas de l'échantillon étudié. On a calculé l'énergie libre d'interphase à partir du point de fusion et de l'épaisseur de la lamelle et on a trouvé une valeur voisine de 1950 cal/mole^{-1} d'unités de la chaîne émergente ou 45 ergs cm^{-2}. Le résultat se compare au 1900 cal. mole^{-1} ou 70 ergs cm^{-2} du polyéthylene. On en conclut que l'energie libre superficielle de divers polymères organiques est très voisine. Quoique la perfection des cristaux lamellaires de polyacrylonitrile soit moindre que celle des cristaux organiques tridimensionnels, il y a analogie de comportement entre les cristaux de ce polymére et des cristaux d'autres polymeres semicristallins. Cette conclusion s'impose par des faits suivants: l'existence d'une relation linéaire entre T_s et T_c, la variation de l'épaisseur des lamelles avec la température de cristallisation et la relation sigmoidale liant le changement fractionnaire du volume spécifique au temps de cristallisation.

Zusammenfassung

Die Auflösungstemperatur kristalliner Polyacrylnitrilplättchen in Propylencarbonat zeigt eine lineare Beziehung zur Kristallisationstemperatur T_c. Die elektronenmikroskopisch gemessene Stufenhöhe ζ der Plättchen nimmt mit zunehmender Kristallisationstemperatur in Übereinstimmung mit der gangigen Theorie der Kristallisation Hochpolymerer in verdünnter Lösung zu. Die Stufenhöhe betrug 100, 130 bzw. 150 A. für ein T_c von 95, 116 bzw. 125°C. Durch Extrapolation der experimentellen Werte von T_s auf den Wert bei $\zeta = \infty$ wird eine charakteristische Konstante $(T_m)\infty$ erhalten. Für die untersuchte Probe war $(T_m)\infty$ in Propylencarbonat 175°C. Die aus dem Schmelzpunkt und der Stufenhöhe berechnete Grenzflachenenergie σ_e liegt in der Grössenordnung von 1950 cal pro Mol heraustragenden Kettenbausteins oder 45 erg cm^{-2} im Vergleich zu 1900 cal Mol^{-1} oder 70 erg cm^{-2} für Polyäthylen. Es scheint, dass die freien Oberflächenenergien verschiedener organischer Polymerer eine bemerkenswerte Ähnlichkeit aufweisen. Obgleich der Grad der kristallinen Vollkommenheit von Polyacrylnitril demjenigen von organischen Kristallen mit dreidimensionaler Ordnung unterlegen ist, zeigt Polyacrylnitril ein dem Kristallisationsverhalten anderer semikristalliner Polymerer ähnliches Verhalten. Diese Schlussfolgerung wird durch die lineare Beziehung zwischen T_s und T_c, die Abhängigkeit der Stufenhöhe von der Kristallisationstemperatur sowie die s-förmige Beziehung für die Änderung des spezifischen Volumens in Abhängigkeit von der Zeit während der Kristallisation gestützt.

Received April 29, 1964
Revised June 2, 1964

JOURNAL OF POLYMER SCIENCE: PART A VOL. 3, PP. 487–499 (1965)

Photoyellowing of Poly(4,4′-Diphenylolpropane Isophthalate): A Novel Polymer Photorearrangement

S. B. MAEROV, *Dacron® Research Laboratory, Textile Fibers Department, E. I. du Pont de Nemours and Company, Inc., Kinston, North Carolina*

Synopsis

The photoyellowing of 4,4′-diphenylolpropane isophthalate (DPP-I) was attributed to a photochemical rearrangement resulting in a polymer containing *o*-hydroxybenzophenones as part of the chain structure. Chain cleavage by photolysis was an accompanying side reaction. *o*-Hydroxybenzophenone derivatives of DPP were prepared to serve as model compounds to confirm the structure of the photorearrangement product. Additional confirmation of the mechanism was obtained by solid phase or solution photorearrangement of the model ester, DPP dibenzoate to its monohydroxybenzophenone derivative. Kinetics of the DPP-I photorearrangement exposed to a xenon high pressure lamp and a carbon arc lamp gave rates of 3.9×10^{-2} and 3.8×10^{-3} mole/l.-hr., respectively. The rate of yellowing in Florida sunlight, open exposure in April, was 1.5×10^{-2} mole/l.-hr.

INTRODUCTION

In the course of our studies of polyesters we found a novel type of molecular rearrangement occurring under the influence of light. Irradiation of polymers by light often results in either polymer discoloration (browning or yellowing), or in photolysis with the usual consequences attendant by a drop in molecular weight. In some cases photolysis and discoloration occur simultaneously. Solarization studies of polyester resins[1] containing unsaturated aliphatic acids crosslinked with polystyrene showed that the yellowing was associated with photosensitive groups present in the formulations. In the case of linear condensation polyesters the structures of the glycol and acid portion have a profound bearing upon the effect of light exposure. Polyesters in which the glycol portion is aliphatic in nature and the acid portion either aliphatic or aromatic generally display good resistance to discoloration by light. Osborne[2] has studied the photolysis of polyethylene terephthalate. The quantum yield found, 5.0×10^{-4}, was remarkably similar to that found for rubber[3] and for cellulose.[4] On the other hand, linear polyesters in which the diacids are aromatic and the glycol replaced by diphenols or bisphenols show a rapid and severe yellowing in sunlight or in artificial light sources having a high intensity of ultraviolet light. The purpose of this work was to study the mechanism of

photoyellowing of poly(4,4′-diphenylolpropane isophthalate) (DPP-I). The preparation of DPP-I (I), via an all-melt acidolysis exchange reaction has been described by Conix; the technique of interfacial polycondensation[6,7] has also been used to prepare DPP-I.

RESULTS AND DISCUSSION

Figure 1 (curve *A*) shows the ultraviolet absorption curve of an unexposed 0.3 mil film of DPP-I. The absorption curve was corrected for scattering by assuming the scattering coefficient of the film to be constant in the region 280–400 mμ. Absorption was at a maximum around 285 mμ, as far as instrument resolution was possible, even with self-supporting films as thin as 0.1 mils. Curve *B* shows the absorption of the same film after irradiation for 4 hr. with a high pressure lamp and subtraction of the original film absorption. An irradiation product was formed which initially showed an absorption maximum at 350 mμ. With additional exposure, the maximum shifted bathochromically to 353.5 mμ. The yellow color formed in irradiated DPP-I was, therefore, due to the tailoff of absorption extending into the visible region of the spectrum due to the chromophoric group being generated.

Figure 2 shows the infrared absorption spectrum of a 1.0 mil DPP-I

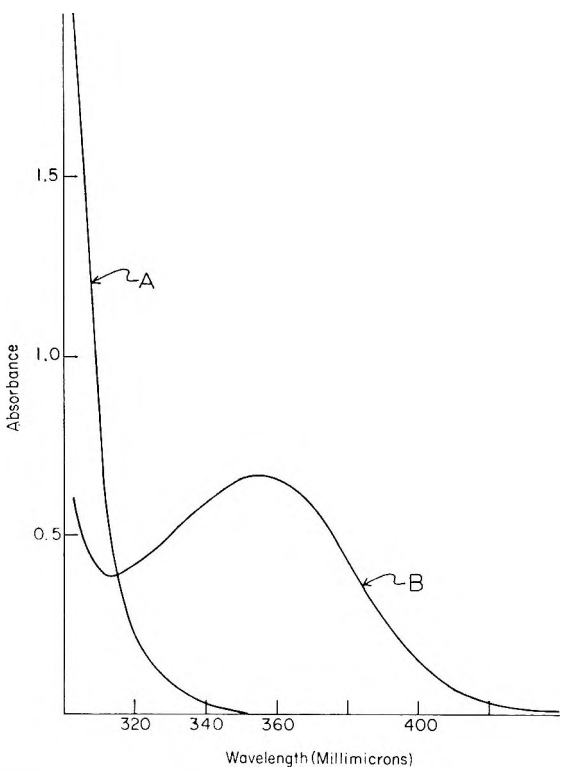

Fig. 1. Ultraviolet absorption of 0.3 mil DPP-I film: (*A*) original film; (*B*) film after 4 hr. exposure to xenon lamp.

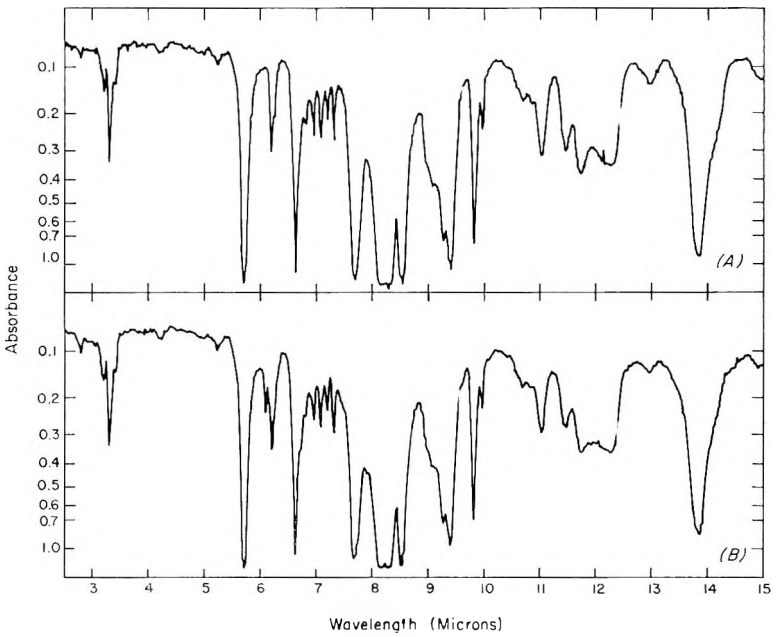

Fig. 2. Infrared spectra of (*A*) 1.0 mil DPP-I film; (*B*) film after 4 hr. exposure to xenon lamp.

film before and after exposure for 4 hr. to a lamp. Among the more notable changes observed after irradiation were (*1*) the increased absorption in the OH region around 2.80μ and (*2*) the appearance of a new, well developed peak at 6.10μ.

It is proposed that irradiation of DPP-I occurred with molecular rearrangement to form a new polymer composed, in part, of linear *o*-hydroxybenzophenone (II) moieties as products. The photochemical rearrangement, shown in reaction (1), is analogous in product formation to the Fries

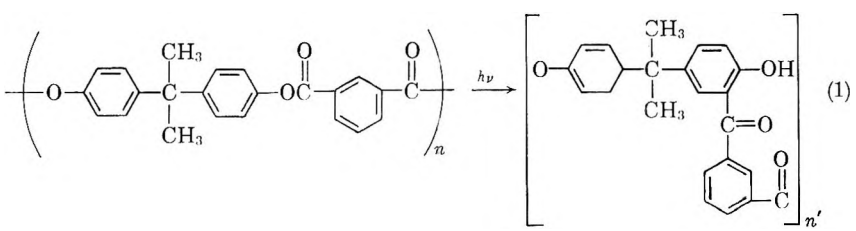

(1)

rearrangement of phenolic esters,[8] however, catalysis by ultraviolet light here replaces the usual Lewis-type acid catalysts.* Evidence supporting the conclusion that *o*-hydroxybenzophenone moieties are photorearrangement products is presented below.

* Although the Lewis acids are commonly referred to as catalysts, they must, in fact, be present in stoichiometric amounts for satisfactory yields in the Fries rearrangement. Similarly, light is a reactant in the photorearrangement of DPP-I, although the stoichiometry between light quanta and moles of ester rearranged is not known.

Model Hydroxybenzophenone Derivatives of Diphenylolpropane

o-Hydroxy-benzophenone derivatives of diphenylolpropane were prepared to serve as model compounds for spectral studies in the ultraviolet, visible, and infrared spectral regions. The compounds prepared were 2,2-bis(3-benzoyl-4-hydroxyphenyl)propane (IIIA), and 2,2-bis(3-*m*-carboxybenzoyl-4-hydroxyphenyl)propane (IIIB). These com-

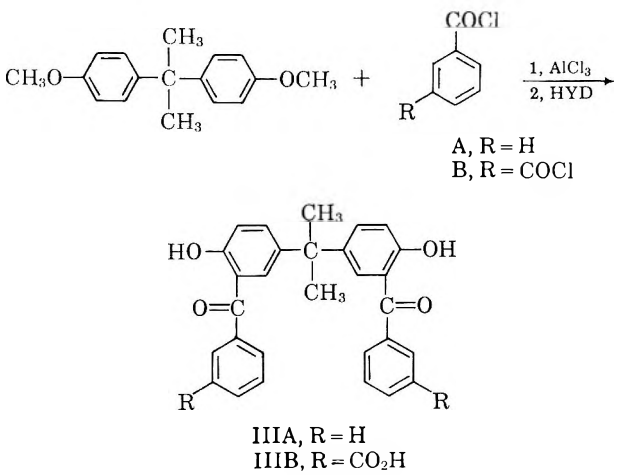

(2)

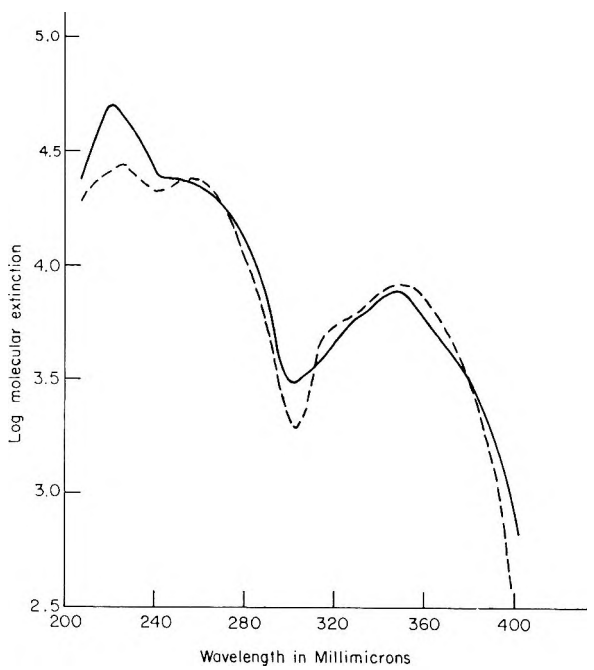

Fig. 3. Ultraviolet absorption spectra in methanol: (——) 2,2-bis(3-benzoyl-4-hydroxyphenyl)propane; (- -)2,2-bis(3-*m*-carboxybenzoyl-4-hydroxyphenyl)propane.

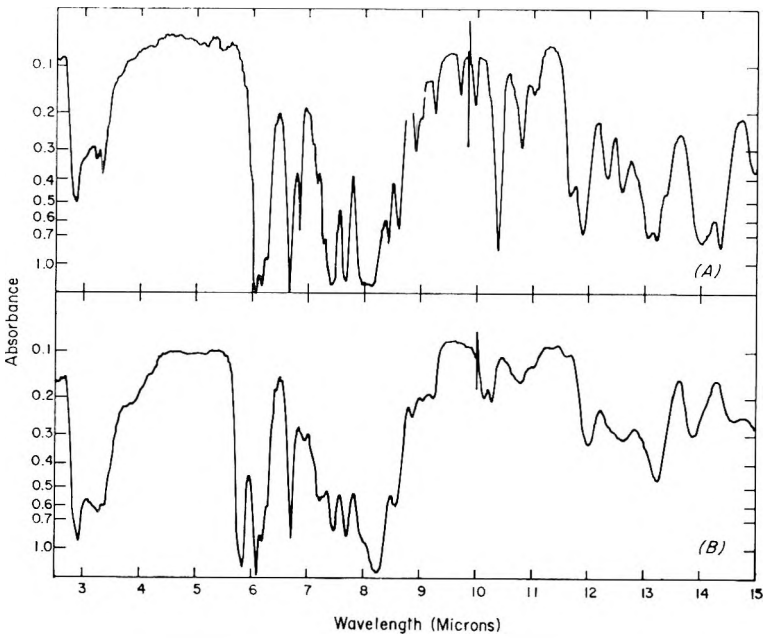

Fig. 4. Infrared absorption of model compounds: (*A*) 2,2-bis(3-benzoyl-4-hydroxyphenyl)propane; (*B*) 2,2-bis(3-*m*-carboxybenzoyl-4-hydroxyphenyl)propane.

pounds were prepared, in low yield, by the simultaneous Friedel-Craft condensation-demethylation reaction of diphenylolpropane dimethyl ether with benzoyl chloride and isophthalolyl chloride, respectively. The ultraviolet absorption spectrum of these compounds in methanol is shown on Figure 3. The similarity in the absorption spectrum in the 300–400 mμ region with that of irradiated DPP-I is apparent. These compounds were characterized by absorption maxima at 348 mμ. Similarly, the infrared absorption spectra of these compounds (Fig. 4) showed a strong, sharp peak at 6.10μ attributed to the highly polarized benzophenone carbonyl group. The spectral data of these model compounds supply confirmatory evidence that *o*-hydroxybenzophenones were formed during photoirradiation of DPP-I.

Photorearrangement of the Model Ester, Diphenylolpropane Dibenzoate

The ester, diphenylolpropane dibenzoate (IV; DPP dibenzoate) was used in irradiation studies as a model monomeric compound resembling DPP-I in structure. Irradiation of DPP dibenzoate in deoxygenated benzene with a Westinghouse Type RS Sunlamp resulted in yellow solutions. Separation by solution chromatography over a silica-base adsorbant column gave a yellow oil (V) besides recovered starting diester, DPP, the monobenzoate ester of DPP and some resinous products of unknown structure. After distillation (V) showed an ultraviolet absorption maximum at 348 mμ, ε carbonyl peak at 6.10 μ in the infrared, and yielded carbonyl

derivatives. Both carbon-hydrogen analysis and the saponification equivalent of V, confirmed its structure to be 3-benzoyl-diphenylolpropane-4′-monobenzoate. No apparent change in the nature of the products was

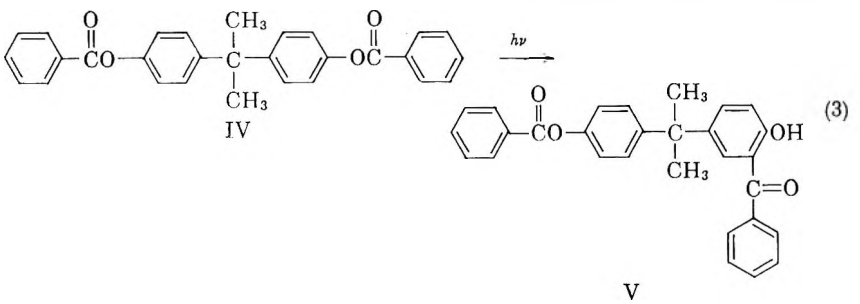

IV V (3)

observed when irradiation of IV was conducted with oxygenated solutions. Further experiments showed that V was also obtained by irradiating DPP dibenzoate as powdered crystalline solid with a Hanovia high-pressure quartz mercury-vapor lamp. The latter experiments confirmed that photorearrangement should be possible in the mixed amorphous-crystalline matrix of a polymer such as DPP-I.

Photochemical Fries Rearrangement

Anderson and Reese[9] reported that irradiation of absolute ethanol solutions of catechol monoacetate yielded catechol (46%), 2,3-dihydroxyacetophenone (22%), and 3,4-dihydroxyacetophenone (18%). Phenyl acetate rearranged at a rate comparable with that of catechol monoacetate suggesting that the photo-induced Fries arrangement may be general in nature. Kobsa[10] studied the photo-induced rearrangement of a series of *p-tert*-butylphenyl esters. Migration to the *ortho* positions occurred whenever both positions were unsubstituted. However, in the case of the 2-chloro- and 2,5-dichloro-*p-tert*-butylphenyl esters, rearrangement occurred with concomitant elimination of a chlorine atom. No elimination of the *p-tert*-butyl group was observed. Schmitt and Hirt[11] reported that 4-*tert*-butylphenylsalicylate undergoes photochemical rearrangement to a dihydroxybenzophenone upon irradiation. Recently[12] *para* rearrangement products were obtained in good yield when both *ortho* positions of the phenolic moiety had methyl substituents; no rearrangement products were observed where all *ortho* and *para* positions of the phenolic moiety were alkyl-substituted or where the acid moiety was the mesitoyl group.

These recent findings add confirmation that the photoyellowing of DPP-I is due to a molecular rearrangement within the polymer chains to form *o*-hydroxybenzophenones.

Kinetics and Discussion of the Mechanism

With the above evidence that hydroxybenzophenone moieties, II, are indeed the products of irradiation of DPP-I, it is possible to calculate the

molar conversion of I to II with time when the molecular extinction coefficient of species II is known. Since the structure of II closely resembles that of the synthesized model compound IIIB, the product was assigned a molecular extinction of one-half the value of this bis compound [λ_{max} 348 mμ (7750)]. This is probably reasonable for nonconjugated chromophors unaffected by electronic interaction through space. Films of DPP-I were exposed to both a carbon arc lamp (Fade-Ometer) and to a high pressure lamp (Xenotest), and the total degree of yellowing was followed

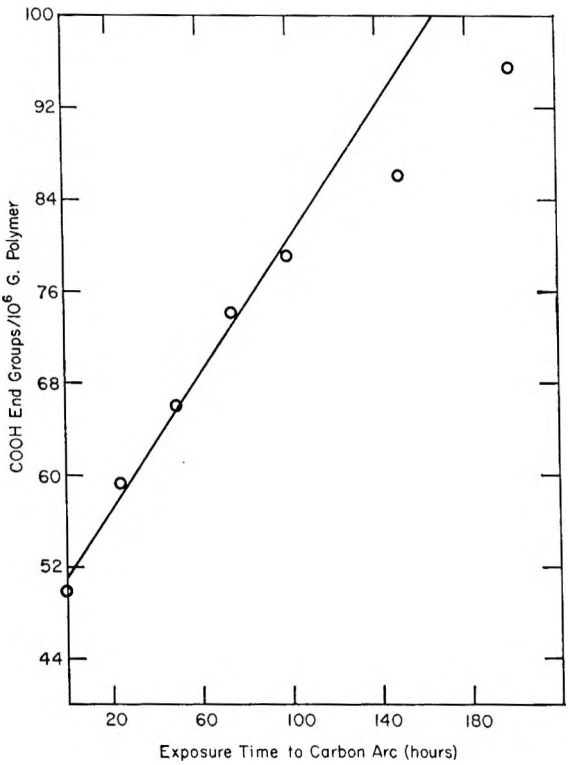

Fig. 5. Carboxyl generation in DPP-I.

spectrophotometrically with time at the observed absorption maximum (350–353 mμ). The concentration of product, II, may be calculated from eq. (1):

$$A_{total} = A_I + A_{II} = (\epsilon_I C_I + \epsilon_{II} C_{II})d \qquad (1)$$

where A = absorbance, ϵ = molecular extinction coefficient, C = concentration in moles/liter (density of DPP-I = 1.20 g./cm.^{3}), and d = film thickness in centimeters.

Since A_I at the absorption maximum of II (350 mμ) is small, and the change in concentration of DPP-I is also quite small, A_I may be considered

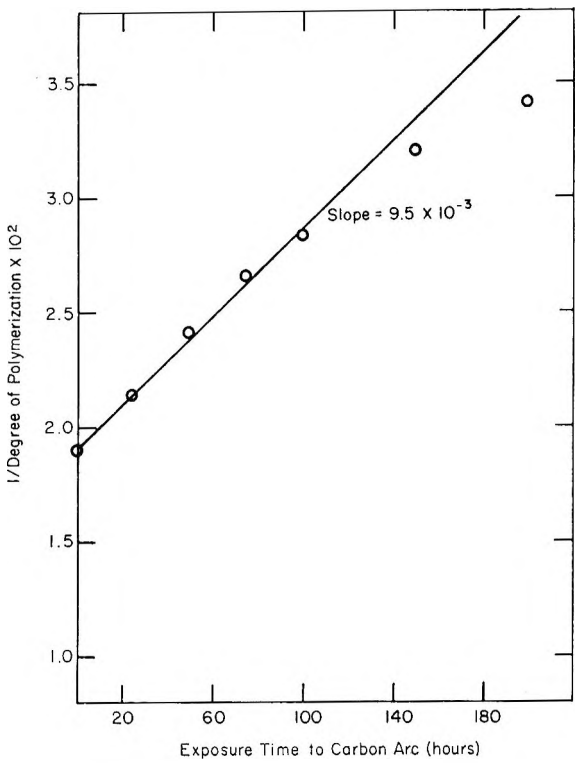

Fig. 6. Rate of chain cleavage of DPP-I.

constant without appreciable error. Therefore, the concentration of product, II, may be obtained from eq. (2):

$$C_{II} = \frac{A_{total} - A_I}{\epsilon_{II} d} \tag{2}$$

A plot of C_{II} versus time for each of the light sources indicated that the formation of photorearranged hydroxybenzophenones followed zero-order kinetics with the following observed rates:* xenon lamp, rate = 3.9×10^{-2} mole/l. hr.; carbon arc lamp, rate = 3.8×10^{-3} mole/l. hr.

Kinetic studies of DPP-I films exposed, open at 45° south, to Hialeah, Florida sunlight in April 1960, gave conversion rates of 1.5×10^{-2} mole/l.-hr.

Photorearrangement was not the exclusive product of irradiation of DPP-I. A rapid chain scission reaction accompanied rearrangement, at

* Actually, the reaction is first order with respect to light quanta. Kobsa[13] determined the rate of rearrangement of DPP-I to be 65000 Einsteins^{-1} cm.^{2} using a General Electric B-H6 high pressure mercury lamp and a spectral band extending in the range 275–285 mμ. Using the molecular extinction coefficient of model compound IIIA, (data supplied by this author), Dr. Kobsa reported a quantum yield, $\phi = 0.016$ for the rearrangement.

least in the early stages of exposure. The degree of photolysis was determined by following both the change in intrinsic viscosity and the determination of chain end carboxyl groups. The plot of COOH groups generated/10^6 g. of polymer with exposure time in the carbon arc lamp is shown in Figure 5. Zero-order kinetics were obeyed up to exposure times of about 100 hr. In order to calculate the molar rate of photolysis the relationship between number-average molecular weight M_n and carboxyl chain ends must be known. DPP-I polymer made by acidolysis polymerization with molecular weight above 10,000, has an average of one COOH per chain.[14] A plot of the reciprocal of the calculated degree of polymerization (D.P.) versus exposure time[15] to the carbon arc lamp is shown in Figure 6. The rate of photolysis was calculated to be 9.5×10^{-3} mole/l.-hr. or about 2.5 times the rate of photorearrangement with the same carbon arc lamp. It is likely that the rate of photolysis fell off at higher exposure times because of the self-screening effect resulting from the formation of the higher absorbing photorearranged moieties. *o*-Hydroxy-benzophenones are efficient ultraviolet light absorbers. As the concentration of the photorearranged product increases, more of the incident light can be internally absorbed and dissipated by these groups. Indeed, carboxyl generation and the change in intrinsic viscosity leveled off at the same time as subjective evaluation of film yellowness reached a maximum. Further irradiation caused only insignificant changes in the polymer molecular weight up to prolonged exposure times.

EXPERIMENTAL*

Preparation of DPP-I Films

DPP-I polymer of intrinsic viscosity 0.99 (in trifluoroacetic acid–methylene chloride, 25/75, v/v) was prepared according to Eareckson's procedure.[7] Clear films were cast from solution (1–5 wt.-%) in TFA–CH_2Cl_2 (25/75, v/v) onto glass plates under a nitrogen atmosphere using a 0.010-in. doctor blade.

DPP-I acidolysis polymer for photolysis studies was prepared by melting together equimolar amounts of diphenylolpropane diacetate and isophthalic acid at 260°C. and removing one-half of the theoretical amount of acetic acid by distillation. The prepolymer was fed in the molten state and applied by a doctor knife as a thin film onto aluminum tape. The coated aluminum tape was exposed in an oven for 1.5 min. at 350°C. while being swept by a countercurrent stream of preheated nitrogen gas to remove acetic acid and other volatile components. Continuous DPP-I films of thickness 0.1–1.0 mils (intrinsic viscosity, 0.50 in TFA–CH_2Cl_2) were obtained by dissolving away the aluminum backing in dilute hydrochloric acid.

* All melting points and boiling points are uncorrected.

Exposure of Films

Xenon lamp exposure was conducted in the Xenotest apparatus (Quarzlampen Gessellschaft M.B.H. Hanau) utilizing a 1500-w. radiator. Radiation intensity on the sample (6.5 cm. sample-to-water filter distance) was 150,000 Lux using the continuous light exposure sequence.

Carbon arc exposure was conducted in the Fade-Ometer (Atlas Electric Devices Co., Chicago). Radiation intensity of the Pyrex-enclosed single violet carbon arc was 167 w./ft.^{2} at a sample-to-globe distance of 25 cm.

Exposure sun hours at Hialeah, Florida in April 1960, were based upon radiation intensities exceeding a minimum of 0.823 Langleys/hr.

Preparation of Intermediates and Model Compounds

Diphenylolpropane Dimethyl Ether. Diphenylolpropane (Monsanto Chemical Co.,; 45.6 g., 0.2 mole) was dissolved in a solution of 250 ml. of water containing 16 g. of sodium hydroxide. The solution was charged to a single-necked, one liter round-bottomed flask fitted with a reflux condenser. After cooling to 0°C., dimethyl sulfate (50.4 g., 0.4 mole) was added and the mixture allowed to warm to room temperature with occasional shaking. The mixture was heated on the steam bath for 1.5 hr. and allowed to stand overnight. The upper organic layer was separated in a separatory funnel and the aqueous layer extracted three times with 100 ml. portions of benzene. The combined organic layer and benzene extracts were dried over anhydrous sodium sulfate, filtered and the benzene removed *in vacuo*. Distillation yielded 40.5 g. (80%) of product, b.p. 163–166°C. (0.6 mm.), $n_D^{28} = 1.5742$ (hazy).

Anal. Calcd. for $C_{17}H_{20}O_2$: C, 79.64%; H, 7.86%. Found: C, 79.65%; H, 7.85%.

2,2-Bis(3-benzoyl-4-hydroxyphenyl)propane, IIIA. In a 500-ml. three-necked flask fitted with an efficient reflux condenser protected by a $CaCl_2$ drying tube, a stirrer, and a 50 ml. dropping funnel there was charged anhydrous aluminum chloride (30.0 g., 0.225 mole) and freshly distilled benzoyl chloride (19.8 ml., 0.170 mole) dissolved in 30 ml. of 1,2-ethylene chloride. At ice bath temperature and with stirring, a solution of diphenylolpropane dimethyl ether (21.0 g., 0.082 moles) in 30 ml. of ethylene chloride was added over a 30-min. period. HCl gas was evolved while stirring was continued for an additional 15 min. at ice bath temperatures. After warming to room temperature and being allowed to stand overnight, the solution was warmed to 45°C. for 1.5 hr. After cooling in an ice bath the mixture was poured over 200 g. of ice containing 100 ml. of concentrated hydrochloric acid. Steam distillation left a viscous dark liquid which was washed by trituration with hot water. After cooling the resinous liquid solidified. Extraction of the solid residue with hot 5% sodium hydroxide solution and charcoal treatment gave a bright red filtrate. The filtrate deposited a cream-colored solid when neutralized with ice water containing

hydrochloric acid. After three recrystallizations from 95% ethanol, the product, 5 g., was obtained as fine yellow crystals, m.p. = 159.5–160.5°C.

ANAL. Calcd for $C_{29}H_{24}O_4$: C, 79.80%; H, 5.54%. Found: C, 80.15%; H, 5.50%.

2,2-Bis(3-*m*-carboxybenzoyl-4-hydroxyphenyl)propane, IIIB. Into the apparatus described for IIIA, there was charged anhydrous aluminum chloride (40.0 g.) and 50 ml. of carbon disulfide. With stirring, at ice bath temperatures there was added over 1 hr. a solution of isophthaloyl chloride (Hooker Chemical Co. recrystallized from hexane; 20.4 g, 0.10 mole), and DPP dimethyl ether (12.4 g., 0.049 moles) in 50 ml. of carbon disulfide. A yellow salt formed, hydrogen chloride gas was evolved, and the mixture became viscous as it was allowed to warm to room temperature. After standing at room temperature for 2 hr., the solvent was refluxed over a 60°C. water bath. The deep red viscous mixture was poured over ice–hydrochloric acid and the carbon disulfide removed by distillation. The viscous oil which solidified on cooling was ground and washed with water and added to 600 ml. of hot 2*N* ammonium hydroxide and filtered. Sufficient charcoal was added to the filtrate to coagulate resinous products and the mixture refiltered. Acidification of the filtrate with dilute hydrochloric acid precipitated a cream-colored solid (12.0 g., 48% yield). After three recrystallizations from 50% aqueous acetic acid, the bright yellow needles melted at 253–255°C.

ANAL. Calcd for $C_{31}H_{24}O_8$: C, 70.98%; H, 4.61%. Found: C, 70.62%; H, 4.76%.

Diphenylolpropane Dibenzoate (IV). This compound was made by conventional Schotten-Baumann technique from sodium diphenoxypropane and benzoyl chloride. After three recrystallizations from benzene–petroleum ether (b.p. 50–60°C.), the colorless crystals melted at 163–163.5°C.

ANAL. Calcd. for $C_{29}H_{24}O_4$: C, 79.80%; H, 5.54%. Found: C, 79.59%; H, 5.53%. Saponification equivalent: Calcd. 218.2. Found 217.1.

Photoirradiation of Diphenylolpropane Dibenzoate (DPP Dibenzoate)

Solution Irradiation under Nitrogen. Finely ground DPP dibenzoate (6.0 g.) was dissolved in 100 ml. of benzene (A.C.S. reagent grade) and charged to a 500 ml. glass-jacketed quartz round-bottomed flask fitted with a straight-walled condenser and a glass inlet tube extending through the entire length of the apparatus. Nitrogen gas was bubbled through the inlet tube which served as both a means of stirring and of deoxygenating the system. The solution was irradiated for 96 hr. with a Westinghouse Type RS sunlamp placed flush against the jacket of the quartz tube through which cooling water was run. After irradiation, the yellow solution was filtered to reclaim 0.4 g. of starting diester, and the filtrate worked up by solution chromatography.

Solution Irradiation in the Presence of Oxygen. The procedure was

TABLE I

Fraction no.	Eluent (vol./vol.)	Wt. obtained, g.	Description or identification of product
1	Benzene	2.5	Reclaimed DPP dibenzoate; m.p. 157–163°C.
2	Benzene–ether (50/50)	1.1	Yellow oil; compound V
3	Ether	0.3	White solid; m.p. 145–153°C.; mixture of DPP and monobenzoate of DPP
4	Ether–chloroform	0.2	White solid; m.p. 290–295°C. (sintered); unknown
5	Acetone–methanol (50/50)	0.35	Dark resinous solid; did not melt below 350°C.

identical with that described above except that dry air was bubbled through the solution in the place of nitrogen.

Irradiation of Crystalline Solid. Finely ground DPP dibenzoate was spread on a glass plate and exposed open, 4 in. from a 450-w. Hanovia high-pressure quartz mercury-vapor lamp (Code L-679A). Every 8 hr. the powder was collected and redistributed over the surface of the glass to expose fresh crystal surfaces. After 96 hr. total exposure time, the yellowed solid (about 2.0 g.) was dissolved in 50 ml. of C.P. benzene.

Solution Chromatography of Irradiated DPP Dibenzoate. A typical chromatographic separation is described. A 4-ft. glass tube (I.D. 26 mm.) was packed with Florisil (125 g. of silica-base adsorbant; Floridin Co., Tallahassee, Florida) dispersed in C.P. benzene. Irradiated DPP dibenzoate (5.0 g./100 ml.) in benzene was added to the column by means of a one-liter separatory funnel. Elution with various solvents gave the products listed in Table I.

Identification of Compound V: 3-Benzoyl-diphenylolpropane-4′-monobenzoate. Fraction 2 from the chromatographic separation was distilled to give a viscous yellow liquid, b.p. 220°C. 0.15 mm. The ultraviolet absorption characteristics in diethyl ether were: (log specific extinction units) λ_{max} 347 mμ (1.82), λ_{min} 307 mμ (1.45), shoulder, λ 270 mμ (2.40), λ_{max} 240 mμ (2.75). The infrared absorption spectrum showed the following bands: 2.80, 3.19, 3.30, 5.72, 6.10, 6.21, 6.60, 6.72, 6.87, 7.08, 7.20, 7.32, 7.48, 7.58, 7.80–8.32 (broad), 8.50, 9.25, 9.38, 9.72, 9.81, 9.95, 10.39. 10.63, 10.82, 11.35, 11.93, 12.25, 13.18, 14.0–14.2 (broad), 14.63, 14.75 μ,

ANAL. Calcd. for $C_{29}H_{24}O_4$: C, 79.80%; H, 5.54%. Found: C, 79.13%; H, 5.95%. Saponification equivalent in alcohol–water with potassium carbonate: Calcd., 436.5. Found: 430.5.

For the 2,4-dinitrophenylhydrazone, red crystals from alcohol, m.p. 207–208°C. analytical data were also obtaind.

ANAL. Calcd. for $C_{35}H_{28}O_7N_4$: C, 68.17%; H, 4.58%; N, 9.09%. Found: C, 68.13%; H, 5.01%; N, 9.11%.

References

1. Hirt, R. C., R. G. Schmitt, and W. L. Dutton, J. Solar Energy, **3**, 19 (1959).
2. Osborne, K. R., *J. Polymer Sci.*, **38**, 357 (1959).
3. Bateman, L., *J. Polymer Sci.*, **2**, 1 (1947).
4. Sauer, H. F., and W. K. Wilson, *J. Am. Chem. Soc.*, **71**, 958 (1949).
5. Conix, A., *Ind. Chim. Belge*, **22**, 1457 (1957); *Ind. Eng. Chem.*, **51**, 147 (1959).
6. Magat, E. E., and D. R. Strachan (assigned to E. I. du Pont de Nemours and Co.), U. S. Pat. 2,708,617 (5/17/55).
7. Eareckson, W. M., III, *J. Polymer Sci.*, **40**, 399 (1959).
8. Blatt, A. H., *Organic Reactions*, Vol. I, Wiley, New York, 1947, Chap. 11.
9. Anderson, J. C., and C. B. Reese, *Proc. Chem. Soc.*, **1960**, 217; *J. Chem. Soc.*, **1963**, 1781.
10. Kobsa, H., *J. Org. Chem.*, **27**, 2293 (1962).
11. Schmitt, R. G., and R. C. Hirt, *J. Polymer Sci.*, **61**, 361 (1962).
12. Finnegan, R. A., and J. J. Mattice, paper presented to Division of Organic Chemistry, 145th Meeting, American Chemical Society, New York, September 9–13, 1963; *Abstracts of Papers*, p. 3Q.
13. Kobsa, H., private communication.
14. Heighton, H. H., private communication.
15. Mark, H., and A. V. Tobolsky, *Physical Chemistry of High Polymeric Systems*, 2nd Ed., Interscience, New York, 1950, p. 462 ff.

Résumé

Le jaunissement à la lumière du DPP-I est attribué au réarrangement photochimique, dû au fait qu'une partie de la chaîne polymérique contient des groupes *o*-hydroxybenzophénones. On constate comme réaction secondaire une rupture de la chaîne par photolyse. On a préparé des dérivés *o*-hydroxybenzophénone du DPP comme substances modéles pour confirmer la structure du produit de photoréarrangement. Une confirmation supplémentaire du mécanisme a été obtenue par réarrangement photochimique en phase solide ou en solution de l'ester modèle, le dibenzoate de DPP en son dérivé monohydroxybenzophenone. Les mesures cinétiques du réarrangement du DPP-I donnent une vitesse de 3.9×10^{-2} moles/l heure pour l'irradiation par une lampe Xénon à heute pression et 3.8×10^{-3} moles/l heure pour une lampe à arc. La vitesse de jainissement sous le soleil de Floride en Avril, était de 1.5×10^{-2} moles/l heure.

Zusammenfassung

Die Lichtvergilbung von DPP-I wurde einer photochemischen Umlagerung unter Bildung eines Polymeren mit *o*-Hydroxybenzophenon als Teil der Kettenstruktur zugeschrieben. Als Nebenreaktion trat Kettenspaltung durch Photolyse auf. Als Modellverbindungen zur Bestätigung der Struktur der Photoumlagerungsprodukte wurden *o*-Hydroxybenzophenonderivate von DPP dargestellt. Zusätzliche Bestätigung des Mechanismus wurde durch die Photoumlagerung des Modellesters DPP-Dibenzoat in ein Monohydroxybenzophenonderivat in fester Phase oder in Lösung erhalten. Kinetische Versuche über die DPP-I-Photoumlagerung unter Bestrahlung mit einer Xenon-Hochdrucklampe und einer Kohlenbogenlampe lieferten eine Geschwindigkeit von $3{,}9.10^{-2}$ bzw. $3{,}8.10^{-3}$ Mol/l.Stunde. Die Vergilbungsgeschwindigkeit im Sonnenlicht von Florida, offene Bestrahlung im April, betrug $1{,}5.10^{-2}$ Mol/l.Stunde.

Received May 18, 1964

JOURNAL OF POLYMER SCIENCE: PART A VOL. 3, PP. 501–511 (1965)

Studies in Cyclocopolymerization. Relative Rates of Addition in the Free Radical-Initiated Copolymerization of 1,4-Dienes and Substituted Olefins*

JOHN M. BARTON, GEORGE B. BUTLER, and EARL C. CHAPIN,†
Department of Chemistry, University of Florida, Gainesville, Florida

Synopsis

A general copolymer composition equation is developed for the cyclocopolymerization of 1,4-dienes (M_1) and monoolefins (M_2). The general equation relates copolymer composition to monomer feed composition in terms of five reactivity ratio parameters. When cyclization is very rapid relative to other chain propagation steps the general equation simplifies to the form: $n = (1 + r_1x)(1 + r_cx)/[r_cx + (r_2/x) + 2]$, where $n = [m_1]/[m_2]$ in the copolymer, $x = [M_1][M_2]$ in the monomer feed, and r_1, r_2, and r_c are reactivity ratios for the chain propagation steps of diene, monoolefin, and cyclized radicals, respectively. The theory is applied to the free radical initiated copolymerization of (A) divinyl ether/maleic anhydride, (B) 1,4-pentadiene/maleic anhydride, (C) divinyl ether/*N*-phenylmaleimide, (D), divinyl ether/acrylonitrile; and (E) 1,4-pentadiene/acrylonitrile. Systems A, B, and C form alternating copolymers of composition $n = 0.5$. For system D, $r_1 = 0.024$, $r_2 = 0.938$, $r_c = 0.017$. For system E, $r_1 \simeq r_c \simeq 0$, $r_2 = 1.13$.

INTRODUCTION

It has been observed that certain 1,4-dienes are capable of copolymerizing with certain monoolefins by a bimolecular alternating inter-intramolecular mechanism.[1–5] In these copolymers a cyclic repeating unit containing both monomers alternates with monoolefin units. The example of copolymerization of divinyl ether and maleic anhydride, shown at the top of the following page, illustrates the general course of the reaction.

General copolymer composition equations have been developed[6,7] for the cyclocopolymerization of 1,6-dienes and monoolefins, when the diene radical can cyclize directly to form a unimolecular cyclic repeating unit. It has been shown that these equations approximate to the classical binary copolymer composition equation when the cyclization of diene radicals is very rapid.

* Presented at the 147th Meeting, American Chemical Society, Philadelphia, Pennsylvania, April 1964.

† Present address: Western New England College, Springfield, Massachusetts.

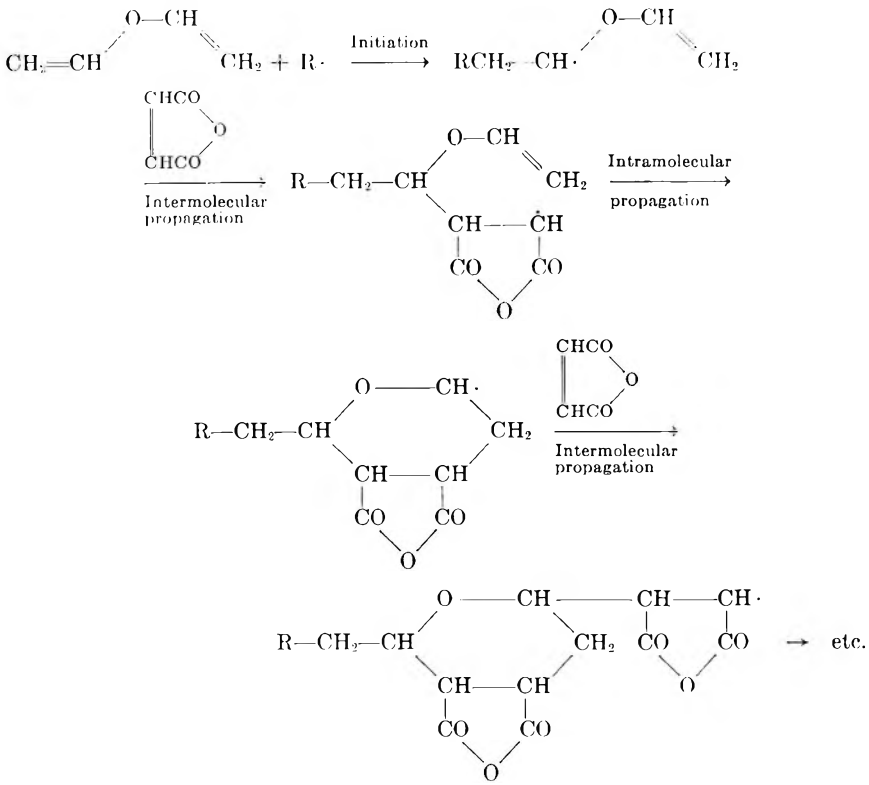

The present work describes a general copolymer composition equation applicable to the cyclocopolymerization of 1,4-dienes and monoolefins where the cyclic repeating unit is bimolecular in construction. This equation does not approximate to the classical binary equation when cyclization is very rapid. The relevance of this theory is demonstrated experimentally for the free radical initiated copolymerization of divinyl ether/maleic anhydride, 1,4-pentadiene/maleic anhydride, divinyl ether/*N*-phenylmaleimide, divinyl ether/acrylonitrile, and 1,4-pentadiene/acrylonitrile.

Although the theory is developed for free radical... initiated copolymerization, it should also apply to appropriate ionically initiated systems and to addition copolymerizations involving nonolefinic unsaturated groups such as epoxide or carbonyl groups, if the same kinetic assumptions apply.

THEORY

The kinetic scheme considered is shown in eqs. (1)–(9).

$$m_1^{\cdot} + M_1 \xrightarrow{k_{11}} m_1^{\cdot} \tag{1}$$

$$m_1^{\cdot} + M_2 \xrightarrow{k_{12}} m_3^{\cdot} \tag{2}$$

$$m_3^{\cdot} \xrightarrow{k_c} m_c^{\cdot} \quad (3)$$

$$m_3^{\cdot} + M_1 \xrightarrow{k_{31}} m_1^{\cdot} \quad (4)$$

$$m_3^{\cdot} + M_2 \xrightarrow{k_{32}} m_2^{\cdot} \quad (5)$$

$$m_c^{\cdot} + M_1 \xrightarrow{k_{c1}} m_1^{\cdot} \quad (6)$$

$$m_c^{\cdot} + M_2 \xrightarrow{k_{c2}} m_2^{\cdot} \quad (7)$$

$$m_2^{\cdot} + M_1 \xrightarrow{k_{21}} m_1^{\cdot} \quad (8)$$

$$m_2^{\cdot} + M_2 \xrightarrow{k_{22}} m_2^{\cdot} \quad (9)$$

M_1 is the diene $CH_2{=}CH{-}X{-}CH{=}CH_2$, where X is CH_2, O, SO_2, etc. M_2 is the monoolefin, CHY = CHZ. The $m_1^{\cdot}$ is the radical $\sim\!\sim CH_2\dot{C}HXCH{=}CH_2$, $m_2^{\cdot}$ is the radical $\sim\!\sim CHY\dot{C}HZ$, $m_3^{\cdot}$ is the radical

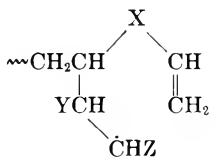

and $m_c^{\cdot}$ is the cyclized radical

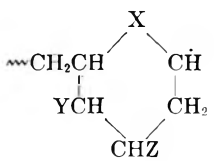

The fate of the intermediate radical, $m_3^{\cdot}$, is governed by the relative rate of cyclization (k_c) and addition to monomers 1(k_{31}) and 2(k_{32}).

Although a six-membered ring is normally the most likely product of cyclization of $m_3^{\cdot}$, if the terminal methylene in $m_3^{\cdot}$ were hindered by bulky substituents or if it were conjugated with an aromatic group, a five-membered ring might be favored. This should not, however, influence the overall kinetics.

If penultimate group effects and crosslinking reactions are neglected, the relative rate of addition of M_1 and M_2 is given by:

$$\frac{d[M_1]}{d[M_2]} = \frac{d[M_1]}{dt} \Big/ \frac{d[M_2]}{dt} = \frac{[M_1]}{[M_2]} \times \frac{\{k_{11}[m_1^{\cdot}] + k_{21}[m_2^{\cdot}] + k_{31}[m_3^{\cdot}] + k_{c1}[m_c^{\cdot}]\}}{\{k_{12}[m_1^{\cdot}] + k_{22}[m_2^{\cdot}] + k_{32}[m_3^{\cdot}] + k_{c2}[m_{c2}][m_c^{\cdot}]\}} \quad (10)$$

or

$$n = \frac{d[M_1]}{d[M_2]} = \frac{K_{11}[m_1^{\cdot}] + K_{21}[m_2^{\cdot}] + K_{31}[m_3^{\cdot}] + K_{c1}[m_c^{\cdot}]}{K_{12}[m_1^{\cdot}] + K_{22}[m_2^{\cdot}] + K_{32}[m_3^{\cdot}] + K_{c2}[m_c^{\cdot}]} \quad (11)$$

where $K_{ij} = k_{ij}[M_j]$.

Making the stationary state assumption that the concentrations of radicals $[m_1^{\cdot}]$, $[m_2^{\cdot}]$, and $[m_c^{\cdot}]$ are constant, leads to:

$$K_{12}[m_1^{\cdot}] - K_{21}[m_2^{\cdot}] - K_{31}[m_3^{\cdot}] = K_{c1}[m_c^{\cdot}] \tag{12}$$

$$K_{21}[m_2^{\cdot}] - K_{32}[m_3^{\cdot}] = K_{c2}[m_c^{\cdot}] \tag{13}$$

$$k_c[m_3^{\cdot}] = (K_{c1} + K_{c2})[m_c^{\cdot}] \tag{14}$$

Solving for $[m_1^{\cdot}]$, $[m_2^{\cdot}]$, and $[m_3^{\cdot}]$, we have:

$$[m_1^{\cdot}] = ([m_c^{\cdot}]/K_{12}kc)(K_{c1} + K_{c2})(K_{31} + K_{32} + k_c) \tag{15}$$

$$[m_2^{\cdot}] = ([m_c^{\cdot}]/K_{21}k_c)\{K_{c2}kc + K_{32}(K_{c1} + K_{c2})\} \tag{16}$$

$$[m_3^{\cdot}] = ([m_c^{\cdot}]/kc)(K_{c1} + K_{c2}) \tag{17}$$

Substituting eqs. (15)–(17) into eq. (11) and simplifying gives:

$$n = \frac{\frac{K_{11}}{K_{12}}\left(1 + \frac{K_{31} + K_{32}}{kc}\right) + \frac{K_{31} + K_{32}}{kc} + 1}{1 + \frac{K_{31} + K_{32}}{kc} + \frac{K_{32}}{kc}\left(\frac{K_{22}}{K_{21}} + 1\right) + \left(\frac{K_{22}}{K_{21}} + 1\right)\left(\frac{K_{c1}}{K_{c2}} + 1\right)^{-1}} \tag{18}$$

This may be further simplified to give:

$$n = \frac{(1 + r_1x)\{1/[M_2] + (1/a)(1 + x/r_3)\}}{(1/a)\{(x/r_3) + (r_2/x) + 2\} + (1/[M_2])\{1 + (1 + r_2/x)(1 + r_cx)^{-1}\}} \tag{19}$$

where $x = [M_1]/[M_2]$, $r_1 = k_{11}/k_{12}$, $r_2 = k_{22}/k_{21}$, $r_3 = k_{32}/k_{31}$, $r_c = k_{c1}/k_{c2}$, $a = k_c/k_{32}$.

Equation (19) is a differential copolymer composition equation which is applicable to the proposed scheme of cyclocopolymerization. The equation may be applied by putting $n \simeq [m_1]/[m_2]$, the fractional ratio of monomers combined in the copolymer at low conversions.

A similar equation can be derived relating the relative rate of addition of diene and the rate of cyclization, as follows. From eq. (10):

$$d[M_1]/dt = K_{11}[m_1^{\cdot}] + K_{21}[m_2^{\cdot}] + K_{31}[m_3^{\cdot}] + K_{c1}[m_c^{\cdot}] \tag{20}$$

Substituting eq. (12) in eq. (20) gives:

$$d[M_1]/dt = (K_{11} + K_{12})[m_1^{\cdot}] \tag{21}$$

Then substituting eq. (15) in eq. (21) gives:

$$d[M_1]/dt = [(K_{11} + K_{12})/K_{12}kc](K_{c1} + K_{c2})(K_{31} + K_{32} + kc)[m_c^{\cdot}] \tag{22}$$

Now the rate of cyclization is given by:

$$d[M_c]/dt = kc[m_3^{\cdot}]$$

which may be substituted in eq. (17) to give:

$$d[M_c]/dt = (K_{c1} + K_{c2})[m_c^{\cdot}] \tag{23}$$

From eqs. (22) and (23) we have:

$$d[M_1]/d[M_c] = [(K_{11} + K_{12})/K_{12}k_c](K_{31} + K_{32} + k_c)$$
$$= (r_1x + 1)\{([M_1]/r_3a) + ([M_2]/a) + 1\} \quad (24)$$

Equation (24) applies at low conversions, where $d[m_1]/d[m_c] \simeq [m_1]/[m_c]$, the ratio of the total fraction of diene (unsaturated and cyclic) to the fraction of diene in cyclized units, in the copolymer.

If precise analytical methods are available for determining both the total fraction of diene in the copolymer and the fraction of either cyclic units or pendant vinyl groups, then by making a series of such measurements for different initial monomer feed compositions, values for r_1, r_3, and a could be obtained from eq. (24). Then the remaining two parameters, r_2 and r_c could be obtained from eq. (19).

In certain special cases eq. (10) may be approximated to simpler forms, as in the following examples.

(*a*) If $k_c \gg k_{32}$ so that a is very large and cyclization is the predominant reaction of the radicals $m_3^{\cdot}$, then eq. (19) gives:

$$n = (1 + r_1x)(1 + r_cx)/[r_cx + (r_2/x) + 2] \quad (25)$$

This is equivalent to considering the addition of monoolefin to diene radicals to be a concerted bimolecular step proceeding through a cyclic transition state and producing the cyclic repeating unit.

(*b*) If in addition there is a strong alternating tendency so that (r_1, r_2, r_c) $\rightarrow 0$ then eq. (25) reduces in the limit to $n = {}^1/_2$. This predicts an alternating copolymer composition of 2:1 molar in contrast to 1:1 for the similar limiting case of the classical binary copolymer composition equation.

(*c*) If the diene has a negligible tendency to add to its own radicals and $r_1 \simeq r_c \simeq 0$, and there is also predominant cyclization, then eq. (25) gives:

$$n = 1/[(r_2/x) + 2] \quad (26)$$

A plot of $1/n$ against $1/x$ should be linear with a slope r_2 and an intercept 2.0.

The application of each of these special cases of the theory is shown for experimental systems in the section on results.

It has been suggested[8] that in reactivity ratio calculations involving nonconjugated dienes the diene concentration should be expressed in equivalents of double bond per liter and not moles per liter. This is so only if the double bonds of the diene act as independent units, and then, to be rigorous, the diene concentration should still be expressed in moles/liter but there should be statistical factors of 2 associated with each of the rate expressions involving diene. This factor does affect the magnitude of the reactivity ratios but not the analytical form of the copolymer composition equation. For example, in eq. (25), $r_1 = 2r_1^*$, $r_c = 2r_c^*$, $r_2 = r_2^*/2$, where r_n is derived for $[M_1]$ in moles/liter, and r_n^* is derived with $[M_1]$ in equivalents double bond/liter.

EXPERIMENTAL

Materials

Monomers and solvents were all readily obtainable in high purity directly or after applying conventional purification techniques.

Polymerization

The monomers and azobisisobutyronitrile initiator were weighed directly into 25 ml. volumetric flasks and diluted to volume with the solvent. Total monomer concentrations were in the range 2–6 moles/l. The solution was transferred by hypodermic syringe to 9 mm. glass tubes, and the tubes were flushed with nitrogen and sealed. The tubes were heated in a water bath at 50 ± 0.05°C., for the appropriate time. The polymer was precipitated in a nonsolvent and dried in a vacuum oven at 50°C. for at least 24 hr. prior to analysis.

The acrylonitrile copolymers which were prepared in dimethylformamide solution, were precipitated in water or methanol. The maleic anhydride and *N*-phenylmaleimide copolymers were precipitated in dry heptane or ether. In all cases care was taken to ensure that the isolated polymer was free of solvents and monomers.

In all copolymerization systems except those in DMF solution the copolymer partially precipitated from solution during polymerization, but the copolymer after isolation was soluble in dimethyl formamide.

Analysis

Elemental analyses were by Galbraith Microanalytical Laboratories, Knoxville, Tennessee. The compositions of the acrylonitrile and *N*-phenylmaleimide copolymers were calculated from their nitrogen content. The compositions of the other copolymers were calculated from their carbon and hydrogen contents.

The copolymers containing maleic anhydride were found almost invariably to be associated with water. This water content was up to 5% w/w and was probably present combined in maleic acid units. From C and H contents, the fractions of combined water and hence the true copolymer compositions were calculated.

Some of the maleic anhydride copolymers were completely hydrolyzed by heating in water. The clear solutions were evaporated to dryness and dried to constant weight *in vacuo* at 60°C. These hydrolyzed samples were then analyzed for C and H and the calculated compositions in terms of maleic acid units were in good agreement with those calculated for the anhydride copolymers after correction for water content.

RESULTS AND DISCUSSION

The relative compositions of the copolymers from various systems have been determined at low conversions and over a wide range of initial mon-

omer feed compositions. The initiator used throughout was azobisisobutyronitrile (AIBN) and the polymerizations were run at 50°C.

Table I shows data for the copolymerization of 1,4-pentadiene and maleic anhydride in tetrahydrofuran.

TABLE I
1,4-Pentadiene (M_1)–Maleic Anhydride (M_2) Copolymers[a]

M_2 (monomer) mole frac.	m_2 (polymer) mole frac.	Reaction time, hr.	Conversion, %
0.249	0.67	17.5	11.1
0.335	0.70	17.5	14.4
0.500	0.655	17.5	20.5
0.667	0.67	17.5	23.7
0.833	0.64	23.0	22.0

[a] [AIBN] = 7.3×10^{-3} mole/l.; total initial monomer concentration: 1.6–3.1 mole/l.

Over a wide range of initial monomer feed composition, $[m_2]$ in the copolymer lies in the range 0.64–0.70 with a mean value of 0.67 which is the predicted value for 2:1 molar alternating copolymers, the special case (*b*) of the theory section.

Data for the copolymerization of divinyl ether and maleic anhydride are given in Table II.

TABLE II
Divinyl Ether (M_1)–Maleic Anhydride (M_2) Copolymers[a]

M_2(monomer) mole frac.	m_2(polymer) mole frac.	[AIBN] $\times$ 10^3, mole/l.	Reaction time, hr.	Conversion, %
0.175	0.70	6.0	3.5	4.5[b]
0.484	0.70	5.4	3.5	5.7
0.504	0.69[c]	5.9	5.5	4.0
0.683	0.70	9.8	3.5	3.3
0.904	0.65	6.6	52.5	4.2
0.976	0.65	8.7	52.5	4.1

[a] Total initial monomer concentration: 2.0–2.8 mole/l.
[b] $[\eta]_{inh} = 0.505$.
[c] Calc. from standard base titration.

Again over a wide variation in initial monomer feed composition, the copolymer composition is approximately constant at 2:1 molar. The mean value for $[m_2]$ (mole frac.) in the copolymer is 0.68.

Table III shows results from the copolymerization of divinyl ether and *N*-phenylmaleimide.

For the three experiments the mean value of $[m_2]$ is 0.70 mole fraction, which is within 5% of the predicted value of 0.67 for alternating copolymers.

TABLE III
Divinyl Ether (M_1)–*N*-Phenylmaleimide (M_2) Copolymers[a]

M_2(monomer) mole frac.	m_2(polymer) mole frac.	(AIBN) × 10^3, mole/l.	Reaction time, hr.	Yield, %	$[\eta]_{inh}$
0.166	0.720	2.9	~30	34.3	—
0.500	0.674	3.2	~30	14.2	0.23
0.665	0.717	2.4	~30	10.8	0.27

[a] Total initial monomer concentration 1.6–2.4 mole/l.

The overall range in values of $[m_2]$ for all of the three copolymerization systems considered above is 0.64–0.72 which is ±4.5% of the theoretical value of 0.67, demonstrating the strong tendency in these copolymerizations to form alternating 2:1 copolymers.

Systems of the type under consideration which do not form constant composition copolymers but where cyclization predominates over side reactions (branching or crosslinking) should be described by eq. (25) at low conversions. The copolymerization of divinyl ether and acrylonitrile appears to be an example of this sort of behavior. Figure 1 illustrates the best fit of the data for this system to eq. (25), obtained by using a digital computer method similar to that applied by Tidwell and Mortimer[9] for the classical binary copolymer composition equation.

The method is essentially a least-squares fit of the data to eq. (25) by a nonlinear (Gauss-Newton) procedure, starting from initial estimates of the values of r_1, r_2, and r_c obtained manually by curve fitting.

The solid line in Figure 1 is drawn for $r_1 = 0.024$, $r_2 = 0.938$, and $r_c = 0.017$. These are the values for which $\sum\Delta^2$, the sum of the squares of the

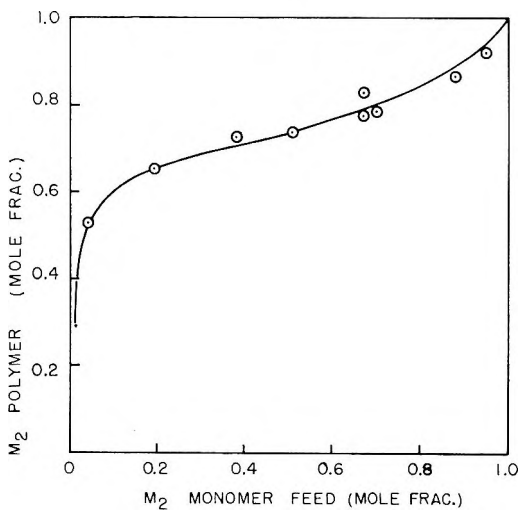

Fig. 1. Divinyl ether (M_1)–acrylonitrile (M_2) copolymers. Points are experimental Line calculated for: $r_1 = 0.024$; $r_2 = 0.938$; $r_c = 0.017$.

differences between observed and computed values of n was a minimum. For the initial estimates $r_1 = 0.04$, $r_2 = 0.90$, and $r_c = 0.01$, $\sum\Delta^2$ was reduced from 0.246462 to 0.0851882 in three iterations of the computing cycle.

Attempts to fit data for the copolymerization of 1,4-pentadiene and acrylonitrile in dimethylformamide solution to eq. (25) by the method described above led to extremely low or negative values for r_1, depending on the initial estimates. Since 1,4-pentadiene does not homopolymerize under these conditions it was thought that this may be a case where cyclization is predominant but $r_1 \simeq 0$, so that eq. (26) should fit the data.

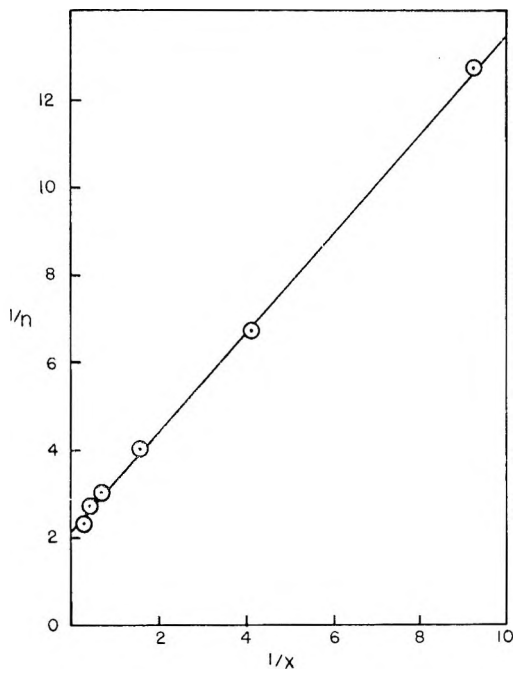

Fig. 2. 1,4-Pentadiene (M_1)–acrylonitrile (M_2) copolymers. $r_2 = 1.129$.

In Figure 2 a plot is shown of $1/n(=[m_2]/[m_1])$ against $1/x(=[M_2]/[M_1])$ for these results. The plot is linear as predicted. The line in Figure 2 is the best fit for the experimental points from a linear regression computation and has a slope $r_2 = 1.13$. The intercept at $1/n = 2.15$ is close to the theoretical 2.00. It is interesting to note that the equivalent limiting case ($r_1 = 0$) of the classical binary equation predicts that $1/n$ should vary linearly with $1/x$ but that the intercept should be 1.00, and it is clear that this case does not fit the present results.

In all of the copolymerization systems considered above the proposed cyclic structure of the copolymers is supported by their solubility in dimethylformamide, the absence of gelation even at high conversion under the conditions of these experiments, and the presence of little or no ab-

sorption in the infrared at 6.1μ for C = C. Further confirmation of the cyclic structure of the copolymers has been obtained by Butler.[5]

The fact that our theoretical expressions in their respective limiting cases, when cyclization is predominant over linear propagation of the radicals $m_3^{\cdot}$, adequately describe the experimental data provides strong support for believing that the postulated mechanism of cyclocopolymerization is essentially correct.

When further values of reactivity ratios for similar systems become available, a comparison of their magnitudes should give valuable information on the influence of the structure of the monomers on the structure of the copolymers. It would be particularly interesting if some data could be fitted to the general equations, eqs. (19) and (24), giving the relative rates of cyclization and linear propagation.

The work was supported by the National Institute of Health under Grant No. CA-06838-01. E. C. C. also acknowledges support by the National Science Foundation Summer Research Participation Program. The authors wish to express their appreciation to Mr. Robert G. Harrell for his aid in the experimental work and to the American Cancer Society for financial support of Mr. Harrell's work under Institutional Grant IN-62-C.

The digital computer program was written and run by Mrs. Eleanore Todarro at the University of Florida Computing Center.

The authors also wish to thank Dr. Frank R. Mayo for valuable discussions during the course of this work.

References

1. G. B. Butler, paper presented at 133rd American Chemical Society Meeting, San Francisco, Calif., April 1958; *Abstracts of Papers*, p. GR.

2. Butler, G. B., and J. J. VanHeiningen, paper presented at 134th American Chemical Society Meeting, Chicago, Ill., September, 1958; *Abstracts of Papers*, p. 32T.

3. Butler, G. B., *J. Polymer Sci.*, **55**, 197 (1961).

4. Chang, E. Y. C., and C. C. Price, *J. Am. Chem. Soc.*, **83**, 4650 (1961).

5. Butler, G. B., in press.

6. Roovers, J., and G. Smets, *Makromol. Chem.*, **60**, 89 (1963).

7. Gibbs, W. E., and R. J. McHenry, *J. Polymer Sci.*, **A2**, 5277 (1964).

8. Wiley, G. R. H., and E. E. Sale, *J. Polymer Sci.*, **42**, 491 (1960).

9. Tidwell, P. W., and G. A. Mortimer, paper presented at 145th American Chemical Society Meeting, New York, September 1963; *Polymer Preprints*, **4**, No. 2, 236.

Résumé

On a développé une équation générale pour la composition des copolymères obtenus dans la cyclocopolymérisation des 1,4-diènes (M_1) et des monooléfines (M_2). L'équation générale relie la composition du copolymère à la composition du mélange réactionnel en employant cinq paramètres du rapport de réactivité. Quand la cyclisation est très rapide par rapport aux autres étapes de propagation de chaîne, l'équation générale devient plus simple: $n = (1 + r_1x)(1 + r_cx)/((r_cx + (r_2/x) + 2)$ où $n = (m_1)/(m_2)$ dans le copolymére, $x = (M_1)(M_2)$ dans le mélange réactionnel et r_1, r_2, et r_c sont les rapports de réactivité pour les étapes de propagation de la chaîne du diène, de la monooléfine et des radicaux cyclisés repectivement. On a appliqué la théorie à la copolymérisation, initiée par des radicaux libres, des systèmes (A) éther divinylique/anhydride maléique (B), 1,4-pentadiène/anhydride maléique (C) éther divinylique/*N*-phenylmalimide (D) éther divinylique/acrylonitrile et (E) 1,4-pentadiéne/acrylonitrile. Les systèmes A, B et C donnent des copolymères alternés de composition $n = 0.5$. Pour le système D, $r_1 = 0.024$, $r_2 = 0.938$, $r_c = 0.017$. Pour le système *E*, $r_1 \simeq r_c \simeq 0$, $r_2 = 1.13$.

Zusammenfassung

Eine allgemeine Copolymerzusammensetzungsgleichung wird für die Cyclocopolymerisation von 1,4-Dienen (M_1) und Monoolefinen (M_2) entwickelt. Die allgemeine Gleichung bildet eine Beziehung zwischen der Copolymerzusammensetzung und der Zusammensetzung des Monomeransatzes mit 5 Reaktivitatsverhältnisparametern. Bei im Verhältnis zu den anderen Kettenwachstumsschritten sehr rascher Cyclisieruug nimmt die allgemeine Gleichung folgende einfache Form an: $n = (1 + r_1x)(1 + r_cx)/[r_cx + (r_2/x) + 2]$, wo $n = m_1/m_2$ im Copolymeren, $x = [M_1][M_2]$ im Monomeransatz und r_1, r_2, und r_c die Reaktivitatsverhältnisse für den Kettenwachstumsschritt des Diens, des Monoolefins bzw. der cyclisierten Radikale sind. Die Theorie wird auf die radikalisch gestartete Copolymerisation von Divinyläther/Maleinsäureanhydrid (A), 1,4-Pentadien/Maleinsäureanhydrid (B), Divinyläther/*N*-Phenylmaleinimid (C), Divinyläther/Acrylnitril (D) und 1,4-Pentadien/Acrylnitril (E) angewendet. Die Systeme A, B, und C bilden alternierende Copolymere mit der Zusammensetzung $n = 0{,}5$. Für das System D ist $r_1 = 0{,}024$, $r_2 = 0{,}938$, $r_c = 0{,}017$. Für das System E ist $r_1 \cong r_c \cong 0$ und $r_2 = 1{,}13$.

Received June 1, 1964

JOURNAL OF POLYMER SCIENCE: PART A VOL. 3, PP. 513–526 (1965)

Stress Relaxation Studies of Chemically Crosslinked Gelatin Films

D. W. JOPLING, *Research Laboratories, Kodak Ltd., Wealdstone, Harrow, Middlesex, England*

Synopsis

Stress relaxation, carried out in 85:15 methyl alcohol–water mixture at 60°C., of gelatin films crosslinked with oxystarch or difluorodinitrobenzene may be represented by the sum of three exponential rates of stress decay. Fresh formaldehyde-crosslinked films relax rapidly and only require two such terms. The second term is shown to be due to the breaking of crosslinks. All excepting 10% of the broken crosslinks do not re-form in unstressed positions as the formaldehyde is easily able to diffuse out of the layer. This 10% is suggested as being due to crosslinks involving a histidine residue. A large percentage of the broken oxystarch crosslinks do re-form because the oxystarch is not easily able to diffuse out of the layer.

INTRODUCTION

Dry gelatin is a brittle, inelastic material with an extension at break of 2–3%. When allowed to equilibrate in an atmosphere of high relative humidity, or when immersed in an alcohol–water mixture to increase its moisture content to about 25%, it becomes more elastic with an extension at break of 25% or more.

When gelatin has been allowed to react with certain bi- and polyfunctional agents the gelatin is no longer soluble in hot water. The process, known as "hardening" in the photographic industry, is similar to the "tanning" of collagen by similar agents.

When films of this type are swollen in a mixture of 85% methyl alcohol and 15% water, the temperature of the mixture may be raised to 60°C. or more without the layer melting. Under these conditions, at temperatures above 40°C., the films may be extended by several hundred per cent, and their behavior is consistent with a model of random flexible chains crosslinked into a three-dimensional network.[1]

The strengths and stabilities of crosslinks formed by various crosslinking agents have now been studied by examining the relaxation of stress in stretched, highly elastic gelatin films. Two of the crosslinking agents used were bifunctional agents, while the third was a polymeric multifunctional agent.

THEORETICAL

Scott and Stein[2] have developed a molecular theory of stress relaxation in polymeric materials based on the kinetic theory of elasticity. The theory applies both to chemical relaxation of crosslinks and to the relaxation of crosslinks of a more transient type, provided that the rate-determining process is slow compared with the rate at which the polymer chains can move to new configurations. Their equation for the stress f at time t approximates to

$$f = N_0kT(\alpha - 1/\alpha^2) \exp\{-\lambda k't\}$$

where N_0 is the initial number of chains per cubic centimeter, k is Boltzmann's constant, T is absolute temperature, α is the extension ratio, λ is a factor of approximately 0.5, and k' is the rate constant for the breaking of crosslinks by a first-order process.

The relative stress decay therefore follows a simple exponential equation

$$f/f_0 = \exp\{-\lambda k't\}$$

where $f_0 = N_0kT(\alpha - 1/\alpha^2)$ is the stress at zero time. For the simultaneous breaking of two or more types of crosslinks having different decay rates, the relative stress decay will be the sum of the individual exponential decay rates

$$f/f_0 = A \exp\{-k_1t\} + B \exp\{-k_2t\} + \ldots$$

where A, B, etc., are the ratios of the two types of crosslinks to the total number. Berry and Watson[3] have shown that such a mechanism with two terms can represent the relaxation of stress in sulfur vulcanizates of natural rubber. They have also applied corrections to the equation for the relative stress decay to allow for the effect of free chain ends.

Relaxation of stress in a stretched crosslinked polymeric material can, however, be due to scission of either the crosslinks or the bonds of the main chain.[4] Berry and Watson[3] consider the case of scission of the bonds in the main chain and derive the expression

$$N/N_0 = p/(p + \exp\{kt\} - 1)$$

where p is the reciprocal of the average number of monomeric units in an effective chain and N is the number of elastically effective chains per cubic centimeter at time t.

EXPERIMENTAL

Materials

The gelatin used was a lime-processed gelatin with an intrinsic viscosity of 0.65 in 1M KCl at pH 7.0, and an isoelectric point of 5.1. It was used without being deionized.

Analytical reagent formaldehyde solution containing not less than 36% HCHO w/v was from British Drug Houses Ltd.

Difluorodinitrobenzene (DFDNB) was supplied by L. Light and Co. Ltd.

Oxystarch[5] was prepared by oxidizing maize starch by the method of Grangaard, Mitchell, and Purves.[6] The product was at least 90% converted.

Preparation of Gelatin Films

The gelatin was swollen for 1 hr. in a suitable amount of water. It was dispersed at 50°C., and the crosslinking agent was added as a solution in water or alcohol. An equivalent quantity of 1*N* sodium hydroxide was then added to react with the liberated acid[7] and the solution was immediately used to prepare the films.

The films were prepared by coating the gelatin solution on level glass plates which had previously been treated with a silicone to prevent adhesion of the dry gelatin to the glass. After chilling at 12°C. to set the gelatin, some were allowed to dry by exposure to the laboratory atmosphere. Others were dried at 50°C. after coating on a level glass plate in an oven. The plate was surrounded by trays containing anhydrous calcium chloride and the air in the oven was circulated by a small fan.

The dry gelatin films, which were approximately 0.3 mm. thick, were cut into strips 2 cm. wide and 10 cm. long.

Determination of Formaldehyde Content of Films

During the drying of films crosslinked with formaldehyde a large part of the formaldehyde was lost to the atmosphere. The formaldehyde contents of these films were therefore determined by chemical analysis.

The gelatin was hydrolyzed by allowing it to stand overnight in 30% sulfuric acid solution. The formaldehyde released was distilled off and determined colorimetrically by the method of Nash.[8]

Apparatus

The apparatus used has already been described (Jopling[9]). The specimen was held between two clamps, the lower of which could be raised or lowered to extend the sample, while the upper clamp was positioned by a servomechanism in conjunction with a differential transformer. The load was read off from the extension of a spring attached to the servomechanism. The specimen was immersed in an 85:15 methyl alcohol–water mixture contained in a double-walled vessel through the outer compartment of which water from a thermostat was circulated.

Measurement of Continuous Relaxation

The gelatin film was held between the two clamps in the methyl alcohol mixture for a predetermined time. Just before the sample was extended, its swollen unstressed length was measured. The servomotor was then switched on and the sample extended by the required amount. The first reading of the extension of the spring was taken after 15 sec. and then at suitable time intervals until the end of the experiment.

Measurement of Intermittent Relaxation

The procedure for measuring intermittent relaxation curves was the same as for continuous relaxation except that the specimen was extended, and readings of the load were taken, at $^1/_4$, $^1/_2$, 1, and 2 min., after which the specimen was released. It was then allowed to recover until the next reading was required when the procedure was repeated. The stress at 1 min. after loading was taken as the "initial stress."

RESULTS

Relaxation of Crosslinked Films at 60°C.

No difference was found between the rates of stress decay of layers dried at 20°C. and at 50°C.

The formaldehyde contents of the dry formaldehyde-crosslinked films are given in Table I together with the amounts of the other agents used. About 20% of the formaldehyde remains behind in the layer after drying.

TABLE I
Concentration of Crosslinking Agent in Crosslinked Films.
Formaldehyde as Determined by Chemical Analysis

Code	Crosslinking agent	Amount HCHO added, mmole/g. gelatin	Amount HCHO determined, mmole/g. gelatin
H	Formaldehyde	0.25	0.058
2H		0.5	0.13
4H		1.0	0.225
6H		1.5	0.34
10H		2.5	0.35
	DFDNB	0.05	
	Oxystarch	$2x$[a]	

[a] Where x is the amount required to prevent the gelatin film from melting in boiling water. Experience has shown that the latter amount corresponds to 0.02–0.025 mmole/g.

The continuous relaxation curves for the films crosslinked with the different agents are shown in Figures 1, 2, and 3. The films were extended and the readings commenced after the films had been in the alcohol–water mixture at 60°C. for 30 min. The stress decay of the freshly prepared formaldehyde-crosslinked film (H) was very rapid, and after the first 30 min. of relaxation followed a less rapid, but still rapid, exponential decay down to less than 2% of the initial stress.

The DFDNB- and oxystarch-crosslinked films (Figs. 2 and 3) relaxed more slowly.

The curves were analyzed as follows. The ratio f/f_0 can be expressed in the form

$$G_0 = f/f_0 = A \exp\{-k_1 t\} + B \exp\{-k_2 t\} + C \exp\{-k_3 t\}$$

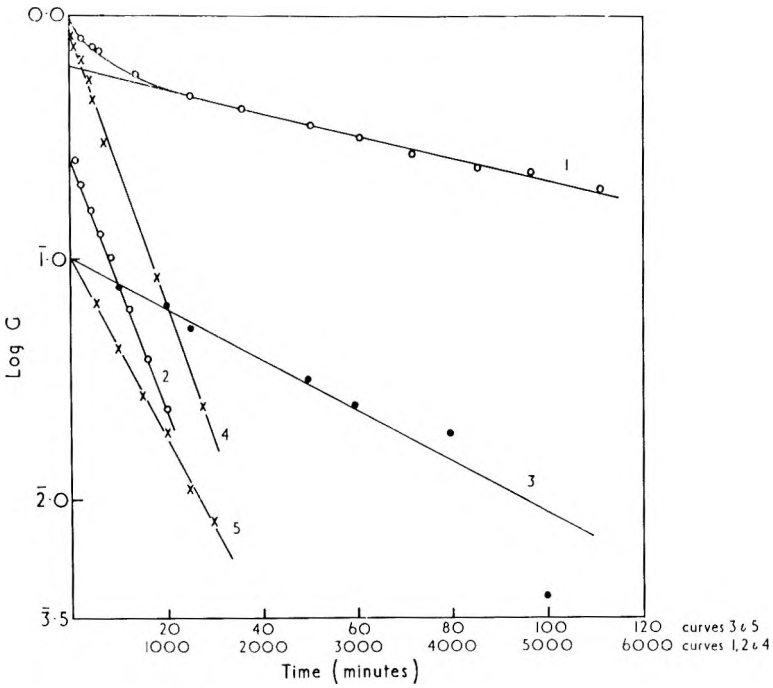

Fig. 1. Graphical analysis of stress relaxation curves for films crosslinked with formaldehyde: (*1*) fresh film, experimental; (*2, 3*) fresh films, derived as per text; (*4*) conditioned film, experimental; (*5*) conditioned film, derived ($G_1 = 0$).

For large values of t, if $k_1 \gg k_2 \gg k_3$, the first two terms will be negligible and we can define

$$G_1 = C \exp \{-k_3 t\}$$

Hence C and k_3 can be calculated from the intercept and slope of the straight-line portion of the plot of log G_0 against t.

The value of G_1 can then be calculated for all values of t and subtracted from the experimental values giving G_2, where

$$G_2 = G_0 - G_1 = f/f_0 - C \exp \{-k_2 t\}$$

The straight-line portion of the plot of log G_2 against t allows B and k_2 to be calculated. A new quantity G_3, where

$$G_3 = G_2 - B \exp \{-k_2 t\}$$

is then derived and a new plot gives A and k_1.

It was thus shown that the curve shapes are consistent with the relaxation being the sum of three exponential processes with relaxation coefficients k_1, k_2, and k_3 and values of A, etc., as given in Table II.

When a freshly prepared formaldehyde-crosslinked film (H) was conditioned in the presence of moisture a third exponential relaxation process (k_3) became apparent. The relaxation curves for film (H) conditioned in

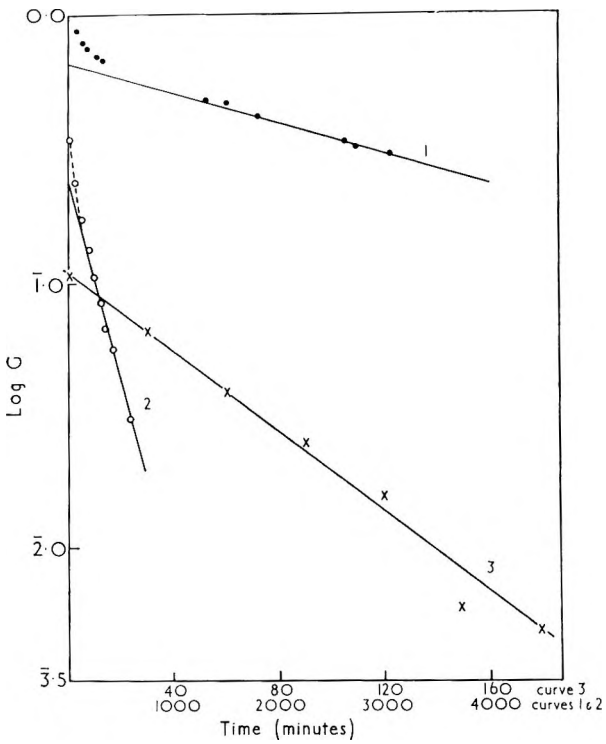

Fig. 2. Graphical analysis of stress relaxation curves for films crosslinked with DFDNB. (*1*) experimental; (*2*, *3*) derived as per text.

TABLE II

Relaxation Coefficients for the Relaxation of Stress in Crosslinked Gelatin Films in 85:15 Methyl Alcohol–Water Mixture at 60°C. Films Extended after 30 min. at 60°C.

Crosslinking agent	k_1, hr.$^{-1}$	A	k_2, hr.$^{-1}$	B	k_3, hr.$^{-1}$	C
Formaldehyde, fresh film H	5.4	0.11	0.16	0.89		
Film H after 90 days in 85% MeOH at 20°C.	1.7	0.11	0.14	0.26	0.013	0.63
DFDNB (0.05 mmole/g.)	1.0	0.11	0.21	0.24	0.014	0.65
Oxystarch	1.9	0.23	0.25	0.28	0.007	0.48

85:15 methyl alcohol–water mixture at 20°C. for 90 days, are included in Figure 1 and the coefficients in Table II. The values of k_3 are very similar to those for films crosslinked with the other agents. k_2 does not change significantly, but the contribution that it makes to the total relaxation is reduced.

Similar conditioning of the films crosslinked with the other agents did not produce any change in the rate of stress decay.

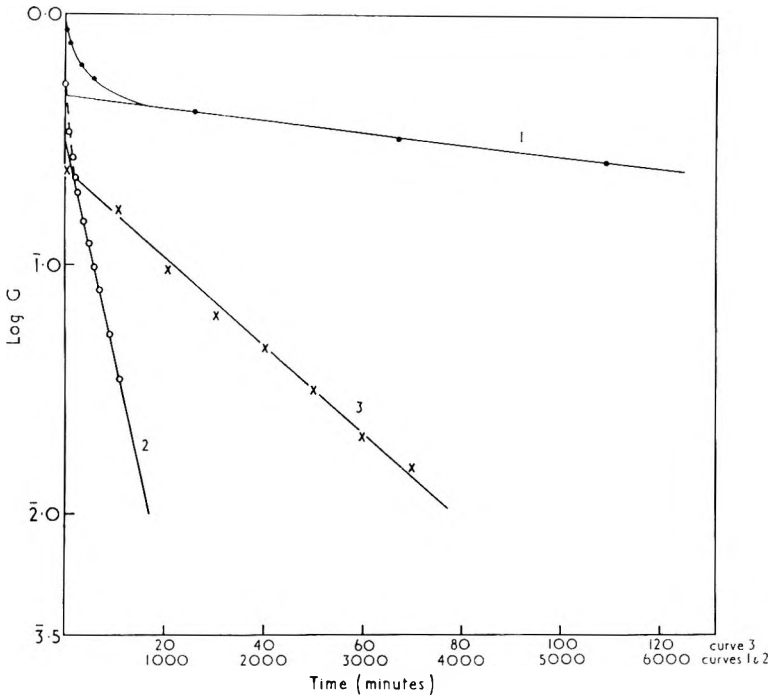

Fig. 3. Graphical analysis of stress relaxation curves for films crosslinked with oxystarch: (*1*) experimental; (*2*, *3*) derived as per text.

Relaxation measurements were made on some of the films H after they had been held in the methyl alcohol–water mixture at 60°C. for different times before extension (Fig. 4). After the first 30 min. after extension all the relaxations are simple exponentials and the values of the coefficients are given in Table III. There is some fall in k_2 with increasing time in the methyl alcohol–water mixture but this is small compared with the large differences between k_1, k_2, and k_3 seen in Table II.

Also included in Table III are some results for the relaxation of film 10H. The values of k_2 for this film are about half those for film H, which contains about one tenth of the amount of reacted formaldehyde. In film 10H, the degree of crosslinking is very high and, therefore, the swelling liquid will have difficulty in penetrating the network. When the swelling is increased by carrying out the relaxation in a medium molar with respect to urea, the relaxation coefficient is increased to a level more comparable with that for film H.

To summarize, the results show that, in general, the relaxation of stress in chemically crosslinked gelatin films may be represented by the sum of three exponential rates of stress decay over the time scale 0–6000 min. With fresh formaldehyde-crosslinked films only two terms, k_1 and k_2, are required to represent the stress decay down to 2% of the initial stress. k_2 is here responsible for 90% of the stress decay. Conditioning the fresh formalde-

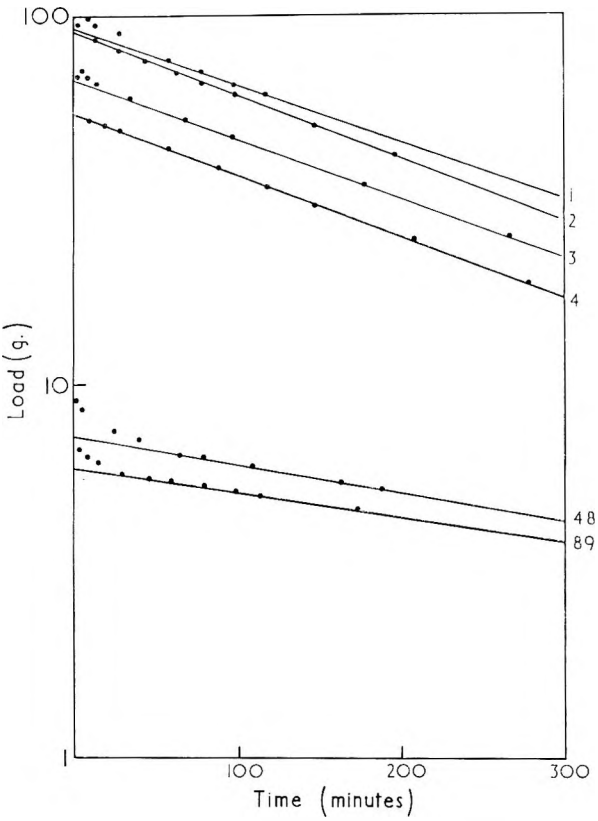

Fig. 4. Relaxation curves for films crosslinked with formaldehyde. Numbers refer to time in hours in 85:15 methyl alcohol–water mixture at 60°C. before extension.

TABLE III
Relaxation Coefficients for the Relaxation of Stress in Formaldehyde-Crosslinked Films after Different Times in 85:15 Methyl Alcohol–Water Mixture at 60°C.

Film	Time in MeOH at 60°C. before extension, hr.	Relaxation coefficient k_2, hr.$^{-1}$
H	$^1/_2$	0.16, 0.25
	1	0.22
	2	0.24
	3	0.22
	4	0.24
	5	0.25
	16	0.19
	48	0.10
	89	0.10
10H	16	0.08
	24	0.07
10H (in 1*M* urea)	16	0.11
10H (in 1*M* urea)	24	0.14

hyde-crosslinked films in the presence of moisture brings them more into line with those incorporating the other two crosslinking agents, the contribution of k_2 to the stress decay decreasing, while the third term k_3 now accounts for over 60% of the stress decay.

Intermittent Relaxation

Figure 5 shows the effect on the initial load to give 50% extension (proportional to the elastic modulus) of holding the stressed formaldehyde-crosslinked films in the methyl alcohol–water mixture at 60°C. for increasing times before extending. It is seen that the modulus falls rapidly to a fairly constant value. This minimum is reached after about 10 hr. for the formaldehyde film H and after about 30 hr. for the film 10H.

The intermittent relaxation curves for the films crosslinked with DFDNB and with oxystarch are given in Figure 6. The relative stress is plotted against the time. The composite curve for films crosslinked by formaldehyde to different degrees, and the curve for a conditioned film H are also included. The continuous relaxation curves are included for comparison.

It is seen that conditioning the formaldehyde cross-linked film greatly reduces the rate of decay of the modulus, in the same way that it reduced the rate of continuous relaxation.

Continuous relaxation is measuring the rate of breaking of bonds, a bond that re-forms in an unstressed configuration not contributing to the modulus. On the other hand, intermittent relaxation is measuring the number of

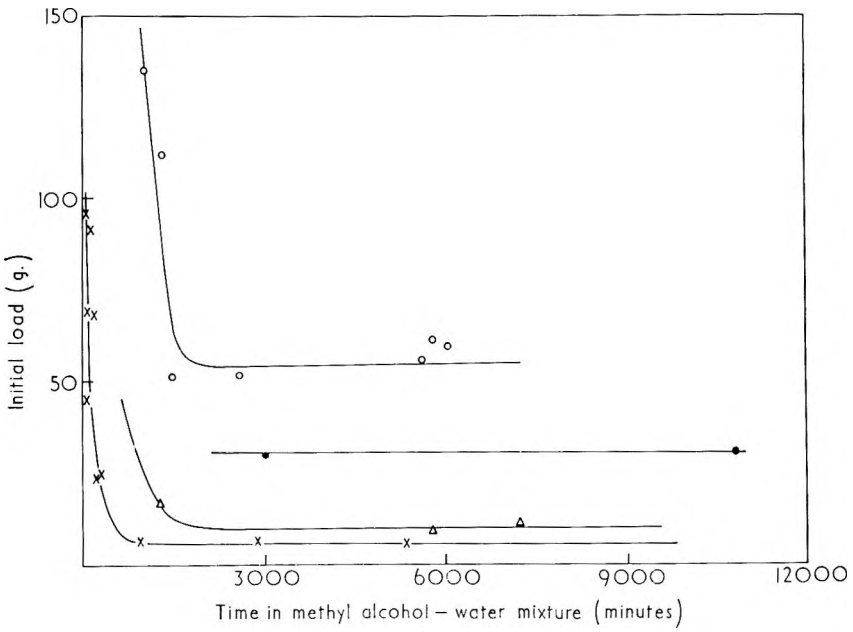

Fig. 5. Variation of initial load with time of immersion in 85:15 methyl alcohol–water mixture at 60°C. Films crosslinked with formaldehyde.

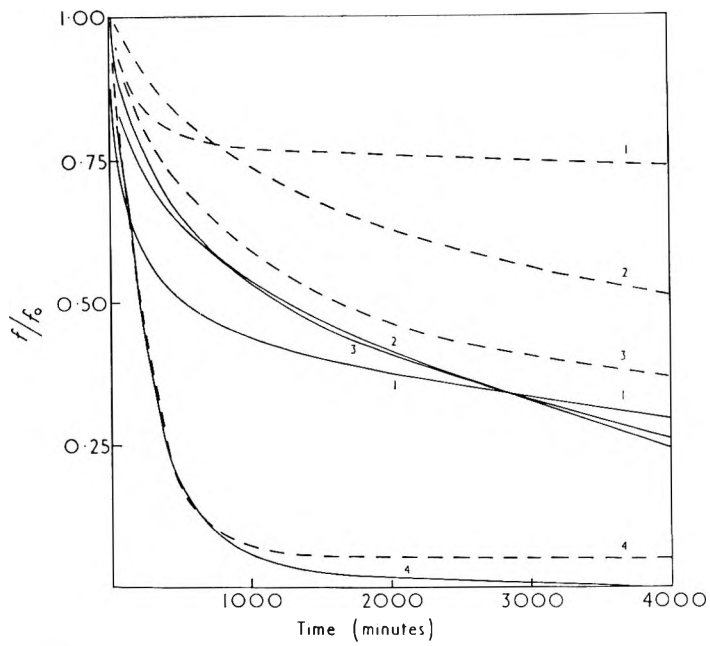

Fig. 6. Stress relaxation curves for crosslinked gelatin films: (- -) intermittent relaxation; (——) continuous relaxation; (*1*) oxystarch; (*2*) DFDNB; (*3*) conditioned formaldehyde; (*4*) fresh formaldehyde.

crosslinks at any particular instant, including crosslinks that may have broken but have re-formed.

In Figure 6 it is seen that the intermittent relaxation curves are in all cases above the continuous relaxation curves. The curves for the fresh formaldehyde crosslinked films are fairly close, indicating that nearly all the bonds that break do not re-form. The intermittent curve does level off, however, at a relative modulus of about 0.08 while the continuous curve decays to zero, showing that a "hard core" of the crosslinks do re-form when broken

The intermittent and the continuous relaxation curves for DFDNB and for oxystarch are widely separated. In the latter case the intermittent curve, after an initial rapid fall, is almost horizontal. It therefore appears that a large number of the broken DFDNB crosslinks and most of the oxystarch crosslinks (after the initial fall in modulus) are re-formed in unstressed configurations.

Activation Energy for the Breaking of Formaldehyde Crosslinks

Freshly prepared formaldehyde-crosslinked films H were also stretched at 40 and 50°C. as well as at 60°C. and the relaxation of stress was measured. The values of k_1 and k_2 are plotted against the reciprocal absolute temperature in Figure 7.

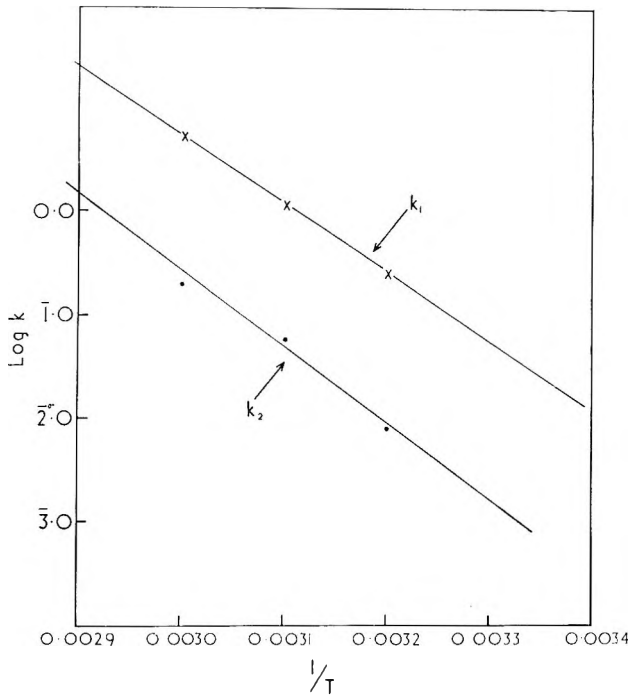

Fig. 7. Arrhenius plot of k_1 and k_2 for fresh formaldehyde-crosslinked films.

Although there are only three points these do allow an estimate to be made of the activation energy for the relaxation processes. The values obtained are 30 kcal. derived from k_1 and 34.4 kcal. from k_2.

The temperature range that could be used was restricted because at temperatures below 40°C. gelatin commences to gel and the plot of log stress against time becomes increasingly non-linear. Above 60°C. degradation of the gelatin is likely to affect the results and would not be possible with the methyl alcohol system.

DISCUSSION

From the evidence available it is not possible to make any inferences as to the mechanisms giving rise to the relaxation terms excepting in one case to be discussed later.

As already discussed, an exponential stress decay will be given by the first-order breaking of crosslinks between chains, whether these crosslinks are chemical crosslinks or points of hydrogen bonding. Stress relaxation arising from cleavage of the main chain gives a more complicated relationship between relative stress and time.

The simple relationship obtained in our experiments would therefore appear to indicate that the three terms are due to the breaking of three different types of crosslink. On the other hand, however, the coefficients ob-

tained when using crosslinking agents of different types are very similar, which would indicate that the nature of the crosslink was unimportant.

Formaldehyde-Crosslinked Films

Fresh formaldehyde-crosslinked films are unique among the layers examined in that they relax very rapidly. At the same time the modulus of the film also decreases rapidly as shown by the intermittent relaxation. Stress decay is therefore due to the breaking of bonds that in general do not re-form.

Our results show that this rapid relaxation is due to the very much greater contribution of k_2 to the relaxation than in the other cases. Apparently a greater number of suitable bonds are available for cleavage. On the assumption, therefore, that the presence of formaldehyde-crosslinks does not increase the chance of main-chain cleavage, it is apparent that this mechanism must be due to the breaking of the crosslinks.

Davis and Tabor[7] have shown that the first stage in the formation of a formaldehyde crosslink is the reversible reaction of a formaldehyde molecule with a side-chain amino group to form a methylol compound. This compound then reacts with the methylol compound of another group, not an amino group, to give a crosslink. Both these reactions are believed to be reversible. They point out that both methylene bridges ($-CH_2-$) and methylene ether crosslinks ($-CH_2-O-CH_2-$) have been proposed for the crosslinking of proteins by formaldehyde and suggest that methylene ether crosslinks, which are supported by the kinetics of the reaction, could later reorganize to form more stable methylene crosslinkages.

The second relaxation process with fresh formaldehyde-crosslinked films ($k_2 = 0.1$–0.25 hr.$^{-1}$) could be associated with the hydrolysis of methylene ether crosslinks. As these linkages rearrange to give methylene crosslinks the contribution of k_2 to the relaxation will decrease since fewer crosslinks will be available to relax. A third exponential term with $k_3 = 0.013$ then becomes apparent, this term becoming increasingly important until, on long conditioning, it accounts for 60% of the relaxation. It could be associated with either the breaking of the methylene crosslink or the scission of bonds in the polypeptide backbone of the gelatin.

Cater[10] has shown that the crosslinkages introduced into collagen by formaldehyde are very much less resistant to hydrolysis than those formed by glutaraldehyde or acrolein. He attributes the differences in stability to differences in the molecular lengths of the bonds formed. He, however, assumes that the formaldehyde crosslinks are simple methylene bridges. In freshly crosslinked layers this is probably not the case.

In Figure 4 the initial rapid fall in the modulus of the films is thus due to the hydrolysis of crosslinkages. This also accounts for k_2 in the continuous relaxation. The crosslinks that remain to give the fairly constant modulus after long times of immersion (Fig. 6) are not associated with the more stable crosslinkages just discussed, because the relaxation of a film in this region (after 89 hr. in 85% methyl alcohol at 60°C.) occurred with a coefficient of

0.1 which is about ten times greater than that for the slow process (k_3). The explanation is related to the case of re-formation of broken crosslinks. When a methylene ether crosslink is broken, because of the reversible nature of the reaction, free formaldehyde will be formed which will then diffuse out of the layer and be lost. If a percentage of the formaldehyde–amino group complexes are more stable, then the formaldehyde from such a broken crosslink will be less likely to diffuse out of the layer and will be able to re-form a crosslink in an unstressed configuration. Thus it will allow relaxation to occur but will still contribute to the static modulus. From Figure 6 it would appear that these more stable compounds should amount to about 10% of the total. They could possibly be associated with crosslinks formed with the imidazole groups of the histidine residues which are approximately one tenth as numerous as amino group side chains. There is evidence that crosslinks, from which the formaldehyde cannot be recovered, are formed by formaldehyde between histidine and amino groups.[11]

Films Crosslinked with DFDNB and Oxystarch

With both of these crosslinking agents the rate of relaxation was low and unaffected by conditioning the films. These agents apparently gave crosslinks that were much less easily broken than those freshly produced by formaldehyde.

Figure 6 shows that the fall in the modulus of an oxystarch-crosslinked film on keeping in 85:15 methyl alcohol–water mixture at 60°C. is fairly rapid at first but becomes very slow after about 400 min. The intermittent relaxation measures the number of crosslinks that are present at any time including those that re-form. Oxystarch is a polymeric material with a large number of functional groups per molecule. Both of these facts will prevent the crosslinking agent from diffusing out of the gelatin layer into the surrounding medium in the way that, say, formaldehyde can. When some of the crosslinks are broken, those remaining will hold the oxystarch molecules to the gelatin network and, even if all the crosslinks were to break on one oxystarch molecule, the size of the molecule would greatly reduce the rate of diffusion through the layer. The oxystarch crosslinks will, therefore, readily re-form in unstressed positions and hence the intermittent relaxation will be much slower. The initial rapid fall of the modulus is probably due to the loss of some of the lower weight fraction of the oxystarch.

References

1. Jopling, D. W., *Bull. Brit. Soc. Rheol.*, No. **46**, 2 (1946).
2. Scott, K. W., and R. S. Stein, *J. Chem. Phys.*, **21**, 1281 (1953).
3. Berry, J. P., and W. F. Watson, *J. Polymer Sci.*, **18**, 201 (1955).
4. Tobolsky, A. V., *J. Appl. Phys.*, **27**, 673 (1956).
5. Jeffreys, R., and B. E. Tabor, Brit. Pat. 928,591 (1962).
6. Grangaard, D. E., J. H. Mitchell, and C. B. Purves, *J. Am. Chem. Soc.*, **61**, 1290 (1939).
7. Davis, P., and B. E. Tabor, *J. Polymer Sci.*, **A1**, 799 (1963).
8. Nash, T., *Biochem. J.*, **55**, 416 (1953).

9. Jopling, D. W., *Rheol. Acta*, **1**, 133 (1958).
10. Cater, C. W., *J. Soc. Leather Trades' Chemists*, **47**, 259 (1963).
11. Fraenkel-Conrat, H., and H. S. Olcott, *J. Biol. Chem.*, **174**, 827 (1948).

Résumé

On a mesuré la relaxation de la tension dans un mélange 85/15 d'alcool méthylique et d'eau à 60°C, de film de gélatine ponté par l'amidon oxydé de la difluorodinitrobenzène. La relation résulte de la superposition de trois modes de relaxation variant exponentiellement. Des films fraîchement pontés par le formaldéhyde se relaxent rapidement et demandent seulement deux modes de relaxation. Le second mode est du à la rupture des ponts. 10% seulement de ces ponts se reforment en position non-tendue étant donné que la formadéhyde diffuse rapidement en dehors du film. Ces 10% seraient dûs aux ponts qui contiennent un résidu histidine. Un pourcentage important de ponts rompus se reforme par suite de l'inaptitude de l'amidon oxydé à diffuser hors du film.

Zusammenfassung

Die Spannungsrelaxation von mit Oxystärke oder Difluordinitrobenzol vernetzten Gelatinefilmen in einer 85:15-Methylalkohol-Wassermischung bei 60°C kann durch die Summe dreier exponentieller Spannungsabfallgeschwindigkeiten dargestellt werden. Frische, mit Formaldehyd vernetzte Filme relaxieren rasch und erfordern nur zwei solcher Terme. Der zweite Term lässt sich auf den Bruch von Vernetzungsstellen zurückführen. Alle mit Ausnahme von 10% der gebrochenen Vernetzungsstellen bilden sich nicht in unbeanspruchten Stellungen zurück, da der Fromaldehyd leicht in der Lage ist, aus der Schicht heraus zu diffundieren. Diese 10% werden auf Vernetzungsstellen unter Beteiligung eines Histidinrestes zurückgeführt. Ein grosser Prozentsatz der gebrochenen Vernetzungsstellen in Oxystärke bildet sich zurück, da die Oxystärke nicht leicht aus der Schicht herausdiffundieren kann.

Received June 8, 1964

JOURNAL OF POLYMER SCIENCE: PART A VOL. 3, PP. 527–549 (1965)

Turbidimetric Titration Method for Determining Solubility Distributions of Polymers

W. H. BEATTIE,* *Synthetic Rubber Division, Shell Chemical Company, A Division of Shell Oil Company, Torrance, California*

Synopsis

A turbidimetric titration method for determining solubility distributions (which are closely related to molecular weight distributions) has been developed. In this method, polymer is precipitated from its solution by addition of a nonsolvent of the same refractive index as that of the solvent. The precipitating particles of swollen polymer are allowed to agglomerate until the turbidity reaches a maximum. It is shown by the use of light-scattering theory that under these conditions the concentration of polymer which is precipitated can be calculated from the maximum turbidity on an absolute basis. The effects of particle size and particle size distribution are discussed. The method was tested by using polystyrene, and is shown to be accurate. In principle the method is applicable to most kinds of polymers.

INTRODUCTION

There is a demand for quick and accurate methods for determining molecular weight distributions of polymers. The search for good methods has produced a variety of methods which have been outlined by Hall.[1] Of these methods, turbidimetric titration is one of the quickest to carry out, and this is probably the major reason for the considerable interest shown in this method.

Like many other methods for determining molecular weight distributions, turbidimetric titration depends upon solubility differences. In the general procedure the turbidity of a dilute polymer solution is measured as it is titrated with a precipitant. The initial turbidity is caused by the precipitation of the high molecular weight species. With increasing volume fraction of precipitant, lower molecular weight species are precipitated and turbidity is increased. The turbidity (with some corrections) is assumed to be proportional to the concentration of precipitated polymer and in this way the weight distribution of solubilities of the polymer molecules is obtained.

The main disadvantages of the turbidimetric method as used in the past have been summarized by Hall[1] as follows.

"(*a*) There will be a change in the refractive index of the solvent

* Present address: Department of Chemistry, California State College at Long Beach. Long Beach, California.

precipitant medium unless the two components have fairly close refractive indices. . . ."

"(*b*) The polymer must have a different refractive index from that of the solvent precipitant medium."

"(*c*) The scattering power of the precipitate may be a function of molecular weight due to a dependence of particle swelling on molecular weight."

"(*d*) Aging, agglomeration or coagulation of precipitate will alter the turbidity without the quantity of precipitate varying."

Point (*a*) has commonly been allowed for with a simple correction. Point (*b*) is a physical limitation to all turbidimetric methods but causes no difficulty. The real difficulty has been that of allowing for points (*c*) and (*d*). For instance, Hall states: "the writer and his colleagues have found turbidity to be closely dependent on the precise experimental technique employed."

In the present method these difficulties have been almost completely eliminated. Point (*a*) is taken care of by choosing a solvent and precipitant of approximately the same refractive index. Point (*c*) will be proven to be of minor significance when this condition is imposed. Point (*d*) is taken care of by making measurements under conditions in which particle size effects do not interfere. It will be shown that these improvements are a result of the application of light-scattering principles and theory to this problem, which places the determination of concentrations from turbidity measurements upon an absolute basis. This approach is based in part upon the work of Meehan and Beattie.[2]

In this paper we will discuss only the determinations of solubility distributions. It is of interest to point out that the method is capable of giving molecular weight distributions provided that a relationship between solubility and molecular weight is known.

THEORY OF TURBIDIMETRY FOR SPHERICAL PARTICLES

During a turbidimetric titration, precipitant is added to a polymer solution until a phase separation occurs, as evidenced by the onset of turbidity. From this point onward the system consists of small particles of polymer rich phase suspended in a medium of polymer poor phase. Since the particles are fluid they will tend to assume the shape having lowest surface energy, the spherical shape. Evidence apparently to the contrary[3] has been discussed in Appendix I and is inconclusive. We therefore make the assumption that the particles are spherical.

Turbidity, τ, is defined as the extinction of light due to scattering. When light passes through a turbid medium of path length l, the intensity I is given by an expression analogous to Lambert's law, i.e.,

$$-dI/dl = \tau I \tag{1}$$

Integration of eq. (1) gives

$$\tau = (1/l) \ln (I_0/I) \tag{2}$$

where I_0 is the incident intensity and I is the intensity after traversing a path of length l. Turbidity is related to apparent absorbance A due to scattering by $\tau = 2.303\ A/l$, where $A = \log (I_0/I)$. In the measurement of I with conventional spectrophotometers the angle of view should be limited to exclude forward scattered light by placing small apertures in the beam.[4]

The relationship between turbidity and particle size is given by the Mie equations.[5] The turbidity of a monodisperse suspension of spherical particles of radius r at infinite dilution is given by

$$\tau = n\pi r^2 K \tag{3}$$

where n = number of particles per milliliter, K = scattering coefficient, a function of m and α (where $m = \mu'/\mu_0$ and $\alpha = 2\pi r\mu_0/\lambda$), μ' = refractive index of particle (polymer-rich phase), μ_0 = refractive index of surrounding medium (polymer-poor phase), and λ = wavelength of light *in vacuo*. In the dilute solutions used for turbidimetric titrations the refractive index of the solvents and the refractive index of the polymer-poor phase are so nearly identical that μ_0 has been used for both.

The scattering coefficient K is the ratio of the scattering cross section of the particle to its geometric cross section. It can be calculated for any size (α) and refractive index ratio (m). If r/λ were less than 1/20, the scattering would follow Rayleigh's law,[6] in which case K would be a simple function of m and α. However, the present method applies only to rather large particles, and K must be calculated from the complicated Mie equations. Since this is a very laborious process, it is fortunate that computations have been tabulated in the range of m and α of interest.[7] The concentrations used in turbidimetric titrations (e.g., $<0.05\%$) are sufficiently dilute to ignore secondary scattering, and we can use eq. (3) without extrapolation to infinite dilution.[8,9]

In general, particles of precipitated polymer-rich phase will be polydisperse, in which case the turbidity and concentration c_p, expressed in grams of precipitated phase per milliliter of solution, are given by:

$$\tau = \sum n_i \pi r_i^2 K_i \tag{4}$$

$$c_p = \sum n_i (4/3)\pi r_i^3 D' \tag{5}$$

where D' represensts the density of the particles of polymer-rich phase. On combining eqs. (4) and (5), the specific turbidity is given by:

$$\tau/c_p = (3/4D')(\sum n_i r_i^2 K_i / \sum n_i r_i^3) \tag{6}$$

This is simplified by using w_i = weight fraction of species i:

$$\tau/c_p = (3/4D') \sum (K_i/r_i) w_i / \sum w_i \tag{7}$$

For our purposes, it is advantageous to substitute the normalized size parameter[5] $\rho = 2\alpha(m - 1)$ for r, which leads to:

$$\tau/c_p = [3\pi\mu_0(m - 1)/D'\lambda](\overline{K/\rho})_w \tag{8}$$

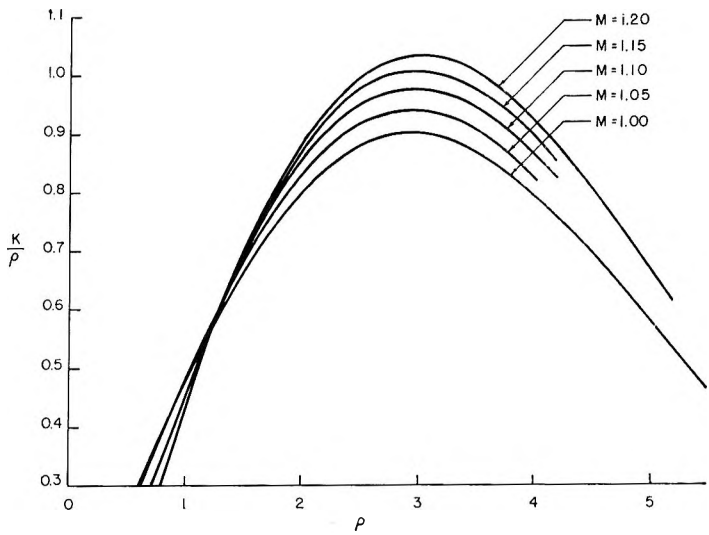

Fig. 1. K/ρ functions for various m.

where $\overline{(K/\rho)}_w = \sum(K/\rho)_i w_i = \int_0^\infty (K/\rho)\, dw$, i.e., the weight average of K/ρ. The value of K/ρ depends only on m and ρ. With increasing ρ, K/ρ increases from zero (at $\rho = 0$) to a maximum (at $\rho \approx 3$), then oscillates about a slowly decreasing value. The first and largest maximum in the K/ρ function is shown on Figure 1 for several values of m between 1.0 and 1.2. The advantage of using K/ρ versus ρ curves instead of K/α versus α curves is that the former have only a small dependence upon m in the region of this maximum.

Equation (8) is a fundamental relationship between τ and c_p,[2] which when $\overline{(K/\rho)}_w$ can be evaluated places turbidimetry for analytical purposes on an absolute basis. It will be shown later that $\overline{(K/\rho)}_w$ in eq. (8) can be evaluated when the particle size distribution is known.

THEORY OF TURBIDIMETRIC TITRATION

The Basic Equation

For the purpose of a turbidimetric titration it is necessary to know the concentration of polymer which is precipitated. This means that eq. (8) is not suitable in its present form because the concentration of precipitated phase (rather than of precipitated polymer) is obtained. In addition τ depends upon m and m depends upon the fraction of polymer in the concentrated phase, which is not generally known. If the refractive index of the solvent and precipitant are almost identical, m can be calculated by using a refractive index mixture rule. The Gladstone and Dale empirical mixture rule has proven accurate with a wide range of compounds[10] and

is assumed to be valid for the polymer-rich phase. It may be stated as follows:

$$\mu' - 1 = (\mu - 1)\phi + (\mu_0 - 1)(1 - \phi) \tag{9}$$

where ϕ = volume fraction of polymer in polymer-rich phase, μ' refractive index of polymer-rich phase, μ_0 = refractive index of solvent and precipitant, μ = refractive index of polymer.
Equation (9) may be rearranged in the form:

$$(m - 1)\mu_0 = \Delta\mu\phi \tag{10}$$

where $\Delta\mu = \mu - \mu_0$. Substitution into eq. (8) gives

$$\tau/c_p = 3\pi\Delta\mu\phi\overline{(K/\rho)}_w/\lambda K' \tag{11}$$

This is further simplified by substituting the equality $c/D = \phi c_p/D'$ where c is the weight (grams) of precipitated polymer per unit volume (milliliters) of original solution and D is the density of pure polymer, giving:

$$c = D\lambda\tau/[3\pi\overline{(K/\rho)}_w\Delta\mu] \tag{12}$$

This is the fundamental equation for the method. All factors on the right-hand side of the equation, except $\overline{(K/\rho)}_w$ are directly measurable. If $\overline{(K/\rho)}_w$ can be known, the concentration of precipitated polymer can be related to the turbidity on an absolute basis.

The relative refractive index of the precipitated particles of polymer-rich phase, m, which appeared in eq. (8), does not appear in eq. (12), and the scattering function K/ρ is almost independent of m for $\rho < 5$ (see Fig. 1). Therefore turbidity is almost independent of m, and the difficult measurement of m can usually be avoided.

It is interesting to note that according to the Gladstone and Dale rule, m is determined by the composition of the particles, e.g., the degree of swelling of the polymer-rich phase. It follows that turbidity is almost independent of the degree of swelling of the particles, even though their size is changed with swelling. Evidently Hall's disadvantage (*c*) is of only minor significance when the solvent and precipitant have nearly identical refractive indices.

Evaluation of $\overline{(K/\rho)}_w$ for Monodisperse Particles

It remains to be shown how the weight-average scattering function, $(K/\rho)_w$, can be evaluated. Let us first consider monodisperse particles (for the purpose of illustrating the method). In this case $\overline{(K/\rho)}_w = K/\rho$. Let us also assume that the approximate value of m is known. Obviously, if ρ were known, K/ρ could be found from Figure 1. Although ρ cannot be measured directly, it will be shown that it is possible to determine it indirectly from certain measurements of turbidity. It should be noted that τ and $\overline{(K/\rho)}_w$ must change in the same way with change in particle size (or change in ρ). All other factors in eq. (12) are independent of particle size. Therefore if particle size can be increased (keeping con-

centration and other parameters constant) τ must increase to a maximum then decrease, in a manner similar to any one curve on Figure 1.

It is experimentally possible to adjust the particle size to the point where turbidity is maximum. A volume of precipitant is added to a polymer solution causing particles of a new phase to form. The particles will generally coalesce and grow, particularly if the solution is stirred. The turbidity is measured until it reaches a maximum value and begins to decrease. It should be understood that the decrease in turbidity is a particle size effect, and is not caused by sedimentation. An example of this measurement is shown on Figure 6. At the maximum turbidity, the scattering function must also be at its maximum value, and the particle size must be such that $\rho = [2\pi r\mu_0(m - 1)/\lambda] = 3$. The maximum value of turbidity which was determined experimentally and the maximum value of K/ρ (taken from Figure 1 or otherwise calculated) are corresponding values which are substituted into eq. (12). The value of ρ does not actually need to be known, but particle size is so adjusted that $\rho \simeq 3$, where K/ρ is known.

Evaluation of $\overline{(K/\rho)}_w$ for Narrow Particle Size Distributions

The requirement that particles be monodisperse is an unrealistic restriction for a system of coalescing particles, where particle volumes must necessarily differ by at least a factor of 2 (and particle diameters must differ by at least a factor of $2^{1/3}$). Let us examine the limits of the particle size distribution for this method. The maxima of the curves on Figure 1 are rather broad, which means that K/ρ varies only slowly with ρ. Hence over a narrow range of ρ (say, from 2.4 to 3.5) K/ρ is almost constant. The turbidity is approximately independent of particle size in the region of the maximum. This means that for a narrow distribution of particle sizes with ρ values corresponding to this range, the average $\overline{(K/\rho)}_w$ will have a value very close to the maximum value of K/ρ. This will be true for particle size distributions of any shape. Evaluation of the average in this way can be done only in the region of the maximum. Therefore this method requiring adjustment of particle size until $\rho \simeq 3$ serves to evaluate not only K/ρ for monodisperse particles, but also $\overline{(K/\rho)}_w$ for narrow distributions of particles. The method does not differ from that outlined for monodisperse particles, and the particle sizes may vary by a factor as high as 1.5. The calculation of $\overline{(K/\rho)}_w$ for broad distributions is somewhat more difficult, and is described below.

Wavelength Dependence

The turbidimetric method may be used at any wavelength where the particles do not absorb (due to color). Since it is the ratio of particle size to wavelength which determines ρ, the condition of maximum turbidity can be attained with small particles at short wavelengths or large particles at long wavelengths. The wavelength should preferably be chosen to fit

the growth rate of the particles, so that a convenient length of time is required to obtain the condition of maximum turbidity.

It is also possible to obtain the condition, $\rho \simeq 3$ by varying wavelength instead of varying particle size. Equation (12) indicates that $(K/\rho)_w$ must vary with λ in the same way that the experimentally determinable quantity $\tau\lambda/\Delta\mu$ varies with λ. If τ is measured over a range of λ and $\Delta\mu$ is known as a function of λ, the quantity $\tau\lambda/\Delta\mu$ can be plotted as a function of λ. The maximum experimental value of $\tau\lambda/\Delta\mu$ and the maximum value of K/ρ are then substituted into eq. (12) to determine c.

The Experimental Method

The concentration calculated from eq. (12) refers to the final volume (solution plus precipitant). In order to calculate the concentration of original solution before precipitant was added, τ must first be corrected by multiplying it by $(v + V)/V$, where V is the volume of solution and v is the volume of added precipitant.

Most of the turbidimetric titration methods described in the literature involve measurement of turbidity either after incremental additions of precipitant or simultaneously with continuous addition of precipitant. Neither of these methods can be used here, for the following reason. At the beginning of the titration the precipitating particles are highly swollen, causing m to be low. Therefore to attain the condition of maximum turbidity given by $\rho = 4\pi r\mu_0(m - 1)/\lambda \simeq 3.0$, the particles must be large. At the end of the titration the opposite is true: m is high and particles must be small. Clearly it is impossible to begin with big particles and end with small particles. Therefore each point in the titration must be done with a new solution, so that the particles can grow to the desired size. This is not considered to be a severe restriction, since each point can usually be measured quickly and simply.

If a series of precipitations are made using different volume fractions of precipitant, the concentration of precipitated polymer can be determined and plotted as a function of volume fraction of precipitant. The resulting curve is a solubility distribution, an example of which is shown on Figure 9 (except that the per cent precipitated has been plotted instead of the absolute concentration precipitated).

There are several advantages to the method of maximum turbidity over empirical turbidimetric methods. (*1*) The method is absolute and therefore calibration which is usually required can be avoided. (*2*) The scattering cross section per unit volume of scattering material is at a maximum when $\rho \simeq 3$. Therefore the sensitivity is the highest attainable by a turbidimetric method. (*3*) The particle size distribution does not affect the result if the distribution is narrow. As a result, small differences in the experimental technique which will cause the particle size distribution to be nonreproducible will have little or no effect upon the turbidity. This eliminates Hall's disadvantage (*d*). (*4*) The wavelength may be selected to correspond to the particle size.

There are several limitations to the method of maximum turbidity: (*1*) the condition of $\rho \simeq 3$ must be attained by particle growth, or adjustment of wavelength, or both (which may not be experimentally possible in some cases); (*2*) particles must be approximately spherical; (*3*) the solvent and precipitant must have approximately the same refractive indices, and these must be distinctly different from the refractive index of the polymer.

Calculation of $\overline{(K/\rho)}_w$ for Broad Distributions

Known Distribution Functions. If the distribution of particle sizes (in ρ) is broader than the maximum in K/ρ, the value of K/ρ is not constant over the range of particle sizes. In this case $\overline{(K/\rho)}_w$ can be calculated only if the particle size distribution is known. Stevenson, Heller, and Wallach[11] discussed the merits of some particle size distribution functions and calculated specific turbidities for one kind of distribution function. Unfortunately their calculations are not extensive enough to be used here. The lognormal distribution is a realistic and convenient distribution function,[12] and we have used this function to illustrate the method. The values of $\overline{(K/\rho)}_{w,m=1}$ have been calculated for lognormal weight distributions of varying weight geometric mean particle sizes ρ_0 and varying distribution widths β. Details of this calculation can be found in Appendix II and the results are illustrated in Figure 2 and tabulated in Appendix II. Inspection of Figure 2 indicates that as the distribution width is increased from monodisperse ($\beta = 0.0$) to broad ($\beta = 1.4$) the value of the maximum is decreased and the curves are broadened.

The distribution width may be obtained using a curve fitting method (originally described by Barns and La Mer[13] in somewhat different form).

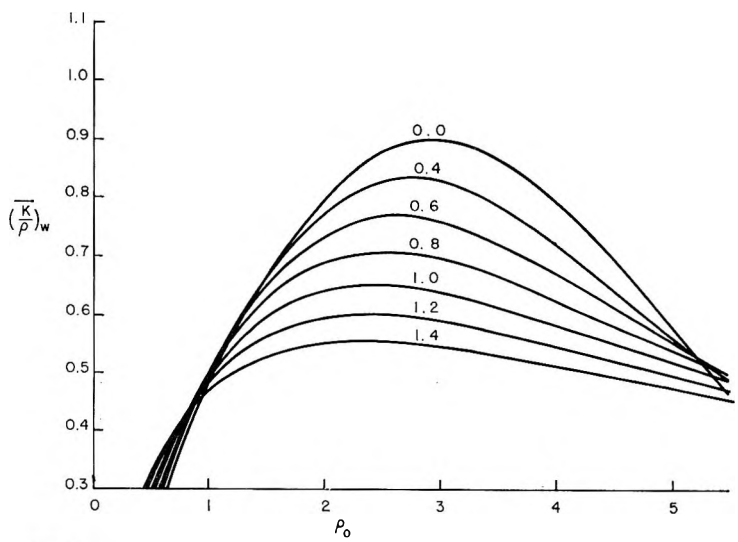

Fig. 2. $\overline{(K/\rho)}_{w,m=1.0}$ for lognormal weight distributions. Width parameters (β) are indicated.

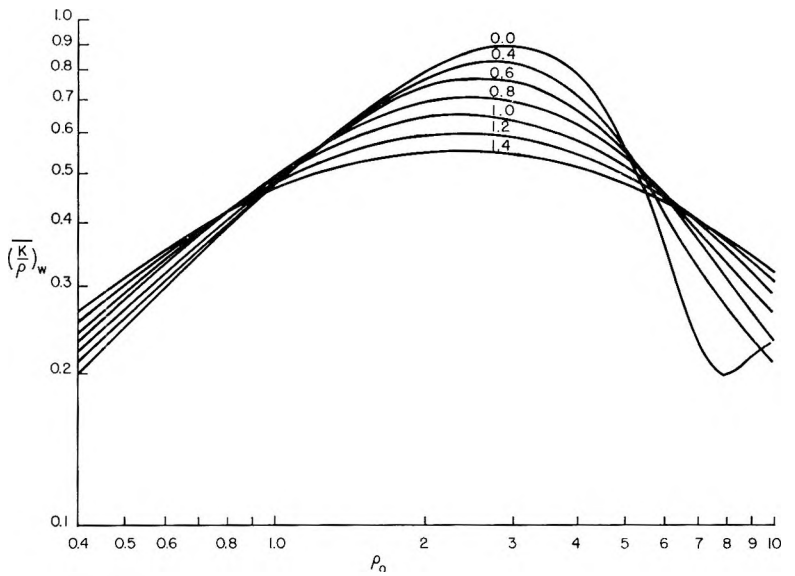

Fig. 3. Log $(\overline{K/\rho})_{w,m=1.0}$ vs. log ρ for lognormal weight distributions. Width parameters (β) are indicated.

From eq. (12) and the definition of ρ we may obtain respectively the following two equations:

$$\log \overline{(K/\rho)}_w - \log (\tau\lambda/\Delta\mu) = \log (D/3\pi c) \tag{13}$$

$$\log \rho - \log (\mu_0/\lambda) = \log [4\pi r(m - 1)] \tag{14}$$

For particles of a particular size the right-hand sides of both equations are constants. Therefore, a plot of log $\overline{(K/\rho)}_w$ versus log ρ will be displaced from a plot of log $(\tau\lambda/\Delta\mu)$ versus log (μ_0/λ) only by constants, but will be of identical shape. The former plot can be calculated from light scattering functions alone, and is shown for various lognormal distributions on Figure 3. The latter plot can be calculated from experimental measurements of the turbidity over a range of wavelengths. The experimental curves can be fitted to the theoretical curves and the distribution width thereby defined. Experimental curves which will not fit any of the theoretical curves indicate non-lognormal distributions.

The maximum $\overline{(K/\rho)}_{w,m=1.0}$ which is found by the process of curve fitting must be corrected to the m of the particles (see below) before substitution into eq. (12).

Effect of m. The maximum of $\overline{(K/\rho)}_w$ depends upon both the distribution width and the refractive index ratio, m. The dependence of $\overline{(K/\rho)}_w$ upon m for monodisperse particles and narrow distributions is shown on Figure 1. For known broad distributions it is necessary that the maximum of $\overline{(K/\rho)}_{w,m=1.0}$ which is obtained by curve fitting be corrected for m. It is reasonable to assume that the small refractive index effects may be treated

separately from polydispersity effects. In this case the maximum $(\overline{K/\rho})_w$ may be calculated by multiplying the maximum $(\overline{K/\rho})_{w,m=1.0}$ corresponding to the particular distribution width under consideration by the ratio of $(K/\rho)_{m=m}$ to $(K/\rho)_{m=1.0}$ for monodisperse particles (obtained by interpolation of the maxima on Figure 1). This ratio, the m correction, will generally be less than 10% of $(\overline{K/\rho})_w$.

The approximation was tested by comparison of $(\overline{K/\rho})_w$ for a lognormal distribution of spheres calculated by the exact Mie theory with those calculated using the approximate method. The exact value of $(\overline{K/\rho})_w$ in the region of the maximum for lognormal distributions with $\beta = 1.0$ and $m = 1.137$, is 0.704.[14] Using the approximation we obtain from Figure 2 $(\overline{K/\rho})_{w,m=1.0} = 0.651$, and the ratio of $(K/\rho)_{m=1.137}$ to $(K/\rho)_{m=1.0} = 1.105$, giving a corrected value of $(K/\rho)_w = 0.720$ for particles of $m = 1.137$, which is only 2% greater than the exact value. Since higher m or much broader distributions are not expected in turbidimetric titrations, it is concluded that the errors arising from the approximation used are negligible.

The refractive index of the precipitated phase depends upon the solvent-to-precipitant ratio (because the swelling volume depends upon this ratio), which means that m will increase from point to point during a titration. Measurement of the refractive index of the precipitated phase at several ratios of solvent to precipitant, and interpolation to intermediate values should be sufficiently accurate for calculation of m and the m correction. It is necessary to know m to 1–2% accuracy which requires that $\mu' - 1$ be known to about 10% accuracy. This may be calculated from eq. (9) and the volume fraction of polymer in the precipitated phases. Approximate volume fractions of polymer can be calculated from the weights of the precipitated phases, the density of pure polymer, estimated densities of mixtures of solvent and precipitant in the precipitated phase, and estimated densities of the precipitated phases. Alternatively, it may be possible to measure the refractive index of the precipitated phase directly.

Unknown Distribution Functions. For broad distributions which are unknown, the maximum $\tau\lambda/\Delta\mu$ is proportional to c, but the proportionality constant must be obtained from the value at 100% precipitation. In this case the method is empirical.

EXPERIMENTAL APPLICATION TO POLYSTYRENE

Materials and Equipment

The equipment required for this method is a modified recording spectrophotometer with an optical cell which can be thermostated to ±0.1°C. and stirred continuously and which has sufficient capacity to allow additions of precipitant. A turbidity cell having these features is shown on Figure 4. Water is pumped through the jacket from an outside thermostat. The cell windows are cemented with epoxy resin (Shell Chemical Co.) to plugs making standard taper joints with the body of the cell. The joints

Fig. 4. Turbidity cell.

were coated with Nonaq stopcock grease (Fisher Scientific Co., New York). By varying the length of the plugs, different optical path lengths can be obtained. This cell has been used in both the Cary Model 14 and the Beckman DU spectrophotometers. In both cases the cell compartment was enlarged by placing a metal box over the top of the compartment.

In our general procedure for the absolute method 25 or 30 ml of a solution having a concentration in the range 0.005% to 0.02% is placed in the turbidity cell and allowed to come to thermal equilibrium. The stirrer is turned on, a volume of thermostated precipitant is added from a pipet or syringe, and the turbidity at a particular wavelength is measured until it reaches a maximum. The stirrer is turned off, and the spectral turbidity of the suspension is recorded. This process is repeated for each point of the titration.

For the purpose of testing the method, titrations were made with Dow Styron 666, a general-purpose polystyrene. The solvent and precipitant used in most of the experiments were methyl ethyl ketone and isopropyl alcohol, respectively. In several preliminary experiments the solvent and precipitant were, respectively, methyl-*n*-propyl ketone and *n*-propyl alcohol. All solvents were reagent grade quality, but not further purified. All measurements were made on the Cary spectrophotometer without use of collimating apertures. Preliminary experiments showed that the use of collimating apertures did not appreciably alter turbidities.

For any given cone of light θ, the correction increases with particle size α. Therefore the correction is larger at the beginning of a titration when m is small and α is large, than it is at the end of a titration when the opposite is true. This correction cannot be used for the optical systems in the Cary or Beckman spectrophotometers, but it gives some idea of the errors which can be made with a poorly collimated beam.

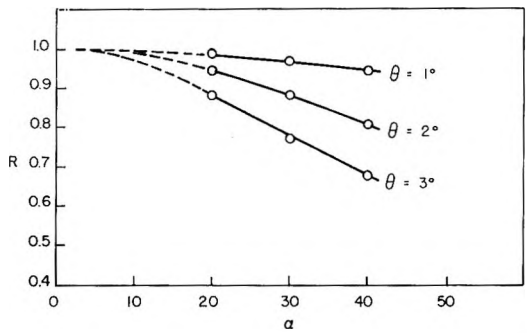

Fig. 5. Forward scattering correction for lens pinhole system.

Under certain experimental conditions (e.g., the lens pinhole system[15] in which the angle intercepted by the phototube is known) Gumprecht and Sliepcevich[16] calculated some corrections to the scattering coefficient to account for forward scattering. They showed that a good approximation to the correction (which depends on α and the half-angle of the cone of light intercepted by the phototube, θ) could be calculated from simple diffraction theory. This correction, R is shown on Figure 5.

Particle Growth

As precipitant is mixed with a dilute polymer solution, nucleation will be expected to occur at a point slightly past the equilibrium precipitation point. The nuclei are particles of new phase which contain one or more polymer molecules. When particles collide some of them may be expected to coalesce. Therefore the rate of particle growth should be closely related to the rate of stirring. This was confirmed in preliminary experiments.

Since it is necessary that particles grow to the size corresponding to the maximum $\tau\lambda/\Delta\mu$, preliminary experiments on particle growth were undertaken. In a typical experiment, a volume of n-propanol was added to an equal volume of 0.0015% polystyrene in methyl-n-propyl ketone in a cell of 10 cm. optical path at 25°C. with continuous stirring. The change in turbidity with time is shown for three wavelengths on Figure 6. The time required for the turbidity to reach a maximum is less at short wavelengths than at long wavelengths because smaller particle sizes are required to obtain the condition that $\rho \approx 3.0$.

Several samples of suspension were removed from the turbidity cell and examined under a microscope. Particles appeared to be polydisperse spheres but no aggregations of particles could be detected. This is evidence in support of the position taken in Appendix I.

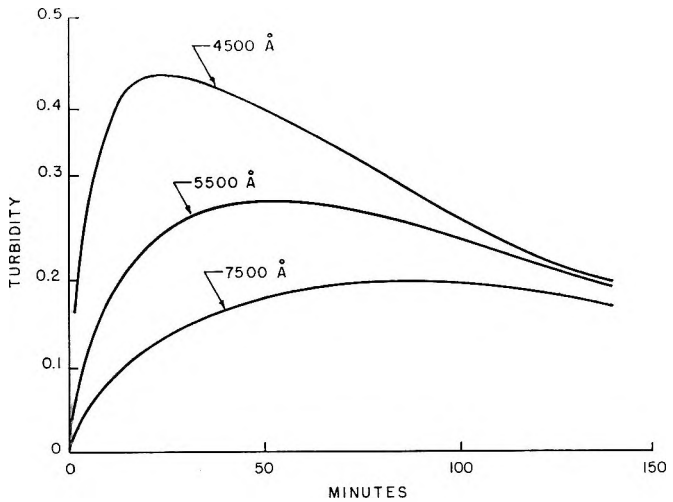

Fig. 6. Change of turbidity with time during stirring.

Particle Size Distribution

We have assumed that the particle size distributions are lognormal. This can be tested by the method of curve fitting previously described. Solutions of polystyrene in methyl ethyl ketone were made up to various concentrations and precipitated at 33°C. in a stirred turbidity cell with a 2-cm. optical path by adding a volume of isopropyl alcohol (IPA) to 30 ml. of solution. Turbidity was measured from 3500 to 7500 A. The turbidities at four wavelengths (expressed in absorbance units, a) are given in Table I.

The average of the refractive indices of the solvents and polymer at 30°C. were interpolated (from values by Timmermans[17]) and Boundy and Boyer[18]) by using plots of μ_0 versus $1/\lambda^2$ and are given in Table II.

TABLE I
Turbidities at Various Wavelengths for Curve Fitting

Curve no.	Polystyrene, %	IPA added, ml.	Turbidity, absorbance units				β
			3500 A.	4500 A.	5500 A.	7500 A.	
1	0.0062	10	0.450	0.370	0.299	0.204	0.6
2	0.0062	15	0.820	0.718	0.600	0.415	0.4
3	0.01	9	0.385	0.316	0.248	0.164	0.6
4	0.01	10	0.712	0.597	0.492	0.334	0.6
5	0.01	15	1.336	1.152	0.960	0.657	0.4
6	0.01	25	1.358	1.217	1.030	0.684	0.4
7	0.02	8	0.146	0.123	0.105	0.072	0.6
8	0.02	8	0.220	0.145	0.105	0.057	0.6
9	0.02	9	0.807	0.652	0.538	0.367	0.6
10	0.02	10	1.306	1.096	0.930	0.662	0.8

The data in Table I was plotted as log $A\lambda/\Delta\mu$ versus log μ_0/λ, on Figure 7 and is indicated by the points. The lines are calculated curves for log-normal distributions of log $(K/\rho)_w$ versus log ρ_0 (i.e., segments of curves in Fig. 3) fitted to the experimental points. The curves fit reasonably well

TABLE II
Refractive Index Differences for Polystyrene in Methyl Ethyl Ketone and Isopropyl Alcohol, 30°C.

λ, A.	μ	$\Delta\mu/\lambda$
3500	0.2583	7380
4500	0.2305	5122
5500	0.2199	3998
7500	0.2095	2797

for different concentrations of polymer and volumes of precipitant indicating that the distributions are close to lognormal. The approximate distribution width parameters β are listed in Table I. It is interesting to note that the width of the distributions does not change much under different conditions.

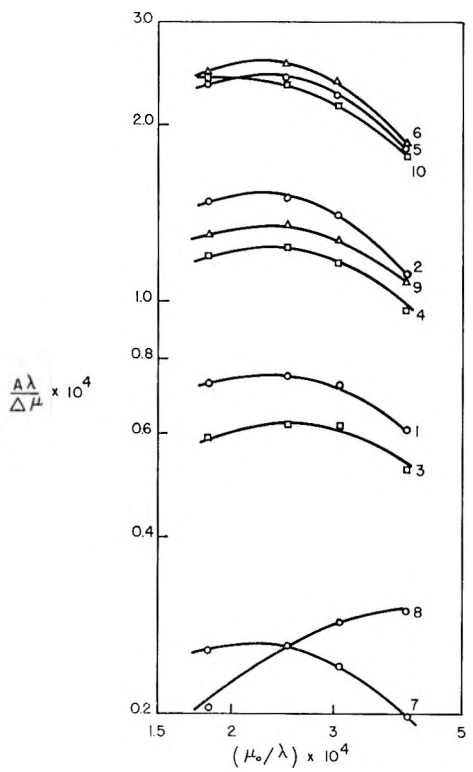

Fig. 7. Illustration of curve fitting procedure.

Refractive Index Ratio

For the purpose of measuring m as a function of per cent precipitant, precipitations were made as follows. A volume of isopropyl alcohol was added to a solution of polystyrene in methyl ethyl ketone. While stirring, or shaking the temperature was increased to 50°C. and then allowed to cool slowly to 30.0°C. The stirring was turned off and the precipitate allowed to settle. The precipitated phase was weighed, dried (to remove solvents), and reweighed.

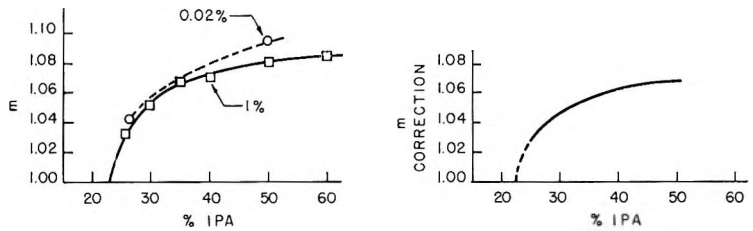

Fig. 8. Refractive index and refractive index correction factor for precipitating polystyrene as a function of per cent isopropyl alcohol (IPA).

The volume fraction of polystyrene in the precipitated phase was calculated (assuming no volume change on mixing) and this was used to calculate the refractive index [eq. (9)], and so m. Results are given on Figure 8. Within experimental error the composition and refractive index of the precipitated phase is the same for 0.02% and 1% polystyrene. (It is interesting to compare the results of Patat and Träxler[19] on the solution fractionation of poly(vinyl alcohol) which indicated that the composition of the precipitated phase at a given solvent/precipitant ratio is independent of the starting concentration and the original molecular weight of the polymer.) The m correction is plotted as a function of volume per cent isopropyl alcohol on Figure 8.

Titrations

Titrations were carried out by adding a volume of isopropyl alcohol to 30 ml. of 0.01 or 0.02% polystyrene in methyl ethyl ketone at 30°C. The mixtures were stirred until the turbidity at 5500 A. reached a maximum. At this time the stirrer was turned off to stop the growth of particles and the turbidity was measured from 3500–7500 A. Finally the stirrer was turned on, the turbidity at 7500 A. was allowed to reach a maximum. After each measurement the turbidity cell was emptied, rinsed, and new additions of solution and precipitant were made.

The turbidities (in absorbance units, A.) and associated data are given in Table III. The distribution width (β) was obtained from the data at 5500 A. by curve fitting, as previously described. It is assumed that this distribution width is valid at both wavelengths. From this value, $(K/\rho)_{w,m=1.0}$ was found and corrected for m, giving $(K/\rho)_w$. Concentra-

TABLE III
Data for Turbidimetric Titrations of 0.01% and 0.02% Polystyrene

Polystyrene, wt.-%	IPA, %	Maximum turbidity, absorbance units 5500 A.	Maximum turbidity, absorbance units 7500 A.	β	m correction factor	$(K/\rho)_w$	Calculated $c \times 10^4$, g./ml. 5500 A.	Calculated $c \times 10^4$, g./ml. 7500 A.	% Precipitated 5500 A.	% Precipitated 7500 A.
0.02	21.9	0	0	—	—	—	0	0	0	0
"	24.1	0.101	0.072	~0.8	1.04	0.74	0.58	0.59	2.9	2.95
"	26.3	0.535	0.380	0.9	1.04	0.71	3.30	3.36	16.5	16.8
"	28.4	0.932	0.689	1.0	1.05	0.68	6.17	6.52	30.8	32.6
"	37.3	1.567	1.226	1.0	1.06	0.69	11.7	13.1	58.5	65.5
"	49.8	1.666	1.27	~1.0	1.08	~0.70	15.3	16.7	76.5	83.5
0.01	24.1	0	—	—	—	—	0	—	0	—
"	26.3	0.248	—	0.9	1.04	0.71	1.53	—	15	—
"	28.4	0.487	—	0.9	1.05	0.71	3.10	—	31	—
"	37.3	0.960	—	0.8	1.06	0.75	6.6	—	66	—
"	49.8	1.008	—	0.7	1.08	0.80	8.1	—	81	—

tions were calculated from eq. (1) and are given in Table III. They are plotted against the per cent isopropyl alcohol (IPA) on Figure 9. The results of the two wavelengths are slightly different at the end of the titration.

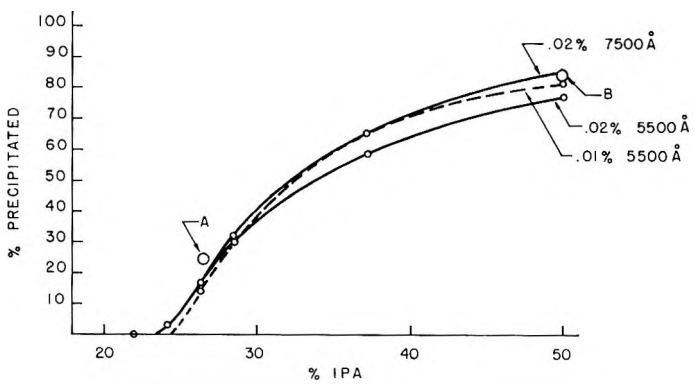

Fig. 9. Turbidimetric precipitation curves of Dow Styron 666.

Reproducibility of the Maximum Turbidity and Concentration

Choice of Wavelength. According to eq. (13) it is possible to use any wavelength, provided only that the refractive indices are known and that neither solvent, precipitant, nor polymer exhibit true absorption. A comparison of the results at three different wavelengths for one precipitation with 26.5% isopropyl alcohol is given in Table IV. At the long wavelengths larger particles had to be formed than at short wavelengths. Since, as was pointed out above, the distribution width at the point of maximum

TABLE IV
Comparison of Precipitates Measured at Different Wavelengths

λ, A.	Maximum turbidity, absorbance units	10^5 c, g./ml.	% Precipitated
3500	1.031	3.66	18.3
5500	0.550	3.60	18.0
7500	0.389	3.65	18.3

turbidity does not change much with the per cent of precipitant, $\overline{(K/\rho)}_w$ will not change much with particle size. Therefore the value of $\overline{(K/\rho)}_w$ at 5500 A. (0.68) was used for all three calculations.

The agreement in Table IV is better than would be expected from considerations of experimental error.

Other Experimental Variables. The effect on the turbidity of some of the variables which cannot be easily controlled were tested. These include rate of stirring, rate of addition, time of addition and temperature control. Table V gives the maximum turbidities (in absorbance units) for various methods of mixing 13 ml. of isopropyl alcohol with 25 ml. of 0.0062% polystyrene in methyl ethyl ketone, making the mixture 28.6% in isopropyl alcohol. Temperatures were maintained constant to ±0.1°C.

TABLE V
Variations in Procedure for Addition of Precipitant

Procedure	Maximum turbidity, absorbance units
Pipet addition with stirring	0.296
Syringe addition with stirring	0.308
Syringe addition with stirring, then no stirring for 8 min., stirring 5 min.	0.312
Dropwise from pipet with stirring	0.309
Dropwise from syringe with stirring	0.312
Fast addition from syringe with slow stirring	0.304
Fast addition from syringe with no stirring for 23 min., then stirring for 3 min.	0.310

Comparison of the precipitations show that variations in the rate of stirring, rate of addition, and procedure used for addition have very little influence upon the resulting maximum turbidities. However, the time required to reach maximum turbidity does vary with these conditions.

In another experiment, addition of the precipitant in one lot was compared with addition in portions. In this experiment, 24 ml. of 0.0053% polystyrene in methyl ethyl ketone was added to the turbidity cell (at 25.0°C.). When 10 ml of isopropyl alcohol was added in one lot, the turbidity reached a maximum value of 0.806. When the alcohol was added

in two lots (of 8 ml. and 2 ml.), allowing time for the turbidity to reach a maximum after each addition, the absorbance after the second addition reached a maximum value of only 0.691. When the alcohol was similarly added in three lots (of 8 ml., 1 ml., and 1 ml.), the turbidity after the third addition reached a maximum value of 0.608. Addition of a second volume of precipitant to a system already containing large particles would be expected to form new small particles and create a broad particle size distribution with resulting decreased maximum turbidity. (In principle a correction for this could be made by the curve-fitting procedure previously described.)

Other experiments indicated that the purification and drying of both the solvent and the precipitant have a large effect upon the fraction of material precipitated.

Accuracy of the Absolute Method

Two points of the precipitation curve were checked by comparison with precipitation according to conventional fractionation techniques. Because precipitations are concentration-dependent, the concentration of polystyrene was the same as that used for the turbidimetric precipitation curve (0.02 g./100 ml. solvent). Precipitations were carried out in a stirred 2-liter flask, held in a 30°C. thermostat, by slowly adding a volume of isopropyl alcohol to 1 liter of polymer solution. With continuing stirring the temperature was raised to ~50°C. and then allowed to drop slowly to 30.0°C. The stirrer was then stopped and the precipitate allowed to settle. The concentration of the supernatant was determined by evaporating 1 liter to dryness under an infrared lamp in a large pan constructed of heavy gauge aluminum foil. The weight of precipitated polymer was determined by sucking off the remaining supernatant, and removing all of the precipitated phase followed by drying and weighing. At the low concentration used, it was necessary to correct for solids in the methyl ethyl ketone. These were determined by evaporation of 1 liter of methyl ethyl ketone to dryness and weighing according to the procedure described above. No solids were found in the isopropyl alcohol. The results are given in Table

TABLE VI
Gravimetric Determination of Solids

	Point A	Point B
Isopropyl alcohol, vol.-%	26.5	50
Wt. total solids per liter of supernatant, g.	0.164	—
Wt. total solids in entire supernatant, g.	0.223	—
Wt. solids per liter methyl ethyl ketone, g.	0.072	—
Wt. polystyrene in entire supernatant, g.	0.151	—
Wt. precipitated polystyrene, g.	0.052	0.167
Total wt. polystyrene recovered, g.	0.203	—
Wt. polystyrene in original solution, g.	0.200	0.200
% polystyrene precipitated	25	84

VI. The concentration in the solvent was not determined for point B because the precipitate was a hard mass which could be easily collected without introducing errors. The check on total solids for point A is excellent. Points A and B are given on Figure 9 for comparison with the turbidimetric precipitation curves. The curve for 0.02% and 7500 A falls below point A, but quite close to point B. Errors in the gravimetric determination are estimated to be 1–3%. Errors in the absolute method are difficult to estimate, but two sources of error can be discussed. In the first place, selection of the particle distribution width, β, is imperfect because (a) the curvature of the plots at the peaks (see Fig. 7) is somewhat dependent upon m (but we assume $m = 1.0$), and (b) in some cases actual distributions may deviate substantially from the lognormal distribution function. In the second place no provisions were made to limit forward scattering in this precipitation curve. In spite of these errors the turbidimetric method agrees quite well with gravimetric analysis.

CONCLUSIONS

The absolute method for calculating the concentration of precipitated polymer from turbidities has been checked. The experimental work with polystyrene indicates that under the specified conditions, the reproducibility of turbidimetric precipitation curves is very good and that the method is accurate. The experimental findings agree with the theory. Additional verification of the theory comes from (*1*) the fact that the concentrations calculated at different wavelengths (and therefore at different average particle sizes) give almost identical results; (*2*) the fact that mixing conditions have very little influence upon the maximum turbidity.

It should be re-emphasized that many of the usual precautions given for turbidimetric titrations[1] are not necessary with this method. The optimum experimental conditions for obtaining the greatest accuracy in a turbidimetric method (absolute or empirical) are (*1*) the solvent and precipitant have equal refractive indices, and (*2*) turbidity is measured when it reaches a maximum. It is doubtful whether optimum conditions have ever previously been attained, and it is not surprising that turbidimetry has often been regarded as a method of doubtful accuracy.

APPENDIX I

Comments on Work by Hastings and Peaker

Hastings and Peaker[3] measured dissymmetries of scattered light during turbidimetric titrations of solutions of polystyrene in benzene by the addition of methanol. At several points during the titrations the ratios of intensities of light scattered at various pairs of angles symmetrical about 90° (i.e., dissymmetries) were measured. They compared curves of dissymmetry versus forward angle with similar curves calculated according to the Rayleigh-Gans theory for spheres. Curves obtained early in the

titrations showed a large decrease in dissymmetry with angle and agreed with theoretical curves for spheres. However, curves late in the titrations showed an initial increase followed by a decrease in dissymmetry with angle, and did not agree with theoretical curves. Hastings and Peaker interpreted the change in the dissymmetry pattern to be the result of a change in the shape of the particles. They apparently confirmed this using electron microscopy which showed chainlike aggregates of spherical particles.

The purpose of this Appendix is to show that an alternative interpretation is also possible. We assume that the particles are spherical as shown in the electron micrograph, but that the aggregation occurred during the process of specimen preparation. The average diameter of the particles on the photograph is of the order of 0.2 μ. In suspension the particles are swollen 6-15 fold which means that the diameters of the particles in solution is of the order of 2μ.

The Rayleigh-Gans theory is valid when the condition $2\alpha(m - 1) \ll 1$ is fulfilled.[5] Assuming that the incident light used was 546 mμ this requires that $(m - 1) \ll 0.3$. The actual $(m - 1)$ for this system is estimated to be <0.02. We will assume the Rayleigh-Gans theory is a rough approximation. In the range of particle sizes considered, the dissymmetries calculated on the basis of the Rayleigh-Gans theory fluctuate several orders of magnitude with small changes in diameter. Therefore experimental dissymmetry curves of a suspension composed of a distribution of particle sizes cannot be compared with the dissymmetry curve corresponding to an average particle size, but should be compared with the dissymmetry curve corresponding to the particle size distribution. The dissymmetry can be calculated for known distributions by the equation:

$$I_\theta/I_{180-\theta} = \left[\sum n_i D_i^6 P(\theta)_i\right]/\left[\sum n_i D_i^6 P(180\text{-}\theta)_i\right]$$

where I_θ is the intensity of light scattered at angle θ, n_i is the number of particles of diameter D_i, and $P(\theta)_i$ is the particle scattering factor for spherical particles of diameter D_i. $P(\theta)$ is given by the relationship:

$$P(\theta) = [(3/x^3)(\sin x - x \cos x)]^2$$

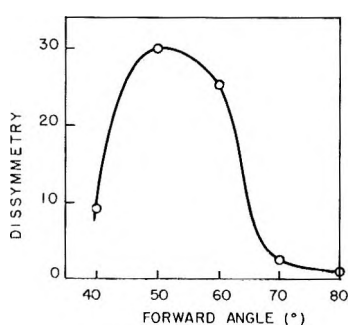

Fig. 10. Dissymmetry curve for a simple distribution.

where

$$x = (2\pi D\mu_0/\lambda) \sin \theta/2$$

Since the particle size distributions in the work of Hastings and Peaker are unknown, we will illustrate the method by calculating the dissymmetry of a simple distribution. We assume that $n_i D_i^6 = 1$ for every i, and that the distribution consists of five species such that $D\mu_0/\lambda$ have values 1.9, 2.0, 2.1, 2.2, 2.3. The dissymmetry curve for this distribution is given on Figure 10. This curve has the same general shape as Hastings and Peaker's curves late in the titrations. We expect that a more sophisticated treatment could produce curves of even greater similarity to the experimental curves.

APPENDIX II

Calculation of $\overline{(K/\rho)}_{w,m=1}$ for Lognormal Weight Distributions of Spheres

The definition of $\overline{(K/\rho)}_w$ is [from eq. (8)]:

$$\overline{(K/\rho)}_w = \sum (K/\rho)_i w_i = \int_0^\infty (K/\rho) dw \tag{18}$$

where w is the weight fraction having a size parameter between ρ and $\rho + d\rho$. The normalized lognormal distribution by weight is given by:[20]

$$dw = (1/\beta\sqrt{\pi}) \exp \{ - \log (\rho/\rho_0)/\beta \}^2 \, d \log \rho \tag{19}$$

where

$$\beta = \sqrt{2} \log \sigma_g$$

and σ_g = geometric standard deviation, ρ_0 = weight geometric mean.

Substitution of eq. (19) into eq. (18) gives:

$$(K/\rho)_w = (1/\beta\sqrt{\pi}) \int_0^\infty K/\rho^2 \exp \{ -\log (\rho/\rho_0)/\beta \}^2 \, d\rho \tag{20}$$

In the limit as $m \rightarrow 1.0$, K is a simple function[5] of ρ as follows:

$$K = 2 - (4/\rho)\sin \rho + (4/\rho^2)(1 - \cos \rho) \tag{21}$$

Substitution into eq. (20) gives

$$\overline{(K/\rho)}_{w,m=1.0} = \frac{1}{\beta\sqrt{\pi}} \int_0^\infty \left[\frac{2}{\rho^2} - \frac{4 \sin \rho}{\rho^3} + 4 \frac{(1 - \cos \rho)}{\rho^4} \right] \cdot \exp \left\{ - \frac{\log (\rho/\rho_0)}{\beta} \right\}^2 d\rho \tag{22}$$

Integration of eq. (22) was carried out numerically by using Simpson's rule.[21] All computations were made on the IBM 650 computer. Results are given in Table VII and on Figure 2.

TABLE VII
Table of $\overline{(K/\rho)}_{w,m=1.0}$ for Lognormal Weight Distributions

ρ_0	β = 0	β = 0.2	β = 0.4	β = 0.6	β = 0.8	β = 1.0	β = 1.2	β = 1.4
0.4	0.198	0.200	0.206	0.215	0.228	0.243	0.254	0.265
0.6	0.294	0.296	0.304	0.315	0.329	0.342	0.352	0.354
0.8	0.386	0.389	0.396	0.408	0.419	0.425	0.425	0.419
1.0	0.473	0.476	0.484	0.490	0.495	0.492	0.481	0.465
1.2	0.554	0.556	0.560	0.562	0.557	0.544	0.523	0.498
1.4	0.627	0.628	0.629	0.623	0.607	0.583	0.553	0.521
1.6	0.693	0.692	0.688	0.673	0.646	0.611	0.574	0.537
1.8	0.751	0.748	0.736	0.711	0.674	0.631	0.588	0.548
2.0	0.799	0.793	0.775	0.740	0.693	0.643	0.596	0.554
2.2	0.838	0.830	0.803	0.758	0.704	0.650	0.601	0.556
2.4	0.867	0.856	0.822	0.768	0.709	0.652	0.601	0.556
2.6	0.887	0.873	0.832	0.771	0.708	0.650	0.599	0.554
2.8	0.897	0.881	0.833	0.768	0.703	0.646	0.595	0.551
3.0	0.899	0.879	0.827	0.760	0.695	0.639	0.589	0.546
3.2	0.892	0.870	0.814	0.747	0.684	0.630	0.582	0.541
3.4	0.877	0.854	0.796	0.730	0.671	0.620	0.574	0.534
3.6	0.855	0.831	0.774	0.711	0.656	0.608	0.565	0.527
3.8	0.826	0.802	0.748	0.691	0.641	0.596	0.556	0.520
4.0	0.793	0.769	0.719	0.669	0.624	0.584	0.547	0.513
4.5	0.691	0.673	0.640	0.611	0.581	0.551	0.522	0.493
5.0	0.576	0.569	0.561	0.553	0.538	0.519	0.496	0.473
5.5	0.464	0.470	0.487	0.499	0.497	0.487	0.472	0.454
6.0	0.365	0.385	0.423	0.450	0.459	0.457	0.448	0.435
6.5	0.287	0.318	0.370	0.407	0.424	0.429	0.425	0.416
7.0	0.235	0.270	0.328	0.369	0.393	0.403	0.404	0.399
7.5	0.206	0.240	0.294	0.337	0.365	0.380	0.384	0.383
8.0	0.197	0.224	0.268	0.309	0.339	0.358	0.366	0.367
8.5	0.202	0.217	0.248	0.285	0.317	0.338	0.349	0.352
9.0	0.212	0.214	0.232	0.265	0.296	0.319	0.332	0.339
9.5	0.223	0.213	0.219	0.247	0.278	0.302	0.318	0.326
10.0	0.229	0.210	0.208	0.232	0.262	0.287	0.304	0.314

The author wishes to thank Dr. Colin Booth, Manchester University, for his comments and criticism.

References

1. *Techniques of Polymer Characterization*, P. W. Allen, Ed., Academic Press, New York, 1959, Chap. II.

2. Meehan, E. J., and W. H. Beattie, *Anal. Chem.*, **33**, 632 (1961).

3. Hastings, G. W., and F. W. Peaker, *J. Polymer Sci.*, **36**, 351 (1959); G. W. Hastings, D. W. Ovenall, and F. W. Peaker, *Nature*, **177**, 1091 (1956).

4. Leviton, A., and H. S. Haller, *J. Phys. Colloid Chem.*, 51, 460 (1947); W. Heller and R. M. Tabibian, *J. Colloid Sci.*, **12**, 25 (1957).

5. van de Hulst, H. C., *Light Scattering by Small Particles*, Wiley, New York, 1957, Chap. 11. (Note: in the notation of van de Hulst, α is x and K is $Q_{ext.}$)

6. Weissberger, A., *Technique of Organic Chemistry*, Vol. I, Part III," 3rd Ed., Interscience, New York, 1960, Chap. 32.

7. Pangonis, W. J., W. Heller, and A. Jacobson, *Tables of Light Scattering Functions*

for Spherical Particles, Wayne State University Press, Detroit, 1957; R. B. Penndorf, *J. Opt. Soc. Am.*, **47**, 603 (1957).

8. Sinclair, D., and V. K. LaMer, *Chem. Rev.*, **44**, 245 (1949).

9. Batemen, J. B., E. J. Weneck, and D. C. Eshler, *J. Colloid Sci.*, **14**, 308 (1959).

10. Weissberger, A., *Technique of Organic Chemistry*, Vol. I, Part II, 3rd Ed., Interscience, New York, 1960, Chap. 18.

11. Stevenson, A. F., W. Heller, and M. L. Wallach, *J. Chem. Phys.*, **34**, 1789, 1796 (1961).

12. Kottler, F., *J. Franklin Inst.*, **250**, 339, 419 (1950).

13. Barns, M. D., and V. K. LaMer, *J. Colloid Sci.*, **1**, 79 (1946).

14. Wales, M., private communication.

15. Chin, J. H., C. M. Sliepcevich, and M. Tribus, *J. Phys. Chem.*, **59**, 841, 845 (1955).

16. Gumprecht, R. O., and C. M. Sliepcevich, *J. Phys. Chem.*, **57**, 90 (1953).

17. J. Timmermans, *Physico-Chemical Constants of Pure Organic Compounds*, Elsevier, New York, 1950.

18. Boundy, R. H., and R. F. Boyer, *Styrene, Its Polymers, Copolymers and Derivatives*, Reinhold, New York, 1952.

19. Patat, F., and G. Träxler, *Makromol. Chem.*, **33**, 113 (1959).

20. Herdan, G., *Small Particle Statistics*, Academic Press, New York, 1960.

21. Hilderbrand, F. W., *Introduction to Numerical Analyses*, McGraw-Hill, New York, 1956, p. 75.

Résumé

On décrit une méthode de titration turbidimétrique pour déterminer les distributions de solubilité (que sont étroitement reliées aux distributions du poids moléculaire). Dans cette méthode, le polymère est précipité de sa solution par addition d'un non-solvant de même indice de réfraction que celui du solvant. On laisse les particules précipitées du polymère gonflé s'agglomérer jusqu'à ce que la turbidité atteigne un maximum. On montre par l'emploi de la théorie de la diffusion lumineuse que dans ces conditions la concentration du polymère qui est précipité, peut être calculée sur une base absolue à partir de la turbidité maximum. On discute de l'influence de la dimension des particules et de la distribution de la dimension des particules. La méthode a été essayée avec succès sur du polystyrène. En principe la méthode peut être appliquée à la plupart des polymères.

Zusammenfassung

Eine Trübigkeitstitrationsmethode zur Bestimmung der Löslichkeitsverteilung (die in enger Beziehunt zur Molekulargewichtsverteilung steht) wurde entwickelt. Bei dieser Methode wird das Polymere aus einer Lösung durch Zusatz eines Nichtlösungsmittels mit gleichem Brechungsindex wie derjenige des Lösungsmittels gefällt. Die ausfallenden Teilchen des gequollenen Polymeren lässt man solange agglomerieren, bis die Trübigkeit ein Maximum erreicht. Anhand der Lichststreuungstheorie wird gezeigt, dass unter diesen Bedingungen die Konzentration des gefällten Polymeren aus der maximalen Trübigkeit auf einer absoluten Grundlage berechnet werden kann. Der Einfluss von Teilchengrösse und Teilchengrössenverteilung wird diskutiert. Die Methode wurde an Polystyrol getestet und erwies sich als zuverlässig. Im Prinzip kann die Methode auf die meisten Polymerarten angewendet werden.

Received May 1, 1964
Revised June 23, 1964

JOURNAL OF POLYMER SCIENCE: PART A VOL. 3, PP. 551–567 (1965)

Determination of the Molecular Weight Distribution of Polyisoprenes from the Sol Dependence on Crosslinking*

NISSIM CALDERON and KENNETH W. SCOTT, *Research Division, The Goodyear Tire & Rubber Company, Akron, Ohio*

Synopsis

A polyisoprene with a narrow molecular weight distribution was prepared with a polyisoprenyl lithium catalyst by the "seeding" technique. Dicumyl peroxide was shown to be a quantitative crosslinking agent for this polyisoprene. The dependence of the sol fraction on the amount of crosslinking introduced by dicumyl peroxide vulcanization was determined and found to give excellent agreement with gel network formation theory. Two procedures for estimating the breadth of the molecular weight distribution from the sol dependence on crosslinking yield the value of 1.05 ± 0.05 for the ratio of the weight-average to number-average molecular weight for this polyisoprene. These results demonstrate that it is possible to determine the molecular weight and molecular weight distribution of polyisoprenes, containing *cis*-1,4, *trans*-1,4, or moderate amounts of 3,4 addition structures, from the sol dependence on the amount of dicumyl peroxide used in crosslinking. Temporary or permanent molecular chain scission that might accompany the crosslinking by dicumyl peroxide was negligible, as there was no evidence of broadening of the molecular weight distribution due to scission. For the most likely set of recombination reactions that might occur it is estimated that less than 0.3% of the dicumyl peroxide is used in reactions leading to temporary molecular chain scission.

INTRODUCTION

A previous paper[1] presented an experimental verification of gel network formation theory and thus established the feasibility of determining the molecular weight distribution of a polymer from the dependence of the sol fraction on the amount of crosslinks introduced. The work of Lorenz and Parks[2,3] offered chemical evidence that dicumyl peroxide is a quantitative crosslinking agent for *cis*-1,4 or *trans*-1,4-polyisoprene, yielding one crosslink for each molecule of dicumyl peroxide decomposed. However, Moore and Scanlan,[4] observing stress relaxation during the crosslinking of stretched natural rubber by dicumyl peroxide, concluded that "degradation of the primary network occurs equivalent to about 10% of the new elastically effective crosslinks formed." While it was possible to show that any degradation or molecular chain scission of a permanent type was

* Presented, in part, at the American Chemical Society national meeting, New York, September 1963.

negligible[1] and hence unlikely to affect the quantitative nature of dicumyl peroxide crosslinking, the possibility that the observed stress relaxation was due to temporary scission cast doubts on the practicality of determining the molecular weight distribution of polyisoprenes from the sol dependence on the amount of dicumyl peroxide used for crosslinking, since temporary scission might alter the molecular weight distribution. The studies reported here support our contention that temporary scission is negligible and that dicumyl peroxide may be used as a quantitative crosslinking agent for determining the molecular weight distributions of polyisoprenes consisting of *cis*-1,4, *trans*-1,4, and moderate amounts of 3,4 addition structures.

EXPERIMENTAL

Preparation and Characterization of Polyisoprene

Isoprene was polymerized for 48 hr. at 25°C. by the "seeded" polymerization technique described by Morton et al.[5] The polyisoprenyl lithium "seed" used had a molecular weight of about 3000. The polymerizing system consisted of 38 vol.-% of isoprene in hexane. A 220-g. sample of polyisoprene was isolated by precipitation in methanol containing 0.2 g./l. of 2,6-di-*tert*-butyl-*p*-cresol as an antioxidant and then drying *in vacuo*. From the amount of polyisoprenyl lithium "seed" used (0.001434 mole), the expected number-average molecular weight, $\bar{M}_k$, of the polyisoprene is 153,000 on the basis that each mole of "seed" yields a mole of polyisoprene. The intrinsic viscosity of the polyisoprene in toluene at 25°C. was 1.38 dl./g., which corresponds to a viscosity-average molecular weight[6] of 144,000 or viscosity-average degree of polymerization, $\bar{y}_v$, of 2118. (Another sample of polyisoprene, prepared by the same procedure and having an expected number-average molecular weight $\bar{M}_k$ of 178,000, was found to have a viscosity-average molecular weight of 175,000 and an osmometrically determined number-average molecular weight of 181,000.) The close agreement of these molecular weights indicates that this polyisoprene has a narrow distribution of molecular weights, while the relative values of these molecular weights suggest that the distribution of molecular weights in this polyisoprene is narrower than that of the fractions used to determine the intrinsic viscosity–molecular weight relationship.[6] An analysis of the infrared spectrum of this polyisoprene gave the following normalized values for the various possible addition structures: *cis*-1,4, 80.5%; *trans*-1,4, 11.9%; 3,4, 7.6%; 1,2, none.

Crosslinking the Polyisoprene

Samples (4 g.) were extracted with acetone to remove any remaining traces of 2,6-di-*tert*-butyl-*p*-cresol from the rubber. The samples were dried *in vacuo* and then dissolved in benzene. The desired amount of dicumyl peroxide was added volumetrically to each sample from a solution of doubly recrystallized dicumyl peroxide in benzene. After thorough

mixing, the cements were evaporated to dryness *in vacuo*, placed in flat sheet molds, and crosslinked by press curing under pressure at 149°C. for 2 hr. A control sample was carried through all of the above operations with the exception that dicumyl peroxide was not added. The intrinsic viscosity of this control sample after the above treatment was 1.36 dl./g., indicating negligible change in the molecular weight during the handling of these samples.

Determination of Sol Fraction and Swelling Value

Weighed pieces of the crosslinked samples (about 1 g.) were extracted three times with 60 cc. acetone containing 100 mg./l. of *N*-phenyl-2-naphthylamine for 48 hr. each time. A fourth extraction with pure acetone followed. The acetone extractions were used to remove the nonpolymeric, soluble reaction products of the crosslinking, primarily 2-phenyl-2-propanol. The samples were dried *in vacuo* at room temperature for 24 hr. and then weighed (W_a). The samples were then extracted twice with 200 cc. benzene containing 50 mg./l. of *N*-phenyl-2-naphthylamine for 24 hr. each time, followed by a third extraction with pure benzene. All extractions were done at room temperature in the dark and after every solvent change the system was purged with carbon dioxide. The swollen samples were rapidly blotted between filter paper and transferred to tared weighing bottles for weighing (W_s). The samples were dried *in vacuo* at room temperature for 72 hr. and then weighed (W_b). The benzene-soluble, polymeric sol fraction S is given by

$$S = (W_a - W_b)/W_a \tag{1}$$

and the swelling value, Q, in grams of benzene per gram of rubber gel network, is given by

$$Q = (W_s - W_b)/W_b \tag{2}$$

For the purpose of this paper we shall empirically use a corrected swelling value, Q_c, which approximates the swelling value which would be obtained for a sample crosslinked to the same extent in the absence of any soluble diluent (here dicumyl peroxide) and is defined by

$$Q_c = v_0(Q + 1) - 1 \tag{3}$$

where v_0 is the volume fraction of rubber gel present during crosslinking. Taking into account the densities of dicumyl peroxide and natural rubber, one obtains the expression

$$v_0 = (1 - S)/(1 + 0.00896C) \tag{4}$$

where C is the dicumyl peroxide concentration (in phr). The experimental and theoretical justification of eq. (3) is reported by Scott, Lorenz, and Parks,[7] but is of no importance to this paper, as almost any empirical relation would suffice here.

RESULTS AND DISCUSSION

Figure 1 is a comparison of the dependence of the reciprocal of the corrected swell value on the dicumyl peroxide concentration used in crosslinking for the polyisoprene of this work and the milled natural rubber used by Lorenz and Parks[3] and Scott.[1] Since the polyisoprene used here has the same number-average molecular weight as the milled natural rubber,[1,3] the corrected swell values will not require further corrections to take in account the free chain ends associated with finite molecular weights. Since dicumyl peroxide has been shown to be a quantitative crosslinking agent for natural rubber,[2,3] the close agreement shown in Figure 1 indicates that dicumyl peroxide is also a quantitative crosslinking agent for the polyisoprene of this work. The close agreement shown in Figure 1 indicates that natural rubber and this synthetic polyisoprene have the same dependence of total crosslinks (physical and chemical) on chemical crosslinks. On the basis of the infrared analysis of this polyisoprene we suggest that dicumyl peroxide is a quantitative crosslinking agent for polyisoprenes consisting of *cis*-1,4, *trans*-1,4, and 3,4 addition structures. The close agreement shown in Figure 1 indicates that crosslinking by polymerization of the vinylidene groups of the 3,4-polyisoprene structures does not contribute significantly to the total number of crosslinks at this moderate level of 3,4 addition structures. Van der Hoff[8] studied the effect of microstructure on the crosslinking reaction of polyioprenes with dicumyl peroxide. He concluded that a polymer with 32% 3,4 addition structure crosslinked at 145°C. with 4 phr of dicumyl peroxide yielded almost the same number of crosslinks as natural rubber, balata, or a high-*cis* 1,4-polyisoprene.

The work of Morton, Bostick, and Clark[5] showed that the polymerization of isoprene, when conducted under highly pure conditions and using

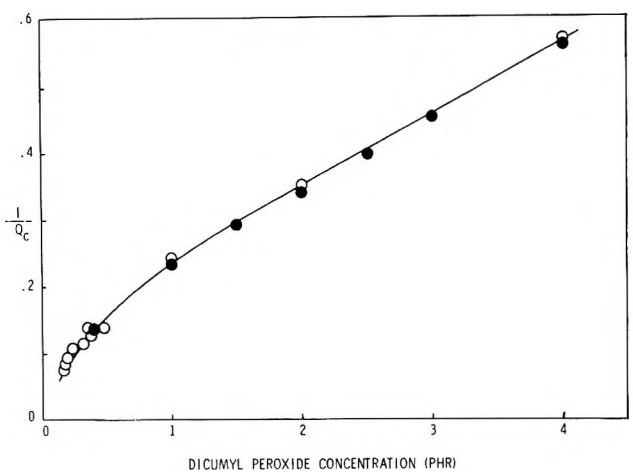

Fig. 1. Dependence of the reciprocal of the corrected swelling value, $1/Q_c$, on the dicumyl peroxide concentration decomposed to crosslink polyisoprenes; (○) this work; (●) natural rubber.[3]

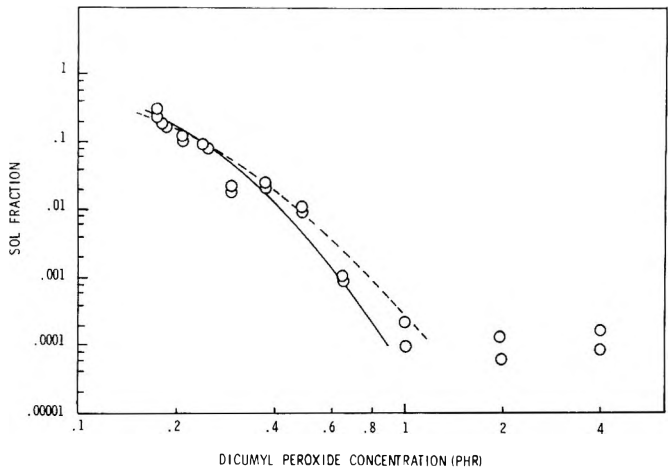

Fig. 2. The dependence of the sol fraction on the dicumyl peroxide concentration decomposed to crosslink polyisoprene: (——) theoretically expected dependence for a homogeneous molecular weight distribution ($\bar{y}_w/\bar{y}_n = 1.0$); (- -) theoretically expected dependence for a Schulz distribution of molecular weights ($\bar{y}_w/\bar{y}_n = 1.1$).

low molecular weight polyisoprenyllithium "seed" as a catalyst in hydrocarbon solvent, leads to a polymer with an extremely sharp molecular weight distribution, since the ratio of viscosity-average to number-average molecular weight approaches one. These findings have been corroborated for the polyisoprene used in this work. A polyisoprene with a sharp or almost homogeneous molecular weight distribution is an ideal material to use for detecting temporary scission since any type of temporary scission accompanying crosslinking would lead to what is equivalent to a broadening of the initial molecular weight distribution.

The experimental sol fraction values obtained from crosslinking the polyisoprene of this work with varying amounts of dicumyl peroxide are plotted in Figure 2. (The small limiting sol fraction at high dicumyl peroxide levels occurs too abruptly to be due to molecular scission,[1] and is most likely due to traces of nonpolymeric material, e.g., residual acetone or 2-phenyl-2-propanol.) The experimental points in Figure 2 are compared with the theoretically expected behavior for a homogeneous distribution of molecular weights (solid line) and also for a Schulz distribution of molecular weights with a weight-average to number-average molecular weight ratio of 1.10 (dashed line). For a homogeneous molecular weight distribution the theoretical behavior[9] is given by

$$q = -\ln S/[y(1-S)] \tag{5}$$

where q is the fraction of the polymeric structural repeat units that have been crosslinked and y is the degree of polymerization. From the stoichiometry of crosslinking polyisoprene by dicumyl peroxide one calculates that

$$q = 0.00504C \tag{6}$$

In Figure 2 the solid line for the homogeneous molecular weight distribution was calculated from eqs. (5) and (6) for a value of $y = \bar{y}_n = 2118$. For a polymer with a Schulz distribution the theoretical behavior[1] is given by

$$q = (1-S^{\epsilon})\epsilon^{-1}(\bar{y}_w)^{-1}S^{-\epsilon}(1-S)^{-1} \tag{7}$$

where $\bar{y}_w$ is the weight-average degree of polymerization and $\epsilon = 1 - (\bar{y}_n/\bar{y}_w)$, where $\bar{y}_n$ is the number-average degree of polymerization. In Figure 2 the dashed line for the Schulz distribution behavior was calculated from eqs. (6) and (7) for $\epsilon = 0.091$, i.e., $\bar{y}_w/\bar{y}_n = 1.1$, and $\bar{y}_w = 2373$. The latter value was selected to give a good fit to the experimental data and was determined by the superposition technique described earlier.[1] Attempts at fitting these data to other theoretical expressions show that molecular weight distributions with weight-average to number-average molecular weight ratios of 1.2 or greater are clearly too broad to be consistent with these data.

The close agreement between the experimental points and theoretical lines over a thousand fold range in sol fraction values in Figure 2 immediately indicates that temporary and permanent scission are negligible here and that the molecular weight distribution of a polyisoprene, of moderate molecular weight and consisting of *cis*-1,4, *trans*-1,4, and moderate amounts of 3,4 addition structures, may, in principle, be calculated from the sol fraction dependence on the amount of dicumyl peroxide decomposed for crosslinking. From the close agreement between the experimental points and theoretical lines of Figure 2 one can estimate that the ratio of weight-average to number-average molecular weight is 1.05 ± 0.05 for this polyisoprene sample. This ratio was also estimated from the slope at various

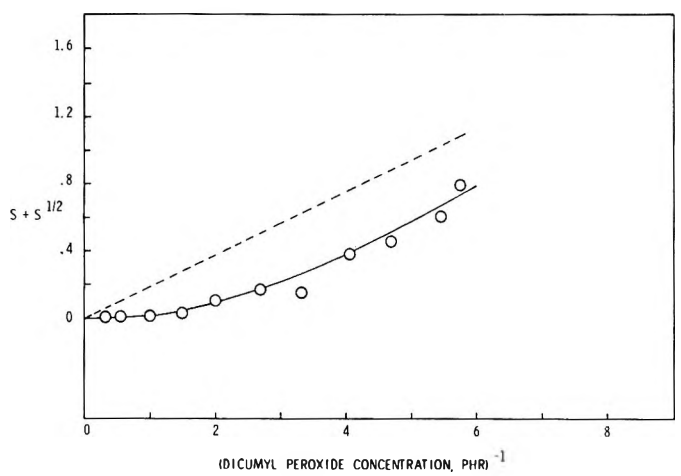

Fig. 3. The relation, suggested by eq. (8), between sol fraction S and dicumyl peroxide concentration decomposed to crosslink polyisoprene: (——) theoretically expected dependence for a homogeneous molecular weight distribution ($\bar{y}_w/\bar{y}_n = 1.0$); (- -) theoretically expected dependence for a most probable distribution of molecular weights ($\bar{y}_w/\bar{y}_n = 2.0$).

sol fraction levels of the experimental points in Figure 2 by a method described earlier.[1] This method also gave a value of 1.05 ± 0.05 for the ratio of weight-average to number-average molecular weight.

The good agreement with theory depicted in Figure 2 for a polyisoprene with an essentially homogeneous distribution of molecular weights when combined with the equally good agreement with theory reported earlier for natural rubber with essentially a random or most probable distribution of molecular weights[1] constitutes an experimental verification of both gel network formation theory and the stoichiometry of crosslinking high molecular weight polyisoprene by dicumyl peroxide, i.e., one chemical crosslink per dicumyl peroxide molecule decomposed.

Figure 3 is a plot of the experimental data in the form suggested by the Charlesby and Pinner theory[10] for the case of simultaneous crosslinking and permanent scission of a polymer with a random or most probable distribution of molecular weights. The solid line is the theoretical behavior expected for a polymer with a homogeneous distribution of molecular weights as given by eqs. (5) and (6) with $y = 2118$. The dashed line is the theoretical behavior[10] expected for a polymer with a random or most probable distribution of molecular weights and is given by

$$S + S^{1/2} = (p/q) + (q\,\overline{y_n})^{-1} \tag{8}$$

where p is the fraction of the polymeric structural repeat units that have undergone permanent scission; in this particular case we have assumed $p = 0$ and $\overline{y_n} = \overline{y_v}/2 = 1059$. The apparent negative intercept obtained by extrapolating the experimental data at high sol values and the positive curvature of the locus of the data points is characteristic of molecular weight distributions that are sharper than the most probable or random distribution and which undergo no scission during crosslinking.

Figure 3 illustrates a point brought out earlier[1] that, in the absence of appreciable chain scission, the apparent intercept obtained by extrapolating experimental data at high sol values is sensitive to the distribution of molecular weights in the polymer used. Recently Bristow[11] reported somewhat higher values for p/q for the natural rubber–dicumyl peroxide system than was reported earlier.[1] His samples consisted essentially of three different molecular weight ranges obtained by milling natural rubber to various degrees. His values of p/q curiously increased with the molecular weight of the rubber samples, and this may be attributed to his assumption that all of his samples had a molecular weight distribution sufficiently close to the most probable one. His reported values of intrinsic viscosity and number-average molecular weight indicate that the molecular weight distribution in his samples broadens as the molecular weight increases. Bristow's data may be accurately fitted with eq. (7), which assumes that chain scission does not occur, with the following, respective values for number-average molecular weight and the ratio, $\overline{y_w}/\overline{y_n}$: 80,000 and 2.13; 201,000 and 2.86; 239,000 and 3.84.

Temporary Scission

In this section we shall attempt to evaluate quantitatively the contribution of temporary scission to these experimental results. Since we have no clear evidence that any temporary scission has occurred at all, our experimental results will only be useful for placing a limit on the maximum amount of temporary scission that could have occurred, consistent with our experimental sensitivity.

The maximum possible effect of temporary scission on our experimental results is assumed to be the altering of the distribution of molecular weights from that of an initially homogeneous distribution to one having a weight-average to number-average molecular weight ratio of 1.05 as observed with the decomposition of up to 1 phr of dicumyl peroxide. It is permissible, for purposes of calculation, to consider the scission processes as occurring first to alter the molecular weight distribution and these, in turn, are then followed by scission-free crosslinking of this altered molecular weight distribution. The extent of alteration of the molecular weight distribution will depend on the amount and specific type of temporary scission taking place. For convenience only, we shall discuss the various types of temporary scission reactions in terms of the most likely chemistry involved, even though only the statistical considerations involved are important in this problem and would still apply if somewhat different chemical details governed scission reactions.

Moore and Scanlan[4] speculated that the scission step involves the unimolecular scission of a polyisoprenyl free radical (I) into a new terminally located polyisoprenyl free radical (II) plus a 1,3-diene structure (III) on the end of the other part of the chain which has undergone scission:

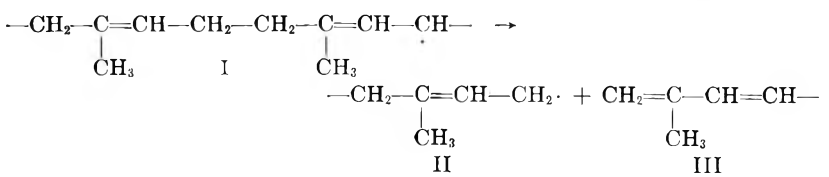

(9)

The scission process will be temporary if species II or III undergo further reactions that will cause them to recombine with other polymeric species. The Appendix describes how the ratio of weight-average to number-average molecular weight is altered for a polymer of a homogeneous molecular weight which has undergone any of the temporary scission processes considered. For the limiting case of small amounts of scission per initial molecule, py, one obtains, in all cases, for the altered ratio of weight-average to number-average degree of polymerization the following expression,

$$\overline{y_w}/\overline{y_n} = 1 + \alpha py \tag{10}$$

where α is a numerical constant depending on the details of the temporary scission process. In Table I the values of α for cases treated in the Appendix are presented, and they fall in the range of $^1/_6$ (for recombination of II with III) to $^8/_3$ (for both II and III recombining with I).

TABLE I
Dependence of the Parameter α of Eq. (10) on the Type of Recombination Reaction

Recombination reaction[a]	α
(II), (III)	$^2/_3$
II + III	$^1/_6$
II + II, (III)	$^5/_{12}$
II + I, III + I	$^8/_3$
II + I, (III)	$^5/_3$
II + II, III + I	$^{17}/_{12}$

[a] Structures in parentheses did not recombine with another polymeric structure, i.e., they remained unreacted or underwent disproportionation with another free radical, e.g., the first line is the case of pure permanent scission with no recombination.

Since the rate constant for termination[12] is of the order of 10^7 times as great as the rate constant for propagation[13] in the free-radical polymerization of dienes and since in butadiene termination is almost exclusively by combination[12] one would expect the most likely reaction following the scission of I to be the recombination of II with another I while III remains unreacted, i.e., the penultimate example in Table I. For this specific case of $\alpha = {}^5/_3$, eq. (10) shows that $py = 0.03$ in order for $\overline{y_w}/\overline{y_n}$ to be equal to 1.05 as observed experimentally. Since $y = 2118$ for the sample used here and $q = 0.00504$ for 1 phr of dicumyl peroxide decomposed we may estimate that the ratio of combined temporary and permanent scissions to crosslinked units, p/q, for this system is less than 0.0028. Over the range of permissible α values this estimate of the upper limit of p/q for scission will vary from 0.0018 to 0.028, depending on the type of temporary scission involved. Hence, we may conclude that temporary scission is negligible for the usually encountered range of molecular weights and that probably less than 0.3% of the polyisoprenyl free radicals (I) undergo scission.

Some Comments

Since this work has shown that both temporary and permanent scission are negligible in the press curing of polyisoprene with dicumyl peroxide, one is left seeking an explanation for the stress relaxation observed by Moore and Scanlan[4] during the crosslinking of stretched natural rubber with dicumyl peroxide in a nitrogen filled apparatus. While there are many factors from a speculative point of view, which might contribute to the stress relaxation observed by Moore and Scanlan, only two are singled out here for consideration, namely, experimental differences between press and nitrogen atmosphere curing conditions and, secondly, difficulties inherent in extracting quantitative information from stress relaxation measurements.

If the nominally oxygen-free nitrogen atmosphere used by Moore and Scanlan contained traces of oxygen, then the observed stress relaxation may be due to oxidative chain scission rather than the reaction shown in eq. (9) as they proposed. The difficulty of attaining a sufficiently low concentra-

tion of oxygen in nitrogen to avoid completely stress relaxation in rubber has been pointed out in the literature.[14] Additionally, oxidative scission and stress relaxation experiments in air[15] have shown that chain scission initiated by oxygen alone is negligible compared to chain scission initiated by the decomposition of added peroxides. It is conceivable that at sufficiently low concentrations of oxygen in nitrogen no stress relaxation would be observed in a reasonable time span for a rubber sample in the absence of free radical initiators; however, in the presence of a free radical initiator, such as dicumyl peroxide, the oxygen content might still be high enough to lead to oxidative scission, detectable by stress relaxation. Experience with a variety of crosslinking systems used under both press and various inert atmospheric conditions teaches that extraordinary precautions are required before the inert atmosphere achieves the same degree of freedom from oxidative degradation effects as is readily achieved in a press.

The history of the utilization of stress relaxation studies to elucidate chemical reactions involving elastomers indicates that such studies have been most fruitful when some chemical evidence regarding the reaction has been combined with a restraint to be satisfied with the qualitative features of the overly simplified models proposed for stress-relaxing systems.[16] The literature contains examples[17,18] where erroneous conclusions on the site of oxidative scission of rubber have been drawn as a result of an undue reliance on the quantitative accord between stress relaxation results and the behavior predicted for a simple model. This past performance suggests that most, if not all, theories for stress relaxation resulting from chemical reactions of a model rubber network cannot be expected to give quantitative agreement with a real system because all pertinent factors have not been adequately included in these simple models.

To analyze their data, Moore and Scanlan utilize the "two-network" theory which, as a consequence of the assumptions inherent in this model, predicts that the stress is unchanged upon adding crosslinks (the second network) to a stretched rubber network (the first network). Now, the two-network theory employs the assumption that the mean-square end-to-end displacement of all network chains between crosslinks in their respective unstrained states is equal to that of the equivalent free polymer chain. While this assumption may or may not be a good approximation for the original first network,[19] it is a less reliable assumption for the second network formed by crosslinking extended polymer chains[20] where non-Gaussian effects may begin to intrude and probably is a poorer assumption for the first network, after the second network crosslinks have been introduced, since the first network must interact to some extent with the second network, i.e., it is unlikely that the two networks can be completely oblivious of each other. Thus, a more refined treatment of the two-network model would predict that the stress will increase or decrease on crosslinking in the strained state, depending on whether the mean-square end-to-end displacement between crosslinks of the first network in its unstrained state increases or decreases upon addition of the second network crosslinks. Theoretical

models proposed for adding crosslinks while in the extended state are apparently still too simple since these models[21,22] predict that the resulting specimen will be isotropic with respect to its equilibrium state of ease (null stress) while experimentally it is observed to be highly anisotropic[23] if crosslinks are introduced in a highly ordered state and probably slightly anisotropic if the crosslinks are introduced at moderate extensions.[21,23]

A second factor which is not taken into consideration in these simple models is the chain entanglement effect.[24,25] The concept of chain entanglements has often been invoked because rubber networks have more elastically effective network chains than can be accounted for by the amount of chemical crosslinks present. It would seem that chain entanglements should be important in several aspects of the elastic properties of rubber in addition to a mere, simple contribution to the number of elastically effective network chains; for instance, the observed difference between experimental stress–strain behavior and that predicted by the kinetic theory of rubber-like elasticity is consistent with the concept that the elastic contribution of chain entanglements decreases on elongation. The vague nature of chain entanglements suggests that they might contribute to stress relaxation in a number of ways.[25]

A chain entanglement will be less effective than a chemical crosslink in contributing to the elastic properties of a rubbery network. In interpreting stress relaxation data it is implicitly assumed that elastically effective network chains resulting from chain entanglements behave exactly like those resulting from permanent chemical crosslinks. This is certainly not completely true. It is further assumed in the interpretation of stress relaxation data that the effectiveness of a given chain entanglement is a constant independent of the amount of chemical crosslinking and this is contrary to studies which showed that, at least for low degrees of crosslinking, the number of potential chain entanglements and probably the effectiveness of a given chain entanglement decrease with the degree of chemical crosslinking.[24,25] On the basis of these latter studies one might expect that chain entanglements associated with the first network could become elastically less effective as the second network crosslinks are introduced and hence might lead to stress relaxation. Because no attempt is made to treat the above complications in the simple two-network theory it is questionable whether the small stress relaxation observed by Moore and Scanlan should be ascribed solely to chain scission.

APPENDIX

We shall estimate here the change in molecular weight distribution accompanying the scission of N polymeric molecules, each of degree of polymerization, y, followed by any of several subsequent recombination steps that might occur. We shall characterize the molecular weight distribution after the scission and recombination steps by the ratio of the resulting weight-average degree of polymerization, $\bar{y}_w$, to the number-average degree of polymerization, $\bar{y}_n$.

Case A: (II), (III)—Permanent Scission

Permanent scission is defined as the case in which neither structure II nor structure III reacts in such a way as to combine with another polymeric species, e.g., if III remains unreacted and II undergoes a disproportionation reaction with another free radical in the system. For the case of permanent scission it has been shown[26,27] that:

$$\overline{y_w}/\overline{y_n} = 2(e^{-py} - 1 + py)(1 + py)(py)^{-2} \qquad \text{(A-1)}$$

where p is the fraction of the polymeric repeat units that have undergone scission. Equation (A-1) may be expressed in series form as

$$\overline{y_w}/\overline{y_n} = 1 + (2/3)py - (1/4)(py)^2 + \ldots \qquad \text{(A-2)}$$

Case B: II + III—Temporary Scission Followed by Recombination of Structures II and III

We consider now the case where a structure II resulting from the scission of a particular structure I recombines on a random basis with a structure III resulting usually from the scission of a different structure I. A nonrandom or selective recombination of II and III from the same I is a simple reversal of the scission process and hence this particular overall combination of scission and recombination would be undetectable.

We shall assume that the scission step is completely random, i.e., each polymeric repeat unit has an equal probability of undergoing scission. The fraction n_b of the molecules that have undergone b scissions after a fraction p of the total number of repeat units have undergone scission is given by the usual expression

$$n_b = p^b(1 - p)^{y-b}y!/(y - b)!b! \qquad \text{(A-3)}$$

We can simplify considerably the computations by considering only those molecules which have never undergone scission and those which have had only one repeat unit undergo scission. The fraction of the molecules having undergone 0 and 1 scission respectively are

$$n_0 = (1 - p)^y \simeq 1 - py$$

$$n_1 = py(1 - p)^{y-1} \simeq py(1 - py) \qquad \text{(A-4)}$$

The approximation is good for the large degrees of polymerization that are of interest. The fraction of the molecules having undergone either no scission or one scission is

$$n_0 + n_1 = (1 - p)^{y-1}(1 - p + py) \simeq 1 - (py)^2 \qquad \text{(A-5)}$$

Since we are concerned here with small values of py equal to about 0.1 scission per molecule it follows from eq. (A-5) that about 99% of the molecules have undergone no scission or only one scission. Accordingly, we shall calculate the ratio $\overline{y_w}/\overline{y_n}$ for this bulk of the material and neglect the fate of those few molecules which have undergone two or more scissions.

This approximation limits the following calculation to small values of py, the number of scissions per molecule.

Out of the original number of molecules, N, in the system, n_1N of them will have undergone one scission to yield $2n_1N$ smaller molecules, hereafter called fragments. Since the scission is random there will be equal numbers ($N_x = 2n_1N/y - 1$) of these fragments for each size from $x = 1$ to $x = y - 1$. (For the sake of simplification and at the expense of exactness we shall not distinguish between scission between polymeric repeat units which leads to integral values of x and scission within the polymeric repeat units which leads to nonintegral values of x. Similarly, we have neglected any difference in probability of scission that an end repeat unit might have compared to the internal repeat units. In any case these omissions are negligible, since we shall later make the assumption that $y \gg 1$ in order to arrive at tractable expressions.) The probability, or mole fraction, of x-mers resulting from the random recombination of fragments by pairs is $(x - 1)/(y - 1)^2$ for $2 \leq x \leq y$ and $(2y - x - 1)/(y - 1)^2$ for $y + 1 \leq x \leq 2y - 2$. The number of x-mers from recombination of the fragments by pairs is

$$N_x = n_1N(x - 1)/(y - 1)^2 \qquad 2 \leq x \leq y$$

and (A-6)

$$N_x = n_1N(2y - x - 1)/(y - 1)^2 \quad y + 1 \leq x \leq 2y - 2$$

The weight-average degree of polymerization of the recombined fragments is

$$\overline{y_w}' = \frac{\sum_x x^2N_x}{\sum_x xN_x} = \frac{\sum_{x=2}^{y} x^2(x - 1) + \sum_{x=y+1}^{2y-2} x^2(2y - x - 1)}{\sum_{x=2}^{y} x(x - 1) + \sum_{x=y+1}^{2y-2} x(2y - x - 1)} \tag{A-7}$$

Carrying out the summations and assuming $y \gg 1$ yields

$$\overline{y_w}' = 7y/6 \tag{A-8}$$

The number-average degree of polymerization of the recombined fragments is y since the number of molecules remains unchanged for the overall process of scission and complete recombination by pairs. The complete system consists of yn_1N parts by weight of these recombined fragments and yn_0N parts by weight of molecules which have not undergone scission hence the weight-average degree of polymerization of the whole system is

$$\overline{y_w} = \frac{\sum_x xw_x}{\sum_x w_x} = \frac{y^2n_0N + (7/6)y^2n_1N}{yn_0N + yn_1N} \tag{A-9}$$

where w_x is the weight of x-mer molecules. Using eq. (A-4) yields

$$\overline{y_w} = y\,\frac{1 + (7/6)py}{1 + py} \simeq y(1 + py/6) \tag{A-10}$$

The number-average degree of polymerization of the whole system is still y, since the number of molecules remains unchanged for the overall process of scission and complete recombination of the fragments by pairs. Hence,

$$\overline{y_w}/\overline{y_n} \simeq 1 + py/6 \tag{A-11}$$

We may expect eq. (A-11) to be an underestimation of $\overline{y_w}/\overline{y_n}$ in the exact treatment since the factor ($^7/_6$) in eq. (A-8) should increase up to a limiting value of $^3/_2$ for larger extents of scission. The general validity of the approximations made in this calculation has been checked by carrying out a similar calculation for the case of permanent scission which yielded

$$\overline{y_w}/\overline{y_n} = 1 + (2/3)py \tag{A-12}$$

which agrees with eq. (A-2) for small values of py.

This type of recombination, II + III, is very unlikely on kinetic grounds. Since the rate constant for termination[12] is of the order of 10^7 times as great as the rate constant for propagation[13] in the polymerization of dienes, it is more likely that the fate of II will be termination rather than addition to III which is present in such small amounts.

Case C: II + II, (III)—Temporary Scission Followed by Recombination of Two Structures of Type II

The case where the recombination step involves the coupling of two type II structures while the type III fragment does not recombine, is resolved by using the same approximations as in case B, and one obtains

$$\overline{y_w}/\overline{y_n} = 1 + (5/12)py \tag{A-13}$$

Case D: II + I, III + I—Temporary Scission Followed by Complete Recombination of the Endlinking Type

Endlinking as defined by Charlesby[28] is the process where either fragment II or III or both combine with a structure of type I. For this process the resulting molecular weight distribution has been reported by Saito[29] and for a polymer with an initial homogeneous degree of polymerization, y, one has

$$\frac{\overline{y_w}}{\overline{y_n}} = \frac{2(1 + py)^2(e^{-py} - 1 + py)(py)^{-2}[1 + (1 - 2\sigma)py]}{[1 + (1 - 2\sigma)py]^2 - 8(1 + py)\sigma^2(e^{-py} - 1 + py)} \tag{A-14}$$

where σ is the fraction of the fragments that react to form endlinks. A series expansion of the exponential terms of eq. (A-14) yields

$$\frac{\overline{y_w}}{\overline{y_n}} = [1 + (1 - 2\sigma)py]\frac{1 + (5/3)py + (5/12)(py)^2 - \ldots}{1 + 2(1 - 2\sigma)py - (1 - 4\sigma)(py)^2 - \ldots} \tag{A-15}$$

When complete endlinking takes place, i.e., both fragments II and III combine with I, $\sigma = 1$ and eq. (A-15) reduces to

$$\overline{y_w}/\overline{y_n} = 1 + (8/3)py + (85/12)(py)^2 - \ldots \tag{A-16}$$

While this is the most likely way for temporary scission to occur exclusively we do not consider this process to be too likely since kinetic grounds again should rule out appreciable contributions from the addition of I to III.

Case E: II + I, (III)—Temporary Scission Followed by Partial Endlinking

If structure I does undergo scission to give structures II and III the most likely subsequent events on kinetic grounds are that III remains unreacted while II undergoes either disproportionation or combination reactions with I, i.e., the scission is partly permanent and partly temporary. This is an example of the endlinking case with σ varying from 0 (pure disproportionation and hence wholly permanent scission) to 1/2 (pure combination). For the case of all structures II combining with structures I, $\sigma = 1/2$ and

$$\overline{y_w}/\overline{y_n} = 1 + (5/3)py + (17/12)(py)^2 - \ldots \qquad \text{(A-17)}$$

This is the most likely process involving the fragments resulting from the scission of I since the literature indicates that in the polymerization of butadiene termination is almost exclusively by combination.[12] For the case of only half the structures II coupling with I, $\sigma = 1/4$ and

$$\overline{y_w}/\overline{y_n} = 1 + (7/6)py + (1/12)(py)^2 - \ldots \qquad \text{(A-18)}$$

Case F: II + II, III + I—Temporary Scission Followed by Recombination and Endlinking

This case is also most unlikely to occur on kinetic grounds but it can be shown that it is the average between cases B and D, and the resulting distribution is expressed by

$$\overline{y_w}/\overline{y_n} = 1 + (17/12)py \qquad \text{(A-19)}$$

Strictly speaking, certain recombinations involving the loss of two free radicals, either by combination or disproportionation, would require a correction to the value of q given by eq. (6) to account for this wastage of free radicals; however, this correction is entirely negligible in the present case, as p/q is only 0.003.

References

1. Scott, K. W., *J. Polymer Sci.*, **58**, 517 (1962).
2. Parks, C. R., and O. Lorenz, *J. Polymer Sci.*, **50**, 287 (1961).
3. Lorenz, O., and C. R. Parks, *J. Polymer Sci.*, **50**, 299 (1961).
4. Moore, C. G., and J. Scanlan, *J. Polymer Sci.*, **43**, 23 (1960).
5. Morton, M., E. E. Bostick, and R. G. Clarke, *J. Polymer Sci.*, **A1**, 475 (1963).
6. Carter, W. C., R. L. Scott, and M. Magat, *J. Am. Chem. Soc.*, **68**, 1480 (1946).
7. Scott, K. W., O. Lorenz, and C. R. Parks, *J. Appl. Polymer Sci.*, **8**, 2909 (1964).
8. Van Der Hoff, B. M. E., *Ind. Eng. Chem. Prod. Res. Develop.*, **2**, 273 (1963).
9. Flory, P. J., *Ind. Eng. Chem.*, **38**, 417 (1946).
10. Charlesby, A., and S. H. Pinner, *Proc. Roy. Soc. (London)*, **A249**, 367 (1959).
11. Bristow, G. M., *J. Appl. Polymer Sci.*, **7**, 1023 (1963).

12. Morton, M., and S. D. Gadkary, paper presented at the 130th American Chemical Society Meeting, Atlantic City, Sept. 1956; *Abstracts of Papers*, p. 25S; R. Livigni, Doctoral Dissertation, Univ. of Akron, 1960.
13. Morton, M., P. P. Salatiello, and H. Landfield, *J. Polymer Sci.*, **8**, 215, 279 (1952).
14. Tobolsky, A. V., I. B. Prettyman, and J. H. Dillon, *J. Appl. Phys.*, **15**, 380 (1944).
15. Tobolsky, A. V., and A. Mercurio, *J. Am. Chem. Soc.*, **81**, 5535, 5539 (1959).
16. Tobolsky, A. V., *J. Appl. Phys.*, **27**, 673 (1956).
17. Berry, J. P., and W. F. Watson, *J. Polymer Sci.*, **18**, 201 (1955).
18. Dunn, J. R., J. Scanlan, and W. F. Watson, *Trans. Faraday Soc.*, **55**, 667 (1959).
19. Treloar, L. R. G., *The Physics of Rubber Elasticity*, Oxford Univ. Press, 1958, Chap. 4.
20. Flory, P. J., *J. Am. Chem. Soc.*, **78**, 5222 (1956).
21. Berry, J. P., J. Scanlan, and W. F. Watson, *Trans. Faraday Soc.*, **52**, 1137 (1956).
22. Flory, P. J., *Trans. Faraday Soc.*, **56**, 722 (1960).
23. Greene, A., and A. Ciferri, *Kolloid-Z.*, **186**, 1 (1962).
24. Scott, K. W., V. R. Allen, and M. Morton, *Proceedings 6th Joint Army Navy Air Force Conference on Elastomer Research and Development*, Boston, Mass., October 1960, p. 78.
25. Allen, V. R., Doctoral Dissertation, Univ. of Akron, 1960.
26. Sakurada, I., and S. Okamura, *Z. Physik. Chem.*, **A187**, 289 (1940).
27. Charlesby, A., *Proc. Roy. Soc. (London)*, **A224**, 120 (1954).
28. Charlesby, A., *Proc. Roy. Soc. (London)*, **A231**, 521 (1955).
29. Saito, O., *J. Phys. Soc. Japan*, **13**, 1451 (1958).

Résumé

On a préparé un polyisoprène possédant une distribution étroite des poids moléculaires au moyen de polyisoprenyl lithium comme catalyseur par une technique d'ensémencement. On a démontré que le peroxyde de dicumyle est un agent de pontage quantitatif par ce polyisoprène. La dépendance de la fraction soluble vis-à-vis de la quantité pontée produite par la vulcanisation à l'aide du peroxyde de dicumyle a été déterminée; elle correspond parfaitement à la théorie de la formation d'un réseau gel. Deux procédés employés pour estimer la largeur de la formation de la distribution des poids moléculaires à partir de la dépendance sol-gel fournissent une valeur de 1,05 ± 0,05 pour le rapport entre les poids moléculaires moyens en poids et en nombre de ces polysioprènes. Cette méthode démontre qu'il est possible de déterminer le poids moléculaire et la distribution des poids moléculaires des polyisoprènes, qui contiennent des structures *cis*-1,4, *trans*-1,4 ou de petites quantités de structures d'addition 3,4 à partir de la dépendance de la fraction sol en fonction de la quantité de peroxyde de dicumyle employée dans le pontage. Une scission de la chaîne moléculaire temporaire ou permanente, pouvant accompagner le pontage par le peroxyde de dicumyle, est à négliger parce qu'on ne trouve pas d'élargissement de la distribution des poids moleculaires par scission de la chaîne. A partir des réactions de recombinaison les plus probables qui peuvent se produire, on estime que moins de 0.3% de peroxyde de dicumyle est consommé dans les réactions conduisant à une scission temporaire de la chaîne moléculaire.

Zusammenfassung

Ein Polyisopren mit enger Molekulargewichtsverteilung wurde mit einem Polyisoprenyllithiumkatalysator nach dem "Keimungs"-Verfahren dargestellt. Dicumylperoxyd erwies sich als quantitatives Vernetzungsmittel für dieses Polyisopren. Die Abhängigkeit der Solfraktion vom Betrag der durch Dicumylperoxydvulkanisation eingeführten Vernetzung wurde bestimmt und stand in ausgezeichneter Übereinstimmung mit der Gelnetzwerk-Bildungstheorie. Zwei Verfahren zur Bestimmung der Breite der Molekulargewichtsverteilung aus der Abhängigkeit des Sols von der Vernetzung liefern

den Wert 1,05 ± 0,05 für das Verhältnis des Gewichtsmittels zum Zahlenmittel des Molekulargew chts für dieses Polyisopren. Diese Ergebnisse zeigen, dass eine Bestimmung des Molekulargewichtes und der Molekulargewichtsverteilung von Polyisoprenen mit *cis*-1,4, *trans*-1,4 oder mässigen Mengen von 3,4 Additionsstrukturen aus der Solabhängigkeit von der Menge des zur Vernetzung benützten Dicumylperoxyd möglich ist. Temporäre oder permanente Molekülkettenspaltung, die zugleich mit der Dicumylperoxydvernetzung auftreten könnte, war vernachlässigbar, da keine durch durch Spaltung bedingte Verbreiterung der Molekulargewichtsverteilung nachgewiesen werden konnte. Für die Reihe der Rekombinationsreaktionen, deren Auftreten am wahrscheinlichsten erscheint, wird ein Verbrauch von weniger als 0,3% des Dicumylperoxyds für Reaktionen, die zu einer temporären Molekülkettenspaltung führen, abgeschätzt

Received June 8, 1964

JOURNAL OF POLYMER SCIENCE: PART A VOL. 3, PP. 569–573 (1965)

Surface Energetics, Adhesion, and Adhesive Joints. III. Surface Tension of Molten Polyethylene

HAROLD SCHONHORN and LOUIS H. SHARPE,
Bell Telephone Laboratories, Incorporated,
Murray Hill, New Jersey

Synopsis

The surface tension of polyethylene has been measured by the ring method over the temperature range 125–193°C. Because of problems with the viscousness of the liquid polyethylene, it was found convenient to use an Instron testing apparatus instead of the usual du Nouy torsion balance. The surface tension of the polyethylene decreased from a value of 28.5 dynes/cm. at 125°C. to 23.3 dynes/cm. at 193°C. with an average temperature coefficient of −0.076 dynes/cm./°C.

Recently, we have extended the adsorption theory of adhesion as applied to the formation of strong adhesive joints.[1,2] A proper understanding of the utility of our particular approach to the formation of strong adhesive joints requires a knowledge of the surface tensions and surface free energies of the liquid adhesives and the solid adherends, respectively. At the present time, the surface free energies of solids are generally inaccessible quantities necessitating the use of various empirical approaches which usually measure a related parameter. The surface tensions at room temperature of ordinary liquid adhesives can usually be measured with considerable ease. Studies at elevated temperatures of the surface tensions of thermoplastic polymers are somewhat more difficult.

This communication reports the surface tension of a molten polyethylene over a wide temperature range as measured with a strain gage-type automatic testing apparatus.[3] The manually operated du Nouy tensiometer was found to be inadequate because of the high viscosity of the liquid polymer and the sluggish response of the film under load, making it difficult to determine the maximum load.[3]

Experimental

The polyethylene employed in this study was supplied by the Union Carbide Plastics Company, Bound Brook, New Jersey. This material, which is designated DYLT, has a number-average molecular weight of 10,000, approximately 45 methyl groups per thousand methylene groups, a melt index of 230, and a room temperature density of 0.917 g./cm.[3]

The strain gage type testing apparatus depicted in Figure 1 is manu-

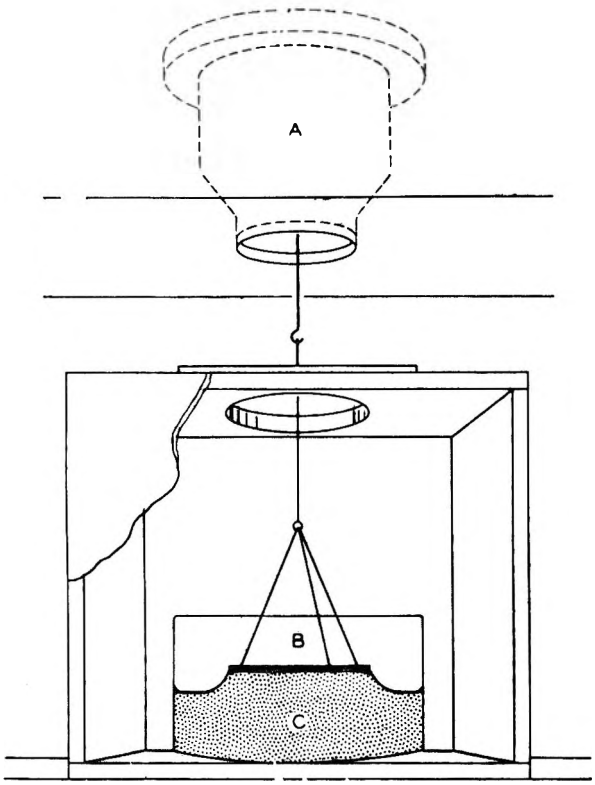

Fig. 1. Molten polyethylene (*C*) contained in a dish which is supported on the moving crosshead of the Instron testing apparatus. Suspended from the load cell (*A*) is a platinum–iridium ring (*B*) which is completely wetted by the polyethylene.

factured by the Instron Engineering Corporation, Canton, Massachusetts. The high sensitivity range of 2 g. full scale (load cell *A*) was used in these experiments. It was only necessary to hang the ring (*B*) from the load cell and immerse it in the liquid (*C*) in a container resting on the lower moving crosshead of the Instron. The load on the ring was continuously recorded as a function of head motion. The lowest available crosshead speed of 0.02 in./min. was used to enable the viscous liquid to relax as it was drawn from the surface. Too rapid pulling may seriously affect the results. The ring and dish containing the molten polyethylene were enclosed in an oven built by Custom Scientific Instrument Company, Kearny, New Jersey, which was controlled to ± 0.5°C. Dry preheated nitrogen was continually passed through the chamber to preclude oxidation of the hot polyethylene. Samples aged for several hours at 166°C. showed no variation of surface tension with time. At 193°C. some increase in surface tension with time was noted if the sample was exposed for longer than 1 hr. Measurements were repeated a minimum of three times for each recorded temperature. The Instron could resolve ± 0.005 g. at its most sensitive setting. The platinum–iridium ring (radius 2.985 cm. and wire diameter 0.0617 cm.)

was manufactured by Englehard Industries, Newark, New Jersey. The liquids used for calibrating this ring were reagent grade and were not purified further.

Results and Discussion

The ring correction data of Harkins and Jordan[4] did not extend sufficiently to employ their tables. The large ring diameter made it necessary to calibrate our system by using liquids of known surface tension. The surface tensions of water, methyl alcohol, ethyl alcohol, ethylene glycol,

TABLE I
Standardization of Ring

Liquid	du Nouy tensiometer surface tension (23°C.), dynes/cm.	Uncorrected Instron surface tension (23°C.), dynes/cm.	Mass, g.	Volume, cm.^{3}	R^3/V	F
Water	72.3	81.4	3.11	3.11	8.55	0.888
Methyl alcohol	21.8	26.6	1.02	1.29	20.6	0.823
Ethyl alcohol	21.4	26.2	1.00	1.27	20.9	0.822
Ethanolamine	48.5	57.8	2.21	2.17	12.2	0.839
Ethylene glycol	45.3	54.2	2.07	1.86	14.2	0.837
Glycerol	63.4	75.3	2.87	2.28	13.1	0.842

glycerol, and ethanolamine were measured by using the standard du Nouy tensiometer, the ring dimensions of which were within those studied by Harkins and Jordan. The measured surface tensions are listed in Table I. The surface tensions of these liquids were then measured in the Instron at 23°C., resulting in the uncorrected surface tensions listed in column 2 of

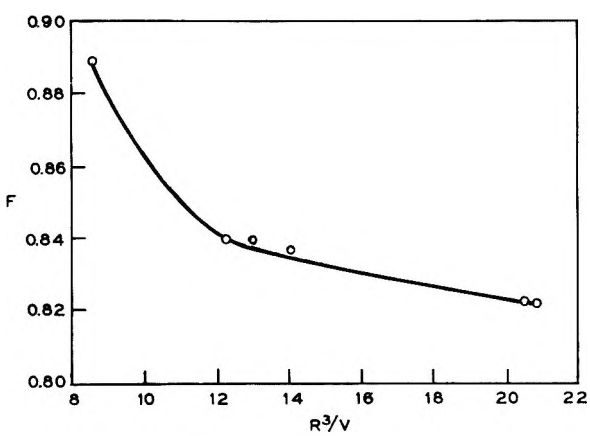

Fig. 2. Plot of the correction factor F vs. R^3/V, where R is the ring radius and V is the volume of the liquid supported by the ring at the recorded maximum. The ratio of the ring radius to the wire radius is 96.8.

Table I. The F factor of Harkins and Jordan, which for this investigation is the ratio of the correct surface tension to the uncorrected Instron value, was treated as usual as a function of R^3/V. R is the radius of the ring and V is the volume of liquid supported by the ring at the temperature of the measurement. A plot of F versus R^3/V is shown in Figure 2. If V is known as a function of temperature, then γ can be calculated as follows:

$$\gamma = (mg/4\pi R)\ F$$

where m is the mass of liquid supported by the ring, g is the gravitational constant, and F is the factor obtained from Figure 2. In this study, no correction was made for the change in the ring radius with temperature since the maximum linear expansion that would be encountered over the range 23–193°C. would be less than 0.2%, and therefore this effect can be neglected.

TABLE II
Results for Molten DYLT Polyethylene

Temp., °C.	Mass, g.	Density, g./cm.^{3}	Volume, cm.^{3}	R^3/V	F	γ, dynes/cm.
125	1.31	0.797	1.645	16.20	0.831	28.5
138	1.26	0.793	1.588	16.75	0.830	27.4
152	1.22	0.788	1.548	17.20	0.828	26.4
166	1.17	0.781	1.498	17.75	0.827	25.3
193	1.10	0.762	1.445	18.42	0.826	23.3

Table II lists the pertinent data for molten polyethylene. The mass of the liquid polymer that is supported by the ring is measured by the load cell in the Instron and recorded automatically on the strip chart. Matsuoka[5] has determined the specific volume of polyethylene as a function of temperature from 20–160°C. Although polyethylenes may differ in

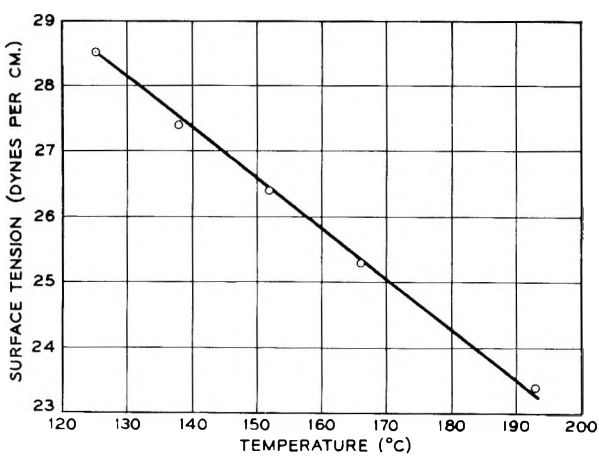

Fig. 3. Surface tension of polyethylene as a function of temperature.

their room temperature densities, their melt densities are essentially the same. Above the melting point the specific volume versus temperature curve is linear. This linearity may be extended to the temperatures we have used, assuming we have avoided any polymer degradation.[6] Hybart and White[7] have measured the surface tension of an unspecified polyethylene by the maximum bubble pressure method and obtained 22.8 dynes/cm. at 150°C. using an estimated density value of 0.85 g./cm.^{3}. This is approximately 7% higher than the density value determined by Matsuoka.[5] Using the correct density, their surface tension value would have approached our value of 26.4 dynes/cm.

Figure 3 is a plot of the surface tension of molten polyethylene as a function of temperature from 125–193°C. For this particular polyethylene, the temperature coefficient was −0.076 dyne/cm./°C., which is quite reasonable since paraffin has a value of −0.0798 dyne/cm./°C. in the melt.[8]

References

1. Sharpe, L. H., and H. Schonhorn, *Adv. Chem. Series*, **43**, 189 (1964).
2. Schonhorn, H., and L. H. Sharpe, *J. Polymer Sci.*, **B2**, 719 (1964).
3. Newman, S. B., and W. M. Lee, *Rev. Sci. Instr.*, **29**, 786 (1958).
4. Harkins, W. D., and H. F. Jordan, *J. Am. Chem. Soc.*, **52**, 1751 (1930).
5. Matsuoka, S., *J. Polymer Sci.*, **57**, 569 (1962).
6. Matsuoka, S., private communication.
7. Hybart, F. J., and T. R. White, *J. Appl. Polymer Sci.*, **3**, 118 (1960).
8. Partington, J. R., *Treatise on Physical Chemistry*, Vol. II, Longmans, Green, London, 1951, p. 194.

Résumé

On a calculé la tension superficielle du polyéthylène fondu par la méthode de l'anneau à des températures variant de 125° à 193°C. Par suite de la grande viscosité du polyéthylène fondu, on a utilisé un appareil d'essai Instron plutrt que la balance de torsion traditionnelle de du Nouy. La tension superficielle du polyéthylène diminue de 28.5 dynes/cm à 125°C jusqu'à 23.3 dynes/cm à 193°C, le coefficient thermique étant voisin de −0.076 dynes/cm/°C.

Zusammenfassung

Die Oberflächenspannung von Polyäthylen wurde nach der Ringmethode im Temperaturbereich von 125°C–193°C gemessen. Wegen der durch die hohe Viskosität des flüssigen Polyäthylens auftretenden Probleme erwies sich die Anwendung eines Instron-Testapparates anstelle der üblichen Nouy-Torsionswaage als angebracht. Die Oberflächenspannung von Polyäthylen nahm von einem Wert von 28,5 dyn/cm bei 135°C auf 23,3 dyn/cm bei 193°C mit einem mittleren Temperaturkoeffizienten von −0,076 dyn/cm.°C ab.

Received June 12, 1964

JOURNAL OF POLYMER SCIENCE: PART A VOL. 3, PP. 575–581 (1965)

Copolymerization of Secondary Fumarates with Styrene

L. F. VANDER BURGH and C. E. BROCKWAY, *Research Center, A. E. Staley Manufacturing Company, Decatur, Illinois*

Synopsis

Reactivity ratios for the copolymerization of styrene (M_1) with some secondary butyl fumarates (M_2) indicate that the r_1 values are more dependent on the inductive effect of the alkyl groups than on the steric effect and that the r_2 values approach zero. Copolymerization rates of the secondary dialkyl fumarates with 65 mole-% styrene were found to be consistent with the r_1 values and the rate of styrene homopolymerization. However, mono(1-methylpropyl) fumarate copolymerized with styrene at a rate more than twice that of styrene homopolymerization; this agrees very well with the modified copolymer equation which is obtained when the terms of the general copolymerization equation which contain r_2 are set equal to zero.

INTRODUCTION

Glycols having secondary hydroxyl groups are widely used in the preparation of fumarate polyester resins. The polyfunctionality of such resins, however, makes a direct study difficult and relatively little information about the copolymerization of comparable monofunctional examples is available. Consequently, it was of interest to study the copolymerization characteristics of some secondary butyl fumarates. Mono(1-methylpropyl), bis(1-methylpropyl), and bis(2-chloro-1-methylpropyl) fumarate were chosen as model compounds and copolymerized with styrene at 60°C. The reactivity ratios and rates of copolymerization of the monomer systems were measured by the isolation and carbon analysis of the copolymers.

EXPERIMENTAL

Materials

Diethyl Fumarate. Diethyl fumarate (Eastman Kodak) was vacuum-distilled twice. The center cut distilling at 112–112.5°C. at 20 mm. pressure was collected, n_D^{30} 1.43637.

Bis(1-methylpropyl) Fumarate. Bis(1-methylpropyl) fumarate was prepared by the acid-catalyzed esterification of fumaric acid with an excess of *sec*-butyl alcohol, the reaction being driven to completion by azeotropic removal of the water with benzene. The product was vacuum-distilled

twice, and a center cut distilling at 153.5–154°C. at 23 mm. was collected, n_D^{30} 1.43801.

ANAL. calc.: C, 63.13%; H, 8.83%. Found: C, 62.89%; H, 8.93%.

Mono(1-methylpropyl) Fumarate. Maleic anhydride (1 mole) was heated to 120°C. in a three-necked flask equipped with a stirrer, condenser, and dropping funnel. *sec*-Butyl alcohol (1 mole) was added by means of the dropping funnel over a period of 30 min. while the temperature was maintained at 115–120°C. After an additional 30 min. at that temperature, the maleate was isomerized to fumarate by PCl_3(7 drops) at 110–115°C. for 15 min. As soon as the mixture had been cooled to ambient temperature in an ice bath it was poured into a slight excess of 10% Na_2CO_3 solution and washed twice with 200-ml. portions of ether to remove the dialkyl fumarate. The aqueous solution was carefully acidified with hydrochloric acid and extracted twice with 200-ml. portions of ether. After drying over anhydrous $MgSO_4$ the ether solution was cooled at −30°C. for 5–6 hr., filtered to remove any residual fumaric acid, evaporated under vacuum on a rotary evaporator at room temperature, and stored at −30°C. An infrared spectrum indicated that the product contained no maleates. It had a refractive index n_D^{30} of 1.45193.

ANAL. Calc.: C, 55.80%; H, 7.03%. Found: C, 56.06%; H, 6.89%.

3-Chloro-2-butanol. Addition of hypochlorous acid to 2-butene (Phillips pure grade) at 5–10°C. was used to prepare 3-chloro-2-butanol. The product was isolated by steam-distilling the reaction mixture, saturating the condensate with NaCl, and vacuum-distilling the dried oily layer. A fraction distilling at 56–58°C. at 29 mm. pressure was collected and used without further purification.

Bis(2-chloro-1-methylpropyl) Fumarate. A mixture of 99 g. (0.647 mole) of fumaryl chloride and 147.5 g. (1.36 mole) of 3-chloro-2-butanol was placed in a three-necked, 250-ml. flask fitted with a thermometer extending into the liquid, a condenser, and a glass capillary tube connected to a dry nitrogen supply. The reaction mixture was heated for 2 hr. at 40–50°C. at a pressure of ~ 130 mm. followed by 5 hr. at 70 mm. The product was distilled under vacuum and redistilled through a spinning band column fitted with a gold-plated Monel band.

An oil was obtained which distilled at 133.5–135°C. at 0.3 mm., n_D^{30} 1.47253.

ANAL. Calc.: C, 48.50%; H, 6.11%; Cl, 23.86%. Found: C, 48.38%; H, 6.04%; Cl, 23.94%.

Styrene. Styrene (Eastman white label) was fractionally vacuum-distilled, and a center cut distilling at 69–70°C. at 52 mm. was collected and stored under refrigeration until used.

2,2′-Azobis(2-methylpropionitrile). Eastman (white label) 2,2′-azobis-(2-methylpropionitrile) was recrystallized from ether, dried *in vacuo*, and stored in the dark until used.

Procedures

Reactivity Ratios. Appropriate quantities of the monomers were weighed into a glass-stoppered Erlenmeyer flask and a quantity of initiator was added to give about 1 g. of 2,2′-azobis(2-methylpropionitrile) per liter of monomers. Approximately 10-g. portions of the master solution were then transferred to tared Pyrex tubes which had a standard taper joint and a constriction near the top. The tubes were reweighed and connected to a vacuum system; their contents were frozen in Dry Ice–acetone. The tubes were evacuated to about 10^{-4} mm. of Hg, closed from the system, and the contents allowed to melt. After a minimum of three freeze-thaw-degassing cycles the samples were sealed from the system at the constriction and placed in a constant temperature bath at 60 ± 0.02°C. for a sufficient time to produce about 5–10 wt.-% of polymer.

Immediately after their removal from the bath the tubes were opened and their contents washed into tared 400 ml. beakers with 10–20 ml. of solvent (benzene for the dialkyl fumarates and methyl ethyl ketone for the monoalkyl fumarates) containing 0.1% *p-tert*-butyl catechol and precipitated by the slow addition of 350–400 ml. of nonsolvent (methanol for the dialkyl fumarates and a 70/30 mixture of benzene and hexane for the monoalkyl fumarates).

The samples were redissolved in 20–30 ml. of solvent and reprecipitated. When the polymers had been precipitated three times, they were dried for a minimum of 16 hr. in a vacuum oven at 40–50°C. and reweighed.

Carbon analyses of the samples (performed by Clark Microanalytical Laboratory, Urbana, Illinois) were used to calculate the amounts of styrene and fumarates in the polymers.

The reactivity ratios for the styrene (r_1) and fumarates (r_2) were calculated by graphically solving eq. (1):[1]

$$(F/f)(f - 1) = r_1(F^2/f) - r_2 \tag{1}$$

where F is the average molar ratio of styrene to fumarate monomer and f is the molar ratio of styrene to fumarate in the polymer.

The azeotropic copolymerization composition was calculated from eq. (2):[2]

$$\text{Mole-\% } M_1 = (1 - r_2)/[(1 - r_1) + (1 - r_2)] \times 100 \tag{2}$$

Rates of Copolymerization. Polymerizations were run in duplicate at 60 ± 0.02°C. according to the method described above except that 25-g. samples were used. The absence of an induction period or Trommsdorff acceleration (during the portion of the polymerization being studied) was confirmed by dilatometry. Densities of the monomer mixtures were measured at 60°C. and used to convert concentrations from a weight/weight basis to a weight/volume basis.)

The average rate of polymerization was calculated by multiplying the amount of polymer (in grams per liter of monomers) by the moles of mono-

mer per gram of polymer (from carbon analysis of the polymer) and dividing by the time in seconds.

RESULTS AND DISCUSSION

Reactivity Ratios

Monomer–polymer compositions of various fumarates copolymerized with styrene are given in Table I.

Reactivity ratios were calculated from the compositions of Table I by the graphical solution of eq. (1) and are given in Table II along with selected values from the literature.[4]

TABLE I
Monomer–Polymer Compositions of Styrene–Fumarate Systems[a]

Fumarate	Average ratio (styrene)/(fumarate) in monomer	Ratio (styrene)/(fumarate) in polymer
Diethyl	4.04, 4.03	2.21, 2.31
Diethyl	0.977, 0.980	1.39, 1.29
Diethyl	0.266, 0.267	1.10, 1.05
Bis(1-methylpropyl)	3.96, 3.96	2.95, 3.01
Bis(1-methylpropyl)	1.00, 1.00	1.58, 1.51
Bis(1-methylpropyl)	0.237, 0.246	1.09, 1.12
Mono(1-methylpropyl)	4.17, 4.20	2.46, 2.38
Mono(1-methylpropyl)	1.86, 1.86	1.70, 1.64
Mono(1-methylpropyl)	0.98, 0.98	1.45, 1.32
Mono(1-methylpropyl)	0.254, 0.255	1.08, 1.11
Bis(2-chloro-1-methylpropyl)	9.08, 9.09	3.17, 3.20
Bis(2-chloro-1-methylpropyl)	3.53, 3.53	1.85, 1.97
Bis(2-chloro-1-methylpropyl)	1.82, 1.90	1.61, 1.68
Bis(2-chloro-1-methylpropyl)	0.264, 0.249	1.30, 1.24

[a] At 60°C. with 1 g./1.2, 2′-azobis(2-methylpropionitrile).

TABLE II
Reactivity Ratios of Styrene (M_1)–Fumarate (M_2) Systems at 60°C.

Fumarate	r_1	r_2	Azeotropic copolymerization composition M_1, mole-%	M_2, mole-%
Dimethyl[a]	0.21 ± 0.02	0.025 ± 0.02	55	45
Monoethyl[a]	0.18 ± 0.10	0.25 ± 0.10	48	52
Diethyl[a]	0.30 ± 0.02	0.07 ± 0.007	57	43
Diethyl	0.31 ± 0.02	0.05 ± 0.02	57	43
Mono(1-methylpropyl)	0.34 ± 0.03	0 ± 0.01	60	40
Bis(1-methylpropyl)	0.50 ± 0.03	0 ± 0.01	66.5	33.5
Bis(2-chloro-1-methylpropyl)	0.25 ± 0.02	−0.05 ± 0.01	60	40

[a] Data of Mayo and Walling.[4]

The techniques used in this study are believed to be reliable, since measurements on the styrene–diethyl fumarate system agree quite well with the value given in the literature.[4] However, the monomer–polymer compositions of the styrene–bis(2-chloro-1-methylpropyl) fumarate system did not give a good straight-line relationship when plotted according to eq. (1) and gave a negative value for r_2. A negative r_2 value is not theoretically possible, but is given here as it best describes the system.

The values in Table II show that r_1 increases as the size and electron-donating ability of the alkyl groups increase. However, the electron donating ability of the alkyl groups is probably more important than the steric factor, since the electron-withdrawing chloro groups in bis(2-chloro-1-methylpropyl) fumarate increase the bulk, but still reduce r_1 to a value which is considerably smaller than that of its nonhalogenated analog. Since only the methyl and ethyl fumarates have measurable r_2 values it can be concluded that the higher alkyl fumarates have very little tendency to homopolymerize and their azeotropic compositions are determined by the r_1 values.

Rates of Copolymerization

In Table III are given the copolymerization rates of some fumarates with styrene.

TABLE III
Copolymerization Rates of Fumarates with 65 Mole-% Styrene at 60°C.[a]

Fumarate	Rate × 10^4, mole/l./sec.
Diethyl[b]	4.7 ± 0.1
Mono(1-methylpropyl)	12.8 ± 0.2
Bis(1-methylpropyl)	2.3 ± 0.1
Bis(2-chloro-1-methylpropyl)	5.6 ± 0.1

[a] With 1 g./l. 2,2′-azobis(2-methylpropionitrile).
[b] Data of Walling and McElhill.[5]

The diethyl, bis(1-methylpropyl) and bis(2-chloro-1-methylpropyl) fumarates copolymerize with styrene at rates which are consistent with the reactivity ratios and electron donating ability of the alkyl groups. However, mono-(1-methylpropyl) fumarate, though it homopolymerizes at a negligible rate ($\sim 0.03 \times 10^{-5}$ mole/l./sec.) copolymerizes with styrene much faster than the dialkyl fumarates and over twice as fast as styrene homopolymerizes under the same conditions (5.9×10^{-5} mole/l./sec.)[5]

Thermal cross-initiation cannot account for the large difference in rate between the initiated monoalkyl copolymerization and the initiated styrene homopolymerization, as the thermal copolymerization rate of 65 mole-% styrene with the monoalkyl fumarate at 60°C. was only 0.6×10^{-5} mole/l./sec. At a fixed rate of initiation the copolymerization of monomers of very different reactivity usually proceeds at a rate slower than the mean of the rates for the separate polymerizations, since the increased rates of

propagation are more than offset by a large cross-termination rate.[6] If we assume that the fumarate radical attacks its own monomer at a negligible rate, that the fumarate radical attacks styrene monomer much faster than the styrene radical attacks fumarate monomer, and that termination involving fumarate radicals is negligible, then the following equation can readily be derived:[4, 7]

$$-d([S] + [F])/dt = \{[S] + (2/r_1 [F])\} (k_p^2 V_i/2k_t)^{1/2} \quad (3)$$

where [S] is the styrene concentration, [F] the fumarate concentration, V_i the rate of initiation, k_p the rate constant for styrene propagation, and k_t the rate constant for styrene radical coupling. This equation is identical to that obtained from the general copolymerization equation when the terms containing r_2 are set equal to zero.[4,7] From the rate of styrene homopolymerization with 1 g./l. of 2,2′-azobis(2-methylpropionitrile) (5.9×10^{-5} mole/l./sec.)[5] and concentration of pure monomer (8.35 mole/l.), the second term of eq. (3) can be calculated as:

$$(k_p^2 V_i/2k_t)^{1/2} = V_p/[M] \quad (4)$$

At 65 mole-% styrene [S] is 4.81 and [F] is 2.58, and eq. (3) gives a value of 1.41×10^{-4} mole/l./sec. for the maximum rate of copolymerization at 60°C. with 1 g./l. of 2,2′-azobis(2-methylpropionitrile). Since the measured value (1.28×10^{-4} mole/l./sec.) agrees very well with the calculated value, it would appear that the relatively large copolymerization rate arises from the fast addition of monoalkyl fumarate radicals to styrene monomer, which in turn keeps the fumarate radical concentration very small, makes termination involving fumarate radicals negligible, and allows the fast cross-propagation terms to increase the overall rate.

It might be inferred from the values in Table III that when styrene is copolymerized with a carboxyl-terminated fumarate polyester the monoalkyl fumarates would be incorporated into the polymer much more rapidly than the dialkyl fumarates. However, since the rapid copolymerization of the monoalkyl fumarate arises from a lack of cross-termination instead of a rapid attack by styrene radicals on fumarate monomer, the ratio of monoalkyl to dialkyl fumarates incorporated into the copolymer would be determined by the r_1 values, when $r_2 = 0$, and not by the overall copolymerization rates.

References

1. Fineman, M., and S. D. Ross, *J. Polymer Sci.*, **5**, 259 (1950).
2. Billmeyer, F. W., *Textbook of Polymer Chemistry*, Interscience, New York, 1957, pp. 221–227.
3. Pinner, S. H., *A Practical Course in Polymer Chemistry*, Pergamon Press, New York, 1961, pp. 90–95 and 114–131.
4. Mayo, F. R., and C. Walling, *Chem. Rev.*, **46**, 191 (1950).
5. Walling, C., and E. A. McElhill, *J. Am. Chem. Soc.*, **73**, 2819 (1951).
6. Flory, P. J., *Principles of Polymer Chemistry*, Cornell Univ. Press, Ithaca, N. Y., 1953, pp. 199–203.
7. Walling, C., *J. Am. Chem. Soc.*, **71**, 1930 (1949).

Résumé

Les rapports de réactivité pour la copolymérisation du styréne (M_1) avec certains fumarates de butyle secondaire (M_2) montrent que les valeurs de r_1 dépendent plus de l'effet inductif des groupements alcoyles que de l'effet stérique et que les valeur r_2 sont proches de zéro. Les vitesses de copolymérisation des fumarates de dialcoyl secondaire avec 65 moles-% de styréne sont en accord avec les valeurs de r_1 et la vitesse de l'homopolymérisation du styréne. Cependant, le mono fumarate de (1-méthylpropyle copolymérise avec le styréne a une vitesse supérieure a deux fois celle de l'homopolymérisation du styréne et est en parfait accord avec l'equation modifiée que l'on obtient en posant égal a zéro les termes de l'équation générale de copolymérisation qui contiennent r_2.

Zusammenfassung

Reaktivitätsverhältnisse für die Copolymerisation von Styrol (M_1) mit einigen Sekundäar-butylfurmaraten (M_2) zeigen, dass die r_1-Werte mehr vom induktiven Effekt der Alkylgruppe als vom sterischen Effekt abhängen und sich die r_2-Werte null nähern. Copolymerisationsgeschwindigkeiten der Sekundäar-dialkylfumarate mit 65 Mol-% Styrol waren mit ihren r_1-Werten und der Geschwindigkeit der Styrolhomopolymerisation konsistent. Mono(1-methyl-propyl)fumarat jedoch copolymerisiert mit Styrol mit einer mehr als doppelt so grossen Geschwindigkeit als der der Styrolhomopolymerisation und zeigt gute Übereinstimmung mit der modifizierten Copolymergleichung, welche durch Nullsetzen der Terme der allgemeinen Copolymergleichung, die r_2 enthalten, erhalten werden.

Received July 23, 1963
Revised July 20, 1964

JOURNAL OF POLYMER SCIENCE: PART A VOL. 3, PP. 583–591 (1965)

Copolymerization of 4-Cyclopentene-1,3-dione with Styrene*

ANTHONY WINSTON and F. LYNN HAMB,† *Department of Chemistry, West Virginia University, Morgantown, West Virginia*

Synopsis

The copolymerization of 4-cyclopentene-1,3-dione (D) with styrene (S) is reported. The copolymers were prepared by heating sealed tubes containing the monomer feeds and azobisisobutyronitrile. The copolymers exhibited infrared bands for the phenyl and β-diketone groups, indicating that copolymerization had occurred. The copolymers were completely insoluble in all solvents. Some swelling was observed in tetrahydrofuran, nitrobenzene, and aqueous sodium hydroxide. From the compositions of the copolymers, as determined from the carbon and hydrogen analyses, it was found that the copolymers were about 40 mole-% styrene over an appreciable range of feed compositions (0.1–0.6 mole fraction styrene). The results at styrene feeds <0.5 were in general agreement with the equation: $d[D]/d[S] = 1^1/_2 + (k_{DD}/2k_{DC}K[S])$. This equation was derived on the basis of monomer complex (C) participating in the propagation and a penultimate effect preventing the occurrence of a sequence of three dione units.

INTRODUCTION

The copolymerization of 4-cyclopentene-1,3-dione with acrylonitrile and methyl methacrylate was reported in a previous paper of this series.[1] These copolymerizations proceeded normally, allowing the determination of reactivity ratios for each system and the assignment of Q and e values to 4-cyclopentene-1,3-dione. In this paper the copolymerization of 4-cyclopentene-1,3-dione with styrene is reported, and a possible correlation of the results with the copolymerization equation, through considerations of complex formation and penultimate unit effects, is suggested.

EXPERIMENTAL

Materials

The preparation and purification of 4-cyclopentene-1,3-dione was described in the previous communication.[1]

Styrene (The Bordon Chemical Company) was distilled under nitrogen at 72°C./65 mm. after the addition of a trace of sulfur. A middle fraction was collected and used immediately.

* Taken from the Ph.D. Dissertation of F. Lynn Hamb (1963).

† NDEA Predoctoral Fellow 1960–1963.

Polymerization Procedure

The desired ratio of styrene and 4-cyclopentene-1,3-dione was dissolved in the minimum amount of pure dry benzene. The solution was placed in a thick-walled tube and 0.05 mole-% of the charge of azobisisobutyronitrile was added. After degassing by alternate cooling and warming under a low pressure of nitrogen, the tube was sealed at 0.1–0.2 mm. and placed in a constant temperature bath at 50 ± 0.1°C. The contents were stirred with a small bar magnet until the reaction had proceeded to an extent of 2 or 3%, as estimated by the precipitation of the insoluble copolymer. The tube was cooled to room temperature and opened. The mixture was poured into a nonsolvent consisting of methanol for high styrene content, ethyl ether for low styrene content, or a mixture of methanol and ethyl ether for intermediate styrene content, and the flocculent tan copolymer was allowed to settle. The polymer was collected by filtration, washed with ethyl ether, dried in air at room temperature, and weighed to determine the per cent conversion.

Characterization of the Copolymers

The characteristic infrared absorptions of the phenyl group at 1650 cm.$^{-1}$ and of the β-diketone group at 1580 cm.$^{-1}$ indicates that both styrene and 4-cyclopentene-1,3-dione have entered the copolymer.

The solubility properties of all copolymers, regardless of the feed compositions, are nearly identical. Common solvents such as benzene, toluene, acetone, methyl ethyl ketone, diethyl carbonate, dimethylformamide, dimethyl sulfoxide, and chloroform have no noticeable effect on the copolymers. They are swollen slightly by the action of tetrahydrofuran, nitrobenzene, and aqueous sodium hydroxide. Molecular weight studies were not feasible because of the extreme insolubility of the copolymers. The

TABLE I
Reactivity Ratio Data for the Copolymerization of Styrene(S) and 4-Cyclopentene-1,3-dione(D)

f_1 Mole fraction S in feed	Time, min.	Conversion, %	Analysis C, %	Analysis H, %	F_1 Mole fraction S in copolymer
0.96[a]	150	1.54	83.09	7.82	0.61
0.90[a]	50	0.87	78.51	6.44	0.52
0.80[a]	130	2.50	77.34	7.11	0.48
0.65[b]	100	1.39	75.87	6.40	0.43
0.35[b]	15	1.46	74.81	7.62	0.40
0.25[b]	60	2.35	74.94	6.35	0.40
0.15[b]	150	2.24	73.16	6.17	0.34
0.08[b]	220	2.06	74.21	6.31	0.37
0.04[b]	45	2.15	73.33	6.24	0.35

[a] No solvent.
[b] Benzene solvent.

swelling action of sodium hydroxide solution indicates the presence of weakly acidic structures characteristic of enolic β-diketones. The swelling effect of tetrahydrofuran and nitrobenzene suggests that there may be cross-linking between polymer chains, perhaps through chain transfer reactions with the active hydrogens of the β-diketone structure. The amorphous, hard polymers are not fusible when heated in a Bunsen flame, but form a brown granular material.

Analysis of the Copolymers

The copolymers were crushed to a fine powder, extracted with refluxing benzene in a Soxhlet apparatus for 8 hr., and dried in air under reduced pressure for 6 hr. The composition of each sample was calculated from the elemental analysis for carbon and hydrogen as determined by Galbraith Laboratories, Inc., Knoxville, Tennessee. The results are reported in Table I.

RESULTS

The mole fraction of styrene in the copolymer (F_1) is plotted in Figure 1 as a function of the mole fraction of styrene in the feed (f_1). Treatment of the copolymer equation by the method of Mayo and Lewis[2] (Fig. 2) and by the method of Fineman and Ross[3] (Fig. 3) afforded values of r_1 and r_2 (Table II).

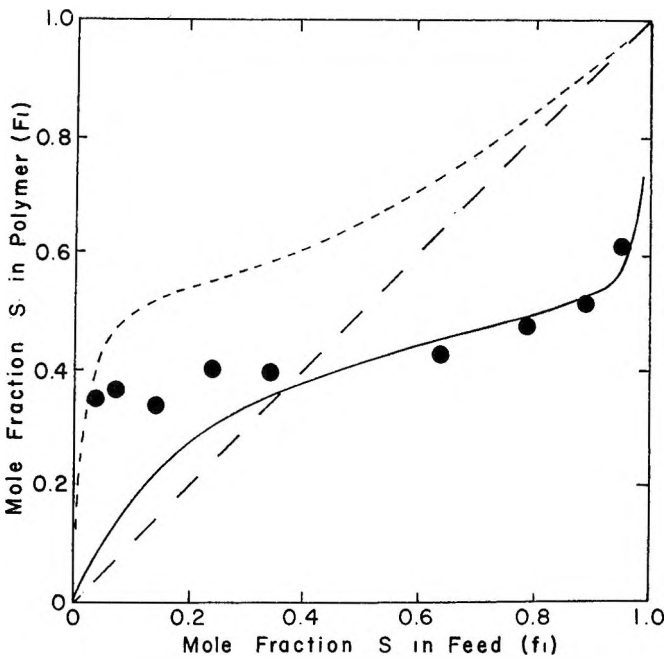

Fig. 1. Copolymerization of styrene (S) with 4-cyclopentene-1,3-dione (D): (——) calculated for $r_1 = 0.02$, $r_2 = 0.4$; (- -) calculated for $r_1 = 1.5$, $r_2 = 0.033$ as determined from the Q and e values of the monomers.

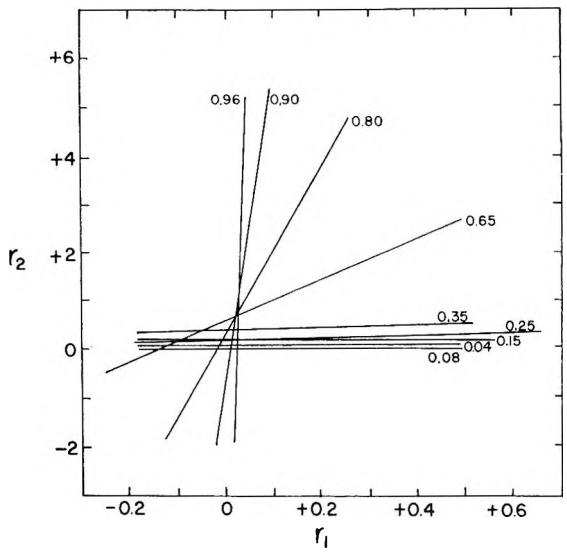

Fig. 2. Mayo-Lewis plot for determining reactivity ratios. The number at each line is the feed composition in mole fraction of styrene. $r_1 = 0.015 \pm 0.015$; $r_2 = 0.4 \pm 0.35$.

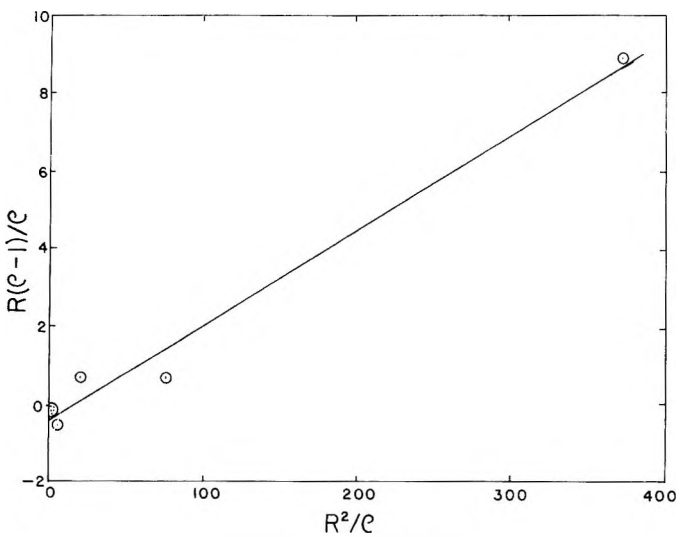

Fig. 3. Fineman-Ross plot for determining reactivity ratios. $r_1 = 0.024$; $r_2 = 0.415$.

By using the IBM 1620 digital computer, numerous combinations of reactivity ratios from $r_1 = 0$–0.15 and $r_2 = 0.01$–0.7 were tested in the copolymer equation, but no combination was found which produced a curve fitting the data over the entire composition range. The unbroken curve of Figure 1, obtained from the reactivity ratios listed in Table II, seemed to be about the best overall fit. Agreement is good in the region above 0.5

TABLE II
Reactivity Ratios for the Copolymerization of Styrene(M_1)–4-Cyclopentene-1,3-dione(M_2)

Method	r_1	r_2
Mayo-Lewis	0.015 ± 0.015	0.4 ± 0.35
Fineman-Ross	0.024	0.415
Curve fitting	0.02	0.4
Alfrey-Price	1.5	0.033

mole fraction of styrene in the feed, but considerable departure from the curve is observed at concentrations below this value.

From the Q and e values of 4-cyclopentene-1,3-dione (Q = 0.20, e = +1.42)[1] and styrene (Q = 1.0, e = −0.8),[4] reactivity ratios were calculated according to the method of Alfrey and Price.[5] These values of r_1 and r_2 (Table II) and the resulting copolymer composition curve (broken curve in Fig. 1) are not consistent with the observed results.

DISCUSSION

The failure to reproduce the experimental curve by the curve-fitting method and the considerable divergence between the experimental curve and the curve predicted by the Q and e values indicate that the copolymer composition equation does not apply in a simple way to the styrene(S)–4-cyclopentene-1,3-dione(D) system. This is further indicated by the ability to fit a curve to the experimental data at high styrene, but not at low styrene feeds. Also, in Figure 2, the r_2 versus r_1 lines seem to fall into two groups: high styrene feeds (0.96, 0.90, 0.80, and 0.65) and low styrene feeds (0.35, 0.25, 0.15, 0.08, and 0.04).

If the structure of the copolymers approached perfect alternation of the monomer units (structure I), F_1 would be 0.5. If II or III represented the structure, F_1 would be 0.33 or 0.40, respectively.

$$\text{-(S—D)-}_n \qquad \text{-(D—S—D—)}_n \qquad \text{-(D—S—D—S—D)-}_n$$
I II III

The occurrence of F_1 values between 0.3 and 0.4 in the region of low to medium values of f_1 (Fig. 1) indicates that the copolymers are partially alternating, and that the average structure is best represented by II or III. The results may be compared with those of Fordyce and Ham,[6] who found that in the copolymerization of the styrene–fumaronitrile system the fumaronitrile content of the copolymers approached 40 mole-% with increasing concentration in the feed.[7] The dione case is different in that it is the styrene concentration that approaches 40 mole-%.

The copolymerization of styrene with sulfur dioxide and of ethylene with carbon monoxide, both of which provide highly alternating copolymers have been interpreted by Barb[8,9] on the basis of a copolymerization between a 1:1 complex and the monomer present in the greater amount. In the case of the styrene(S)–sulfur dioxide (SO_2) system, a 1:1 complex of

TABLE III
Feed and Copolymer Composition Data for the System
Styrene(S)–4-Cyclopentene-1,3-dione(D)

Monomer feed				Copolymer	
f_1	[S], mole/l.	[D], mole/l.	1/[S]	F_1	n
0.35	2.08	3.87	0.418	0.40	1.53
0.25	0.97	2.89	1.03	0.40	1.51
0.15	0.64	3.62	1.56	0.34	1.94
0.08	0.35	3.99	2.86	0.37	1.68
0.04	0.17	4.18	5.88	0.35	1.90

the two monomers copolymerized with styrene in a perfectly alternating fashion to form a copolymer having an average structure:

$$\text{—[S—SO}_2\text{]——S—}_n$$

where the brackets enclose the complex residue. By writing the individual rate equations in terms of a 1:1 styrene–sulfur dioxide complex (C) and through an assumption that the reaction of complex radical with complex was negligible, Barb derived the expression

$$n = d[\text{S}]/d[\text{SO}_2] = 2 + (k_{\text{SS}}/k_{\text{SC}}K[\text{SO}_2]) \quad (1)$$

where K is the equilibrium constant for formation of the complex:

$$[\text{C}] = K[\text{S}][\text{SO}_2] \quad (2)$$

The plot of n versus $1/[\text{SO}_2]$ was found to be linear with an intercept of 2.

Walling[10] has shown that an equation of the same kinetic form as that of Barb can be derived through a sequence which includes two reversible steps and a penultimate unit effect. The fit of the data to both of these equivalent kinetic schemes makes difficult a choice between the two proposals.

If the styrene(S)–4-cyclopentene-1,3-dione(D) system in the region of low styrene concentration is analogous to styrene–sulfur dioxide, a plot of

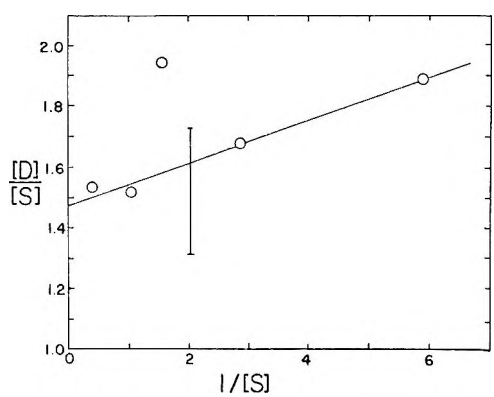

Fig. 4. Plot of [D]/[S] in the polymer as a function of 1/[S] in the feed according to eq. (9). The bracket spans a range equivalent to ±1% error in the carbon analysis.

n, the ratio of the dione to styrene in the copolymer, as a function of $1/[S]$ at constant dione concentration should be linear with an intercept of 2. The information required for this plot is given in Table III.

Although the dione concentrations are not constant, they are close enough to test this proposal. The plot of n versus $1/[S]$ (Fig. 4) is linear within reasonable experimental error. However, since the n intercept is not 2, but 1.48, the treatment of Barb[8] or Walling[10] does not apply to this system.

Retaining the idea of the complex and writing the kinetic equation for the copolymerization in terms of the individual structural units, where the complex or complex residue in the polymer is enclosed in parentheses, eqs. (3)–(6) are obtained for the region of low styrene concentration ($f_1 < 0.5$).

$$\text{D—D}\cdot + \text{D} \xrightarrow{k_{DD}} \text{D—D—D}\cdot \tag{3}$$

$$\text{D—D}\cdot + (\text{S—D}) \xrightarrow{k_{DC}} \text{D—D—(S—D}\cdot) \tag{4}$$

$$(\text{S—D}\cdot) + (\text{S—D}) \xrightarrow{k_{CC}} (\text{S—D})\text{—(S—D}\cdot) \tag{5}$$

$$(\text{S—D}\cdot) + \text{D} \xrightarrow{k_{CD}} (\text{S—D—D}\cdot \tag{6}$$

This scheme includes the assumption that styrene enters the copolymer only through complex and that the complex units add to the growing chain through the styrene end of the complex, as would be predicted on the basis of steric effects.

Assuming for the moment that penultimate group effects are negligible, then the rates of eqs. (4) and (5) would be equal, since both involve the addition of the complex to the same chain radical. Thus:

$$k_{DC}[D\cdot][C] = k_{CC}[C\cdot][C] \tag{7}$$

The copolymer equation can now be written as:

$$d[D]/d[C] = (k_{DD}[D\cdot][D] + k_{CD}[C\cdot][D])/2k_{DC}[D\cdot][C] \tag{8}$$

Elimination of radical concentration with the steady-state expression, conversion of the left-hand side to a ratio of the structural units, and replacement of [C] on the right-hand side with the equilibrium expression for the formation of the complex leads to eq. (9).

$$n = d[D]/d[S] = 1 + (d[D]/d[C]) = 1\tfrac{1}{2} + (k_{DD}/2k_{DC}\,K\,[S]) \tag{9}$$

With the exception of one point, the results plotted in Figure 4 are in general agreement with the requirements of eq. (9).

On this same basis, eqs. (3) and (6) might also be expected to be equal, since both equations represent the addition of the dione monomer to dione chain radicals. The result would be, however, that the rates of all four of the competing reactions, eqs. (3)–(6), would be equal, and eq. (8) would reduce to $n = 2$, which is inconsistent with the observed results.

If the previous reasoning concerning the mode of addition of this complex is correct, the inequality of eqs. (3) and (6) can be interpreted on the

basis of a penultimate unit effect of considerably greater significance than that expected in the case of eqs. (4) and (5). This effect can be attributed to steric factors which suppress the addition of a dione unit to a chain radical already ending in two dione units, eq. (3). A strong steric effect operating in eqs. (4) and (5), the addition of a relatively nonbulky styrene end of the complex to the chain, would not be as important. A detectable penultimate effect in this copolymerization is not unreasonable in view of the results of Barb[11] and Ham.[7,12,13]

The data as plotted in Figures 1 and 4 are consistent with the average structure III for the copolymer in the region of $0.5f_1$ with a trend directed toward structure II with decreasing styrene in the feed.

Correlation of the data for high styrene feeds with the proposed 1:1 complex is not as successful as for low styrene feeds. The Mayo-Lewis plot (Fig. 2) in which the reactions were assumed to involve styrene and 4-cyclopentene-1,3-dione monomers shows a well-defined intersection for the high styrene feeds (0.96, 0.90, 0.80, 0.65) corresponding to $r_1 = 0.03$ and $r_2 = 0.8$. The high value of the apparent reactivity ratio, r_2, is difficult to explain in view of the recognized low reactivity of the dione.[1]

With more data in the high styrene region, correlation with the sequence distribution treatment as proposed by Berger and Kuntz[14] and supported by Ang and Harwood[15] to distinguish between the terminal model and the penultimate model for copolymerization might be feasible. If the dione system is at all similar to the case of maleic anhydride, then such an analysis might easily indicate the simple terminal model of copolymerization. However, the proposal of a penultimate effect at low styrene feeds would not be jeopardized, since the penultimate effect as proposed here operates only to prevent a sequence of three dione units from occurring, an unlikely event in any case at high styrene feeds. A knowledge of the number of dione units in sequences for copolymers prepared at various feed ratios would be most valuable in attempting to support the penultimate group effect.

The services of the West Virginia University Computer Center are greatfully acknowledged.

References

1. Hamb, F. L., and A. Winston, *J. Polymer Sci.*, **A2**, 4475 (1964).
2. Mayo, F. R., and F. M. Lewis, *J. Am. Chem. Soc.*, **66**, 1594 (1944).
3. Fineman, M., and S. S. Ross, *J. Polymer Sci.*, **5**, 259 (1950).
4. Price, C. C., *J. Polymer Sci.*, **3**, 772 (1948).
5. Alfrey, T., and C. C. Price, *J. Polymer Sci.*, **2**, 101 (1947).
6. Fordyce, R. G., and G. E. Ham, *J. Am. Chem. Soc.*, **73**, 1186 (1951).
7. Ham, G. E., *J. Polymer Sci.*, **45**, 177 (1960).
8. Barb, W. G., *Proc. Roy. Soc. (London)*, **A212**, 66 (1952).
9. Barb, W. G., *J. Am. Chem. Soc.*, **75**, 224 (1953).
10. Walling, C., *J. Polymer Sci.*, **16**, 315 (1955).
11. Barb, W. G., *J. Polymer Sci.*, **11**, 117 (1953).
12. Ham, G. E., *J. Polymer Sci.*, **45**, 169 (1960).

13. Ham, G. E., *J. Polymer Sci.*, **45**, 183 (1960).
14. Berger, M., and I. Kuntz, *Polymer Division Preprints*, **4** (1), 73 (1963).
15. Ang, T. L., and Harwood, H. J., *Polymer Division Preprints*, **5** (1), 306 (1964).

Résumé

On décrit la copolymérisation du 4-cyclopentène-1,3-dione (D) avec le styrène (S). Les copolymères sont préparés en chauffant des tubes scellés contenant les mélanges des monomères et de l'azobisisobutyronitrile. Les copolymères montrent dans l'infrarouge des bandes caractéristiques du groupe phényle et du groupe β-dicétone, ce qui indique que la copolymèrisation a eu lieu. Les copolymères sont tout-à-fait insolubles dans tous les solvants. On a observé un léger gonflement dans le tétrahydrofurane, le nitrobenzène, et l'hydroxyde de sodium en solution aqueuse. A partir de la composition des copolymères, déterminée par des analyses de carbone et d'hydrogène, on montre que les copolymères contiennent à peu près 40 mole-% de styrène dans un domaine assez étendu de compositions du mélange de départ (fraction molaire de styrène 0.1 à 0.6) Les résultats pour des compositions en styrène <0.5 sont en bon accord avec l'équation: $d[D]/d[S] = 1^1/_2 + k_{DD}/2\,k_{DC}K[S]$ Cette équation est obtenue sur la base de l'existence d'un complexe monomérique (C) participant à la propagation et d'un effet de l'unité pénultième qui empêcherait la formation d'une séquence composé de trois unités dione.

Zusammenfassung

Es wird über die Copolymerisation von 4-Cyclopenten-1,3-dion (D) mit Styrol (S) berichtet. Die Copolymeren wurden durch Erhitzung des Monomeransatzes mit Azobisisobutyronitril in zugeschmolzenen Röhren dargestellt. Die Copolymeren weisen für Phenyl- und β-Diketongruppen charakteristische Infrarotbanden auf, was für den Eintritt einer copolymerisation spricht. Die Copolymeren waren in allen Lösungsmitteln völlig unlöslich, eine gewisse Quellung wurde in Tetrahydrofuran, Nitrobenzol und wassrigem Natiumhydroxyd beobachtet. Die Zusammensetzung der Copolymeren wurde durch Kohlenstoff- und Wasserstoffanalysen bestimmt und zeigte, dass die Copolymeren über einen betrachtlichen Zusammensetzungsbereich des Monomeransatzes (0,1 – 0,6 Molenbruch Styrol) einen Gehalt von etwa 40 Mol-% Styrol besassen. Die Ergebnisse bei einem Styrolgehalt des Ansatzes < 0,5 waren im allgemeinen mit der Gleichung $d[D]/d[S] = 1^1/_2 + k_{DD}/2k_{DC}K[S]$ inÜbereinstimmung. Diese Gleichung wurde unter der Annahme abeleitet, dass ein Monomerkomplex (C) am Wachstum teilnimmt und ein Einfluss des vorletzten Gliedes das Auftreten einer Sequenz von drei Dioneinheiten verhindert.

Received June 19, 1964

JOURNAL OF POLYMER SCIENCE: PART A VOL. 3, PP. 593–603 (1965)

Modification of Polymers via the Wittig Reaction*

L. X. MALLAVARAPU and A. RAVVE, *Metal Research & Development Laboratories, Continental Can Company, Chicago, Illinois*

Synopsis

Representative macromolecules containing either aldehyde or ketone groups were subjected to the Wittig reaction. As expected, the carbonyl content of the reaction products was drastically decreased, with concomitant increase in unsaturation. This is shown by spectral and chemical evidence. However, the molecular weights of the polymers before and after reaction showed significant differences; some degree of cross-linking was also noted.

Introduction

The Wittig reaction[1] provides the means for the direct conversion of carbonyl compounds to the corresponding olefins through replacement of the doubly bonded oxygen by carbon in the carbonyl groups, thus introducing the olefinic linkage. Whereby the disclosure of this reaction in 1953[2] prompted numerous publications, attention so far has focussed only on the synthesis of low molecular weight olefins from the corresponding carbonyls.

Due to special properties of large molecules, where effects due to bulk, among others, can have an important bearing on polymer reactivity,[3–5] it was desirable to study the applicability of the Wittig reaction to the macromolecules.

Results and Discussion

The reaction of phosphorus ylenes with carbonyls was discovered by Wittig[6] and discussed elsewhere.[7–17]

In this investigation two types of macromolecules were used: polymers bearing (1) aldehyde and (2) ketone groups. The polyaldehydes were represented by two copolymers of styrene and acrolein. These differed in molecular weights, that of polymer A being 1900 and that of polymer B being 1100, and in the ratios of the aldehyde to styrene. The higher molecular weight polymer was expected to possess on the average 8 aldehydes (but later found to possess 13) per mole and the lower molecular weight polymer 4.9 aldehydes per mole.

* Presented in part at the 147th Meeting of the American Chemical Society, Philadelphia, April 1964.

The reactions carried out on polymers A, B, and C can be illustrated by eq. (1):

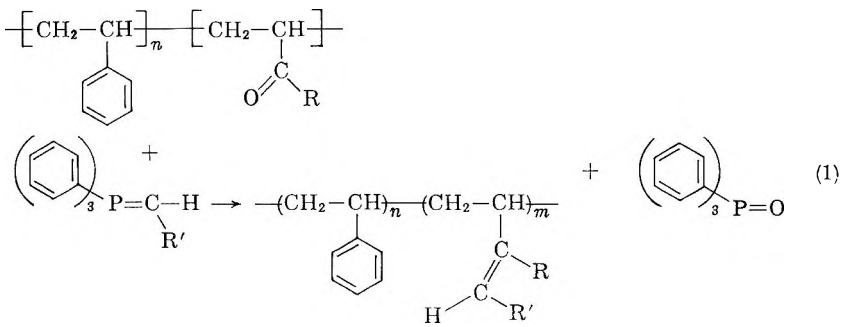

(1)

where for polymers A and B, R = H; R′ = H and for polymer C, R = CH_3; R′ = H, CH_3. The reaction carried out on polymer D can be represented as shown in eq. (2):

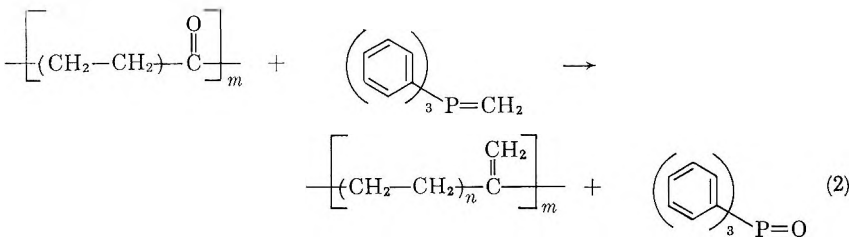

(2)

Stereospecificity is not possible with products from the above described reactions. Substitution of an ethyl halide for the methyl analog in the preparation of the Wittig reagent should on the other hand lead to vicinally substituted olefins with the resultant *cis* and/or *trans* isomers.

A reagent from triphenylphosphine and ethyl bromide was prepared, therefore, and reacted with polymer C. The infrared spectrum, shown in Figure 1, did not enable us, however, to conclude whether either isomer predominated.

The properties of the starting materials and their reaction products are summarized in Table I.

Comparisons of molecular weights of the starting materials and their products indicate differences. Specifically, lower molecular weights were observed in the products from polymers A and B than those of the starting materials. On the other hand, the molecular weights of the products from polymer C are higher than that of the parent compound. The nature of this we can not explain readily. In addition, gel formation was observed to accompany the reactions. Actually, due to these gel formations, only the soluble fractions of the products comprising approximately 75% of the product could be used for molecular weight determinations.

The tendency to crosslink can perhaps be attributed to the presence of the organometallic compounds during the course of the reaction. Such

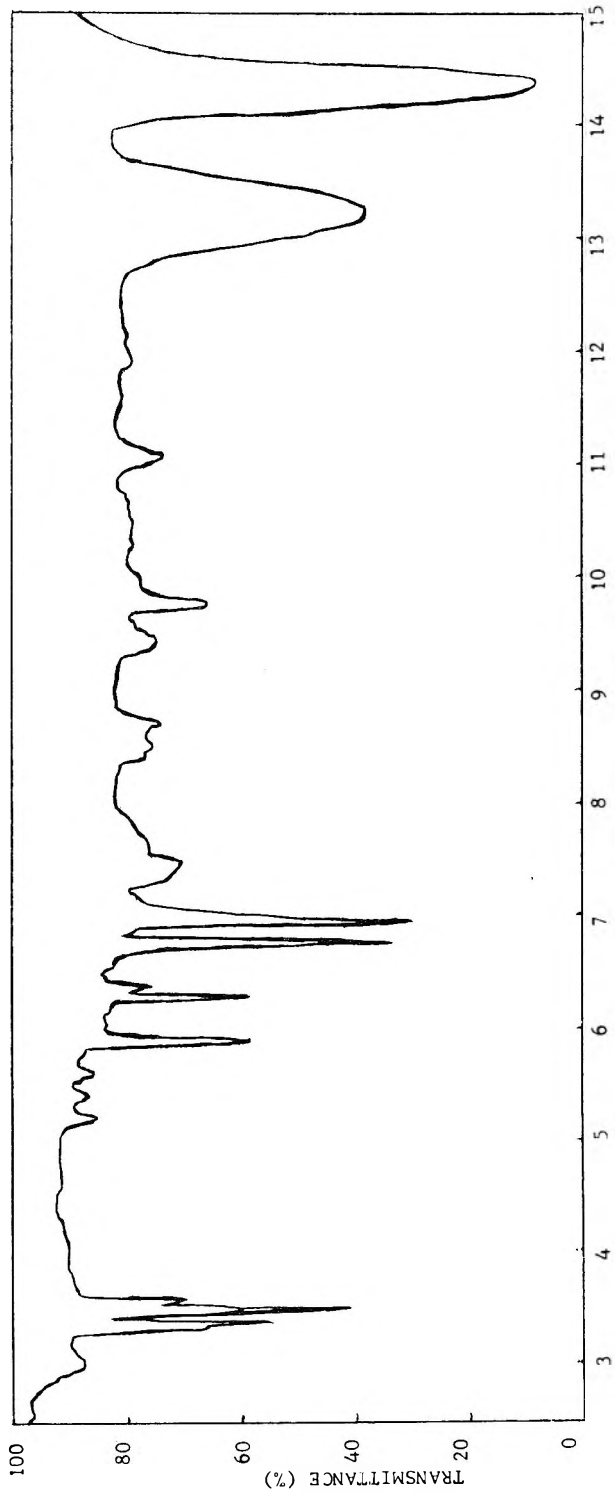

Fig. 1. Infrared spectrum of polymer C after the Wittig reaction (2).

TABLE I

Polymer	Calculated C, %	Calculated H, %	Calculated O, %	Found C, %	Found H, %	Found O, %[a]	Mol. wt.	Softening point, °C.	Iodine no.	Infrared spectra
Polymer A[b]	81.4	7.48	11.11	81.51	8.23	10.75	1900 ± 10%	122	14.7	Strong peak at 5.65–5.85 μ
Polymer A after Wittig reaction[c]	91.01	8.99	—	84.01	8.20	6.39	632 ± 10%	195	45.0	Weak peak at 5.65-5.85 μ; New peaks at 6.05, 10.75 μ
Polymer B	85.37	7.56	7.09	83.70	8.17	8.34	1100 ± 10%	96	25.1	Strong peak at 5.65–5.85 μ
Polymer B after Wittig reaction[c]	91.47	8.53	—	84.48	8.59	5.21	940 ± 10%	195	43.0	Weak carbonyl; new peaks at 6.05–6.10 μ, 10.95 μ
Polymer C	90.80	7.75	—	90.44	7.97	—	34,000 ± 3%	118	<1.0	Strong peak at 5.65–5.85 μ
Polymer C after Wittig reaction (1)[d]	92.06	7.94	—	91.09	7.97	—	38,700 ± 3%	120	47.0	New peaks at 6.65, 9.05–9.10, 11.25 μ
Polymer C after Wittig reaction (2)[ac]	91.96	8.04	—	89.15	7.82	—	45,500 ± 3%	120	145.0	Weak peak at 5.65–5.85 μ
Polymer D	76.19	11.11	—	78.93	12.03	—	3200 ± 10%	95	—	Strong peak at 5.65–5.85 μ
Polymer D after Wittig reaction[e]	87.10	12.90	—	77.37	11.83	—	Polymer crosslinked	—	—	New peaks at 6.05-6.10, 11.25 μ

[a] Oxygen, where determined, is by direct oxygen analysis; [b] Calculated on the basis of 13 aldehydes/mole; [c] Phenyllithium was used in preparation in the ylene. Toluene-soluble portion comprised 75% of the product; [d] *n*-Butyllithium was used in preparation at the ylene. The product was completely toluene-soluble; [e] *n*-Butyllithium was used. 70% of the product was toluene-soluble.

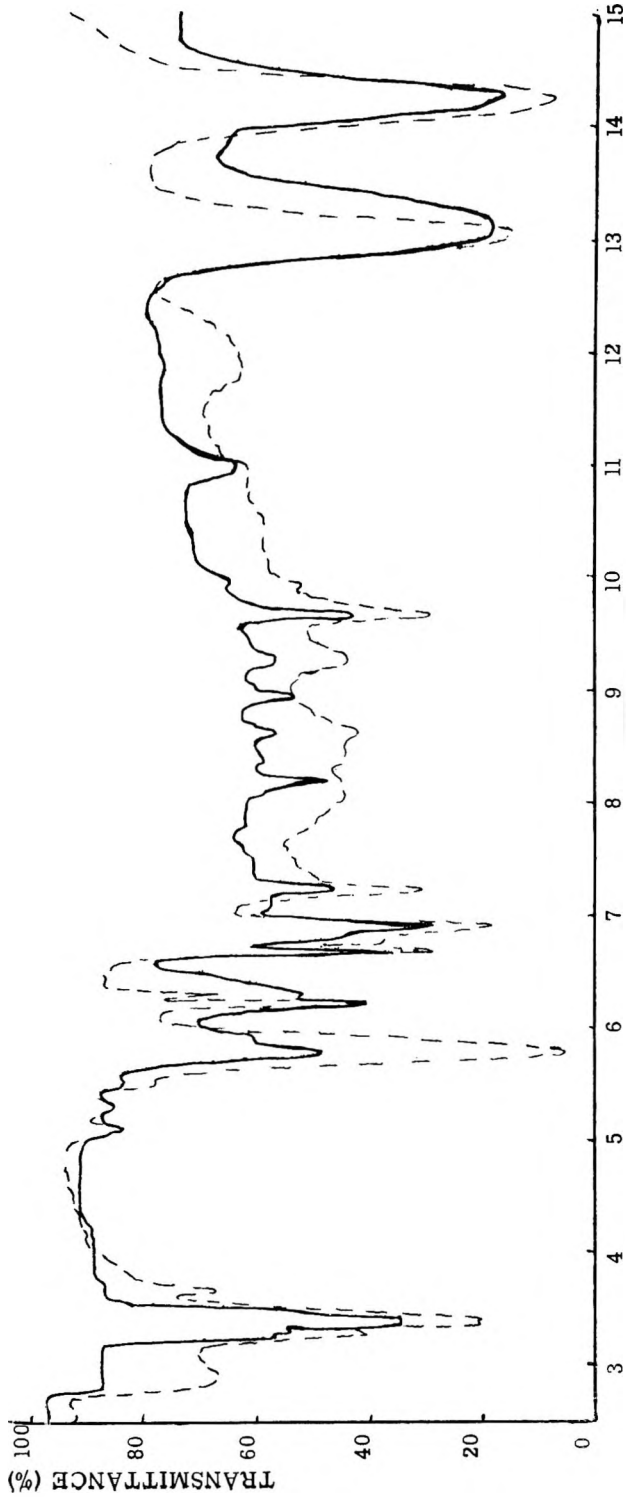

Fig. 2. Infrared spectra of polymer A (– –) before and (——) after the Wittig reaction.

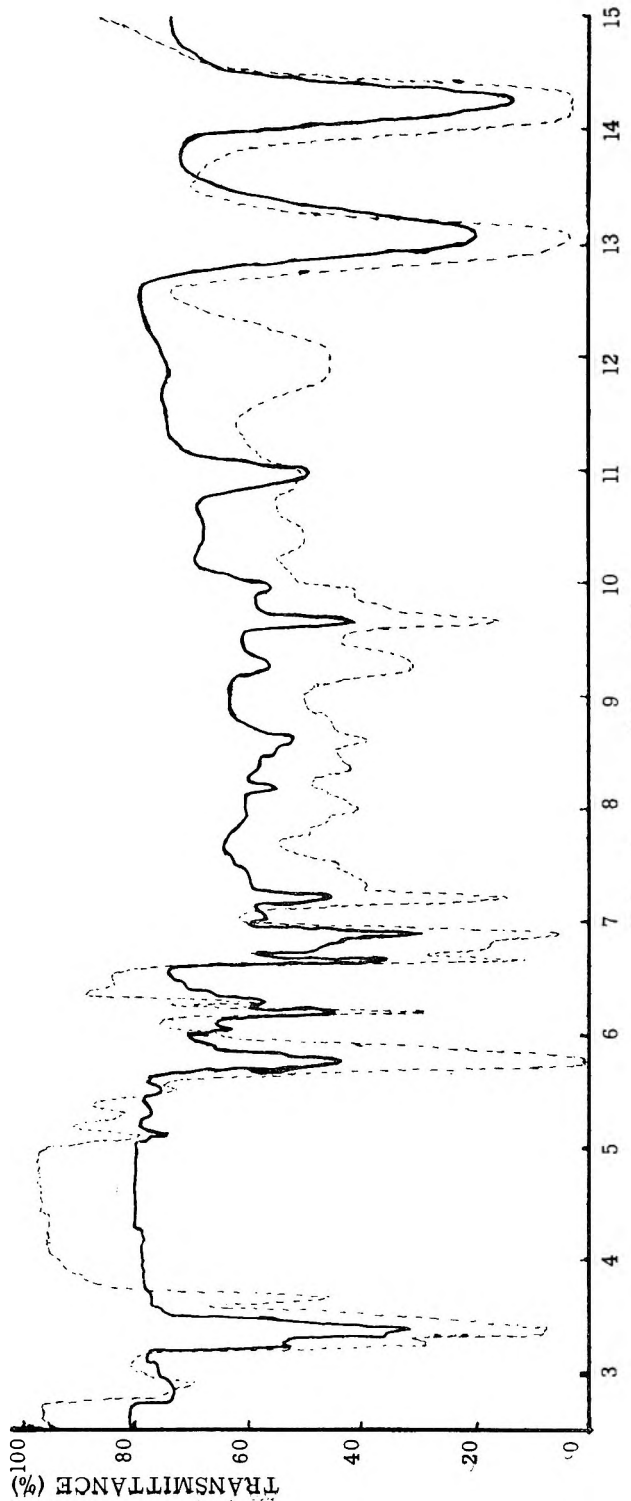

Fig. 3. Infrared spectra of polymer B(– –) before and (——) after the Wittig reaction.

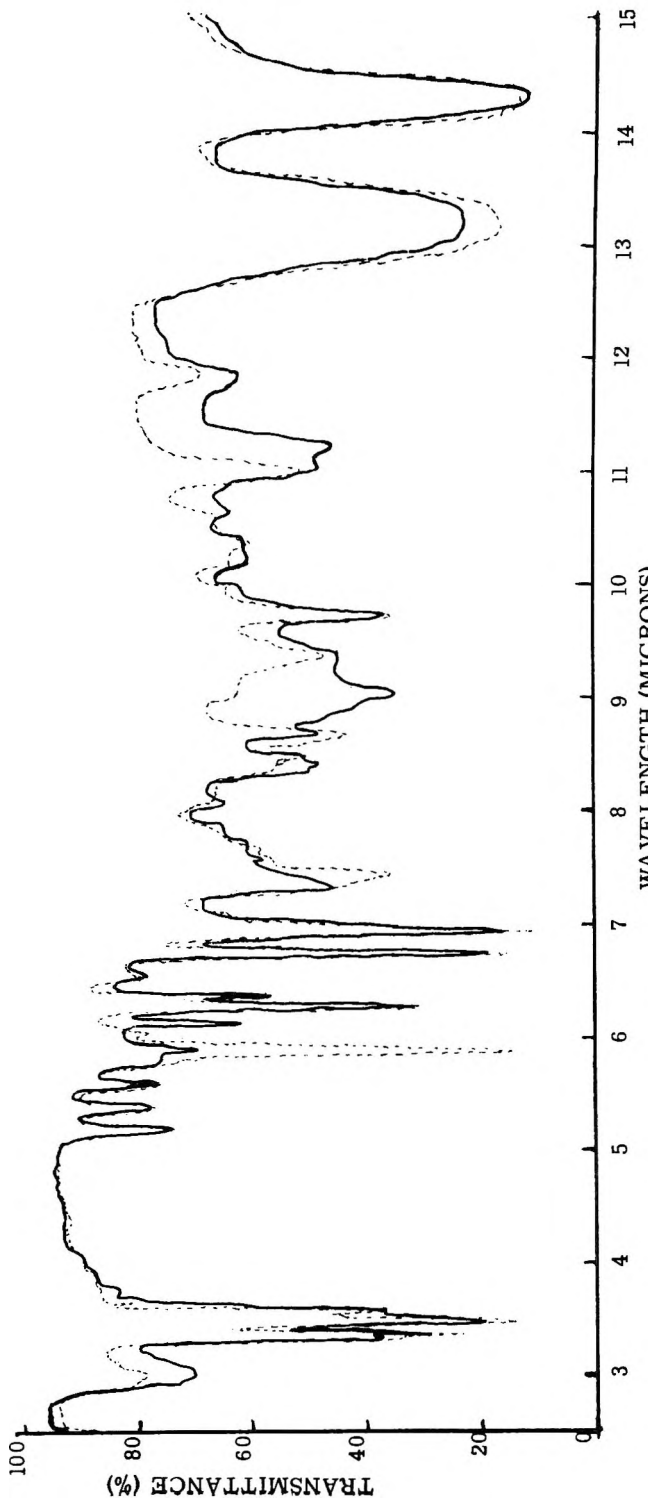

Fig. 4. Infrared spectra of polymer C (--) before and (——) after the Wittig reaction.

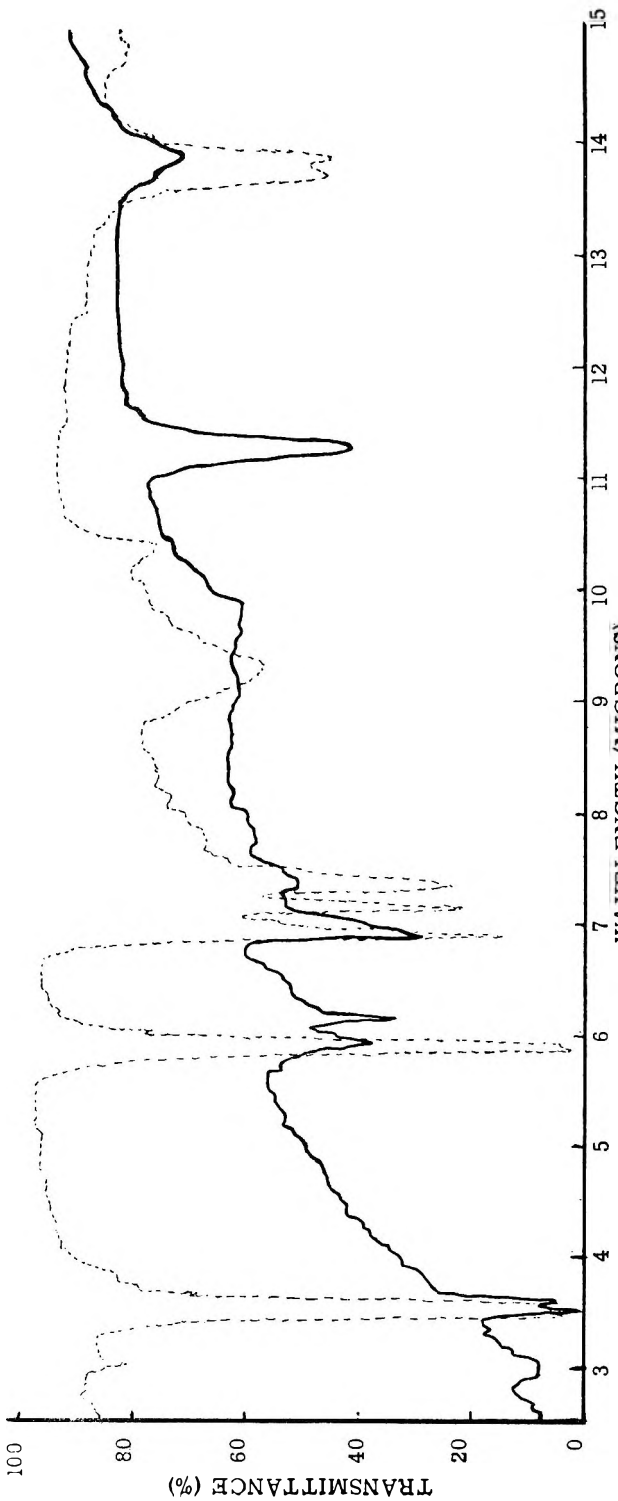

Fig. 5. Infrared spectra of polymer D (--) before and (——) after the Wittig reaction.

organometallic compounds are known to catalyze olefin polymerizations. In carrying out the reaction on simple, low molecular weight compounds this can perhaps result in the formation of small amounts of tars and then might be ignored. In dealing, however, with macromolecules, even a small amount of crosslinking will significantly affect the properties of the products.

Infrared spectra of the materials studied are shown in Figures 1–5.

The yields of the olefins, based upon amounts of carbonyls replaced by methylenes, and judged from the infrared spectra appear to be within the ranges reported for low molecular weight compounds.[18] This would suggest that within the molecular weight ranges studied, the bulk of the molecule had little, if any, effect on the reactivity.

A further study of the infrared spectra of the five products of the reaction indicates that with this decrease in the carbonyl absorption, simultaneously new peaks appear which can be attributed to C = CHR.[19] In particular, Figure 2 discloses new peaks at 6.05 and 10.95 μ for polymer A. Figure 3 shows a new strong peak at 10.95 μ and a weak peak at 6.05–6.10 μ indicating C=C absorption.[20] Figure 4 (for polymer C and its products) shows in addition a new band at 11.25 μ which is assigned to out-of-plane deformation of R'R"C=CH_2 and a new peak at 6.05 μ. We also note in Figure 4 a third new peak at 9.05–9.10 μ which cannot be readily explained. A band in the 10 μ region was identified with the group C=CH—CH_3 by Lecomte and Naves[21] and ascribed to the CH_3—C stretching frequency.[19] Gunzler et al.[22] find that a reasonably constant absorption occurs near 8.75 μ for fully substituted ethylenes carrying a methyl group. Whether a shift to 9.01–9.10 μ does occur for CH_3—C=CH_2 is not established. Figure 5 also shows a strongly decreased carbonyl absorption and two new peaks at 6.10 μ for C=C absorption and a strong new peak at 11.25 μ for the out-of-plane deformation of the disubstituted olefin R'R"C=CH_2. In addition, it is interesting to note the virtual disappearance of the peak at 7.10 μ which is associated with active methylene groups adjacent to a carbonyl.[23]

The iodine values were determined on the products, and they confirm further an increase in olefinic unsaturation after the Wittig reaction.

Experimental

The experimental procedure involved the synthesis of triphenylmethylphosphonium bromide and triphenylethylphosphonium bromide and subsequent conversion of the bromide to the corresponding ylene in the Wittig reaction proper. Triphenylphosphorus, required for the preparation of the bromide, was purchased from M & T Chemicals. The conversion of the bromide to the corresponding ylene was carried out by the use of phenyllithium, prepared according to the procedure of Gilman et al.[24] or with butyllithium in hexane (Foote Mineral Co., Philadelphia) according to the procedure described by Hauser et al.[25] The triphenylmethylphosphonium bromide and triphenylethylphosphonium bromide were synthesized in

virtually quantitative yields according to the procedure of Field, described by Marvel et al.[26]

General Procedure for the Wittig Reaction

The reaction was carried out in all cases as follows: 0.1 mole of the polymer (based on the carbonyl content) was dissolved in either dry 1,2-dimethoxyethane or tetrahydrofuran and added to the stoichiometric amount of the Wittig reagent in the same solvent. The reaction was then allowed to proceed first at room temperature and then at reflux under nitrogen for approximately 18–20 hr. The product was then precipitated with 95% ethyl alcohol, water washed, and dried.

Polymers A and B. Polymers A and B were obtained from Shell Chemical Company. These materials were copolymers of styrene and acrolein. They were characterized by melting points, infrared spectra, combustion analysis, and molecular weight determinations.

Polymer C. This copolymer of styrene (90%) and methyl vinyl ketone (10%) was prepared by solution polymerization in boiling xylene with 2% di-*tert*-butyl peroxide as initiator. The product was precipitated with methyl alcohol, washed, and dried. The infrared spectrum, molecular weight, and melting point were determined on this material.

Polymer D. This polymer was obtained from du Pont & Company. It is a copolymer of ethylene and carbon monoxide in ratios of 3.5:1. Combustion analysis, infrared spectrum, melting point, and molecular weight were obtained on this polymer as well.

Molecular Weight Determinations. Molecular weight determinations were carried out on polymers A, B, and D and their products with a vapor phase osmometer (Mechrolab Model 301A).

Molecular weight determination on Polymer C and its products were carried out with a membrane osmometer (Mechrolab Model 501, 37°C. thermostat) in toluene solution, with the use of a UA very dense S&S membrane.

References

1. Wittig, G., and U. Schollkopf, *Ber.*, **37**, 1318 (1954).
2. Wittig, G., and G. Geissler, *Ann.*, **580**, 44 (1953).
3. Kern, W., R. C. Schultz, and D. Braun, *J. Polymer Sci.*, **48**, 91 (1960).
4. Smets, G., *Makromol. Chem.*, **34**, 190 (1959).
5. Plesch, P., *Chem. Ind. (London)*, **1958**, 954.
6. Wittig, G., and W. Haag, *Ann.*, **588**, 1964 (1955).
7. Schollkopf, U., *Angew. Chem.*, **71**, 260 (1959).
8. Yanoskaya, L. A., *Usp. Khim.*, **30**, 813 (1961).
9. Levissalles, J., *Bull. Soc. Chim. France*, **1958**, 1021.
10. Wittig, G., *Angew. Chem.*, **68**, 505 (1958).
11. Denney, D. B., and M. J. Boskin, *Chem. Ind. (London)*, **1959**, 330.
12. Speriale, A. J., and K. W. Ratts, *J. Am. Chem. Soc.*, **84**, 844 (1962).
13. Johnson, A. W., and A. B. La Count, *Tetrahedron*, **9**, 130 (1961).
14. Yanovskaya, L. A., *Russ. Chem. Rev. Engl. Transl.*, **1961**, 347.

15. Trippett, S., *Quart. Rev.*, **17**, 406 (1963).
16. Bergelson, L. D., V. A. Vaver, L. D. Barsukov, and M. M. Shemyakin, *Dokl. Akad. Nauk SSSR*, **143**, 111 (1962).
17. Bergelson, L. D., and M. M. Shemyakin, *Tetrahedron*, **19**, 149 (1963).
18. Antonucci, J. M., Ph.D. Dissertation, Univ. Maryland, 1959.
19. Bellamy, L. J., *The Infra-Red Spectra of Complex Molecules*, Wiley, New York, 1958.
20. Barnes, R. B., R. C. Gore, U. Liddel, and V. Z. Williams, *Infra-red Spectroscopy*, Reinhold, New York, 1944.
21. Lecomte, J., and Y. R. Naves, *J. Chim. Phys.*, **53**, 462 (1956).
22. Gunzler, H., M. Kinitz, and E. Nebaus, Naturwiss., **43**, 299 (1956).
23. Francis, J., *J. Chem. Phys.*, **19**, 942 (1951).
24. Gilman, H., E. A. Zoeliner, and W. M. Selby, *J. Am. Chem. Soc.*, **54**, 1957 (1932).
25. Hauser, C. F., T. W. Brooks, M. L. Miles, M. A. Raymond, and G. B. Butler, *J. Org. Chem.*, **28**, 372 (1963).
26. Marvel, C. S., and E. J. Gall, *J. Org. Chem.*, **24**, 1494 (1959).

Résumé

On a soumis certaines macromolécules contenant des fonctions aldéhydiques ou cétoniques à la réaction de Wittig. Comme on s'y attendait, la teneur en carbonyle des produits de réaction est fortement diminué et est accompagnée d'une augmentation de l'insaturation. Ceci a été mis en évidence par des études spectrales et chimiques. Cependant, les poids moléculaires des polyméres avant et aprés la réaction montrent des différences importantes; on note aussi un certain degré de pontage.

Zusammenfassung

Repräsentative Makromoleküle mit Aldehyd- oder Ketongruppen wurden der Wittig-Reaktion unterworfen. Wie zu erwarten, war der Carbonylgehalt der Reaktionsprodukte stark herabgesetzt und gleichzeitig die Zahl der Doppelbindungen erhöht, was durch Spektralergebnisse und chemisch bewiesen wurd. Das Molekulargewicht der Polymeren vor und nach der Reaktion zeight signifikante Unterschiede; ein gewisser Grad an Vernetzung wurde ebenfalls festgestellt.

Received April 6, 1964
Revised June 16, 1964

JOURNAL OF POLYMER SCIENCE: PART A VOL. 3, PP. 605–614 (1965)

Some Statistical Properties of Flexible Ring Polymers

EDWARD F. CASASSA, *Mellon Institute, Pittsburgh, Pennsylvania*

Synopsis

The conventional "string-of-beads" statistical model for flexible chain polymers is modified for derivation of configurational and thermodynamic properties of long-chain ring molecules (i.e., flexible linear chains with ends joined) in dilute solution near the Flory temperature. The effect of the intramolecular excluded volume on the mean-square molecular radius is obtained to the first order of approximation; the second virial coefficient is given to the "double contact" approximation; and the angular intensity distribution for Rayleigh scattering is determined for the unperturbed molecule. Qualitatively, all these properties, in comparison to those for linear chains of the same mass, are affected as anticipated from the more compact nature of the ring model.

Introduction

In this note we discuss three properties relating to a dilute solution of a homogeneous ring polymer: the mean-square molecular radius, the second virial coefficient, and the angular intensity distribution for Rayleigh scattering. The recent discovery that some natural macromolecules, deoxyribonucleic acids from the bacteriophage ϕX174[1] and from a polyoma virus,[2] occur in closed rings makes the consideration of such questions something more than simply an intellectual exercise. It is conceivable, too, that synthetic long-chain ring polymers could be synthesized in controlled fashion by anionic methods; perhaps by reacting a difunctional terminator with a difunctional polymeric anion at extreme dilution. Finally, without regard to the practical possibilities, it is of some interest to compare theoretical calculations for rings with recent studies of various branched chain structures.[3,4]

The molecular model to be used is the familiar statistical chain—a sequence of N segment vectors characterized by a Gaussian length distribution—with the special requirement that the vectors form a closed ring. Except at the Flory temperature Θ, any pair of statistical segments exhibits a mutual volume of exclusion.

In the succeeding calculations, we shall require various combinations of random-flight probabilities. They are conveniently formulated by using a theorem of Wang and Uhlenbeck,[5] as generalized by Fixman,[6] for multivariate Gaussian distributions. Essentially, the theorem is used to express the simultaneous probability of occurrence of vectors formed by linear combinations of the Gaussian segment vectors describing one or more poly-

mer chains. Thus, forming s vectors, $\mathbf{V}_1, \mathbf{V}_2, \ldots, \mathbf{V}_s$, each of which is a linear combination of N segment vectors $\mathbf{r}_1, \mathbf{r}_2, \ldots, \mathbf{r}_N$, e.g.,

$$\mathbf{V}_p = \sum_{t=1}^{N} \psi_{pt}\mathbf{r}_t \tag{1}$$

one obtains the probability density for the simultaneous occurrence of $\mathbf{V}_1, \mathbf{V}_2, \ldots, \mathbf{V}_s$:

$$P_s(\mathbf{V}_1,\mathbf{V}_2, \ldots, \mathbf{V}_s) = (3/2\pi b^2)^{3s/2} C_s^{-3/2} \exp\left\{-(3/2b^2C_s) \sum_i \sum_j C^{ij}\mathbf{V}_i \cdot \mathbf{V}_j\right\} \tag{2}$$

where C^{ij} is the cofactor of the element C_{ij} of the determinant C_s of order s with

$$C_{ij} = \sum_{t=1}^{N} \psi_{it}\,\psi_{jt} \tag{3}$$

and b is the root-mean-square length of a segment vector. In the applications to be made here, the coefficients ψ are either unity or zero. The determinants C_s then all have similar structure: each diagonal element C_{ii} is the number of segments in the closed loop formed by the chain (or chains) and the vector $\mathbf{V}_i$; and each off-diagonal element is the number of segments common to two such loops.

Immediately, the probability density, which we denote by $P(\text{ring})$, for the probability that a linear chain of N segments forms a closed loop—that the sum of the segment vectors is zero—is seen to be given by

$$P(\text{ring}) = (3/2\pi b^2)^{3/2}(1/N^{3/2}) \tag{4}$$

Precisely, $P(\text{ring})d\mathbf{L}$ is the probability that the separation L of the ends of the chain lies in the differential element $d\mathbf{L}$ as $\mathbf{L}$ approaches zero. Throughout, other random-flight probabilities, conditional on the occurrence of this event, will have to be evaluated.

Mean-Square Radius of the Molecule

In this calculation we consider the single molecule with segments numbered consecutively from 1 to N around the ring. (We can, of course, visualize the ring as formed by joining elements 1 and N of a linear chain.) We use the definition of the mean-square radius:

$$\langle R^2\rangle = (1/2N^2) \sum_i \sum_j \langle L_{ij}^2\rangle \tag{5}$$

where $\langle L^2_{ij}\rangle$ is the mean-square separation of segments i and j. This quantity can be expressed as a series, given by Fixman,[6]

$$\langle L_{ij}^2\rangle = \int L_{ij}^2 P(\mathbf{L}_{ij}|\text{ring})d\mathbf{L}_{ij} - \beta/2 \sum_{\substack{k \\ k<l}} \sum_{l} \int L_{ij}^2 [P(\mathbf{L}_{ij},0_{kl}|\text{ring}) - P(\mathbf{L}_{ij}|\text{ring})\, P(0_{kl}|\text{ring})]d\mathbf{L}_{ij} + O(\beta^2) \tag{6}$$

in which β is the excluded volume for any pair of segments. The symbol 0_{kl} is used to symbolize a contact between segments k and l. Thus, $P(\mathbf{L}_{ij},0_{kl}|\text{ring})$ relates to the probability of occurrence of the vector distance $\mathbf{L}_{ij}$ between segments i and j and the contact between segments k and l, when segments **1** and N are also joined. Evidently, the first term of the series gives the unperturbed mean-square separation $\langle L_{ij}^2\rangle_0$ while the following terms provide successive orders of correction arising from the prohibition of those random-flight configurations in which chain vectors intersect within a volume element β. The assumptions implied by eq. (6) are the usual ones: that the potentials of average force between segments are of short range and that they are additive pairwise.[7]

To evaluate $\langle L_{ij}^2\rangle_0$ we require the probability density

$$P(\mathbf{L}_{ij}|\,\text{ring}) = P(\mathbf{L}_{ij},\text{ring})/P(\text{ring})$$

$$= (3/2\pi b^2)^{3/2}\left[\frac{N}{aN - a^2}\right]^{3/2} \exp\left\{-[3N/2b^2(aN - a^2)]L_{ij}^2\right\} \qquad (7)$$

where a is the number of segments intervening between segments i and j, measured over either path around the ring. Substitution into eq. (6) and integration over space leads to

$$\langle L_{ij}^2\rangle_0 = b^2(aN - a^2)/N \qquad (8)$$

Averaging $\langle L_{ij}^2\rangle_0$ over all i and j, according to eq. (5), gives

$$\langle R^2\rangle_0 = Nb^2/12 \qquad (9)$$

for large N. Hence, the unperturbed mean-square radius of the ring polymer is only half that of the linear chain with N segments. This result was obtained earlier by Zimm and Stockmayer.[8]

Calculation of the second term in eq. (6) is more intricate in that we now need the probability $P(\mathbf{L}_{ij},0_{kl}|\,\text{ring}) = P(\mathbf{L}_{ij},0_{kl},\text{ring})/P(\text{ring})$, which

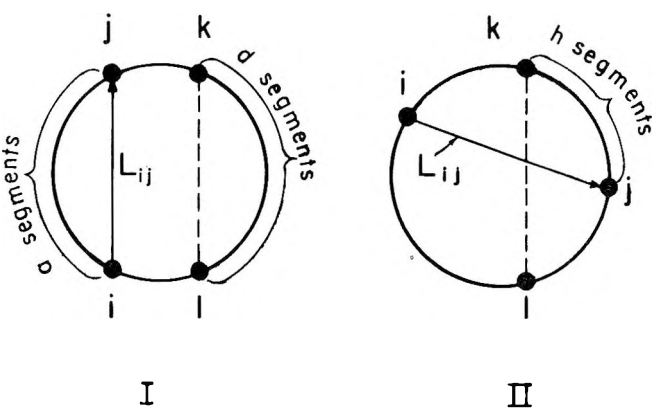

Fig. 1. Schematic diagrams illustrating the two categories of configurations of a ring molecule with one intramolecular contact (indicated by dashes) and one intramolecular segment separation simultaneously specified.

assumes two forms depending on the topological relations among segments i, j, k, and l. The two situations are illustrated schematically in Figure 1. In configurations of type I, the two loops closed by the vector $\mathbf{L}_{ij}$ and by the contact between segments k and l can be chosen so as not to intersect, but an intersection cannot be avoided in the type II diagram. Consequently, the third-order determinant associated with $P(\mathbf{L}_{ij},0_{kl},$ ring)

$$C_3 = \begin{vmatrix} a & h & a \\ h & d & d \\ a & d & N \end{vmatrix} \tag{10}$$

(a and d being the numbers of segments in each of these two loops, and h the number in the intersection) has the elements h equal to zero for type I configurations.

Integration over $d\mathbf{L}_{ij}$ in the second term of eq. (6) and substitution in eq. (5) gives

$$\langle R^2\rangle = \langle R^2\rangle_0 - \frac{b^2 z}{4N} \sum_i \sum \sum_k \sum_l \left[\frac{C_3}{(Nd - d^2)^{5/2}} - \frac{Na - a^2}{N(Nd - d^2)^{3/2}} \right] + \cdots \tag{11}$$

where z denotes

$$(3/2\pi\, b^2)^{3/2}\, \beta\, N^{1/2}$$

Since we always assume N to be large it is permissible to replace summations by integrations and to simplify the limits by regarding quantities of order $1/N$ as zero. The symmetry of the ring model facilitates the work further in that any configuration with the relative positions of three segments along the chain contour specified in a particular way with respect to the fourth can be obtained in N different ways. Then, the three remaining variables to be considered can be taken as a, d, and h. In any type I configuration with one segment, say k, and the associated contour length d, held fixed, a takes on values from 1 to $N - d$; and each a can be obtained in $N - d - a$ distinguishable ways. Then d is allowed to vary from 1 to $N - 1$, and the final factor N is included. It follows that the contribution to the quadruple sum in Eq. (11) can be expressed as the double integral

$$I_1 = -N^2 \int_{v=0}^{1} \int_{u=0}^{1-v} [(1 - v - u)u^2v^2/(v - v^2)^{5/2}]du\,dv \tag{12}$$

Here we have introduced reduced dummy variables with the upper limit unity instead of N.

If we hold k and l fixed with $d < N/2$ in the type II diagram shown in Figure 1, we can distinguish two subgroups of configurations. For $a < d$ there are a distinct ways to obtain a given a, each with a different h in the range $1 \leqslant h \leqslant a$; and similarly for $a > d$ there are d configurations for every a, with $1 \leqslant h \leqslant d$. Contributions from each group are multiplied by 2 to account for the equivalent configurations with segment i lying within the d contour. Then, d is allowed to vary from unity to $N/2$ and

the factor N is introduced to allow for the N distinguishable ways of choosing any given d. Finally, these contributions to the quadruple sum in eq. (11) reduce to triple integrals:

$$I_2 = -2N^2 \int_{v=0}^{1/2} \int_{u=0}^{v} [1/(v - v^2)^{5/2}] \left[u^3v^2 + \int_0^u (y^2 - 2uvy)dy \right] dudv \tag{13}$$

and

$$I_3 = -2N^2 \int_{v=0}^{1/2} \int_{u=v}^{1/2} [1/(v - v^2)^{5/2}] \left[u^2v^3 + \int_0^v (y^2 - 2uvy)dy \right] dudv \tag{14}$$

which can be evaluated by reference to standard tabulated forms.

The integrated result is

$$I_1 + I_2 + I_3 = -N^2\pi/24 \tag{15}$$

In terms of the usual expansion factor α for the mean-square radius, $\alpha^2 \equiv \langle R^2 \rangle / \langle R^2 \rangle_0$, this gives

$$\alpha^2 = 1 + (\pi/2)z + \ldots \tag{16}$$

The coefficient of z in the corresponding series for a linear chain is 134/105. The larger value for the ring polymer is close to 1.559, the number calculated by Berry and Orofino[4] for a regular star molecule with eight branches (eight linear chains attached at one end to a common junction).

Second Virial Coefficient

In this section we calculate the second virial coefficient A_2, the coefficient of the linear term in the virial equation of state, e.g., for the osmotic pressure Π

$$\Pi/RTc = (1/M) + A_2c + O(c^2) \tag{17}$$

where c is the concentration in units of mass/volume and M is the molecular weight. For any flexible chain structure, A_2 can be expressed as a series in integral powers of β(or of z) the successive terms relating to configurations with increasing numbers of contacts specified between segments of two molecules.[7] Specifically, for the ring polymer we can write:

$$A_2 = (\beta N_0/2M^2) \sum_{i_1} \sum_{i_2} \Big[1 - \beta/2 \sum_{j_1} \sum_{j_2} \mathrm{P} \times (0_{j_1 j_2} | 0_{i_1 i_2}, \mathrm{ring}_1, \mathrm{ring}_2) + O(\beta^2) \Big] \tag{18}$$

where N_0 denotes Avogadro's number and the subscripts 1 and 2 refer to the two molecules of the bimolecular cluster. Hence,

$$P(0_{j_1 j_2} | 0_{i_1 i_2}, \mathrm{ring}_1, \mathrm{ring}_2) = \frac{P(0_{j_1 j_2}, \mathrm{ring}_1, \mathrm{ring}_2 | 0_{i_1 i_2})}{P(\mathrm{ring}_1, \mathrm{ring}_2 | 0_{j_1 j_2})} = \frac{P(0_{j_1 j_2}, \mathrm{ring}_1, \mathrm{ring}_2 | 0_{i_1 i_2})}{P(\mathrm{ring}_1) P(\mathrm{ring}_2)} \tag{19}$$

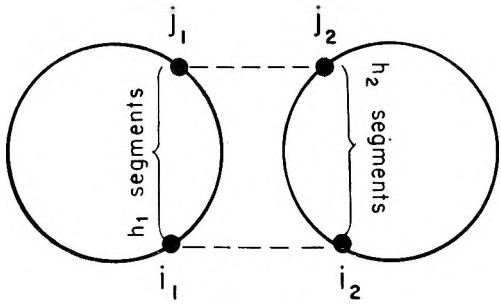

Fig. 2. A double contact configuration of two ring molecules. The dashed lines denote the segment pairs in contact.

is the random-flight probability that segments j_1 and j_2 of molecules 1 and 2 respectively, are in contact, given that segments i_1 and i_2 are in contact and that both molecules 1 and 2 form closed rings. The last equality in eq. (19) is justified by the obvious circumstance that the formation of rings and the existence of the initial contact between segments i_1 and i_2 are independent events. From eq. (2), we have

$$P(0_{j_1 j_2}, \text{ring}_1, \text{ring}_2 | 0_{i_1 i_2}) = (3/2\pi b^2)^{9/2} C^{-3/2} \tag{20}$$

in which

$$C = \begin{vmatrix} h_1 + h_2 & h_1 & h_2 \\ h_1 & N & 0 \\ h_2 & 0 & N \end{vmatrix} \tag{21}$$

where h_1 and h_2 are, respectively, the numbers of segments separating segments i_1 and j_1, and i_2 and j_2 along each chain contour, as shown in Figure 2.

The symmetry of the ring model again simplifies the multiple summations (or integrations). A configuration with two intermolecular contacts, is characterized by the two quantities h_1 and h_2, which each can be realized independently in N different ways. The quadruple sum in eq. (18) is then given by

$$\sum_{i_1} \sum_{j_2} \sum_{j_1} \sum_{j_2} (N^2/C)^{3/2} = N^{5/2} \int_0^1 \int_0^1 (u + v - u^2 - v^2)^{-3/2} du dv$$
$$= 2^{3/2} \pi N^{5/2} \tag{22}$$

and finally the virial coefficient is

$$A_2 = (N_0 B N^2/2M^2)[1 - Bz + O(z^2)] \tag{23}$$
$$B = \pi\sqrt{2} = 4.457$$

The coefficient B found here is much larger than the value 2.865 for linear chains. Comparison with B for branched star molecules, which we have calculated elsewhere,[3] shows that the ring model behaves in this

respect nearly like the star model with five arms. The ring and this star are also quite similar in the ratio of the unperturbed mean-square radius to that of the linear chain of the same mass: for the star this ratio is 0.52.

Angular Distribution of Rayleigh Scattering

We turn last to discussion of the angular distribution of scattered radiation from a dilute solution in which A_2 is zero: i.e., under such conditions that configurations of solute molecules are uncorrelated and are described by unperturbed random-flight statistics. With some, not very restrictive, assumptions about the electromagnetic properties of the scattering units, the excess intensity (that from the solution less that from the solvent alone) scattered through the angle θ, from incident radiation polarized perpendicular to the plane containing both incident and scattered rays, is proportional to the function[9,10]

$$P(\theta) = (1/N^2) \sum_k \sum_l P(\mathbf{L}_{kl}|\text{ring}) e^{i\mathbf{s}\cdot\mathbf{L}_{kl}} d\mathbf{L}_{kl} \tag{24}$$

normalized to unity at $\theta = 0$. The conventionally used symbol $P(\theta)$ is not to be confused with the probability densities. As before, $\mathbf{L}_{kl}$ is the vector separation of segments k and l of the same molecule; the exponent i indicates $\sqrt{-1}$; and $\mathbf{s}$ is the vector difference between unit vectors in the direction of incident and of scattered rays, multiplied by $2\pi/\lambda'$, with λ' the wavelength of light in the medium.

The integration over space can be done immediately; and since the argument of the double sum depends only on the separation a of segments k and l along the contour, the scattering function for the ring polymer can be expressed as a single sum.

$$P(\theta) = (1/N) \sum_{a=1}^{N-1} \exp\{-[s^2 b^2 (aN - a^2)/6N]\} \tag{25}$$

After conversion to an integral and a minor transformation of the variable, this becomes

$$P(\theta) = (2/u^{1/2}) e^{-u/4} (\mathcal{E} u^{1/2}/2) \tag{26}$$

where

$$u = [8\pi^2/3(\lambda')^2] N b^2 \sin^2(\theta/2) \tag{27}$$

and

$$\mathcal{E}(x) = \int_0^x e^{l^2} dl \tag{28}$$

Although the irreducible integral $\mathcal{E}(x)$ is relatively unfamiliar, it has been tabulated. In the present application, the most useful compilation is that of Miller and Gordon,[11] who give the function $e^{-x^2}\mathcal{E}(x)$, which appears directly in $P(\theta)$ and also has the advantage, for interpolation, of

approaching a finite limit $1/2x$ as x becomes large. A useful asymptotic series for $\mathcal{E}(x)$ is

$$\mathcal{E}(x) = \frac{e^{x^2}}{2x}\left[1 + \frac{1}{2x^2} + \frac{3.1}{(2x^2)^2} + \frac{5\cdot 3\cdot 1}{(2x^2)^3} + \ldots\right] \tag{29}$$

By expanding the integrand of eq. (28) in series and integrating term by term, it is confirmed that $P(\theta)$ is given by

$$P(\theta) = 1 - (1/3)\langle R^2\rangle[(4\pi/\lambda') \sin (\theta/2)]^2 + O[\sin (\theta/2)]^4 \tag{30}$$

as is required for any molecular model whatsoever.[10] At large u, according to eqs. (28) and (29), the scattering function approaches the asymptotic form

$$P(\theta) \sim (2/u)[1 + (2/u) + (12/u^2) + \ldots] \tag{31}$$

which may be compared with the expression for the linear chain[9,10]

$$P(\theta)_{\text{lin}} = (2/u^2)(e^{-u} - 1 + u) \rightarrow (2/u)[1 - (1/u)] \tag{32}$$

Both scattering functions asymptotically approach $2/u$, the limiting behavior that holds, in fact, for any chain structure made up of sequences

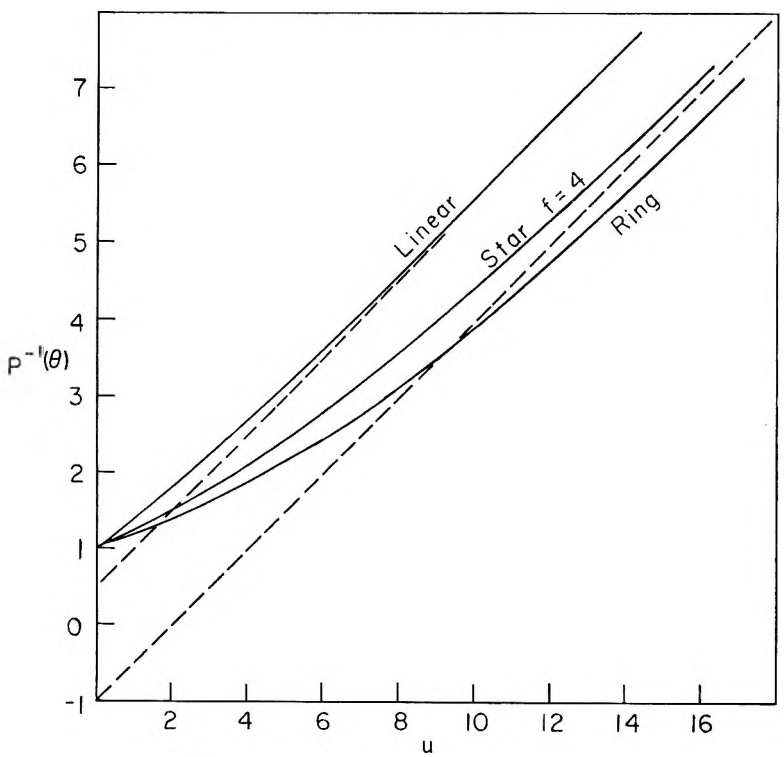

Fig. 3. Reciprocal scattering functions for linear chains, tetrafunctional stars, and rings [eqs. (32), (35), and (26)]. The upper dashed line is the asymoptote for the linear model; the lower one, for both tetrastars and rings.

of random-flight steps, no matter how they may be interconnected to form rings or branches. It is more informative, however, to compare the reciprocal functions:

$$P^{-1}(\theta) \sim (1/2)(u - 2) + O(1/u) \tag{33}$$

for the ring, and

$$P^{-1}(\theta)_{\text{lin}} \sim (1/2)(u + 1) + O(1/u) \tag{34}$$

for the straight chain. The limiting straight lines representing these functions plotted against u will obviously have the same slope but very different intercepts.

It is interesting that eq. (33) is precisely the asymptotic reciprocal function for the regular star model with four arms. In general, for the f-functional star, a result obtained by Benoit[12] reduces to

$$P(\theta)_{\text{star}} = (2/u^2)[(1/2)f(f-1)e^{-2u/f} - f(f-2)e^{-u/f} + u + (1/2)f(f-3)] \tag{35}$$

from which we obtain

$$P^{-1}(\theta)_{\text{star}} \sim (u/2) - [(f^2 - 3f)/4] + O(1/u) \tag{36}$$

In Figure 3, we show graphs of the reciprocal scattering functions and their linear asymptotic forms for linear chains, rings, and tetrafunctional stars. An additional point revealed by the plot is that while the straight chain and star functions approach their asymptotes monotonically from above, $P^{-1}(\theta)$ for the ring crosses the asymptotic line when u is about 9, and eventually approaches the limiting behavior from below. Over the finite range shown in the plot, $P(\theta)$ for a pentafunctional star actually coincides much more closely with the ring function than does the function for the tetrafunctional star. On the scale of Figure 3, the two reciprocal plots would diverge sensibly only beyond $u = 8$, as $P^{-1}(\theta)$ for the penta-star approaches its asymptotic limit $(u - 5)/2$.

This work was aided by support from the U. S. Air Force, Air Force Systems Command, Research and Technology Division, under Contract No. AF 33(657)-10661. It is a pleasure to acknowledge the benefit of conversations with Dr. Victor Bloomfield and Dr. D. P. Wyman.

References

1. Fiers, W., and R. L. Sinsheimer, *J. Mol. Biol.*, **5**, 424 (1962).
2. Weil, R., and J. Vinograd, *Proc. Natl. Acad. Sci. U. S.*, **50**, 730 (1963).
3. Casassa, E. F., *J. Chem. Phys.*, **37**, 2176 (1962).
4. Berry, G. C., and T. A. Orofino, *J. Chem. Phys.*, **40**, 1614 (1964).
5. Wang, M.-C., and G. E. Uhlenbeck, *Revs. Modern Phys.*, **17**, 323 (1945).
6. Fixman, M., *J. Chem. Phys.*, **23**, 1656 (1955).
7. Zimm, B. H., *J. Chem. Phys.*, **14**, 164 (1946).
8. Zimm, B. H., and W. H. Stockmayer, *J. Chem. Phys.*, **17**, 1301 (1949).
9. Zimm, B. H., R. S. Stein, and P. Doty, *Polymer Bull.*, **1**, 90 (1945).
10. Debye, P., *J. Phys. Colloid Chem.*, **51**, 18 (1947).
11. Miller, W. L., and A. R. Gordon, *J. Phys. Chem.*, **35**, 2785 (1931).
12. Benoit, H., *J. Polymer Sci.*, **11**, 50 (1953).

Résumé

On a modifié le modèle statistique conventionnel "en chapelet" proposé pour les chaînes flexibles de polymére dans le but de déterminer les propriétés thermodynamiques et configurationnelles de longues chaînes fermées (c.à.d. chaînes linéaires flexibles mais dont les terminaisons sont jointes) en solution diluée aux environs de la température de Flory. On a déterminé avec un premier ordre d'approximation l'effet du volume exclu intramoléculaire sur le carré moyen du rayon moléculaire; le second coefficient viriel est donné jusqu'à l'approximation de "double contact"; la distribution angulaire de l'intensité pour la dispersion de Rayleigh a été déterminée dans le cas de la molécule non perturbée. Qualitativement on peut dire que toutes ces propriétés sont modifiées par rapport à celles des chaînes linéaires de même masse comme le laissent prévoir la nature plus compacte du modéle cyclique.

Zusammenfassung

Das konventionelle statistische Perlschnurmodel für flexible Kettenpolymere wird zur Ableitung thermodynamischer und Konfigurationseigenschaften langkettiger Ringmoleküle (d.h. flexibler linearer Ketten mit vereinigten Enden) in verdünnter Lösung in der Nähe der Flory-Temperatur modifiziert. Der Einfluss des intramolekular ausgeschlossenen Volumens auf das mittlere Quadrat des Molekülradius wird in erster Näherung erhalten; der zweite Virialkoeffizient wird in der Näherung des "Doppelkontakts" berechnet; schliesslich wird die Winkelverteilung der Intensität für die Rayleigh-Streuung ungestörter Moleküle bestimmt. Qualitativ werden alle diese Eigenschaften im Vergleich zu denjenigen von linearen Ketten der gleichen Masse so beeinfluss, wie von der kompakteren Natur des Ringmodells erwartet werden kann.

Received June 1, 1964

JOURNAL OF POLYMER SCIENCE: PART A VOL. 3, PP. 615-628 (1965)

Vinyl Polymerization. XCII. Polymerization of Propenyl Chloride Isomers

TAKAYUKI OTSU, AKIHIKO SHIMIZU, and MINORU IMOTO,
Faculty of Engineering, Osaka City University, Sugimoto-cho, Sumiyoshi-ku, Osaka, Japan

Synopsis

The effect of the substituent on polymerization of isopropenyl chloride (IPC), *cis*-propenyl chloride (CPC), and *trans*-propenyl chloride (TPC) has been investigated. These monomers homopolymerized only very slightly in the presence of radical or ionic catalyst, and only a low molecular weight polymer of IPC was isolated. However, these monomers copolymerized with radical initiator with vinyl acetate, vinyl chloride, and acrylonitrile, and their reactivities towards the poly(vinyl acetate) radical decreased in order of IPC $\gg$ TPC $\geq$ CPC. The Q, e values for the monomers were estimated as follows: for IPC, $Q = 0.06$, $e = -0.85$; for CPC, $Q = 0.005$, $e = -1.66$; for TPC, $Q = 0.009$, $e = -1.33$. Further results on copolymerization with maleic anhydride indicated that the steric effect of the substituent for these monomers increased in order IPC $\ll$ TPC $\leq$ CPC. On radical polymerization of IPC, its degradative chain transfer reactivity was suggested to be also significant.

INTRODUCTION

Previous papers have reported on the effect of an *endo*- or *exo*-substituent on radical polymerizations of bicyclo-[2.2.1]-heptane-2-carboxylates[1] and of bornyl methacrylates.[2] In radical polymerizations of bornyl methacrylates,[2] the results indicated that an *endo*-bornyl substituent showed the same electric and steric effects on the rate and the reactivity as a methyl substituent, but the *exo*-bornyl substituent showed somewhat increased steric effect.

In order to elucidate further the steric effect of the substituent on the vinyl polymerization, a study of the effect of the substituent in isopropenyl chloride (IPC), *trans*-propenyl chloride (TPC), and *cis*-propenyl chloride (CPC) on their polymerizations was taken up in the present work. Several studies on polymerization of IPC or an isomeric mixture of propenyl chlorides have been reported,[3-6] but no detailed study as to the polymerizations of the respective pure propenyl chloride isomers under similar conditions has been found. The present paper deals with the effect of the substituent on polymerization and copolymerization of the various propenyl chloride isomers.

EXPERIMENTAL

Preparation of IPC, CPC, and TPC

The isomeric mixture of propenyl chlorides was prepared by dehydrochlorination of 1,2-dichloropropane. The dehydrochlorination was carried out by dropping 1,2-dichloropropane (1 mole) into 20% alcoholic solution of potassium hydroxide (1.5 mole) maintained at 74°C. (81% yield). The percentages of the various propenyl chloride isomers in the resulting isomeric mixture were found by gas chromatography to be 18.1 (IPC), 59.6 (TPC), and 22.3% (CPC). The crude mixture was then fractionated by using a precision fractionation column having a theoretical plate number of more than 50 into IPC, CPC, and TPC.

TABLE I
Purities and Properties of the Propenyl Chloride Isomers

Monomer	Purity, %	b.p., °C.	d_4^{20}	n_D^{20}	Relative retention volume[a]
IPC	99.84	22.5–23.0	0.931	—	156
TPC	99.42	37.0–38.0	0.932	1.4112	374
CPC	99.38	32.4–33.0	0.947	1.4069	294

[a] Relative retention volume of the propenyl chloride isomers was calculated by assuming that the retention time for air was unity.

The physical properties of the resulting pure monomers are shown in Table I, in which their purities determined by gas chromatography are also indicated. Gas chromatography of the respective propenyl chloride isomers was determined by using a tricresyl phosphate (TCP) column in a stream of hydrogen (30 ml./min.) at 40°C. The infrared spectra (Fig. 1) showed characteristic absorption bands at 798 cm.$^{-1}$ for IPC, 1179 cm.$^{-1}$ for TPC, and 685 cm.$^{-1}$ for CPC, in good agreement with the reported values.[7]

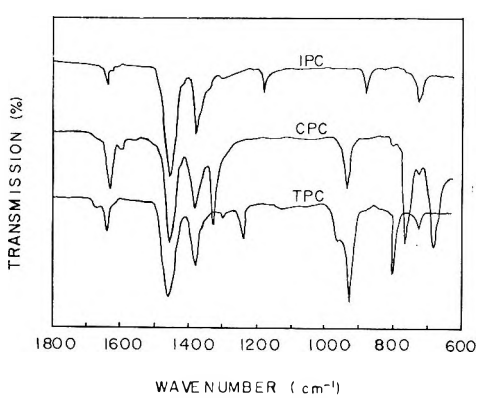

Fig. 1. Infrared spectra of propenyl chloride isomers (Nujol mull).

Other Materials

Vinyl acetate (VAC), vinyl chloride (VC), acrylonitrile (AN), and maleic anhydride (MAH) used as comonomers were purified by the conventional methods.[8] Azobisisobutyronitrile (AIBN) was recrystallized from ethanol. Boron trifluoride–diethyl etherate was used after distillation. Butyllithium (Hans Heinrich Hutte), diethylaluminum chloride (Texas Alkyl Co.), and titanium trichloride (Stauffer Chem. Co.) were used without further purification.

Polymerization Procedure

Polymerization and copolymerization were carried out in a sealed tube of 20 ml. capacity. The required amounts of initiator, solvent, and comonomers were placed in the tube, and this tube was connected to a vacuum system. After degassing of its content by repeating freezing and thawing, the required amount of monomer which had been weighed beforehand in a vacuum system was charged into the tube by distillation, and the tube was then sealed off. In the case of ionic polymerization, a hard glass tube provided with rubber stopper from which catalyst was charged through a syringe next to the connection to the vacuum system was used.

Polymerization and copolymerization were carried out with shaking in a thermostat maintained at a constant temperature for a given time. After polymerization, the contents of the tube were poured into a large amount of methanol (ether was used in copolymerization with MAH) to precipitate the polymer. The resulting polymer was washed thoroughly, filtered, dried under vacuum at room temperature, and then weighed.

Analysis of the Polymer

The composition of the resulting polymer and copolymer was determined by elementary analyses for C, H, N, and Cl. Monomer reactivity ratios (r_1 and r_2) were calculated by the Fineman-Ross method.[9]

The content of 1,2-dichloride unit in the copolymers with VC was determined as follows.[10] A given amount of the copolymer (0.2–0.3 g.) was placed in a glass tube containing about 1 g. of potassium iodide and 15 ml. of peroxide-free dioxane. The content of the tube was degassed by alternate freezing and thawing and then sealed off. The reaction was carried out for 96 hr. in boiling water and then the contents of the tube were poured into a mixture of 20 ml. of chloroform and 100 ml. of water. The free iodine was titrated with 0.05N sodium thiosulfate, 5% aqueous starch solution being used as an indicator. The percentage of 1,2-dichloride units present (Δ) was calculated from the equation:

$$\Delta = {}^1/_2(\text{free } I_2 \text{ eq./g. of polymer})(76.5\ dM_1 + 62.5\ dM_2) \times 100$$

where dM_1 and dM_2 are mole fractions of propenyl chloride and VC in the copolymer, respectively.

RESULTS

Polymerization of IPC, TPC, and CPC

The results of the homopolymerization of these propenyl chloride monomers with radical or ionic initiators are summarized in Table II. These monomers were found to be not polymerized by the presence of butyllithium (1.0×10^{-2} mole/l. in toluene at $-78°$C. for 65 hr.), boron trifluoride–diethyl etherate (5.0×10^{-2} mole/l. in toluene at 26–27°C. for 120 hr.), and diethylaluminum chloride–titanium trichloride (Al/Ti = 2) (0.167 mole/l. in *n*-heptane at 60°C. for 30 hr.).

TABLE II
Results of Polymerization of Propenyl Chloride Monomers

Initiation	Monomer[a]	Temp., °C.	Time, hr.	Yield, %	η_{sp}/c of polymer[b]	Analyses of polymers[c] C, %	H, %	Cl, %
[AIBN] =	IPC	60	100	2.1	0.017	74.42	8.92	16.47
1.84×10^{-2}	TPC	60	100	0.02	—	—	—	—
mole/l. in bulk	CPC	60	100	Nil	—	—	—	—
γ-ray ($5.089 \times$	IPC	26–27	96	4.8	0.026	52.12	8.25	24.95
10^5 r/hr.) in	TPC	26–27	96	0.04	—	—	—	—
bulk	CPC	26–27	96	Nil	—	—	—	—
$[(C_2H_5)_2AlCl]$ =	IPC	−78	79	Nil	—	—	—	—
5.0×10^{-2}	IPC	0	15	9.8	0.037	63.87	8.58	26.38
mole/l. in *n*-	IPC	26–27	192	1.9	—	—	—	—
heptane	TPC	−78	122	Nil	—	—	—	—
	TPC	26–27	136	Nil	—	—	—	—
	CPC	−78	122	Nil	—	—	—	—
	CPC	26–27	42	Nil	—	—	—	—

[a] Monomer concentrations were as follows: [IPC] = [TPC] = 12.2 mole/l., [CPC] = 12.4 mole/l. in bulk; [IPC] = [TPC] = 6.1 mole/l., [CPC] = 6.2 mole/l. in *n*-heptane.

[b] Determined by viscosity measurement of 0.2% benzene solution at 30°C. in an Ubbelohde viscometer.

[c] Calculated value for polypropenyl chloride: C, 47.06%; H, 6.54%; Cl, 46.40%.

From these results it was clear that these monomers polymerized slightly in the order IPC $\gg$ TPC $\geq$ CPC. During the polymerization of these monomers by AIBN or by ionic initiator, the polymerization mixtures changed in color from yellow to brown, and the colored polymer of IPC which showed a quite low specific viscosity were isolated. This polymer was also gradually converted to a deep-colored crosslinked polymer on being allowed to stand in air at room temperature.

Infrared spectra of the polymers which were allowed to stand in air for a week at room temperature are shown in Figure 2. Strong absorption bands attributed to carbon–carbon double bonds (1610, 1630 cm.$^{-1}$) and carbonyl group (1720, 1740 cm.$^{-1}$) were observed. These observations were also supported by the fact that the observed chlorine contents in the

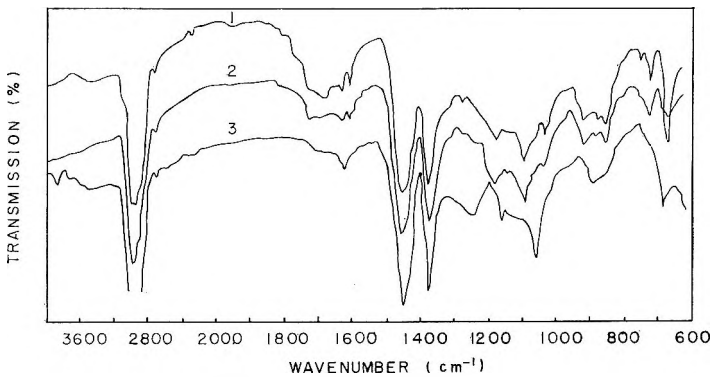

Fig. 2. Infrared spectra of poly(isopropenyl chlorides) obtained under various conditions (KBr disk): (*1*) polymer obtained with AIBN, (*2*) polymer obtained by γ-irradiation; (*3*) polymer obtained with Et_2AlCl.

polymers were less than those calculated for propenyl chloride as indicated in Table II. These results might indicate that the dehydrochlorination and oxidation of the resulting IPC polymer occurred during the polymerization or on standing in air.

Copolymerization with VAC

The results of the radical copolymerization of these monomers with VAC at 60°C. are shown in Table III. There is some question regarding the analytical values of the copolymers of IPC, because dehydrochlorination of the homopolymer took place readily, as stated above. In order to confirm this point, the observed carbon and hydrogen contents in the copolymers were compared with those calculated from their observed chlorine contents. The results shown in Table IV indicate that both values for

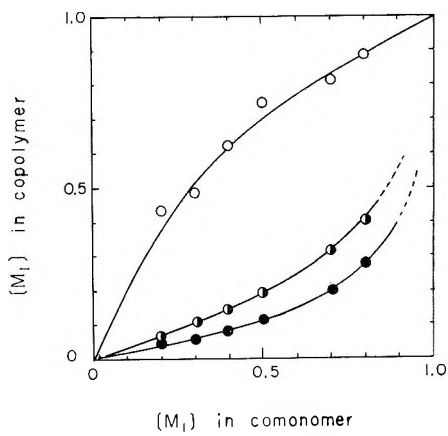

Fig. 3. Monomer–copolymer composition curves for copolymerization of propenyl chlorides (M_1) and VAC (M_2) initiated by AIBN at 60°C.: (O) IPC–VAC system; (◑) TPC–VAC system; (●) CPC–VAC system.

TABLE III. Results of Copolymerization of the Propenyl Chloride Monomers with VAC, VC, and AN at 60°C. in Benzene

Polymerization system	$[M_1]$ in comonomer, mole-%	Time, hr.	Yield, %	Rate of copolymerization, %/hr.	Copolymer Cl, %	Copolymer $[M_1]$, mole-%
IPC(M_1)–VAC(M_2)	20.0	12.0	11.4	1.0	18.7	43.1
	30.1	14.8	9.2	0.6	21.1	48.3
	39.9	15.5	5.7	0.4	27.4	61.9
	50.0	20.5	11.0	0.5	33.5	74.4
	70.2	40.9	2.7	0.07	36.6	80.8
	80.0	54.5	1.9	0.03	40.4	88.4
TPC(M_1)–VAC(M_2)	19.9	5.5	13.4	2.4	3.2	7.7
	30.2	6.0	10.3	1.7	4.7	11.1
	40.0	7.3	8.1	1.1	6.0	14.7
	50.0	17.8	10.2	0.6	8.1	19.6
	70.4	69.7	7.1	0.1	13.2	31.3
	80.0	83.2	2.9	0.03	17.1	40.4
CPC(M_1)–VAC(M_2)	20.2	4.0	11.0	2.8	1.8	4.3
	30.4	6.0	9.8	1.6	2.5	6.0
	40.1	10.0	9.4	0.9	3.4	8.2
	50.0	22.0	11.9	0.5	4.8	11.2
	70.8	37.5	4.3	0.1	8.2	19.7
	80.4	37.5	1.9	0.05	11.8	28.2
IPC(M_1)–VC(M_2)	10.0	3.0	15.6	5.2	52.3	38.7
	20.0	4.0	14.4	3.6	50.4	56.5
	30.1	5.0	10.8	2.2	49.1	70.2
	49.5	11.5	7.8	0.7	46.8	95.5
	69.8	39.2	7.4	0.2	38.1	—
	79.6	40.9	4.7	0.1	37.1	—
TPC(M_1)–VC(M_2)	10.1	2.0	13.5	6.8	56.8	0.1
	20.0	2.5	12.3	4.9	56.2	5.2
	30.2	5.0	10.6	2.1	55.4	11.5
	49.9	11.8	10.7	0.9	54.6	18.4
	70.0	24.0	4.0	0.2	52.6	35.7
	80.2	45.0	1.0	0.02	50.2	58.7
CPC(M_1)–VC(M_2)	10.1	1.2	5.7	5.0	57.3	1.0
	20.2	2.4	7.9	3.3	56.6	1.7
	30.4	4.5	10.7	2.4	56.1	5.7
	50.1	5.0	4.5	0.9	56.0	6.3
	70.4	16.8	3.1	0.2	54.8	16.7
	80.5	37.8	0.9	0.02	51.9	42.4
IPC(M_1)–AN(M_2)	9.9	0.3	2.8	9.3	10.4	7.5
	19.8	0.6	2.2	3.7	21.1	15.6
	41.6	0.6	1.2	2.0	35.0	27.2
	49.5	1.4	2.0	1.4	40.4	31.9
	69.3	2.0	1.6	0.8	46.5	37.7
	79.2	5.3	3.0	0.6	49.7	40.7
TPC(M_1)–AN(M_2)	10.0	0.3	2.0	6.7	1.5	1.1
	19.8	0.6	2.6	4.3	1.9	1.3
	29.7	0.6	1.5	2.5	3.0	2.1
	49.6	1.4	1.8	1.3	5.5	3.9
	69.4	2.0	0.9	0.5	14.2	10.3
	79.3	5.3	0.9	0.2	22.8	17.0

TABLE III (*continued*)

Polymerization system	$[M_1]$ in comonomer, mole-%	Time, hr.	Yield, %	Rate of copolymerization, %/hr.	Copolymer Cl, %	Copolymer $[M_1]$, mole-%
CPC(M_1)–AN(M_2)	10.0	0.3	7.2	24.0	1.3	0.9
	20.1	0.6	7.5	12.5	1.7	1.2
	30.2	0.6	3.9	6.5	2.4	1.6
	50.4	1.4	3.7	2.6	4.4	3.1
	70.5	2.0	1.2	0.6	8.4	6.0
	80.6	5.3	0.9	0.2	14.7	10.7

carbon and hydrogen are the same within experimental error, and hence no dehydrochlorination of the copolymer occurred.

As is clearly shown in Table III, the rates of copolymerization of the monomers with VAC markedly decreased as the concentration of the propenyl chloride monomer increased. The resulting monomer–copolymer composition curves based on the results of Table III are shown in Figure 3. The resulting copolymers were almost colorless powders and were soluble in acetone, benzene, and tetrahydrofuran. Their infrared spectra showed no absorption band due to the carbon–carbon double bond.

TABLE IV
Comparison of the Carbon and Hydrogen Contents in the Copolymers of IPC with VAC

Carbon, %		Hydrogen, %		Chlorine, %
Obs.	Calcd.[a]	Obs.	Calcd.[a]	(obs.)
52.73	52.29	6.97	6.80	18.68
52.20	51.84	6.75	6.78	21.06
51.26	50.64	6.59	6.72	27.41
50.36	49.50	6.86	6.66	33.45
49.73	48.91	6.87	6.63	36.60
49.16	48.19	6.79	6.60	40.44

[a] Calculated from the observed chlorine contents.

Copolymerization with VC

The results are shown in Table III. The resulting monomer–copolymer composition curves are shown in Figure 4. Figure 4 indicates that the copolymerization of the propenyl chloride monomers with VC followed almost the same trend as with VAC. The resulting copolymers were colorless or light yellow powders and were soluble in cyclohexanone, tetrahydrofuran, and nitrobenzene.

In order to determine the regularity of the head-to-tail configuration on radical polymerization of the monomers, the content of 1,2-dichloride unit in the copolymers with VC was determined by the potassium iodide method. The results are shown in Figure 5; the content of 1,2-dichlorides

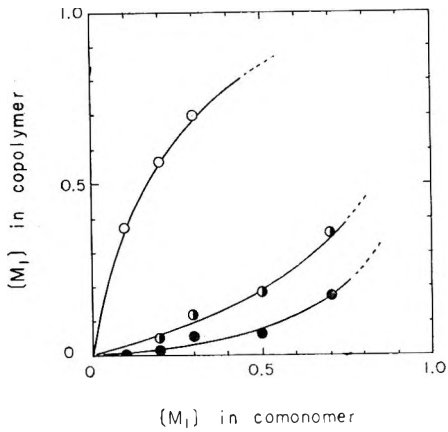

Fig. 4. Monomer-copolymer composition curves for copolymerization of propenyl chlorides (M_1) with VC (M_2) initiated by AIBN at 60°C.: (O) IPC–VC system; (◑) TPC–VC system; (●) CPC–VC system.

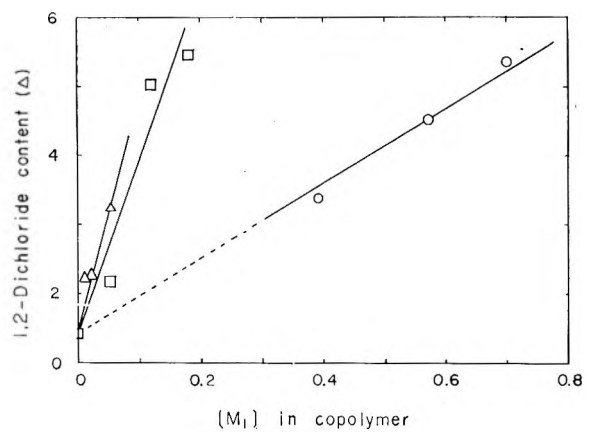

Fig. 5. Relationship between the percentage of 1,2-dichloride unit and the concentration of propenyl chloride (M_1) in copolymer with VC: (O) IPC–VC copolymer; (□) TPC–VC copolymer; (△) CPC–VC copolymer.

increased linearly with an increase of the propenyl chloride content in the copolymers. The slopes of these straight lines, which might indicate the rate of formation of the 1,2-dichloride unit, were observed to become greater in the order of IPC $\ll$ TPC $\leq$ CPC. By extrapolating these lines to [PC] = 0, the same intercepts were obtained as 1.49 which showed the content of the 1,2-dichloride unit for poly(vinyl chloride).

Copolymerization with AN

The results are shown in Table III; the monomer–copolymer composition curves are shown in Figure 6. The resulting colorless or light yellow copolymers were soluble in dimethylformamide.

Copolymerization with MAH

The results of copolymerizations of the propenyl chloride monomers with MAH initiated by AIBN at 60°C. are shown in Table V, and the monomer–copolymer composition curves are shown in Figure 7.

As can be seen from Table V, IPC copolymerized quite readily with MAH to give a colorless polymer which showed a relatively high specific viscosity. However, TPC and CPC copolymerized at rather slow rates and light red-colored copolymers having a lower specific viscosity were obtained.

TABLE V

Results of Copolymerization of Propenyl Chlorides (M_1) with MAH (M_2) at 60°C.; [AIBN] = 1.68×10^{-2} mole/l. in Benzene

M_1	$[M_1]$ in comonomer, mole-%	Time, hr.	Yield, %	Rate of copolymerization, %/hr.	Copolymer Cl, %	Copolymer $[M_1]$, mole-%	Copolymer η_{sp}/c[a]
IPC	19.9	3.5	48.4	13.8	18.7	45.6	—
	39.9	3.5	84.1	24.0	20.0	49.2	0.51
	61.4	3.5	73.1	20.9	20.5	50.0	—
	80.0	3.5	39.3	11.2	22.5	54.3	—
TPC	19.9	20	2.9	0.15	12.5	32.0	—
	40.0	20	6.0	0.30	16.9	42.3	0.065
	61.4	20	7.8	0.39	19.3	47.8	—
	79.9	20	5.3	0.27	21.8	53.2	—
CPC	20.2	20	4.1	0.21	11.8	30.5	—
	40.3	20	7.4	0.37	15.2	38.5	0.046
	61.8	20	10.2	0.51	17.4	43.5	—
	80.3	20	7.5	0.38	19.1	47.3	—

[a] Determined by viscosity measurement of 0.4% tetrahydrofuran solution in an Ubbelohde viscometer.

From Table V, the composition of the resulting copolymers was found to be independent of monomer feed ratio and to consist of 1:1 molar composition of MAH and propenyl chloride monomer.

Monomer Reactivity Ratios and Q–e Values for Propenyl Chloride Isomers

According to the Fineman-Ross method,[9] the monomer reactivity ratios (r_1 and r_2) were calculated for these copolymerization systems. The results are summarized in Table VI. From the r_1 and r_2 values obtained, Q and e values for the monomers were calculated by assuming the values: VAC($Q_2 = 0.026$, $e_2 = -0.22$);[11] VC($Q_2 = 0.044$, $e_2 = 0.20$);[11] AN($Q_2 = 0.6$, $e_2 = 1.2$).[11] In Table VI, the reported values for allyl chloride (AC) which may be considered a propenyl chloride isomer are also indicated.

As understood from this table, the values of Q_1 for the propenyl chloride isomers and the values of $1/r_2$ which might indicate the reactivity of the propenyl chloride isomers to polymer radicals were found to be of the same

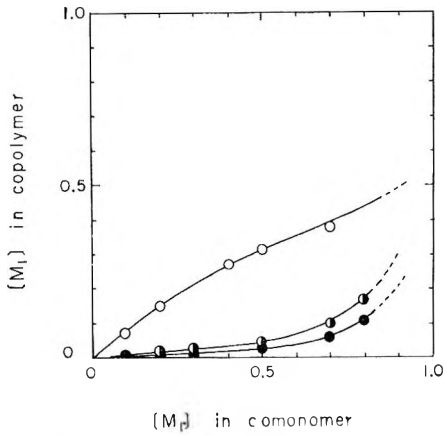

Fig. 6. Monomer–copolymer composition curves for copolymerization of propenyl chloride (M_1) with AN (M_2) initiated by AIBN at 60°C.; (○) IPC–AN copolymer; (◑) TPC–AN copolymer; (●) CPC–AN copolymer.

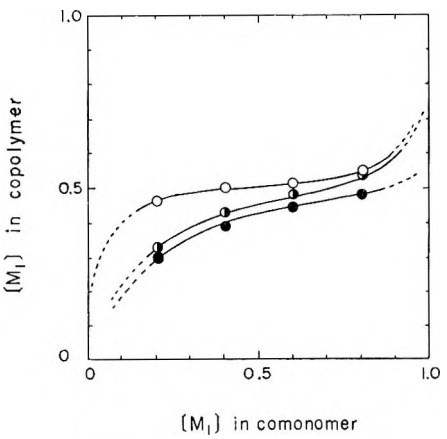

Fig. 7. Monomer–copolymer composition curves for copolymerization of propenyl chloride (M_1) with MAH (M_2) initiated by AIBN at 60°C.; (○) IPC–MAH copolymer; (◑) TPC–MAH copolymer; (●) CPC–MAH copolymer.

order as their reactivities for homopolymerization. The products r_1r_2 which are used as a measure of alternative tendency for copolymerization were calculated as 0.0004 for IPC–MAH, 0.013 for TPC–MAH, and 0.0002 for CPC–MAH copolymerization systems.

TABLE VI
Monomer Reactivity Ratios(r_1, r_2) and Q_1, e_1 Values for Propenyl Chloride Isomers

M_1	M_2	r_1	r_2	$1/r_2$	Relative reactivity	Q_1	e_1
IPC	VAC	1.84	0.22	4.55	33	0.06	−0.85
IPC	VC	5.21	0.18	5.56	67	0.24	−0.14
IPC	AN	0.01	1.4	0.72	21	0.04	−0.86
IPC	MAH	0.06	0.06	16.7	6.8	—	—
TPC	VAC	0.08	3.56	0.28	2	0.009	−1.33
TPC	VC	0.18	4.0	0.25	3	0.01	−0.37
TPC	AN	0.01	18.0	0.057	2	0.008	−0.11
TPC	MAH	0.05	0.26	3.84	1.6	—	—
CPC	VAC	0.01	7.0	0.14	1	0.005	−1.66
CPC	VC	0.08	12.1	0.083	1	0.004	0.02
CPC	AN	0.005	29.5	0.034	1	0.005	−0.18
CPC	MAH	0.004	0.41	2.44	1	—	—
AC	VAC	0.67[a]	0.7[a]	1.43	10	0.056[b]	0.11[b]
AC	AN	0.05[a]	3.0[a]	0.33	9.7	0.056[b]	0.11[b]

[a] Data of Agron et al.[12] (68°C.).
[b] Data of Chapin et al.[13] (60°C.).
[c] Data of Young.[11]

DISCUSSION

As can be seen from Table II, the reactivities of these propenyl chloride isomers for their homopolymerization were quite low and decreased in the order of IPC $\gg$ TPC $\geq$ CPC. The same reactivity order was also found for their copolymerizations (Table VI). The low reactivities of TPC and CPC which were 1,2-disubstituted ethylene monomer might be understood by an increased steric effect of the substituent in their monomers.

From Table VI, TPC was about two or three times as reactive towards the polymer radicals as CPC. This difference coincided with the results on *cis*- or *trans*-1,2-dichloroethylene observed by Lewis and Mayo,[14] who reported that the *trans* isomer was six times as reactive as the *cis* isomer towards attack of the poly(vinyl acetate) radical. Accordingly, the rather low reactivity of CPC compared to TPC might be understood by a decreased resonance stabilization energy in its transition state as the result of the steric effect of the *cis* substituent. It might be also supported by the lower Q value for CPC than TPC as indicated in Table VI.

However, in radical polymerization of IPC which is known to have a smaller steric effect than TPC or CPC, the degradative monomer chain transfer (allylic termination) might be indicated as an important factor in the lower reactivity as well as that for AC:

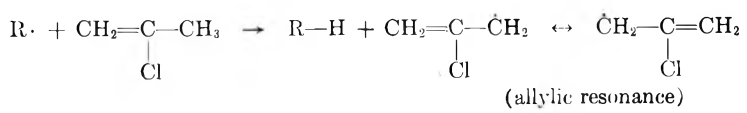

where R· is an initiator or polymer radical. This fact could be supported by the results that IPC copolymerized without retardation more easily with MAH than TPC or CPC to yield a high molecular weight alternating copolymer. However, it was found that the rates of copolymerizations with VAC, VC, and AN decreased with increasing concentration of the propenyl chloride monomer, indicating that the degradative PC monomer chain transfer reactivity and the steric effect of the substituent might be also important for the copolymerizations.

Let us consider the growing polymer ends for each of the isomers to be as shown in I–IV:

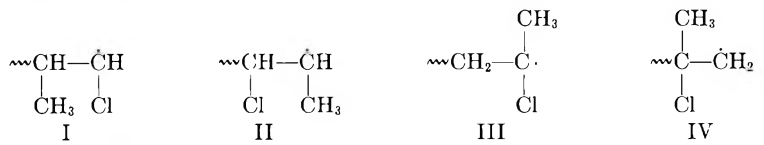

where structures I and II are those for TPC and CPC, and structure III and IV are alternative ones for IPC.

As can be expected from the observed Q values (Table VI), the difference in resonance stabilization energy was not so large between the structures of I and II in the *cis* and *trans* isomers. In the case of IPC, however the structure of III was more stable than that of IV and also than the structures of I and II. These differences might be expected to give the irregularity of the head-to-tail configuration in the repeated monomer unit of the resulting polymer chain.

This possibility was checked by the determination of the 1,2-dichloride content in the copolymers with VC. As clearly indicated in Figure 5,

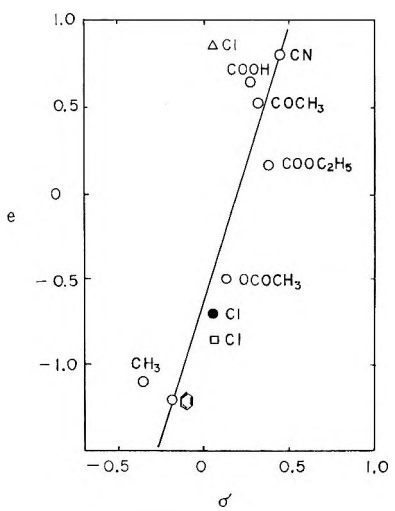

Fig. 8. Relationship between e values and σ constants for substituted isopropenyl monomers: (△) Young's value; (●) calculated from Tkachenko's data;[5] (□) observed value.

the rate of formation of the 1,2-dichloride unit in the propenyl chloride copolymers with VC increased in the order IPC $\ll$ TPC $\leq$CPC, which was found to be an order which is the reverse of their reactivities for polymerization.

Although the observed e values for TPC and CPC were in agreement with the reported value for the isomeric propenyl chloride mixture, the e value (-0.85) for IPC was quite different from this value (0.86).[11] In order to check this point, the reported e values for substituted isopropenyl monomers were plotted against the σ values of the substituent. As shown in Figure 8, the result indicated that there was clearly a linear relationship between the e values of the monomers, including that for IPC, obtained in this study and the σ values of the substituent. Accordingly, it was concluded that the e value obtained in this study was the appropriate value.

The homopolymer of IPC was very unstable and dehydrochlorination and oxidation leading to formation of a colored polymer took place easily during the polymerization, or on standing afterwards. However, it was suggested that the IPC unit in the polymer chain was stabilized by copolymerization with the other monomers.

References

1. Imoto, M., T. Otsu, and W. Fukuda, *J. Polymer Sci.*, **B1**, 225 (1963); *Kogyo Kagaku Zasshi*, **66**, 832 (1963).
2. Imoto, M., T. Otsu, K. Tsuda, and T. Ito, *J. Polymer Sci.*, **A2**, 1407 (1964).
3. Starkweather, H. W., *J. Am. Chem. Soc.*, **56**, 1870 (1934).
4. Aelterman, M., and G. Smets, *Bull. Soc. Chim. Belg.*, **60**, 459 (1952).
5. Tkachenko, G. V., P. M. Khomikovskiĭ, A. D. Abkin, and S. S. Medvedev, *Zhur. Fiz. Khim.*, **31**, 242 (1957).
6. Gilbert, H., F. F. Miller, S. J. Averill, E. J. Carlson, V. L. Folt, H. J. Heller, F. D. Stewart, R. F. Schmidt, and H. L. Trumbull, *J. Am. Chem. Soc.*, **78**, 1669 (1956).
7. Spell, H. L., *Anal. Chem.*, **31**, 1442 (1959).
8. Blout, E. R., W. P. Hohenstein, and H. Mark, *Monomers*, Interscience, New York, 1949; T. Otsu and K. Takemoto, *Experimental Method of Vinyl Polymerization*, Kyoritsu, Tokyo, Japan, 1960.
9. Fineman, M., and S. D. Ross, *J. Polymer Sci.*, **5**, 269 (1950).
10. Mayo, F. R., and K. E. Wilzbach, *J. Am. Chem. Soc.*, **71**, 1124 (1949); C. S. Marvel, J. H. Sample, and M. F. Roy, *J. Am. Chem. Soc.*, **61**, 3241 (1939).
11. Young, L. J., *J. Polymer Sci.*, **54**, 411 (1961).
12. Agron, P. T., T. Alfrey, Jr., J. Bohrer, H. Haas, and H. Weehsler, *J. Polymer Sci.*, **3**, 157 (1948).
13. Chapin, E. C., G. E. Ham, and C. L. Mills, *J. Polymer Sci.*, **4**, 597 (1949).
14. Lewis, F. M., and F. R. Mayo, *J. Am. Chem. Soc.*, **70**, 1533–1536 (1948).

Résumé

On a étudié l'influence du substituant sur la polymérisation du chlorure d'isopropenyle (IPC), du chlorure de *cis*-propényle (CPC) et du chlorure de *trans*-propényle (TPC). Ces monomères homopolymérisent fortement en présence de catalyseurs radicalaires ou ioniques: on a pu isoler seulement un polymère de faible poids moléculaire de l'ICP. Cependant ces monomères copolymérisent par initiation radicalaire avec l'acétate de vinyle, le chlorure de vinyle et l'acrylonitrile, et leurs réactivités vis-à-vis du radical de l'acétate de polyvinyle diminuent dans l'ordre IPC $\gg$ TPC > CPC. Les valeurs de Q

et de e pour ces monomères sont les suivantes: IPC: $Q = 0.06$, $e = -0.85$; CPC: $Q = 0.005$, $e = -1.66$; TPC: $Q = 0.009$, $e = -1.33$. A partir des résultats obtenus lors de la copolymérisation avec l'anhydride maléique, l'effet stérique du substituant pour ces monomères augmente dans l'ordre IPC $\ll$ TPC $\leq$ CPC. Lors de la polymérisation radicalaire de l'IPC, la réactivité du transfert de chaîne dégradant est également important.

Zusammenfassung

Der Einfluss des Substituenten auf die Polymerisation von Isopropenylchlorid (IPC), *cis*-Propenylchlorid (CPC) und *trans*-Propenylchlorid (TPC) wurde untersucht. Diese Monomeren zeigten in Gegenwart von radikalischen oder ionischen Katalysatoren kaum eine Homopolymerisation: lediglich ein liedrigmolekulares Polymeres von IPC wurde isoliert. Mit radikalischen Startern trat jedoch eine Copolymerisation dieser Monomeren mit Vinylacetat, Vinylchlorid und Acrylnitril ein, wobei ihre Reaktivität gegen das Polyvinylacetatradikal in der Reihenfolge IPC $\gg$ TPC $\geq$ CPC abhanm. Für diese Monomeren wurden folgende Q- und e-Werte bestimmt: IPC: $Q = 0{,}06$, $e = -0{,}85$; CPC: $Q = 0{,}005$, $e = -1{,}66$; TPC: $Q = 0{,}009$, $e = -1{,}33$. Ergebnisse bei der Copolymerisation mit Maleinsäureanhydrid zeigen weiters, dass der sterische Effekt des Substituenten bei diesen Monomeren in der Reihenfolge IPC $\ll$ TPC $\leq$ CPC zunimmt. Für die radikalische Polymerisation von IPC wurde auch eine charakteristische degradative Kettenübertragung angenommen.

Received April 8, 1964
Revised July 9, 1964

JOURNAL OF POLYMER SCIENCE: PART A VOL. 3, PP. 629–640 (1965)

Rubber Elasticity of Preswollen Polymer Networks: Highly Crosslinked Vinyl–Divinyl Systems*

M. C. SHEN† and A. V. TOBOLSKY, *Frick Chemical Laboratory, Princeton University, Princeton, New Jersey*

Synopsis

The rubber elasticity of highly crosslinked, preswollen network polymers is studied. Copolymers of tetraethylene glycol dimethacrylate with ethyl acrylate, *n*-butyl acrylate, methyl methacrylate, and styrene covering the whole range of composition are investigated. Dioctyl phthalate is used to preswell the polymers up to 50% by volume. Both shear moduli and front factors are found to increase with increasing crosslink concentration but to decrease with increasing diluent content. Crosslinking efficiencies are determined by a modified Loshaek-Fox method. They are relatively invariant with the degree of preswelling. Factors contributing toward these observations are discussed.

INTRODUCTION

Most of the published work on rubber elasticity has been concerned with systems having low degrees of crosslinking. Statistical theories[1,2] have been derived with the assumption that the network chains are all sufficiently long to assume Gaussian conformation. Recently, in order to examine the applicability of these theories in the highly crosslinked network polymers, we have reported the rubber elasticity of epoxy resins,[3] polyesters,[4] as well as several vinyl–divinyl systems which covered the entire range of degree of crosslinking.[5–7] Rubbery plateau regions were found to occur at high temperatures for very highly crosslinked polymers. Front factors were calculated from the equation of state of rubber elasticity. Data on the vinyl–divinyl systems included those on poly(ethyl acrylate) crosslinked by dimethacrylates of varying chain lengths[6] and on four different vinyl polymers crosslinked by tetraethylene glycol dimethacrylate.[5,7] These network polymers were all prepared in bulk.

The physical properties of network polymers prepared in the presence of diluents, however, can be expected to differ from those of polymers prepared in bulk. Swelling behavior of preswollen polymers has been reported.[8–10] In previous papers from this laboratory,[11,12] we have studied the rubber elasticity of lightly crosslinked, preswollen polymers. In this

* This article is based on part of a dissertation submitted by M. C. Shen for the partial fulfillment of the requirements for the degree of Doctor of Philosophy at Princeton University.

† Harvard Chemistry Fellow, 1961–1962.

paper, we shall present our results on that of highly crosslinked preswollen polymers.

The equation of state of rubber elasticity for shear modulus is:[1]

$$G = \phi nRT \tag{1}$$

where G is the shear modulus, n is the concentration of effective network chains in moles per cubic centimeter, R is the ideal gas constant, and T is the absolute temperature at which the measurement of G is made. The front factor, ϕ, is under simple conditions approximated by the following equation:[1,2]

$$\phi = G/nRT \approx \bar{r}_i^2/\bar{r}_f^2 \tag{2}$$

where $\bar{r}_i^2$ and $\bar{r}_f^2$ are the mean square end-to-end distances of the network chain and of a free chain, respectively. For polymers that obey stipulations of the kinetic theory, ϕ is unity. The concentration of network chains per cubic centimeter is given by the expression:

$$n = c'z = ecz \tag{3}$$

where c is the number of moles per cubic centimeter of crosslinker, e is the crosslinking efficiency, and z depends on the functionality of the crosslinker. c' is defined by eq. (3) and may be known as the effective crosslinker concentration. Equation (1) therefore reads:

$$G = \phi eczRT \tag{4}$$

The front factor ϕ may also be affected by the presence of "trapped entanglements" and by ineffective "cyclized" network chains, as discussed in the remainder of this paper.

EXPERIMENTAL METHODS

Sample Preparation

Monomers ethyl acrylate (EA), *n*-butyl acrylate (BA), methyl methacrylate (MMA), styrene (STY), and tetraethylene glycol dimethacrylate (TEGDM) were obtained from the Borden Chemical Co. Dioctyl phthalate (DOP) from Eastman Chemical was used as the diluent. Photopolymerizations were carried out between Pyrex glass plates in front of a G.E. RS sunlamp for approximately two days. Benzoin (Matheson) was used as photosensitizer. Unpolymerized monomer was removed by heating in a vacuum oven. Preswollen polymers were made that contain various diluent contents and cover the whole range of crosslinking densities. In a few cases where both the diluent content and degree of crosslinking were very high, some evidence of incompatibility was observed.

Efficiency of Crosslinking Measurements

In this study, we have used tetraethylene glycol dimethacrylate (TEGDM) as the divinyl crosslinker. At low concentrations of TEGDM, the length of the TEGDM chain is negligible with respect to the length of network chains made of monofunctional vinyl monomers. Here z can be

taken to be 2. At intermediate values of c', the length of the TEGDM chain becomes comparable to the other network chains, z may perhaps be 3. At very high degrees of crosslinking, TEGDM chains are the only ones with appreciable length, and z approaches unity. The precise assignment of z values at various degrees of c', however, is a difficult task. In data presented below, we prefer to leave z unspecified.

It is well known that in the copolymerization of a difunctional monomer with a monofunctional monomer, the number of crosslinks actually produced is not equal to the number of difunctional molecules employed.[13-17] An experimental procedure is available[13] to evaluate quantitatively the efficiency of crosslinking e. For the preswollen network polymers, a modified Loshaek-Fox method for measuring e is presented.

It was found[6] that the volume contraction associated with the complete polymerization of a mole of double bonds is nearly the same for methacrylates of similar structure: $\Delta V = 22.50$ cc./mole at 25°C. This apparent volume contraction is assumed to be the same for the double bonds of difunctional methacrylates if the polymerization is complete. In practice the contractions are lower. The relation between the observed contraction and the contraction associated with complete conversion can then be used to calculate the degree of conversion.

An equation for the efficiency of crosslinking can now be derived. If p is the fraction of all the vinyl groups which have reacted, then it can be represented by the following equation:

$$p = (\bar{v}_m - \bar{v}_p)/(N_M \Delta V_M + N_D \Delta V_D) \tag{5}$$

where $\bar{v}_m$ and $\bar{v}_p$ are the specific volumes of monomer mixture and polymer, respectively, N_M and ΔV_M are the number of moles of double bonds and the molar volume contraction of the monofunctional vinyl compounds, whereas N_D and ΔV_D are corresponding values for the difunctional ones. N_M and N_D are calculated by:

$$N_M = m_M/(m_M M_M + m_D M_D + m_S M_S) \tag{6}$$

and

$$N_D = 2m_D/(m_M M_M + m_D M_D + m_S M_S) \tag{7}$$

where m represents the number of moles of each component in the monomer mixture, M their molecular weights, and the subscripts M,D,S refer to monofunctional monomer, difunctional monomer, and solvent (diluent), respectively.

We assume, with good evidence,[13] that all monofunctional monomers have polymerized, and that all the difunctional monomers have at least reacted once. Obviously all the additional reacted double bonds now form crosslinks; hence the efficiency can be expressed by the following equation:

$$e = [p(m_M + 2m_D) - (m_M + m_D)]/m_D \tag{8}$$

Specific volumes of all the monomer mixtures and copolymers were determined by displacement density measurements at 25°C. Molar volume contractions due to polymerization previously determined[6] were used in this study. They are: 22.50 cc./mole for MMA; 16.64 cc./mole

TABLE IA
Rubber Elasticity Data of the System *n*-Butyl Acrylate (BA)–Tetraethylene Glycol Dimethacrylate (TEGDM)–Dioctyl Phthalate (DOP)

No.	DOP, vol.-%	Mole fraction TEGDM, %	c_{TEGDM}, mole/cc. $\times 10^5$	Sp. vol. monomer, cc./g.	Sp. vol. polymer, cc./g.	G, dynes/cm.^{2}	e	c', mole/cc. $\times 10^5$	$z\phi$
1	0	1.2	9.94			4.85×10^6	(0.75)	(7.47)	(1.03)
2	0	2.6	23.1			6.66×10^6	(0.75)	(17.3)	(0.61)
3	0	12.1	85.9	1.067	0.917	3.69×10^7	0.76	64.9	1.60
4	0	19.3	126	1.044	0.897	6.50×10^7	0.83	105	1.74
5	0	25.5	159	1.026	0.883	1.09×10^8	0.77	122	2.52
6	0	46.3	245	0.984	0.848	2.32×10^8	0.82	200	3.27
7	0	64.4	298	0.958	0.831	4.56×10^8	0.73	117	5.93
8	0	86.4	346	0.935	0.818	6.67×10^8	0.67	231	8.15
9	0	100.0	375	0.924	0.808	1.07×10^9	0.72	270	11.19

TABLE IB
Rubber Elasticity Data of the System *n*-Butyl Acrylate (BA)–Tetraethylene Glycol Dimethacrylate (TEGDM)–Dioctyl Phthalate (DOP)

No.	DOP, vol.-%	Mole fraction TEGDM, %	c_{TEGDM}, mole/cc. $\times 10^5$	Sp. vol. monomer, cc./g.	Sp. vol. polymer, cc./g.	G, dynes/cm.^{2}	e	c', mole/cc. $\times 10^5$	$z\phi$
1	11.4	2.0	13.6			5.30×10^6	(0.74)	(10.1)	(0.82)
2	11.1	5.2	34.4			1.20×10^7	(0.74)	(25.4)	(0.73)
3	10.9	11.1	71.3	1.064	0.930	1.42×10^7	0.62	44.8	0.89
4	11.2	53.3	237	0.978	0.855	2.46×10^8	0.86	226	3.08
5	10.9	78.1	296	0.950	0.838	3.84×10^8	0.73	260	4.17

TABLE IC

Rubber Elasticity Data of the System *n*-Butyl Acrylate (BA)–Tetraethylene Glycol Dimethacrylate (TEGDM)–Dioctyl Phthalate (DOP)

No.	DOP, vol.-%	Mole fraction TEGDM, %	c_{TEGDM}, mole/cc. $\times 10^5$	Sp. vol. monomer, cc./g.	Sp. vol. polymer, cc./g.	G, dynes/cm.^{2}	e	c', mole/cc. $\times 10^5$	$z\phi$
1	30.6	2.1	11.6			1.52×10^6	(0.93)	(10.8)	(0.34)
2	29.2	8.2	41.5			7.60×10^6	(0.93)	(38.6)	(0.48)
3	31.8	19.1	82.7	1.035	0.937	1.87×10^7	0.93	48.5	1.09
4	34.4	40.8	143	1.004	0.909	3.68×10^7	0.97	128	0.81
5	31.6	57.4	185	0.984	0.892	9.40×10^7	0.95	159	1.66
6	33.2	82.5	217	0.963	0.879	1.73×10^8	0.88	157	3.11

TABLE ID

Rubber Elasticity Data of the System *n*-Butyl Acrylate (BA)–Tetraethylene Glycol Dimethacrylate (TEGDM)–Dioctyl Phthalate (DOP)

No.	DOP, vol.-%	Mole fraction TEGDM, %	c_{TEGDM}, mole/cc. $\times 10^5$	Sp. vol. monomer, cc./g.	Sp. vol. polymer, cc./g.	G, dynes/cm.^{2}	e	c', mole/cc. $\times 10^5$	$z\phi$
1	48.9	1.7	6.86			8.66×10^5	(0.77)	(5.29)	(0.28)
2	50.3	3.8	13.6			1.64×10^6	(0.77)	(10.5)	(0.26)
3	50.6	7.5	25.4			2.30×10^6	(0.77)	(19.6)	(0.19)
4	50.2	14.3	45.7			4.47×10^6	(0.77)	(35.2)	(0.22)
5	49.6	20.5	61.7			4.75×10^6	(0.77)	(47.6)	(0.17)
6	51.2	40.0	86.7	1.013	0.943	8.24×10^6	0.78	67.4	0.12
7	50.2	61.2	130	0.991	0.924	2.38×10^7	0.85	111	0.61
8	47.7	75.2	154	0.980	0.913	4.20×10^7	0.73	112	1.05
9	52.7	100.0	163	0.971	0.913	6.43×10^7	0.71	116	1.56

TABLE IIA
Rubber Elasticity Data of the System Ethyl Acrylate (EA)–Tetraethylene Glycol Dimethacrylate (TEGDM)–Dioctyl Phthalate (DOP)

No.	DOP vol.-%	Mole fraction TEGDM, %	c_{TEGDM}, mole/cc. $\times 10^5$	Sp. vol. monomer, cc./g.	Sp. vol. polymer, cc./g.	G, dynes/cm.^{2}	e	c', mole/cc. $\times 10^5$	$z\phi$
1	12.0	1.0	10.3			4.32×10^6	(0.79)	(8.15)	(0.93)
2	11.7	2.4	22.9			5.78×10^6	(0.79)	(18.1)	(0.56)
3	11.9	27.3	175	1.001	0.856	1.18×10^8	0.84	147	2.27
4	11.6	52.1	251	0.966	0.838	2.39×10^8	0.83	207	3.26
5	11.5	76.2	294	0.945	0.832	3.56×10^8	0.71	210	4.79

TABLE IIB
Rubber Elasticity Data of the System Ethyl Acrylate (EA)–Tetraethylene Glycol Dimethacrylate (TEGDM)–Dioctyl Phthalate (DOP)

No.	DOP, vol.-%	Mole fraction TEGDM, %	c_{TEGDM}, mole/cc. $\times 10^5$	Sp. vol. monomer, cc./g.	Sp. vol. polymer, cc./g.	G, dynes/cm.^{2}	e	c', mole/cc. $\times 10^5$	$z\phi$
1	34.8	0.8	6.09	1.064	0.929	2.36×10^6	(0.87)	(5.30)	(0.95)
2	34.1	3.1	22.0	1.058	0.916	8.75×10^6	(0.87)	(19.1)	(0.97)
3	34.0	14.5	71.9	1.033	0.898	1.95×10^7	(0.87)	(62.5)	(0.67)
4	33.7	28.4	135	1.004	0.885	5.13×10^7	1.00	135	1.07
5	33.0	53.4	192	0.974	0.871	1.52×10^8	0.87	166	2.60
6	32.8	75.0	225	0.961	0.868	2.01×10^8	0.73	164	3.45

TABLE IIIA

Rubber Elasticity Data of the System Methyl Methacrylate (MMA)–Tetraethylene Glycol Dimethacrylate (TEGDM)–Dioctyl Phthalate (DOP)

No.	DOP, vol.-%	Mole fraction TEGDM, %	c'_{TEGDM}, mole/cc. $\times 10^5$	Sp. vol. monomer, cc./g.	Sp. vol. polymer, cc./g.	G, dynes/cm.^{2}	e	c', mole/cc. $\times 10^5$	$z\phi$
1	11.9	0.7	7.41			9.40×10^6	(0.76)	(5.64)	(2.12)
2	12.2	2.8	28.2			1.48×10^7	(0.76)	(21.6)	(1.12)
3	10.1	3.3	31.7			1.46×10^7	(0.76)	(24.1)	(0.99)
4	12.4	13.6	111	1.012	0.840	8.18×10^7	0.84	92.8	2.82
5	11.5	27.2	179	0.986	0.835	1.56×10^8	0.74	133	3.32
6	11.2	53.0	258	0.956	0.828	3.74×10^8	0.72	185	5.71
7	10.7	77.8	305	0.939	0.824	5.97×10^8	0.73	222	7.60

TABLE IIIB

Rubber Elasticity Data of the System Methyl Methacrylate (MMA)–Tetraethylene Glycol Dimethacrylate (TEGDM)–Dioctyl Phthalate (DOP)

No.	DOP, vol.-%	Mole fraction TEGDM, %	c_{TEGDM}, mole/cc. $\times 10^5$	Sp. vol. monomer, cc./g.	Sp. vol. polymer, cc./g.	G, dynes/cm.^{2}	e	c', mole/cc. $\times 10^5$	$z\phi$
1	29.9	1.4	10.7			5.19×10^6	(0.66)	(7.05)	(0.91)
2	29.7	3.8	28.2			1.46×10^7	(0.66)	(18.6)	(0.96)
3	31.5	9.2	60.6	1.013	0.873	1.88×10^7	0.75	45.5	1.61
4	28.1	28.1	141	0.986	0.869	1.01×10^8	0.60	83.5	3.41
5	28.5	53.2	195	0.960	0.863	1.92×10^8	0.60	117	4.63
6	32.7	78.5	229	0.949	0.860	2.70×10^8	0.68	156	4.89

TABLE IVA
Rubber Elasticity Data of the System Styrene (STY)–Tetraethylene Glycol Dimethacrylate (TEGDM)–Dioctyl Phthalate (DOP)

No.	DOP, vol.-%	Mole fraction TEGDM, %	c_{TEGDM}, mole/cc. $\times 10^6$	Sp. vol. monomer, cc./g.	Sp. vol. polymer, cc./g.	G, dynes/cm.^{2}	e	c', mole/cc. $\times 10^5$	$z\phi$
1	11.2	0.7	5.10			4.07×10^6	(0.73)	(3.72)	(1.64)
2	12.1	3.4	28.			1.61×10^7	(0.73)	(20.9)	(1.15)
3	11.	10.9	82.			4.09×10^7	(0.73)	(60.4)	(1.02)
4	10.9	27.6	16	1.009	0.884	1.40×10^6	0.75	126	3.13
5	11.9	53.4	250	0.96	0.851	2.89×10^8	0.75	1	4.33
6	11.4	78.5	315	0.946	0.835	5.01×10^8	0.73	230	6.15
7	9.5	100.0	336	0.933	0.829	7.02×10^8	0.68	227	8.73

TABLE IVB
Rubber Elasticity Data of the System Styrene (STY)–Tetraethylene Glycol Dimethacrylate (TEGDM)–Dioctyl Phthalate (DOP)

No.	DOP, vol.-%	Mole fraction, TEGDM, %	c_{TEGDM}, mole/cc. $\times 10^5$	Sp. vol. monomer, c./g.	Sp. vol. monomer, cc./g.	G, dynes/cm.^{2}	e	c', mole/cc. $\times 10^5$	$z\phi$
1	32.1	0.8	4.98			2.64×10^6	(0.89)	(4.44)	(1.33)
2	32.3	3.1	19.9			8.21×10^6	(0.89)	(17.7)	(1.03)
3	31.0	10.4	61.2			2.26×10^7	(0.89)	(54.5)	(0.93)
4	32.1	28.7	135	1.008	0.899	6.15×10^7	0.96	129	1.35
5	31.8	53.5	190	0.978	0.882	1.22×10^8	0.86	163	2.11
6	33.3	78.5	229	0.961	0.868	2.38×10^8	0.84	191	3.52
7	27.9	100.0	249	0.950	0.857	2.85×10^8	0.88	219	3.67

for STY; and 20.75 cc./mole for both EA and BA. That for the double bonds of dimethacrylates is assumed to be 22.50 cc./mole. Crosslinking efficiencies determined by this method are expectedly less accurate for preswollen polymers due to the presence of diluents.

Shear Modulus Measurements

The 10-sec. shear moduli were measured at 150°C. for all samples by a modified Gehman apparatus.[18] Data are collected in Tables I–IV. Figure 1 summarizes results for the BA copolymers.

RESULTS AND DISCUSSION

Efficiency of Crosslinking in Preswollen Network Polymers

From our data it is clear that the crosslinking efficiency is quite high for all the network polymers studied. This is partially attributable to the long, flexible chain TEGDM possesses between the two vinyl groups. These long, flexible chains have sufficiently large domains in which neighboring groups can be found, so that it is possible for them to react with other vinyl groups.[13]

To our surprise, e seems to be relatively unaffected by the presence of diluents (Tables I–IV). As the diluent content increases, one might expect that there would be fewer reactants within each domain, and therefore lower crosslinking efficiency should result. However, this is probably in part offset by the high mobility of the chains due to the presence of these diluents. Also, one should take into account the fact that preswollen polymers have lower glass transition temperatures. The low diffusibility of the pendant vinyl groups of the dimethacrylates at temperatures below T_g was shown to restrict the extent of degree of crosslinking.[13]

For copolymers containing lower contents of TEGDM, the accuracy required for calculating e is beyond our experimental method. This has already been discussed in a previous publication.[6] In this paper we choose to assign an average value for efficiencies of crosslinking in less crosslinked samples. This assumption is at least partially justified by the constancy of e throughout the entire range of mole per cent TEGDM at a given diluent content. These values are given in parenthesis as shown in the Tables. This method of presentation facilitates a convenient way for comparison of the data.

Effect of Preswelling on Elastic Moduli

It was found in our studies on lightly crosslinked network polymers that their elastic moduli decrease as diluent contents increase.[12] Similar situations prevail in highly crosslinked systems (Tables I–IV and Fig. 1). We have already pointed out previously that two factors may have contributed to this decrease in modulus: (*1*) increase in the formation of intramolecular loops that contribute nothing to stress; and (*2*) decrease in the concentration of physical crosslinks, i.e., the lowering of the degree of entanglement coupling as the diluent content increases.

For highly crosslinked systems, another type of intramolecular loop formation becomes significant. The pendant vinyl group of the dimeth-

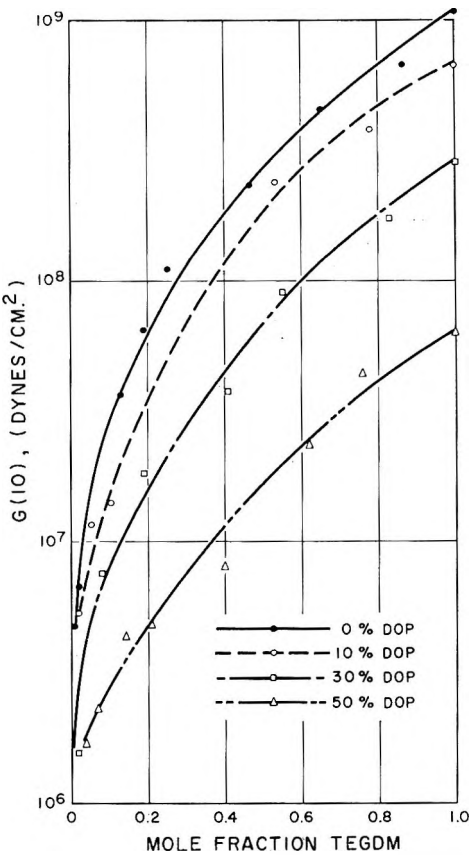

Fig. 1. Plots of 10-sec. shear moduli of polymer networks of TEGDM–*n*-butyl acrylate–dioctyl phthalate system vs. mole fractions of TEGDM.

acrylate molecule may curl back and react with the other vinyl group that has already reacted. In other words, the crosslinker itself may form a ring. This situation is quite possible for the long, flexible chain of TEGDM. Experimental evidence for such a reaction has been given for diallyl phthalate.[19] For preswollen polymers, it is obvious that increases in the diluent content will be favorable to such a kind of ring formation. This is an additional factor that causes the decrease in the elastic moduli.

Application of the Equation of State of Rubber Elasticity to Preswollen Network Polymers

As we have mentioned earlier, the kinetic theories of rubber elasticity were derived for lightly crosslinked polymers. The range of experiments in this paper is probably beyond the applicability of these theories.[6] Nevertheless, we thought it would be interesting to interpret our data in the light of these theories.

Front factors calculated from eq. (4) are collected in the Tables. Data are compared on the basis of mole fractions of TEGDM so that network chains are all on the average of the same length. Front factors are pre-

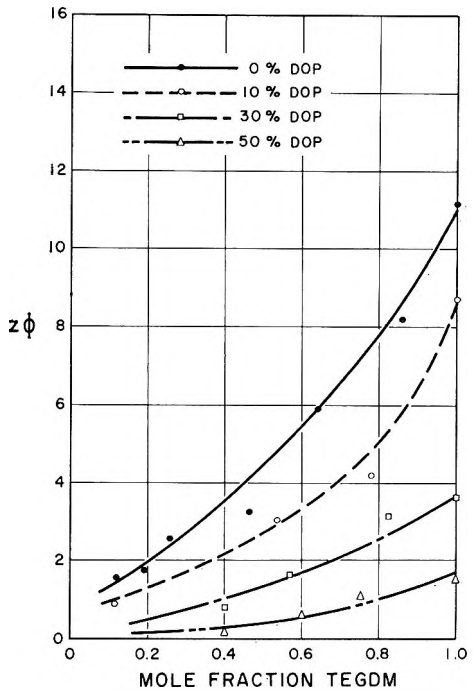

Fig. 2. Front factors $z\phi$ of polymer networks of TEGDM–*n*-butyl acrylate–dioctyl phthalate system vs. mole fraction of TEGDM.

sented as $z\phi$. Figure 2 shows the variation of $z\phi$ as a function of mole fraction TEGDM for BA copolymers.

It has been found that front factors increase with increasing crosslinking concentration,[5,7] but decrease as diluent content increases.[12] Figure 2 illustrates these trends very well. Noteworthy are, however, the slopes of $z\phi$–TEGDM curves. Clearly they are more gradual at higher degrees of preswelling. We have already shown that ϕe is approximately constant up to 12 mole-% of dimethacrylates for unswollen polymers.[6] It seems that for preswollen polymers this constancy will extend to higher contents of crosslinking concentration.

This phenomenon is not surprising if we consider the process of network formation. In the case of bulk polymerization, chains formed in the beginning were solvated by the unpolymerized monomers. They were able to assume random configurations. During the later stages of polymerization, however, both the increasing rigidity of the network and the decreasing solvating effect act to change the chain conformation. Possibly there is a greater tendency for coiling and entanglement. This situation is alleviated if diluents are present during the polymerization. Here the network is less rigid, and chains are more mobile. A more "ideal" network is formed.

In conclusion, we can say that preswollen polymer networks are more "ideal" in that they have less chain entanglements, but only at the expense of increasing the extent of "wastage reactions." Although front factors are lowered by increasing degrees of preswelling, they remain constant in value up to higher crosslink concentration for higher diluent contents.

The support of the Goodyear Rubber and Tire Co. and the Office of Naval Research is gratefully acknowledged.

References

1. Tobolsky, A. V., D. W. Carlson, and N. Indicator, *J. Polymer Sci.*, **54**, 175 (1961).
2. Ciferri, A., *J. Polymer Sci.*, **55**, 149 (1961).
3. Tobolsky, A. V., D. Katz, R. Thach, and R. J. Schaffhauser, *J. Polymer Sci.*, **62**, 174 (1962).
4. Katz, D., and A. V. Tobolsky, *Polymer*, **4**, 417 (1963).
5. Katz, D., and A. V. Tobolsky, *J. Polymer Sci.*, **A2**, 1587 (1964).
6. Katz, D., and A. V. Tobolsky, *J. Polymer Sci.*, **A2**, 1595 (1964).
7. Tobolsky, A. V., D. Katz, M. Takahashi, and R. J. Schaffnauser, *J. Polymer Sci.*, **A2**, 2749 (1964).
8. Lloyd, W. G., and T. Alfrey, Jr., *J. Polymer Sci.*, **62**, 301 (1962).
9. Millar, J. R., D. G. Smith, W. E. Marr, and T. R. E. Kressman, *J. Chem. Soc.*, **1963**, 218.
10. Kwei, T. K., *J. Polymer Sci.*, **A1**, 2977 (1963).
11. Tobolsky, A. V., D. W. Carlson, N. Indicator, and M. C. Shen, *J. Polymer Sci.*, **61**, S23 (1962).
12. Shen, M. C., and A. V. Tobolsky, *J. Polymer Sci.*, **A2**, 2513 (1964).
13. Loshaek, S., and T. G Fox, *J. Am. Chem. Soc.*, **75**, 3544 (1953).
14. Butler, G. B., *J. Polymer Sci.*, **48**, 279 (1960).
15. Hwa, J. C. H., and L. Miller, *J. Polymer Sci.*, **55**, 197 (1961).
16. Hwa, J. C. H., *J. Polymer Sci.*, **58**, 715 (1962).
17. Gordon, M., and R. J. Roe, *J. Polymer Sci.*, **21**, 75 (1956).
18. *ASTM Standards*, American Society for Testing Materials, Philadelphia, 1958, Designation D1053-58.
19. Simpson, W., T. Holt, and R. J. Zetie, *J. Polymer Sci.*, **10**, 489 (1953).

Résumé

On étudie le comportement élastique de réseaux polymériques hautement ramifiés et prégonflés. On a procédé à une étude systématique de copolymères de diméthacrylate d'éthylène-glycol avec l'acrylate d'éthyle, l'acrylate de *n*-butyle, le méthacrylate de méthyle et le styrène, la composition des copolymères couvrant l'entièreté du domaine. On a utilisé le phtalate de dioctyle pour prégonfler les polymères jusqu'a un taux de 50% (en volume). On a trouvé que et le module de cisaillement et le facteur de front augmentaient avec la densité du pontage, mais diminuaient lorsqu'on augmentait la quantité de diluant. On a déterminé l'efficacité du pontage par la méthode de Loshaek-Fox modifiée. Cette efficacité dépend peu du degré de prégonflement. On discute les facteurs qui contribuent à ces résultants expérimentaux.

Zusammenfassung

Die Kautschukelastizität stark vernetzter vorgequollener Polymernetzwerke wird untersucht. Die Untersuchung bezieht sich auf Copolymere von Tetraäthylenglycoldimethacrylat mit Äthylacrylat, *n*-Butylacrylat, Methylmethacrylat und Styrol über den ganzen Zusammensetzungsbereich. Zur Vorquellung bis 50 Volums% wird Dioctylphthalat verwendet. Schubmodul wie auch Frontfaktor nehmen mit steigender Vernetzungskonzentration zu, mit steigendem Verdünnungsmittelgehalt jedoch ab. Vernetzungsausbeuten werden mit einer modifizierten Loshaek-Fox-Methode bestimmt. Sie hängen verhältnismässig wenig vom Vorquellungsgrad ab. Die Faktoren, die diesen Beobachtungen zugrunde liegen, werden diskutiert.

Received May 27, 1964
Revised July 13, 1964

JOURNAL OF POLYMER SCIENCE: PART A VOL. 3, PP. 641–646 (1965)

Effect of Constraints on the Equilibrium Swelling of Rubber Vulcanizates

E. SOUTHERN and A. G. THOMAS, *The Natural Rubber Producers' Research Association, Welwyn Garden City, Hertfordshire, England*

Synopsis

The swelling of natural rubber vulcanizates under equal two-dimensional compression has been investigated. The degree of crosslinking of the vulcanizate and the nature of the swelling liquid have both been varied. The reduction in equilibrium swelling produced by the stresses is found to agree well with theoretical predictions, except for high degrees of swelling. This divergence from theory has been explained on the basis of surface instability, which takes the form of wrinkles of the rubber surface.

INTRODUCTION

When a sheet of a rubber vulcanizate is immersed in a solvent, the surface layer takes up its equilibrium amount of liquid virtually instantaneously. The liquid subsequently diffuses into the bulk of the rubber. The rate of diffusion is dependent on the concentration of liquid in the surface, and in the early stages of the diffusion the swollen layer is prevented from expanding laterally by the constraint imposed by the underlying bulk of unswollen rubber, so that the lateral dimensions of the layer remain substantially unchanged. It is known that the imposition of such stresses affect the equilibrium swelling attained by a vulcanizate, so that the surface concentration is not that in a freely swelling sample. In the course of an investigation into the diffusion of liquids into rubber vulcanizates[1] this surface concentration had to be determined. This paper describes a study of the effect of this form of constraint on the equilibrium swelling.

THEORY

The general theory for the effect of applied stress on swelling has been given by Treloar, and he has also carried out experiments for the cases of simple extension and compression and equal two-dimensional extension.[2] For good swelling agents the agreement between the predicted and the experimentally obtained dependence on strain is excellent. The particular case of interest here, that is, when the lateral dimensions are unchanged, has not previously been studied.

The theory[2] relates the equilibrium volume fraction of rubber v, the prin-

cipal stresses t_i, and the extension ratios λ_i referred to the dry unstressed state by the equation

$$t_i = (RT/V)[\ln (1 - v) + v + \mu v^2] + \rho(RT/M_c)v\lambda_i^2 \qquad i = 1,2,3 \tag{1}$$

where R is the gas constant, T the absolute temperature, V the molar volume of the liquid, ρ the density of the rubber, M_c the molecular weight between crosslinks, and μ is the rubber–liquid interaction parameter. For the present case we have

$$\lambda_1 = \lambda_2 = 1 \tag{2}$$

$$t_3 = 0 \tag{3}$$

$$\lambda_3 = 1/v \tag{4}$$

and thus the volume fraction of rubber at equilibrium v_c is given by

$$(M_c/\rho V)[\ln (1 - v_c) + v_c + \mu v_c^2] + (1/v_c) = 0 \tag{5}$$

where the subscript c indicates that the rubber is subject to constraints according to eq. (2) and (3). If a sample of the same rubber is allowed to swell freely, i.e., with $t_1 = t_2 = t_3 = 0$, the equilibrium value of v, denoted now by v_f, is given by

$$M_c/\rho V = -v_f^{1/3}/[\ln (1 - v_f) + v_f + \mu v_f^2] \tag{6}$$

Elimination of $M_c/\rho V$ between eqs. (5) and (6) gives the relation between the free swelling v_f and the constrained swelling v_c for a series of rubbers with various degrees of crosslinking.

EXPERIMENTAL

In order to constrain the rubber in the required manner when swollen it was bonded during vulcanization to mild steel backing plates $^1/_{16}$ in. thick and $1^1/_2$ in. square with Desmodur R bonding agent (manufactured by Fabenfabriken Bayer). Thus the rubber specimens, in the form of 1 mm. thick sheets, were, except for the edges, prevented from expanding laterally by these rigid plates and therefore the conditions specified by eq. (2) were satisfied. Near the edges, the constraints were not fully effective and the specimen did expand somewhat. To prevent this, an adjustable collar was made to fit tightly around the specimen in order to constrain these edges. It could be removed rapidly when weighings were made. The equilibrium swellings were obtained by weighing, about 24 hr. immersion being sufficient to reach equilibrium. The masses of rubber in the bonded specimens were found by prior weighing of the backing plates individually.

The vulcanizates used were of natural rubber cured with dicumyl peroxide, the formulations being as shown in Table I.

The specimens were produced by laying four of the backing plates, treated with bonding agent, in a 6 × 6 in. mold of suitable thickness and then, after applying the compounded rubber, the vulcanization was carried out. In this way a set of virtually identical specimens was produced.

TABLE I
Composition of Vulcanizates

Vulcanizate	A	B	C	D	E	F
RSS1, parts by weight	100	100	100	100	100	100
Dicumyl peroxide, parts by weight	1	1.5	2	3	4	6
Time of cure at 140°C. min.	50	50	50	50	50	50

RESULTS AND DISCUSSION

Swelling in *n*-Decane

The results are shown in Figure 1, where each point gives the v_e and v_f values for a particular rubber with *n*-decane as the swelling liquid. The v_f values were obtained for unbonded rubber from the sheet containing the bonded samples. The curve *A* is derived from eqs. (5) and (6) with $\mu = 0.42$.[3]

The experimental points are seen to be consistently below it. There appears to be two sources of this discrepancy. First, the state of strain is not strictly that defined by eqs. (2) and (4) because the rubber-to-metal bond is formed at the temperature of vulcanization, and, as rubber and metal have different coefficients of thermal expansion, stresses are set up on cooling. Secondly, at high degrees of swelling ($v_e < 0.42$) the surface

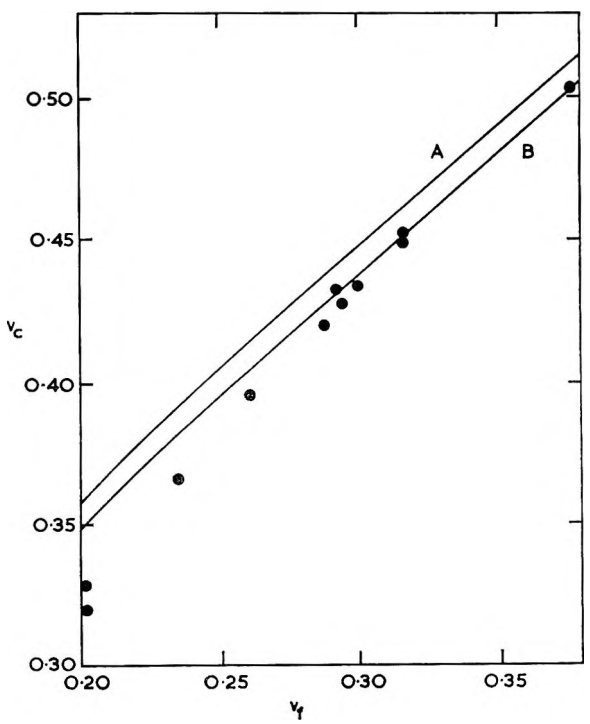

Fig. 1. Relation between v_f and v_e for various degrees of crosslinking.

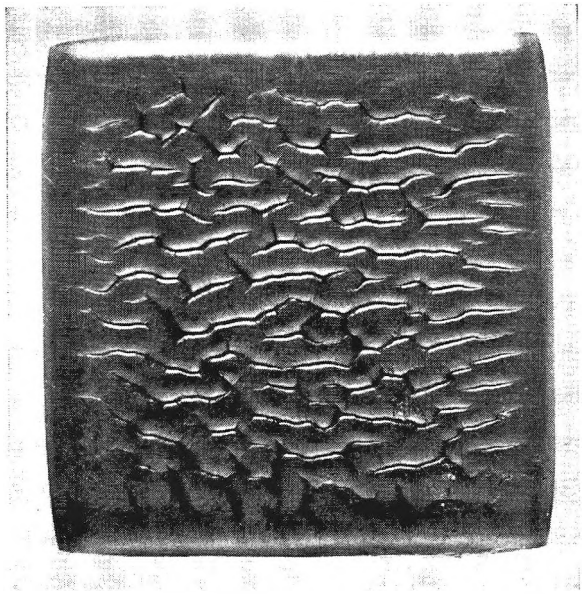

Fig. 2. Surface instability of bonded sample swollen in *n*-decane.

of the rubber is no longer plane but becomes wrinkled. The first effect can be allowed for by modifying eqs. (2) and (4). The differences in the thermal expansion of the rubber and metal would increase λ_1 and λ_2 by about 2.5%; measurements of the dimensions of a sample of rubber (vulcanizate 1) removed from its backing plate indicated about a 3.5% change. The extra 1% is due to nonrubber constituents being extracted by the swelling liquid. The precise amount extracted will depend somewhat on the vulcanizate, but for the present series of experiments the differences are relatively slight and will be neglected. If λ_1 and λ_2 are taken to be 1.035, instead of eq. (5) we have

$$(M_c/\rho V)(1.035)^4[\ln (1 - v_c) + v_c + \mu v_c^2] + (1/v_c) = 0 \qquad (5a)$$

and this gives curve *B* in Figure 1 for the relation between v_c and v_f. This shows good agreement with experiment for v_c values greater than about 0.42. Below this, v_c is less than predicted, i.e., the swelling is greater. Bonded specimens giving v_c values less than 0.42 show wrinkles on their surfaces when swollen, more lightly crosslinked rubbers giving more pronounced wrinkles. Figure 2 is a photograph of the surface of a bonded specimen (vulcanizate A).

This effect appears to be one of surface instability. Green and Zerna[4] find, in a theoretical study of indentation of a strained highly elastic block, that the indenting force becomes zero for a certain critical value of the two-dimensional compressive strain. They suggest this shows that at compressive strains greater than the critical value the surface becomes unstable. The critical strain predicted by their theory is equivalent in the present case to a v_c value of 0.295. In fact, it appears from the present

investigation that instability occurs at lower compressive strains, equivalent to the v_c value 0.42 given above. This is not surprising, as the observed instability takes the form of a network of wrinkles, whereas the theory is concerned with spherical indentations.

In the initial stages of swelling, unbonded specimens also show this surface instability due to the constraints imposed on the surface layer by the unswollen bulk of the rubber.

Swelling in Other Liquids

The equilibrium swellings of one of the above vulcanizates (D) in various other liquids have been measured. Because some of these liquids caused only slight swelling, the presence of a few per cent of extractable material in the rubber gave rise to inaccurate results. The samples were therefore extracted in hot acetone for 24 hr. in an atmosphere of nitrogen. Also, the bonded sample was cut from its backing plate after the v_c value had been obtained and swollen without constraint to obtain the v_f value. The original weight of rubber in the freely swollen sample was obtained by allowing the liquid to evaporate until the sample reached constant weight.

From the observed v_f values in decane and a particular liquid, the μ value for the liquid–rubber system was calculated. Hence, from eq. (5a), the v_c value could be found. Table II shows the results together with the μ values for the various liquids. Comparing the predicted swellings v_c with the observed values, it is seen that there is good agreement. For poor swelling agents both the predicted and experimentally found effects of constraint are very slight.

Repeat measurements on samples taken from different parts of the same sheet show that the molecular weight between crosslinks M_c, calculated from free swelling data, may vary by $\pm 5\%$. This would lead to an error of $\pm 1\%$ in the calculated value of v_c.

It appears from the present work that Treloar's general theory for the effect of stresses on equilibrium swelling accounts well for the results obtained from measurements in two-dimensional compression, both for variations in the degree of crosslinking and in the nature of the swelling liquid.

TABLE II
Equilibrium Swelling Data for Various Liquids

Liquid	μ	v_f	v_c Calculated	v_c Measured
Decane	0.42	0.278	0.419	0.410
Dodecane	0.38	0.2735	0.421	0.429
Tetradecane	0.42	0.309	0.448	0.438
Hexadecane	0.43	0.332	0.468	0.479
Diethyl ether	0.57	0.306	0.423	0.413
Ethyl acetate	0.79	0.560	0.596	0.594
Acetone	1.37	0.837	0.837	0.837
Aniline	1.79	0.909	0.909	0.913

This work forms part of a program of research undertaken by the Board of the Natural Rubber Producers' Research Association.

References

1. Southern, E., and A. G. Thomas, to be published.
2. Treloar, L. R. G., *The Physics of Rubber Elasticity*, 2nd Ed., Oxford, 1958, Chap. 7.
3. Mullins, L., *J. Appl. Polymer Sci.*, **2**, 1 (1959).
4. Green, A. E., and W. Zerna, *Theoretical Elasticity*, Oxford, 1954, pp. 135–138.

Résumé

On a étudié le gonflement du caoutchouc naturel vulcanisé, comprimé de façon égale sous deux dimensions. On a fait varier le degré de pontage du vulcanisat ainsi que la nature du liquide de gonflement. On a trouvé que la diminution de l'équilibre de gonflement, produite par les forces de tension, étaient en bon accord avec les prévisions théoriques, sauf pour les hauts degrés de gonflement. On a expliqué cette divergence avec la théorie sur la base d'une instabilité de surface qui prend la forme de plis à la surface du caoutchouc.

Zusammenfassung

Die Quellung von Naturkautschukvulkanisaten unter gleichmassigerzweidimensionaler Kompression wurde untersucht. Vernetzungsgrad des Vulkanisates und Natur des Quellungsmittels wurde variiert. Die durch die Spannung erzeugte Herabsetzung der Gleichgewichtsquellung stimmt mit Ausnahme der hohen Quellungsgrade gut mit den theoretischen Aussagen überein. Die Abweichung von der Theorie wurde auf Grundlage einer Oberflacheninstabilität erklärt, welche die Form von Runzeln auf der Kautschukoberfläche annimmt.

Received May 25, 1964

JOURNAL OF POLYMER SCIENCE: PART A VOL. 3, PP. 647-658 (1965)

Application of Transmission Electron Microscopy to Polymer Thin Sections. I. Observations on Nylon 66, Bulk and Filament Forms

JOHN A. RUSNOCK* and DAVID HANSEN, *Interdisciplinary Materials Research Center, Rensselaer Polytechnic Institute, Troy, New York*

Synopsis

A study was made on the internal morphology of molding pellets and filaments of nylon 66 by using transmission electron microscopy on ultrathin sections and polarized light microscopy. Nylon specimens embedded in an epoxy–phenolic resin alloy were sectioned to below 500 A. in thickness on an ultramicrotome with a 48° diamond knife. This resin combined good sectioning properties with strong adhesion to the nylon due to the interaction between the phenolic and the nylon. It was established that success in sectioning depended on embedding in a medium with proper wetting characteristics (to permit floating sections away from the knife edge) and obtaining a strong adhesive bond between specimen and embedding material. Contrast in the electron micrographs was enhanced by staining the nylon sections with phosphotungstic acid. Observations on nylon 66 molding pellets resolved the fibrillar structure of spherulites at the 100 A. level. Observations on undrawn monofilaments indicated a cylindrical rather than spherical symmetry of spherulitic crystallization. When the filaments were cold-drawn, these spherulites retained their radial symmetry but were reduced in diameter.

INTRODUCTION

The morphology of crystallinic high polymers has been the subject of considerable research and much debate. Because the crystals in high polymer materials are usually very small, most of the knowledge of crystal growth and arrangements of crystals has been obtained from indirect evidence. In studies of crystallite sizes and growth patterns in melt-crystallized polymers a variety of experimental techniques have been employed, including low-angle x-ray diffraction, light microscopy, and electron microscopy. Light microscopy has been particularly useful in studying gross, crystal growth patterns such as spherulites. However, most light microscope observations have been made on specially prepared thin films, and the correspondence between morphology in these essentially two-dimensional structures and their three-dimensional counterparts in a bulk material is not clear.

Electron microscopy appears to be an ideal tool for studying polymer morphology. However, the difficulties of specimen preparation have

* Present address: Shell Chemical Co., Woodbury, New Jersey.

severely limited direct observations on polymer samples by transmission electron microscopy, and most investigations have been limited to variations of standard replication and shadow casting techniques. Although much useful information has been gained from such observations (see Geil[1]), they have been limited to replicas of unrestrained growth surfaces, fracture surfaces, etched surfaces, and solution-grown crystals.

In this paper ultramicrotoming techniques for preparing thin sections of polymers, suitable for electron microscopy, are presented. Since no reliable techniques for cutting such samples of crystalline polymeric materials have been set forth to date, the microtoming process is descriptively analyzed in order that the several aspects of the successful system employed here can be better understood. Staining of these sections to enhance contrast between structural areas in the electron microscope image is also considered. While replication and shadow casting are limited to observations of surface features, this technique permits direct observation of the interior structural features of bulk materials. Although there are difficulties and limitations inherent in these techniques, they are considered to be valuable in the study of the morphology of melt-crystallized bulk polymers, particularly with respect to the influences of mechanical and thermal treatments.

Some observations on bulk nylon 66 and drawn and undrawn nylon 66 filaments are presented to demonstrate the capabilities of the technique in studying polymer morphology by direct transmission electron microscopy.

SPECIMEN PREPARATION

Sectioning

Specimens for direct study by transmission electron microscopy are limited to 0.1 μ in thickness because of the poor transmission of electrons through matter. In addition, when internal structure is to be resolved, the thickness must be reduced to less than 500 A. to avoid interpretation difficulties due to the overlapping of structural regions. Ultramicrotomes are available for cutting thin sections in the 200 A. range, and these instruments have been widely used in preparing biological specimens for electron microscopy.

The interaction between microtome knife and the material being cut is a complex one. However, aside from the cutting itself, good thin sections are not obtained unless they can be effectively withdrawn from the knife edge as they are being cut. In this respect, ultrathin sections are most easily handled by floating them from the knife edge on a liquid surface. Hence, the good sectioning characteristics of methacrylates and epoxies are associated, at least in part, with their wetting characteristics. Conversely, direct thin sectioning of such polymers as polyamides, polyesters, and polyolefins is prevented by their wetting characteristics; when a polymer specimen of this type is brought near the cutting edge of the knife, the meniscus of the collecting liquid is pulled up to the specimen, liquid spills over the

knife edge forming a barrier between knife and specimen, and no cutting results. In order to make the cutting edge of the knife accessible to these types of materials, it is necessary to encapsulate small specimens in a matrix of a methacrylate or epoxy resin or other material of suitable sectioning characteristics. In comparison to the biologists' technique then, the purpose of an embedding medium for ultramicrotomy of polymeric samples is not primarily to serve as a supporting matrix with proper sectioning characteristics but rather to afford a clean contact with the knife.

Attempts to section nylon and other polymers by direct embedding in methacrylate, epoxy, or other resins with suitable cutting characteristics are not successful. While the embedding medium is readily cut and floated back and away from the knife edge, the specimen is not cut or, generally, appears to be pulled out from the embedding matrix. A physical analysis of the cutting operation leads to an explanation for the complete failure of the ultramicrotoming procedure in these cases. During cutting, a plane of maximum shear stress exists normal to the rake face of the knife extending from the cutting edge to the outer surface of the section.[2] This means that at every instant of cutting the specimen–embedding interface is experiencing a maximum shear stress directed parallel to its smallest dimension, with failure at the interface resembling a lifting of the specimen directly out of the embedding. Hence, it is apparent that an adhesive bond of high shear strength is required between specimen and embedding matrix if the ultramicrotoming procedure is to be successful. Although the adhesion problem was recognized by Scott and Ferguson[3] in their attempts at sectioning synthetic fibers and limited experimental success was achieved by coating fibers with a thin layer of silica before embedding in polystyrene, they apparently did not explain the reasons necessitating improvement of bond strength. Similarly, Botty, Felton, and Anderson[4] used a latex coating and methacrylate embedding on acrylic fibers, but did not obtain sections suitable for high magnification observations. Most recently, Harris[5] succeeded in cutting 500 A. thick sections of coated nylon fibers, but experienced considerable folding of specimens.

By embedding nylon in a mixture of epoxy resin and phenolic resin, it was possible to cut sections less than 500 A. in thickness almost routinely. The epoxy–phenolic resin alloy consisted of Araldite 6005 (Cargille Laboratories NYSEM epoxy embedding kit), 30.75 vol. %; dodecenyl succinic anhydride, 30.75 vol. %; *N*-benzyl dimethylamine, 1.55 vol. %; and a laboratory–prepared, resol type phenol–formaldehyde resin, 36.95 vol. %. After properly positioning a nylon specimen in a gelatin capsule filled with the resin alloy, the mixture was cured for 24 hr. at 50°C. and 24 hr. at 100°C. It is believed that the success with this embedding system for nylon was due to the solvent action of the phenolic resin on the surface of the nylon, which, after curing, resulted in an exceptionally strong bond between the specimen and embedding matrix. Sectioning was carried out on a Porter-Blum ultramicrotome with the use of a 48° diamond knife. Nylon specimens were less than 0.1 mm. square in cross section and were surrounded by

epoxyphenolic embedding trimmed to approximately 0.5 mm. for sectioning. Complementary light microscope sections were cut from the same specimens by employing the ultramicrotome and dry glass knives.

The successful sectioning of nylon in the epoxy–phenolic embedding material suggests that many other polymers can be thin-sectioned by applying the embedding technique, provided a strong adhesive bond between specimen and embedding can be obtained. As has been shown, one way of acquiring a high shear strength bond is to incorporate in the embedding medium a material which will, for a limited time, act as a solvent for the specimen.

Staining

Contrast in the final image produced by the electron microscope results from electrons being scattered out of the focused beam by different parts of the specimen. Polymer thin sections must be stained with reagents containing atoms of high scattering capabilities in order to make them visible in the electron microscope and, in addition, preferential staining is required to obtain contrast between structural areas. Primarily because replication and shadow casting have dominated the preparative methods used in the electron microscope studies of crystalline polymers, very little has been published in the area of specific electron stains for these materials. Hess and co-workers[6,7] have reported staining disintegration products of polyamides with phosphotungstic acid and rayon and poly(vinyl alcohol) with iodine. During the course of this work, Spit[8] reported the successful staining of nylon 6 thin films with phosphotungstic acid. The effectiveness of these reagents as preferential electron stains is based on the relative accessibility of different structural regions, regions of high crystalline order being less accessible than disordered regions.

In this work nylon 66 was successfully stained with phosphotungstic acid. It is believed that this staining reagent, as well as other metallo-acids such as chloroauric acid, chloroplatinic acid, and chlorostannic acid, are highly efficient electron stains for polyamides because of their ability to behave as the acid dyes used in the coloring of nylon. The staining procedure used here was a 1-hr. treatment of the ultrathin sections in a 5% aqueous solution of phosphotungstic acid at 95°C.

OBSERVATIONS

Bulk Nylon

Figure 1 is a light micrograph, as viewed between crossed polars, of a section cut directly from a commercial molding pellet of nylon 66 (du Pont Zytel 101). All spherulites were determined to be of the positive type from orthoscopic observations in which a first-order red plate was used. Those spherulites showing a clear Maltese cross extinction pattern are believed to represent diametral sections through a three-dimensional spherulite. The light microscope observations made on the spherulites in this nylon molding

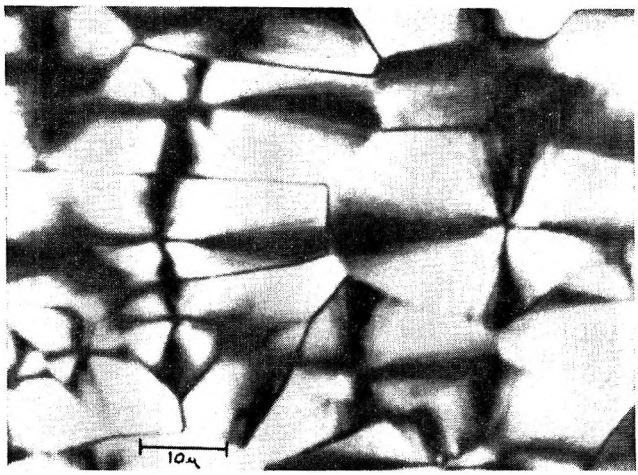

Fig. 1. Micrograph of section of nylon 66 molding pellet. Crossed polars, polarization and cutting directions vertical.

pellet indicate that these three-dimensional, polycrystalline regions and their two-dimensional counterparts grown in thin films are similar. The spherulites found here correspond to the simple, straight extinction cross type whose optical properties have been thoroughly investigated in thin film studies.

Microtoming effectively compresses the cut sections slightly in the cutting direction; this effect is hardly noticeable in Figure 1 where the cutting direction and polarizer direction are parallel. When the section is rotated so that the cutting direction is at an angle of 45° to the polarization direction the Maltese cross extinction pattern changes to a hyperbolic type extinction due to the optical anisotropy introduced by compression during sectioning. However, the seemingly undisturbed radiating structure and an analysis of the change in extinction pattern indicates that the microtoming artifact is small and no appreciable damage is done to morphological units.

Figure 2 is an electron micrograph of a diametral section of a spherulite in the same nylon 66 molding resin. The specimen, prepared according to the procedures described above, was approximately 300–400 A. thick and stained with phosphotungstic acid. (All electron micrographs are presented as positive prints, the light or unstained regions corresponding to crystalline or high density regions.) The center of the spherulite is clearly defined as the intense white region, and a radiating, splayed fibrillar structure is found emanating for some distance before the structure becomes confused and less well developed. Microtoming appears to have had little effect on the central sheaf as it forms an almost perfectly circular region. Figure 3 is a higher magnification electron micrograph taken near the center of the same spherulite. In these micrographs the radiating structure can be seen to be composed of clearly defined fibrillar lamellae approximately 100 A. thick.

In these electron micrographs the light areas correspond to unstained material. Since the stain (phosphotungstic acid) would be expected to be

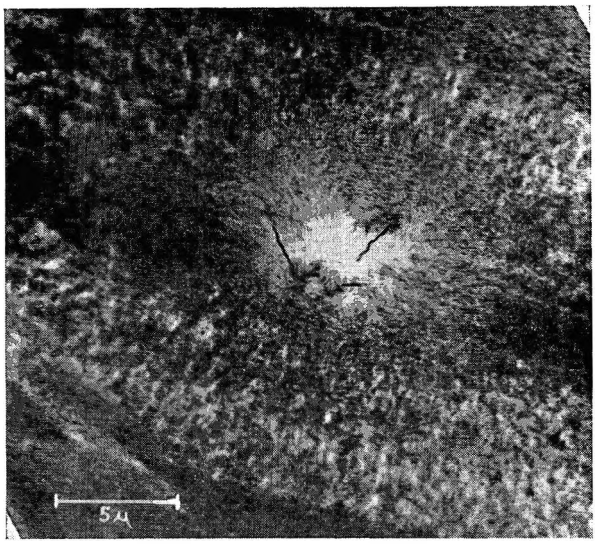

Fig. 2. Electron micrograph of spherulite in nylon 66 molding pellet.

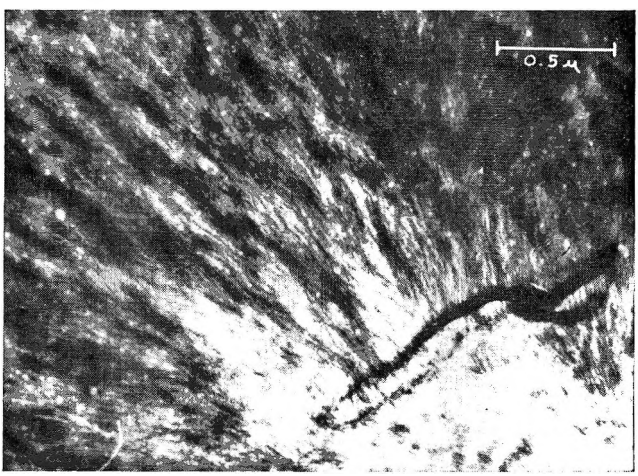

Fig. 3. Electron micrograph of portion of nylon 66 spherulite.

more heavily concentrated in the least ordered or least dense areas, the micrographs would be darkest in the least dense regions. On this basis, the observed spherulites show the highest crystalline order at the center, with order or density decreasing radially outward. This observation is in agreement with the recently proposed theory of spherulitic crystallization by Keith and Padden.[9] Nucleation occurs at the center of each spherulite, with radial growth taking place by branching and splaying of the lamellar crystals. During this growth, impurities, which may be low molecular weight fractions, diffuse away from the crystallization areas to be eventually deposited at the spherulite boundaries or between growing lamellae, depending on the conditions of crystallization. Secondary crystallization,

occurring mostly after the size of the spherulite is determined, or during annealing, may improve the crystalline order throughout the spherulite. Spherulite growth in this manner, particularly in the absence of annealing, would be expected to give the type of density variations observed in these micrographs.

Undrawn Filaments

Nylon 66 monofilaments of 2–3 mils diameter were prepared in the laboratory from the same molding pellets (du Pont Zytel 101). The filaments

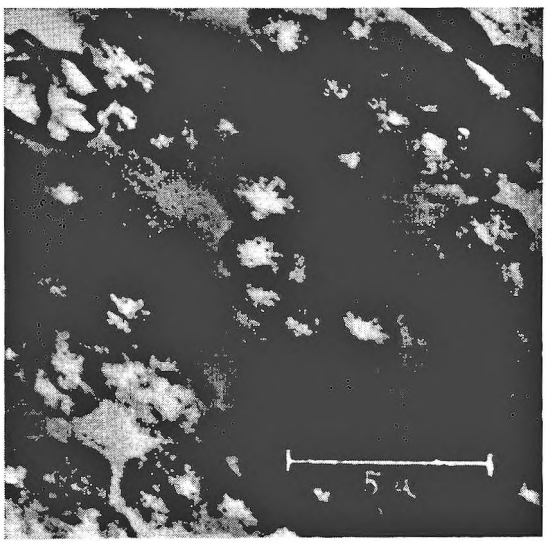

Fig. 4. Electron micrograph of undrawn nylon 66 cross section.

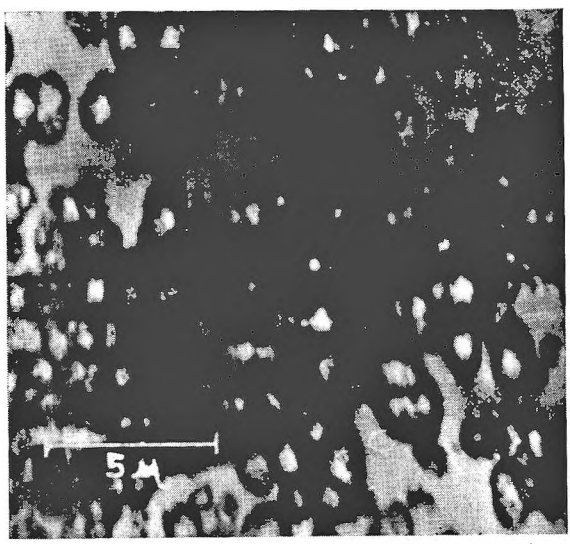

Fig. 5. Electron micrograph of undrawn nylon 66 longitudinal section, fiber axis horizontal.

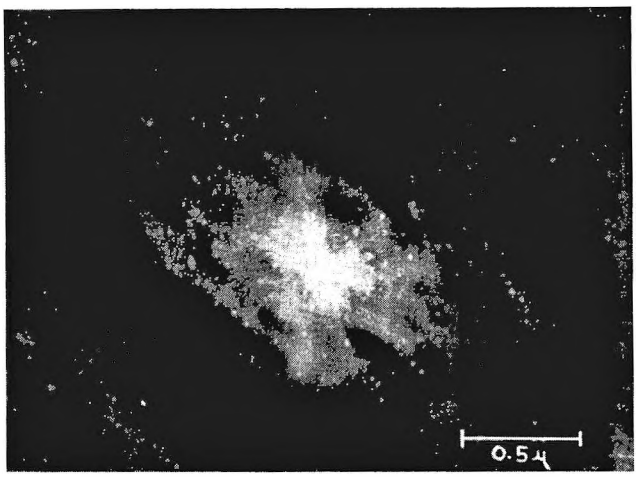

Fig. 6. Electron micrograph of undrawn nylon 66 cross section including diametral section of spherulite.

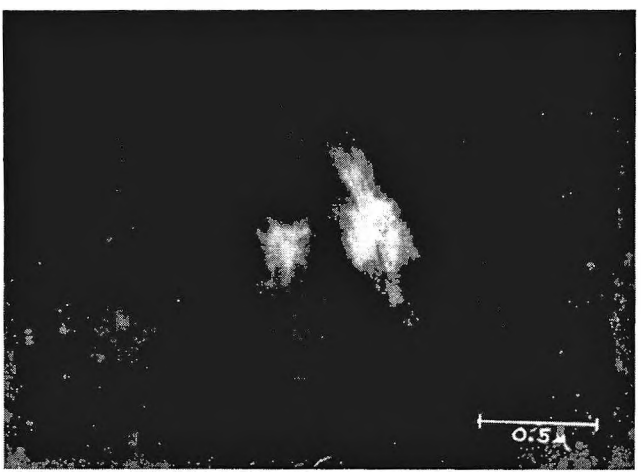

Fig. 7. Electron micrograph of undrawn nylon 66 longitudinal section including diametral sections of adjacent spherulites, filament axis horizontal.

were extruded through a small furnace nozzle at about 280°C. and allowed to air cool. Light microscope observations (crossed polars) on the monofilament showed tiny, but very distinct, positive spherulites scattered throughout the cross section in no apparent pattern. In the longitudinal section very few distinct spherulite extinction patterns were seen, but there appeared to be an arrangement of columns paralleling the filament axis. This arrangement was made strikingly clear by electron microscopy employing the preparative techniques described above. Figures 4 and 5 are electron micrographs of a cross section and a longitudinal section, respectively, of the monofilament. Figure 6 is a higher magnification electron micrograph of a diametral section of a spherulite in the cross section of the

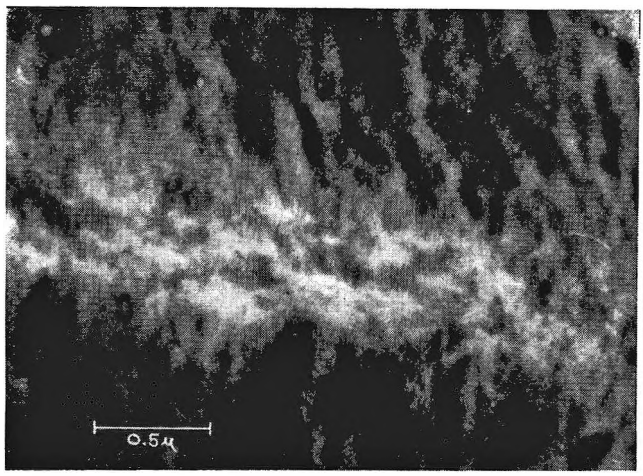

Fig. 8. Electron micrograph of elongated spherulite in longitudinal section of undrawn nylon 66

filament. Figure 7 is a similar longitudinal section showing two adjacent spherulites. Elongated spherulites (Fig. 8) were also observed in longitudinal sections.

The evidence presented here indicates that the spherulites in these extruded monofilaments have a cylindrical rather than spherical symmetry and correspond to the "row-orientation" described by Keller.[10] The axial grouping of spherulites and the elongated spherulites observed in the longitudinal sections are probably due to the orientation of nucleation sites along flow lines and the temperature profiles that exist in the monofilaments during extrusion. The fibrillar or lamellar structure seen in the spherulites of the bulk nylon (Fig. 3) is not as evident, or as clearly resolved, in the electron micrographs of these much smaller spherulites. This may be due to a finer structure in these spherulites as a result of their growth at high degrees of supercooling. The observed differences in order, as evidenced by the amount of stain density, are in agreement with the theory of spherulitic crystallization. Note that, in the filaments, the small spherulites are less dense at their boundaries than the surrounding nonspherulitic material because of the effect of diffusion of impurities in the spherulite growth mechanism.

Drawn Filaments

Light microscope observations on the nylon 66 filaments after cold drawing approximately 300% indicated that in the cross section spherulites retained their radial symmetry but were reduced in diameter in proportion to the draw ratio. In the longitudinal direction the spherulites appear to have been elongated proportionately. Electron microscope observations on longitudinal sections of drawn filaments showed a homogeneous structure in which drawn-out spherulites could be identified. Attempts to thin section drawn filaments normal to the filament axis were unsuccessful.

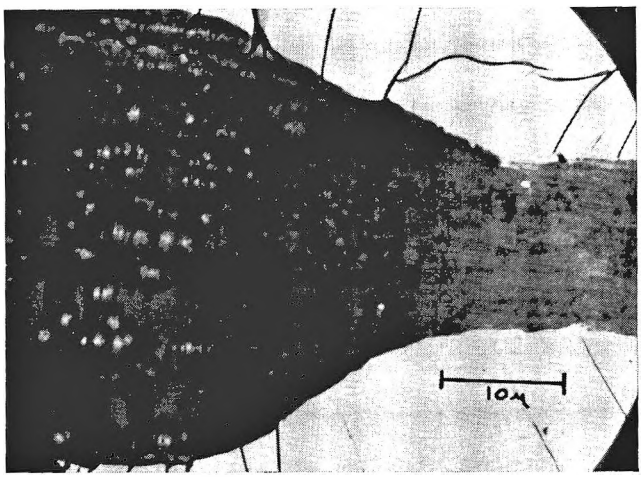

Fig. 9. Electron micrograph of neck region in nylon 66 filament.

Neck Regions

When nylon 66 filaments are cold-drawn they generally develop a sharp neck across which the filament goes from its undrawn diameter to the final drawn diameter. Similar behavior is observed in other polymeric filaments. Light microscope extinction patterns of sections cut through neck regions indicated an essentially random molecular orientation (on the average) in the undrawn filament. Across the neck there is an orientation at 45° to the filament axis, and in the drawn filament the orientation is parallel to the filament axis. The 45° orientation is observed in a band about 25 μ wide.

Figure 9 is typical of the results obtained in taking electron micrographs of thin sections through the neck region. A transition from a structure of clustered spherulites to a more homogeneous, oriented structure is seen to occur across the neck.

CONCLUSIONS

The results presented in this report demonstrate the feasibility and potential of transmission electron microscopy of stained thin sections as a tool in studies of polymer morphology. By this method structure can be studied directly as it exists in three-dimensional polymer samples; it is not limited to specimens prepared specifically for their convenience in observation (e.g., cast, thin films). For this reason, it is believed that the technique is particularly suited to studies of structural changes as influenced by mechanical deformations or heat treatments.

It has been shown that nylon 66 can be thin sectioned in an ultramicrotome by standard procedures after embedding in an epoxy–phenolic resin alloy. Nylon 66 can be effectively stained for electron microscopy with phosphotungstic acid.

The general techniques developed here for nylon 66 specimens should be applicable to other polymers as well. The primary requirements are establishing a good adhesive bond between specimen and an embedding medium of good sectioning properties and choosing a staining reagent which will preferentially enter the less ordered regions of the polymer structure.

Financial support of this research by the National Aeronautics and Space Administration is gratefully acknowledged. (Grant NSG 100-60).

References

1. Geil, P. H., *Polymer Single Crystals*, Interscience, New York, 1963.
2. Phillips, R., *Brit. J. Appl. Phys.*, **12**, 554 (1961).
3. Scott, R. G., and W. A. Ferguson, *Textile Res. J.*, **26**, 284 (1956).
4. Botty, M. C., C. D. Felton, and R. E. Anderson, *Textile Res. J.*, **30**, 959 (1960).
5. Harris, P. H., paper presented at Fifth Intern. Congr. Electron Microscopy, Philadelphia, 1962.
6. Hess, K., and H. Mahl, *Naturwiss.*, **41**, 86 (1954).
7. Hess, K., E. Gutter, and H. Mahl, *Naturwiss.*, **46**, 70 (1959).
8. Spit, B. J., paper presented at Fifth Intern. Congr. Electron Microscopy, Philadelphia, 1962.
9. Keith, H. D., and F. J. Padden, Jr., *J. Appl. Phys.*, **34**, 2409 (1963).
10. Keller, A., *J. Polymer Sci.*, **15**, 31 (1955).

Résumé

On a fait une étude sur la morphologie interne de paillettes de moulage et de filaments de nylon 66, en utilisant un microscope de transmission électronique sur des lamelles ultrafines, et un microscope à lumière polarisée. Des échantillons de nylon, incorporés dans une résine époxyphénolique ont été coupés en lamelles d'épaisseur inférieure à 500 A. au moyen d'un ultramicrotome muni d'une lame en diamant à 48°. Cette résine présente de grandes facilités lors du sectionnement et une forte adhésion au nylon, grâce à l'interaction entre la résine phénolique et le nylon. On a établi que le succès lors du sectionnement dépend de l'incorporation dans un milieu possédant des propriétés caractéristiques d'humidité (pour permettre aux lamelles de se détacher facilement du bord de la lame) et dépend d'une force d'adhésion élevée entre l'échantillon et le matériau qui l'englobe. Le contraste dans les micrographies électroniques sont augmentés lorsqu'on teint les lamelles de nylon avec de l'acide phosphotungsténique. À partir d'observations sur les paillettes de moulage de nylon 66, on peut résond la structure fibrillaire des sphérulites jusqu'à un niveau de 100 A. Des observations sur des monofilaments non-étirés indiquent que les sphérulites cristallisent avec une symétrie cylindrique plutôt que sphérique. Lorsque les filaments sont étirés à froid, ces sphérulites gardent leur symétrie radiale, mais leur diamètre est réduit.

Zusammenfassung

Eine Untersuchung der internen Morphologie von Nylon-66-Presspellets und fäden wurde unter Verwendung der Transmissionselektronenmikroskopie an ultradünnen Schnitten und der Mikroskopie in polarisiertem Licht ausgeführt. In einem Epoxy-Phenolharz eingebettete Nylonproben wurden mit einem Ultramikrotom mit einem 48°-Diamantmesser auf Dicken unterhalb 500 A. geschnitten. Dieses Harz vereinigte gute Schnitteigenschaften mit einer starken auf der Wechselwirkung wischen dem Phenolharz und Nylon beruhenden Adhäsion. Es wurde gefunden, dass der Erfolg bei der Herstellung der Schnitte von der Einbettung in ein Medium mit geeigneter Vernetzungs-

charakteristik (um eine Fortbewegung der Schnitte von der Messerkante zu ermöglichen) und von der Erzielung einer starken Adhäsivbindung zwischen Probe und Einbettungsmaterial abhängt. Die Kontraste in den elektronenmikroskopischen Aufnahmen wurden durch Anfärbung der Nylonschnitte mit Phosphorwolframsäure verstärkt. Die Beobachtungen an den Nylon-66-Presspellets zeigten eine Auflösung der Fibrillenstruktur der Sphärolithe bis zu Bereichen von 100 A. Die Beobachtungen an ungereckten Monofilamenten zeigten Zylinder- und nicht Kugelsymmetrie der Sphärolithkristallisation. Bei kalter Reckung behielten diese Sphärolithe ihre Radialsymmetrie, ihr Durchmesser wurde jedoch verkleinert.

Received May 21, 1964
Revised June 30, 1964

JOURNAL OF POLYMER SCIENCE: PART A VOL. 3, PP. 659–670 (1965)

Thermal Conductivity of High Polymers

DAVID HANSEN and CHONG C. HO,* *Interdisciplinary Materials Research Center, Rensselaer Polytechnic Institute, Troy, New York*

Synopsis

The thermal conductivities of linear high polymers were studied experimentally and theoretically. A theory of thermal conductivity in linear amorphous high polymers was derived based on a simple model of molecular structure. Predictions on the effects of molecular weight and molecular orientation on thermal conductivity taken from the theory agree with available experimental data. New data on the thermal conductivity of linear polyethylene and some polyethylene–wax blends are presented. Temperature dependence of the thermal conductivity in polyethylene was analyzed by the per cent crystallinity concept to obtain results which are in accord with the phonon theory of thermal conductivity in dielectric crystals.

Introduction

Data on thermal conductivity have been reported for many high polymers, but surprisingly little has been said about the relationship of thermal conductivity to such parameters as molecular weight, crystallinity, and molecular orientation. Most of the thermal conductivity data which have been reported were obtained on samples for which these parameters were unknown or at least not reported. Yet, some reports specifically demonstrate the sensitivity of thermal conductivity to these parameters.

Ueberreiter, Laupenmuhlen, and Purucker[1,2] obtained data on fractionated polystyrene which indicate an increase in thermal conductivity with molecular weight of the polymer. The data of Tautz[3] and those of Hellwege and Knappe[4–7] show that, when a polymer is oriented, the thermal conductivity increases in the direction of molecular orientation with a corresponding decrease in directions normal to the orientation.

Existing theories of thermal conductivity of matter in condensed states fall into two categories. On the one hand there are the theories of quantized lattice vibrations whereby the resistance to thermal energy transport is analyzed in terms of phonon scattering. These analyses are particularly designed for crystalline dielectric solids. On the other hand are liquid-state theories such as that of Bridgman[8] or the more recent analysis by Horrocks and McLaughlin.[9] These analyses are based on a model of liquid structure wherein each molecule vibrates about a mean

* Present address: U. S. Rubber Company, Wayne, New Jersey.

equilibrium position, colliding and exchanging energy with nearest neighbor molecules.

The simple models of molecular structure on which these theories are based are best suited to simple low molecular weight compounds. For substances composed of larger molecules they are inadequate, although some success has been noted in applying essentially empirical corrections to these theories in order to correlate data on liquids of fairly large molecular weight. For high polymers these theories are completely inadequate. The models on which they are based do not include any features which consider the effects of molecular weight and molecular orientation.

This paper deals first with a theoretical approach to analyzing the thermal conductivity of linear, amorphous high polymers. Supporting evidence for the theory is provided by data obtained in this laboratory and data reported by other workers. Second, data on linear polyethylene at temperatures above and below the crystal melting range are presented and analyzed.

Theory of Thermal Conductivity for Linear Amorphous High Polymers

Consider a single segment in an amorphous linear high polymer mass. The segment has two kinds of nearest neighbors. First, it has two neighbors on the same molecule to each of which it is chemically bonded. Second, the segment is surrounded by other segments on other molecules. To these segments it is bonded only by secondary forces. In a fashion similar to that employed in treatments of the thermal conductivity of liquids composed of simple molecules it is assumed that a given segment interacts with each of its nearest neighbors at some frequency designated by ν. However, the frequency of interaction with neighbors on the same molecule will probably be different from the frequency of interaction with other neighbor segments. These two frequencies will be designated ν_1 and ν_2, respectively.

Further, if it is assumed that the energy transferred in each interaction is proportional to the energy difference between the interacting segments, then a segment by segment energy balance on a given molecule at steady state would read:

$$\begin{aligned}
&\nu_1 p_1(e_2 - e_1) + \nu_2 p_2(\epsilon_1 - e_1) = 0 \\
&\nu_1 p_1(e_1 - e_2) + \nu_1 p_1(e_3 - e_2) + \nu_2 p_2(\epsilon_2 - e_2) = 0 \\
&\vdots \\
&\nu_1 p_1(e_{n-1} - e_n) + \nu_1 p_1(e_{n+1} - e_n) + \nu_2 p_2(\epsilon_n - e_n) = 0 \qquad (1) \\
&\vdots \\
&\nu_1 p_1(e_{N-2} - e_{N-1}) + \nu_1 p_1(e_N - e_{N-1}) + \nu_2 p_2(\epsilon_{N-1} - e_{N-1}) = 0 \\
&\qquad \nu_1 p_1(e_{N-1} - e_N) + \nu_2 p_2(\epsilon_N - e_N) = 0
\end{aligned}$$

where the symbols are defined as follows: e_i is the energy of segment i; ϵ_i is the average energy of neighbors to segment i which are not on the same molecule; p_1, p_2 are proportionality factors.

In the above, terminal segments on a molecule have been treated as identical to nonterminal segments except that they have only one directly bonded nearest neighbor. Terminal segments could be considered separately (assigned distinct ν and p) but this would unduly complicate the analysis since the number of terminal segments in a high polymer is small compared to the number of nonterminal segments. Proceeding, the total energy flux through each segment would be:

$$\begin{aligned}
q_1 &= {}^1/_2\nu_1 p_1 |e_2 - e_1| + {}^1/_2\nu_2 p_2 |\epsilon_1 - e_1| \\
q_2 &= {}^1/_2\nu_1 p_1 |e_1 - e_2| + {}^1/_2\nu_1 p_1 |e_3 - e_2| + {}^1/_2\nu_2 p_2 |\epsilon_2 - e_2| \\
&\vdots \\
q_n &= {}^1/_2\nu_1 p_1 |e_{n-1} - e_n| + {}^1/_2\nu_1 p_1 |e_{n+1} - e_n| + {}^1/_2\nu_2 p_2 |\epsilon_n - e_n| \qquad (2) \\
&\vdots \\
q_{N-1} &= {}^1/_2\nu_1 p_1 |e_{N-2} - e_{N-1}| + {}^1/_2\nu_1 p_1 |e_N - e_{N-1}| \\
&\qquad + {}^1/_2\nu_2 p_2 \epsilon_{N-1} - e \\
q_N &= {}^1/_2\nu_1 p_1 |e_{N-1} - e_N| + {}^1/_2\nu_2 p_2 |\epsilon_N - e_N|
\end{aligned}$$

q_i being the energy flux through segment i.

Over a reasonably small range the energies may be linearly related to temperatures:

$$\begin{aligned}
e_i &= \epsilon_0 + c_s\theta_i = c_s(T_0 + \theta_i) \\
\epsilon_i &= \epsilon_0 + c_s T_i = c_s(T_0 + T_i) \qquad (3)
\end{aligned}$$

where θ_i is a temperature corresponding to the energy of segment i, T_i is a temperature corresponding to the average energy of the neighbors (not on the same molecule) to segment i, T_0 is an arbitrary reference temperature, ϵ_0 is an arbitrary reference energy, and c_s is the heat capacity per segment.

For a linear temperature gradient, the energies ϵ_i are a simple function of temperature gradient and position:

$$\epsilon_i = \epsilon_0 + c_s g_T x_i = c_s(T_0 + g_T x_i) \qquad (4)$$

where g_T is temperature gradient and x_i is the distance, in the direction of the temperature gradient, of segment i from some reference point. Note that this relationship is written only for ϵ_i and not for e_i. That is, it is effectively assumed that the average energy of the neighbor segments is the same as the macroscopic average energy corresponding to the position of these segments. Segment i itself is not necessarily at this energy.

Substituting from eqs. (3) and (4) in eq. (1) yields:

$$\begin{aligned}
&\nu_1 p_1(\theta_2 - \theta_1) + \nu_2 p_2(g_T x_1 - \theta_1) = 0 \\
&\vdots \\
&\nu_1 p_1(\theta_{n-1} - \theta_n) + \nu_1 p_1(\theta_{n+1} - \theta_n) + \nu_2 p_2(g_T x_n - \theta_n) = 0 \qquad (5) \\
&\vdots \\
&\nu_1 p_1(\theta_{N-1} - \theta_N) + \nu_2 p_2(g_T x_N - \theta_N) = 0
\end{aligned}$$

Letting $\nu_2 p_2/\nu_1 p_1 = a$, g_T = unity, and rearranging yields:

$$\begin{aligned}
&(1 + a)\theta_1 - \theta_2 = ax_1 \\
&\vdots \\
&-\theta_{n-1} + (2 + a)\theta_n - \theta_{n+1} = ax_n \\
&\vdots \\
&-\theta_{N-1} + (1 + a)\theta_N = ax_N
\end{aligned} \tag{6}$$

Similarly eqs. (2) can be rewritten with g_T equal to unity:

$$\begin{aligned}
q_1' &= |\theta_2 - \theta_1| + a|x_1 - \theta_1| \\
&\vdots \\
q_n' &= |\theta_{n-1} - \theta_n| + |\theta_{n+1} - \theta_n| + a|x_n - \theta_n| \\
&\vdots \\
q_N' &= |\theta_{N-1} - \theta_N| + a|x_N - \theta_N|
\end{aligned} \tag{7}$$

where

$$q_i' = 2q_i/c_s\nu_1 p_1$$

The average energy flux $\bar{q}$ through a segment in the macromolecule is, with unit temperature gradient:

$$\bar{q} = (c_s\nu_1 p_1/2N) \sum_{i=1}^{N} q_i' \tag{8}$$

On this basis then, the macroscopic energy flux, which at unit temperature gradient is the thermal conductivity k, is:

$$k = v^{-2/3}\bar{q} \tag{9}$$

$$k = (c_s\nu_1 p_1/2v^{2/3}N) \sum_{i=1}^{N} q_i' \tag{10}$$

where v is the volume occupied by a segment. A calculation of thermal conductivity could be made by first solving eqs. (6) for the θ_i, evaluating the q_i from eqs. (7), and then inserting these values in eq. (10). In such a calculation the conductivity would be based on the average energy flux through one macromolecule. Since all molecules in a polymer are not equivalent, it is further required to average over many molecules. It is apparent that the numerical calculations are extensive since eqs. (6) represent N simultaneous equations to be solved for the θ_i. A further difficulty is that $\nu_1 p_1$ and a are not known, nor is it apparent how to evaluate them.

However, to a first approximation, the only factors in the calculation of k which would be affected by molecular weight or molecular orientation are N itself and the x_i which characterize the conformations of the molecules. (Extreme orientation, or crystallization, would affect other parameters.)

In particular note that in an affine, elastic deformation, where the molecular extension would correspond to the macroscopic deformation,

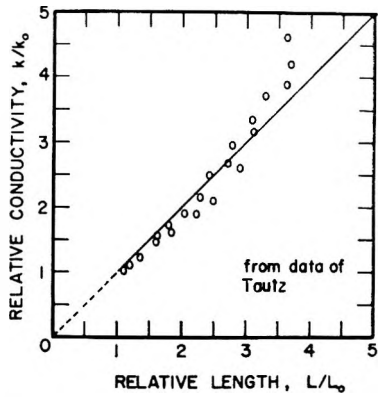

Fig. 1. Thermal conductivity of lightly vulcanized rubber as a function of extension.

these equations would predict that the thermal conductivity would increase in proportion to the extension. This point is evident from eqs. (6). If the molecular deformation is proportional to the macroscopic deformation, then the x_i increase in proportion to the macroscopic extension. Hence, the result of extension, with respect to eqs. (6), is to multiply through by the extension ratio. This effect of multiplication by the extension ratio carries directly through eqs. (7, 8, and 9). A lightly vulcanized rubber in tension should closely approximate such an affine elastic deformation. In Figure 1 some data on lightly vulcanized natural rubber from a paper by Tautz[3] have been plotted. On the basis of the above conclusion, the data on this plot would be expected to fall on a 45° line through the origin. Tautz drew a curved line through these data, but, the 45° line drawn in Figure 1 gives a reasonable fit at least up to a relative extension of 300%.

In a viscoelastic deformation the macroscopic deformation is not so simply related to the microscopic deformations. However, if a viscoelastic deformation is considered to consist of an elastic, affine deformation followed by a viscous flow and all molecular orientation is associated with the elastic deformation, then for any constant volume, orienting deformation of the above equations would predict the following relationships between thermal conductivity in direction of extension and thermal conductivity in the directions normal to the extension:

$$k_0/k_\perp = (k_\parallel/k_0)^{1/2} \tag{11}$$

or:

$$k_0^{3/2}/k_\perp k_\parallel^{1/2} = 1 \tag{12}$$

where k_0 is the thermal conductivity of the unoriented material and $k_\parallel$ and $k_\perp$ are the thermal conductivities measured parallel and normal to the orientation, respectively.

Table I presents some data from a paper by Eiermann and Hellwege[10] on oriented poly(methyl methacrylate). The data agree with eqs. (11)

TABLE I
From Data of Eiermann and Hellwege on Thermal Conductivity of Poly(methyl methacrylate)

	Conductivities, cal. cm.$^{-1}$ sec.$^{-1}$ °C.$^{-1}$ × 10^4					
T, °C.	k_0	$k_\parallel$	$k_\perp$	$\frac{k_0}{k_\perp}$	$\left(\frac{k_\parallel}{k_0}\right)^{1/2}$	$\frac{k_0^{3/2}}{k_\perp k_\parallel^{1/2}}$
−150	3.86	4.73	3.50	1.10	1.11	0.99
−100	4.27	5.45	3.86	1.11	1.13	0.98
−50	4.55	6.00	4.05	1.12	1.16	0.97
0	4.65	6.45	4.14	1.12	1.18	0.95
50	4.77	6.81	4.19	1.14	1.20	0.95

and (12) within experimental error in determination of the thermal conductivity values.

To estimate the magnitude of the influence of molecular weight on thermal conductivity some calculations were made from eqs. (6)–(9). The x_i values were obtained by effectively building molecules on a digital computer using a random walk procedure. Calculations were made for a value of the parameter $a = 0.01$ and for molecular weights (number of segments in a molecule) of 20, 50, 100, and 200. Taking conductivity at molecular length 20 segments as a reference, the calculated relative conductivity at other molecular weights was plotted versus molecular weight on a logarithmic scale with the results shown by the solid line in Figure 2. (The vertical bars indicate probable error limits on the calculations due to the limited number of calculations or "molecules" on which average values were determined.)

A limiting value of the dependence of thermal conductivity on molecular weight can be calculated by taking the parameter $a = 0$. This is equivalent to assuming that energy transfer between bonded segments (on the same molecule) is infinitely easier than energy transfer between neighboring, unbonded segments. With this assumption a derivation similar to the one above yields:

$$k = (\nu_2 p_2 c_s / 2v^{2/3})(\overline{|x - y|}) \tag{13}$$

where x and y represent the distances (in the direction of the temperature gradient) between two interacting segments and the respective centers of gravity of the associated molecules. $(\overline{|x - y|})$ represents the average absolute values of the difference between these distances. In eq. (13) the factor $(\overline{|x - y|})$ is the only one which is sensitive to molecular weight. Calculations based on this equation and the statistics of the freely jointed, freely rotating, polymer molecule configurations yield a thermal conductivity increasing as the $^1/_2$ power of molecular weight. For mixtures of different size molecules the dependence is on the $^1/_2$ power of the weight-average molecular weight. For purposes of comparison with the previous calculation, the $^1/_2$ power dependence is indicated on Figure 2 by the

straight line. (Further details on the derivations and calculations may be found in a thesis by Ho.)[11]

The predictions of the above theory on the influence of molecular weight on thermal conductivity may be compared with the data in Figures 3 and 4. Figure 3 is a plot of data taken in this laboratory on a series of melts of linear polyethylene–paraffin wax blends. The polyethylenes were a commercial linear type provided by Phillips Chemical Company (Marlex 6050, 6030, 6015, and 6009). Weight-average molecular weights of the polyethylenes were determined from intrinsic viscosity measurements in α-chloronaphthalene at 125°C. and the equation suggested by

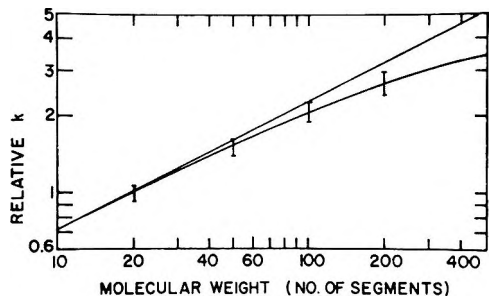

Fig. 2. Calculated dependence of thermal conductivity on molecular weight.

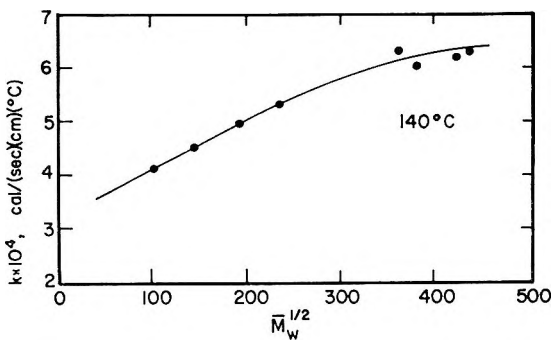

Fig. 3. Thermal conductivity of molten linear polyethylene as a function of molecular weight.

Atkins et al.[12] Polyethylene–wax blends were prepared from the above polyethylenes combined with a paraffin wax of molecular weight approximately 350. Thermal conductivities were measured in a twin guarded hot plate, 8 in. × 8 in. with samples $^1/_4$ in. thick, the temperature difference across the sample thickness was 2°C. The measurements are estimated to be accurate ±4% with a reproducibility of ±2%.

The data in Figure 3 clearly show a linear dependence of thermal conductivity on the $^1/_2$ power of the weight-average molecular weight which falls off as the molecular weight goes above about 100,000. This is in agreement with the predictions of the theory as shown in Figure 2.

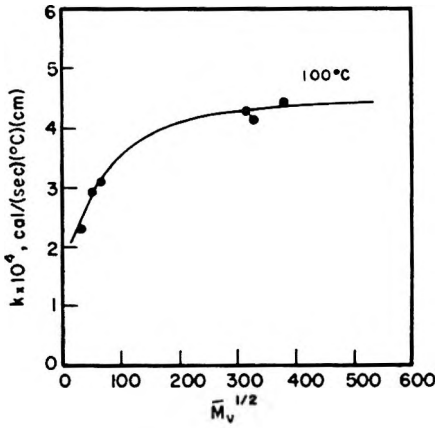

Fig. 4. Thermal conductivity of polystyrene as a function of molecular weight.

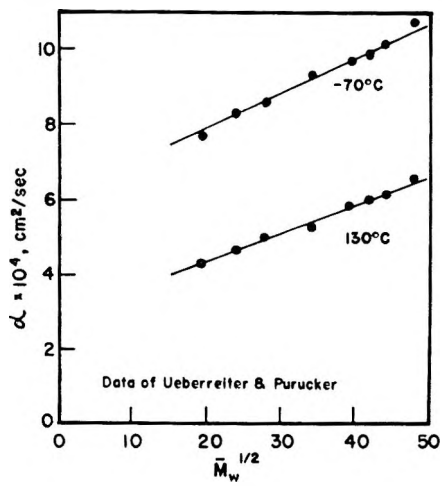

Fig. 5. Thermal diffusivity of polystyrene–hexachlorodiphenyl solutions as a function of molecular weight.

Figure 4 presents a few data on polystyrene some of which were determined in this laboratory and some of which were taken from a paper by Ueberreiter and Laupenmuhlen.[1] These data are not as complete as those on polyethylene, nor were the samples as well characterized. Note that the conductivity is plotted versus the intrinsic viscosity-average molecular weight. The data show the same general behavior as noted for the polyethylene, although it appears that the molecular weight influence falls off more rapidly with increasing molecular weight in polystyrene than it does in polyethylene. This may be explained in terms of the relatively large influence of the benzene group on interchain energy transfer in polystyrene which would lead to a higher value of a, and hence, a less extensive influence of molecular weight on thermal conductivity in polystyrene compared to polyethylene.

Some further evidence in support of the theory is given in Figure 5,

which is a plot of data by Ueberreiter and Purucker[2] on the thermal diffusivity of some polystyrene–hexachlorodiphenyl solutions. A linear relationship between the weight-average molecular weight and the thermal diffusivity is evident, but direct comparison with the theory is not possible on two counts: (*1*) hexachlorodiphenyl is not a polystyrene, and hence the solution has two components; (*2*) the thermal diffusivity rather than thermal conductivity was measured.

Temperature Effects on the Thermal Conductivity of Linear Polyethylene

Figure 6 presents data obtained on the thermal conductivity of linear polyethylene (Phillips Marlex 6050) as a function of temperature. These data were obtained in the guarded hot plate apparatus with the use of twin samples 8 in. × 8 in. × $^1/_4$ in. thick. The temperature drop across the samples during measurement was 2°C. The samples were prepared by vacuum molding at 180°C. and slow cooling under nitrogen (cooling time from 180°C. to room temperature was about 15 hr.). By intrinsic viscosity measurement in α-chloronaphthalene at 125°C., the weight-average molecular weight of this sample was estimated at 132,000. The density of the samples at 27°C. after vacuum molding was 0.975 g./cc.

The data in Figure 6 show the thermal conductivity decreasing with temperature above 60°C. and falling rapidly as the melt temperature is approached. Above the melting point there is a small increase with temperature. These data were analyzed further in terms of the crystallinity of the sample. Volume dilatometry yielded the results presented in Figures 7 and 8 for the specific volume V and per cent crystallinity γ as functions of temperature. The "per cent crystallinity" was calculated from the expression:

$$V = \gamma V_c + (1 - \gamma) V_a \tag{14}$$

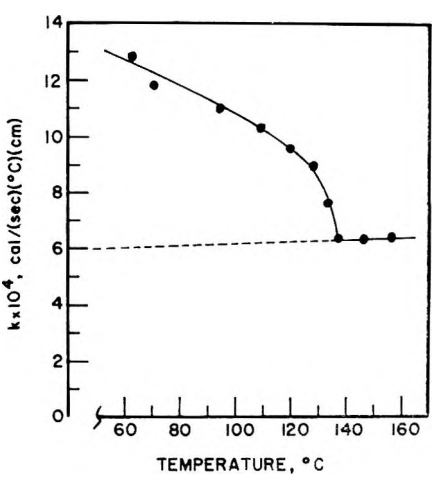

Fig. 6. Thermal conductivity of linear polyethylene as a function of temperature.

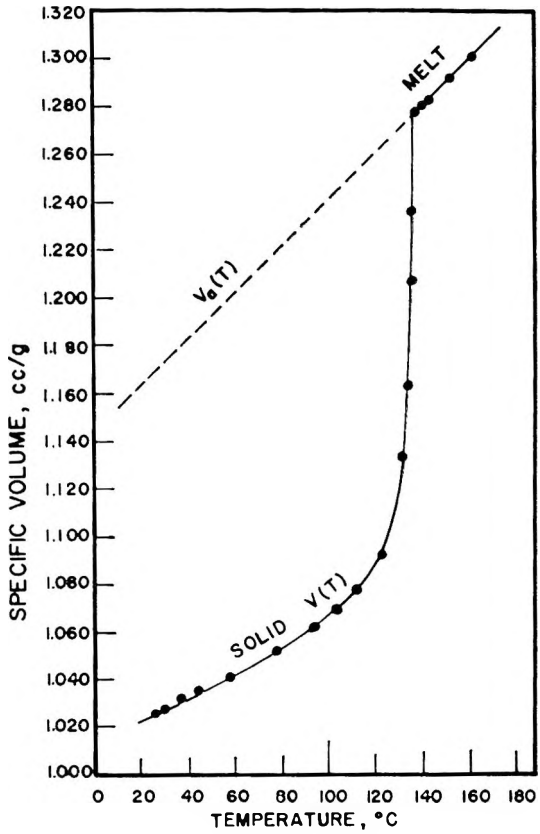

Fig. 7. Specific volume of linear polyethylene as a function of temperature.

relating per cent crystallinity γ to the specific volume of the sample V and the specific volumes of completely amorphous polyethylene and perfectly crystalline polyethylene, V_a and V_c, respectively. V_a values were taken from extrapolation of the specific volume of molten polyethylene in Figure 7. V_c values were taken from Swan's x-ray data.[13]

In a manner analogous to the calculation of per cent crystallinity from specific volumes, one can write for the thermal conductivity:

$$k = \gamma k_c + (1 - \gamma)k_a \tag{15}$$

By using this expression, the measured values of k, and extrapolation of the k data on molten polyethylene for k_a, values of k_c were calculated. These values of k_c, presumably an extrapolated estimate of the thermal conductivity of perfectly crystalline polyethylene, are plotted versus reciprocal temperature in Figure 9. A linear relationship is evident, which is in agreement with the phonon theory of thermal conductivity in dielectric crystals. Hence, it would appear that in perfectly crystalline polyethylene the thermal conductivity behavior is the same as that which has been observed for nonpolymeric, dielectric crystals. For incompletely crystallized polyethylene the thermal conductivity can be related to specific volume by the per cent crystallinity concept. Identical results

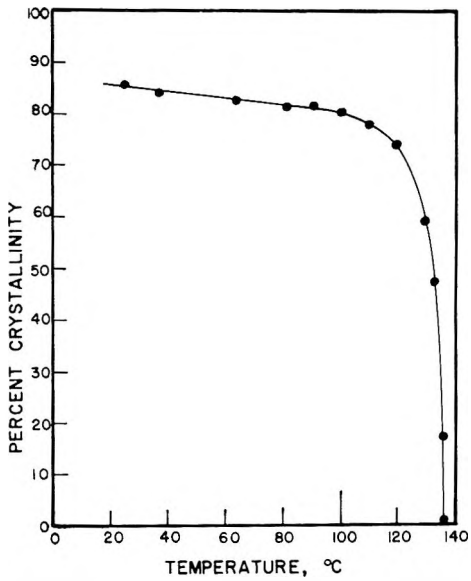

Fig. 8. Per cent crystallinity of linear polyethylene as a function of temperature.

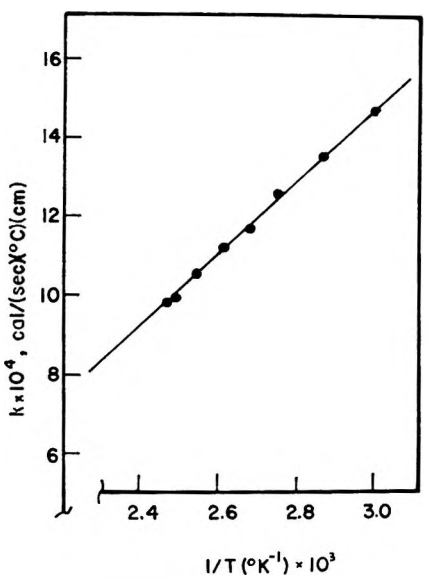

Fig. 9. Thermal conductivity of crystalline polyethylene vs. reciprocal temperature.

were obtained with three other polyethylene samples of different molecular weights (Marlex 6009, 6015, and 6035).

Conclusions

A theory has been postulated which predicts the effects of molecular weight and molecular orientation on the thermal conductivity of linear, amorphous high polymers. The predictions of the theory agree with available experimental data.

The temperature behavior of the thermal conductivity of one crystalline polymer, linear polyethylene, is in accord with the phonon theory of energy transport in dielectric crystals. Data on this polymer indicate that the thermal conductivity of semicrystalline polymers can be analyzed in terms of the thermal conductivities of the crystalline and amorphous fractions by the per cent crystallinity concept.

Financial support of this work by a grant from the National Aeronautics and Space Administration to Rensselaer Polytechnic Institute (NSG 100-60) is gratefully acknowledged.

References

1. Ueberreiter, K., and O. Laupenmuhlen, *Z. Naturforsch.*, **8a,** 664 (1953).
2. Ueberreiter, K., and S. Purucker, *Kolloid-Z.*, **144,** 120 (1955).
3. Tautz, H., *Exptl. Tech. Physik.*, **7,** 1 (1959).
4. Hellwege, K. H., W. Knappe, and V. Semjonow, *Z. Angew. Phys.*, **11,** 285 (1959).
5. Hellwege, K. H., J. Hennig, and W. Knappe, *Kolloid-Z. Polymere*, **188,** 121 (1963).
6. Knappe, W., *Plaste Kautschuk*, **4,** 189 (1962).
7. Knappe, W., *Z. Angew. Phys.*, **12,** 508 (1960).
8. Bridgman, P., *The Physics of High Pressure*, MacMillan, New York, 1931.
9. Horrocks, J. K., and E. McLaughlin, *Trans. Faraday Soc.*, **56,** 206 (1960).
10. Eiermann, K., and K. H. Hellwege, *J. Polymer Sci.*, **57,** 99 (1962).
11. Ho, C. C., Ph.D. Thesis, Rensselaer Polytechnic Institute, 1964.
12. Atkins, J. G., L. T. Muus, C. W. Smith, and E. T. Pieski, *J. Am. Chem. Soc.*, **79,** 5089 (1957).
13. Swan, P. R., *J. Polymer Sci.*, **56,** 403 (1962).

Résumé

On a étudié d'un point de vue expérimental et théorique les conductivités thermiques des hauts polymères linéaires. On en a tiré une théorie de la conductivité thermique dans les hauts polymères linéaires amorphes, basée sur un modèle simple de structure moléculaire. Les prévisions sur les effets du poids moléculaire et de l'orientation moléculaire sur la conductivité thermique, obtenues à partir de la théorie, sont en accord avec les résultats expérimentaux. Nous avons présenté des nouvelles données sur la conductivité thermique de polyéthylènes linéaires et de certains mélanges de cires de polyéthylène. L'influence de la température sur la conductivité thermique du polyéthylène a été déterminée par une étude du "pourcentage de cristallinité," ce qui a fourni des résultats qui sont en accord avec la théorie du phonon concernant la conductivité thermique dans les cristaux diélectriques.

Zusammenfassung

Die Wärmeleitfähigkeit linearer Hochpolymerer wurde experimentell und theoretisch untersucht. Eine auf einem einfachen Molekülstrukturmodell beruhende Theorie der Wärmeleitfähigkeit bei linearen amorphen Hochpolymeren wurde aufgestellt. Die Voraussagen der Theorie bezüglich des Einflusses von Molekulargewicht und Molekülorientierung auf die Wärmeleitfähigkeit stimmen mit den vorhandenen Versuchsdaten überein. Für die Warmeleitfahigkeit von linearem Polyäthylen und einigen Polyäthylen-Wachsmischungen werden neue Ergebnisse vorgelegt. Die Temperaturabhängigkeit der Wärmeleitfähigkeit von Polyäthylen wurde anhand des "prozentuellen Kristallinitäts"-Konzepts analysiert, und dabei Ergebnisse in Übereinstimmung mit der Phononentheorie der Wärmeleitfähigkeit dielektrischer Kristalle erhalten.

Received June 1, 1964
Revised July 13, 1964

JOURNAL OF POLYMER SCIENCE: PART A VOL. 3, PP. 671–679 (1965)

Differential Thermal Analysis of the Cocrystal Peak in Linear–High Pressure Polyethylene Blends*

BERT H. CLAMPITT, *Research and Development Department, Spencer Chemical Company, Merriam, Kansas*

Synopsis

A DTA study of over 60 linear–high pressure polyethylene blends is reported. From this study a preliminary phase diagram for this type of system is derived; however, the main emphasis is on the nature of the cocrystal peak. The results appear to indicate that there are two classes of cocrystals in linear–high pressure polyethylene blends with the linear component being responsible for the division of the blends into two groups. The property of the linear component which is responsible for this division is related to the crystallite size of the pure linear crystal. While the division of the blends into two groups is primarily dependent on the linear component, the magnitude of the cocrystal peak height is dependent on the high pressure polyethylene component. Low melt index and low branching of the high pressure polyethylene favor large cocrystal formation. Indeed, resins containing 30 methyls per 1000 carbons do not possess a cocrystal peak.

Introduction

In a previous communication it was shown that differential thermal analysis (DTA) curves on annealed samples of linear–high pressure polyethylene blends could be resolved into three peaks.[1] These peaks come at 115, 124, and 134°C. The 115°C. peak was associated with the high pressure polyethylene, whereas the 134°C. peak was shown to be proportional to the linear content of the system. The nature of the 124°C. peak is not clear, but may be associated with cocrystal formation in these blends. It is the purpose of the present paper to shed some further light on the nature of the 124°C. transition by extending the measurements to a large number of linear–high pressure polyethylene blends.

Experimental

The DTA apparatus and general procedure are the same as described previously.[1] The DTA samples were all cast at 190°C., but the key step in sample preparation was the annealing of the cast samples for 30 min. at 120°C. prior to the determination. This annealing procedure gives well resolved DTA peaks and appears to be ideal for studying linear–high pressure polyethylene blends.

*Paper presented at the 148th National American Chemical Society Meeting, Chicago, Ill., August 30–Sept. 4, 1964.

The actual blending of the components was done on a Brabender mixer, and product was of very uniform composition. The linear polyethylenes used in this study are listed in Table I together with some of their properties. Similarly, the high-pressure polyethylenes used in this investigation are listed in Table II. Over 60 blends of these components were made and analyzed by DTA.

TABLE I
Linear Polyethylenes

Polyethylene	Type	Density, g./cc.[a]	Melt index[a]
Hifax 2000	Ziegler	0.962	9.0
Hifax 1800	Ziegler	0.945	0.4
Koppers 6060	Ziegler	0.956	6.0
Hifax 2600E	Ziegler	0.962	0.2
Grex 50-090	Phillips	0.950	9.0
Grex 60-002	Phillips	0.960	0.2
Phillips 6050	Phillips	0.960	5.0
Grex 50-004	Phillips	0.950	0.4
Alathon 7040	Ziegler	0.957	6.0
Alathon 7011	Ziegler	0.950	0.5

[a] Manufacturer's data.

TABLE II
High Pressure Polyethylenes (HPPE)

Polyethylene	Melt index	CH_3/1000 carbons
PE-5206	2	10
PE-5392	2	20
PE-1005	2	30
PE-1408.5	20	20
PE-1008.5	20	30

Results and Discussion

A typical DTA curve of a linear-high-pressure polyethylene blend is shown in Figure 1. The particular peak of interest in this study is the 124°C. (cocrystal) peak; however, data are included for the other peaks as well. Because of the difficulty of assigning an area to the 124°C. peak, the results are reported in arbitrary units of peak height, and this proves to be a very convenient and informative parameter.

In the first series of experiments, the high pressure polyethylene component was kept constant (i.e., PE-5392 was used), and blends at the 5, 17.5, and 30% linear level were made with the linear polyethylenes listed in Table I. Results of the thermograms in these systems are given in Table III.

Two aspects of the data given in Table III are of special interest. First, it will be noted that in the 30% blends, the cocrystal heights cluster near two values, namely 17 and 35. Furthermore, these same values persist in

TABLE III
DTA Results on Linear-PE 5392 Blends

Linear		% Linear	Height			Temp., °C.		
			HPPE	Cocrystal	Linear	HPPE	Cocrystal	Linear
Hifax	2000	30	20	17	88	115	123	135
Hifax	1800	30	24	35	53	116	124	129
Koppers	6060	30	20	35	63	116	124	131
Hifax	2600E	30	20	17	68	114	124	135
Grex	50–090	30	20	38	68	115	124	131
Grex	60–002	30	22	20	75	115	124	135
Phillips	6050	30	22	17	87	116	124	134
Grex	50–004	30	20	32	67	116	124	131
Alathon	7040	30	16	15	78	115	124	135
Alathon	7011	30	17	14	77	115	124	135
Hifax	2000	17.5	28	14	45	116	124	133
Hifax	1800	17.5	32	36	36	116	124	127
Koppers	6060	17.5						
Hifax	2600E	17.5	26	15	48	116	124	133
Grex	50–090	17.5	29	39	39	116	124	129
Grex	60–002	17.5	29	16	50	116	124	133
Phillips	6050	17.5	28	17	44	116	124	133
Grex	50–004	17.5	35	36	49	116	124	129
Alathon	7040	17.5	24	19	56	115	124	133
Alathon	7011	17.5	25	12	47	116	124	133
Hifax	2000	5	39	17	10	116	124	130
Hifax	1800	5	42	23	—	116	124	—
Koppers	6060	5	41	26	—	117	124	—
Hifax	2600E	5	43	18	12	117	124	130
Grex	50–090	5	41	30	—	117	124	—
Grex	60–002	5	42	17	6	117	124	130
Phillips	6050	5	40	20	9	116	124	130
Grex	50–004	5	44	26	—	116	124	—
Alathon	7040	5	39	18	11	116	124	130
Alathon	7011	5	40	15	16	116	124	131

TABLE IV

Group I	Group II
Hifax 2600E	Hifax 1800
Grex 60–002	Grex 50-004
Hifax 2000	Koppers 6060
Phillips 6050	Grex 50–090
Alathon 7040	
Alathon 7011	

the 17.5% blends. The 5% blends are slightly different in that the systems showing a peak height of 17 appear to be unaltered; while the systems previously showing a peak height of 35 have a value lower than 35. Significantly, the systems which previously had a peak height of 35 have no linear (130°C.) peak in the 5% blends. All of these data, therefore,

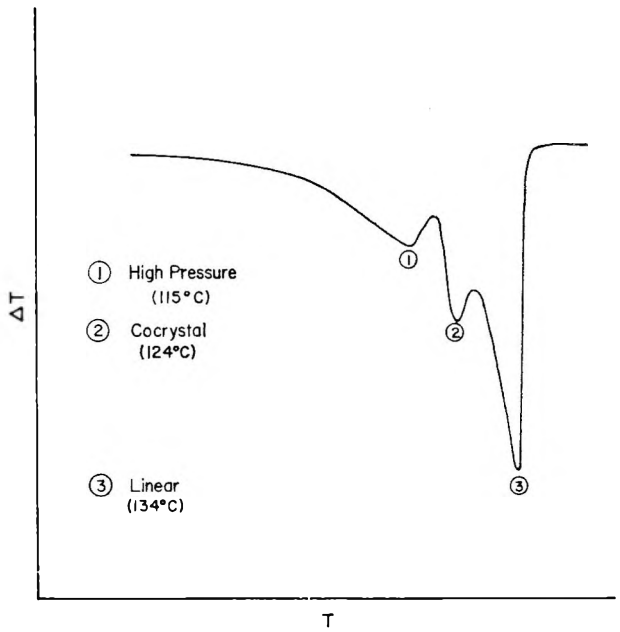

Fig. 1. Typical thermogram of a linear–high pressure polyethylene blend.

strongly suggest that the linears listed in Table I may be divided into two groups as shown in Table IV.

These groups do not correspond to any division based on linear type, density class, or melt index. Similarly, the DTA crystallinity or even the x-ray crystallinity of the pure components do not divide the linear polyethylenes into the groups listed above. Crystallite size of the pure linear polyethylenes (Table V), as measured by peak broadening of the x-ray diffraction pattern,[2] do however, appear to divide them along the above lines.

These data indicate that the linear components of the group II systems have a smaller crystallite size than the group I systems, and also they are more compatible with the high pressure polyethylene (i.e., a larger

TABLE V

Linear polyethylene	Crystallite size, A.
Hifax 1800	276
Grex 50–004	275
Koppers 6060	275
Grex 50–090	275
Hifax 2600E	314
Grex 60–002	322
Hifax 2000	328
Phillips 6050	314
Alathon 7040	328
Alathon 7011	301

TABLE VI
DTA of Linear–PE 5392 Blends Over the Entire Concentration Range

Linear	% Linear	Height			Temp., °C.		
		HPPE	Cocrystal	Linear	HPPE	Cocrystal	Linear
Hifax							
2000	0	56	—	—	119	—	—
	5	39	17	10	116	124	130
	17.5	28	14	45	116	124	133
	30	20	17	88	115	123	135
	50	17	16	108	112	123	136
	70	8	17	104	107	123	137
	85	—	—	115	—	—	138
	95	—	—	115	—	—	138
	100	—	—	120	—	—	138
Grex							
60–002	0	56	—	—	119	—	—
	5	42	17	6	117	124	130
	17.5	29	16	50	116	124	133
	30	22	20	75	115	124	135
	50	16	19	99	111	123	135
	70	11	25?	106	109	123	136
	85	—	—	110	—	—	137
	95	—	—	135	—	—	138
	100	—	—	138	—	—	140
Hifax							
1800	0	56	—	—	119	—	—
	5	42	23	—	116	124	—
	17.5	32	36	36	116	124	127
	30	24	35	53	116	124	129
	50	21	37	72	113	124	130
	70	14	40	85	111	123	131
	85	11	40	85	113	123	132
	95	11?	38?	90	113	123	133
	100	—	—	111	—	—	133
Grex							
50–090	0	56	—	—	119	—	—
	5	41	30	—	117	124	—
	17.5	29	39	39	116	124	129
	30	20	38	68	115	125	131
	50	18	35	80	115	125	132
	70	13	38	112	112	125	133
	85	9	38	111	111	124	133
	95	9?	28?	124	111	123	134
	100	—	—	135	—	—	135

cocrystal peak is observed). This would appear to indicate that the more poorly crystallized linear systems could be better accommodated in the cocrystals than the others. Indeed, in the 5% blends, the group II linears are completely incorporated in the cocrystal. This is a rather reasonable conclusion, but *a priori* it would be difficult to predict.

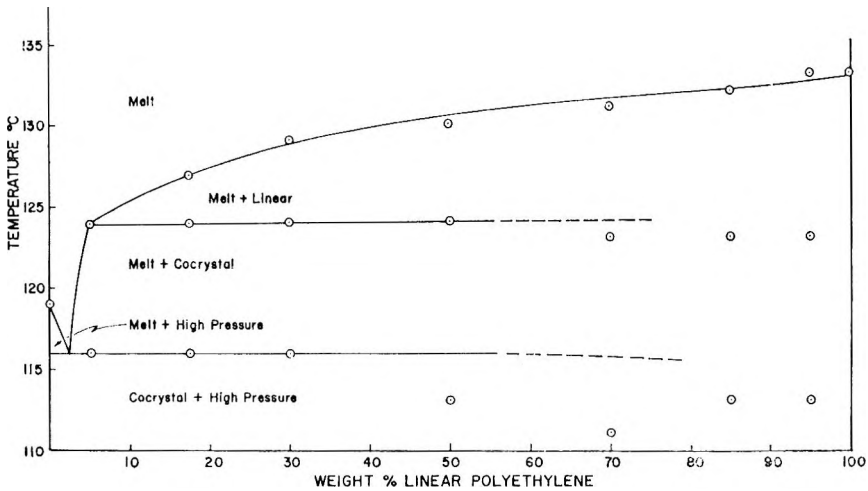

Fig. 2. Phase diagram of a linear–high pressure polyethylene system.

Not only do the cocrystal peak heights appear to cluster near two values, but also these values tend to be independent of composition. To further check this last point, blends of PE-5392 and four of the linears previously investigated (two from each group) were prepared to cover the entire concentration range. The DTA results are given in Table VI, and it is evident that the cocrystal peak height is truly independent of composition. The DTA peaks become more diffused at very high percentage linears, and it is not possible to detect a point where only the cocrystal and linear polyethylene peaks are present. Nevertheless, on the basis of the data given in Table VI, it is possible to draw a preliminary phase diagram for a linear–higher pressure polyethylene blend. The Hifax 1800-PE 5392 data from Table VI are plotted in Figure 2 and it is seen that a reasonable phase diagram is obtained. Further work will be necessary to clarify the high percentage linear region of the diagram and to locate exactly the position of the eutectic. Nevertheless, the qualitative aspects of the diagram are correct, and the existence of a peritectic appears clear.

The results discussed so far have been confined to a given high pressure polyethylene (PE-5392) and various linear polyethylenes. In order to complete the picture, it was decided to prepare linear blends with other high pressure polyethylenes. As the cocrystal peak height appears to be independent of composition only 30% linear–70% high pressure polyethylene blends were prepared. The same four linears used previously were blended with all of the high pressure polyethylenes listed in Table II. Results of the thermograms are given in Table VII.

From the data in Table VII it is clear that the previously designated linear groups are valid, regardless of the high pressure polyethylene (HPPE) component (i.e., for a given high pressure polyethylene, the cocrystal peak height is larger in the Grex 50–090 and Hifax 1800 linear systems than

TABLE VII
DTA of Various Linear–High Pressure Polyethylene Blends

Composition		Height			Temp., °C.		
30% Linear	70% HPPE	HPPE	Cocrystal	Linear	HPPE	Cocrystal	Linear
Grex 60-002	PE-5206	25	44	92	115	123	134
"	PE-5392	22	20	75	115	124	135
"	PE-1005	11	—	121	105	—	134
"	PE-1408.5	25	12	80	114	121	135
"	PE-1008.5	21	—	80	105	—	135
Hifax 2000	PE-5206	24	38	75	115	123	134
"	PE-5392	20	17	88	115	123	135
"	PE-1005	6	—	119	104	—	134
"	PE-1408.5	21	15	79	114	122	134
"	PE-1008.5	16	—	68	104	—	135
Grex 50-090	PE-5206	25	62	84	115	124	131
"	PE-5392	20	38	68	115	124	131
"	PE-1005	12	—	109	108	—	131
"	PE-1408.5	21	21	63	114	122	131
"	PE-1008.5	20	—	67	104	—	131
Hifax 1800	PE-5206	24	61	56	116	124	128
"	PE-5392	24	53	53	116	124	129
"	PE-1005	16	—	100	105	—	128
"	PE-1408.5	23	26	57	113	124	128
"	PE-1008.5	15	—	46	104	—	128

in the Grex 60–002 and Hifax 2000 systems). Another interesting feature of the data in Table VII is that for a given linear polyethylene, the cocrystal peak heights depend upon the high pressure component which is present. Indeed, the cocrystal peak heights for a given linear polyethylene are in the order PE-5206 > PE-5392 > PE-1408.5 > PE-1008.5 = PE-1005, regardless of the linear polyethylene studied, e.g., in the Grex 60–002–high pressure polyethylene blends, the cocrystal peak heights are 44, 20, 12, 0, and 0 for the PE-5206, PE-5392, PE-1408.5, PE-1008.5, and PE-1005 systems, respectively.

Probably the most interesting aspect of the data in Table VII is the fact that systems containing PE-1008.5 and PE-1005 do not possess a cocrystal peak in any of the blends which have been studied. Apparently the greater the methyl content of the high pressure component, the less high pressure polyethylene will fit into a cocrystal lattice, and therefore, the lower the cocrystal peak height. This is clearly seen by comparing the methyl content of the various high-pressure polyethylene components listed in Table II with the observed order of cocrystal peak heights listed in Table VII. At 30 methyls per 1000 carbon atoms, none of the high pressure polyethylene molecules will fit into a cocrystal lattice and, therefore, only the high pressure polyethylene and linear polyethylene peaks are observed in the PE-1008.5 and PE-1005 systems. While methyl content is of prime importance, the cocrystal height is also apparently related to

melt index, and the results suggest that the larger the melt index, the lower the cocrystal peak height. Results on PE-5392 and PE-1408.5 show this, as they have the same methyl content (i.e., 20 methyls per 1000 carbon atoms), but the PE-1408.5 has a larger melt index and correspondingly a lower cocrystal peak height.

In summary, it appears that there are two classes of cocrystals in linear–high pressure polyethylene blend. The linear component is apparently responsible for the division of the blends into the two groups. The property of the linear component which is responsible for this division is not easy to discern, since it is independent of linear type, density, melt index, and crystallinity; however, it is related to the crystallite size of the pure linear crystal. Indeed, the more poorly crystallized linear systems are more easily incorporated in the cocrystal than are the well crystallized linears. While the division of the blends into two groups is primarily dependent on the linear component, the magnitude of the cocrystal peak height is dependent on the high pressure polyethylene component. Low melt index and low branching of the high pressure polyethylene favors large cocrystal formation. Indeed, resins containing 30 methyls per 1000 carbons do not appear to possess a cocrystal peak. Not only is DTA valuable in studying the cocrystal, but the entire phase diagram of linear–high pressure polyethylene blends can profitably be studied by this technique.

The author wishes to express his gratitude to Dr. R. H. Hughes and Mr. D. E. German for the x-ray data and for helpful discussions regarding the DTA results. Appreciations are also expressed to Dr. H. D. Anspon, Mr. Charles Mosier, and Dr. W. A. Pavelich for suggestions regarding the overall design of the program and for aid in the interpretation of the data. A special measure of thanks is extended to Mr. Nathan Scarritt for much of the experimental work.

References

1. Clampitt, B. H., *Anal. Chem.*, **35**, 1834 (1963).
2. Bunn, C. W., and T. C. Alcock, *Trans. Faraday Soc.*, **41**, 317 (1945).

Résumé

On a effectué une étude par analyse thermique différentielle de 60 mélanges de polyéthylène linéaire et de polyéthylène haute pression. Un diagramme de phase préliminaire valable pour ce genre de système en a été déduit; cependant l'accent a été mis principalement sur la nature du maximum du cocrystal. Les résultats semblent indiquer l'existence de deux classes de cocristaux dans les mélanges de polyéthylènes linéaire et haute pression, la fraction linéaire étant responsable de la division des mélanges en deux groupes. La propriété des polyéthylènes linéaires qui est à l'origine de cette division, est liée à la taille des cristallites dans le cristal totalement linéaire. Alors que la subdivision des mélanges en deux groupes est due principalement à la présence de polyéthylène linéaire, l'importance du maximum du cocristal dépend de la présence de polyéthylène haute pression dans le mélange. Un indice de fusion faible et une ramification peu importante du polyéthylène haute pression favorisent la formation de grands cocristaux En effet, les résines possédant 30 méthyles pour 1000 carbones ne présentent pas de maximum dû aux cocristaux.

Zusammenfassung

Es wird über eine DTA-Untersuchung an 60 Linear–Hochdruck-Polyäthylenmischungen berichtet. Aus dieser Untersuchung wird ein vorläufiges Phasendiagramm für den vorliegenden Systemtyp abgeleitet. Das Hauptgewicht wird jedoch auf die Natur des Cokristallmaximums gelegt. Die Ergebnisse scheinen zu zeigen, dass es zwei Klassen von Cokristallen bei Linear–Hochdruck-Polyäthylenmischungen gibt, wobei die lineare Komponente für die Teilung der Mischungen in zwei Gruppen verantwortlich ist. Die Eigenschaft der linearen Komponente, welche für diese Teilung verantwortlich ist, wird zur Kristallitgrösse des reinen linearen Kristalls in Beziehung gesetzt. Während die Teilung der Mischungen in zwei Gruppen primär von der linearen Komponente abhängt, hängt die Höhe des Cokristallmaximums von der Hochdruck-Polyäthylenkomponente ab. Niedriger Schmelzindex und geringe Verzweigung des Hochdruck-Polyäthylens begünstigen eine grosse Cokristallbildung. Tatsächlich besitzen Harze mit 30 Methylgruppen auf 1000 Kohlenstoffatome kein Cokristallmaximum.

Received June 8, 1964
Revised July 23, 1964

JOURNAL OF POLYMER SCIENCE: PART A VOL. 3, PP. 681–696 (1965)

Comparison of Some Mechanical and Flow Properties of Linear and Tetrachain Branched "Monodisperse" Polystyrenes

D. P. WYMAN and L. J. ELYASH, *Mellon Institute, Pittsburgh, Pennsylvania*, and W. J. FRAZER, *Marbon Chemical Company, Washington, West Virginia*

Synopsis

The strength and flow properties of narrow distribution polystyrenes have been studied as functions of molecular weight and branching (tetrachain star-type molecules). Most of the mechanical properties of linear and branched narrow distribution polystyrenes were essentially the same as those for a broad distribution general-purpose polystyrene. For the narrow distribution linear polymers the value of a given property increased rapidly with molecular weight until ca. $M = 1.6 \times 10^5$. Thereafter the magnitude of the property increased only slightly for rather large increases in M and asymptotically approached a maximum. The same was true of the branched polymers except that certain properties, e.g., tensile strength, were found to level off in value at higher molecular weights than for the corresponding linear polymers. Studies of apparent melt viscosity, η, made with a capillary rheometer showed that at low shear rates ($\dot{\gamma} < 10$ sec.$^{-1}$), the branched polymers exhibited much lower apparent values of η than linear polymers of the same total molecular weight. At high shear rates ($\dot{\gamma} \sim 2000$ sec.$^{-1}$), this difference essentially disappeared and η approached a constant value independent of M (1.5×10^5–4.5×10^5) and branching. Melt viscosity data for both the linear and branched narrow distribution polymers when plotted in the form of reduced viscosities versus a function of $\dot{\gamma}$ (as suggested by Bueche) fell upon one master curve.

INTRODUCTION

Since anionic polymerization techniques are capable of yielding polystyrenes with narrow chain length distributions,[1–3] it has been of considerable interest to assess the effects of molecular weight distribution on various polymer properties.[4–6] The nonterminating nature of anionic polymerizations is such that at the completion of a polymerization one has available a solution of macromolecular organometallic compounds which can be reacted with suitable terminating agents to prepare branched polymers with narrow molecular weight distribution,[7–10] viz.,

$$4\text{PSLi} + \text{Ph}(\text{CH}_2\text{Cl})_4 \rightarrow \text{Ph}(\text{CH}_2\text{PS})_4 + 4\text{LiCl}$$

where PS denotes R—(CH_2—CHPh)$_n$—CH_2—CH(Ph), n is a variable integer, and R is an alkyl (or aryl) group.

In this paper we give the results of a comparative investigation of some

mechanical and melt flow properties of several linear ($\bar{M}_v$ = 1.6 × 10^5–8.9 × 10^5) narrow distribution polymers with two ($\bar{M}_v$ = 2.04 × 10^5 and 4.3 × 10^5) narrow distribution tetrachain star-type branched polymers. This study was prompted, in part, by previous reports[11] that branched polymers exhibit significantly lower melt viscosities than linear polymers of the same total molecular weight. Such a decrease in η might be of considerable value in fabricating operations such as extrusion wherein higher through-puts and/or decreased operating temperatures could be possible. However, it was necessary to determine (*1*) what, if any, differences existed in the mechanical properties of linear and branched polystyrene at ordinary temperatures and (*2*) whether the differences in η observed at low values of $\dot{\gamma}$ persisted at higher values of $\dot{\gamma}$, i.e., would there be a real advantage under the shear conditions found in normal extrusion operations?

EXPERIMENTAL

Narrow-Distribution Polymers

Linear Polymers. Narrow molecular weight distribution anionic polystyrenes reported in the literature,[1] with few exceptions,[3,4] have been prepared in high vacuum. The larger sample sizes required in the measurements made in this study mitigated against vacuum line operations; therefore, all preparations were conducted at atmospheric pressure under pure inert gases (argon and/or nitrogen).

The polymerization vessel was a 12-liter flask equipped with a large glass-covered magnetic stirrer and several ground glass joints whose function is described below. Included was an inert gas inlet and outlet. The inlet was such that in operation the gas was bubbled through the reaction solution. It was found that storage of the reaction flask in an oven at 120°C. for several days was not sufficient to remove adsorbed moisture. Therefore, the flask was removed from the oven just before use and placed in position for the polymerization under pure argon. The argon was purified by bubbling it through a concentrated tetrahydrofuran (THF) or THF–benzene solution of α-methylstyrylsodium dianions prepared by the reaction of excess sodium–potassium alloy (eutectic) with α-methylstyrene. While under a blanket of pure argon all surfaces of the polymerization vessel were rinsed with a concentrated solution of butyllithium and polystyryllithium. The solution was forced out of the reaction flask under argon at the completion of this step.

Benzene served as solvent for the polymerization. It was purified as follows. Reagent grade material was dried for several days over calcium hydride and then transferred to a 12-liter flask. The predried solvent was vigorously stirred with sodium–potassium alloy for several days and then forced into the polymerization flask under nitrogen. Pure argon was bubbled through the well stirred liquid in order to degas it. For most polymerizations a sufficient quantity of solvent was used so that the

final concentration of polymer was ~10% (w/v). Thus, typically, for the preparation of 500 g. of polystyrene, 5 liters of benzene were used.

Styrene monomer was purified by fractional distillation *in vacuo*, nitrogen being used as the carrier gas to control the pressure (at ~60 mm.). The middle cut, used for polymerization, was collected in a flask equipped with a gas inlet and siphon tube extending from the bottom of the flask to a ground glass joint. With this apparatus distilled styrene could be forced into the polymerization vessel under nitrogen without exposure to air. After the introduction of the monomer the solution which resulted was degassed as described above.

A small amount (usually 5 ml./500 g. styrene) of pure THF, distilled from a THF solution of sodium α-methylstyrene was added next.[14] If polymer with $\bar{M}_n < 1 \times 10^5$ was being prepared, the styrene–benzene–THF solution was cooled in an ice bath before adding the initiator, butyllithium (obtained from the Foote Mineral Company in the form of a hexane solution). In the case of higher molecular weight polymers, cooling was used at the beginning of polymerization. The quantity of butyllithium (which was introduced by syringe in one portion) was based on eq. (1):[1]

$$\text{Molecular weight} = \text{g. monomer/moles butyllithium} \qquad (1)$$

Often, a 10% excess of butyllithium over that required by eq. (1) was used in order to purge the small amounts of impurities present before polymerization. In the case of low molecular weight polymers, e.g., $\bar{M}_n = 25{,}000$, the ice bath was removed about 15 min. after the polymerization commenced, and the remainder of the reaction was allowed to proceed at room temperature. For the higher molecular weight polymers ($M > 1 \times 10^5$) the polymerization was started at room temperature. Occasionally reaction temperatures rose quite rapidly and cooling with cold water was necessary in order to keep them below 40°C. After 1–2 hr. of stirring, termination of the polystyryllithium was accomplished by the introduction of methanol. Polymer was recovered by precipitation in a 10-fold excess of methanol and then vacuum-dried.

Tetrachain Star-Type Polymers. The apparatus described above for the preparation of linear polymers was modified to include an attachment to a 1-liter round-bottomed dropping funnel which was in turn attached through a condenser to a 12-liter flask. Prior to attachment to the polymerization flask this apparatus was charged with about 8 liters of THF, several milliliters of α-methylstyrene, and sodium–potassium alloy. The glass surfaces were thoroughly cleaned (under argon) by distilling pure THF throughout the apparatus. After about 1 liter had been distilled, the apparatus was assembled.

Polystyryllithium of appropriate molecular weight (Table I) was prepared as described above. The resultant solution was then cooled in an ice–salt bath and a volume of THF about equal to that of the solution was distilled in rapidly under argon. This step, involving 5–6 liters of THF, required about 1½ hr. An additional 500 ml. of THF was then distilled

TABLE I. Properties of Various Polystyrenes[a]

Property	Linear narrow distribution						Linear broad distribution (Styron 666[b])	Tetrachain narrow distribution		ASTM method
	2	5	10	9	14	8		16	17	
$\bar{M}_v \times 10^{-3}$	81	85	160	330	539	888	229	204	430	
Tensile strength at 72°F., psi ?	3100–4300[c]	5050[c]	7750[c] (380°F., 425 psi) 6650[c] (500°F., 650 psi)	7950[c] 435°F., 950 psi) 7100[c] (550°F., 725 psi)	64–8400[c] (930°F., 095 psi) 7400[c] (550°F., 700 psi)	7650[c] (550°F., 725 psi)	6600	4900	6100–7300	D-638
Tensile modulus at 73°F., psi	400,000[c]	420,000[c]					350,000	410,000	420,000	D-638
Flexural modulus at 73°F., psi	500,000	500,000	460,000	480,000	470,000	480,000	460,000	470,000	490,000	D-790
Flexural yield strength at 73°F., psi ($^1/_8 \times 1 \times 4$ in. base)	5,300	7,100	12,200	12,200	11,100–13,500	13,600	9,750			D-790
Deflection temp., °F.										
Unannealed 264 psi		191			194	188	178			D-648
66 psi	194	200	207	210	210	208	192	208	208	
Deflection temp., °F., ($^1/_8 \times ^1/_2 \times 4^3/_4$ in. base)										
Annealed 264 psi						213	192			
66 psi	203	210			215		207	218	222	
Rockwell hardness	R-120 L-95	R-120 L-95	R-122 L-95	R-122 L-98	R-121 L-98	R-121 L-98	R-119 L-97	R-121 L-97	R-121 L-98	D-785
Density, g. ice; 25°C.		1.046	1.046					1.047	1.046	
217°C.		0.966						0.966		
T_g, °C.		101						100	101	
Volatiles, %		0.92	0.18	0.21				0.04	0.14	

[a] Unless otherwise specified, test samples were compression molded. [b] Product of Dow Chemical Company. [c] Injection-molded.

into the dropping funnel and then a small excess of pure tetrachain coupler, 1,2,4,5-tetra(chloromethyl)benzene[12] was rapidly added and dissolved. The stoichiometric quantity of coupling agent was calculated according to eq. (2):

A small aliquot of the polystyryllithium was forced out under argon and terminated in methanol. This sample was used for evaluating the average chain length and molecular weight distribution of the linear precursor. The temperature of the polystyryllithium–benzene–THF solution was then raised to 40–45°C. by warming in a warm water bath and the THF-coupling agent [1,2,4,5-tetra(chloromethyl)benzene] solution was added dropwise until the characteristic red color of polystyryllithium was discharged. As discussed below, 60–70% of the theoretical coupling agent required by eq. (2) was necessary for this to occur. The polymer was recovered by precipitation in a 10-fold excess of methanol.

Polymer Characterizations

Intrinsic viscosities $[\eta]$ of the polymers were determined in cyclohexane at 34.5°C. (theta) and/or benzene at 25°C. in Ubbelohde viscometers. Kinetic energy corrections were applied. Viscosity-average molecular weights $\bar{M}_v$ of the linear polymers were computed from eq. (3)[13] for polymers with $\bar{M} \sim 25{,}000$

$$[\eta]_{\text{benzene},25^\circ\text{C.}} = 4.2 \times 10^{-4} \bar{M}_v^{0.6} \tag{3}$$

and from eqs. (4) or (5)[14] for polymers with $\bar{M}_v > 40{,}000$

$$[\eta]_{\text{benzene},25^\circ\text{C.}} = 8.5 \times 10^{-5} \bar{M}_v^{0.75} \tag{4}$$

$$[\eta]_\theta = 8.5 \times 10^{-4} \bar{M}_v^{0.5} \tag{5}$$

For tetrachain polymers, the average number of branches $\bar{P}$ and $\bar{M}_v$ was computed from eqs. (6) and (6a):[15]

$$X = [\eta]_{\theta\text{branched polymer}} / [\eta]_{\theta\text{linear polymer}} = K(\bar{P}M_1)^{1/2} g^{1/2} / KM_1^{1/2} \tag{6}$$

where

$$g = 3/\bar{P} - 2/\bar{P}^2$$

hence

$$X = g^{1/2}\bar{P}^{1/2} = \sqrt{3-(2/\bar{P})}$$

or

$$\bar{P} = 2/(3 - X^2)$$

$$\bar{M}_{v\text{(branched}} = \bar{P}\bar{M}_{v\text{(linear precursor)}} \tag{6a}$$

Molecular weights were also estimated from ultracentrifugal sedimentation constants, s_0. These experiments were performed with a Spinco Model E analytical ultracentrifuge. Cyclohexane was used as solvent, and experi-

ments were performed at 35°C. The sedimentation constants, s_0, were computed from eq. (7):

$$s_0 = \ln (Y/Y_0)/\omega^2 r \tag{7}$$

where Y_0 and Y are the distances from the center of rotation of the peak initially and at time t, and ω is the angular velocity. The value of $\bar{P}$ was also computed from eq. (8)[16]

$$s_{0_{\text{branched}}}/s_{0_{\text{linear}}} = (M_{\text{branched}}/M_{\text{linear}})^{1/2}\, g^{-1/6} \tag{8}$$

Molecular weight distributions were estimated from comparisons of the ultracentrifugal sedimentation profiles (measured in cyclohexane at 35°C.) with those of well characterized[1-3] anionic polystyrenes. In all cases it was apparent that for the polymers prepared in this program $\bar{M}_w/\bar{M}_n \leq 1.1$.

While attempts were made to carry the coupling reactions to completion, this goal was not realized experimentally (possibly because of small traces of impurities in the THF) and consequently a mixture consisting mostly of tetrachain (60–70%) and linear precursor (30–40%) polymers resulted. For example, the control chains (linear precursor) from which sample 16 was prepared had $[\eta]_{\text{benzene}} = 0.297$, $\bar{M}_v$ 54,000 [eq. (4)]. This sample also had $[\eta]\theta = 0.193$. The total polymer after the branching reaction had $[\eta]_{\text{benzene}} = 0.469$. The benzene–THF solution of this polymer mixture was slowly added to 8 volumes of acetone, and the polymer-rich phase which separated was precipitated in methanol and dried. It had $[\eta]_{\text{benzene}} = 0.570$ [eq. (4)]. A portion of this polymer was redissolved in a 50/50 (v/v) mixture of THF and benzene (ca. 10% solution w/v) and again precipitated in an 8-fold excess of acetone. The precipitate from this step had $[\eta]_{\text{benzene}} = 0.569$; $[\eta]_\theta = 0.305$. From eq. (6a) it is seen that P, the average degree of branching, = 3.86, in excellent agreement with the theoretical value of 4, and that $\bar{M}_{v(\text{actual})} = 204{,}000$ [eq.(6a)]. A portion of the acetone-soluble polymer (actually, an acetone–THF–benzene mixture) was isolated by precipitation in benzene and found to have $[\eta]_{\text{benzene}} = 0.321$; $\bar{M}_v = 59{,}000$; i.e., nearly the same as the linear precursor. These values indicate that this polymer was mostly linear precursor. The ultracentrifuge sedimentation patterns (Schlieren optics) of the tetrachain star-type polymer fraction and the original linear precursor in cyclohexane (34.5°C., theta) were very sharp and narrow, as has been found to be the case with narrow distribution polystyrenes in theta solvents. The ratio of sedimentation constants of the branched to linear polymers was 2.13, which is in excellent agreement with the theoretical value of 2.16 predicted from eq. (8). The yield of tetrachain star-type polymer fraction in this experiment was 60%.

Tetrachain star-type polymer 17 was treated in the same way. The control or precursor chains had $[\eta]_{\text{benzene}} = 0.517$; $\bar{M}_v = 111{,}000$. The gross polymer from the coupling reaction had $(\eta)_{\text{benzene}} = 0.786$. The first acetone insoluble polymer isolated had $[\eta]_{\text{benzene}} = 0.949$. A second

treatment with acetone (in exactly the same way as described above for sample 16) yielded polymer with $[\eta]_{\text{benzene}} = 0.999$. The corresponding value in cyclohexane was $[\eta]_\theta = 0.446$. The linear precursor had $[\eta]_\theta = 0.283$, consequently, the value of $\bar{P}$ for this fraction was 3.86 [eq. (6)]. The molecular weight [eq. (6a)] was 430,000. The ultracentrifuge pattern (cyclohexane, 34.5°C.) for this fraction showed only one sharp peak and the ratio of the sedimentation constant of branched to linear polymer was 2.10 (compared to 2.16, theory). The portion of polymer soluble in an acetone–benzene–THF mixture had $[\eta]_{\text{benzene}} = 0.549$; $\bar{M}_v = 120{,}000$, i.e., mostly linear precursor. The isolated yield of tetrachain star-type polymer in this case was 62%.

Volatiles Content

The percentage (by weight) of volatile components in several of the polymers was measured. Carefully weighed samples were placed in tared tubes which were in turn placed in larger tubes attached to the high vacuum line. The latter tubes were placed in a resistance furnace and heated to 220 ± 1°C. The molten polymers were heated *in vacuo* at this temperature for 2 hr. and then allowed to cool to room temperature before reweighing them. At no time were the polymers exposed to air at temperatures higher than room temperature. In all cases the volatiles content was less than 1%, and in most volatiles constituted approximately 0.2–0.3%.

Density Determinations

The densities of samples 5, 16, and 17 were determined on polymers recovered from the glass temperature experiments (see below), whereas the densities of samples 7, 9, and 10 were run on polymers recovered from experiments in which per cent volatiles were determined. In all cases a hydrostatic weighing technique was used for room temperature measurements; the relations used were:

$$\text{Vol. of polymer} = \frac{\text{wt. of sample in air} - \text{wt. of sample in water}}{\text{density of water at test temperature}}$$

$$\text{Density of polymer} = \text{wt. of polymer sample/vol. of polymer sample}$$

High temperature densities of samples 5 and 16 were measured by a pycnometer method[17] at 217°C. (boiling naphthalene bath). The volume

TABLE II

Polymer	Density	Specific volume (= 1/density), cc./g.
5	0.966	1.036
16	0.966	1.036
Reference 18		1.037

of the molten samples was determined at 217°C. and the mass was measured at room temperature. The results were as given in Table II.

Glass Transition Temperatures

The glass transition temperatures of various samples were determined by the method of Fox and Flory.[19] Approximately 2 g. of bubble-free sample was placed in the bulb of a dilatometer equipped with a mercury reservoir. The dilatometer was sealed off under high vacuum and then tipped to introduce the mercury. The assembly was heated to 150°C. and the position of the mercury in the capillary was recorded. The height of the mercury column and temperature was recorded at 10° intervals above and below T_g and at more frequent intervals near T_g. The temperature at which a pronounced change in slope occurred in the temperature–height of mercury column plot was taken as T_g (see Table I).

Physical Properties Measurements

The polymers were originally isolated as powders. These were compacted by compression molding in order to facilitate handling. It was established (by intrinsic viscosity determinations) that compression molding did not degrade the samples.

The test methods used were standard ASTM procedures as given in the last column of Table I.

Injection-molded test specimens were made by grinding the compacted sample prior to injection molding in a 1-oz. capacity Minijector machine at the temperatures shown in Table I. The mold temperature was 180°F.

Compression-molded specimens were machined to the appropriate ASTM geometry from $^1/_8 \times 7 \times 7$ in. slabs. Conditions for molding were 1 min. at 280°F. and 40,000 psi. This operation was conducted with a semipositive mold between the steam-heated platens of a hydraulic press. All physical properties of injection or compression-molded samples were measured at 73°F. and 50% R. H. unless otherwise specified in the ASTM procedure.

Tensile properties were obtained with the Instron machine following ASTM D-638 except that the jaw separation was 4 in. rather than $4^1/_2$ in. The crosshead rate was 0.2 in./min. Flexural properties were also obtained with the Instron machine according to ASTM D-790. Test specimens for these measurements were compression-molded $^1/_8 \times 1 \times 4$ in. bars. The crosshead speed and distance between supports were 0.5 in./min. and 2 in., respectively. Hardness specimens were compression molded $^1/_4 \times ^1/_2 \times 2^3/_4$ in. bars.

Viscosity versus rate of shear data was obtained with an Instron capillary rheometer. In most cases an orifice with a 0.060 in. diameter was used. In a few cases, however, this diameter was 0.030 in. Shear stress, S or τ, at the wall was computed from eq. (9):

$$S = F/4A_p(L_c/d_c) = \tau \tag{9}$$

where S is shear stress (in pounds per square inch), F is the force on the plunger (in pounds), A_p is the plunger area (0.11 in.^{2}), L_c is the length of the capillary (in inches), and d_c is the diameter of the capillary (in inches). Shear rate was computed from eq. (10):

$$D = 2VXhd_p^2/15d_c^3 = \dot{\gamma} \tag{10}$$

where D = shear rate = $\dot{\gamma}$ (per second), VXh is the speed of the crosshead (in inches per minute) and d_p is the diameter of plunger (0.375 in.). Apparent melt viscosity (in poises) was computed from eq. (11):

$$\text{Apparent melt viscosity} = (\text{shear stress/shear rate}) \times 6.9 \times 10^4 = \eta \tag{11}$$

RESULTS

The linear and branched narrow molecular weight distribution polymers used in this program (Table I) were all prepared and characterized as described in the Experimental section. The broad distribution general-purpose polystyrene was a commercial sample, Styron-666 (product of the Dow Chemical Co.). Its molecular weight was determined viscometrically here. It was assumed that for this sample $\bar{M}_w/\bar{M}_n \sim 2$.

The results of the measurements of various mechanical properties of the polymers used in this investigation are compiled in Table I. No significant

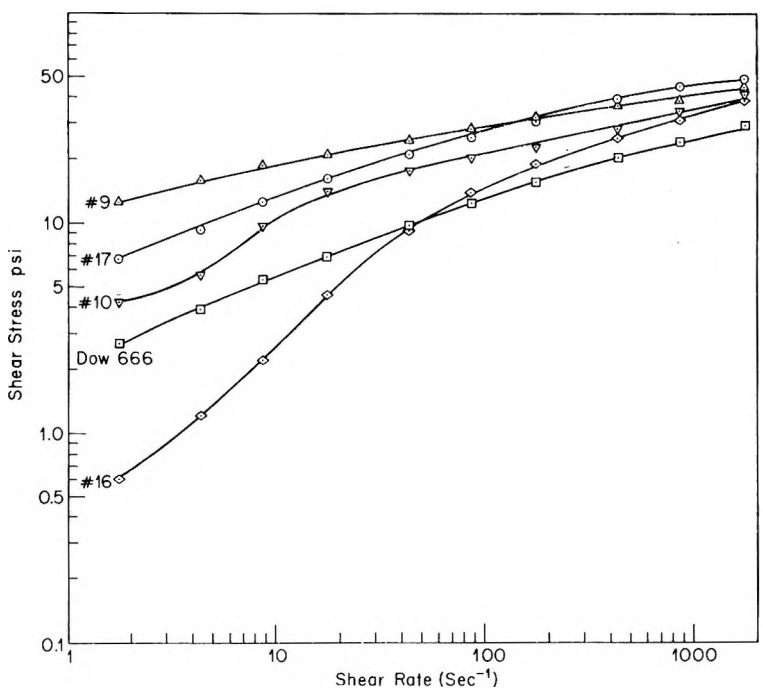

Fig. 1. Shear stress (psi) vs. shear rate (sec.$^{-1}$) for broad and linear and tetrachain branched narrow distribution polymers.

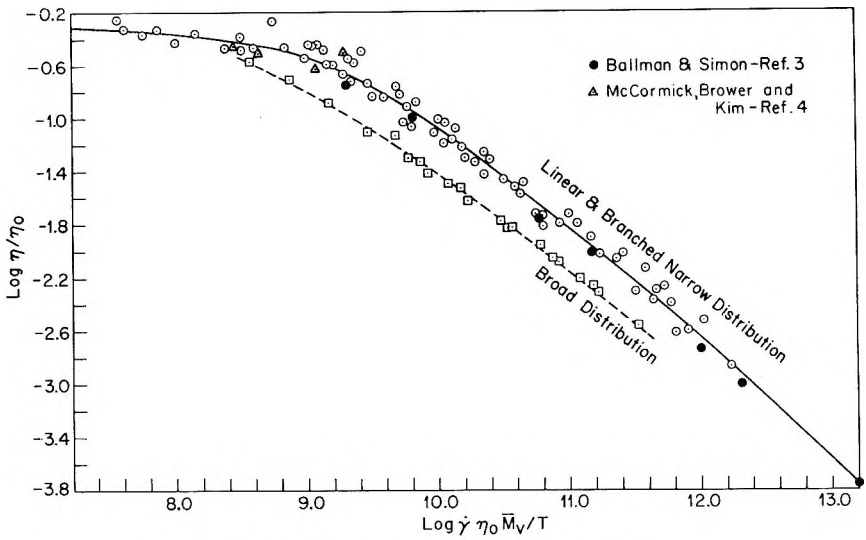

Fig. 2. "Master" η vs. $\dot{\gamma}$ curves for various polystyrenes.

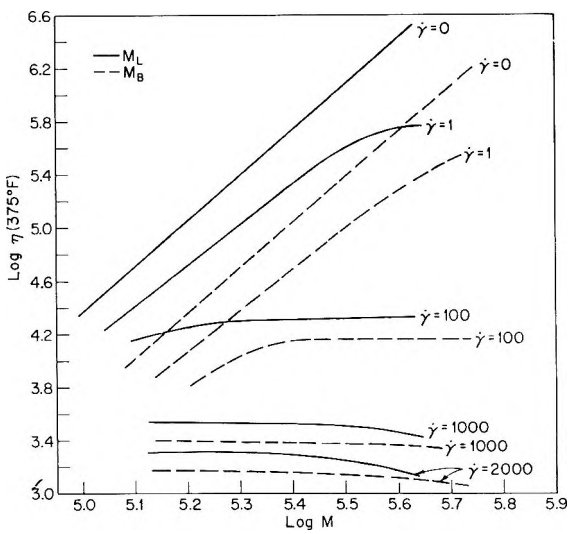

Fig. 3. Plots of log η vs. log M at varying $\dot{\gamma}$ for linear and tetrachain branched narrow distribution polystyrene.

differences between narrow and broad distribution polymers were found in their values of tensile strength, flexural modulus, deflection temperature, and hardness as long as the molecular weights of the polymers compared were in the asymptotic region of the property versus molecular weight curve. The narrow distribution polymers had higher values for flexural yield strength at a given $\bar{M}_v$ than the broad distribution polymer. The tensile modulus values of the lower molecular weight ($\bar{M}_v = 8.1 \times 10^4$

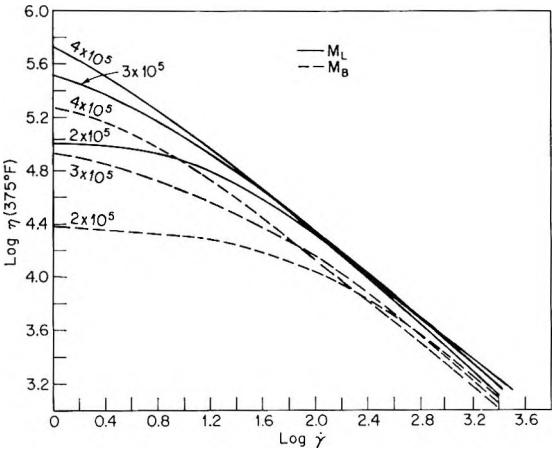

Fig. 4. Plots of log η vs. log $\dot{\gamma}$ at varying molecular weights for linear and tetrachain branched narrow distribution polystyrenes.

and 8.5×10^4) narrow distribution polymers appeared to be higher than that obtained for the higher molecular weight general-purpose polymer. However, the general-purpose material was compression-molded, whereas the lower molecular weight samples were injection-molded and, consequently, the differences may be due to orientation. On the other hand, the difference between general-purpose and narrow distribution tetrachain polymers (with regard to tensile modulus) seems to be real (compression-molded specimen used in each case).

The magnitudes of the properties of the branched polymers (Table I) were generally about the same as for the linear polymers of the same molecular weight. One notable exception was that the lower molecular weight ($\bar{M}_v = 2.04 \times 10^5$) tetrachain polymer exhibited a tensile strength which was much lower than expected. In fact, the value was about the same as obtained for a linear polymer (e.g., polymer 5, Table I) of $\sim$ $^1/_2$ the molecular weight.

Apparent values of η for different values of $\dot{\gamma}$ and temperature were obtained for the various polymers with a capillary rheometer. Typical data are presented graphically in Figures 1–4.

DISCUSSION

The results obtained from measurements of the mechanical properties of the linear polymers reported here are in general agreement with those of McCormick, Brower, and Kim,[4] and it is apparent that little practical advantage strengthwise can be derived by use of narrow rather than broad distribution polymers.

It has long been realized that the magnitude of a given mechanical property of a polymer rises rapidly with molecular weight until an asymptotic region is reached wherein further increases in M result in only very small

increases in the value of the given property. It is apparent that this is true also of the branched polymers but that for them certain properties (notably tensile strength) level off at higher molecular weights than for a linear polymer of the same molecular weight. Thus, at least in the case of tensile strength the property versus molecular weight curves of linear and branched polymers have about the same general shape, but the rate of change of the property with increasing M is less for branched than for linear polymers. Since the glass temperature (Table I) of the linear and branched narrow distribution polymers and of the broad distribution general-purpose polystyrene were the same (within experimental error), it is clear that this factor is not involved in the "curve shifts" described above. Whether the smaller size of the branched polymers, relative to linear ones of the same total molecular weight, is involved in causing the shift in the value at which the asymptotic region of the property versus molecular weight curve begins is speculative at this point.

Measurements of η as a function of $\dot{\gamma}$ were obtained for five polymers at three different temperatures. A typical plot of $\dot{\gamma}$ versus τ (shear stress) is shown in Figure 1. The tendency for the curves for different molecular weight polymers to converge at high values of $\dot{\gamma}$ has been noted before by Rudd[20] and Ballman and Simon.[5]

It was of interest and convenience to try to correlate all of the data obtained for the five polymers with measurements made at several values of $\dot{\gamma}$ and two or three temperatures into one useful curve. This was done on the basis of the molecular theory of Bueche[21] by plotting log η/η_0 versus log $\dot{\gamma}\eta_0 M/T$, where T is the absolute temperature, η_0 was computed from eq. (13), and M was the viscosity-average molecular weight, $\bar{M}_v$. This plot (Fig. 2) has several interesting features. First, the rather large number of data accumulated experimentally do indeed fall without systematic deviation about one smooth curve. Equally interesting is that the linear and branched narrow distribution polymers fall on the same curve, whereas the broad distribution linear polymer clearly does not. Similar observations as regards narrow and broad distribution linear polymers have been reported by Ballman and Simon.[5] Indeed, their data for narrow distribution linear polymers fit the curve in Figure 2 very well. Also, as observed by these workers, the Bueche-Harding "master curve"[22] does not fit Figure 2.

The melt behavior of narrow and broad distribution linear polystyrenes as a function of shear rate (or shear stress) was also studied by McCormick, Brower, and Kim.[4] While their data were treated in a different way, the results were similar (indeed, their data falls on the master curve, Fig. 2). Thus, especially at high shear stresses it was found that narrow and broad distribution polymers did not fall on one curve when η versus $\bar{M}_w$ plots were constructed and that the flow behavior of narrow distribution linear polymers was generally more Newtonian than that of broad distribution linear polymers.

In preparing Figure 2 we found it convenient to use viscosity-average

molecular weights (in the expression $\dot{\gamma}\eta_0\bar{M}_v/T$). Since these are normally rather close in magnitude to weight-average molecular weights, it appears that an average molecular weight greater than the weight average would have to be used in order to get one "master curve" to fit broad and narrow distribution polymers. As a first approximation, the z-average molecular weight,[23] $\bar{M}_z$, might be applicable.

The value of η_0 (zero shear melt viscosity) was computed from eq. (13):[24]

$$\log \eta_0 = 3.4 \log(Zg) + 2.7 \times 10^{16}/T^6 - 9.51 \qquad (13)$$

where Z, the number of chain atoms for polystyrene is given by

$$Z = M/52$$

The fact that extrapolations of experimental data to zero shear rates do not give values which particularly agree well with those computed from eq. (13) (which was based on measurements performed with "zero shear viscometers") casts some doubt on the quantitative validity of values of η obtained at low (>10 sec^{-1}) values of $\dot{\gamma}$. The deviations probably arise from frictional problems which exist in the capillary rheometer. It is believed that the values obtained in the middle region, e.g., $\dot{\gamma}$ = 10–500 sec.^{-1} are more reliable.

Since the branched narrow distribution polymers and linear narrow distribution polymers fell on the same master curve it was possible (and convenient) to choose values of $\dot{\gamma}$ and molecular weight and compute η for a linear and branched polymer of the same molecular weight and then systematically to determine (from the master curve, Figure 2) the effect of increasing $\dot{\gamma}$ on η. This kind of treatment is shown in Figure 3, wherein $\log \eta$ is plotted versus $\log M$ as a function of $\dot{\gamma}$ for both linear and branched (tetrachain) polymers. The $\dot{\gamma} = 0$ lines (slope = 3.4)[21] are shown for comparison. As shear rates are increased, the sizeable differences in η between the linear and tetrachain polymers decrease very markedly. Furthermore, η tends to become very much less dependent on molecular weight (as well as of branching) as $\dot{\gamma}$ becomes 1000 sec.^{-1}, or greater. There was, in fact, some tendency for η to be slightly less for higher molecular weight polymers at high $\dot{\gamma}$ than for lower molecular weight polymers. While it cannot be stated with certainty from this work whether or not this is an artifact caused perhaps by viscous heating of the higher polymers at higher shear rates, there is some precedence for such behavior in measurements of dynamic mechanical properties. Thus, for example, Cox, Nielsen, and Keeney[25] have shown logarithmic plots of dynamic viscosity versus reduced frequency which actually show cross-overs, i.e., η_{dynamic} for higher molecular weight polymers becomes less than for lower as frequency is increased.

Figure 4 is a logarithmic plot of η versus $\dot{\gamma}$ for a series of linear and tetrachain polymers with molecular weights of 2×10^5–4×10^5. This representation (with values again taken from Figure 2) clearly shows that large differences in η at low values of $\dot{\gamma}$ which arise from differences in molec-

ular weight and structure become nearly negligible at higher ($\dot{\gamma} = 1 \times 10^3$–$2 \times 10^3$ sec.$^{-1}$) shear rates. Once again, as in Figure 3, evidence for cross-overs or inversions with respect to molecular weight appear. It should be pointed out that similar plots of the actual data (not taken from Figure 2) were of exactly the same form.

A very notable difference between linear and branched polymers was that the former exhibited "melt fracture" upon extrusion whereas the latter did not. A rationalization of this difference is beyond the scope of the present work, but clearly the basis for this behavior is not due to apparent viscosity differences at relative high ($\dot{\gamma} \sim 1000$ sec.$^{-1}$) shear rates.

Thus, it has been found in a comparison of linear and tetrachain star-type branched polystyrene of narrow molecular weight distribution that most of the mechanical properties are very similar in the asymptotic region (i.e., the region in which the magnitude of the property in question changes only negligibly with further increases of molecular weight) although the molecular weight at which this plateau is reached begins at higher molecular weights for branched polystyrenes than for linear ones. At relatively high values of $\dot{\gamma}$, η is not very sensitive to molecular weight or extent of branching. However, η_0/η is very sensitive to both molecular weight and the extent of branching at high $\dot{\gamma}$ and there is less departure from Newtonian flow for lower molecular weight linear polystyrene and for branched polystyrenes. As described above, one consequence of this is that the branched polystyrenes were less prone to melt fracture during extrusion than linear polystyrenes of the same or even greater total molecular weights.

We are indebted to Drs. T. G Fox and H. Markovitz for many helpful discussions concerning this work. The assistance of Mr. R. E. Kerwin (ultracentrifuge measurements) and Miss E. Frommell (intrinsic viscosities) is also acknowledged. The assistance and advice of Mrs. S.-P. S. Yen was of great aid during the syntheses.

References

1. Wenger, F., and S.-P. S. Yen, *Makromol. Chem.*, **43**, 1 (1961).
2. Worsfold, D. J., and S. Bywater, *Can J. Chem.*, **38**, 1891 (1960).
3. Wyman, D. P., and T. Altares, Jr., *Makromol. Chem.*, **72**, 68 (1964).
4. McCormick, H. W., F. M. Brower, and L. Kin, *J. Polymer Sci.*, **39**, 87 (1959).
5. Ballman, R. L., and R. H. M. Simon, paper presented at the 145th meeting American Chemical Society, Division of Coatings and Plastics Chemistry, New York, Sept. 1963; *Preprints*, **23**, No. 2, 26 (1963).
6. Porter, R. S., and J. F. Johnson, paper presented at the 145th meeting, American Chemical Society, Division of Coatings and Plastics Chemistry, New York, Sept. 1963; *Preprints*, **23**, No. 2, 41 (1963).
7. Morton, M., T. E. Helminiak, S. D. Gadkary, and F. Bueche, *Conference on High Temperature Polymer and Fluid Research*, Dayton, Ohio, May 1962, Vol. 1, p. 165.
8. Wenger, F., and S.-P. S. Yen, *Preprints, American Chemical Society, Polymer Division*, **3**, No. 1, 162 (March 1962).
9. Yen, S.-P. S., *Preprints, American Chemical Society, Polymer Division*, **4**, No. 2, 332 (Sept. 1963).

10. Wyman, D. P., T. Altares, Jr., V. R. Allen, and K. Meyersen, to be published.
11. Allen, V. R., and T. G Fox, Technical Report No. 7, Office of Naval Research, Contract Nonr 2693(00), Sept. 1961–Feb. 1962.
12. Kulka, M., *Can. J. Res.*, **23B**, 106 (1945).
13. Pepper, D. C., *Sci. Proc. Roy. Dublin Soc.*, **25**, 239 (1951).
14. Altares, T., Jr., D. P. Wyman and V. R. Allen, *J. Polymer Sci.*, **A2**, 4533 (1964).
15. Zimm, B. H., and R. W. Kilb, *J. Polymer Sci.*, **37**, 19 (1959).
16. Zimm, B. H., and R. W. Kilb, *J. Polymer Sci.*, **17**, 1301 (1949).
17. Flory, P. J., *J. Am. Chem. Soc.*, **62**, 1057 (1940).
18. Fox, T. G, and P. J. Flory, *J. Appl. Phys.*, **21**, 581 (1950).
19. Fox, T. G, and P. J. Flory, *J. Polymer Sci.*, **14**, 315 (1954), and refs. therein.
20. Rudd, J F., *J. Polymer Sci.*, **60**, 57 (1962).
21. Bueche, F., *J. Chem. Phys.*, **22**, 1570 (1962).
22. Bueche, F., and S. W. Harding, *J. Polymer Sci.*, **32**, 177 (1958).
23. Flory, P. J., *Principles of Polymer Chemistry*, Cornell Univ. Press, Ithaca, N. Y., 1953, p. 307.
24. Fox, T. G, S. Gratch, and S. Loshaek, in *Rheology*, F. R. Eirich, Ed., Academic Press, New York, 1956, p. 456; T. G Fox, and V. R. Allen, *J. Chem. Phys., in press.*
25. Cox, W. P., L. E. Nielsen, and R. Kenny, *J. Polymer Sci.*, **26**, 365 (1957).

Résumé

Les propriétés de force et d'écoulement de polystyrènes de distribution étroite ont été étudiées en fonction du poids moléculaire et de la ramification (molécules du type étoile à quatre branches). La plupart des propriétés mécaniques des polystyrènes linéaires et ramifiés à distribution étroite sont en général les mêmes que celles d'un polystyrène de large distribution. Pour les polymères linéaires de distribution étroite, la valeur d'une propriété donnée augmente rapidement avec le poids moléculaire jusqu'à $M = 1.6 \times 10^5$. Après cela la grandeur de la propriété donnée augmente très lentement pour de grandes augmentations de M et tend asymptotiquement vers un maximum. On trouve la même chose pour les polymères ramifiés à l'exception de quelques propriétés, comme la force de tension, qui tendent à se niveler pour des valeurs plus grandes du poids moléculaire que dans le cas des polymères linéaires correspondants. L'étude à l'état fondu de la viscosité apparente, η, faite au moyen d'un rhéomètre capillaire, montre que pour de faibles vitesses de cisaillement, $\dot{\gamma} < 10\ \text{sec}^{-1}$, les polymères ramifiés présentent des valeurs apparentes beaucoup plus basses pour η que les polymères linéaires de même poids moléculaire total. À des vitesses de cisaillement élevées, $\gamma \sim 2000\ \text{sec}^{-1}$, cette différence disparaît et η tend vers une valeur constante indépendante de M (à partir de $1.5\text{–}4.5 \times 10^5$) et de la ramification. Les résultats de la viscosité a l'état fondu pour les polymères linéaires aussi bien que pour les polymères ramifiés de distribution étroite, portés graphiquement sous forme de viscosités réduites en fonction de $\dot{\gamma}$ (suivant Buche), tombent sur une courbe maîtresse.

Zusammenfassung

Festigkeit und Fliesseigenschaften von Polystyrolen mit enger Verteilung wurde als Funktion des Molekulargewichts und der Verzweigung (Vierkettensternmoleküle) untersucht. Die meisten mechanischen Eigenschaften der linearen und verzweigten Polystyrole mit enger Verteilung sind im wesentlichen die gleichen wie diejenigen der allgemein verwendeten Polystyrole mit breiter Verteilung. Bei den eng verteilten linearen Polymeren nehmen die Werte einer gegebenen Eigenschaft bis zu $M = 1{,}6.10^5$ rasch zu. Danach steigen die Werte der Eigenschaft für ziemlich grosse Zunahme in M nur schwach an und erreichen asymptotisch ein Maximum. Das Gleiche gilt für verzweigte Polymere mit der Ausnahme, dass gewisse Eigenschaften, wie Zugfestigkeit erst bei höheren Molekulargewichten als für die entsprechenden linearen Polymeren konstant wurden. Eine Untersuchung der scheinbaren Schmelzviskosität η mit einem Kapillar-

rheometer zeigte, dass bei kleiner Schubgeschwindigkeit, $\dot{\gamma} < 10$ sec^{-1}, das verzweigte Polymere viel niedrigere scheinbare Werte von η aufwiesen als lineare Polymere mit dem gleichen Gesamtmolekulargewicht. Bei hoher Schubgeschwindigkeit, $\dot{\gamma} \sim 2000$ sec^{-1}, verschwanden diese Unterschiede im wesentlichen, und η näherte sich einem konstanten, von M (von 1,5 bis 4,5.10^5) und der Verzweigung unabhängigen Wert. Bei Auftragung der Schmelzviskositätsergebnisse für lineare und verzweighte eng verteilte Polymere als reduzierte Viskosität gegen eine Funktion von $\dot{\gamma}$ (wie von Bueche vorgeschlagen wurde), fielen diese auf eine Masterkurve.

Received June 10, 1964
Revised July 13, 1964

JOURNAL OF POLYMER SCIENCE: PART A VOL. 3, PP. 697–701 (1965)

Sound Velocity in Polyethylene at Ultrasonic Frequencies

A. LEVENE, W. J. PULLEN, and J. ROBERTS, *Ministry of Aviation, Explosives Research & Development Establishment, Waltham Abbey, Essex, England*

Synopsis

An ultrasonic interferometer was used to measure the sound velocity at 1.45 Mcycle/sec. and 20°C. in small disk samples of polyethylene. A plot of sound velocity versus density does not conclusively show that the relationship is linear or cubic. The velocities were converted to dynamic Young's moduli by using Poisson's ratios given by Schuyer. Comparison of these results with the lower frequency moduli of Davidse, Waterman, and Westerdijk indicates that the test conditions may well be close to those pertaining when the viscoelastic effects have been more or less eliminated.

Introduction

The difficulties that can arise when comparing two sets of dynamic moduli for nominally the same polymers are well illustrated by considering the ultrasonic moduli for polyethylenes given by Schuyer[1] and the lower frequency values given by Davidse, Waterman, and Westerdijk.[2]

The former results were obtained by measuring sound velocity by means of a pulsation technique,[3] the test frequency and temperature being 2 Mcycle/sec. and 20°C., respectively. The polyethylenes tested were Alkathene 2, Poly-Eth, Super Dylan, and Marlex 50. The results are approximately described by curve *I* in Figure 1. The moduli of Davidse et al. were obtained by measuring sound velocity by a technique in which longitudinal oscillations are generated electrodynamically in a bar specimen. The test frequency depends on the stiffness of the material so there is a frequency range of 2.7–10.9 Kcycle/sec. The experiments, carried out at room temperature, gave results approximately described by curve *II* of Figure 1. The materials tested were various grades of low density I.C.I. polyethylenes, Eastman Tenite, Zeigler, and Marlex 50.

General experience would suggest that curve *I* should lie above curve *II* for all densities. However the reverse is the case for densities $\rho > 0.945$ g./cm.^{3}, although both investigations use Marlex 50 in this high density range.

With such experimental evidence it is difficult to initiate theoretical studies. In order to clarify the position it was decided to make further measurements of sound velocity by means of the ultrasonic interferometer

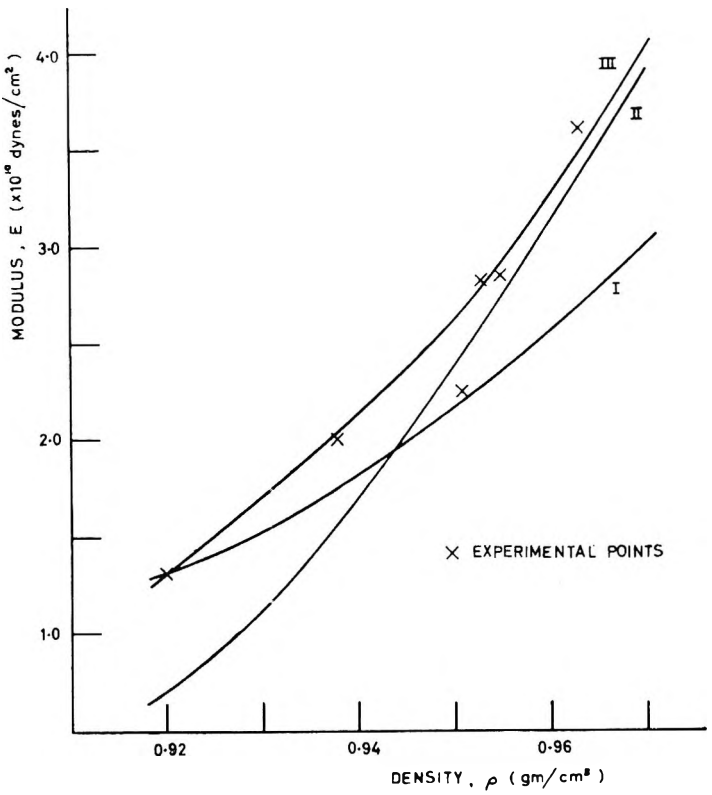

Fig. 1. Dynamic Young's modulus of polyethylene.

which is being used in this laboratory[4] for the study of polymer mechanical properties at ultrasonic frequencies.

The Interferometer

The general design of the apparatus used[4] is due to Hubbard and Loomis[5] A piezoelectric crystal, mounted at the base of a vertical cylindrical chamber containing a silicone oil M.S.550, is energized by a constant frequency source which is indirectly coupled to it. Loose coupling is used to minimize the effects of a variable load on the source frequency. At the top of the chamber is a steel reflecting plate which can be moved parallel to the axis of the chamber by means of a micrometer screw.

Ultrasonic waves produced by the crystal in the oil column form a standing wave system in the presence of the reflector plate. When the path length between the crystal and the reflector is an integral number of quarter wavelengths there is a voltage maximum, or minimum, indicated on a valve voltmeter connected in parallel with the crystal. This effect is due to the changes in the loading on the crystal.

The movement of the reflector plate is measured by means of a dial indicator gauge so that as the plate is moved the positions of the nodal

and antinodal planes can be plotted. This information together with the measured exciting frequency enables the wave velocity in the oil to be calculated.

A thin disk-shaped specimen of the solid polymer introduced with its plane surface perpendicular to the axis of the oil column, causes an effective change in the path length and hence a shift in the positions of the noda and antinodal planes. The wave velocity in the solid is calculated from the measurements of this shift and the wave velocity in the oil as below.

Theory

According to Klein and Herschberger,[6] a specimen of thickness d inserted in a liquid column gives a shift D of the nodal and antinodal planes, away from the crystal, where:

$$D = d(U - 1)/U \tag{1}$$

in which U is the ratio V_S/V_L, V_S and V_L being the velocities of sound in the solid and liquid, respectively. The compressibility K can be calculated from eq. (2):

$$K = 3(1 - \nu)/\rho(1 + \nu)V_S^2 \tag{2}$$

if Poisson's ratio ν is known. The corresponding Young's modulus E is calculated from eq. (3):

$$E = 3K(1 - 2\nu) \tag{3}$$

Experimental Results

The six different types of commercially available polyethylene tested were Alkathene 2, YHG31, Hilex, Rigidex, Ziegler, and Marlex 50 having densities of 0.920, 0.938, 0.951, 0.953, 0.955, and 0.963 g./cm.^{3}, respectively. The experiments were carried out at room temperature, nominally 20°C. The test samples were disks, punched from sheet material, with diameters and thicknesses of the order of 2.24 and 0.15 cm.

The crystal used in the present experiments set the exciting frequency at 1.45 Mcycle/sec. The sound velocity in the oil at 20°C. was found to be $V_L = 1256$ m./sec.

The measured sound velocities V_S given in Table I are average values as the results for a material can vary by as much as $V_S \pm 2$–4%. The Poisson's ratio required to calculate compressibilities from these velocities were obtained from the empirical equation

$$\nu = 1.143 - 0.757\rho \tag{4}$$

which is found to describe results given by Schuyer.[1] The ratios given by eq. (4) are within the expected range suggested by the assumptions that Poisson's ratio of a polyethylene for which $\rho \sim 0.85$ g./cm.^{3} is of the order $\nu = 0.49$, as for soft rubber,[7] and the ratio for a polyethylene where $\rho \sim 1$ g./cm.^{3} is of the order $\nu = 0.39$, as for a hard rubber.[7]

The required Young's moduli are listed in Table I, and plotted as the points shown in Figure 1. Curve *III* is taken to represent the general trend indicated by the results. Hilex with a density of 0.951 g./cm.^{3} is the one exception to this trend.

TABLE I
Results for Polyethylene

Density of material ρ, g./cm.^{3}	Velocity of sound V_S, m./sec.	Compressibility K, cm.^{2}/dyne $\times 10^{11}$	Young's modulus E, dyne/cm.^{2} $\times 10^{-10}$
0.920	2237	2.51	1.31
0.938	2477	2.10	2.00
0.951	2470	2.14	2.24
0.953	2742	1.71	2.81
0.955	2777	1.69	2.84
0.963	2951	1.50	3.60

Discussion

It was suggested by Davidse et al.[2] that the variation of the longitudinal wave velocity with density is a linear function. On the other hand, Schuyer[1] suggests a cubic relation. If the result for Hilex is omitted the present sound velocities can be equally well represented by either type of function. Thus it does not appear that such an approach is at all conclusive.

Plotting the results as Young's moduli (Fig. 1) does show, as might be expected, that the general trend is above the lower frequency values of curve *II*. Curve *II* only approaches curve *III* for the materials of higher density. From this it would appear that, in the main, viscoelastic effects may well have been largely eliminated at 1.45 Mcycle/sec. The fact that the modulus for Hilex lies close to curve *I* suggests that this material may be of a similar type to those used by Schuyer. However, at present, there is no completely satisfactory explanation for this result.

The unexpected divergence of curve *I* from curves *II* and *III*, particularly for $\rho > 0.945$ g./cm.^{3}, must be considered in conjunction with the fact that in all three investigations the high density material Marlex 50 was used. Perhaps the effect is related to the conditioning, or lack of conditioning, of samples before an experiment. Thus for curve *I* the samples were heated *in vacuo* for 1 hr. at a temperature slightly below the softening point, cooled slowly, and then ground plane parallel to 5 mm. thickness. Samples for curve *III* were not subjected to any such preliminary processing.

Poisson's ratios calculated from eq. (4) assume that the materials have properties similar to those used by Schuyer. Comparison of moduli as above shows that this is not the case, or that with high density material Schuyer's method tends to underestimate modulus. If it is the latter then the values of ν given by eq. (4) seem to be of the correct order because they

are calculated not from an individual velocity but from the ratio of the longitudinal and transverse wave velocities.

Conclusions

The experiments show that the ultrasonic interferometer can be a convenient method for the measurement of the ultrasonic sound velocity in disk samples of polymer materials.

It has been shown that no satisfactory conclusions can be drawn from empirical equations describing sound velocity versus density results for polyethylene.

A comparison of the Young's moduli obtained with those of Davidse et al. suggests that curve *III* of Figure 1 may well be close to the curve giving the moduli when viscoelastic effects have been more or less eliminated.

Further experiments on batches of samples each with a particular type of pre-experimental treatment are clearly required.

References

1. Schuyer, J., *J. Polymer Sci.*, **36**, 475 (1959).
2. Davidse, P. D., H. I. Waterman, and J. B. Westerdijk, *J. Polymer Sci.*, **59**, 389 (1962).
3. Schuyer, J., H. Dijkstra, and D. W. van Krevelen, *Fuel*, **33**, 409 (1954).
4. Pullen, W. J., J. Roberts, and T. E. Whall, *Polymer*, **5**, 471 (1964).
5. Hubbard, J. C., and A. L. Loomis, *Phil. Mag.*, **5**, 1177 (1928).
6. Klein, E., and W. D. Hershberger, *Phys. Rev.*, **37**, 760 (1931).
7. Schmidt, A. X., and C. A. Marlies, *Principles of High-Polymer Theory and Practice*, McGraw-Hill, New York, 1948.

Résumé

On a utilisé un interferomètre à ultrason pour mesurer la vitesse du son à 1.45 Mc/sec et 20°C, dans de petits échantillons circulaires en polyéthylène. L'établissement d'un graphique vitesse du son—densité ne permet pas de conclure à une relation linéaire ou cubique. Les vitesses sont converties en module dynamique de Young au moyen du rapport de Poisson donné par Schuyer. La comparaison de ces données avec les modules de Davidse, Waterman, et Westerdijk relatifs à une fréquence plus basse, semble indiquer que les conditions réalisées dans nos expériences correspondent à une élimination plus ou moins poussée des effets viscoélastiques.

Zusammenfassung

Ein Ultraschallinterferometer wird zur Messung der Schallgeschwindigkeit bei 1,45 MHz und 20°C in kleinen scheibenförmigen Polyäthylenproben benützt. Eine Auftragung der Schallgeschwindigkeit gegen die Dichte zeigt nicht eindeutig, ob die Beziehung linear oder kubisch ist. Mit dem von Schuyer angegebenen Poisson-Verhältnis werden die Geschwindigkeiten in dynamische Young-Moduln umgewandelt. Ein Vergleich der Ergebnisse mit den Moduln bei niedriger Frequenz von Davidse, Waterman, und Westerdijk zeigen, dass die Testbedingungen eng bei denjenigen liegen, bei welchen die viskoelastischen Effekte mehr oder weniger eliminiert wurden.

Received June 11, 1964

JOURNAL OF POLYMER SCIENCE: PART A VOL. 3, PP. 703–710 (1965)

Kinetics of Alternating Copolymerization*

M. G. BALDWIN, *Rohm & Haas Company,*
Redstone Arsenal Research Division, Huntsville, Alabama

Synopsis

The rates of copolymerization of three monomer pairs which form only alternating copolymers have been studied. The monomer pairs were vinyl isobutyl ether–diethyl fumarate, vinyl isobutyl ether–maleic anhydride, and 1-octene–maleic anhydride. It was shown that the maximum copolymerization rate occurs at $[M_1]/[M_2]$ ratios which differ significantly from unity, for a fixed total monomer concentration ($[M_1] + [M_2]$). An equation for the rate of copolymerization for alternating systems is given and the results are discussed in terms of the equation.

INTRODUCTION

Certain monomer pairs copolymerize readily while the individual monomers do not polymerize alone at appreciable rates under the same conditions. The copolymers which are formed consist of alternating units of the two monomers, regardless of the initial monomer concentration ratio.[1,2] Few kinetic data for copolymerization of systems of this type have been published, although the kinetics of systems which contain one monomer which can undergo homopolymerization (styrene–maleic anhydride, for example) have been studied.[3–5]

This paper describes a dilatometric study of the rates of copolymerization of three alternating pairs for different starting monomer ratios. The monomer pairs that were studied were diethyl fumarate–vinyl isobutyl ether, maleic anhydride–vinyl isobutyl ether, and maleic anhydride–1-octene.

Before describing the experimental results it will be well to define precisely what is meant by the copolymerization rate as used in this paper. The rate R_p is simply the rate of formation of polymer,

$$R_p = d(\text{polymer})/dt = -d([M_1] + [M_2])/dt$$

where $[M_1]$ and $[M_2]$ are the monomer concentrations. It should be borne in mind that in alternating systems such as these the polymerization proceeds only until the monomer in the lesser amount is completely consumed. There will thus be unreacted monomer at the completion of the reaction, a situation which is different from the usual copolymerization system.

* This work was performed under the sponsorship of the U. S. Army under Contract No. DA-01-021 ORD-11878.

EXPERIMENTAL

Materials

Vinyl isobutyl ether, diethyl fumarate, and solvents were all taken from commercial sources and distilled through a 40-plate column before use. Maleic anhydride was recrystallized from a 1:1 carbon tetrachloride–chloroform mixture.

Dilatometric Procedure

The dilatometer and technique used in polymerization rate determinations have been described previously.[6] In calculating copolymerization rates from the shrinkage data that were obtained in the dilatometric studies, the assumption was made that the amount of polymer formed at a given time is proportional to the polymerization shrinkage that has occurred at that time. The total shrinkage per mole of polymer formed was obtained from polymerizations which were carried to completion in the dilatometer. Polymerization shrinkages (as cubic centimeters per mole of M_1—M_2 bonds formed) for the systems studied here were: diethyl fumarate–vinyl isobutyl ether, 20.6 cc./mole; maleic anhydride–vinyl isobutyl ether, 21.6 cc./mole; and maleic anhydride–octene, 22.7 cc./mole.

RESULTS

Vinyl Isobutyl Ether (VIBE)–Diethyl Fumarate (DEF)

Table I shows the results of VIBE–DEF studies. The copolymerization rates were determined from the slopes of the initial portions of the polymerization–time curves.

The experiments described in Table I were run at 60°C., with benzene as the solvent and with an azobisisobutyronitrile (AIBN) concentration

TABLE I
Vinyl Isobutyl Ether–Diethyl Fumarate Copolymerization in Benzene at 60°C. at [AIBN] = 0.0122 mole/l.

[DEF], mole/l.	[VIBE], mole/l.	$\frac{[VIBE]}{[DEF]}$	Copolymerization rate $\frac{-d([M_1] + [M_2])}{dt}$, mole/l./sec.
5.0	0	—	0
2.90	0.30	0.10	0.22
2.60	0.67	0.25	0.27
2.03	1.42	0.70	0.67
1.70	1.90	1.12	0.76
0.60	2.61	4.35	4.1
0.28	3.12	11.1	3.9
0	5.0	—	0

of 0.0122 mole/l. It should be noted that in this series of runs, and in those described below, the ratio of starting monomer concentration $[M_1]/[M_2]$ was varied over a wide range, but the total starting monomer concentration ($[M_1] + [M_2]$) was held approximately constant.

The data in Table I are not sufficient to define the [VIBE]/[DEF] ratio for which the rate is a maximum, but it appears to lie in the range of [VIBE]/[DEF] = 4–10 and is certainly greater than unity.

Maleic Anhydride–Vinyl Isobutyl Ether (MA–VIBE)

Table II contains the data for the MA–VIBE copolymerizations which were run at 60°C. with [AIBN] = 6.6×10^{-3} mole/l. Ethyl acetate was used as the solvent, in which both monomers and polymer were soluble. It is noted that the polymerization rate maximum occurs at [VIBE]/[MA] = ca. 4, and drops off rapidly at ratios less than unity, similar to the behavior of the DEF–VIBE system.

TABLE II
Copolymerization of Maleic Anhydride and Vinyl Isobutyl Ether in Ethyl Acetate at 60°C. at [AIBN] = 6.6×10^{-3} mole/l.

[MA], mole/l.	[VIBE], mole/l.	$\frac{[VIBE]}{[MA]}$	Copolymerization rate $\frac{d([M_1] + [M_2])}{dt}$, mole/l./sec. $\times 10^4$
0.0	5.0	—	0.0
0.5	4.5	9.0	3.4
1.0	4.0	4.0	4.2
1.5	3.5	2.3	3.3
2.0	3.0	1.5	3.0
2.5	2.5	1.0	3.0
3.0	2.0	0.67	2.1
3.5	1.5	0.43	1.3
4.0	1.0	0.25	0.78
4.5	0.5	0.11	0.24
5.0	0.0	—	0.00

Maleic Anhydride–1-Octene

Table III shows the polymerization results from the maleic anhydride–1-octene system. The polymerizations were run at 60°C. in ethyl acetate solution with AIBN concentration of 0.0310 mole/l. The monomers and polymer were soluble in the medium. The polymerization rate was much lower than in the other two systems, and the rate maximum occurred at a [octene]/[MA] ratio somewhat less than unity.

It was noted that the polymerization curves from which the rate data were taken appeared to be linear over a wide range of per cent reaction,

TABLE III
Copolymerization of Maleic Anhydride and 1-Octene at 60°C. in Ethyl Acetate at [AIBN] = 0.031 mole/l.

[MA], mole/l.	[1-Octene], mole/l.	$\frac{[1\text{-Octene}]}{[MA]}$	Copolymerization rate, mole/l./sec. $\times 10^4$
0	5.0	—	0.0
0.5	4.5	9.0	1.6
1.0	4.0	4.0	3.2
1.5	3.5	2.3	3.5
2.0	3.0	1.5	4.2
2.5	2.5	1.0	4.8
3.0	2.0	0.67	5.1
3.5	1.5	0.43	4.8
4.0	1.0	0.25	2.3
4.5	0.5	0.11	1.3
5.0	0.0	—	0.0

especially in the VIBE–DEF and VIBE–MA systems. This phenomenon was investigated in more detail by carrying out experiments so designed that the reactions could be closely followed to completion. Results are shown in Figure 1 for the VIBE–DEF and VIBE–MA systems and in Figure 2 for MA–1-octene.

In the MA–1-octene run for Figure 2, benzoyl peroxide was substituted for AIBN. This was necessary for dilatometric observation of the entire reaction, since nitrogen evolution from the AIBN at the high concentrations that were necessary to get a suitably high copolymerization rate gave rise to bubbles before polymerization was complete, thus precluding valid dilatometric data.

The almost constant polymerization rate and abrupt cessation of reaction

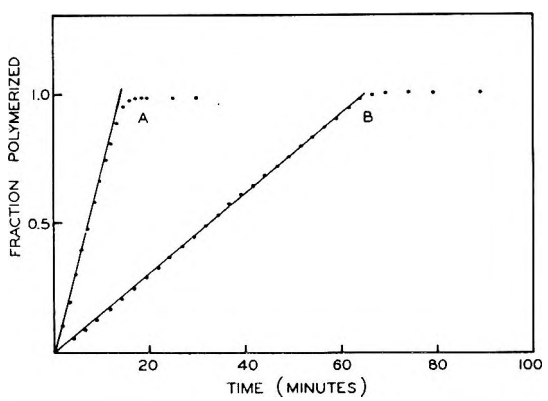

Fig. 1. Alternating copolymerizations at 60°C.: (*A*) vinyl isobutyl ether 1.69 mole/l.; maleic anhydride 0.308 mole/l., AIBN, 0.0158 mole/l., in ethyl acetate; (*B*) vinyl isobutyl ether 9.50 mole/l., diethyl fumarate 0.379 mole/l., AIBN 0.0136 mole/l.

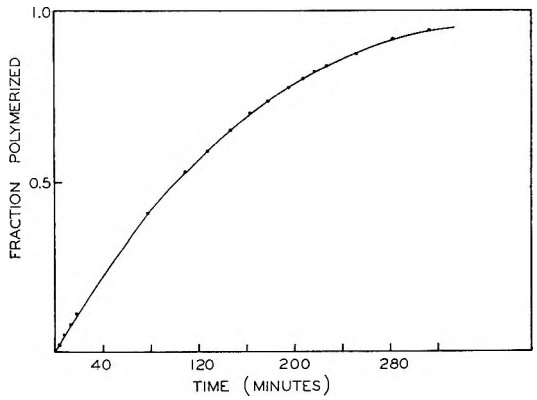

Fig. 2. Alternating copolymerization at 60°C.; 1-octene 4.44 mole/l., maleic anhydride 0.98 mole/l., benzoyl peroxide 0.13 mole/l., in ethyl acetate.

are apparent in the VIBE–DEF and VIBE–MA systems, while the 1-octene–MA system does not exhibit a significant linear portion. The unusual apparent zero-order kinetics approached in the curves in Figure 1 must be considered in any discussion of the mechanism of the reaction.

DISCUSSION

The kinetic scheme shown in eqs. (1)–(8) (neglecting transfer reactions) describes the copolymerization of monomer systems which form only alternating copolymer.

Initiator Decomposition:

$$\mathrm{I} \xrightarrow{k_d} 2\mathrm{R}\cdot \tag{1}$$

Chain Initiation:

$$\mathrm{R}\cdot + \mathrm{M}_1 \xrightarrow{k_{i_1}} \mathrm{M}_1\cdot \tag{2}$$

$$\mathrm{R}\cdot + \mathrm{M}_2 \xrightarrow{k_{i_2}} \mathrm{M}_2\cdot \tag{3}$$

Chain Propagation ($-\mathrm{M}_2\mathrm{M}_1\cdot$ and $-\mathrm{M}_1\mathrm{M}_2\cdot$ refer to growing chain radicals):

$$-\mathrm{M}_2\mathrm{M}_1\cdot + \mathrm{M}_2 \xrightarrow{k_{21}} -\mathrm{M}_1\mathrm{M}_2\cdot \tag{4}$$

$$-\mathrm{M}_1\mathrm{M}_2\cdot + \mathrm{M}_1 \xrightarrow{k_{12}} -\mathrm{M}_1\mathrm{M}_2\cdot \tag{5}$$

Chain Termination:

$$-\mathrm{M}_2\mathrm{M}_1\cdot + -\mathrm{M}_2\mathrm{M}_1\cdot \xrightarrow{k_{t_{11}}} \text{polymer} \tag{6}$$

$$-\mathrm{M}_2\mathrm{M}_1\cdot + -\mathrm{M}_1\mathrm{M}_2\cdot \xrightarrow{k_{t_{12}}} \text{polymer} \tag{7}$$

$$-\mathrm{M}_1\mathrm{M}_2\cdot + -\mathrm{M}_1\mathrm{M}_2\cdot \xrightarrow{k_{t_{22}}} \text{polymer} \tag{8}$$

It is noted that this scheme differs from that for usual copolymer systems in that the propagation rate constants k_{11} and k_{22} are considered to have the value zero.

These equations may be used to derive an expression for the overall rate of copolymerization in a manner analogous to the derivation of the general copolymerization rate equations.[7] The chain initiation step is neglected in the treatment, since it is unimportant for long kinetic chain processes such as those studied here. The expression obtained is

$$R_p = \frac{2k_{12}k_{21}[M_1][M_2]R_i^{1/2}}{(2k_{t_{11}}k_{21}^2[M_1]^2 + 2k_{t_{12}}^2[M_1][M_2] + 2k_{t_{22}}k_{12}^2[M_2]^2)^{1/2}} \quad (9)$$

which is seen to differ from the general expression only in the absence of terms containing k_{11} and k_{22}.

Two important characteristics of the alternating systems studied here that were considered in light of eq. (9) are: (*1*) the copolymerization rate maxima occur at monomer concentration ratios other than unity (for given fixed total monomer concentrations); (*2*) the apparent kinetic order of the reaction approaches zero in M_2 when M_1 is present in large excess in the VIBE(M_1)–DEF(M_2) and VIBE(M_1)–MA(M_2) systems, but not in the 1-octene–MA system.

Equation (9) contains five constants, none of which are known. Not only are they not known individually, there are no ratios of the constants which are known. Thus quantitative description of the results is not possible, but certain qualitative conclusions can be drawn.

It can be stated, for instance, that cross termination ($k_{t_{12}}$) is not the only operative termination mechanism in any of the three systems. If only cross termination occurred (i.e., if $k_{t_{11}}$ and $k_{t_{22}}$ were zero) the equation would be symmetrical with respect to $[M_1]$ and $[M_2]$, for ($[M_1] + [M_2]$) = constant, and the maximum rate would occur when $[M_1]/[M_2] = 1$.

The data presented here tell nothing of the relative values of the rate constants for cross termination ($k_{t_{12}}$) compared to termination by like radicals ($k_{t_{11}}$ and $k_{t_{22}}$). Presumably, cross termination is favored because of polarity effects, but the situation could nevertheless exist in which most termination would be by coupling of like radicals. It is postulated that this occurs in systems 1 and 2 and gives rise to the linear rate plots shown in Figure 1. If in these systems the rate constants k_{12} are much greater than k_{21}, the reaction shown in eq. (10) would occur very rapidly:

$$\text{—}M_2M_1\cdot + M_2 \xrightarrow{k_{12}} \text{—}M_1M_2\cdot \quad (10)$$

and the concentration of —$M_2M_1\cdot$ radicals would be very small compared to —$M_1M_2\cdot$. There would thus be little opportunity for cross termination to occur.

An extreme case of such a situation is described by eq. (9) if the first

two terms in the denominator are negligible with respect to the third term. In that case eq. (9) reduces to

$$R_p = 2k_{12}k_{21}[M_1][M_2]R_i^{1/2}/(2k_{t_{22}}k_{12}^2[M_2]^2)^{1/2}$$
$$= 2k_{21}[M_1]R_i^{1/2}/(2k_{t_{22}})^{1/2} \quad (11)$$

Equation (11) predicts that for a constant rate of initiation, the rate of polymerization would be independent of $[M_2]$, and that for an excess of $[M_1]$ would be essentially constant. This was closely approached in the experiments described in Figure 1.

If eq. (11) accurately describes the situation, the ratio $k_{21}^2/k_{t_{22}}$ can be calculated for systems which copolymerize at a rate independent of $[M_2]$ over a significant range in $[M_2]$. This has been done for the VIBE–DEF and VIBE–MA systems. The values that were obtained are given in Table IV.

TABLE IV

System	$k_{12}^2/k_{t_{22}}$
VIBE(M_1)–DEF(M_2)	1.8×10^{-3}
VIBE(M_1)–MA(M_2)	140×10^{-3}

The value for R_i for AIBN at 60°C. that was used in the calculation for Table IV was 1.20×10^{-5}. These values are comparable to corresponding values k_p^2/k_t for common monomers at 63°C., several of which were calculated from k_p and k_t values and are listed in Table V.[8]

TABLE V

Monomer	$k_p^2/k_t \times 10^3$
Vinyl acetate	180
Methyl methacrylate	2.8
Styrene	7.0
Methyl acrylate	930

References

1. Seymour, R. B., F. Harris, and I. Branum, *Ind. Eng. Chem.*, **41**, 1509 (1949).
2. Martin, M. M., and N. P. Jensen, *J. Org. Chem.*, **27**, 1201 (1962).
3. Barb, W. G., *J. Polymer Sci.*, **11**, 117 (1953).
4. Blackley, D. C., and H. W. Melville, *Makromol. Chem.*, **18–19**, 16 (1956).
5. Barnett, G. M., and H. R. Gersmann, *J. Polymer Sci.*, **28**, 655 (1958).
6. Baldwin, M. G., *J. Polymer Sci.*, **A-1**, 3209 (1963).
7. Walling, C., *J. Am. Chem. Soc.*, **71**, 1930 (1949).
8. Walling, C., *Free Radicals in Solution*, Wiley, New York, 1957, p. 95.

Résumé

On a étudié les vitesses de copolymérisation de trois paires de monomères qui forment uniquement des copolymères alternés. Les paires de monomères sont l'éther vinyl-isobutylique, le fumarate de diéthyle, l'éther vinyl isobutylique–anhydride maléique et

le 1-octène–anhydride maléique. La vitesse maximum de copolymérisation a lieu pour des rapports $[M_1]/[M_2]$ qui diffèrent fortement de l'unité pour une concentration totale en monomère $[M_1] + [M_2]$ constante. On donne une équation pour la vitesse de copolymérisation des systèmes alternés et on discute des résultats sur la base de l'équation.

Zusammenfassung

Die Copolymerisationsgeschwindigkeit dreier Monomerpaare, die nur alternierende Copolymere bilden, wurde untersucht. Die Monomerpaare waren Vinylisobutyläther-diäthylfumarat, Vinylisobutyläthermaleinsäureanhydrid, und 1-Octenmaleinsäureanhydrid. Es wurde gezeigt, dass die maximale Copolymerisationsgeschwindigkeit für eine bestimmte totale Monomerkonzentration $[M_1] + [M_2]$ bei einem $[M_1]/[M_2]$-Verhältnis auftritt, welches merklich von eins abweicht. Die Gleichung für die Copolymerisationsgeschwindigkeit in alternierenden Systemen wurde angegeben, und die Ergebnisse anhand dieser Gleichung diskutiert.

Received June 15, 1964

JOURNAL OF POLYMER SCIENCE: PART A VOL. 3, PP. 711–722 (1965)

Rate of Densification of Gel during Coagulation of Viscose*

MAHARAJ K. GUPTA, LEON MARKER, ERIC WELLISCH, and ORVILLE J. SWEETING,† *Olin Mathieson Chemical Corporation, New Haven, Connecticut*

Synopsis

We have developed a simple method which permits measurement of the rate of densification of the gel forming during the coagulation of viscose and in effect experimentally separates the coagulation process from the regeneration process. The method is based on changes in density of a drop of viscose as it passes through a column of a salt solution. In devising the experimental program, three assumptions have been made: (*1*) Stokes' law is assumed to be valid for the movement of a drop of viscose through a column of a salt solution; (*2*) the volumes of sodium cellulose xanthate and water are assumed additive in viscose, permitting the calculation of the density of anhydrous xanthate; (*3*) the mechanics of loss of water initially from a surface are assumed to be the same whether the area is planar or spherical, i.e., a drop of viscose initially dehydrates in the same manner as does a thin film. Using this experimental technique, we have studied the coagulation of viscose as a function of salt index, ripening temperature, type of salt, and concentration of salt.

INTRODUCTION

In cellulose film, a combination of properties such as toughness, durability, and good dimensional stability is required. Further, the base sheet should be compatible with the after-treatments which give the additional properties of moistureproofness, heat sealing, and other surface characteristics. Because of the specific end-use, the property requirements of film are markedly different from those of rayon fiber, and different structural requirements are therefore needed. Whereas low lateral order and high orientation are necessary for a tough, strong rayon fiber,[1] low orientation and low lateral order are the requisites in a regenerated film.[2,3]

Lateral order in rayon for a given cellulose is determined primarily by the degree of xanthation of the cellulose in the viscose and by the nature of the coagulating and regenerating baths; orientation is produced as a result of stretch after a filament has been formed. It is well known that the degree of molecular order in cellulose regenerated from viscose depends not only on the molecular weight of cellulose but also quite markedly on

* Presented at the 145th Meeting of the American Chemical Society, New York New York, September 11, 1963.

† Present address: Yale University, New Haven, Conn.

the conditions prevailing during coagulation and regeneration and on subsequent treatments,[4] and in particular, on the rate at which the densification of the gel occurs during coagulation and regeneration in relation to the speed of casting.

The rate of coagulation and regeneration, and therefore the rate of formation, of film will depend on the concentration and ionic strength of the coagulating salt solution, on the hydrogen ion concentration of the regeneration bath, and on the rate of diffusion of hydrogen ions through the coagulated viscose.

Although coagulation and regeneration usually occur simultaneously, they do not occur at the same rate. The absolute concentrations and the nature and ratio of acid to salts determine which of these reactions predominates and in turn determine the shrinkage characteristics of the gel and the strength and quality characteristics of the final regenerated cellulose.[5,6] We report here an analytical method which has been developed to study the rate of loss of water of the coagulating gel in a variety of salt solutions and during regeneration in the presence of acid. By use of this method, the rate of densification of the gel has been measured as a function of salt index,* ripening temperature, and type and concentration of salts and acid in the coagulating bath.

METHOD OF MEASUREMENT

The method finally adopted to measure the rate of coagulation of viscose is based on changes in density of a drop of viscose as it passes through a column of the coagulating bath. Very simply, as coagulation proceeds, the viscose drop begins to dehydrate and its density increases with decrease in volume, resulting in a change in rate of fall, which can be determined and used to measure the rate of densification of the gel as coagulation and dehydration proceed.

In using these data, we have made assumptions as follows: (*1*) that Stokes' Law is valid for the movement of a drop of viscose through a column of salt solution; (*2*) that the volumes of sodium cellulose xanthate and water are additive in viscose, permitting the calculation of the density of dry xanthate as shown in the appendix; (*3*) that the mechanics of loss of water initially from a surface is the same whether the area is plane or spherical. Thus, we assume that a drop of viscose initially dehydrates in the same manner as does a thin film (the use of thin films in this work was impossible because of the extremely rapid rate of coagulation).

It should be mentioned that adoption of this procedure followed experiments in which attempts were made to follow density changes directly with a spring balance and cathetometer and also by observing changes in pH of the coagulating bath as alkaline solution was transferred from the gel to the bath. Neither of these procedures was sufficiently precise or reproducible.

* Salt index is a measure of the degree of xanthation related empirically to its rate of coagulation in a given sodium chloride solution.

EXPERIMENTAL PROCEDURE

Viscose Preparation

The viscose used in these experiments was standard commercial viscose as used for casting cellophane. It was prepared from Cellunier F pulp (manufactured by Rayonier, Inc.) with an alkali cellulose press ratio of 2.7 (cellulose basis), an unaccelerated aging time of 45 hr., a carbon disulfide concentration of 30%, a final alkalinity of 5.25, a blender viscosity of about 240 sec. at 18°C. (standard viscosity tube) and a cellulose content of 9%; the salt index prior to ripening was between 5.0 and 6.0.

High-xanthate viscose was prepared similarly except that the carbon disulfide concentration was increased to 45%, as described elsewhere.[7] The salt index prior to ripening was usually between 12 and 16.

Additional data for the viscose used are given in Tables III, IV, and VI.

Coagulation

The apparatus consisted of a glass tube $1^1/_4$ in. in diameter closed at one end, on which two etch marks had been made 30 in. apart. The tube was filled with coagulating bath, stoppered and fastened to a stand with a pivoted clamp by which it could be quickly inverted. The bath had a known density greater than that of viscose, the density of which had also been determined.

A drop of viscose of known average weight was added to the solution, and the tube was quickly stoppered and inverted; at the same instant a stop watch was started. The time when the drop passed the first etch mark was recorded; the time was next recorded when the drop passed the upper etch mark. The tube was then quickly inverted and the process was repeated, with stop watch readings being taken at the time when the drop passed each of the two etch marks again in its upward travel. This operation was repeated several times as desired. The data obtained for a typical experiment are given in Table I. As coagulation of a drop proceeds, the density increases and the velocity changes in accord with Stokes' Law. At any instant the drop has a definite density and moves with a definite velocity. Changes in radius taking place are small as compared to changes in density, but have been accounted for in the mathematical development (Appendix).

By plotting the time intervals Δt as a function of the elapsed time t, and extrapolating to zero time, the initial time interval Δt_0 is obtained as shown in a typical plot (Fig. 1). The value of Δt_0 is proportional to the reciprocal steady-state velocity of the viscose drop prior to the onset of coagulation.

Changes in density are calculable from the values of Δt by using eq. (A-5) (Appendix):

$$\Delta t_0/\Delta t = G(1 - F\theta_{ij})/(1 + \theta_{ij})^{1/3} \qquad \text{(A-5)}$$

TABLE I
Time of Travel of Viscose Drop in a Typical Experiment

Recorded times, sec.	Time to travel 30 in., Δt, sec.	Avg. recorded time t, sec.[a]
16		
39	23	27
—[b]		
47		
73	26	60
—[b]		
82		
108	26	95
—[b]		
114		
146	32	130
—[b]		
153		
200	47[c]	176
—[b]		
213		
246	33	229
—[b]		
258		
294	36	276
—[b]		
302		
340	38	321
—[b]		
350		
392	42	371

[a] Since the rate of rise is constantly changing between readings, it was convenient to calculate an average of the recorded times for each 30-inch traverse, t, computed as the arithmetic average of the readings at start and end of a traverse, e.g., $t = (16 + 39)/2 = 27$; $(47 + 73)/2 = 60$; etc.

[b] Tube is inverted in this interval and drop changes direction.

[c] This value for elapsed time Δt is evidently incorrect and results from the drops of viscose adhering to the wall for a few seconds. The method of recording the traverse time continuously and calculating t allows us to ignore this particular value of Δt in obtaining an accurate plot of Δt for an entire experiment as a function of t.

F is a differential density factor, a constant equal to $(\rho_s - \rho_w)/(\rho_x - \rho_s)$, where ρ_s, ρ_w, ρ_x are densities of solution, water, and xanthate, respectively. $\theta = \rho_x/\rho_w$, y is the ratio of weight of water in viscose to weight of sodium cellulose xanthate in viscose, and y_0 is the value of y at time zero, whereupon G, the degree of coagulation (expressed in terms of y) can be given by eq. (1):

$$G = (1 + \theta y_0)^{1/3}/(1 - F\theta y_0) \tag{1}$$

Equation (A-5) relates G and y to Δt, the time interval required for a droplet to traverse the distance between two graduations on the tube.

The cumbersome solution of the cubic equation can be avoided by a graphical solution. If eq. (1) is rewritten in the form

$$\Delta t_0/G\ \Delta t = (1 - F\theta y)/(1 + \theta y)^{1/3} \tag{2}$$

and $\Delta t_0/G\ \Delta t$ and θy are considered the variables, eq. (2) has a single pa-

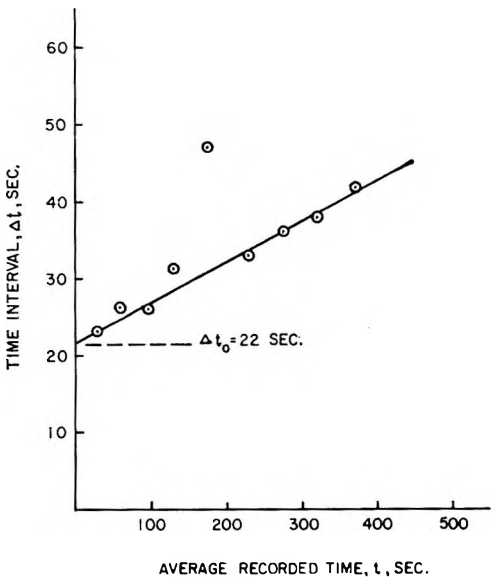

Fig. 1. Time required for a drop of viscose to travel through 30-in. intervals in a coagulation bath, plotted as a function of elapsed time.

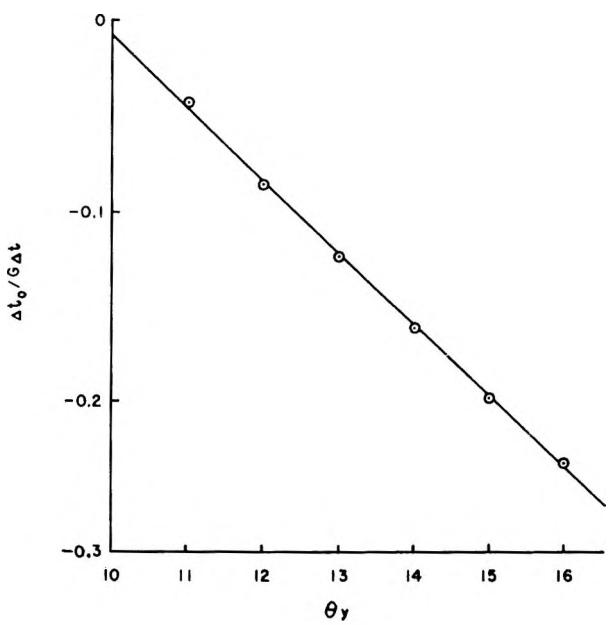

Fig. 2. Calculated theoretical F curve for $F = 0.1$.

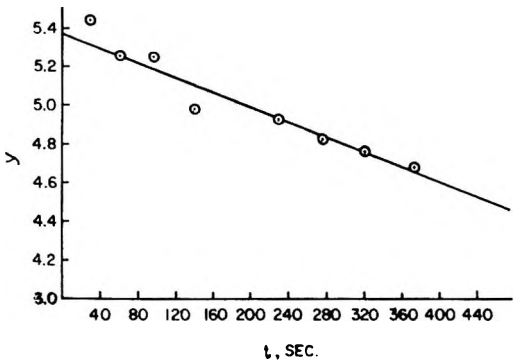

Fig. 3. Dehydration curve of viscose, relating y, the weight ratio of water to xanthate in a given drop of viscose, and t, the total elapsed time in the coagulating bath.

rameter F. For each of a series of values of F, a curve, e.g., Figure 2 for $F = 0.1$, can be constructed to relate the variables. From curves like Figure 2, θy values can be obtained for every experimental value of $\Delta t_0/G\,\Delta t$. From θ, y can then be calculated for any time interval Δt. A series of y values can thus be calculated for the Δt's and related to the total time measurement t as exhibited in Table II and Figure 3. From the slope

TABLE II
Determination of Rate of Coagulation of Commercial Viscose

Δt, sec.	$t_0/G\Delta t$	θy from graph	$y = \theta y/\theta$	t, sec.
23	0.1775	14.40	5.44	27
26	0.1565	13.90	5.26	60
26	0.1565	13.90	5.26	95
32	0.1274	13.15	4.97	130
47[a]	0.0867	12.15	4.59	176
33	0.1235	13.05	4.92	229
36	0.1133	12.80	4.82	276
38	0.1073	12.65	4.77	321
42	0.0972	12.40	4.68	371

[a] This point omitted in Fig. 3, for reason stated in Table I, footnote c.

of this line (Fig. 3), the rate of loss of water dy/dt can be calculated by multiplying the slope by the amount of xanthate present in the drop of viscose and dividing by the surface area of the drop. And if we let W_v be the average weight of a drop of viscose, the amount of xanthate in a drop of viscose is $W_v/(y_0 + 1)$. Also, letting ρ_v be the density of viscose and since the volume of a drop of viscose is $V = W_v/\rho_v$, the area of a drop of viscose is $(4\pi)^{1/3}(3V)^{2/3}$, or $(4\pi)^{1/3}/(3W_v/\rho_v)^{2/3}$. Thus, for the representative example given above, the slope of the line (Fig. 3) is 19.7×10^{-4}. From the average weight of a drop of viscose (0.06251 g.) and its volume (0.06251 g./1.113 g./ml. = 0.05616 ml.), the area of the drop of viscose is 2.325 ($3 \times$

TABLE III
Data Used in Calculating Coagulation Rate of Viscose

Type of viscose	Density of viscose, g./ml.	H_2O in viscose, %	Area of drop, cm.^{2}	F value	Coagulation bath: Concentration, %	Coagulation bath: Density, g./ml.
			$(NH_4)_2SO_4$ Solution as Coagulating Bath			
Std. coml. viscose	1.113	83.7	0.669	0.1540	40	1.220
Std. coml. viscose	1.113	83.7	0.669	0.1190	30	1.176
High-xanthate viscose	1.110	83.3	0.660	0.1780	40	1.220
High-xanthate viscose	1.110	83.3	0.629	0.1377	30	1.176
High-xanthate viscose	1.110	83.3	0.673	0.0866	20	1.116
High-xanthate viscose	1.110	83.3	0.683	0.0738	16.7	1.096
			Na_2SO_4 Solution as Coagulating Bath			
Std. coml. viscose	1.113	83.7	0.709	0.1133	18	1.168
Std. coml. viscose	1.113	83.7	0.709	0.0985	15	1.148
Std. coml. viscose	1.113	83.7	0.709	0.0812	13	1.124
Std. coml. viscose	1.113	81.4	0.646	0.1584	18	1.168
Std. coml. viscose preheated for 3 min.	1.143	76.4	0.658	0.1584	18	1.168

$0.05616)^{2/3}$ or 0.7093 cm.^{2}. The amount of xanthate in this drop of viscose is $0.06251/5.37 = 9.82 \times 10^{-3}$ g., and thus the rate of dehydration of viscose is $(19.7 \times 9.82 \times 10^{-7})/0.7093$, or 27.3×10^{-6} g.H_2O/cm.^{2} -sec.

Data used in the calculations that were made are presented in Table III.

RESULTS

Using the technique described, we have determined the rates of coagulation of different types of viscose. The effect of salt index and ripening temperature and the effect of salt type and concentrations in the coagulating solutions were also studied. The results are summarized in Tables IV–VII.

The rate of coagulation of standard commercial viscose is independent of its ripening temperature. The rate is independent of the salt index when the latter is greater than unity, but slows down when the salt index is less than unity, probably because partial coagulation has already occurred at these low indexes.

The rate of coagulation of viscose increases with increasing salt concentrations in the coagulating solutions. On a molar equivalent basis, sodium sulfate is more effective than ammonium sulfate, but owing to its greater solubility, the latter results in a faster rate of dehydration.

The rate of coagulation of high-xanthate viscose is faster than that of standard viscose; here also the rate is concentration-dependent. The effect of salt index by ripening (ranging from 19.6 to 3.6) does not appear to be significant.

TABLE IV
Rate of Coagulation of Standard Viscose as a Function of Salt Index at Constant Ripening Temperatures

Ripening temp., °C.	Salt index	Rate in 18% Na_2SO_4 solution, g.H_2O × 10^6/cm.²-sec.
4	4.40	35.70
4	3.40	32.80
4	2.30	32.07
4	1.25	33.90
18	4.40	35.70
18	3.70	31.25
18	2.30	29.92
18	1.15	33.45
18	0.75	24.20
18	0.50	26.20

TABLE V
Rate of Coagulation of Standard Viscose and Hydroxyethyl Cellulose as a Function of Salt Type and Concentration

Salt solution	Salt concentration, %	Rate, g. H_2O × 10^6/cm.²-sec.	
		Viscose	HEC[a]
Sodium sulfate	13.0	22.90	15.16
	15.0	27.27	22.52
	16.0	34.24	—
	18.0	36.34	25.25
Ammonium sulfate	16.7	8.41	5.80
	30.0	30.57	29.35
	40.0	40.00	39.52

[a] Rayonier product containing about 4% ethylene oxide adduct.

TABLE VI
Rate of Coagulation of High-Xanthate Viscose

Salt index	$(NH_4)_2SO_4$ concentration, %	Rate, g. H_2O × 10^6/cm.²-sec.
19.6	40.0	45.92
8.7	40.0	44.36
4.5[a]	40.0	47.80
3.6[b]	40.0	48.69
8.7	30.0	39.20
8.7	20.0	8.38
8.7	16.7	7.06

[a] Stored in refrigerator for one month.

[b] Ripened at room temperature. It should be noted that only ammonium sulfate solution can be used for high-xanthate viscose, since it remains dissolved even in saturated sodium sulfate solution.

TABLE VII
Rate of Coagulation of Preheated Viscose in 18% Sodium Sulfate

Treatment	Salt index		Rate, g. H_2O $\times 10^6$/cm.^{2}-sec.
	Before treatment	After treatment	
Control	3.92		36.34
Heated 1 min. in infrared	3.98	0	26.80
Heated 3 min. in infrared	3.98	0	16.44
Dielectric (30 sec.)	3.98	2.5	32.10
Dielectric (60 sec.)	3.98	2.5	27.70
Dielectric (180 sec.)	3.98	0	24.85

Preheating of viscose by infrared treatment slows down the rate of coagulation appreciably. Concurrent with the treatment there is a drop in salt index probably caused by partial dexanthation. Infrared treatment for 180 sec., which lowers the salt index to a zero value, reduces the rate by almost one-half.

Coagulation and Regeneration

In the treatment given above it was assumed that the change of y with time in the course of the experiment is almost linear and therefore that the slope of a plot of y as a function of t is a measure of the initial rate of water

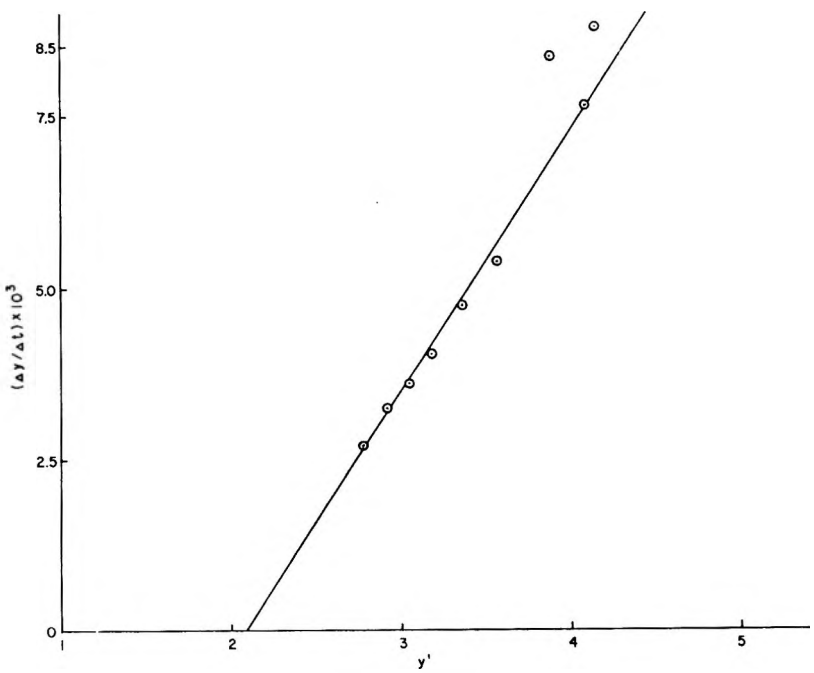

Fig. 4. Curve relating change of y with time to y'.

loss. There are circumstances under which this assumption does not hold and then it is necessary to determine the initial slope of the y–t curve.

From a set of data an average value for the instantaneous rate of change of moisture content $\Delta y/\Delta t$ was determined by dividing the difference between successive values of y by the time elapsed between successive measurements. The values of $\Delta y/\Delta t$ were plotted against the corresponding values of y' where $y' = (y_1 + y_2)/2$ is the average moisture content for the interval under consideration. The value of $\Delta y/\Delta t$ when $y = y_0$ is the initial rate of moisture loss of the viscose. The value of y when $\Delta y/\Delta t$ is extrapolated to zero is the equilibrium moisture content.

Tables VII and VIII present data from experiments with a regenerating bath containing acid: 20% sodium sulfate and 12.5% sulfuric acid. When a viscose droplet is placed in this bath, rapid surface regeneration takes place. Changes in density therefore reflect both a loss of water with coagulation and also a change in the chemical composition of the droplet. The film formed is highly permeable to water, and the equilibrium moisture content is rapidly approached.

Data for the coagulation of viscose in one acid regenerating bath are: water in viscose, 81.53%; y_0 ratio, 4.41; density of acid–salt bath, 1.274 g./ml.; weight of viscose drop, 0.05601 g.; weight of xanthate in drop, 0.0103 g.; area of drop, 0.6545 cm.^{2}. The calculated values are given in Table VIII and Figure 4.

The rate of dehydration can be obtained from the initial rate of coagulation (Fig. 4), i.e., from $\Delta y/\Delta t$ at $t = 0$, when $y' = y_0$. The value of

TABLE VIII
Calculated Rate Data for the Coagulation of Viscose in Acid–Salt Bath

Δy	Δt	$\Delta y/\Delta t \times 10^3$	y'
0.176	20	8.80	4.15
0.153	20	7.65	4.08
0.335	40	8.37	3.84
0.216	40	5.40	3.56
0.190	40	4.75	3.36
0.162	40	4.05	3.18
0.109	30	3.63	3.05
0.162	50	3.24	2.91
0.108	40	2.70	2.78

TABLE IX
Rate of Coagulation and Equilibrium Moisture Content of Viscose Coagulated in Acid–Salt Bath

$\Delta y/\Delta t$ at $y' = y_0$	8.85×10^{-3}
y' ratio at $\Delta y/\Delta t = 0$	2.08
Rate of dehydration, g. H_2O/cm.^{2}-sec.	137.1×10^{-6}
Final equilibrium moisture content, %	67.7

y' at $\Delta y/\Delta t = 0$ gives the value for the ratio of moisture content to the amount of xanthate at equilibrium; from this the final equilibrium moisture content after complete coagulation can be calculated. These data and calculations are summarized in Table IX.

APPENDIX

Development of a Velocity–Density Equation for Calculation of Rate of Densification of Gel

According to Stokes' Law, a drop of viscose of density ρ_v, moving under the urging of gravity through a salt solution of density ρ_s, travels with a velocity V given by the equation,

$$V = 2ga^2(\rho_v - \rho_s)/9\eta \tag{A-1}$$

where g is the acceleration caused by gravity, a the radius of the drop, and η the viscosity of the salt solution. If the volumes of cellulose xanthate and water are assumed to be additive,

$$\rho_v = (W_w + W_x)/(U_w + U_x) = \rho_x(y + 1)/(\theta y + 1) \tag{A-2}$$

where W_w and W_x are the respective weights of water and xanthate in the viscose drop, U_w and U_x are the corresponding volumes, y is the weight ratio of water to xanthate, ρ_w and ρ_x are the densities of water and xanthate respectively, and $\theta = \rho_x/\rho_w$.

Since we have assumed the volume of viscose, U_v, to equal $U_w + U_x$, then $U_v = (W_x/\rho_x)(\theta y + 1)$.

Setting $U_v = (4/3)\pi a^3$,

$$a^2 = [(3W_x/4\pi\rho_x)(\theta y + 1)]^{2/3} \tag{A-3}$$

When the drop is first placed in the solution it has a water content y_0, a radius a_0, and moves through the solution with a velocity V_0. On taking the ratio V/V_0 and substituting the values of ρ_v and a^2 from eqs. (A-2) and (A-3):

$$V/V_0 = [(\theta y_0 + 1)/(\theta y + 1)]^{1/3} \\ [(y + 1 - A\theta y - A)/(y_0 + 1 - A\theta y_0 - A)]$$

where $A = \rho_s/\rho_x$.

This may be written

$$V/V_0 = \frac{(\theta y_0 + 1)^{1/3}}{1 - [\theta y_0(A\theta - 1)/\theta(1 - A)]} \cdot \frac{1 - [\theta y(A\theta - 1)/\theta(1 - A)]}{(\theta y + 1)^{1/3}}$$

or

$$V/V_0 = G(1 - F\theta y)/(1 + \theta y)^{1/3} \tag{A-4}$$

where

$$F = (A\theta - 1)/\theta(1 - A) = [(\rho_s/\rho_x)(\rho_x/\rho_w) - 1]/(1 - \rho_s/\rho_x)(\rho_x/\rho_w) \\ = (\rho_s - \rho_w)/(\rho_x - \rho_s)$$

and

$$G = (1 + \theta y_0)^{1/3}/(1 - F\theta y_0)$$

Since the velocity is related to the measured time interval by $V = \Delta l/\Delta t$, l being the distance traversed in time t,

$$V/V_0 = \Delta t_0/\Delta t = G(1 - F\theta y)/(1 + \theta y)^{1/3} \qquad \text{(A-5)}$$

References

1. Sisson, W. A., *Textile Res. J.*, **3,** 153 (1960).
2. Miller, M., and V. C. Haskell, *J. Appl. Polymer Sci.*, **18,** 627 (1961).
3. Price, C. R., and V. C. Haskell, *J. Appl. Polymer Sci.*, **18,** 635 (1961).
4. Marrinan, H. J., *Recent Advances in the Chemistry of Cellulose and Starch,* J. Honeyman, Ed., Interscience, New York–London, 1959.
5. Moore, C. L., *Silk and Rayon*, **9,** 19 (1935).
6. Bronnert, E., U. S. Pat. 1,393,197, October 11, 1922; *Chem. Abstr.*, **16,** 837 (1922).
7. Ingersoll, H. G. (to E. I. du Pont de Nemours and Company), U. S. Pat. 2,991,510 (July 11, 1961).

Résumé

Nous avons mis au point une méthode simple permettant la mesure de la vitesse de densification du gel pendant la coagulation de la viscose et séparant expérimentalement le processus de coagulation du processus de régénération. La méthode est basée sur les variations de densité d'une goutte de viscose lorsqu'elle passe par une colonne remplie d'une solution de sel. En élaborant le programme expérimental, trois suppositions ont été faites: (*1*) La loi de Stokes est considérée comme valable pour le mouvement d'une goutte de viscose à travers la colonne d'une solution de sel: (*2*) les volumes du xanthate sodique de cellulose et de l'eau sont considérés comme additifs dans la viscose, ce qui permet le calcul de la densité du xanthate anhydre; (*3*) les mécanismes de perte d'eau par la surface sont supposés initialement les mêmes si la surface est plane ou sphérique, c'est à dire: une goutte de viscose se déshydrate initialement de la même manière qu'un film mince. En utilisant cette technique expérimentale, nous avons étudié la coagulation de la viscose en fonction de l'indice de sel, de la température de maturation, du type de sel et de la concentration en sel.

Zusammenfassung

Eine einfache Methode, welche eine Messung der Verdichtungsgeschwindigkeit des während der Koagulation von Viskose gebildeten Gels gestattet, sowie eine experimentelle Trennung des Koagulationsprozesses vom Regenerations-prozess ermöglicht, wurde entwickelt. Die Methode beruht auf der Dichteänderung eines Viskosetropfens beim Durchgang durch eine Säule einer Salzlösung. Bei der Aufstellung des Versuchsprogrammes wurden drei Annahmen gemacht. (*1*) Die Gültigkeit des Stokes-Gesetzes für die Bewegung des Viskosetropfens durch eine Salzlösungssäule wird vorausgesetzt. (*2*) Es wird angenommen, dass in der Viskose die Volumina von Natriumzellulosexanthat und Wasser sich additiv verhalten und so die Berechnung der Dichte des wasserfreien Xanthats erlauben. (*3*) Der Mechanismus des anfänglichen Wasserverlusts aus einer Oberfläche wird für eine ebene und eine sphärische Fläche als gleich angenommen, d.h. ein Viskosetropfen dehydratisiert sich anfänglich in der gleichen Weise wie eine dünner Film. Mit dieser Versuchsmethode wurde die Koagulation von Viskose als Funktion von Salzindex, Reifungstemperatur, Salztyp und -konzentration untersucht.

Received October 23, 1963
Revised July 28, 1964

JOURNAL OF POLYMER SCIENCE: PART A VOL. 3, PP. 723–733 (1965)

Polymerization of 1-Methylene-4-Vinylcyclohexane by a Cyclic Polymerization Mechanism*†

GEORGE E. BUTLER, MARION L. MILES, and WALLACE S. BREY, JR., *Department of Chemistry, University of Florida, Gainesville, Florida*

Synopsis

1-Methylene-4-vinylcyclohexane was prepared by the following reaction sequence: (1) conversion of 4-methylene-cyclohexane methanol to the tosylate, (2) oxidation of the tosylate to 4-methylenecyclohexane carboaldehyde by the method of Kornblum, and (3) reaction of the aldehyde with the ylide from triphenylmethylphosphonium bromide in a Wittig reaction to produce the diene. Polymerization of 1-methylene-4-vinylcyclohexane was attempted with the use of free radical, anionic, cationic, and Ziegler-type initiators. Polymers were obtained from the cationic (boron trifluoride) and Ziegler (titanium tetrachloride and triethylaluminum complex)-initiated reactions. The polymer obtained by polymerization of this monomer with gaseous boron trifluoride as the initiator led to a solid polymer which was soluble in a number of organic solvents and had a softening temperature of 150°C. The infrared spectrum of this polymer gave absorption bands for terminal unsaturation. NMR analysis indicated that the unsaturation ratio was one double bond per two monomer units. The NMR analysis also indicated that this unsaturation was due to vinyl rather than methylene groups. Polymerization of this monomer by use of a Ziegler catalyst (titanium tetrachloride and triethylaluminum) led to a solid polymer of which 10% was soluble in a number of organic solvents. Although the infrared spectrum of this polymer indicated the presence of some terminal unsaturation, an NMR analysis indicated only an extremely small amount of residual unsaturation. The essential absence of unsaturation in this linear polymer supports an intramolecular interaction in this monomer, since Ziegler-type initiators do not ordinarily initiate polymerization of the isobutylene type. These results can be interpreted as additional evidence for the nonbonded interaction concept as a driving force to cyclic polymer.

INTRODUCTION

Cyclopolymerization or intra-intermolecular polymerization is a phenomenon observed with certain 1,5- and 1,6-dienes by which a polymer is formed having cyclic recurring units. The original proposal[1] that such a mechanism could lead to soluble, fully saturated polymers containing recurring five- or six-membered cyclic units has now been fully substantiated.[2] A

* From the Ph.D. Dissertation of Marion L. Miles, Department of Chemistry, University of Florida, April 1963.

† The support of this work by the National Science Foundation under NSF Grant No. 10011 is kindly acknowledged. This paper was presented before the Division of Polymer Chemistry, American Chemical Society, Atlantic City, New Jersey, September 1962; *Polymer Preprints*, 3 No. 2, p. 288.

wide variety of monomers structurally capable of undergoing cyclopolymerization and a wide variety of initiators for these systems have been studied[3] and all confirm the proposed mechanism.

A recent report[4] presented evidence that certain trienes undergo polymerization in presence of Ziegler-type initiators to produce soluble, linear polymers containing cyclic units produced during the propagation step by a mechanism which involves alternating 1,2- and 1,4-addition polymerization steps. For example, *trans*-1,3,8-nonatriene produced a polymer possessing a structure which could be accounted for only on the basis of the proposed mechanism.

It was the purpose of this investigation to synthesize monomers which are structurally capable of undergoing cyclic polymerization to produce bicyclic systems during the propagation step. 1-Methylene-4-vinylcyclohexane is a monomer which meets the structural requirements. During the course of this work, the synthesis and polymerization of 1,4-dimethylenecyclohexane was reported.[5] These authors presented evidence that this monomer produced a polymer containing bicyclo[2.2.1]-heptane units by cationic initiation, and that this structure could be accounted for on the basis of a cyclic polymerization mechanism.

More recently other bicyclic polymers produced through the cyclopolymerization or copolymerization mechanism have been published. Frazier and O'Neill[6] have described the bicyclo-copolymerization of sulfur dioxide and *cis*, *cis*-1,5-cyclooctadiene. Reichel and Marvel[7] have described the transannular polymerization of 1,5-cyclooctadiene. Graham, Buhle, and Pappas[8] have described high molecular weight, soluble polymers of 2-carbethoxybicyclo[2.2.1]-2,5-heptadiene believed to contain nortricyclene repeating units, formed by transannular polymerization. Attempted polymerization of structures similar to this compound suggested that this type of transannular polymerization of bicycloheptadienes requires activation of the double bonds and resonance stabilization of radicals formed during the polymerization. These results support the earlier proposal[2] that such nonbonded interactions may contribute to the driving force for cyclic polymerization in general. Further evidence to support this proposal is included in this paper.

RESULTS AND DISCUSSION

1-Methylene-4-vinylcyclohexane (I) would be expected to undergo cyclic polymerization to produce a polymer possessing the structural units II:

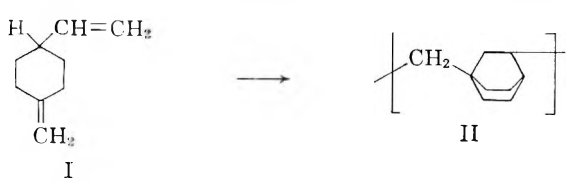

I II

However, other structural units which may arise are represented by formulas III and IV. Structure III could arise through initiation at the exo-methylene group alone, and

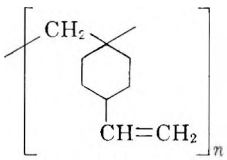

III

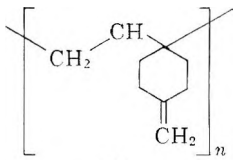

IV

propagation through this group only, thus leaving the vinyl group pendent. Due to the structural similarity of this portion of the monomer molecule to isobutylene, this type of initiation would likely occur predominantly through cationic initiation. Structure IV could arise by a similar process involving the vinyl group alone, and would likely occur predominantly through Ziegler-type initiation. A structure including structural units II and III could arise through initiation at the exo-methylene group alone as in III; however, in this case certain monomer units are required to cyclize through the vinyl groups, while others do not. This type of structure would be expected to predominate in a cationic-initiated polymerization. Another structure including structural units II and IV could arise through initiation at the vinyl group alone, followed by cyclization of certain monomer units through the exo-methylene group, and failure of certain other monomer units to cyclize. This structure would be expected to predominate in a Ziegler-type initiation.

The monomer was synthesized by oxidation of 4-methylenecyclohexane-1-methanol to the corresponding aldehyde, followed by the Wittig synthesis, employing the ylide of methyltriphenylphosphonium bromide. Polymerization was accomplished by use of both cationic and Zeigler-type initiators, although the former was more successful. Free radical and conventional anionic initiators were not effective in polymerization of this monomer, as might be predicted on the basis of its structure.

The polymer obtained by polymerization of this monomer with gaseous boron trifluoride as the initiator led to a solid polymer which was soluble in a number of organic solvents and has a softening temperature of 150°C. The infrared spectrum of this polymer gave absorption bands for terminal unsaturation. NMR analysis based upon sp^2:sp^3 hydrogen ratios indicated that the unsaturation ratio was approximately one double bond per two monomer units, and that this unsaturation was due to vinyl rather than methylene groups. The peak for the sp^3-bonded hydrogens was very broad and occurred at a value of τ of approximately $8.6\tau \pm 1\tau$ while the sp^2-bonded hydrogens usually gave rise to two peaks at τ of approximately 4.5 and 5.2. The observed sp^2:sp^3 ratio was found to be 1:7.5. The calculated ratios for structures III, IV, a structure which includes equal numbers of II and III, and a structure which includes equal numbers of II and IV, respectively, are 1:3.7, 1:6, 1:8.3, and 1:13. The evidence leads to the

conclusion that the structure of the polymer obtained through cationic initiation can be best represented by a structure which includes both structural units II and III. These results are consistent with predictions based upon the similarity of the exo-methylene portion of this monomer to isobutylene. The results, however, offer no evidence for a regularly alternating structure of units II and III but a structure which can only be interpreted that the polymer chain is made up of bicyclic and cyclic units but in an unknown order. However, an examination of scale molecular models of these structures indicates that considerable steric interference exists when two bicyclic units are joined together. On the other hand, a regularly alternating structure of structural units II and III can be constructed readily from the models. The results, therefore, strongly suggest that the structure is that of an approximately regularly alternating copolymer of bicyclic and cyclic units, with the cyclic units predominating.

Calculations of the per cent cyclization can be accomplished by using eq. (1):

$$100\ (dc - b)/(dc - b + a) = \%\ \text{cyclization} \qquad (1)$$

where a = number of sp^3 hydrogens in the saturated unit; b = number of sp^3 hydrogens in the unsaturated unit; c = number of sp^2 hydrogens in the unsaturated unit; and d = sp^3 to sp^2 hydrogens ratio as determined by NMR. By use of this method a value of 40% cyclization in the cationic-initiated polymer of 1-methylene-4-vinylcyclohexane is obtained. It should be clearly understood that these calculations represent only a good approximation of the extent of cyclization in these polymers since the data used in the calculations are not based on highly accurate experimental data.

Polymerization of this monomer by use of a Ziegler catalyst (titanium tetrachloride and triethylaluminum) led to a solid polymer of which 10% was soluble in a number of organic solvents. Although the infrared spectrum of this polymer indicated the presence of some terminal unsaturation, an NMR analysis indicated only an extremely small amount of residual unsaturation. The soluble fraction of this polymer had an intrinsic viscosity of 0.09, and the NMR spectrum indicated a rather high degree of cyclization, showing a sp^2:sp^3 ratio of 1:37. By use of eq. (1), the polymer is shown to consist of 88% cyclic units. The essential absence of unsaturation in this linear polymer supports an intramolecular interaction in this monomer, since Ziegler-type initiators do not ordinarily initiate polymerization of the isobutylene type. These results can be interpreted as additional evidence for the nonbonded interaction proposal[2] as a driving force to cyclic polymer, the nonbonded interaction providing a lower energy pathway to polymer through cyclization. The conditions used and results of the polymerization experiments are recorded in Table I.

X-ray diffraction studies on these polymers did not indicate any appreciable degree of crystallinity. The physical properties of the soluble polymers obtained from this monomer are recorded in Table II.

TABLE I. 1-Methylene-4-vinylcyclohexane Polymerizations[a]

Polymer number	Solvent ml.	Initiator		Catalyst aging		Reaction conditions		Polymer	
		System	Quant. used (mmole)	Temp., °C.	Time, min.	Temp., °C.[b]	Time	Yield, %	Soluble, %
	None	Benzoyl peroxide	0.02			68	14 days	None	
	THF, 10	Li-naphthalene	0.04			R.T.	20 hr.	None	
	THF, 10	Na-naphthalene	[c]			R.T.	16 hr.	None	
	n-Heptane, 12	$TiCl_4$	0.085			0	6 hr.		
							then		
		$Al(C_2H_5)_3$	0.15	0	45	R.T.	40 hr.	0.3	
	n-Heptane, 5	$TiCl_4$	0.085						
		$Al(C_2H_5)_3$	0.15	98	5	R.T.	7 days	1	
7a	*n*-Heptane, 5	$TiCl_4$	0.17						
		$Al(C_2H_5)_3$	0.11	98	5	R.T.	7 days	11	20[d]
7b	*n*-Heptane, 5	$TiCl_4$	0.17						
		$Al(C_2H_5)_3$	0.11	R.T.	20	R.T.	14 days	61[e]	10
7c	*n*-Heptane, 5	$TiCl_4$	0.17						
		$Al(C_2H_5)_3$	0.11	0	20	R.T.	18 days	33	12
	n-Heptane, 5	$TiCl_4$	0.15	R.T.	5	R.T.	6 days	Trace	
		$Al(i\text{-}Bu)_3$	0.15						
7d	*n*-Heptane, 5	$TiCl_4$	0.17						
		$Al(i\text{-}Bu)_3$	0.11	R.T.	20	R.T.	18 days	10	30[b]
7e	CH_3Cl_2,5	BF_3	Gas			−70	24 hr.	5	95[b]
7f	CH_2Cl_2,5	BF_3	Gas			−70	1 hr.	79	70
							then		
						R.T.	4 hr.		

[a] All polymerizations carried out with 7.4 mmole of monomer except where indicated; [b] R.T. = room temperature; [c] A solution of approximately 0.1*M* was perpared of the catalyst in THF; After the monomer and solvent had been placed in the reaction flask, the catalyst solution was injected until the faint bluish color presisted; [d] Total yield of polymer was too small to determine this percentage accurately; [e] Polymerization carried out with 14.8 mmole of monomer.

TABLE II
Physical Properties of soluble Polymers of 1-Methylene-4-vinylcyclohexane

Polymer number	Polymer melt temperature, °C.	Intrinsic viscosity	Elemental Analysis			
			Calculated		Found	
			C, %	H, %	C, %	H, %
7a	132	N.D.[a]	88.45	11.55	88.42	11.52
7b	104	0.09	88.45	11.55	88.29	11.69
7c	147	0.11	88.45	11.55	N.D.	
7d	138	N.D.	88.45	11.55	88.42	11.56
7e	130	0.06	88.45	11.55	N.D.	
7f	132	0.08	88.45	11.55	88.44	11.49

[a]N.D. = not determined.

EXPERIMENTAL

Equipment and Data

All temperatures herein are uncorrected and reported in degrees centigrade. Pressures are expressed in millimeters of mercury, having been determined by means of either a Zimmerli or McLeod gauge. Infrared spectra were obtained with a Perkin-Elmer Infracord double-beam infrared recording spectrophotometer or a Perkin-Elmer Model 21 double-beam infrared recording spectrophotometer. Refractive indices were obtained with a Bausch and Lomb Abbe 34 refractometer equipped with an achromatic compensating prism. Gas–liquid chromatographic (GLC) analyses were made with a Wilkens Aerograph Model A-110-C gas chromatographic instrument with helium as the eluent gas. Unless otherwise indicated, gas–liquid chromatographic analyses were made on a 5-ft. column packed with 20% Silicone GE SF-96 on firebrick and on a 10-ft. column packed with 20% Carbowax 1000 on 42/60 firebrick.

Nuclear magnetic resonance (NMR) spectra were obtained with a Varian DP-60 nuclear magnetic resonance spectrometer at a frequency of 56.4 M-cycles with carbon tetrachloride as solvent. Melting point determinations of monomeric compounds were carried out in open capillary tubes in a Thomas-Hoover melting point apparatus. Polymer softening points and melting ranges reported were determined in a similar manner. The polymer melt temperatures were determined by means of a Kofler micro hot stage. The polymer melt temperature is defined as the lowest temperature at which a wet streak is left on a hot stage upon pressing a sample of polymer with a spatula. This technique was adopted for the present work, since most of the polymers studied contained some pendent double bonds, and if these materials are heated slowly over a long period of time, there is high probability for crosslinking to occur, and elevation of the apparent melt temperature. Intrinsic viscosities were calculated from efflux times of solutions through a Cannon-Ubbelohde semi-micro dilution viscometer set in a 25°C. constant temperature bath. X-ray diffraction spectra were obtained with a Norelco

x-ray diffractometer, Model 12045 using a proportional counter. Elemental analyses were performed by Galbraith Laboratories, Knoxville, Tennessee.

Source and Purification of Materials

Tetrahydrofuran was obtained from Fisher Scientific Company. It was dried over sodium ribbon and then distilled. Allyl bromide, triphenylphosphine, titanium tetrachloride, and phosphorus tribromide were obtained from Peninsular Chem-Research, Inc. The allyl bromide and phosphorus tribromide were distilled before use, and the triphenylphosphine and titanium tetrachloride were used as received. *n*-Butyllithium was obtained from Foote Mineral Company and used as received. Methyl bromide was obtained from Dow Chemical Company and used as received. 1-Methylene-4-cyclohexanemethanol and *p*-toluenesulfonyl chloride were obtained from Distillation Products Industries division of Eastman Kodak Company. The 1-methylene-4-cyclohexanemethanol was distilled before use, and the *p*-toluene sulfonyl chloride was used as received. Boron trifluoride (gas) was obtained from The Matheson Company and used as received. Triisobutylaluminum and triethyl-aluminum were obtained from Ethyl Corporation and used as received. Nitrogen used as a sweep gas in the polymerization experiments was Airco prepurified grade containing less than 20 ppm of oxygen.

Preparation of 1-Methylene-4-vinylcyclohexane

1-Methylene-4-cyclohexanemethyl Tosylate. To a vigorously stirred mixture of 1-methylene-4-cyclohexanemethanol (252 g.; 2 moles) and dry pyridine (632 g.; 8 moles) cooled to 10°C. was added tosyl chloride (401 g.; 2.1 moles) at such a rate that the reaction temperature did not exceed 20°C. After the addition was completed, the resulting mixture was stirred 4 hr. at 20°C. The reaction slurry was poured into a solution prepared by adding 1200 ml. of concentrated hydrochloric acid (12*M*) to 4 liters of water. The tosylate which precipitated was collected, washed with cold water, and recrystallized from 1100 ml. of methanol. Yield 475 g., 85%, m.p. 61–63°C.

ANAL. Calcd. for $C_{15}H_{20}O_3S$: C, 64.26%; H, 7.19%. Found: C, 64.48%; H, 7.17%.

1-Methylene-4-cyclohexanemethanal. The reaction used is a modification of the method developed by Kornblum.[9] A freshly prepared mixture of sodium bicarbonate (177 g.; 2.1 moles) and dimethyl sulfoxide (850 ml.) was heated to 150°C. Dry nitrogen gas was bubbled through the slurry, and 1-methylene-4-cyclohexanemethyl tosylate (280 g.; 1 mole) was added with vigorous stirring. The reaction mixture was maintained at 150°C. for 15 min. after the addition was completed and then allowed to cool to room temperature. The mixture was filtered, 1 liter of water was added, and the resulting solution was continuously extracted with 450 ml. of diethyl ether for 48 hr. The organic extracts were combined and dried over

anhydrous sodium sulfate, filtered and distilled through a 23-plate spinning band column to yield 1-methylene-4-cyclohexanemethanal (43 g.; 33%) b.p. 61°C./12 mm.; n_D^{20} 1.4892. Infrared analysis revealed the following absorption bands assignable to the expected structure: 2720 cm.$^{-1}$(CHO), 1700 cm.$^{-1}$ (CHO), 1650 cm.$^{-1}$(C=C), 890 cm.$^{-1}$ (C=CH_2).

ANAL.: Calcd. for $C_8H_{12}O$: C, 77.37%; H, 9.74%. Found: C, 77.21; H, 9.72.

1-Methylene-4-vinylcyclohexane. A stirred slurry of 35.7 g. (0.1 mole) of methyltriphenylphosphonium bromide in 400 ml. of absolute ethyl ether, in a dry nitrogen atmosphere, was treated with 65 ml. of an approximately 15% solution of *n*-butyllithium in *n*-hexane. To the resulting reddish-orange solution of the triphenylphosphorusmethylide, at room temperature, was added a solution of 12.4 g. (0.1 mole) of 1-methylene-4-cyclohexanemethanal in 30 ml. of dry ethyl ether. This mixture was stirred for 20 min., and a 500-ml. portion of water was then added. Upon addition of the water, two layers were formed and the organic layer was removed. The aqueous layer was extracted with two 200 ml. portions of ether, and these extracts were combined with the organic layer. The combined ethereal portions were then dried for 24 hr. over anhydrous sodium sulfate. The ether and *n*-hexane were removed by distillation through a 80-cm. vacuum-jacketed Vigreux column. The residue was distilled through a 23-plate spinning-band column under reduced pressure to yield 5 g. (41%) of 4-methylene-1-vinylcyclohexane, b.p. 70–71°C./58 mm. or 140–141°C./atmospheric, n_D^{20} 1.4674.

GLC analysis of the product by use of two different columns revealed only one peak, and quantitative hydrogenation resulted in the reaction of 1.95 moles of hydrogen per mole of sample. The NMR spectrum using an external benzene standard has two peaks with chemical shifts located at 1.73 and 2.21 parts per million (ppm) and a larger peak at 4.73 ppm. The integrated peak area ratio for sp^2 to sp^3 hydrogens was 1:2 (theoretical = 5:9). The infrared spectrum of this compound has the following absorption bands which are assignable to the proposed structure: 1645 cm.$^{-1}$(C=C), 995 cm. $^{-1}$(CH=CH_2), 910 cm.$^{-1}$(CH=CH_2), 885 cm.$^{-1}$(C=CH_2).

ANAL. Calcd. for C_9H_{14}: C, 88.45%; H, 11.55%. Found: C, 88.58%; H, 11.61%

Polymerization of 1-Methylene-4-vinylcyclohexane

Polymerization of 1-methylene-4-vinylcyclohexane was attempted by use of various types of initiators—free radical, cationic, anionic, and Ziegler. High conversion to soluble polymer was obtained only with the cationic initiator, gaseous boron trifluoride. Polymerization of this monomer by use of a Ziegler-type initiator (titanium tetrachloride and triethylaluminum) led to a solid polymer of which approximately 10% was soluble in a number of organic solvents.

Attempted Free Radical-Initiated Polymerization. Benzoyl peroxide (4 mg.) and 1-methylene-4-vinylcyclohexane (1 ml.; 0.9 g.) were charged

to a Pyrex tube which was swept with nitrogen, sealed, and placed in an oven set at 68°. After two weeks at this temperature, no apparent increase in viscosity had occurred. Upon cooling and pouring the resulting solution into methanol, no polymer precipitation occurred.

Attempted Anionic Initiated Polymerization. (1) A small piece of lithium metal was placed in 10 ml. of dry tetrahydrofuran containing 8 mg. of resublimed naphthalene under a dry nitrogen atmosphere. After stirring for 1 hr., 0.9 g. of 1-methylene-4-vinylcyclohexane was added to the solution. Stirring at room temperature was continued for 26 hr., after which the solution was poured into 200 ml. of methanol. No precipitation of polymer occurred.

(2) A procedure similar to that reported by Field[3] was used. An initiator solution was prepared by adding 1 g. (0.043 mole) of sodium metal to 6.4 g. (0.05 mole) of naphthalene in 100 ml. of dry tetrahydrofuran under a blanket of dry nitrogen. The formation of sodium naphthalene was indicated by formation of a very dark blue-green color. To 10 ml. of dry tetrahydrofuran under nitrogen was added the initiator solution until a faint green color persisted. To this 1 ml. (0.9 g.) of 1-methylene-4-vinylcyclohexane was added, and the resulting solution was stirred overnight (16 hr.) at room temperature. After this time, the solution was poured into 200 ml. of methanol. No precipitation of polymer occurred.

Polymerization with Boron Trifluoride. In a 50 ml. flask equipped with stirrer, condenser, under a cover of dry nitrogen and protected by a mercury bubbler, boron trifluoride gas was introduced over a solution of 1 ml. (0.91 g.) of monomer in 5 ml. of methylene chloride maintained at Dry Ice–acetone bath temperature. After 1 hr. at this temperature the bath was removed and then after 4 hr. at room temperature the polymer was precipitated by pouring the contents of the flask into 20 ml. of methanol. The polymer was isolated and washed with 50 ml. of pure methanol and then dried for three days in a vacuum oven at 60°C. The yield was 0.73 g. (79%). The polymer was dissolved in 10 ml. methylene chloride, the solution filtered, and reprecipitated by pouring the solution into 50 ml. of methanol. The yield was 0.5 g. of soluble polymer (70% of total polymer was soluble). After being further purified by another reprecipitation from methylene chloride and two reprecipitations from benzene, the resulting polymer had an intrinsic viscosity of 0.08 in benzene, softening point of 150°C., and melting range of 150–190°C. with decomposition.

ANAL.: Calcd. for $(C_9H_{14})_n$: C, 88.45%; H, 11.55%. Found: C, 88.44%; H, 11.49%.

The infrared spectrum of this compound in a potassium bromide disk indicated a slight degree of unsaturation with the following bands: 2960, 2900 (sh.), 1640, 1455, 912, and 994 cm.$^{-1}$. An NMR spectrum of the polymer gave an integrated peak area ratio for sp^2 to sp^3 hydrogens of 1:7.5.

Polymerization with a Ziegler-Type Initiator. (1) Titanium tetrachloride (0.034 g.; 0.17 mmole) was added to 5 ml. of spectral grade *n*-

hexane under a dry nitrogen atmosphere (dry box). To this solution was added triethylaluminum (0.013 g.; 0.11 mmoles). The catalyst was aged for 20 min. and then 1 ml. of 1-methylene-4-vinylcyclohexane (0.91 g.; 7.4 mmole) was added. The reaction was allowed to proceed for 18 days and then the reaction mixture was poured into 100 ml. of methanol. The polymer which precipitated was removed, washed with fresh methanol, and dried at 60°C. in a vacuum oven. The yield was 0.35 g. (39%). Approximately 10% of this polymer was soluble in hot toluene. An NMR spectrum of the soluble polymer indicated a negligible amount of unsaturation.

(2) To 12 ml. of dry *n*-heptane under a dry nitrogen atmosphere was added 0.15 ml. of 1*M* solution of triethyaluminum in *n*-heptane (0.15 mmole). The resulting solution was cooled to 0°C., and 0.01 ml. (0.016 g.) of titanium tetrachloride (0.085 mmole) was added. This solution was "aged" for 45 min. 1-Methylene-4-vinylcyclohexane, 1 ml. (0.9 g.; 7.4 mmole) was then added. The solution was maintained at 0°C. for 6 hr. and then was permitted to warm to room temperature. After 40 hr. the solution was clear, and the reaction mixture was poured into 200 ml. of methanol. The yield of precipitated polymer was 3 mg.

(3) To 5 ml. of dry *n*-heptane under a dry nitrogen atmosphere was added triethylaluminum and titanium tetrachloride in the quantities indicated in procedure (2) above. The resulting solution was heated to reflux, cooled to room temperature, and 1 ml. (0.9 g.; 7.4 mmole) of 1-methylene-4-vinylcyclohexane added. The reaction vessel was sealed under dry nitrogen, and stirred for one week at room temperature. The reaction mixture was poured into 200 ml. of methanol. The yield of precipitated polymer was 10 mg.

(4) To 5 ml. of dry *n*-heptane under dry nitrogen was added triisobutylaluminum (0.15 ml. of 1*M* solution in *n*-heptane; 0.15 mmole), titanium tetrachloride (0.3 ml. of 0.5*M* solution in *n*-heptane; 0.15 mmole). After "aging" for 5 min., 1 ml. (0.9 g.; 7.4 mmole) of 1-methylene-4-vinylcyclohexane was added and the reaction vessel sealed under nitrogen. After six days, the contents of the vessel were poured into 200 ml. of methanol. No appreciable amount of polymer precipitated.

References

1. Butler, G. B., and R. J. Angelo, *J. Am. Chem. Soc.*, **79**, 3128 (1957).
2. Butler, G. B., *J. Polymer Sci.*, **48**, 279 (1960).
3. Field, N. D., *J. Org. Chem.*, **25**, 1006 (1960).
4. Butler, G. B., and T. W. Brooks, paper presented at Washington Meeting, Division of Polymer Chemistry, American Chemical Society, Washington, D. C., March 1962; *J. Org. Chem.*, **28**, 2699 (1963).
5. Ball, L. E., and H. J. Harwood, papers presented at St. Louis Meeting Division of Polymer Chemistry, American Chemical Society, St. Louis, Missouri, March 1961; *Polymer Preprints*, **1**, No. 2, 59 (1961).
6. Frazier, A. H., and W. P. O'Neill, *J. Am. Chem. Soc.*, **85**, 2613 (1963).
7. Reichel, B., and C. S. Marvel, *J. Polymer Sci.*, **A1**, 2935 (1963).
8. Graham, P. J., E. L. Buhle, and N. Pappas, *J. Org. Chem.* **26**, 4658 (1961).
9. Kornblum, N., W. J. Jones, and G. J. Anderson, *J. Am. Chem. Soc.*, **81**, 4113 (1959).

Résumé

On a préparé le 1-méthylène-4-vinylcyclohexane par la voie suivante (1) conversion du 4-méthylène cyclohexyl carbinol en tosylate, (2) oxydation du tosylate en 4-méthylènecyclohexane-carboaldéhyde par la méthode de Kornblum, et (3) réaction de l'aldéhyde avec l'ylide dérivé du bromure de triphénylméthylphosphonium (réaction de Wittig) pour former le diène. On a essayé de polymériser le 1-méthylène-4-cyclohexane à l'aide d'initiateurs radicalaires, anioniques, cationiques et du type Ziegler. On obtient des polymères dans les réactions catalysées par les initiateurs cationiques (trifluorure de bore) et du type Ziegler (complexe tétrachlorure d'étain et triéthylaluminium). Le polymère obtenu par polymérisation de ce monomère à l'aide de trifluorure de bore gazeux comme initiateur, est un polymère solide qui se dissout dans beaucoup de solvants organiques et se ramollit à 150°C. Les spectres infra-rouges de ces polymères révèlent la présence de bandes d'absorption typique d'une oléfine terminale. Le spectre NMR indique que le taux d'insaturation est celui d'une double liaison par deux unités monomériques. L'analyse du spectre NMR indique aussi que cette insaturation est due à un groupe vinyle plutôt qu'aux groupes méthylènes. La polymérisation du monomère à l'aide de catalyseur du type Ziegler (tétrachlorure de titane et triéthylaluminium) forment un polymère solide dont 10% seulement sont solubles dans certains solvants organiques. Bien que le spectre infra-rouge indique la présence d'insaturation terminale, l'analyse du spectre NMR indique seulement la présence d'une très petite quantité d'insaturation résiduelle. Pratiquement l'absence d'insaturation dans ce polymère linéaire supporte l'hypothèse d'une interaction intramoléculaire dans le monomère puisque les initiateurs du type Ziegler n'initient pas habituellement la polymérisation dy type "isobutylène." Ces résultats peuvent être interprêtés comme un argument supplémentaire en faveur du concept de l'interaction entre atomes non-liées, force motrice de la cyclopolymérisation.

Zusammenfassung

1-Methylen-4-vinylcyklohexan wurde nach folgender Reaktionssequenz dargestellt: (1) Umwandlung von 4-Methylencyklohexanmethanol zum Tosylat, (2) Oxydation des Tosylats zum 4-Methylencyklohexancarboaldehyd nach der Methode von Kornblum und (3) Reaktion des Aldhyds mit dem Ylid aus Triphenylmethylphosphoniumbromid in einer Wittig-Reaktion unter Bildung des Diens. Die Polymerisation von 1-Methylen-4-vinylcyklohexan wurde mit radikalischen, anionischen und kationischen Startern sowie solchen vom Ziegler-Typ anzuregen versucht. Polymere wurden aus kationisch (Bortrifluorid) und Ziegler- (Titantetrachlorid und Triäthylaluminiumkomplex) gestarteten Reaktionen erhalten. Das durch Polymerisation des Monomeren mit gasförmigem Bortrifluorid als Starter erhaltene Polymere bildet ein festes, in einer Anzahl organischer Lösungsmittel lösliches Polymeres mit einer Erweichungstemperatur von 150°C. Das Infrarotspektrum des Polymeren besass für endständige Doppelbindungen charakteristische Absorptionsbanden. NMR-Analyse zeigte, dass auf zwei Monomereinheiten eine Doppelbindung enthalten war. Weiters zeigte die NMR-Analyse, dass es sich dabei um Vinyl- und nicht um Methylengruppen handelte. Polymerisation des Monomeren mit einem Zieglerkatalysator (Titantetrachlorid und Triäthylaluminium) führte zu einem festen Polymeren, von welchem 10% in einer Anzahl organischer Lösungsmittel löslich waren. Obgleich das Infrarotspektrum dieses Polymeren die Anwesenheit endständiger Doppelbindungen erkennen liess, zeigt die NMR-Analyse nur einen extrem kleinen Betrag an restlichen Doppelbindungen. Das fast völlige Fehlen von Doppelbindungen bei diesem linearen Polymeren spricht für eine intramolekulare Wechselwirkung im Monomeren, da Starter vom Ziegler-Typ normalerweise die Polymerisation von Verbindungen vom Isobutylentyp nicht anregen. Die Ergebnisse können als zusätalicher Beweis für das Konzept der "non-bonded"-Wechselwirkung als treibende Kraft zur Bildung eines zyklischen Polymeren betrachtet werden.

Received March 9, 1964
Revised August 7, 1964

JOURNAL OF POLYMER SCIENCE: PART A VOL. 3, PP. 735–752 (1965)

Stereospecific Polymerization of 1,3-Butadiene. I. New Catalysts Based on $TiCl_4$, AlI_3, and Some Aluminum Hydride Derivatives

W. MARCONI, A. MAZZEI, M. ARALDI, and M. DE MALDÉ, *SNAM-Laboratori Riuniti Studi e Ricerche, S. Donato, Milano, Italy*

Synopsis

Some ternary catalytic systems used in the polymerization of butadiene to a prevailingly 1,4-*cis* product are described. They make use of some aluminum hydride derivatives, aluminum iodide, and titanium tetrachloride. For each catalytic system we have adopted conditions to obtain the maximum yield of polymer and the highest content of 1,4-*cis* units. Such optimum conditions are achieved at certain molar ratios of aluminum hydrides/$TiCl_4$ and $AlI_3/TiCl_4$. In particular, for a constant amount of AlI_3 and $TiCl_4$, the choice of the optimum ratio of hydride/$TiCl_4$ depends on the quantity of active hydrogens present in the aluminum compounds while it does not depend on the type substituents, e.g., chloro, amino groups, etc. The presence of Lewis bases, which tend to stabilize some aluminum hydrides and make them soluble in the reaction medium, does not influence the course of polymerization provided such bases are present in stoichiometric amount with respect to the aluminum. If, however, these complexing agents are in excess, a decrease of the catalytic activity and 1,4-*cis* content is noticed. This is more so, the stronger the basicity of the complexing Lewis base added. The results obtained in the polymerization of butadiene by means of numerous laboratory runs were confirmed by pilot-plant runs.

INTRODUCTION

The use of aluminum hydride complexes as catalysts for the stereospecific polymerization of butadiene is well known. For example, complexes of aluminum hydride with lithium[1] and of boron hydride and lithium,[2] together with titanium salts, are active catalysts which can produce polymers having a prevailingly 1,2-,1,4-*trans* structure[1] or a 1,4-*cis* one.[3]

We refer[4] particularly to those catalytic systems consisting of $LiAlH_4$, I_2, and $TiCl_4$ and to the method for the isolation of aluminum iodohydride (complexed with Lewis bases) in the reaction between $LiAlH_4$ and I_2. These complexes, successively synthesized by the reaction of AlH_3 and AlI_3 in determined molar ratios,[5] represent together with $TiCl_4$, active catalysts for the preparation of polybutadiene having excellent technological properties and with a substantially 1,4-*cis* structure.[6] A similar activity has also been shown by catalytic systems based on TiI_4 or TiI_2Cl_2 together with halogenhydrides or amidohydrides, as well as three-component systems consisting of $TiCl_4$ substituted hydrides, and elemental I_2.

It was also found that a still greater stereospecificity and a higher rate

of reaction are obtained with those ternary catalytic systems which are analogous to the previous ones with the exception that inorganic iodides, in particular AlI_3, are used instead of I_2. The results so far obtained in the polymerization of butadiene with such catalytic systems are herein described.

EXPERIMENTAL

Materials

The aluminum hydrides were prepared according to the methods reported in the literature.[5–7]

Pure commercially available $TiCl_4$ was used without further purification.

The commercially available sublimed I_2 was further sublimed in the presence of KI and used in benzene solution. The aluminum iodide was prepared by the direct combination of the elements and successively distilled under vacuum. It was also used in benzene or toluene solution. The other inorganic iodides used were pure products which were kept under vacuum at 150°C. for 24 hr. to remove any traces of water.

Solvents were purified and dehydrated according to usually acceptable methods.

Polymerizations

Our polymerization runs were carried out in beverage bottles, as previously described.[8] With preformed catalysts the order of addition was: solvent, $TiCl_4$, AlI_3, and, with stirring, the solution of the cocatalyst by means of a graduated syringe-type pipet. With catalysts prepared *in situ*, the order of addition was: solvent, butadiene, the solution of the cocatalyst, and successively the solution containing $TiCl_4$ and AlI_3 in the desired ratios.

In those runs in which we used inorganic iodides, such as BiI_3, LiI, HgI_2, and CaI_2, which were insoluble in the reaction solvent, the catalyst was prepared separately under an inert atmosphere, aged for 15 min. at 50°C., then siphoned into the reactor in the absence of monomer.

Physicochemical Measurements

The viscometric measurements were carried out in an Ubbelohde viscometer with toluene solutions at 30°C. Equation (1) was used for the calculation of the viscometric molecular weight.[9]

$$[\eta] = 3.05 \times 10^{-4} \bar{M}^{0.725} \tag{1}$$

The infrared spectra of the polymers were obtained in CS_2 solutions by means of a Perkin-Elmer model 21 instrument.

RESULTS AND DISCUSSION

Catalytic System $AlHCl_2 \cdot (C_2H_5)_2O$–$TiCl_4$–$AlI_3$

It has previously been reported that the reaction between $TiCl_4$ and $AlHCl_2 \cdot (C_2H_5)_2O$ in hydrocarbon solution brings about the immediate re-

duction of titanium.[10] The mixture so prepared is not too selective for the polymerization of butadiene and it produces a polymer whose structure is a combination of 1,4-*cis* and *trans*.

With the combined system AlI_3–$TiCl_4$, the action of the chloroalane etherate brings about a darkening of the red solution, and the catalyst so obtained is soluble in the reaction solvent if prepared in the presence of a little monomer. In the absence of monomer one obtains a black precipitate in appreciable though small quantity.

In both cases, though at different rates, the mixture so formed polymerizes butadiene to a product which is substantially 1,4-*cis*.

The order of addition of the single components is practically unimportant for the catalytic activity; however in order to have complete homogeneity it is preferable to add to the solvent in the order: monomer, $TiCl_4$, AlI_3, and lastly the reducing agent. When AlI_3 is added to $TiCl_4$ in the absence of monomer and reducing agent, one notices the formation of an oily black product if the solution is concentrated. If the AlI_3 is added to the $AlHCl_2$, a white precipitate is formed, probably due to the insoluble aluminum halogenhydride which is not complexed with ether.

Variations in the Molar Ratios of the Components. The variation in the molar ratios of the components of the catalytic complex determines

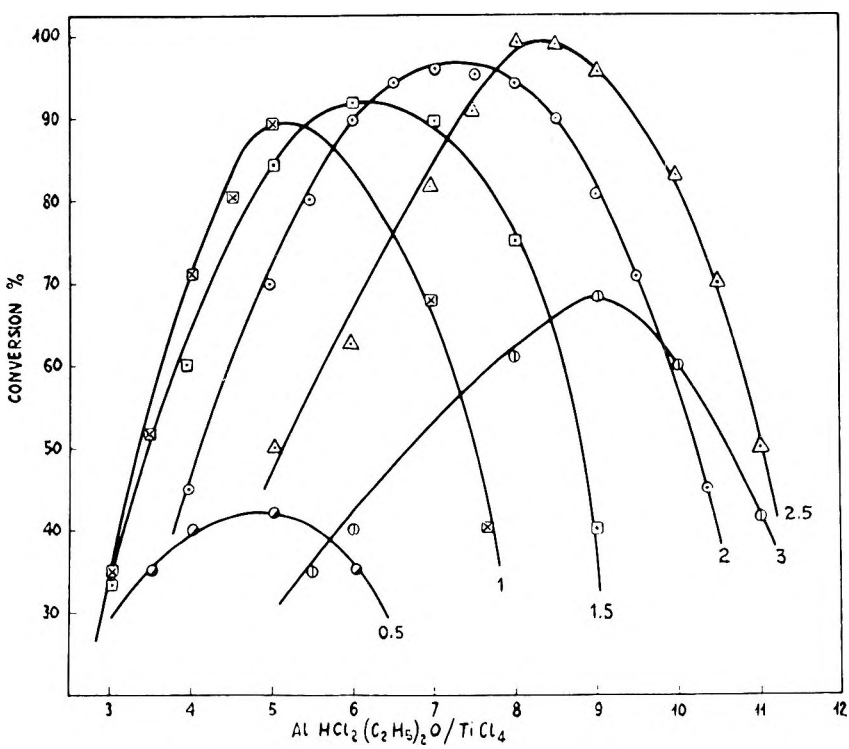

Fig. 1. Yield of solid polymer as a function of the $AlHCl_2 \cdot Et_2O/Ti$ ratios at various $AlI_3/TiCl_4$: (◒) 0.5; (⊠) 1; (⊡) 1.5; (⊙) 2; (◬) 2.5; (⏀) 3. Conditions: toluene 100 ml.; butadiene 15 g.; $TiCl_4$, 2.27×10^{-4} mole; temperature +5°C.; time 2 hr.

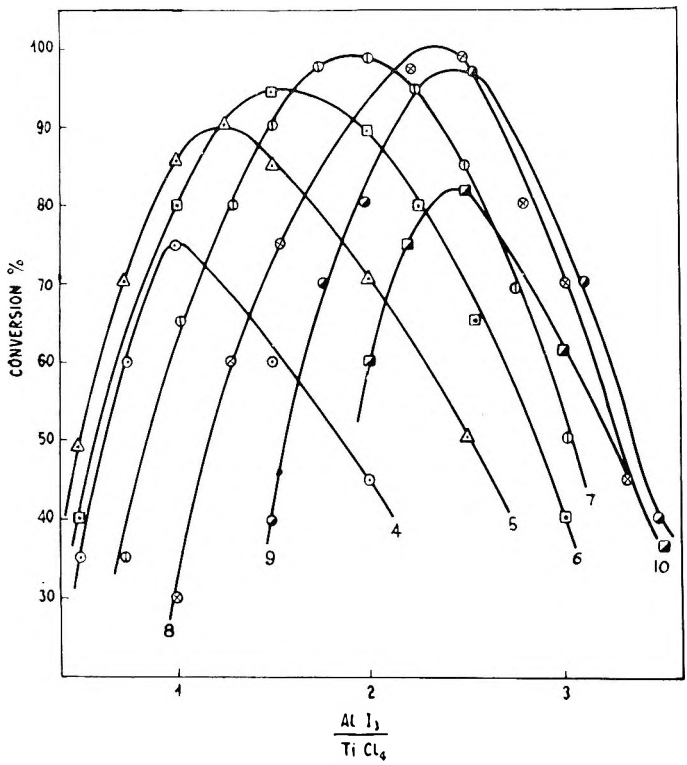

Fig. 2. Yield of solid polymer as a function of the $AlI_3/TiCl_4$ ratios at various $AlHCl_2 \cdot (C_2H_5)_2O/TiCl_4$: (⊙) 4; (△) 5; (⊡) 6; (◫) 7; (⊗) 8; (O) 9; (◪) 10. Conditions as in Figure 1.

significant changes in the conversion of the solid polymer, in its intrinsic viscosity, and to a certain extent in the percentage of the 1,4-*cis* form.

Numerous runs were made with the amount of one of the components ($TiCl_4$), the temperature, and the reaction time being kept constant and the amount of the other two components being varied. For each run we calculated the yield of the solid polymer, as coagulated in methyl alcohol, and its structure was determined by infrared analysis.

In Figure 1 are shown curves relative to the per cent conversion of the solid polymer as a function of the molar ratio $AlHCl_2 \cdot (C_2H_5)_2O/TiCl_4$, for those runs in which the concentration of $TiCl_4$ and AlI_3 were constant; analogous conversion curves as a function of the molar ratio $AlI_3/TiCl_4$ for constant quantities of $TiCl_4$ and $AlHCl_2 \cdot (C_2H_5)_2O$ are shown in Figure 2.

In Figure 3 are shown curves of points having the same per cent conversion with varying $AlHCl_2 \cdot (C_2H_5)_2O/TiCl_4$ and $AlI_3/TiCl_4$ molar ratios for runs carried out at 0°C. and for constant time of polymerization (2 hr.) and constant initial quantity of butadiene.

These average curves were obtained by taking into consideration a certain number of statistical runs and by extrapolating the missing points by a graphical method of analysis.[11]

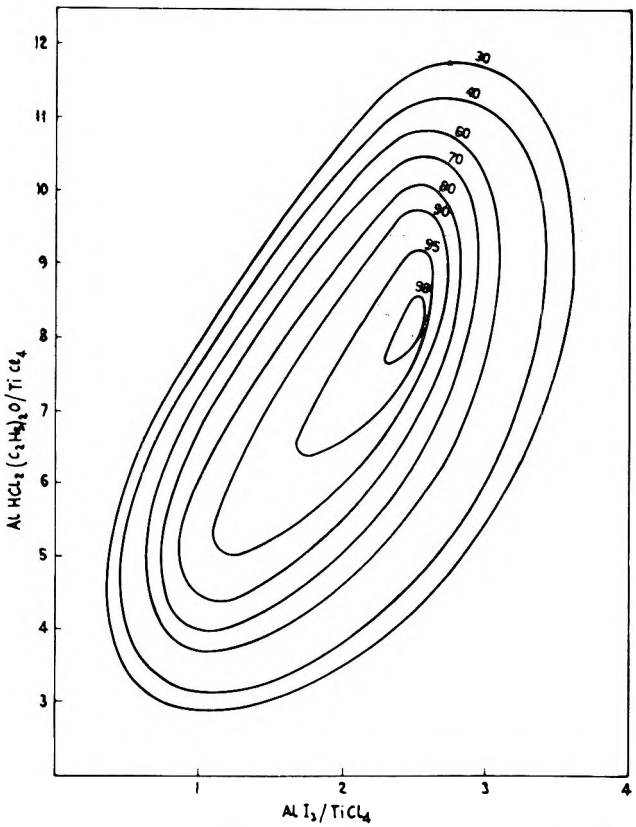

Fig. 3. Regions of equal conversions at variable ratios of $AlHCl_2 \cdot Et_2O/TiCl_4$ and $AlI_3/TiCl_4$. Conditions as in Figure 1.

It is possible to deduce from an examination of the graphs that the quantity of polymer obtained varies with the molar ratio $AlHCl_2 \cdot (C_2H_5)_2O/TiCl_4$ and with the ratio $AlI_3/TiCl_4$.

Practically no solid polymer is obtained when the molar ratio $AlHCl_2/TiCl_4$ is less than 3, independently of the quantity of AlI_3; thus the yield increases with an increase of such a ratio up to a maximum value of 8–9 (which corresponds to $AlI_3/Ti = 2.5$) while it tends to diminish for higher $AlHCl_2/TiCl_4$ values.

A change in this ratio does not appear to modify the steric structure of the polymer, which remains constantly at about 95% 1,4-*cis*.

On the contrary, a change in the molar ratio $AlI_3/TiCl_4$ influences both the structure of the polymer and the yield. For low values of this ratio, little polymer is obtained, and the yield increases with an increase in the ratio; thus for each $AlI_3/TiCl_4$ ratio, curves are obtained whose maximum values are relative to the amount of aluminum hydride present.

We have already said that when AlI_3 is not present in the catalytic system, little nonstereoregular polymer is obtained. The percentage of 1,4-

cis polymer increases up to a value of $AlI_3/Ti = 1$, after which it remains practically constant (Fig. 4).

The polymerization seems to assume a cationic character when the ratio AlI_3/Ti is greater than 4; indeed there is found an immediate increase in the reaction temperature (at times almost in an explosive way), and only low polymers which cannot be coagulated in methanol are obtained.

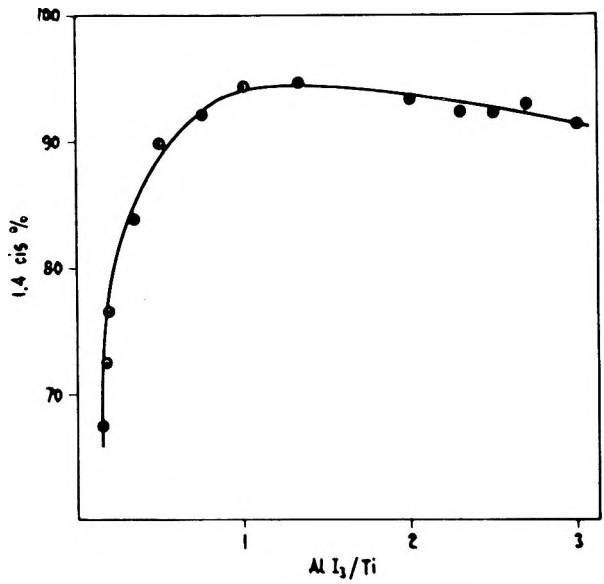

Fig. 4. Change of 1,4-*cis* content as a function of the molar ratio AlI_3/Ti. Conditions: molar ratio $AlHCl_2 \cdot Et_2O/Ti$ 6; benzene 100 ml.; $TiCl_4$ 2.27 $\times$ 10^{-4} mole; butadiene 12 g.; temperature +5°C.; time 18 hr.

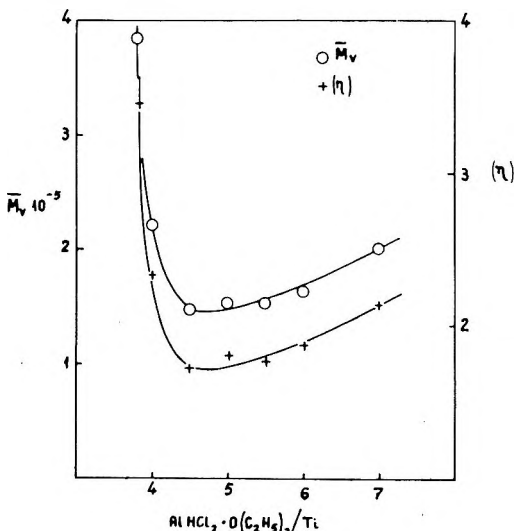

Fig. 5. Variation of $[\eta]$ and $\bar{M}_v$ as a function of the molar ratio $AlHCl_2 \cdot Et_2O/Ti$. Molar ratio $AlI_3/Ti = 1$; other conditions as in Figure 1.

Variation of the Molecular Weight of Polymers. The values of the intrinsic viscosity (measured in toluene at 30°C.) definitely depend on the molar ratios of $AlHCl_2 \cdot (C_2H_5)_2O/Ti$ and AlI_3/Ti used.

In Figure 5 is shown the change of $[\eta]$ with the change of the $AlHCl_2/Ti$ ratio, with quantities of the AlI_3 and $TiCl_4$ being kept constant.

Analogously, in Figure 6, is shown the change of $[\eta]$ as a function of the

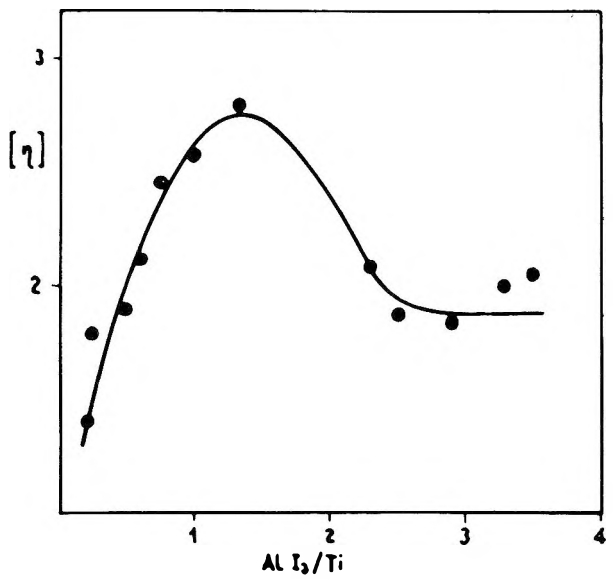

Fig. 6. Variation of $[\eta]$ as a function of the molar ratio AlI_3/Ti for constant $AlHCl_2 \cdot Et_2O/Ti = 6$.

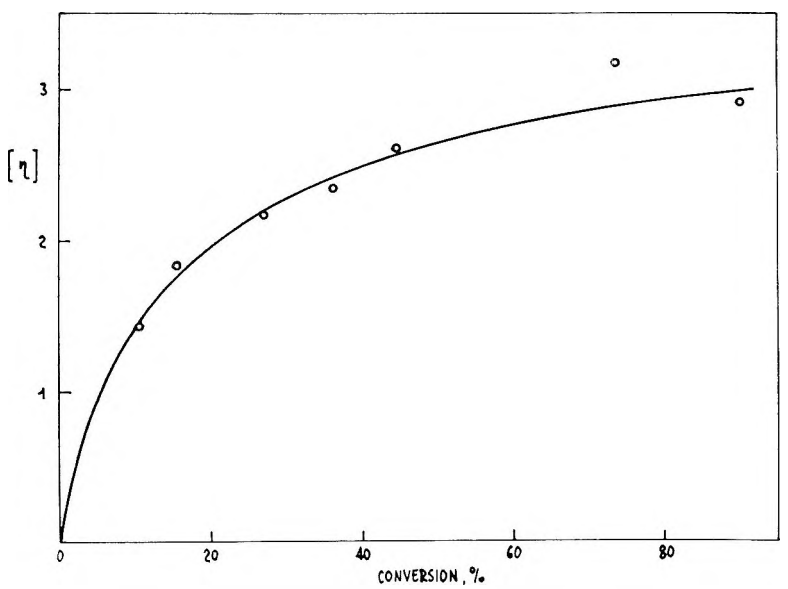

Fig. 7. Variations of $[\eta]$ with the conversion. Conditions as in Figure 1,

TABLE I
Variation of $[\eta]$ and of $\bar{M}_v$ as a Function of Catalyst Concentration[a]

Run no.	$TiCl_4$, mmole	$[\eta]$, dl./g.	$\bar{M}_v \times 10^{-3}$
1	0.0682	7.2	1.075
2	0.1365	6.44	930
3	0.159	4.46	555
4	0.182	3.86	455
5	0.2275	3.43	386
6	0.2842	3.15	343
7	0.3412	1.62	137
8	0.455	0.88	59

[a] Conditions: temperature +5°C.; time 20 hr.; molar ratio AlH_3/Ti = 1.3, $AlHCl_2 \cdot (C_2H_5)_2O/Ti$ = 5.5; toluene 120 ml.; butadiene 20 g.

molar ratio AlH_3/Ti, with the quantities of $AlHCl_2 \cdot (C_2H_5)_2O$ and $TiCl_4$ constant.

It was also observed that the intrinsic viscosity increases with the increase in yield, as shown in Figure 7.

Also, analogously to what has been found in the polymerization of isoprene[10] and to what has been reported by other authors,[12] the molecular weight of the polymer decreases with an increase of the total amount of catalyst (at constant molar ratio of the components), as is shown in the data of Table I.

Influence of Polar Solvents. Lewis base complexes of aluminum alkyl are known,[12,13] as is also the catalytic activity which the base confers to the catalytic system and the relationship which exists with the strength of the base itself.[14]

However, we did not observe with our catalytic system any difference in activity with the change of complexing agents used, if the base is present in stoichiometric amount with respect to the aluminum hydride.

However, if the Lewis base is in large excess with respect to the amount of aluminum hydride present, simultaneously a decrease in yield and 1,4-*cis* content is observed. A greater percentage of 1,4-*trans* units appears up to the point that crystalline polymers having a prevailing 1,4-*trans* structure, are obtained. The percentage of 1,2 addition remains approximately the same.

From the data reported in Table II, it is further possible to observe that the ability to inhibit the polymerization increases in the same sense as the basicity of the Lewis base and that it becomes stronger when the catalyst is prepared in the absence of monomer.

Catalytic Systems of Other Aluminum Hydride Derivatives

In addition to the dichloroalane etherate, we have also investigated other halo derivatives as well as amidoalanes not containing complexing agents. As complexing agent of the aluminum hydride and its derivatives, in addition to diethyl ether, tertiary aliphatic amines were used—for example trimethylamine—in order to obtain more soluble and

TABLE II
Influence of Polar Solvents in the Polymerization of Butadiene with the Catalytic System $AlHCl_2 \cdot$ donor + AlI_3 + $TiCl_4$[a]

Run no.	Cocatalyst with $TiCl_4$ and AlI_3	Complexing agent added		Yield, %	Infrared analysis				$[\eta]$, dl./g.
		Type	mmole		1,4-*cis*, %	1,4-*trans*, %	1,2, %	Total unsat.	
1	$AlHCl_2 \cdot O(C_2H_5)_2$	—	None	93	93	2.5	4.5	96	2.24
2		$O(C_2H_5)_2$	0.227	80	88	8	4	93	1.77
3[b]	1.14 mmole	"	2.27	63	66	30	4	94	1.08
4[b]		"	10.24	55	34	62	4	98	1.11
5[b]		"	33.6	35	12	81[c]	7	98	1.00
6	$AlHCl_2 \cdot N(C_2H_5)_3$	—	None	98	91	5	4	91	1.17
7		$N(CH_3)_3$	0.74	0	—	—	—	—	—
8	1.48 mmole	$N(C_2H_5)_3$	0.74	42	77	18	5	92	1.33
9		"	1.48	20	66	28	6	92	0.93
10		$N(n\text{-}C_4H_9)_3$	1.48	67	75.5	20	4.5	92	1.43
11		"	7.35	46	59	37	4	97	1.18
12		"	29.4	0	—	—	—	—	—
13		$N(C_6H_5)_3$	1.48	97	92.5	3	4.5	97	1.75
14		"	7.35	92	92	3	5	92	1.70

[a] Conditions: toluene 100 ml.; butadiene 15 g.; AlI_3 0.227 mmole; $TiCl_4$ 0.227 mmole; polymerization temperature +5°C.; time 2 hr.; catalyst prepared in the presence of monomer.

[b] Comparison tests in which the catalyst was prepared in the absence of monomer gave traces of polymer with a prevailing 1,4-*trans* structure.

[c] Examined by x-rays: 1,4-*trans* crystalline.

more stable compounds. [The AlH_3 etherate is insoluble due to its polymeric nature, and the $AlH_2Cl \cdot (C_2H_5)_2O$ is not too stable.]

It is also known that halogenalanes free from donor molecules have not been obtained;[15] to establish therefore the possible influence of the com-

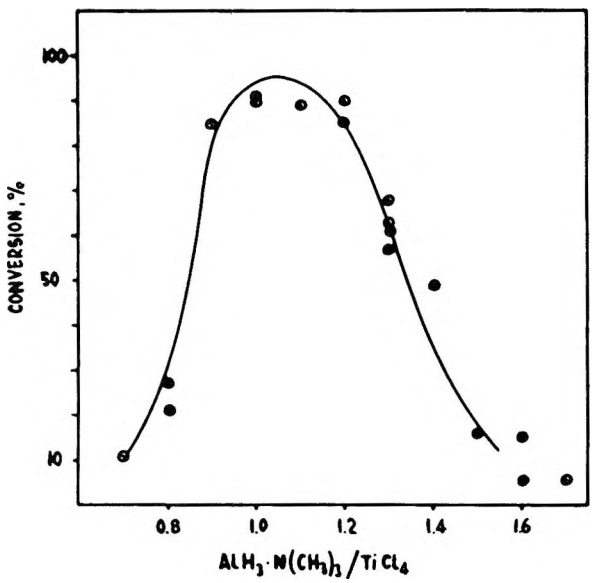

Fig. 8. Yield of solid polymer as a function of the molar ratio $AlH_3 \cdot N(CH_3)_3/Ti$. Molar ratio $AlI_3/Ti = 1$; other conditions as in Figure 1.

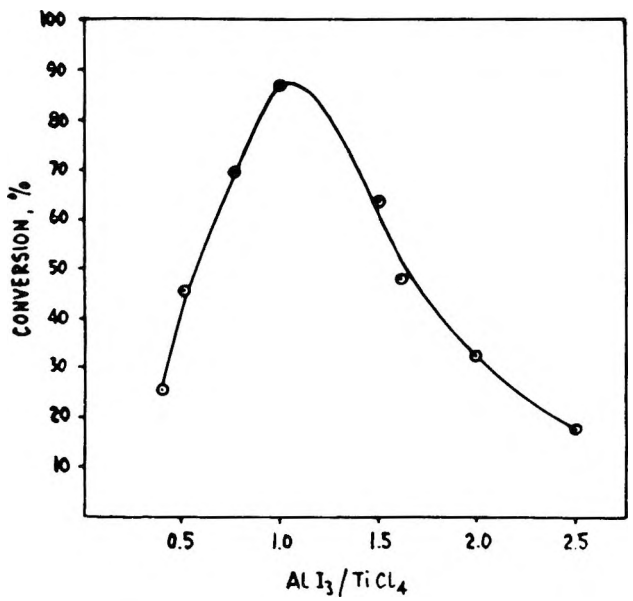

Fig. 9. Yield of solid polymer as a function of the molar ratio AlI_3/Ti, at constant AlH_3/Ti ratio.

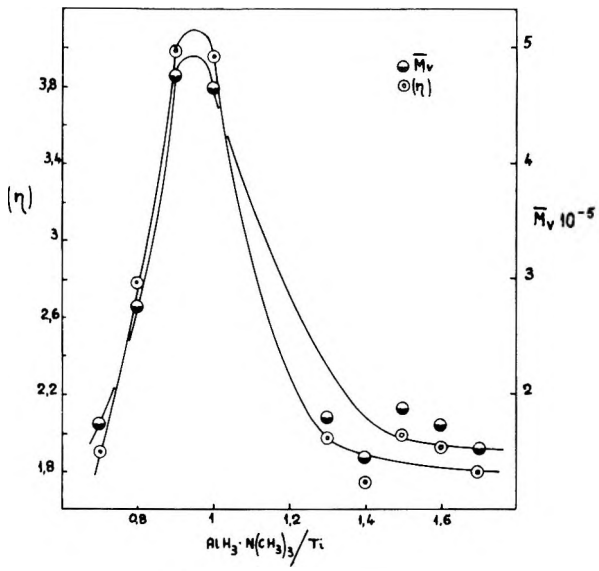

Fig. 10. Variation of $[\eta]$ and $\bar{M}_v$ as a function of the molar ratio $AlH_3 \cdot N(CH_3)_3/Ti$. Conditions as in Figure 8.

plexing agent, which is necessary for stabilization, we have synthesized amidoalanes by the reaction of AlH_3 with secondary aliphatic amines.[7] These derivatives do not coordinate with Lewis bases, due to the phenomenon of association with the formation of autocomplexes. A typical example is $AlH_2N(CH_3)_2$, which is a trimer in benzene solution, and its cocatalyst activity was compared with those systems mentioned above. For each catalyst system, we studied the range of molar ratios for which the best conditions of stereospecificity and yield of solid polymer are obtained.

$AlH_3 \cdot N(CH_3)_3$–$TiCl_4$–AlI_3. In Table III are shown results of some polymerization runs of butadiene in the presence of such a catalytic system.

The course of the conversion of solid polymer as a function of the only variable amount of aluminum hydride (at a constant ratio $AlI_3/Ti = 1$) is reported in Figure 8. It is of interest to point out that the curve is valid within a narrow range of ratios ($AlH_3/Ti = 0.8$–1.6), in agreement with the presence of three active hydrogen atoms in the hydride molecule.

Figure 9 shows the change in yield with the change in the molar ratio AlI_3/Ti (at constant ratio $AlH_3/Ti = 1.1$). The steric structure of the polymers obtained is practically constant within the range of ratio considered.

Figure 10 shows the change of the viscosity as a function of the change in the amount of $AlH_3 \cdot N(CH_3)_3$ in the catalyst.

$AlH_2Cl \cdot N(CH_3)_3$–$TiCl_4$–AlI_3. This ternary system was briefly investigated. Due to the presence of two active hydrogens in the cocatalyst, the values of the molar ratio AlH_2Cl/Ti (for constant ratios of AlI_3/Ti),

TABLE III
Influence of the Ratios $AlH_3 \cdot N(CH_3)_3/TiCl_4$ and $AlI_3/TiCl_4$ on the Conversion and Structure of the Polymer[a]

Run no.	$AlH_3 \cdot N(CH_3)_3$ / $TiCl_4$ molar ratio	AlI_3 / $TiCl_4$ molar ratio	Butadiene, g.	Yield, %	Infrared analysis: 1,4-*cis*, %	1,4-*trans*, %	1,2, %	Total unsat.	[η], dl./g.
1	0.7	1	12.9	10	93.2	2.7	4.1	—	1.90
2	0.8	1	11.4	20.8	94.8	1.1	4.1	95	2.78
3	1	1	12	89.6	94.3	1.2	4.5	96	3.95
4	1.2	1	12.2	98.7	93.7	1.8	4.5	94	4.20
5	1.3	1	11	62.8	93	2.5	4.5	94	1.97
6	1.4	1	13	48.5	91.8	3	5.2	89	1.74
7	1.5	1	12.4	15.4	85.4	9.6	4.5	95	1.99
8	1.6	1	16	15.6	92.9	2.2	4.9	97	2.43
9	1.7	1	12	6	87.8	7	5.2	97	1.80
10	1.1	0.4	11.16	25	92.6	3.4	4	97	3.73
11	1.1	0.75	5.48	69.5	93.5	2	4.7	95	3.33
12	1.1	1	12.6	86.9	94.1	1.5	4.4	96	4.23
13	1.1	1.5	14.2	63.4	94.8	1.2	4.0	99	4.22
14	1.1	2	11.9	33.3	94	2	4.0	96	1.71
15	1.1	2.5	14.3	18.5	93.8	2.2	4.0	97	1.83

[a] Conditions: $TiCl_4$ 0.2275 mmole; benzene 100 ml.; temperature 5°C.; time 2 hr.

for which the greatest conversion is obtained, fall within the range of 2.5–3.2, with a maximum at ratio = 3.

If the molar ratio of $AlI_3/TiCl_4$ is varied (for $AlH_2Cl/TiCl_4 = 3$) the maximum yield is obtained in the range of 1.7–2.5.

TABLE IV
Influence of $AlH_2Cl \cdot N(CH_3)_3/TiCl_4$ and $AlI_3/TiCl_4$ ratios on the Yield and on the Microstructure of Polymers[a]

Run no.	$AlH_2Cl \cdot NR_3$ / $TiCl_4$ molar ratio	AlI_3 / $TiCl_4$ molar ratio	Yield, %	Infrared analysis: 1,4-*cis*, %	1,4-*trans*, %	1,2, %	Total unsat.
1	2	2	15.34	94.6	1.2	4.1	100
2	2.5	2	71.8	94.0	1.3	4.6	99
3	3	2	79.3	94.0	1.6	4.4	98
4	3.5	2	31.5	94.2	1.5	4.3	100
5	3	0.8	[b]	—	—	—	—
6	3	1	15.3	86.5	9.1	4.4	99
7	3	1.3	61	90.0	5.3	4.6	100
8	3	2	91.8	90.3	5.4	4.3	99
9	3	2.5	60.5	94.1	1.4	4.5	98
10	3	3	28.4	92.6	2.5	4.9	97
11	3	3.5	29	93.6	1.8	4.6	98

[a] Conditions: $TiCl_4$ 0.2275 mmole; butadiene 11 g.; benzene 100 ml.; temperature +5°C.; time 2 hr.

[b] Not calculated.

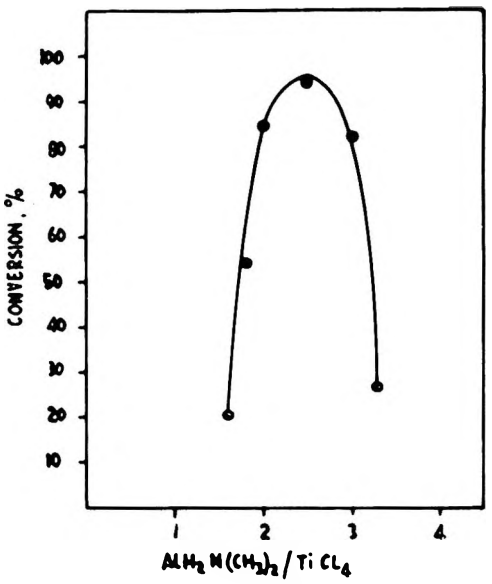

Fig. 11. Yield of solid polymer as a function of the molar ratio $AlH_2N(CH_3)_2/Ti$. Conditions: toluene 100 ml.; butadiene 10 g.; $TiCl_4$ 1.82 × 10^{-4} mole; molar ratio $AlI_3/Ti = 2$; temperature +5°C.; time 1 hr.

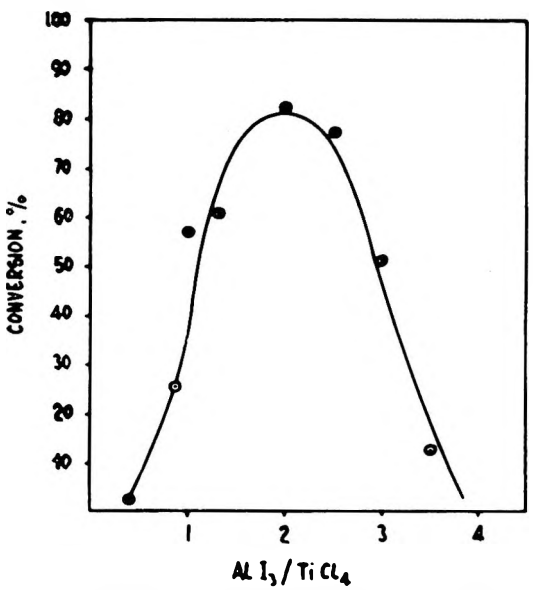

Fig. 12. Change of conversion as a function of the molar ratio AlI_3/Ti, at constant ratio $AlH_2N(CH_3)_2/Ti = 3$.

The microstructure of the polymers does not vary much within the range of the ratios mentioned (Table IV).

$AlH_2N(CH_3)_2$–$TiCl_4$–AlI_3. A close analogy was found between this system and the one described previously. The change in yield versus the change in the molar ratios of the components is shown in Figures 11 and 12.

The structure of the polymers has a high 1,4-*cis* content and it remains so in the ratio range studied by us. From a comparison of the various systems reported, we can deduce that the structure of the polymer is independent of the particular type of cocatalyst used and the yield is related to the active hydrogen present.

Catalytic Systems Having Metallic Iodides Other than AlI_3

In those polymerization runs described up to now, we have always used AlI_3 as the third catalytic component. This choice was made on the basis of its solubility in benzene, in which the catalyst is prepared (by the feeding of benzene solutions of the three components). We have however extended our study to other metallic iodides and we have observed their behavior in the polymerization process.

Some results are given in Table V. Those catalysts prepared with the use of insoluble iodides such as LiI and NaI were allowed to age in heat, in the absence of monomer, and then added by means of a siphon to the polymerization vessel.

Not much can be said at the present regarding the dependence of the catalytic activity on the type of iodide used. From the results obtained one can see that the solubility of the salt in benzene is not a determining condition (if only for practical reasons) in its choice as the catalytic component. Based on our preceding considerations,[4] one could suppose that even in this case, an exchange reaction between the inorganic iodide and the aluminum hydride derivative takes place, with the formation of iodohydrides. These latter compounds, together with $TiCl_4$, would form the true, active catalyst in the polymerization.

A direct exchange, on the other hand, between iodide and $TiCl_4$ would be equally probable.

Pilot-Plant Runs

A significant amount of 1,4-*cis* polybutadiene was produced in a pilot plant by using an $AlHCl_2 \cdot (C_2H_5)_2O$–$TiCl_4$–$AlI_3$ catalytic system. This has allowed us to study at length the properties of the polymer and to compare with 1,4-*cis*-polybutadienes obtained with other known catalytic systems.

The pilot-plant polymerizations have shown an analogous behavior regarding the yield and the structure of the polymer with respect to laboratory runs. In particular, it was possible to reduce the total amount of catalyst (to less than 1% by weight with respect to the monomer), polymers with Mooney viscosity between 43 and 55 being obtained.

Figure 13 shows the course of the conversion and of the Mooney viscosity versus the reaction time in a typical example of a pilot-plant polymerization.

The polymers so obtained were vulcanized according to the recipe: 100 polymer, 50 HAF carbon black, 2 stearic acid, 3 ZnO, 1 antioxidant, 5

TABLE V

Polymerization of Butadiene with $TiCl_4$, $AlHCl_2 \cdot (C_2H_5)_2O$, and Inorganic Iodides Other than AlI_3[a]

Run no.	Iodide Me^nI_n Type	Amt., mmole	$TiCl_4$, mmole	$AlHCl_2 \cdot (C_2H_5)_2O$ mmole	Me^nI_n/Ti molar ratio	Al/Ti molar ratio	Butadiene, g.	Time, hr.	Yield, %	Infrared analysis 1,4-*cis*, %	1,4-*trans*, %	1,2, %	Total unsat.	[η], dl./g.
1	LiI	0.916	0.2275	1.49	4	6.5	12	19	25	93.2	2.4	4.4	97	2.52
2	BiI_3	0.475	0.2275	1.59	2	7	9	20	30	94.7	1.3	4.0	96	7.15
3	MgI_2	0.89	0.357	2.32	2.5	6.5	7	24	10	82	10	8	—	—
4	NaI	1.2	0.3	1.95	4	6.5	13	24	15	55	19	26	—	—
5	HgI	0.57	0.285	1.71	2	6	9.5	48	[b]					
6	PI_3	0.29	0.2275	1.365	1.33	6	11	48	[c]					
7	$[(CH_3)_4N]I$	0.91	0.2275	1.365	4	6	12	48	[b]					
8	NH_4I	0.91	0.2275	1.365	4	6	14	48	[b]					
9	CoI_2	0.52	0.2275	1.56	2	7	11	17	30	90.7	5.0	4.3	95	2.2

[a] Conditions: toluene 100 ml.; temperature +5°C.

[b] No polymer obtained.

[c] Trace amounts of polymer obtained.

TABLE VI
Technological Determinations of a Tread-Type Compound

Property	Value	Method of test
ML 1 + 4 (100°C.) polymer	47.5	ASTM D 927-57T
ML 1 + 4 (100°C.) compound	83.5	" "
300% Modulus, kg./cm.^{2}	97	ASTM D 412-51T
Tensile strength, kg./cm.^{2}	164	" "
Elongation at break, %	430	" "
Hardness Shore A	64	ASTM D 676-55T
Rebound, %	67	*Proceeding Intern. Rubber Conf. Wash.*, 1959, p. 162
Heat build-up ΔT, °C.	22	ASTM D 623-58 (15 min.)
Abrasion loss, mm.^{3}	25	DIN 53-516 (1 kg.)

disproportionated rosin acid, 5 aromatic oil, 1.75 sulfur, 0.8 *N*-oxydiethylene benzothiazole sulfonamide, 0.09 benzothiazole-disulfur; the vulcanization temperature was 144.5°C.; the time was 50 min.

The determinations made on the vulcanized product are reported in Table VI.

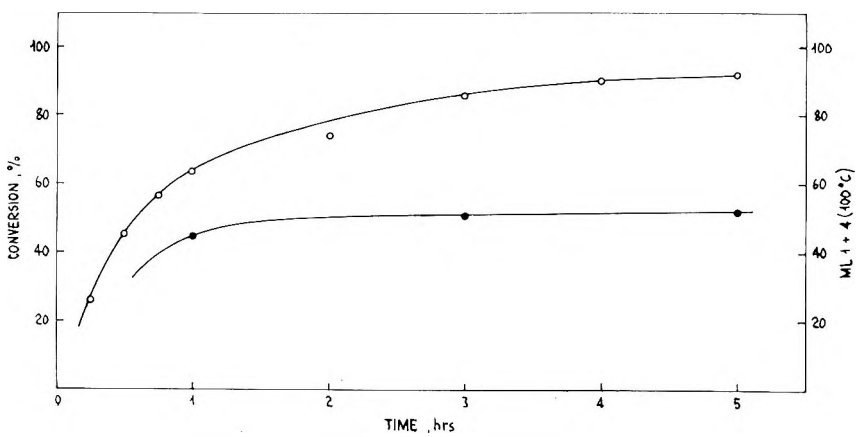

Fig. 13. Change of conversion and of Mooney viscosity with reaction time in a typical run carried out in a pilot plant: (O) Conversion; (●) Mooney.

CONCLUSIONS

A catalytic complex, capable of polymerizing butadiene to polymers having a high 1,4-*cis* content, is obtained by the interaction of aluminum hydrides and its derivatives with $TiCl_4$ and AlI_3. If the catalytic complex is prepared in the presence of monomer, then the polymerization takes place in a homogeneous phase.

The presence of an iodide compound is necessary for the polymerization to be homogeneous and to obtain 1,4-*cis* polymers. When these iodides

are absent, the yields are lowered and the per cent of 1,4-*trans* units in the polymer tends to increase.

The aluminum hydrides show an excellent activity for yields as well as for the structure of the polymer obtained, relative to a determined value of the aluminum hydride/$TiCl_4$ and $AlI_3/TiCl_4$ molar ratios.

For a given ratio of $AlI_3/TiCl_4$, the optimum value of the ratio aluminum hydride/$TiCl_4$ depends on the number of active hydrogens present in the molecule. The optimum value of the ratio H_{active}/Ti is independent of the nature of the substituents of the aluminum (chlorine atoms or secondary amines) and of the complexing agent.

The aluminum hydrides which we employed in the polymerizations are generally complexed with Lewis bases. Contrary to the behavior with aluminum alkyls, we did not notice any differences in activity in experiments carried out with complexed hydrides and those with noncomplexed hydrides such as AlH_2NR_2.

If the Lewis base was in excess, a decrease in yields and in 1,4-*cis* content in the polymer was noted. Such an inhibiting effect increases in the same direction as the basicity of the Lewis base.

The optimum conditions for the described polymerization process were confirmed by numerous runs carried out in a pilot plant, especially with respect to the yield and the structure of polymer.

References

1. Phillips Petroleum Co., Belgian Pat. 551,851 (Oct. 17, 1956).
2. The Distillers Co., French Pat. 1,186,323 (Aug. 20, 1959).
3. SNAM-L.R.S.R., Belgian Pat. 616,725 (Oct. 22, 1962).
4. Marconi, W., A. Mazzei, M. Araldi, and M. De Maldé, *Chim. Ind.* (*Milan*), **46,** 245 (1964).
5. Wiberg, E., *Z. Naturforsch.*, **6b,** 458 (1951).
6. SNAM-L.R.S.R., French Pat. 1,333,265 (June 17, 1963).
7. Ruff, J. K., and M. F. Hawthorne, *J. Am. Chem. Soc.*, **82,** 2141 (1960); *ibid.*, **83,** 535, 2835 (1961); W. Marconi, A. Mazzei, S. Cucinella, and M. De Maldé, *Gazz. Chim. Ital.*, **92,** 1062 (1962).
8. Marconi, W., M. Araldi, A. Béranger, and M. De Maldé, *Chim. Ind.* (*Milan*), **45,** 522 (1963).
9. Danusso, F., G. Moraglio, and G. Giannotti, *J. Polymer Sci.*, **51,** 475 (1961).
10. Marconi, W., A. Mazzei, S. Cucinella, and M. De Maldé, *Makromol. Chem.*, **71,** 118 (1964); *ibid.*, **71,** 134 (1964).
11. Bertsch, P., E. I. Du Pont de Nemours, Bulletin BL 355, June 1959.
12. Henderson, J. F., paper presented at the International Symposium of Macromolecular Chemistry, Paris, July 1–5, 1963; *J. Polymer Sci.*, **C4,** 233 (1964).
13. Zambelli, A., G. Natta, and I. Pasquon, paper presented at the International Symposium of Macromolecular Chemistry, Paris, July 1–5, 1963; *J. Polymer Sci.*, **C4,** 411 (1964).
14. Schoemberg, E., D. L. Chalfant, F. Fazson, J. B. Pyke, and R. H. Mayor, paper presented at the American Chemical Society Symposium on Metal Alkyl-Catalyzed Polymerization, New York, Sept. 11, 1963.
15. Wiberg, E., K. Modritzer, and R. Uson, *Rev. Acad. Ciencias Ex., Fis. Quim. Nat.* (*Zaragoza*), **9,** 91 (1954).

Résumé

On décrit quelques systèmes catalytiques ternaires employés dans la polymérisation du butadiène en vue d'obtenir un produit de structure prédominante 1,4-*cis*. On utilise des dérivés de l'hydrure d'aluminium, de l'iodure d'aluminium et du tétrachlorure de titane. Pour chaque système catalytique, on a employé des conditions nécessaires à l'obtention d'un rendement maximum en polymère et la teneur la plus élevée en unités 1,4-*cis*. Les conditions optimales sont obtenues par détermination des rapports molaires $AlH_3/TiCl_4$ et $AlI_3/TiCl_4$. En particulier, pour une quantité constante en AlI_3 et en $TiCl_4$, le choix du rapport optimum hydrure/$TiCl_4$ dépend de la quantité d'hydrogènes actifs présents dans le composé de l'aluminium, tandis qu'il ne dépend pas de la nature des substituants tels que: chlore, groupements aminés, etc. La présence des bases de Lewis, qui tendent à stabiliser certains hydrures d'aluminium, et qui les rendent solubles dans le milieu réactionnel, n'influence pas le cours de la polymérisation, pourvu qu'elles soient présentes en quantité stoéchiométrique par rapport à l'aluminium. Néanmoins, si les agents complexants sont en excès, on constate une diminution de l'activité catalytique et de la teneur en 1,4-*cis*; cela est d'autant plus prononcé qye la basicité de la base de Lewis complexante ajoutée est plus grande. Les résultats obtenus dans la polymérisation du butadiène au laboratoire sont confirmés par les expériences effectuées en usine pilote.

Zusammenfassung

Einige ternäre katalytische, bei der Polymerisation von Butadien zu einem vorwiegenden 1,4-*cis*-Produkt verwendete Systeme werden beschrieben. Dazu werden gewisse Aluminiumhydridderivate, Aluminiumjodid und Titantetrachlorid verwendet. Für jedes katalytische System wurden die Bedingungen zur Bildung der maximalen Ausbeute an Polymerem und des höchsten Gehalts an 1,4-*cis*-Einheiten eingehalten. Solche optimalen Bedingungen werden durch bestimmte Molverhältnisse Aluminiumhydrid/$TiCl_4$ und $AlJ_3/TiCl_4$ erreicht. Im besonderen hängt für eine konstante Menge von AlJ_3 und $TiCl_4$ die Wahl des optimalen Verhältnisses Hydrid/$TiCl_4$ von der Menge des in der Aluminiumverbindung vorhandenen aktiven Wasserstoffs, nicht aber vom Typus seiner Substituenten wie Chlor-, Aminogruppen etc. ab. Die Anwesenheit von Lewis-Basen, welche eine Tendenz zur Stabilisierung gewisser Aluminiumhydride haben und sie im Reaktionsmedium löslich machen, beeinflusst den Verlauf der Polymerisation nicht, vorausgesetzt, dass sie in stöchiometrischen Mengen in bezug auf das Aluminium anwesend sind. Bei Vorhandensein eines Überschusses dieses Komplexierungsmittels tritt jedoch eine Abnahme der katalytischen Aktivität und des 1,4-*cis*-Gehaltes ein. Diese ist umso grösser, je stärker die Basizität der zugesetzten komplexierenden Lewis-Base ist. Die in zahlreichen Laboratoriumsversuchen für die Polymerisation von Butadien erhaltenen Ergebnisse wurden durch Technikumsversuche bestätigt.

Received April 6, 1964
Revised May 27, 1964

JOURNAL OF POLYMER SCIENCE: PART A VOL. 3, PP. 753–766 (1965)

Stereospecific Polymerization of 1,3-Butadiene. II. Kinetic Studies

A. MAZZEI, M. ARALDI, W. MARCONI, and M. DE MALDÉ,
SNAM-Laboratori Riuniti Studi e Ricerche, S. Donato, Milano, Italy

Synopsis

The kinetics of the polymerization of butadiene with catalysts prepared from some aluminum hydride derivatives, AlI_3, and $TiCl_4$ was investigated. It was found that the reaction rate is first-order with respect to monomer and catalyst concentration when the catalyst is prepared in the presence of monomer. In such a case the polymerization takes place in a homogeneous medium. When the catalyst is prepared in the absence of monomer, the reaction takes place in an heterogeneous medium and the rate is still first order with respect to monomer concentration, while the dependence on the catalyst concentration is no longer linear. The activation energy of the entire process is about 8500 cal./mole. In addition, a comparison is made of the polymerization rate of catalysts obtained from AlI_3, $TiCl_4$, and various aluminum hydride derivatives.

INTRODUCTION

The kinetic study of the polymerization of diolefins with stereospecific catalytic systems has been the object of several publications in recent years.

It was found,[1] in the polymerization of isoprene with the catalytic system $TiCl_4$–Al (isobutyl)$_3$, that a linear dependence exists between the rate of reaction and the monomer concentration at a constant Al/Ti molar ratio. The dependence of the rate of reaction with temperature was also studied, and the activation energy was calculated to be 14 kcal./mole. This value, which is definitely lower than that found for the free-radical polymerization of isoprene, would provide further evidence for the ionic nature of the catalytic system based on aluminum alkyls and titanium salts.

The same system was also studied for the polymerization of 1,3-butadiene.[2] It is known that with this catalytic system, some variations in the microstructure of polybutadiene are obtained with the change in the Al/Ti molar ratio.[3] These variations are also found in the kinetic order of the reaction of polymerization; with Al/Ti ratios varying between 1 and 1.5, the rate of polymerization is first-order with respect to the concentration of the monomer and of the catalyst, and the resulting polymer is essentially 1,4-*trans*. When the Al/Ti ratio is over 2, the rate of the disappearance of monomer is proportional to the square concentration of butadiene; for Al/Ti ratios between 1.6 and 2, there exists a transition interval where the dependence of the rate on the monomer concentration goes gradually from first to second order.

As we have noted previously,[4] it has been possible to obtain butadiene polymers with a high 1,4-*cis* content by using a three-component catalytic system based on halogen-derivative complexes of aluminum hydride, titanium salts, and aluminum iodide. After our first note[5] on the kinetics of polymerization with these new catalytic systems, we wish to report further data from our studies. Our investigation is limited to the catalytic system $AlHCl_2 \cdot (C_2H_5)_2O + TiCl_4 + AlI_3$. A comparison is also made between this system and others which use different hydrides.

CONDITIONS SELECTED FOR THE POLYMERIZATION RUNS

As it was previously reported, the yield of solid polymer depends on the molar ratio of the three components of the catalytic system. For this reason, the kinetic runs were made at constant ratios: $AlHCl_2 \cdot (C_2H_5)_2O/TiCl_4 = 5.5$ and $AlI_3/TiCl_4 = 1.3$. Such values are not exactly the same as those for which the best yield is obtained with comparable time limit, but they are very close to them and within the area of the average curve relative to a 90% yield in 2 hr.[4]

We have chosen these values due to the economy of the catalyst, the excellent molecular weight, and the high 1,4-*cis* content in the polymer obtained.

The solvent used in all cases was toluene, which enhances experimentation at low temperature. The use of benzene, for runs carried out at room temperature, leads to a rate slightly better than with other aromatic hydrocarbon solvents. The apparatus used is entirely made of glass, and it consists of a reactor with a mixer, addition funnel, and a siphoning device operating under inert gas pressure. In the experimental part, a typical polymerization run is described in detail. All the monomer is introduced into the reactor at the beginning by absorbing it into the solvent at low temperature.

The course of polymerization was followed by removing aliquots from the reaction mixture and weighing them after evaporation of the monomer and of solvent. In following this method it is important to operate with dilute solutions which are not too viscous and to limit the course of the reaction to a relatively short time (generally not to exceed 50% conversion). For longer time or for greater monomer concentration, the data obtained do not fit the presupposed path.

The polymerization runs were carried out either with preformed catalysts (aging time 2–3 min.), or with catalysts prepared in the presence of monomer.

RESULTS AND DISCUSSION

The following equation was considered for the kinetics of the stereospecific polymerization of butadiene in solution:

$$-dM/dt = K[M]^{\alpha}[Cat]^{\beta} \qquad (1)$$

where M = grams of monomer present at time t; t = time of polymerization (minutes); K = rate constant; [Cat] = the sum of concentrations of the components in the catalyst (moles/liter of solution); α and β = constants.

The order of the reaction with respect to monomer and to catalyst was determined, and the value of K and the activation energy were calculated.

Catalysts Prepared in the Presence of Monomer

The catalyst was directly prepared in the reactor in the presence of monomer, the reagents being added in the following order: solvent, chloroaluminum hydride etherate, butadiene, and the toluene solution of $TiCl_4$ and AlI_3, the latter by means of an addition funnel which has been kept at the desired temperature.

An immediate slight rise in temperature due to catalyst formation was noticed; the mixture, however, was brought back to its initial temperature setting by a thermostatted bath.

Under these conditions, the polymerization takes place in a homogeneous phase. Runs in which the catalyst was prepared in the presence of very little monomer followed by successive filtration or centrifugation on porous G4 settings did not leave any catalyst residue.

Determination of the Reaction Order with Respect to Monomer

In Figure 1 and in Table I the per cent conversion is given as a function of time for those runs made at constant $AlHCl_2 \cdot (C_2H_5)_2O/TiCl_4/AlI_3$ molar ratios and at 0°C. for initial concentrations of catalysts at variable conditions.

TABLE I
Polymer Conversion at Various Concentrations of Initial Catalyst and at Constant Temperature[a]

Run no.	$TiCl_4$, mmole/l.	Total catalyst mmole/l.	Polymer conversion at given times, %							
			5 min.	10 min.	15 min.	20 min.	25 min.	30 min.	35 min.	45 min.
1	0.214	1.681	2.6	—	4.95	—	7.9	—	10.4	13.1
2	0.32	2.495	—	8.1	—	16.7	20.3	23	26	30.6
3	0.423	3.363	4.8	9.4	13.6	18.8	—	27	—	—
4	0.64	4.99	—	—	18.3	23.7	28.5	33.2	38	—
5	0.856	6.726	8.25	15	22.25	28.7	35.7	40.1	—	—
6	1.295	10.08	15.1	26.8	34.4	41.5	45.3	53	—	—
7	1.712	13.45	20	32.15	42	49.9	57	64.3	—	—

[a] Polymerization conditions: butadiene 1.327 mole/l., temp. °C.

By supposing $\alpha = 1$, eq. (1) can be integrated between the initial time t_0 and t, giving:

$$\ln (M_0/M) = K [\text{Cat}]^{\beta} t \qquad (2)$$

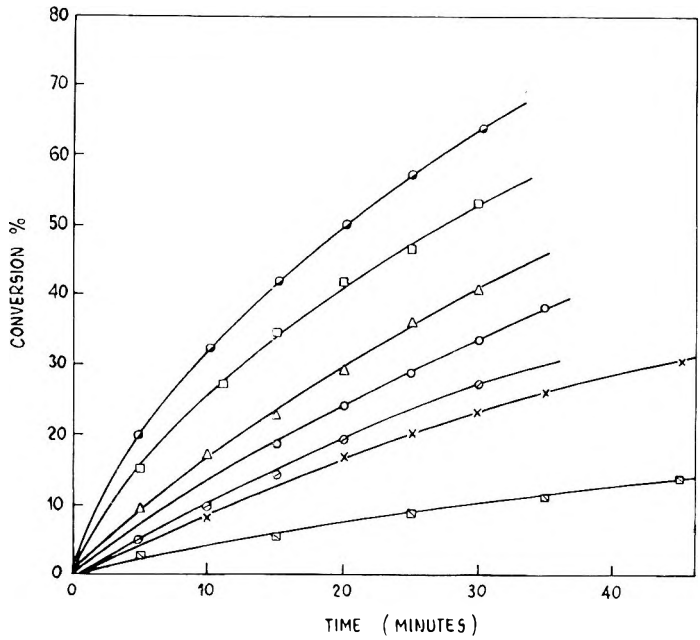

Fig. 1. Course of the conversion as a function of time at various $TiCl_4$ concentrations: (□) 0.214 mmole/l.; (×) 0.32 mmole/l.; (⊘) 0.428 mmole/l.; (○) 0.64 mmole/l.; (△) 0.856 mmole/l.; (□) 1.295 mmole/l.; (◕) 1.712 mmole/l. Conditions: butadiene 1.327 mole/l.; $AlHCl_2.O(C_2H_5)_2/TiCl_4 = 5.5$; $AlI_3/TiCl_4 = 1.3$; temperature 0°C.

where, M_0 = weight of monomer (grams) present initially at time $t_0 = 0$. In Figure 2, $\ln (M_0/M) = f(t)$ is given; this plot indicates, from the linearity of the curves, that the reaction is truly of the first order with respect to monomer.

Determination of the Reaction Order with Respect to Catalyst

Since the polymerizations are carried out at constant temperature (0°C.) and initially at constant amount of monomer, the lines in Figure 2 show a dependence of the reaction rate on the catalyst concentration. The angular coefficient of these lines is equal to:

$$\ln (M_0/M)/t = K\ [\mathrm{Cat}]^{\beta} \tag{3}$$

as can be deduced from eq. (2).

In Figure 3, we show the values of the angular coefficient of the lines as a function of the catalyst concentration, expressed as the sum of $AlHCl_2$–$TiCl_4$–AlI_3 at constant ratios of 5.5 and 1.3.

Since the points fall on a straight line, we can conclude that β must be equal to 1, that is to say, the polymerization rate with respect to the catalyst concentration is of the first order. The angular coefficient of the straight line in Figure 3 is the following:

$$\frac{\ln(M_0/M)/t}{[\mathrm{Cat}]} = K = 2.25 \text{ min.}^{-1} \text{ mole}^{-1}$$

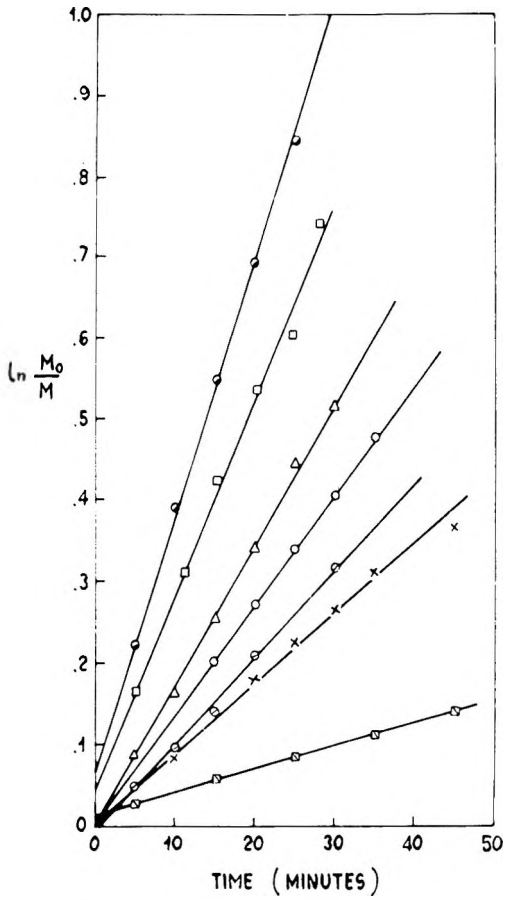

Fig. 2. Diagram of the polymerization of butadiene as a first-order reaction. Conditions and symbols as in Figure 1.

Determination of the Activation Energy

The activation energy is determined according to the Arrhenius equation:

$$K = f(T) = Ae^{-E/RT} \tag{4}$$

where T is absolute temperature.

For this purpose, polymerization runs were made at various temperatures (−6, 0, 12, 18, 21°C.), at constant concentration of catalyst and monomer (Table II).

In Figure 4 we report ln (M_0/M) as a function of time at various temperatures. By multiplying both sides of eq. (4) by [Cat] = constant, we obtain:

$$K[\text{Cat}] = A[\text{Cat}]e^{-E/RT} = Be^{-E/RT}$$

where B is a constant,

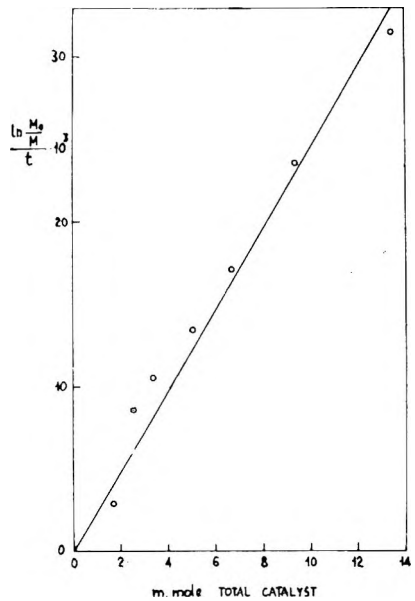

Fig. 3. Plot of $\ln(M_0/M)$ as a function of total catalyst at constant molar ratios of $AlHCl_2.(C_2H_5)_2O/Ti = 5.5$; $AlI_3/Ti = 1.3$.

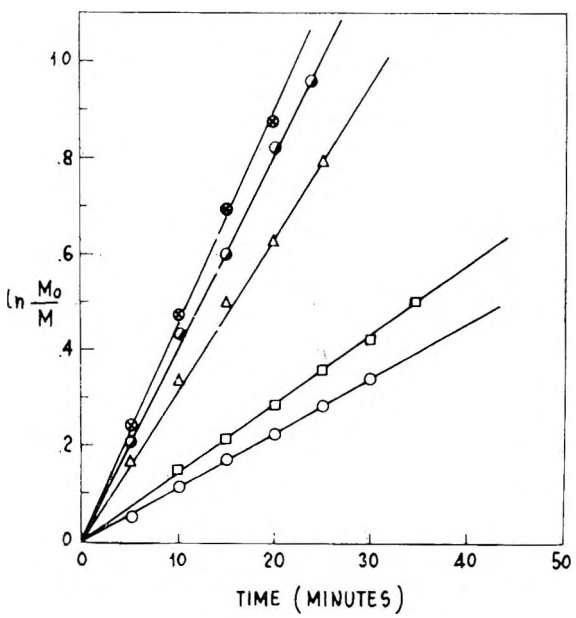

Fig. 4. Effect of temperature on the reaction rate: (O) −6°C.; (□) 0°C.; (△) +12°C.; (◪) +18°C.; (⊗) +21°C. Conditions: butadiene 1.327 mole/l.; $TiCl_4$ 0.64×10^{-3} mole/l.

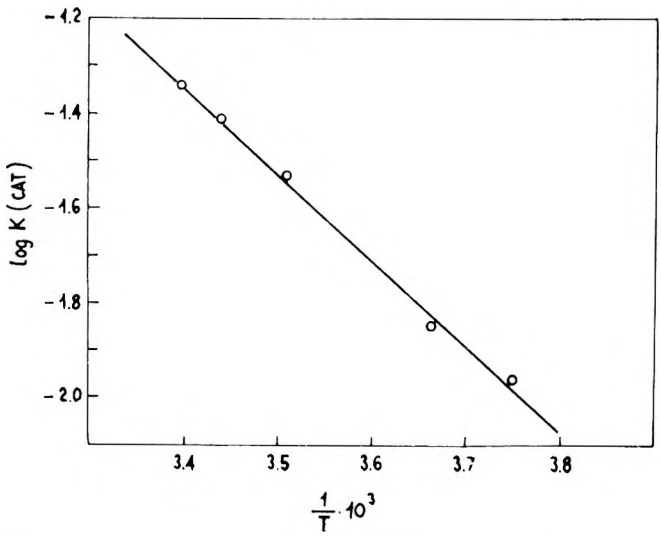

Fig. 5. Logarithm of the rate of polymerization as a function of the reciprocal of the absolute temperature.

TABLE II
Polymer Conversion at Different Polymerization Temperatures at Initial Constant Catalyst Concentration[a]

Run no.	Temperature of polymerization, °C.	Polymer conversion at given times, %					
		5 min.	10 min.	15 min.	20 min.	25 min.	30 min.
1	−6	5.4	11.05	15.95	20.82	24.7	28.6
2	0	—	—	18.3	23.7	28.5	33.2
3	+12	9	21.5	32.5	38.8	42.5	—
4	+18	25.7	41.7	50	61	65.3	—
5	+21	28.2	43.8	54.4	62.6	—	—

[a] Polymerization conditions: $TiCl_4$ 0.64 mmole/l.; total catalyst 4.99 mmole/l.; butadiene 1.327 mole/l.

This was done because we have arbitrarily used as catalyst concentration the sum of the concentrations of all three components instead of the concentration of the active catalyst which was unknown. This mathematical device does eliminate any effect of the arbitrariness of the catalyst concentration on the determination of the activation energy.

Reporting in the graph of Figure 5, values of log K [Cat] as a function of $1/T$, a straight line is obtained, whose slope is $\tan \alpha = -E/2.3R = -1865$, from which $E = 8{,}500$ cal./mole.

Catalyst Prepared in the Absence of Monomer

In this series of runs the catalyst was prepared separately in the absence of monomer, reagents being added in the following order: $TiCl_4$, AlI_3, and

$AlHCl_2 \cdot (C_2H_5)_2O$ with 100 cc. of solvent. The total mixture was then added to the solution of monomer and the remaining solvent. For these runs we can consider that the catalyst had been aged for 2–3 min. By so doing there is a lack of homogeneity in the catalyst; in fact, it was possible to notice in the reaction mixture the appearance of a small amount of a very fine brown precipitate. This was more evident if the catalyst was prepared in small amount of solvent or if the runs were carried out at high catalyst concentration. In any case the quantity of precipitate formed was always very small. The heterogeneity of the catalytic system influences the course of polymerization in a rather substantial way.

Determination of the Order of the Reaction with Respect to Monomer

The polymer conversion with preformed catalysts varies with time as is shown in Figure 6.

The polymerization reaction is still of the first order with respect to monomer, even though in every case the rate is lower than the one of the corresponding runs with catalysts prepared *in situ*.

Determination of the Order of the Reaction with Respect to Catalyst

In the same Figure 6 are shown results of some polymerizations carried out with different quantity of initial catalyst. In this case the dependence of the reaction rate on the catalyst concentration is no longer linear.

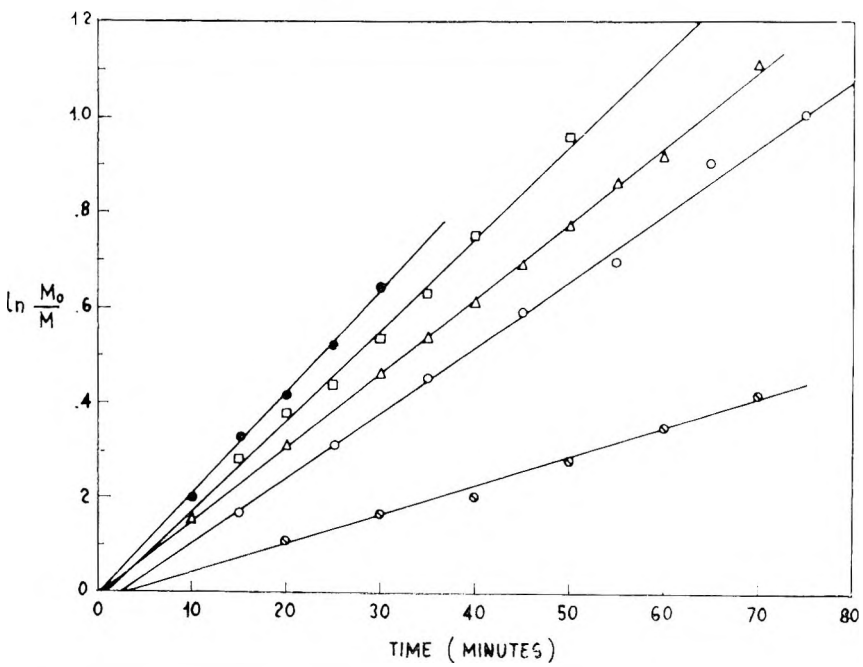

Fig. 6. Diagrams of the reaction rate with catalysts prepared in the absence of monomer at various $TiCl_4$ concentrations: (⊘) 0.428 mmole/l.; (○) 0.64 mmole/l.; (△) 0.856 mmole/l.; (□) 1.295 mmole/l.; (●) 2.151 mmole/l. Conditions: butadiene 1.327 mole/l.; temperature 0°C.

When eq. (2) is plotted in the form of $\ln(M_0/M)t$ versus [Cat], the obtainable curve is not a straight line, at least for the high concentration values. We think that this is related to the heterogeneity of the catalyst for these

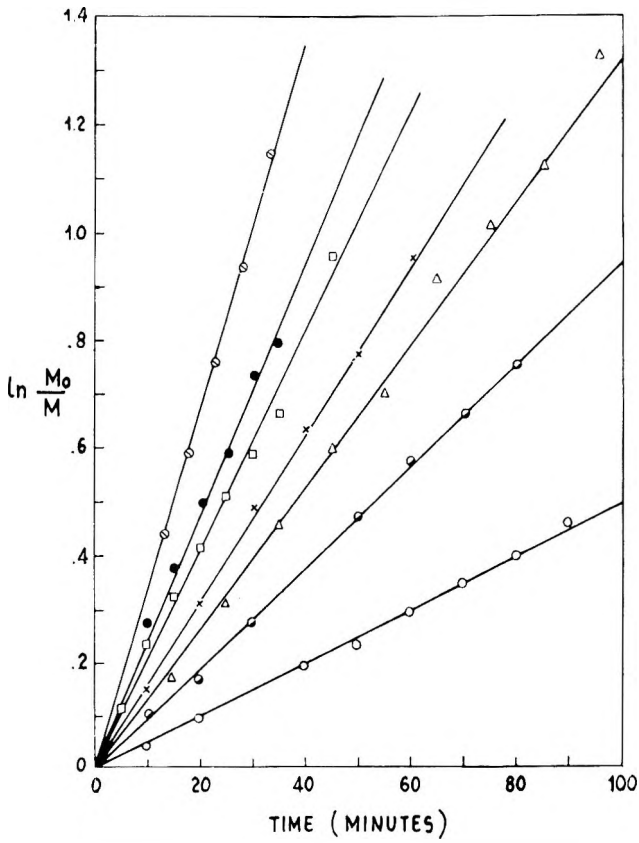

Fig. 7. Influence of the temperature of polymerization on the reaction rate (preformed catalysts): (O) −10°C.; (◕) −5°C.; (△) 0°C.; (×) +5°C.; (□) +10°C.; (●) +13°C.; (⊗) +17°C. Conditions: butadiene 1.327 mole/l.; $TiCl_4$ 0.64 × 10^{-3} mole/l.

runs. This would imply a decrease in the active surface, to the extent that it is more evident as the concentration of the catalyst is higher due to formation of aggregated particles having an even higher magnitude.

Determination of the Value of the Activation Energy

The influence of the temperature on the course of polymerizations with preformed catalysts is shown in Figure 7. By diagramming log K[Cat]/$1/T$, the straight line of Figure 8 is obtained. From this it is possible to calculate the slope to a value of $E = +8750$ cal./mole. This value is practically the same as the one found in polymerizations in the homogeneous phase reported earlier.

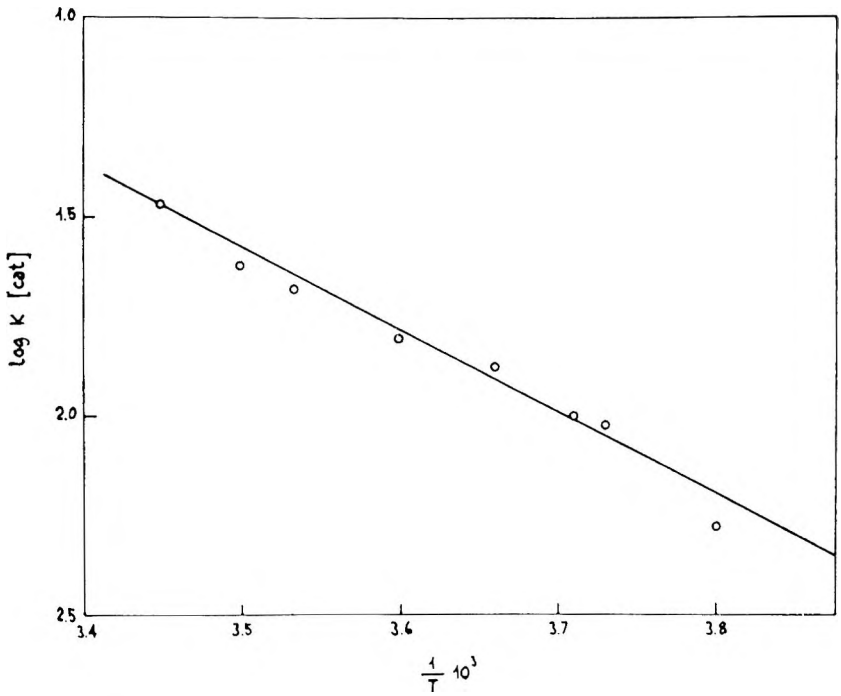

Fig. 8. Logarithm of the rate of polymerization as a function of the reciprocal of the absolute temperature (preformed catalysts).

Comparison with Other Catalytic Systems

In the previous paper[4] we described polymerization runs of butadiene with catalysts made of $TiCl_4$, AlI_3, and aluminum hydride derivatives complexed with trialkylamines or dialkyl amido hydrides.

This study showed that the catalytic activity of these systems changes as a function of the active hydrogen present and the particular nature of the co-catalyst. We now report a kinetic comparison of these catalyst systems with that described previously made of $AlHCl_2 \cdot (C_2H_5)_2O$. The examined hydrides and the respective molar ratios with $TiCl_4$ for which the maximum conversion is obtained are as follows: $AlHCl_2 \cdot N(CH_3)_3/TiCl_4 = 5.5$, $AlH_2Cl \cdot N(CH_3)_3/TiCl_4 = 2.5$, $AlH_3 \cdot N(CH_3)_3/TiCl_4 = 1.1$, $AlH_2N(CH_3)_2/TiCl_4 = 2.5$.

For all these catalytic systems we kept the quantity of $TiCl_4$ constant (0.856×10^{-3} mole/l.) and the molar ratio $AlI_3/TiCl_4 = 1.3$.

In Figure 9 are given the results obtained and from these it is possible to deduce, by means of the values of $\ln (M_0/M)/t$, a scale of the rate of polymerization according to the following decreasing order: $AlHCl_2 \cdot N(CH_3)_3 > AlH_2Cl \cdot N(CH_3)_3 > AlH_2N(CH_3)_2 > AlHCl_2 \cdot (C_2H_5)_2O > AlH_3 \cdot N(CH_3)_3$. In these runs the catalyst was always prepared in the presence of the monomer and the polymerization took place in a homogeneous phase.

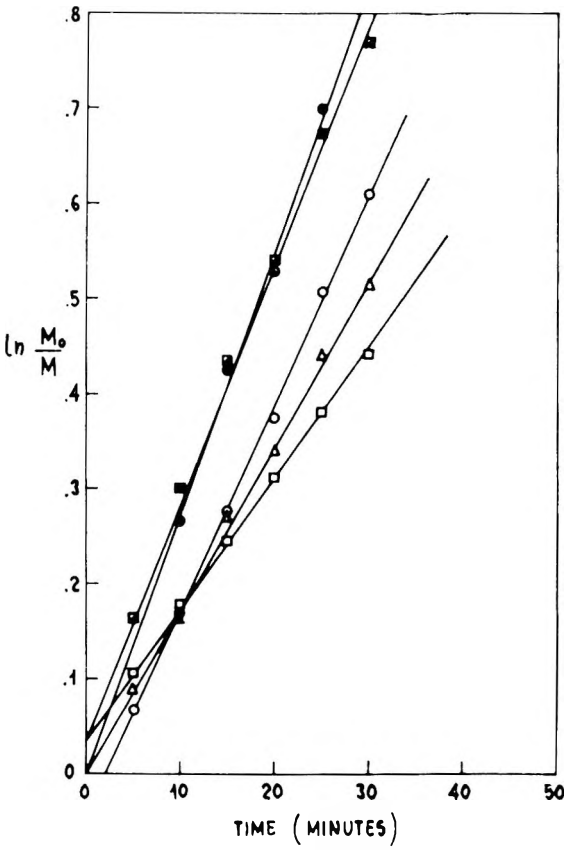

Fig. 9. Comparison of the polymerization rate for catalysts prepared from different aluminum hydrides: (□) $AlH_3 . N(CH_3)_3$; (△) $AlHCl_2 . O(C_2H_5)_2$; (○) $AlH_2N(CH_3)_2$; (◪) $AlH_2Cl . N(CH_3)_3$; (●) $AlHCl_2 . N(CH_3)_3$. Conditions: butadiene 1.327 mole/l.; $TiCl_4$ 0.856×10^{-3} mole/l.; temperature 0°C.

EXPERIMENTAL

Materials

As solvent sodium-dehydrated toluene was used. Before each run the needed quantity was again distilled on $LiAlH_4$. The residual water content was never over 15 ppm.

Butadiene was the 98% product dehydrated by being run through an alumina column.

RP Erba $TiCl_4$ product was used as received.

AlI_3 was prepared from Al and I_2 according to the literature.[6] The salt was distilled under vacuum and the benzene solutions, which were slightly pink in color, were kept under N_2 away from the light.

$AlHCl_2 \cdot (C_2H_5)_2O$ was prepared from $AlCl_3$ and $LiAlH_4$ in diethyl ether as described.[7] The preparation of other derivatives of AlH_3 used as cocatalysts was according to the literature.[8]

Kinetic Measurements

A glass apparatus consisting of a 400-ml.-four-necked cylindrical reactor a spiral type stirrer, a 100-ml. jacketed addition funnel, a siphon used for introducing the monomer and to take aliquots under a N_2 pressure, and a long-stemmed thermometer for measuring the temperature inside the mixture was used. The entire apparatus was connected to a mercury manometer in order to maintain a slight pressure of N_2 in the system.

In the polymerization run with 0.64×10^{-3} moles of $TiCl_4$ (Fig. 2), 393 ml. of toluene was distilled into the reactor and 0.356 ml. of $AlHCl_2 \cdot (C_2H_5)_2O$ (5.93 M) added while the temperature was kept at about $-5°C$. by means of an external bath. Then 32 g. butadiene was slowly introduced through the siphon. At the same time a mixture of 1.68 ml. of a toluene solution of $TiCl_4$ (0.383×10^{-3}M) and 17.25 ml. of AlI_3 solution (0.498×10^{-3} *M*) was prepared in the addition funnel. On addition of the AlI_3 a red solution was obtained which became brown in the presence of the chloroaluminum hydride etherate without a precipitate being formed.

TABLE III
Dependence of Polymer Conversion on the Time of Polymerization[a]

Sample no.	Time, min.	Solution tested, g.	Polymer and catalyst in the solution tested, g.	Total polymer, g.[b]	Yield, %	ln (M_0/M)[c]
1	5	16.69	0.139	2.6	8.20	0.0871
2	10	13.22	0.1859	4.8	15	0.1623
3	15	17.30	0.3470	7.12	22.25	0.252
4	20	16.46	0.4185	9.18	28.7	0.338
5	25	20.78	0.6471	11.4	35.7	0.442
6	30	28.11	0.9743	12.85	40.1	0.513

[a] Polymerization conditions: total volume 447 cc. (385 g.); temp. 0°C.; total catalyst 6.726 mmole/l. (2% respect to monomer); butadiene 1.327 mole/l. (32 g.).

[b] After taking out 0.64 g. due to the catalyst.

[c] M_0 = initial monomer; M = M_0 − polymer.

The time was measured as soon as the catalyst was dripped into the reactor. Every 5 min. aliquots of the reaction mixture were taken and the amount of sample withdrawn weighed. After the addition of methanol, the samples were evaporated and then dried under vacuum to constant weight.

The weight was then converted to the total volume of the reaction mixture, taking out the quantity due to the catalyst (Table III). At the end of the run methanol was added to the reaction mixture remaining, and the coagulated polymer, after further purification with benzene–methanol, was dried at 30°C. overnight.

CONCLUSIONS

A systematic study of the polymerization of butadiene with catalysts prepared from aluminum hydride derivatives, AlI_3, and $TiCl_4$ was made.

From the results obtained in the described experimental conditions we can conclude that when the catalyst is prepared in the presence of the monomer, the polymerization takes place in a homogeneous phase. It was found that the reaction rate is first-order with respect to monomer and to catalyst concentration. For catalyst prepared in the absence of monomer, the reaction takes place in a heterogeneous phase, and the dependence of the polymerization rate on the monomer concentration is still first-order, while the dependence on the catalyst concentration is no longer linear, especially at high concentrations.

The activation energy of the entire process is about 8500 cal./mole in both cases.

A comparison of the catalytic activity of some aluminum hydride derivatives together with AlI_3 and $TiCl_4$ in the polymerization of butadiene is given.

References

1. Saltman, W. M., W. E. Gibbes, and J. Lal, *J. Am. Chem. Soc.*, **80,** 5615 (1958).
2. Gaylord, N. G., T.-K. Kwei, and H. F. Mark, *J. Polymer Sci.*, **42,** 417 (1960).
3. Natta, G., L. Porri, and A. Mazzei, *Chim. Ind. (Milan)*, **41,** 398 (1959).
4. Marconi, W., A. Mazzei, M. Araldi, and M. De Maldé, *J. Polymer Sci.*, **A3,** 735 (1964).
5. Mazzei, A., M. Araldi, W. Marconi, and M. De Maldé, *J. Polymer Sci.*, **B1,** 79 (1963).
6. Brauer, G., *Präparativen Anorganischen Chemie*, F. Enke, Stuttgard, 1960, p. 723.
7. Wiberg, E., K. Moedritzer, and R. Uson, *Rev. Acad. Ciencias Ex. Fis. Quim. Nat. (Zaragoza)*, **2** (1) 91 (1954); E. Wiberg and A. May, *Z. Naturforsch.*, **106,** 234 (1954).
8. Ruff, J. K., and M. F. Hawthorne, *J. Am. Chem. Soc.*, **82,** 2141 (1960); *ibid.*, **83,** 1798 (1961); *ibid.*, **83,** 535 (1961); *ibid.*, **83,** 2835 (1961).

Résumé

On a étudié la cinétique de polymérisation du butadiène avec des catalyseurs préparés à partir de certains dérivés de l'hydrure d'aluminium, de l'AlI_3 et de $TiCl_4$. On a trouvé que la vitesse de réaction est du premier ordre par rapport à la concentration en monomère et en catalyseur, quand la catalyseur est préparé en présence du monomère. Dans ce cas la polymérisation a lieu en phase homogène. Lorsque le catalyseur est préparé en absence de monomère, la réaction se fait en phase hétérogène et la vitesse reste du premier ordre par rapport à la concentration en monomere, tandis que la dépendance vis-à-vis de la concentration en catalyseur n'est plus linéaire. L'énergie d'activation du processus entier est d'environ 8500 cal/mole. De plus on fait une comparaison entre la vitesse de polymérisation pour les catalyseurs obtenus à partir d'AlI_3 et de $TiCl_4$ et différents dérivés de l'hydrure d'aluminium.

Zusammenfassung

Die Kinetik der Polymerisation von Butadien mit Katalysatoren aus gewissen Aluminiumhydridderivaten, AlJ_3 und $TiCl_4$ wurde untersucht. Bei Darstellung des Katalysators in Gegenwart des Monomeren erwies sich die Reaktion als von erster Ordnung in

bezug auf Monomer- und Katalysatorkonzentration. In diesem Fall findet die Polymerisation in homogener Phase statt. Bei Darstellung des Katalysators in Abwesenheit des Monomeren verläuft die Reaktion in heterogener Phase, wobei die Geschwindigkeit immer noch erster Ordnung in bezug auf die Monomerkonzentration ist, während von der Katalysatorkonzentration keine lineare Abhängigkeit mehr besteht. Die Aktivierungsenergie des Bruttovorgangs ist etwa 8500 cal/Mol. Zusätzlich wird ein Vergliech der mit Katalysatoren aus AlJ_3, $TiCl_4$ und verschiedenen Aluminiumhydridderivaten erhaltenen Polymerisationsgeschwindigkeiten durchgeführt.

Received April 6, 1964
Revised June 23, 1964

JOURNAL OF POLYMER SCIENCE: PART A VOL. 3, PP. 767–776 (1965)

Heat and Entropy of Fusion of Isotactic Polypropylene

W. R. KRIGBAUM and ICHITARO UEMATSU, *Department of Chemistry, Duke University, Durham, North Carolina*

Synopsis

Heats and entropies of fusion of polymers are customarily evaluated through melting point depression measurements with the assumption that the observed and thermodynamic melting points are nearly identical. However, it has recently become evident that the crystal surface free energy is not negligible, so that apparent melting points measured dilatometrically or calorimetrically are low by perhaps 5–15°C. The status of the accumulated body of thermodynamic data is rendered still more uncertain by the possibility that the surface free energy may vary in a systematic manner with diluent concentration. To investigate this question, dilatometric data were obtained by two procedures for tetralin solutions of isotactic polypropylene. The first set of measurements was performed upon samples which had been slowly cooled from the melt, while in the second procedure the apparent melting point was measured as a function of the isothermal crystallization temperature. Extrapolation of the latter data gave $t_M^\circ = 186 \pm 2$°C., a value of 12°C. higher than the apparent melting temperature observed according to the first procedure; however, the heats of fusion obtained by the two methods agreed to within the experimental error. A possible explanation for this behavior may be offered by the observations that both the parameter β of Hoffman and Weeks, and the ratio of the temperature of maximum crystallization rate to the melting temperature, are independent of diluent concentration over the range investigated. This suggests that the addition of diluent does not affect the distribution of fold lengths. If this behavior proves to be general, dilatometric heats of fusion will be reinstated as valid thermodynamic data for polymers.

Introduction

One of the several important applications of the Flory-Huggins treatment of polymer solutions involves use of the expression derived for the chemical potential of an amorphous polymer in a two component system to predict the melting point depression relationship. As pointed out some years ago by Flory,[1] the melting point depression of a semicrystalline polymer due to the presence of a low molecular weight diluent at volume fraction v_1 may be written as:

$$(1/T_M) - (1/T_M^0) = (R/\Delta H_u)(V_u/V_1)[v_1 - (BV_1/RT_M)v_1^2] \qquad (1)$$

Here T_M and T_M^0 are the melting points in the presence and absence of the diluent, respectively, ΔH_u and V_u are the heat of fusion and volume per

mole of repeating unit, V_1 is the molar volume of the diluent, R is the gas constant, and B is a polymer–solvent interaction parameter. This relation permits one to evaluate the heat of fusion from melting point depression data. Since the two phases are in equilibrium at the melting point, $\Delta F_u = 0$ and the entropy of fusion is given by $\Delta S_u = \Delta H_u/T_M^0$. Finally, eq. (1) affords a means of estimating T_M^0 by extrapolation of melting point depression data, and this can be quite useful for those polymers which degrade at temperatures below the melting point.

Equation (1) has been employed to accumulate a considerable body of thermodynamic data for polymers through melting point depression studies, particularly by Mandelkern and co-workers.[2] Implicit in this application is the assumption that the experimentally observed melting temperatures correspond to, or at least closely approximate, the true thermodynamic melting points referred to by the theory. This means, in particular, that the crystal surface free energy is of negligible magnitude. It was believed that the thermodynamic melting point could be approached arbitrarily closely by allowing sufficient time for recrystallization near the melting point to improve the perfection of the crystallites. More recently it has become apparent that, due to the lamellar nature of the crystalline domains, one dimension of the crystallite tends to be quite small. Thus, it is impossible to eliminate the surface energy by any practical means now at our disposal.

The effect of the surface energy upon the apparent melting point of a bulk polymer has been examined by Mandelkern[3] and by Hoffman and Weeks.[4] These authors have presented treatments which predict how the observed melting point (measured in the absence of recrystallization) should vary with the crystallization temperature for isothermally crystallized samples. They also propose extrapolation procedures by which the true thermodynamic melting point can be estimated. Application of these procedures indicates that, although recrystallization near the melting point may reduce the influence of the initial crystallization conditions, even the slowest heat schedule which is at all practical in the laboratory will lead to an apparent melting point which is 5–15°C. too low. Hence, we can be certain that all the melting points reported earlier are somewhat in error. Of more importance to the melting point depression studies is the fact that it is by no means evident how the addition of a diluent will affect the crystal surface energy. This casts a serious doubt upon the validity of the thermodynamic parameters deduced from polymer melting point depression data.

These developments demand a reexamination of the melting point depression procedure as a source of thermodynamic data. We report here a study of solutions of isotactic polypropylene in tetralin. Depression measurements were performed by two procedures. The first involved samples which were crystallized by slow cooling from the melt, while in the second the apparent melting points of isothermally crystallized samples were measured as a function of the crystallization temperature, a rapid heating rate being used to minimize recrystallization.

Experimental and Results

Hercules Profax polypropylene was dissolved in tetralin, filtered, and reprecipitated. This was extracted for 24 hr. with boiling *n*-heptane and the residue was used for preparation of the samples. Tetralin was added at 175°C. under streaming nitrogen and, when the desired concentration was attained, the tube was sealed and the sample was maintained at 175–180°C. for two days to ensure that the diluent concentration was uniform throughout the sample.

The specific volume relationships used for crystalline and amorphous polypropylene are those of Danusso et al.:[5]

$$\bar{v}_c = 1.059 + 4.25 \times 10^{-4}t$$

$$\bar{v}_a = 1.1340 + 9.28 \times 10^{-4}t$$

(where t is the temperature in Centigrade) while the value for tetralin was measured dilatometrically:

$$\bar{v}_T = 1.0113 + 6.889 \times 10^{-4}t + 1.044 \times 10^{-6}t^2$$

The samples used for the first series of measurements were slowly cooled from the melt over a period of 5 hr. The dilatometric data appear as a plot of specific volume, $\bar{v}$, versus temperature in Figure 1, from which we obtain an apparent melting point of 174°C. for isotactic polypropylene. The melting point depressions measured in a similar manner for five tetralin solutions are represented by the open circles in Figure 2, where $[(1/T_M) - (1/T_M{}^0)]/v_1$ appears plotted against v_1/T_M. According to eq. (1) the inter-

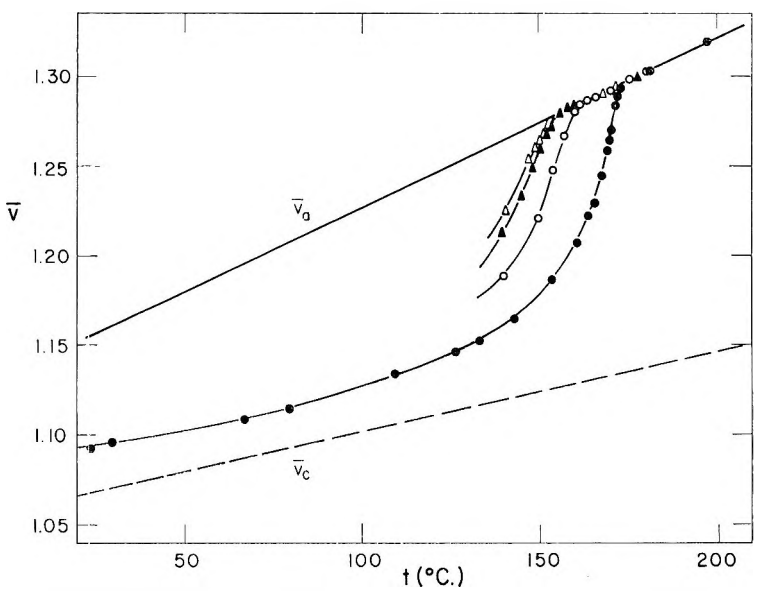

Fig. 1. Specific volume of slowly cooled polypropylene solutions having various polymer weight fractions (△) 0.622; (▲) 0.697; (○) 0.799; (●) 1.000.

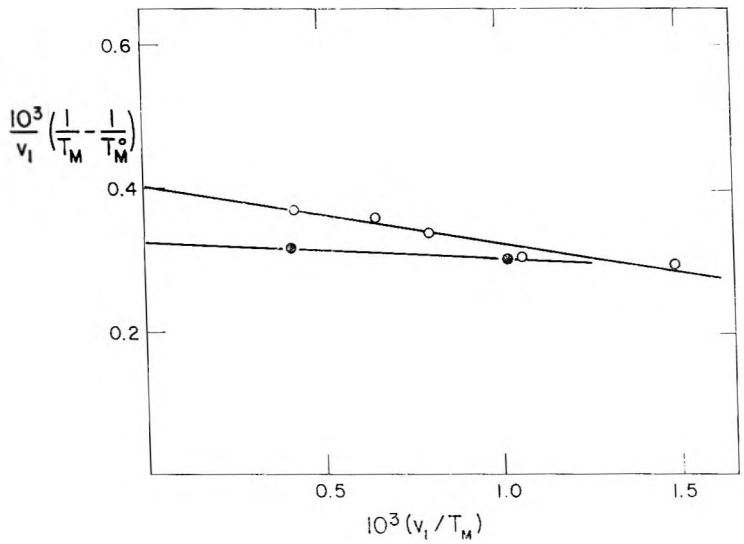

Fig. 2. Plot according to eq. (1) for samples (O) cooled slowly from the melt and (●) crystallized isothermally (see Fig. 4).

cept equals $(R/\Delta H_u)(V_u/V_1)$. From the line drawn in Figure 2 we obtain $\Delta H_u = 2.0 \pm 0.3$ kcal./mole.

We next consider the data obtained using isothermally crystallized samples. Both Mandelkern[3] and Hoffman and Weeks[4] begin with the following expression for the melting point depression of a bulk polymer due to surface energy:

$$T_M = T_M^0(1 - 2\sigma_e/\Delta h_f l') \tag{2}$$

where σ_e is the surface energy (in ergs/square centimeter), Δh_f is the heat of fusion (in ergs/cubic centimeter), and l' is the fold length (in centimeters) of the last crystallites to melt. It has been pointed out to me that one of the early derivations of this relation was due to Tamman.[6] Hoffman and Weeks[4] deduce the following relation for the largest fold length

$$l' = (4\beta\sigma_e/\Delta h_f)[T_M^0/(T_M^0 - T_x)] \tag{3}$$

where β is a constant and T_x is the isothermal crystallization temperature. Combination of eq. (2) and (3) yields

$$T_M = T_M^0[1 - (1/2\beta)] + (T_x/2\beta) \tag{4}$$

Hence, a plot of T_M versus T_x should form a straight line which extrapolates to T_M^0 at the intersection with the line $T_M = T_x$ having a slope of 45°.

Data were obtained by rapidly heating (1°C./5 min.) polypropylene samples which had been isothermally crystallized at different temperatures. Values of the specific volume of bulk polypropylene appear plotted against temperature in Figure 3. Similar measurements (not shown) were performed upon two tetralin solutions having polymer weight fractions w_2 of

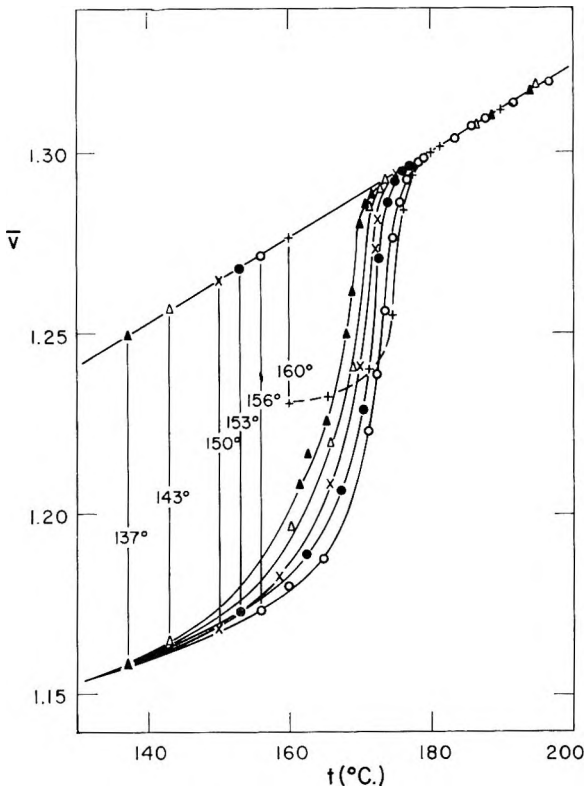

Fig. 3. Specific volume vs. temperature for polypropylene crystallized isothermally at the temperatures indicated.

0.799 and 0.530. These melting points appear plotted as t_M versus t_x in Figure 4. The thermodynamic melting point, as determined by extrapolation of the data for bulk polypropylene, is 186 ± 2°C., which is to be compared with the apparent melting point, 174°C., as determined by the first procedure. The intercepts shown in Figure 4 for the tetralin solutions yield t_M values of 174 ± 2°C. for $w_2 = 0.799$ and 158.5 ± 2°C. for $w_2 = 0.530$. These data are represented by the filled circles in Figure 2, which extrapolate to an intercept yielding $\Delta H_u = 2.1 \pm 0.3$ kcal./mole. This compares quite well with the value 2.0 ± 0.3 kcal./mole obtained through the first procedure.

We conclude that while neglect of the surface free energy results in an underestimation of the thermodynamic melting temperature, it does not seriously affect the values derived for the heat of fusion. This carries the rather surprising implication that the depression due to surface free energy is independent of diluent concentration over a considerable range, at least for the present system. In this connection it is interesting to observe that the same slopes are obtained in Figure 4 for the bulk polymer and the tetralin solutions. Hence the parameter β, which in the treatment of Hoffman and

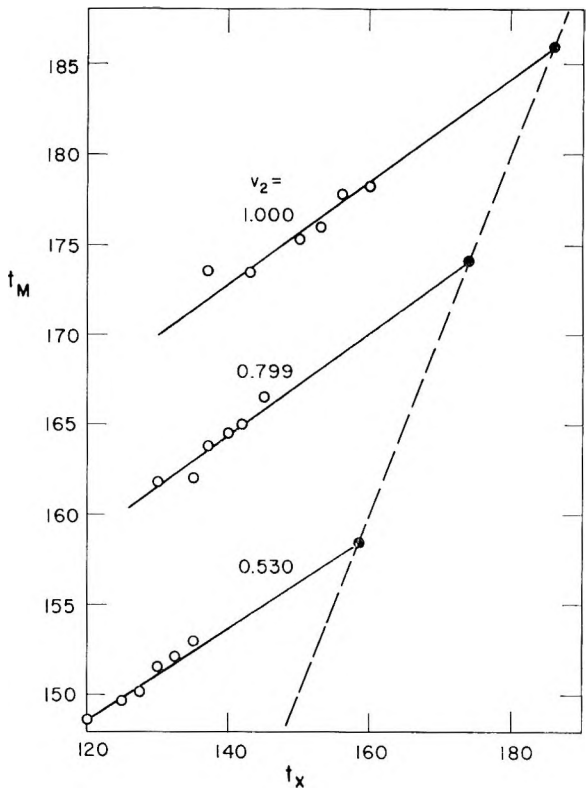

Fig. 4. Observed melting temperature vs. isothermal crystallization temperature for solutions having the polymer weight fractions indicated.

Weeks is related to the range of the crystalline fold lengths, is unaffected by the presence of diluent. Turning next to the samples crystallized by slow cooling, it seems necessary to invoke some type of "corresponding states" hypothesis to explain the success of the first procedure in evaluating heats of fusion. We have attempted to verify this hypothesis by a qualitative study of crystallization rates from the cooling curves. Table I gives the melting temperatures, the temperature T_x^* at which the crystallization rate attains its maximum value, and the T_x^*/T_M ratios. The fourth column indicates that T_x^*/T_M is nearly independent of diluent concentration. If eq. (3) may

TABLE I
Temperatures of Melting and Maximum Crystallization Rate for Polypropylene Solutions

w_2	T_M, °K.	T_x^*, °K.		(T_x^*/T_M)
1.000	459	408		0.889
0.799	447	398		0.890
0.530	432.5	388		0.897
			Avg.	0.892

be applied to a two-component system, and if σ_e is not significantly altered by the presence of diluent, we might expect that the fold period in crystallites formed by slow cooling from solution should be independent of diluent concentration over a considerable range. It should be pointed out that we have not examined dilute solutions. It is possible that these would exhibit a completely different behavior.

Let us designate the apparent melting temperatures measured for slowly cooled samples by a prime. According to eqs. (2)–(4) these may be related to the thermodynamic melting temperatures as follows:

$$T_M'/T_M = 1 - (1/2\beta)[1 - (T_x^*/T_M)] = \zeta \quad (5)$$

If ζ is constant over the range of diluent concentrations of interest, eq. (1) may be recast for application to the first procedure

$$(1/T_M') - (1/T_M^{0\prime}) = (R/\zeta\Delta H_u)(V_u/V_1)[v_1 - (BV_1\zeta/RT_M')v_1^2] \quad (6)$$

From Figure 4 β is found to be 1.8 and, using the average value $T_x^*/T_M = 0.89$ found in Table I, we obtain $\zeta = 0.97$. This suggests that the value of ΔH_u obtained through application of the first procedure will be low by only

TABLE II
Thermodynamic Data for Saturated Polyhydrocarbons

Polymer	t_M' or t_M^0, °C.	ΔH_u, kcal./mole	ΔS_u, e.u.	Procedure[a]	Reference
Polyethylene	137.5	1.88 ± 0.06	4.8 ± 0.15	a	12
	134.9	1.59	3.9	b	15
	143 ± 2	—	—	c	4
	141 ± 1.2	—	—	e	16
	145.5 ± 0.1	—	—	e	17
Polypropylene	186 ± 2	2.1 ± 0.3	4.6 ± 0.6	c	This work
	176	2.6 ± 0.1	5.8 ± 0.2	a	7
	176	1.8$_5$	4.1	b	8
	174	1.9	4.2	b	18
	166	1.7	3.9	b	19
	178.4 ± 0.3	—	—	d	20
Poly-1-butene (modification 1)	135.5	1.45 ± 0.15	3.6 ± 0.3	a	13
	134.7	1.71	4.2	b	21
		1.65 ± 0.08	4.0	a	21
2	124	1.5 ± 0.3	3.8 ± 0.7	a	13
3	106.5	1.55 ± 0.15	4.1 ± 0.3	a	13
Polystyrene	240	2.15 ± 0.1	4.2 ± 0.2	a	14

[a] Procedures used were: (a) Dilatometric measurements; (b) specific heat measurements; (c) dilatometric data by the method of Hoffman and Weeks; (d) DTA, method of Hoffman and Weeks; (e) extrapolation of melting points of orthorhombic normal paraffins.

3% due to the use of apparent melting temperatures, and this error is trivial in comparison with the usual experimental errors.

We next turn to a comparison with the results of other workers. Table II lists the thermodynamic values obtained for saturated polyhydrocarbons. The present measurements yield for polypropylene $t_M^0 = 186°C.$ and $\Delta H_u = 2.1 \pm 0.3$ kcal./mole. Wyckoff[20] has measured the melting point of polypropylene using the method of Hoffman and Weeks. He obtained a lower value, $t_M^0 = 178.4°C.$ However, he followed the melting process by DTA, which appears to be rather insensitive to the disappearance of the last crystallites, so the discrepancy is in the expected direction. Danusso, Moraglio, and Flores[7] investigated the melting point depression of polypropylene by three solvents using the conventional procedure. They obtained $t_M' = 176°C.$ and $\Delta H_u = 2.6 \pm 0.1$ kcal./mole. Passaglia and Kervorkian[18] state that the data of Danusso et al. could be extrapolated to obtain a somewhat higher melting point, $t_M' = 178°C.$, and a lower value for the heat of fusion, $\Delta H_u = 2.2$ kcal./mole. This latter value would be in better agreement with that deduced in the present work, and with the value $\Delta H_u = 1.9$ kcal./mole obtained by Passaglia and Kervorkian[18] by specific heat measurements. This latter value is in excellent agreement with the value $\Delta H_u = 1.8_5$ kcal./mole computed by Wilkenson and Dole[8] through combination of the value $dp/dT = 25$ atm./deg., as measured by Fortune and Malcolm,[9] with $\Delta V_f = 0.163$ cc./mole as determined by Newman.[10] From their own specific heat measurements Wilkenson and Dole[8] deduced a lower value, $\Delta H_u = 1.5$ kcal./mole. Wilski[19] reported $\Delta H_u = 1.7$ kcal./mole from calorimetric measurements.

In general, the heats of fusion obtained calorimetrically appear to be somewhat smaller than those deduced by dilatometric measurement of melting point depressions. The assumptions involved in deducing the heat of fusion from specific heat measurements have been enumerated by Passaglia and Kervorkian.[18] The more recent calorimetric values appear to be higher, perhaps due to an improvement in apparatus. In any event, the most recent value obtained for modification 1 of isotactic poly-1-butene by Wilski[21] represents the only case in which the dilatometric value was exceeded.

Schaefgen[11] has presented an empirical procedure for estimating the heat of fusion. His estimate for polypropylene, 2.37 kcal./mole, falls in the range of the experimental values. On the other hand, his estimate for poly-1-butene was too large by a factor of two.

Table II also lists values for the entropies of fusion for saturated polyhydrocarbons. Within this restricted class of compounds the variations of ΔS_u are small, and may be within the experimental error, so that most of the observed differences in the melting temperatures of these compounds must be ascribed to variations of ΔH_u.

Financial support for this investigation through National Science Foundation grant NSF-G20533 is gratefully acknowledged.

References

1. Flory, P. J., *J. Chem. Phys.*, **17**, 223 (1949).
2. See L. Mandelkern, *Chem. Rev.*, **56**, 903 (1956); *Rubber Chem. Technol.*, **32**, 1392 (1959).
3. Mandelkern, L., *J. Polymer Sci.*, **47**, 494 (1960).
4. Hoffman, J. D., and J. J. Weeks, *J. Res. Natl. Bur. Std.*, **66A**, 13 (1962).
5. Danusso, F., G. Moraglio, W. Ghiglia, L. Motta, and G. Talamini, *Chim. Ind.*, **41**, 74 (1959).
6. Tamman, G., *Z. Anorg. Allgem. Chem.*, **110**, 166 (1920).
7. Danusso, F., G. Moraglio, and E. Flores, *Atti Accad. Nazl. Lincei, Rend. Sci. Fis. Mat. Nat.*, **25**, 520 (1958).
8. Wilkenson, R. W., and M. Dole, *J. Polymer Sci.*, **58**, 1089 (1962).
9. Fortune, L. R., and G. N. Malcolm, *J. Phys. Chem.*, **64**, 934 (1960).
10. Newman, S., *J. Polymer Sci.*, **47**, 111 (1960).
11. Schaefgen, J. R., *J. Polymer Sci.*, **38**, 549 (1959).
12. Quinn, F. A., and L. Mandelkern, *J. Am. Chem. Soc.*, **80**, 3178 (1958).
13. Danusso, F., and G. Gianotti, *Makromol. Chem.*, **61**, 139 (1963).
14. Danusso, F., and G. Moraglio, *Atti. Accad. Nazl. Lincei, Rend. Sci. Fis. Mat. Nat.*, **27**, 381 (1959).
15. Wunderlich, B., and M. Dole, *J. Polymer Sci.*, **24**, 201 (1957).
16. Broadhurst, M. G., *J. Chem. Phys.*, **36**, 2578 (1962).
17. Flory, P. J., and A. Vrij, *J. Am. Chem. Soc.*, **85**, 3548 (1963).
18. Passaglia, E., and H. K. Kervorkian, J. Appl. Phys., **34**, 90 (1963).
19. Wilski, H., *Kunststoffe*, **50**, 335 (1960).
20. Wyckoff, H. W., *J. Polymer Sci.*, **62**, 83 (1962).
21. Wilski, H., and T. Grewer, paper presented at the 145th Meeting of the American Chemical Society, New York, N. Y., Sept. 8–13, 1963, 250, Abstracts of Papers.

Résumé

On évalue usuellement les chaleurs latentes et les entropies de fusion à partir des mesures d'abaissement du point de fusion en postulant l'identité du point de fusion expérimental et du point de fusion thermodynamique. Cependant des observations récentes ont montré que l'énergie libre de surface ne pouvait être négligée et que les point de fusion expérimentaux mesurés soit par dilatométrie soit par calorimétrie étaient abaissés de 5 à 15°C. L'incertitude qui pèse sur l'ensemble des résultats thermodynamiques est encore augmentée si on considère que l'énergie libre de surface peut varier de manière systématique avec la concentration en diluant. En vue d'élucider ce problème, on a procédé à des mesures dilatométriques sur des solutions de polypropylène isotactique dans la tétraline suivant deux processus expérimentaux. On a effectué la première série d'expériences sur des échantillons refroidis lentement en partant de polymères fondus, tandis que suivant le second processus, on mesurait le point de fusion apparent en fonction de la température de la cristallisation isotherma. En extrapolant cette dernière série de résultats, on obtient un point de fusion $t°_M = 186 \pm 2$°C, c.à.d. une valeur supérieure de 12°C à la valeur obtenue par l'autre procédé. Néanmoins, on a obtenu par les deux méthodes une valeur identique des chaleurs de fusion, ceci dans la limite des valeurs expérimentales. On pourrait peut-être expliquer ce comportement en observant que le paramètre β de Hoffman et Weeks et que le rapport température de cristallisation maximum/température de fusion sont indépendants de la concentration en diluant. Ceci suggère que la présence de diluant ne change pas la distribution de la longueur des repliements. Si ce comportement se généralise, la mesure dilatométrique des chaleurs de fusion des polymères reposerait sur des bases thermodynamiques valables.

Zusammenfassung

Schmelzwärmen und -entropien von Polymeren werden gewöhnlich aus Schmelzpunkterniedrigungsmessungen unter der Annahme berechnet, dass der beobachtete und der thermodynamische Schmelzpunkt nahezu identisch sind. In letzter Zeit wurde jedoch festgestellt, dass die freie Kristalloberflächenenergie nicht vernachlässigt werden kann, sodass die scheinbaren dilatometrisch oder kalorimetrisch gemessenen Schmelzpunkte um vielleicht 5 bis 15° zu niedrig liegen. Die Bedeutung der angesammelten thermodynamischen Daten wird durch die Möglichkeit, dass sich die freie Oberflächenenergie systematisch mit der Verdünnungsmittelkonzentration ändern kann, noch ungewisser gemacht. Zur Untersuchung dieser Frage wurden dilatometrische Messungen nach zwei Methoden an Tetralinlösungen von isotaktischem Polypropylen durchgeführt. Die erste Messreihe wurde an langsam aus der Schmelze abgekühlten Proben ausgeführt, während beim zweiten Verfahren der scheinbare Schmelzpunkt als Funktion der isothermen Kristallisationstemperatur gemessen wurde. Eine Extrapolation letzterer Daten ergab $t_M° = 186 \pm 2°C$, ein Wert, der um 12° höher liegt als die nach dem ersten Verfahren beobachtete scheinbare Schmelztemperatur. Die nach den beiden Methoden erhaltenen Schmelzwärmen stimmen jedoch innerhalb der Versuchsfehler überein. Eine mögliche Erklärung für dieses Verhalten kann durch die Beobachtung geliefert werden, dass sowohl der Parameter β von Hoffman und Weeks, als auch das Verhältnis der Temperatur maximaler Kristallisationsgeschwindigkeit zur Schmelztemperatur im untersuchten Bereich von der Verdünnungsmittelkonzentration unabhängig sind. Das zeigt, dass die Zusammensetzung des Verdünnungsmittels die Verteilung der Faltlängen nicht beeinflusst. Falls sich dieses Verhalten als allgemein erweist, können dilatometrische Schmelzwärmen wieder als richtige thermodynamische Daten für Polymere angesehen werden.

Received May 6, 1964
Revised June 27, 1964

JOURNAL OF POLYMER SCIENCE: PART A VOL. 3, PP. 777–791 (1965)

Gel Formation in Polyolefins Exposed to Ionizing Radiation

B. J. LYONS, *Research and Development Division, Raychem Corporation, Redwood City, California*

Synopsis

It is shown that a reasonable value for the ratio of main chain scission to crosslinking rates in a number of polyolefins at infinite dose is close to zero. Moreover, the sum of the sol fraction (s) and its square root ($\sqrt{s}$) in almost all of the polymers studied is proportional to some fractional power of reciprocal dose. There is some slight evidence to suggest that $s + \sqrt{s}$ in relatively low molecular weight polyolefins, which initially contain small amounts of reactive carbon–carbon unsaturation and have random distributions, may be proportional to the square root of the reciprocal dose. There is already good evidence that main chain scission rates in polypropylene and poly-1-pentene decrease with increasing dose: such a variation may account for the observed relationship in these polymers and presumably also in polyethylene. Another possible explanation is that the chance of a molecule becoming attached to the crosslinked network depends not only on the number of monomer units it contains, but also on the chance that a previous radiation event (such as *trans*-vinylene formation) has already occurred in that molecule.

INTRODUCTION

The variation of gel fraction with dose was first used by Charlesby[1] in 1954 as a means of measuring the ratio of main chain scission to crosslinking rates (called in his notation p_0/q_0) and the results obtained were found to be best accounted for on the assumption that this ratio in polyethylene was 0.35. Later Basket and Miller[2] subjected the gels from polyethylene lightly crosslinked by ionizing radiation to further irradiation and separated the low molecular weight fraction thereby obtained by solvent extraction. The limiting soluble fraction of these gels at high doses was used to derive a value of p_0/q_0 equal to 0.18–0.20. However, Charlesby[3] has pointed out that part of the sol fraction obtained in these experiments may result from degradation occurring during the extraction process. Alexander and Toms[4] and Schumacher[5] irradiated thin films under vacuum and found that the sol fraction steadily decreased towards zero, which result suggests that main chain scission is of little importance.

Balwit, Lawton, and Miller[6] examined the gaseous fragments produced in the radiolysis of polymethylene, octacosane, and polyethylene. These authors concluded that permanent main chain scissions are unimportant in these materials as only negligible amounts of saturated or unsaturated volatile hydrocarbons containing more than seven carbon atoms were

obtained. These low molecular weight compounds were considered to arise from cleavage at chain ends and side chain branch points.

Chapiro[7] has pointed out that the fine structure of electron paramagnetic resonance spectra obtained from radicals trapped in polyethylene after irradiation at liquid nitrogen temperatures indicates that carbon–carbon bond scissions are negligible under these experimental conditions.

This problem was reconsidered by Charlesby and Pinner[8] in 1958. Assuming a random process, they derived the theoretical relationship:

$$s + \sqrt{s} = 1/\gamma' \tag{1}$$

where s is the sol fraction and γ' the crosslinking index when both crosslinking and main chain scission occur in the polymer. If the rate of main chain scission and crosslinking is constant with dose, eq. (1) for a polymer of random distribution may be written:

$$s + \sqrt{s} = (p_0/q_0) + (1/q_0 u r_1) \tag{2}$$

where p_0, q_0 are the main chain scission and crosslinking probabilities per monomer unit radiation dose, respectively, u_1 is the initial number-average degree of polymerization of the polymer, and r is the radiation dose. Though few, if any, commercial polymers possess a random molecular weight distribution, Charlesby and Pinner estimated that for doses much in excess of $3p_0/q_0$ times the gelation dose a linear relationship between $s + \sqrt{s}$ and $1/r$ could be expected.[8]

However, Inokuti, in a recent theoretical study,[9] has thrown some doubt on this last conclusion of Charlesby and Pinner. He has shown that for polymers with $\bar{M}_w/\bar{M}_n$ ratios much greater than two, even when appreciable main chain scission accompanies crosslinking, the statistical theory predicts that there is not a linear relationship between $s + \sqrt{s}$ and $1/r$, even at relatively high doses.

A preliminary examination of the variation of $s + \sqrt{s}$ with dose in a commercial polyethylene carried out in this laboratory indicated that a more correct value for p_0/q_0 at infinite dose would be close to zero. Subsequently, it was found that $s + \sqrt{s}$ in this polymer was linearly related not to the reciprocal dose, but to a fractional power of the reciprocal dose. This finding prompted a general survey of the gelation behavior of low and high density polyethylenes and a re-examination of the data obtained by previous workers with this and other polyolefins.

EXPERIMENTAL

Materials and Irradiation Procedure

The materials examined comprised a variety of commercial polyethylenes including high and low density forms. The specimens were hydraulically pressed into sheets 0.5 mm. thick. Samples were either sealed in masking tape (which is very permeable to hydrogen, but much less so to oxygen) and mounted on a drum which was rotated in a 1 kw. beam of 0.61 Mv.

electrons from a General Electric resonant transformer (average dose rate 80 Mrad/hr.), or placed in a water-cooled evacuated (0.05 torr) cell and continuously irradiated at a dose rate of 105 Mrad/hr. The geometry of the cell was such that the samples were pressed against the cooled base of the cell by the thin (0.1) mm. aluminum window, small channels being left to facilitate removal of hydrogen. Dosimetry was established by monitoring *trans*-vinylene growth in Marlex 6002 (the variation of reciprocal vinylene concentration with reciprocal dose is accurately linear in the range 10–150 Mrad). Higher doses were monitored by summing estimates from samples irradiated to suitable fractions of the total dose. The variation of dose with time of irradiation was found to be linear.

Analysis of Gel Fractions

The method used was basically that of Charlesby and Pinner;[8] however, the xylene was stabilized with 1% di-β-naphthyl-*p*-phenylenediamine, boiled under reflux, and changed four times at twelve hourly intervals. After the last extraction, the samples were placed in boiling xylene for 30 min. to remove any antioxidant traces remaining in the gels. The gels were dried under vacuum at 70°C. and 0.01 torr until no further weight loss occurred, then removed from the cotton bags and weighed. Gel fractions were normally measured in duplicate. Whatever the gel fraction, the results usually agreed to within ±0.001. Thus the percentage scatter in the sol fraction was below ±1% at low doses but increased to a maximum of about ±10% at the highest dose used although, even at this level, the average scatter was ±4%.

DISCUSSION

Polyethylene

Figure 1 shows the variation of $s + \sqrt{s}$ with r^{-1} for four low and high density polyethylenes irradiated to doses up to 1000 Mrad on a revolving drum; in Figure 2 these results are compared with an empirical equation:

$$s + \sqrt{s} = Kr^{-k} \tag{3}$$

where k has the values given in the legend.

The results of a general survey of a number of commercial polyethylenes up to moderate dose levels are shown in Figure 3 and Table I.

Table I also gives the manufacturer's estimates of molecular weight and molecular weight distribution where available. It should be stressed that most of these estimates are acknowledged to be approximate. Moreover, most, if not all, of these polymers contain small amounts (of the order of 0.05%) of antioxidants; however, at this level the effect of such additives should be negligible and, in any case, limited to a dose range below that of the gel measurements. The values of the exponent k seem to bear little or no relation to molecular weight or molecular weight distribution.

To establish that the experimental conditions or other factors were not having some effect on the results, similar analyses were carried out on the basis of the measurements of Charlesby and Pinner[8] (kindly supplied by Dr. Pinner), those of Lawton, Balwit, and Powell[11] on Marlex 50 and Plax polyethylene film, and of Chappell, Sauer, and Woodward[12] also on Marlex 50.

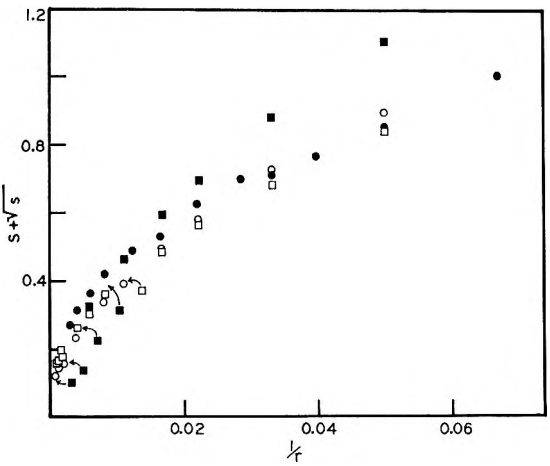

Fig. 1. Charlesby-Pinner plot for four polyethylene samples covered with masking tape and irradiated intermittently in air: (●) I, Marlex 6002; (○) II, Alathon 34; (■) III, Alathon 7020; (□) IV, DYNK.

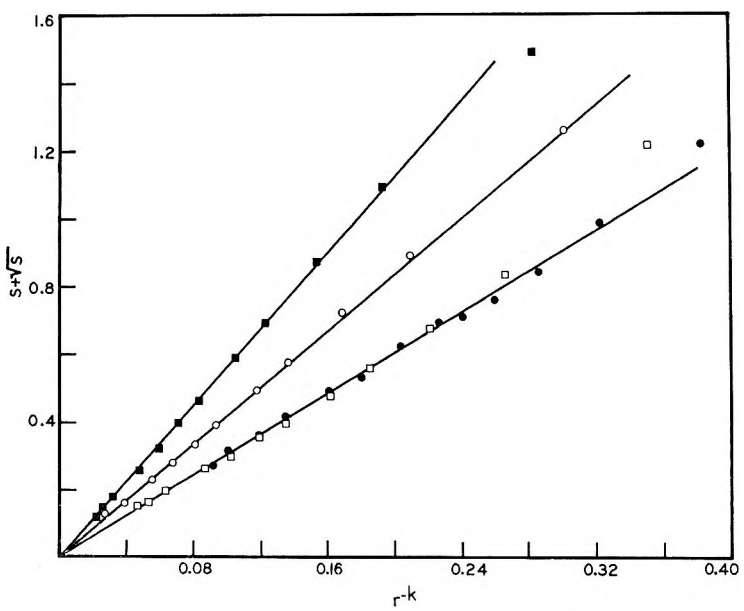

Fig. 2. $s + \sqrt{s}$ values for these four polymers plotted against r^{-k}: (●) I, $k = 0.42$; (○) II, $k = 0.52$; (■) III, $k = 0.55$; (□) IV, $k = 0.44$.

TABLE I

Polymer name	Supplier	$\bar{M}_n \times 10^{-4}$	$\bar{M}_w \times 10^{-5}$	$\bar{M}_w/\bar{M}_n$	Melt index	k
Tenite 3300	Tennessee Eastman Co.	—	—	4[a]	0.2	
Tenite 3310	Tennessee Eastman Co.	—	—	8[a]	0.7	0.44
HiFax 1400E	Hercules Powder Co.	1.75	1.75	10	0.6	0.60
HiFax 2600A	Hercules Powder Co.	1.40	2.80	20	0.2	0.30
DYNK	Union Carbide Co.	—	—	—	0.3	0.43
Alathon 7030	E. I. du Pont de Nemours Co., Plastics Division	—	—	Medium[b]	3.0	0.48
Marlex 6002	Phillips Chemical Co.	—	1.65	Broad[b]	0.2	0.42
Marlex 5003[c]	Phillips Chemical Co.	1.01	1.94	19	0.3	0.43

[a] Based on molecular weight fractionation by means of a chromatographic technique.[10] No information is available regarding the techniques used in other estimations. As they were presumably derived from light-scattering data the estimates are likely to be too high.[10]

[b] The term "medium" probably implies a ratio in the range of 10–20, whereas "broad" probably implies a ratio between 20 and 30.

[c] A copolymer of ethylene with small amounts of 1-butene.

Charlesby and Pinner[8] studied well characterized polymers provided by Dr. Mussa.[13] Their results are compared with eq. (3) in Figure 4, and Table II summarizes available information and compares the total dose range of these measurements with that in which good agreement with eq. (3) is obtained.

TABLE II
Analysis of Data of Charlesby and Pinner

Sample designation[a]	Type[b]	$\bar{M}_w/\bar{M}_n$	$\bar{M}_n \times 10^{-3}$	k	Plot linear over dose range, Mrad[c]	Total dose range of measurements, Mrad
A	HPL	2.00	11	0.49	8.0–300.	8.0–300.
B	HPL	2.12	17	0.48	5.0–100.	5.0–300.
F	HPB	3.12	40	0.27	1.0–300.	0.2–300.
G	HPB	—	50	0.29	4.0–300.	0.2–300.
H	—	—	—	0.25	1.0–300.	1.0–300.

[a] These designations are those used by Mussa.[13]

[b] HPL = high pressure polymer linear; HPB = high pressure polymer, branched.

[c] This refers to the dose range in which $s + \sqrt{s}$ varies linearly with r^{-k}.

The results of Lawton and co-workers[11] and of Woodward and co-workers[12] are compared with eq. (3) by means of a logarithmic plot in Figure 5. Table III summarizes pertinent experimental parameters and gives the values found for the exponent k.

A comparison of the results at 150°C. appears to indicate a considerable dependence of gel formation on radiation quality; this conflicts with the

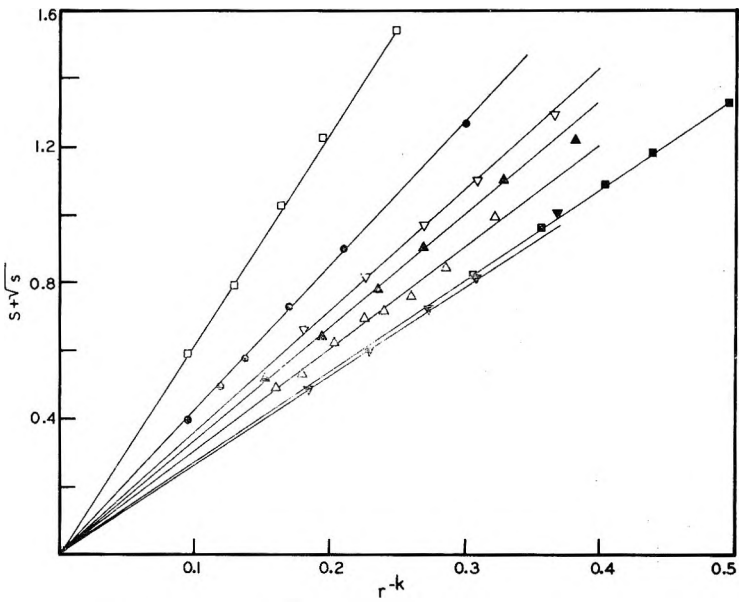

Fig. 3. $s + \sqrt{s}$ variation with r^{-k} for a number of commercial polyethylenes: (△) Marlex 6002; (▽) Tenite 3310; (▲) Alathon 7030; (□) Hifax 1400E; (■) Hifax 2600A1; (●) DYNK; (▼) Marlex 5003.

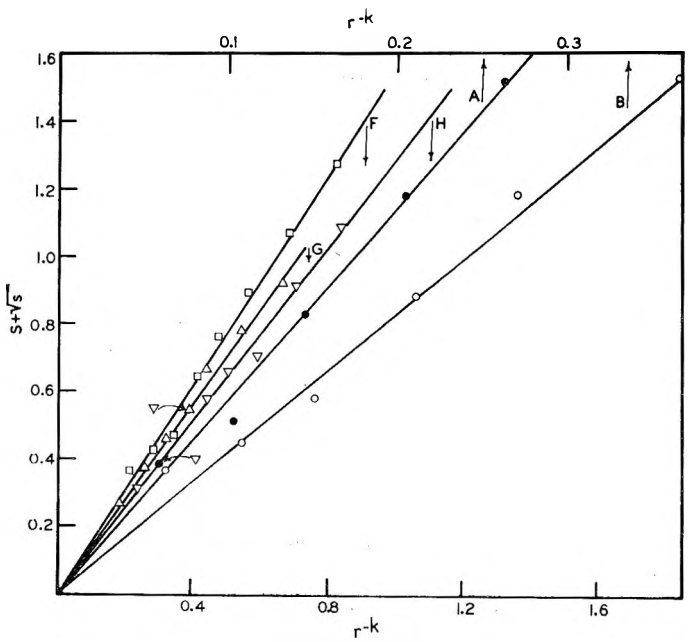

Fig. 4. Results of Charlesby and Pinner compared with eq. (3).

TABLE III

Polymer	Temperature of irradiation, °C.	$\bar{M}_\nu \times 10^{-4}$	Radiation quality	k	Reference
Marlex 50	25	3.5	Electrons	0.43	11
Marlex 50	150	—	Electrons	0.73	11
Plax Film	25	2.1	Electrons	0.42	11
Plax Film	150	—	Electrons	0.41	11
Marlex 50	30–50	—	Pile radiation	0.36	12
Marlex 50	150	—	Pile radiation	0.44	12

conclusions of several authors who studied the radiolysis of polyethylenes at room temperature.[14,15] In all probability the observed differences are rather a result of differences in experimental conditions such as in the pressure of radiolytically produced hydrogen in the samples during irradiation.

Unpublished work by the author in this laboratory has demonstrated that *trans*-vinylene growth in continuous irradiations in vacuum is very dependent upon sample thickness (when more than 0.25 mm.). The characteristics of the dependence (as sample thickness is increased the rate of increase in concentration of *trans*-vinylene groups with dose and their extrapolated concentration at infinite dose is reduced) suggest that this behavior can be attributed to changes in the concentration of radiolytically produced hydrogen in the samples. Additional confirmation comes from the observation that if the aluminum window of the irradiation cell, which

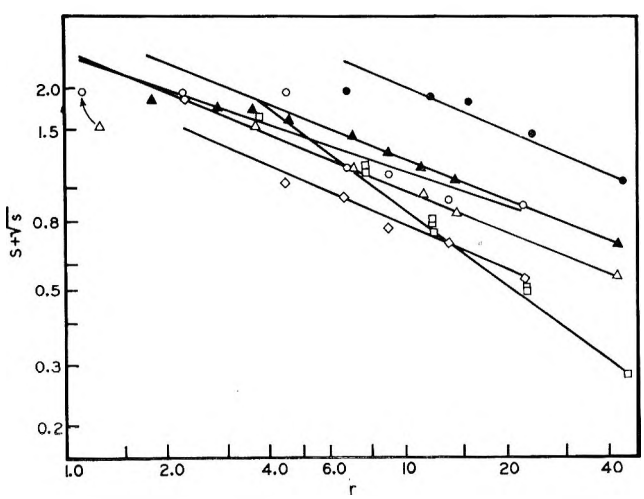

Fig. 5. Variation of $s + \sqrt{s}$ for Plax polyethylene film and Marlex 50 with dose: (▲) Plax film irradiated at 25°C.; (△) Plax film irradiated at 150°C.; (●) Marlex 50 irradiated at 25°C.; (■) Marlex 50 irradiated at 150°C.; (○) Marlex 50 irradiated at 30–50°C.; (□) Marlex 50 irradiated at 150°C.

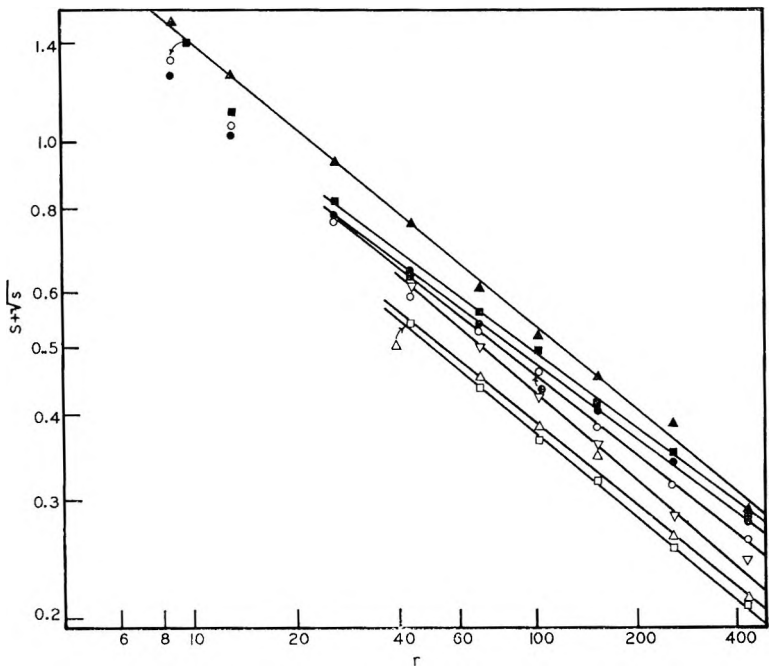

Fig. 6. Effect of sample thickness of the variation of $s + \sqrt{s}$ with dose in continuous vacuum irradiation: (●) Marlex 6002, 30 mil; (○) Marlex 6002, 20 mil; (□) Marlex 6002, 10 mil; (▲) Tenite 3310, 30 mil; (▽) Tenite 3310, 10 mil; (■) Tenite 3300, 30 mil; (△) Tenite 3300, 10 mil, △.

is held in close contact with the samples by atmospheric pressure, is replaced by a polyethylene window of equal electron absorbance, still lower rates of *trans*-vinylene growth are observed. An examination was made of the effect of varying sample thickness on gel formation in continuous vacuum irradiations. Reference to experimental absorbed dose–penetration depth curves indicated that, neglecting back scattering, the difference in absorbed dose between the thickest and thinnest samples used was not greater than 10%. The results are presented in Figure 6.

On comparing the 30 and 20 mil thick Marlex 6002 samples (irradiated simultaneously) it is seen that at low doses the thicker sample has a lower sol fraction; at medium dose levels both give much the same sol fraction, whereas at high dose levels, the thinner sample gives the lower sol fractions. A higher absorbed dose or average temperature during irradiation in the thicker samples would result in uniformly lower sol fractions. The observed effect is not uniform and at high doses the thickest samples give the highest sol fractions. Examination of the infrared absorption band at 10.35 μ indicated that the thicker the sample, the lower the *trans*-vinylene concentration at a given dose level. At levels of 150 Mrad and over the *trans*-vinylene concentration in the thinnest films was about 30% greater than that in the thickest films. It is considered that these results can only

TABLE IV
Variation of k with Thickness of Polymer in Continuous Vacuum Irradiations

Polymer type	Thickness, mils	Dose range, Mrads	k
Marlex 6002	30	10–500	0.36
	20	10–500	0.38
	10	50–500	0.41
Tenite 3300	30	10–500	0.37
	10	50–500	0.40
Tenite 3310	30	10–500	0.41
	10	50–500	0.42

be attributed to the effect of changes in the concentration of radiolytically produced hydrogen. The variation of sol fraction with dose in continuous vacuum irradiation can still be represented by eq. (3), and Table IV gives the values of the constant k for various thicknesses of polymer.

It will be noted that the k values for the thinner films continuously irradiated in the vacuum cell approach the values for films of varying thickness irradiated intermittently in air.

Polypropylene

A possible explanation of the observed gelation behavior of polyethylene is that the rate of main chain scission decreases as the dose is increased, though there is at least one other possibility which will be discussed later. No experimental evidence for varying main chain scission rates in polyethylene has been obtained thus far. Indeed, as pointed out in the introduction, there is some disagreement about the existence of this reaction. It has been shown, however, that main chain scission is a major feature of the radiolysis of polypropylene[16,19] at low doses; moreover, there are good grounds for concluding that the main chain scission rate varies with dose.

The radiation chemistry of polypropylene was originally studied by Black and Lyons.[16,17] In a study of the effect of ionizing radiation on viscosity-average and weight-average molecular weight,[17] they suggested that chain scission and crosslinking in this polymer are not directly proportional to dose but that the chain scission rate, initially high, decreased markedly on irradiation while the crosslinking rate increased. They attributed these changes to a competitive reaction whereby radiolytically formed unsaturation forms endlinks or crosslinks by reaction with excited or ionized species which otherwise lead to main chain fracture. Their equation expressing the variation of molecular weight of polypropylene with dose indicated that a polypropylene of initial number-average molecular weight in the range 1.0×10^4–1.4×10^4 would show no decrease in molecular weight up to the gel point if each molecule initially contained one vinylidene group. Recently Salovey and Dammont[20] found that the initial number-average molecular weight (11,000) of an atactic polypropylene did not decrease more than 10% up to the gel point during exposure to ionizing radiation.

Black and Lyons did not allow for changes in molecular weight distribution during radiolysis in their analysis. However, their light-scattering results indicated that the $\bar{M}_w/\bar{M}_n$ ratio tended to 2 above a dose of 2 Mrads, though this was not reported at the time. Later, Dole and Inokuti,[18] in a more detailed analysis of intrinsic viscosity changes in atactic and isotactic polypropylene when exposed to ionizing radiation, concluded that only a part of the observed behavior could be attributed to chain branching and molecular weight distribution changes. They also suggested that the rate of main chain scission decreased with dose (in carrying out this analysis they assumed that the crosslinking rate was independent of dose).

TABLE V

Polypropylene type	Reference	Symbol in Fig. 7	k	$\Sigma d^2_{s+\sqrt{s}}$ from eq. (3)	$\Sigma d^2_{s+\sqrt{s}}$ from eq. (2)	No. of observations	F ratio	Probability of improvement occurring by chance, %
Atactic	20	○	0.42	0.0432	0.0762	16	7.37	<1
Atactic	19	▲	0.49	0.0326	0.0471	7	2.16	10
Isotactic[a]	19	□	0.38	0.0329	0.0580	10	4.75	1
Isotactic	17	■	0.45	0.0079	0.0155	6	3.43	10
Isotactic[a,b]	12	△	0.38	0.0450	0.0897	14	7.46	<1
Isotactic	12	●	0.5-0.6	—	—	7	—	[c]

[a] Woodward[22] has suggested that the samples of Profax polypropylene film examined by the authors of references 12 and 19 are identical. The identical dose exponents using gamma and pile radiation support this conclusion.

[b] These experimental results were obtained at two dose rates corresponding to nuclear pile power levels of 100 and 200 kw.

[c] Mainly due to the effect of one measurement at the highest dose, nonzero intercepts were obtained in fitting these results to eq. (3). Although with $k = 0.6$, this result, possessing more than 3 times the mean variance of the other measurements, could justifiably be omitted, omission was not justifiable when the results were plotted against the reciprocal dose. Forcing the best fit to eq. (3) to pass through the origin gave a considerably greater variance than did the fit to eq. (1).

A criticism of the theory of Black and Lyons, not previously noted, is that the concentration of vinylidene unsaturation, which their mechanism requires to remain constant at doses above the gelling dose, actually, as their results show, continues to increase above this dose. We infer either that their theory is incorrect or that $s + \sqrt{s}$ for this polymer does not vary linearly with reciprocal dose. All authors who have published $s + \sqrt{s}$ curves for this polymer have assumed this variation to be linear. However extrapolated p_0/q_0 values for isotactic polypropylene vary between 0.75 and 1.0, and there is even greater divergence between the two published values for the atactic polymer: 0.40[21] and 0.80.[20] Woodward[22] obtains extrap-

olated p_0/q_0 values for Profax isotactic polypropylenew hich differ for the quenched (0.45) and annealed (0.75) polymer. He tentatively associates this difference with crystallinity changes. However, such an explanation cannot account for differing ratios obtained with atactic polypropylene. A possible explanation is that $s + \sqrt{s}$ does not vary linearly with r^{-1}.

Table V shows the values for the exponent k which give best agreement between the results of Black and Lyons,[16] Dole and Schnabel,[19] Salovey and Dammont,[20] and Woodward and co-workers[12] with eq. (3). This table also gives the total variance in $s + \sqrt{s}$ when the results are plotted in the

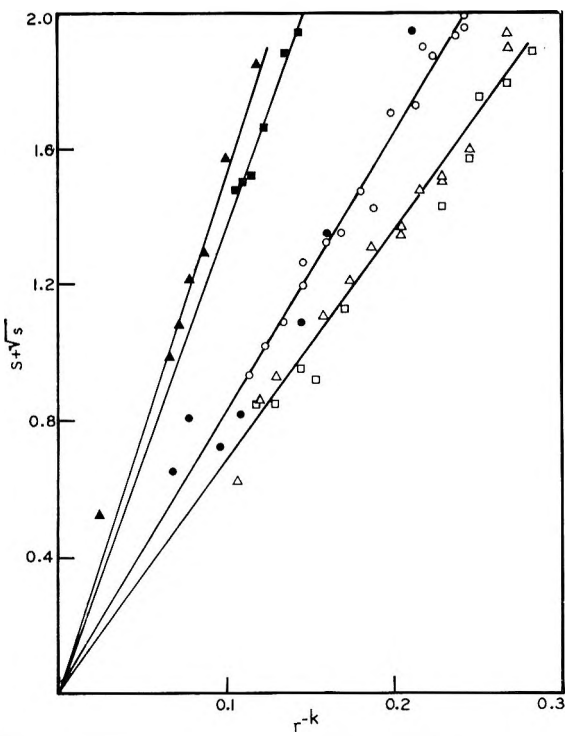

Fig. 7. $s + \sqrt{s}$ values for polypropylene plotted against a power of the reciprocal dose (lines drawn to intersect the origin). Table V identifies the symbols.

normal fashion and against a fractional power of reciprocal dose and includes an estimate of the statistical significance of any improvement in variance. A comparison in this form is necessary because most of these investigators only measured a limited range of sol fractions. $s + \sqrt{s}$ values are plotted against reciprocal dose to the appropriate power in Figure 7.

In only one out of the six sets of observations analyzed did eq. (3) give a poorer fit to the experimental results than eq. (2). Moreover, this set of observations was the only one to yield an $s + \sqrt{s}$ intercept at infinite dose significantly different from zero when fitted to eq. (3).

Other Polyolefins

Poly-1-hexene and poly-1-pentene have been studied by Cooper and Gilbert.[23] Their results were analyzed in detail by Dole and Inokuti[18,21] who showed that G (chain scissions) in the former polymer falls markedly with increasing dose in the pre-gel range They also noted that gel formation in both polymers[21] failed to yield good agreement with the modified Charlesby-Pinner equation of Inokuti.[9] The variation of $s + \sqrt{s}$ with fractional powers of the reciprocal dose is shown in Figure 8. Whereas

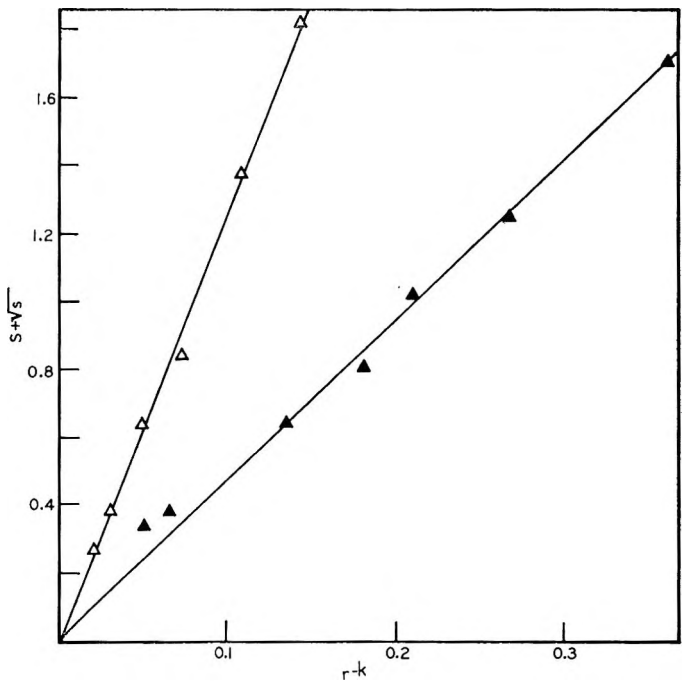

Fig. 8. Variation of $s + \sqrt{s}$ with a fractional power of reciprocal dose for (△) poly-1-pentene, $k = 0.53$ and (▲) poly-1-hexene, $k = 0.43$.

poly-1-pentene shows excellent agreement with eq. (3), deviations occur at very high doses with poly-1-hexene. In view of the close similarity between these two polymers, this difference is somewhat surprising. There were, however, slight differences in the irradiation conditions used. Poly-1-pentene was irradiated as an unsupported film, but poly-1-hexene—a gum —was irradiated as films cast in small flat-bottomed dishes, and this may have influenced the results.

GENERAL COMMENTS

The preceding analysis of Charlesby and Pinner's results with the high pressure polymerized linear polyethylenes A and B of Mussa, which had

closely random distributions, could be taken to indicate that eq. (3) for polyolefins of random distribution may be rewritten:

$$s + \sqrt{s} = Kr^{-1/2} \tag{4}$$

However, the evidence that the relationship may be affected by temperature, hydrogen pressure, and other factors raises the possibility that the above relationship is coincidental. The samples F, G, and H of Mussa, which were all high pressure branched commercial polyethylenes with much broader distributions and much higher molecular weights, gave dosage exponents between 0.25 and 0.3. On the other hand, most of the polyethylenes studied by the author also had broad molecular weight distributions, but yielded values between 0.4 and 0.6 for this exponent. It seems no coincidence that most (but not all) of these polymers were prepared by low pressure polymerization and contained vinyl or vinylidene groups (probably one per molecule). Dole and Williams[24] have presented evidence which indicates that in such circumstances rapid endlinking or crosslinking occurs, so that above about 15 Mrad dose (when unsaturation decay is substantially complete), the variation of sol with dose may correspond to a distribution much narrower than that indicated by the initial $\bar{M}_w/\bar{M}_n$ ratio.

It has been shown that there are reasonable grounds for concluding that the observed dependence of $s + \sqrt{s}$ on some fractional power of reciprocal dose is associated with varying main chain scission rates. However, the occurrence of dose dependent main chain scission rates in polyethylene would be expected to lead to a nonlinear dependence of elastic modulus in the melt on the radiation dose. All reported measurements imply a linear dependence of elastic modulus in the melt on the radiation dose, and the melt modulus of all the polyethylenes examined by the author was found to vary linearly with dose in the range of 10–100 Mrad. At higher doses some nonlinearity could be detected (modulus increased at a faster rate than that implied by the linear relationship), but the experimental error in this range is so large that no firm conclusions can be drawn. For this reason we cannot exclude the alternative explanation that the chance of a molecule becoming part of the crosslinked network depends not only on its molecular weight but also on the probability that some previous radiation event (such as *trans*-vinylene formation) has already occurred in that molecule.

It is suggested that the relatively large increases in gel which occur at low doses when hydrogen is prevented from diffusing out of the polymer are a result of increased vinyl decay (Dole[25] has already shown that preventing the escape of hydrogen from Marlex 50 during radiolysis increases vinyl decay). The increased hydrogen concentration may increase the decay by facilitating radical migration by means of exchange reactions.[26,27] The inhibitory effect of hydrogen on gel formation at higher doses may be due to an increased participation of *trans*-vinylene groups in crosslinking reactions (i.e., by hydrogen atom or alkyl radical scavenging). This would increase the probability of crosslinking occurring in the high molecular

weight fraction of the polymer which would already be part of the crosslinked network and reduce the probability of crosslinks occurring in the soluble low molecular weight fraction. Another possibility is that the rate of main chain scission is inversely dependent on the *trans*-vinylene group concentration. Hence, less chain scission occurs when hydrogen is allowed to diffuse out readily because *trans*-vinylene growth is greater.

Thus, any or all of the preceding factors may be involved in determining the growth of gel in polyolefins during irradiation. Gel formation in polyolefins is certainly a more complex process than is generally assumed and, therefore, inferences drawn on the basis of extrapolations of Charlesby-Pinner plots may be considerably in error.

The author thanks Mr. Alvah Lawrence for his assistance with the experimental work and Dr. E. C. Stivers for his interest in and encouragement of this work.

References

1. Charlesby, A., *Proc. Roy. Soc.* (*London*), **A222,** 60 (1954).
2. Baskett, A. C., and C. W. Miller, *Nature*, **174,** 364 (1954).
3. Charlesby, A., *Atomic Radiation and Polymers*, Pergamon Press, New York, 1960, p. 212.
4. Alexander, P., and D. Toms, *J. Polymer Sci.*, **22,** 343 (1956).
5. Schumacher, K., *Kolloid Z.*, **157,** 16 (1958).
6. Balwit, J. S., E. J. Lawton, and A. A. Miller, *J. Phys. Chem.*, **60,** 599 (1956).
7. Chapiro, A., *Radiation Chemistry of Polymeric Systems*, Interscience, New York, 1962, p. 421.
8. Charlesby, A., and S. H. Pinner, *Proc. Roy. Soc.* (*London*), **A249,** 367 (1959).
9. Inokuti, M., *J. Chem. Phys.*, **38,** 2999 (1963).
10. Guillet, J. E., R. L. Coombs, D. F. Slonaker, and H. W. Coover, Jr., *J. Polymer Sci.*, **47,** 307 (1960).
11. Lawton, E. J., J. S. Balwit, and R. S. Powell, *J. Polymer Sci.*, **32,** 257 (1958).
12. Chappel, S. E., J. A. Sauer, and A. E. Woodward, *J. Polymer Sci.*, **A1,** 2805 (1963).
13. Mussa, C., *J. Polymer Sci.*, **28,** 587 (1958).
14. Chapiro, A., *J. Chem. Phys.*, **52,** 246 (1955).
15. Atchinson, G. J., *J. Polymer Sci.*, **35,** 557 (1959).
16. Black, R. M., and B. J. Lyons, *Nature*, **180,** 1346 (1957).
17. Black, R. M., and B. J. Lyons, *Proc. Roy. Soc.* (*London*), **A253,** 322 (1959).
18. Dole, M., and M. Inokuti, *J. Polymer Sci.*, **A1,** 3289 (1963).
19. Dole, M., and W. Schnabel, *J. Phys. Chem.*, **67,** 295 (1963).
20. Salovey, R., and F. R. Dammont, *J. Polymer Sci.*, **A1,** 2155 (1963).
21. Dole, M., and M. Inokuti, *J. Chem. Phys.*, **38,** 3006 (1963).
22. Woodward, A. E., *J. Polymer Sci.*, **B1,** 621 (1963).
23. Cooper, G. D., and A. R. Gilbert, *J. Polymer Sci.*, **38,** 275 (1959).
24. Dole, M., and T. F. Williams, *J. Am. Chem. Soc.*, **81,** 2919 (1959).
25. Arvia, A. J., M. Dole, and T. F. Williams, *Proc. Intern. Conf. Peaceful Uses Atomic Energy* (*Geneva*), Vol. 29, 171 (1958).
26. Koritskii, A. T., Yu. N. Molin, V. N. Shamshev, N. Ya. Bulen, and V. V. Voevodskii, *Akad. Nauk, SSSR, High Molecular Compounds*, **1,** 1182 (1952).
27. Cracco, F., and M. Dole, *J. Phys. Chem.*, **66,** 193 (1962).

Résumé

On a démontré qu'une valeur raisonnable pour le rapport entre les vitesses de scission de la chaîne principale et de pontage pour un certain nombre de polyoléfines à des doses

infinies, est pratiquement égal à zéro. En plus, la somme de la fraction sol (s) et de sa racine carrée ($\sqrt{s}$) est pour presque tous les polymères étudiés proportionnelle à une certaine puissance fractionnaire de l'inverse de la dose. Il existe quelque évidence pour suggérer que ($s + \sqrt{s}$) pour des polyoléfines de poids moléculaire relativement bas, qui contiennent initialement des petites quantités d'insaturation réactionnelle carbone-carbone et possèdent une distribution statistique, serait proportionnel à la racine carrée de l'inverse de la dose. Il est clair que les vitesses de scission de la chaîne principale dans le polypropylène et le poly(1-pentène) diminuent avec un accroissement de la dose: une telle variation peut expliquer la relation observée pour ces polymères et probablement aussi pour le polyéthylène. Une autre explication est que la probabilité pour une molécule de s'attacher à un réseau ponté, ne dépend pas uniquement du nombre, d'unités monomériques qu'elle contient mais aussi de la probabilité qu'une irradiation antérieure (formation de *trans*-vinylène aie) déjà en lieu dans cette molécule.

Zusammenfassung

Es wird gezeigt, dass der wahrscheinliche Wert für das Verhältnis von Hauptkettenspaltungs- zu Vernetzungsgeschwindigkeit bei einer Anzahl von Polyolefinen bei unendlicher Dosis nahe bei null liegt. Ausserdem ist die Summe der Solfraktion (s) und ihrer Quadratwurzel ($\sqrt{s}$) bei fast allen untersuchten Polymeren einer bestimmten gebrochenen Potenz der reziproken Dosis proportional. Es bestehen schwache Hinweise dafür, dass $s + \sqrt{s}$ bei verhältnismässig niedrigmolekularen Polyolefinen, welche anfänglich kleine Mengen aktiver C=C-Doppelbindungen enthalten und eine statistische Verteilung besitzen, zur Quadratwurzel der reziproken Dosis proportional ist. Es gibt schon gute Belege dafür, dass die Hauptkettenspaltungsgeschwindigkeit bei Polypropylen und Poly(1-penten) mit steigender Dosis abnimmt: Eine solche Abhängigkeit kann die bei diesen Polymeren und wahrscheinlich auch bei Polyäthylen beobachtete Beziehung erklären. Eine weitere Erklärungsmöglichkeit besteht darin, dass die Wahrscheinlichkeit, dass ein Molekül an das Netzwerk gebunden wird, nicht nur von der Zahl der Monomereinheiten, die es enthält, sondern auch von der Wahrscheinlichkeit, dass ein vorangegangenes Strahlungsereignis (wie *trans*-Vinylenbildung) schon in der betreffenden Molekel stattgefunden hat, abhängt.

Received June 3, 1964

JOURNAL OF POLYMER SCIENCE: PART A VOL. 3, PP. 793-801 (1965)

Properties of Semicrystalline Polyolefins. III. Plasticization and Crystallization Phenomena in Sterically Hindered Polyolefins

I. KIRSHENBAUM, R. B. ISAACSON, and W. C. FEIST, *Chemicals Research Division, Esso Research and Engineering Company, Linden, New Jersey*

Synopsis

Increasing crystallinity and spherulite growth in rigid polymers can lead to increased resistance to deformation. Crystallization is facilitated by plasticization which, by increasing chain or segmental mobility, may promote both nucleation and the rate of crystal growth. Evidence points to the latter effect of increased rate of crystal growth being the more important when the plasticization is effected via sequential copolymerization techniques. In a number of copolymer systems, the increased extent of crystal growth more than compensates for the plasticization effects on molecular mobility and as a result, the "copolymers" show higher crystalline melting points, higher heat distortion temperatures, and increased modulus.

A special feature of spherulite structures in polyolefins is their specific appearance when viewed under a polarizing microscope. The appearance and structural elements of the spherulites have been studied in some detail by Keller, Price, and others.[1-3] Studies have been carried out relating the effect of crystallization conditions on the formation of various spherulite structures. However, little has been done relating spherulite growth with structural modifications effected by copolymerizations. Initial studies along these lines were reported in a previous paper.[4] Of the many different methods that have been used to study the development of crystallinity and spherulites in polymers, microscopic or photomicrographic observation of the size, number, and rate of growth of spherulites has a number of advantages. This is especially true when these observations are coupled with a measurement of the birefringence of the crystalline polymer sample. Photomicrographic studies involving the birefringence of 4-methyl-1-pentene polymers have been published.[4]

Although poly-4-methyl-1-pentene is a comparatively highly crystalline polymer, little spherulite growth has been observed with this polymer when conventional modes of preparation were used. Likewise, isotactic polystyrene can be prepared in semicrystalline form, and again spherulite growth is limited. A study was, therefore, carried out to find methods of promoting the growth of spherulites. Our studies have shown that co-

polymerization procedure involving sequential addition techniques can lead to enhanced spherulite growth with extremely interesting effects on the physical and mechanical properties of the polymers. This report discusses these findings for copolymer systems involving 4-methyl-1-pentene, styrene, and propylene.

EXPERIMENTAL

All polymerizations were performed in a dry, oxygen-free nitrogen atmosphere. The reactions were carried out in a stirred glass reactor which was assembled while hot in a stream of dry nitrogen. Styrene monomer was distilled from $LiAlH_4$ under nitrogen immediately before use. Propylene and ethylene were purified by percolation through solutions of $Al(i\text{-}Bu)_3$ in a light hydrocarbon oil. Hydrocarbon diluents were percolated through activated alumina and stored over freshly cut sodium ribbon. Sequential addition copolymers of the A. . .B, A. . . B. . .A, and B. . .A type were prepared with alkyl aluminum–transition metal catalysts, the principal comonomer (A) being 4-methyl-1-pentene, propylene, or styrene.

Propylene–Hexene-1 and Propylene–Octene-1 (A. . .B) Copolymers

In a typical A. . .B type copolymerization, the hydrocarbon diluent was saturated with dry propylene (monomer A) at 60°C. The catalyst was added as a hydrocarbon slurry and the temperature raised to 80°C. over a 5-min. period. The propylene flow was continued and the polymerization was allowed to proceed for 20–40 min. in the presence of excess propylene. At the end of the initial polymerization period, the propylene feed was cut off and the polymer slurry flushed for 5 min. with dry nitrogen. The second monomer (B) was then charged to the reactor in one portion and the polymerization allowed to proceed. After the second polymerization period, the catalyst was deactivated by the addition of acetyl acetone and isopropyl alcohol. The polymer slurry was cooled and the polymer precipitated with 2 liters of isopropyl alcohol. After filtration and washing with alcohol, the polymer was stabilized and dried *in vacuo* for 16 hr. at 40°C.

Ethylene–Styrene (B. . .A) Copolymers

In a typical preparation, the catalyst was suspended in a dry hydrocarbon diluent and the whole heated to 80°C. Ethylene (diluted with nitrogen) was monitored to the reactor until a desired conversion level had been reached. The ethylene feed was removed, the polymerization mixture flushed with a stream of dry nitrogen, and styrene (monomer A) introduced into the reactor. After several hours the polymerization was terminated by addition of a small quantity of methanol. The solid polymer was dried *in vacuo* at 40°C. after isolation by precipitation with a large excess of methanol and subsequent filtration.

4-Methyl-1-pentene–Propylene (A. . .B. . .A) Copolymers

In a typical preparation, the catalyst was suspended in a hydrocarbon diluent and the whole heated to 80°C. 4-Methyl-1-pentene (Phillips Petroleum, pure grade, Bartlesville, Okla.) was added to the reactor and the reaction allowed to proceed until almost complete conversion. Propylene (diluted with nitrogen) was introduced into the polymerization mass. After removal of the propylene feed and flushing of the reactor with nitrogen, an additional charge of 4-methyl-1-pentene was introduced into the reactor. The reaction was quenched with methanol and the polymer isolated as indicated above.

The test methods are described in the previous publications.[4] The pencil scratch hardness used in these studies is similar to that developed for measuring the hardness of a film. Pencils are available in all degrees of hardness from 7B to 9H. Sharp pencils of varying degrees of hardness were used to scratch the surface of a polymer sample. The hardness of the test specimen was defined as that of the pencil which will just fail to leave a visible deformation.

RESULTS AND DISCUSSION

Poly-4-methyl-1-pentene

The 4-methyl-1-pentene homopolymer, homopoly-4-MP, as prepared by the procedures described, melts at 238°C. This is the crystalline melting point as measured by the loss of birefringence, observed on a Kofler hot stage under a polarizing microscope.[4] This melting point is, of course, lower than the true thermodynamic melting point of the large perfect crystal. It is nevertheless meaningful insofar as comparisons are made with related polymers. The experimental poly-4-MP exhibits little spherulite growth even when the crystallinity is about 50%. Molded pads are very clear, and even extensive annealing of a film does not cause much haze. The photomicrograph of poly-4-MP in Figure 1*a* shows the typical appearance of homopolymer annealed at 200°C. for 12 hr. No spherulitic growth is apparent although several areas exhibit weak birefringence. Spherulite growth of poly-4-MP can, however, be promoted by sequential copolymerization using propylene as the comonomer. Figure 1*b* shows the large, well-defined spherulites of poly-4-MP in a copolymer formed by the A. . .B. . .A sequential addition technique. In these experiments, 4-MP was polymerized with an aluminum alkyl–titanium halide catalyst system, and a small quantity (~7 wt.-%) of propylene was introduced into the polymerization mixture before the final stage of the polymerization. An additional amount of 4-MP was added after the propylene had been consumed. The result was a mixture of polypropylene, poly-4-MP, and copolymers of the two monomers, with about 30% of the propylene present as copolymer. The crystalline melting points of the poly-4-MP in a polymeric mixture of this type are 2–6°C. higher than that

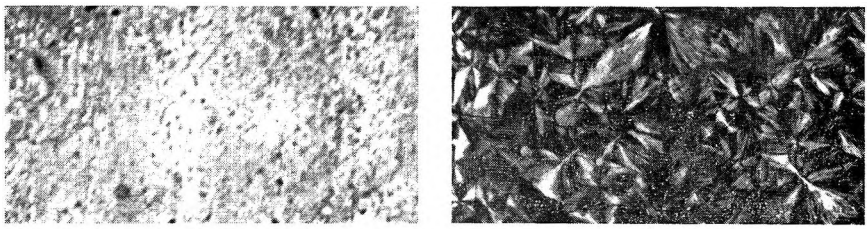

a *b*

Fig. 1. Polymer samples annealed at 200°C. for 12 hr.: (*a*) poly-4-MP; (*b*) A . . . B . . .A polymer.

normally observed for homopoly-4-MP made with the same catalyst system. The poly-4-MP in these copolymer mixtures melts in the range of 240–244°C. as compared with 238°C. for homopoly-4-MP.

It is well known that the addition of a diluent can lower the melting point of a crystalline solid. If, however, the diluent acts as a plasticizer, it can increase the mobility of the crystallizing molecules and thus increase the size and/or the perfection of the resultant crystallites. This effect could result in a higher observed crystalline melting point. Thus the presence of a diluent can either raise or lower the observed crystalline melting point of a polymer, depending upon how the diluent affects the overall morphology. It is, of course, important that the plasticizing diluent be rejected by the crystallite if an increase in melting point is to be observed. These phenomena are related to the recent work of Keith and Padden,[11] who studied the effect of impurities on spherulitic crystallization from the melt.

Extraction of the polymeric mixture with *n*-heptane and subsequent reblending gave the results shown in Table I.

We believe that the development of well-defined spherulite structures in A. . .B. . .A polymers is the result of effective plasticization by the propylene homopolymers and copolymers present. This mixture serves as a highly compatible plasticizer which may promote both nucleation and the rate of growth, but the latter effect is probably the more important. Emphasis, however, must be on the concept of high compatibility, which assures the highly effective plasticization observed. Thus solution blend-

TABLE I
Extraction of A. . .B. . .A Polymer (93% 4-MP–7% Propylene)

Treatment	*Tm*, °C.	Birefringence	Spherulites
None	240	Strong	Yes
n-Heptane, 98°C., 40 hr.			
45% Soluble	None	None	None
55% Insoluble	231	Weak	None
Blend			
50% Heptane-soluble	240	Strong	Yes
50% Heptane-insoluble			

ing of poly-4-MP and polypropylene did not result in any obvious promotion of spherulite growth of the poly-4-MP. The addition of dioctyl phthalate by physical mixing with poly-4-MP also was ineffective. The failure in both of these systems to promote spherulitic growth may be attributed to the lack of compatibility of the added "plasticizers" with poly-4-MP. Also, from a thermodynamic viewpoint, if two homopolymers are incompatible, this incompatibility in a block copolymer (where the two incompatible blocks are attached) may be a driving force to increase crystallization of the principal monomer.

The suggestion has been made[5,6] that nuclei once formed may persist in the molten polymer and may require temperatures well above the melting point to destroy them. This "memory" effect was observed photographically in the present study. The spherulites of both poly-4-MP and polypropylene in the A. . .B. . .A polymer reappeared in the same locations and had the same dimensions after several successive melting and cooling cycles.

Polystyrene

A second system in which this effect of promoting crystallization by sequential addition polymerization has been observed is that of styrene and ethylene. Homopolystyrene of high tacticity crystallizes with difficulty and, as might be expected, the extent of spherulitic growth depends upon thermal history. Figure 2*a* is a photomicrograph of a sample of isotactic polystyrene (m.p. 225°C.) that had been heated to 240°C. and then cooled rapidly (~5°C./min.) to 200°C. and annealed at this temperature for 4 hr. Figure 2*b* is the photomicrograph of the same isotactic polystyrene given the same treatment except that the maximum temperature attained was 270°C. The heating to this higher temperature was carried out in an attempt to destroy "memory" of the sample's previous thermal history. Whereas the first sample was fibrous and had a tensile

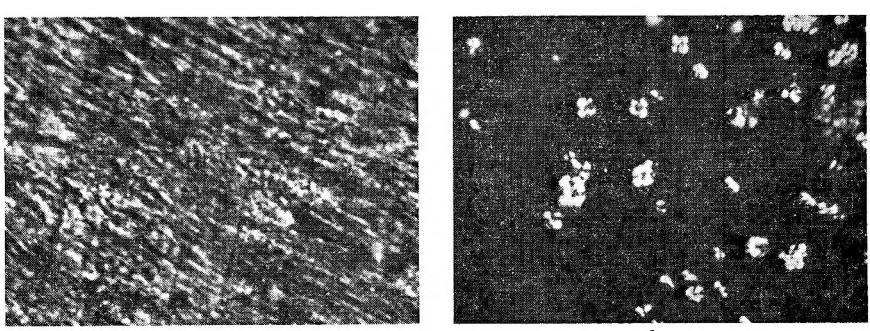

a *b*

Fig. 2. Effect of thermal history on morphology of isotactic polystyrene: (*a*) maximum melt temperature 240°C., annealed at 200°C. for 4 hr., modulus 22,000 psi; (*b*) maximum melt temperature 270°C., annealed at 200°C. for 4 hr., modulus 298,000 psi, spherulite size 0.03 mm.

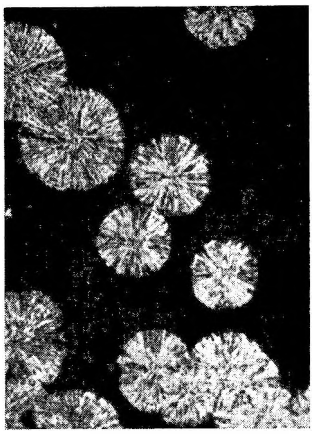

Fig. 3. Spherulite growth promoted by copolymerization (spherulite size 0.15 mm.).

modulus of only 22,000 psi, the second sample showed spherulite growth and had a tensile modulus of almost 300,000. Other experiments indicated that the transition from one form to the other starts at about 250°C. under the experimental conditions used. It would be expected that the temperature required for this change of morphology would depend upon the residence time at the temperature and upon the melt viscosity of the polymer. The higher the molecular weight, the longer the time or the higher the required temperature. It might be noted that in all cases the isotactic polystyrene had not been heated prior to the described experiments. The fibrous structure was also observed by Kargin et al.[7] in their study of unplasticized isotactic polystyrene.

Sequential copolymerization of the styrene and ethylene to introduce 5% ethylene by the B. . .A technique promoted spherulite growth of the polystyrene. As shown in Figure 3, the size of the spherulites increased fivefold (0.15 as compared to 0.03 mm.). This increased spherulite growth led, directionally, to an increased modulus and increased surface hardness. As shown by the data in Table II, the melting point was the same for the small (Fig. 2*b*) and large (Fig. 3) spherulites.

TABLE II
Spherulitic Growth Promoted by Copolymerization

Properties	Polymer[a]	
	Isotactic polystyrene (30% crystalline)	Ethylene–styrene B. . .A copolymer (5.3 wt.-% ethylene)
Spherulite size, mm.	0.03	0.15
Modulus, psi	298,000	317,000
Scratch hardness	5H	6H
Melting point, °C.	225	225

[a] Thermal history: maximum melt temperature, 270°C., annealing conditions; 200°C. for 4 hr.

In the B. . .A copolymerization, ethylene was polymerized first and styrene was then introduced into the polymerization zone.

At low levels of plasticization, chain mobility appears to be sufficiently enhanced to promote a more rapid chain packing. This phenomenon is sufficient to explain the effects observed in the B. . .A polymers. Actually studies by Guenwald[8] and by Kozlov[9] have shown that the addition of small amounts of plasticizer to poly(vinyl chloride) or polycarbonates results in an initial increase in modulus (accompanied by a decrease in impact strength). One must not, however, overlook the distinct possibility that in our A. . .B. . .A and B. . .A polymers, internally plasticized copolymers may have also served as nucleating centers for the A hompolymers (poly-4-MP or polystyrene). However, if the copolymers, possessing high internal mobility, aligned themselves into crystallization nuclei and facilitated the nucleation step, we would expect an increased number of spherulites in the sequential addition polymer systems. The experimental evidence is to the contrary in the B. . .A ethylene–styrene polymers. Many more, albeit very much smaller, spherulites were observed for homopolystyrene than for the B. . .A polymers. Thus, there were fewer nuclei in the B. . .A system, but the rate of spherulitic growth was higher.

Kargin's work[7] showed that spherulite growth in isotactic polystyrene could be promoted by the addition of 20% plasticizer (e.g., cetyl chloride). The plasticizer increased spherulite size by four to six times (in diameter). This is in agreement with our fivefold increase by internal plasticization. It should be noted, however, that internal plasticization appears to be a more efficient plasticization process, in that large spherulites were obtained with only 5% ethylene addition.

Propylene

The phenomenon of promoting crystallization processes by sequential addition copolymerization is not restricted to systems which crystallize with difficulty. It has also been observed in the use of A. . .B and A. . .B . . .A polymers in which polypropylene is the major constituent. Thus, the sequential polymerization of propylene and hexene-1 promotes crystal growth in polypropylene as reflected in a significant increase in the heat distortion temperature (HDT) of the polypropylene. The HDT is a property that is strongly dependent upon crystallinity. It would normally be expected that internal plasticization would lower the HDT because plasticization increases molecular mobility. Thus, in the case of random copolymerization, the HDT is lowered for the propylene–hexene system. However, in the case of the A. . .B and A. . .B. . .A polymers, the increased chain packing or crystal growth appears to have more than compensated for the plasticization effects on molecular mobility *per se*. As shown by the data in Table III, the sequential addition copolymers have HDT values of 122–131°C. as compared to 110°C. for homopolypropylene and 103°C. for the random copolymer.

TABLE III
Effect of Sequential Addition Polymerization on HDT

Polymer	Copolymer type	Comonomer in feed, wt.-%	HDT at 66 psi, °C.	Crystalline m.p., °C.
Propylene	Control	0	110	165
Propylene–hexene	A...B	10	131	166
	A...B...A	10	122	165
	Random	10	103	158

There is probably a fine balance between the extent of plasticization which enhances chain mobility sufficiently to increase chain packing and the extent of plasticization which so increases chain mobility that it now interferes with crystallization. Thus, Goldberg[10] found that the introduction of low levels of internal plasticization (i.e., a polyether block) into polycarbonates produced a more rigid structure, whereas at higher concentrations of the polyether blocks, chain mobility apparently became sufficiently energetic to prevent a high degree of structural order. The effects of these various phenomena on the propylene–octene system are shown in Table IV.

TABLE IV
Comparison of Propylene–Octene Polymers (Total Polymer)

	Polypropylene control	Copolymer A...B	Copolymer A...B...A	Copolymer Random	Blend[a]
Octene, wt.-%	0	3.5	4.4	2.7	3.5
Melting point, °C.	165	170	167	160	163
Tensile, psi at yield	4260	3570	3280	3070	2440
Heptane-insoluble, %	83	80	79	70	—

[a] Blended at 177°C.

Extraction of an A...B...A copolymer with hot heptane for 24 hr. and infrared analysis of the heptane-insoluble fraction showed it to contain 25–50% of the original octene-1.

CONCLUSION

The sequential addition technique provides a convenient method of altering the morphology of a base polymer. The technique leads to a mixture of homopolymer and block copolymers which introduces plasticization into the base polymer. This plasticization, especially at low levels, can promote crystal growth. Depending upon the polymer system, the increased crystal growth may be reflected in a higher crystalline melting point, higher heat distortion temperature, increased modulus, etc. There is, however, as pointed out previously, a balance between increased chain

mobility that leads to improved polymer properties because of greater crystal growth and a further increase in chain mobility that results in lower rigidity and increased flow under load. Thus, the increased crystallinity or spherulite size may, under certain conditions, also be associated with a lower heat distortion temperature, modulus, or flexural stiffness.[1]

References

1. Price, F. P., *J. Polymer Sci.*, **37**, 71 (1959).
2. Geil, P. H., *Polymer Single Crystals*, Interscience, New York, 1963.
3. Keller, A., *Makromol. Chem.*, **34**, 1 (1959).
4. Isaacson, R. B., I. Kirshenbaum, and W. C. Feist, *J. Appl. Polymer Sci.*, **8**, 2789 (1964).
5. Hartley, F. D., F. W. Lord, and L. B. Morgan, *Phil. Trans. Roy. Soc. London*, **A247**, 23 (1954).
6. Price, F. P., *J. Am. Chem. Soc.*, **74**, 311 (1952).
7. Kargin, V. A., T. I. Sogolova, and G. S. Talipov, *Vysokomolekul. Soedin.*, **5** (12), 1809 (1963).
8. Guenwald, I. G., *Kunstoffe*, **50**, 381 (1960).
9. Kozlov, P. V., R. M. Asimova, and A. H. Perepelkin, *SPE Trans.*, 2, 227 (1962).
10. Goldberg, E. P., *J. Polymer Sci.*, **C4**, 707 (1964).
11. Keith, H. D., and F. J. Padden, Jr., *J. Appl. Phys.*, **35**, 1270, 1286 (1964).

Résumé

L'augmentation de la cristallinité et de la croissance des sphérulites dans les polymères rigides peut augmenter la résistance à la déformation. La cristallisation est rendue plus facile per plastification qui, en augmentant la mobilité des chaines ou des segments, peut favoriser non seulement la formation des noyaux, mais aussi la vitesse de la croissance des cristaux. On démontre comme évident que ce dernier effet d'augmentation de la vitesse de cristallisation est le plus important quand on effectue une plastification par les techniques de copolymérisation séquencée. Dans un certain nombre de systèmes de copolymères, l'augmentation de la croissance des cristaux est plus important que les effets produits par la plastification sur la mobilité moléculaire et a comme résultat que les copolymères présentent un point de fusion des cristaux plus élevé, des températures de distortion thermiques plus élevées et une augmentation du module.

Zusammenfassung

Erhöhte Kristallinität und erhöhtes Sphärolithwachstum kann bei starren Polymeren zu erhöhter Beständigkeit gegen Deformation führen. Kristallisation wird durch Weichmachung erleichert, welche durch Erhöhung der Ketten- oder Segmentbeweglichkeit sowohl Keimbildung erleichtern als auch Kristallwachstumsgeschwindigkeit erhöhen kann. Letzterer Einfluss, nämlich die erhöhte Kristallwachstumsgeschwindigkeit scheint bei Weichmachung über eine Sequenz von copolymerisationsverfahren der wichtigere zu sein. Bei einer Reihe von Polymersystemen wird der Einfluss der Weichmachung auf die Molekülbeweglichkeit durch das erhöhte Ausmass des Kristallwachstums mehr als kompensiert, und als Folge zeigen die "Copolymeren" höhere kristalline Schmelzpunkte, höhere Wärmebeständigkeitstemperaturen und einen erhöhten Modul.

Received May 29, 1964
Revised August 6, 1964

JOURNAL OF POLYMER SCIENCE: PART A VOL. 3, PP. 803–811 (1965)

Investigation of Comonomer Distribution in Ethylene Copolymers with Thermal Methods

KARL J. BOMBAUGH and BERT H. CLAMPITT, *Research and Development Division, Spencer Chemical Company, Merriam, Kansas*

Synopsis

This paper is an extension of an earlier work in which thermal pyrolysis gas chromatography and differential thermal analysis were combined to elucidate comonomer distribution in ethylene–acrylate copolymers. In this work consideration is given to the thermal degradation products of ethylene–acrylate and ethylene–vinyl acetate copolymers. The influence of cracking temperature is considered in terms of the utility of the data. The DTA measurements are primarily concerned with the crystallization of the ethylene chains between the branch points. Indeed, a linear relationship between DTA crystallinity and branching is indicated.

INTRODUCTION

In an earlier work thermal pyrolysis gas chromatography and differential thermal analysis (DTA) were combined to elucidate comonomer distribution in ethylene–acrylate copolymers.[1] The major pyrolyzate was shown to be inversely related to the number of ethylene–acrylate junctions. The DTA first-order transition was shown to be related to the polyethylene chain length. Under the conditions of pyrolysis, the degradation profiles of block copolymers were similar to those of equivalent concentration mixtures of their respective homopolymers. The term block copolymer is applied here to copolymers with the fewest acrylate–ethylene junctions and which therefore contain long sequences of both acrylate and ethylene units.

On the surface, these findings, particularly the thermal pyrolysis data may appear to be in conflict with other current published work in the field.[2–6] For example, Strasburger and Brauer[2] reported that they were able to distinguish copolymers from equivalent concentration mixtures of homopolymers, while Barrall, Porter, and Johnson[3] reported no difference between random copolymers and random copolymer mixtures. These are just a sample of the seeming differences developing in the literature around the application of thermal pyrolysis to the study of the composition and structure of high polymers. The need for clarification seems evident.

It is the purpose of this work to examine some of the apparent discrepancies and by careful consideration of the products of degradation and cracking conditions to shed some light on the problems of interpretation. I shall, therefore, set forth a working hypothesis and provide data in support of the hypothesis.

Statement of the Hypothesis

Copolymer pyrolyzate composition is a function of the composition, the configuration of the copolymer, and of the conditions of pyrolysis. No single set of cracking conditions is preferred for all work. The optimum conditions to determine monomer content are not the same as those for determining comonomer distribution.

In general, monomer content is best determined at relatively lower cracking temperatures than those required to determine distribution. At the lower temperature only the weakest bonds are broken, and cracking patterns are somewhat simpler than at higher temperatures. However, to gain information on structural configuration it seems advantageous to crack the molecule more severely to gain more fragments, which in spite of this more complex cracking pattern, provide more information on configuration.

EXPERIMENTAL

Apparatus for Pyrolysis—GLC

The pyrolysis apparatus is similar to that described previously.[1] It was comprised of a CEC Model 201 gas chromatograph equipped with a heated multiport sample valve fitted with a thermal cracker, similar to that used by

TABLE I

Polymers examined[a]	Precut column	Analytical column
PolyEMA	6 in. DNP	136 in. ODPN + 20 in. PEG 1000
PolyEMA	78 in. DNP	78 in. Silica gel
PolyEMMA	6 in. DNP	78 in. DNP
PolyEEA	6 in. DNP	136 in. ODPN + 20 in PEG 1000
PolyEVA	12 in. Silicone	78 in. PEG 20M

[a] EMA = ethylene–methyl acrylate; EMMA = ethylene–methyl methacylate; EEA = ethylene–ethyl acrylate; EVA = ethylene–vinyl acetate; PEG = polyethylene glycol; DNP = dinonyl phthalate; ODPN = oxydipropion nitrile.

Strassberger and co-workers. The cracker is powered with a simple continuously variable power supply of our own design. Chromatograms are presented on a 1-mv. L & N Recorder.

The columns used for the separations are $^1/_4$ in. packed columns of appropriate length and composition (Table I) to effect the needed separation.

The equipment is generally operated at the condition shown in Table II.

Analytical Procedure

The cracker was isolated from the system by placing the multiport valve in the purge position. The filament assembly was removed and a polymer sample of 5–6 mg. ($^1/_4$ in. × $^1/_8$ in. 5 mils) inserted in the filament spiral.

TABLE II

Operating conditions	
Forward flow rate	72 ml./min. helium
Back flush flow rate	50 ml./min. helium
Detector voltage	12 v.
Flash heater	Off position
Column temperature	90°C.
Cracking temperature	90°C. to 600°C. in 48 sec.
Cracking time	48 sec.
Forward flow time till back flush 4 min.	

The assembly was returned to the cracking chamber and secured with a clamp. The multiport valve was turned to the sample position for about 5 min. to sweep air and volatile materials from the cracking chamber. The power leads were attached to the filament terminals and a 5.4 v. potential applied across a 2.2-ohm filament for 48 sec. producing a temperature rise from 90 to about 600°C., at which time the power was turned off. After a total of 4 min. from the time power was applied to the filament, the sample valve was returned to the purge position. This allowed the pyrolyzates of interest to be carried through the analytical column while the heavy fragments were back flushed from the precut column. With the cracker isolated from the flow system, the filament assembly was removed from the cracking chamber and power applied to the filaments to burn off any residual polymer. One minute at red heat was adequate. On completion of the chromatograms of the pyrolyzate, areas of the peaks of interest were determined with a polar planimeter and used in subsequent calculations.

Apparatus for DTA

The DTA apparatus was the same as described previously[7] and consists of a large aluminum block which is heated by circulating oil at a rate of 2.4°C./min. Sample preparation consisted of weighing 0.70 g. of polymer in the sample tube, melting at 190°C. for 10 minutes, compressing to give a compact, bubble-free sample, cooling to room temperature, reheating to 190°C. for 5 min. immediately prior to placing the warmed thermocouples into the molten polymer, and placing in the DTA apparatus.

RESULTS AND DISCUSSION

Characterization of Pyrolyzate from Ethylene–Methyl Acrylate Copolymer

The pyrolyzate produced as described above was examined first with a 2*M* dinonyl phthalate (DNP) column. The precut column was sized to pass materials eluting before C_9. Tables III and IV show a typical composition as calculated from chromatographic peak areas.

TABLE III
Light Ends Which Represent 35% Total Pyrolyzates

	Area % in gas	Area % in sample
CO	4.9	1.7
CH_4	11.0	3.9
Ethane	10.0	3.5
CO_2	17.4	6.1
Ethylene	24.3	8.5
Propane	18.7	6.5
Propylene	13.7	4.8
	100.0	35.0

TABLE IV
Composition of Pyrolyzates Below C_{16}

Peak no.		Area %
1	Light gases, CO, CO_2	17 } Gases in
2	C_3	18 } Table III
3	C_4	13
4	C_5 + methanol	8
5	C_6 + methyl acetate	16
6	Methyl acrylate	3
7	C_7	9
8	Methyl methacrylate	3.6
9	C_8	6
10	Higher ester	2
11	C_{10}	4
		100[a]

[a] The back flushed heavy ends contained higher hydrocarbons and a homologous series of esters tentatively identified as α-alkyl acrylate esters.

Several observations may be made from these data in spite of the incomplete resolution of several peaks. First, methyl methacrylate and methyl acrylate are produced in nearly equal yield. This suggests chain scission as one mode of decomposition which may proceed as follows.

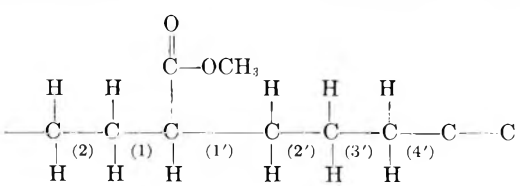

A cleavage at position 1 could be followed by cleavage at 1′ or 2′. Cleavage at 2 could be followed by cleavage at 1′ or 2′. The presence of higher esters allows cleavage at 2, 2′, 3′, or 4′, etc. producing higher α-alkyl acrylates. It can be seen that methyl acetate results from a 1, 1′ cleavage, methyl acrylate from either a 1, 2′, or 2, 1′ cleavage, while methyl methacrylate results from a 2, 2′ cleavage. Methanol, the major pyrolyzate

from MA homopolymer, results from a cleavage of the C–O ether linkage. However, the CO produced did not correlate with the amount of methanol produced. The amount of carbon dioxide produced was greater than the carbon monoxide. Therefore, the scission following cleavage of the ether linkage is not apparent from our data.

Ethylene–Ethyl Acrylate Copolymer

Barral et al.,[3] in the studies with ethylene–ethyl acrylate copolymer, reported the production principally of ethylene with a trace of ethanol and suggested cleavage primarily of the alkyl linkage with the resulting formation of the acid on the residual polymer chain. In our work, though cracking only 3 mg. of sample, we showed increased cleavage at the other side of the oxygen linkage yielding considerably more ethanol, which was analogous to our results with ethylene–methyl acrylate copolymer. Barral's conditions are advantageous for composition analysis; ours are preferred for configurational analysis since we fragmented the carbon skeletal chain.

Ethylene–Methyl Methacrylate Copolymer

Many workers have established that at relatively low cracking temperatures methyl methacrylate unzips to >99% monomer. We demonstrated that at our slightly higher cracking temperature (600°C. top temperature) we could effect a decrease in MMA monomer yield when the MMA unit was separated by ethylene units. This occurred when the cracking temperature was high enough to crack the polyethylene chain as well as to unzip the MMA portion of the chain. It may appear that one could distinguish between a homopolymer mixture and a copolymer by the amount of MMA produced on pyrolysis relative to the amount of MMA in the resin. In reality, pyrolysis cannot differentiate between a block copolymer and a homopolymer mixture. The analytical limitation may be overlooked, since in practice one seldom encounters a block ethylene–methyl methacrylate copolymer because the reactivities of the respective monomers favor formation of a random copolymer.

Vinyl Acetate–Ethylene Copolymer

Vinyl acetate–ethylene copolymer, when pyrolyzed at temperatures as low as 300°C., yields acetic acid and a light hydrocarbon (methane).[3] The pyrolyzate produced at 600°C. also includes a series of hydrocarbons, as is shown in Figure 1. The comparative ease with which the side chain is removed may present an obstacle to structural analysis even at higher temperatures. Nevertheless, the basic premise holds that lower cracking temperatures are desirable for composition analysis. If structural information is to be gained, it must be done at conditions at which the skeletal carbon chain is fragmented.

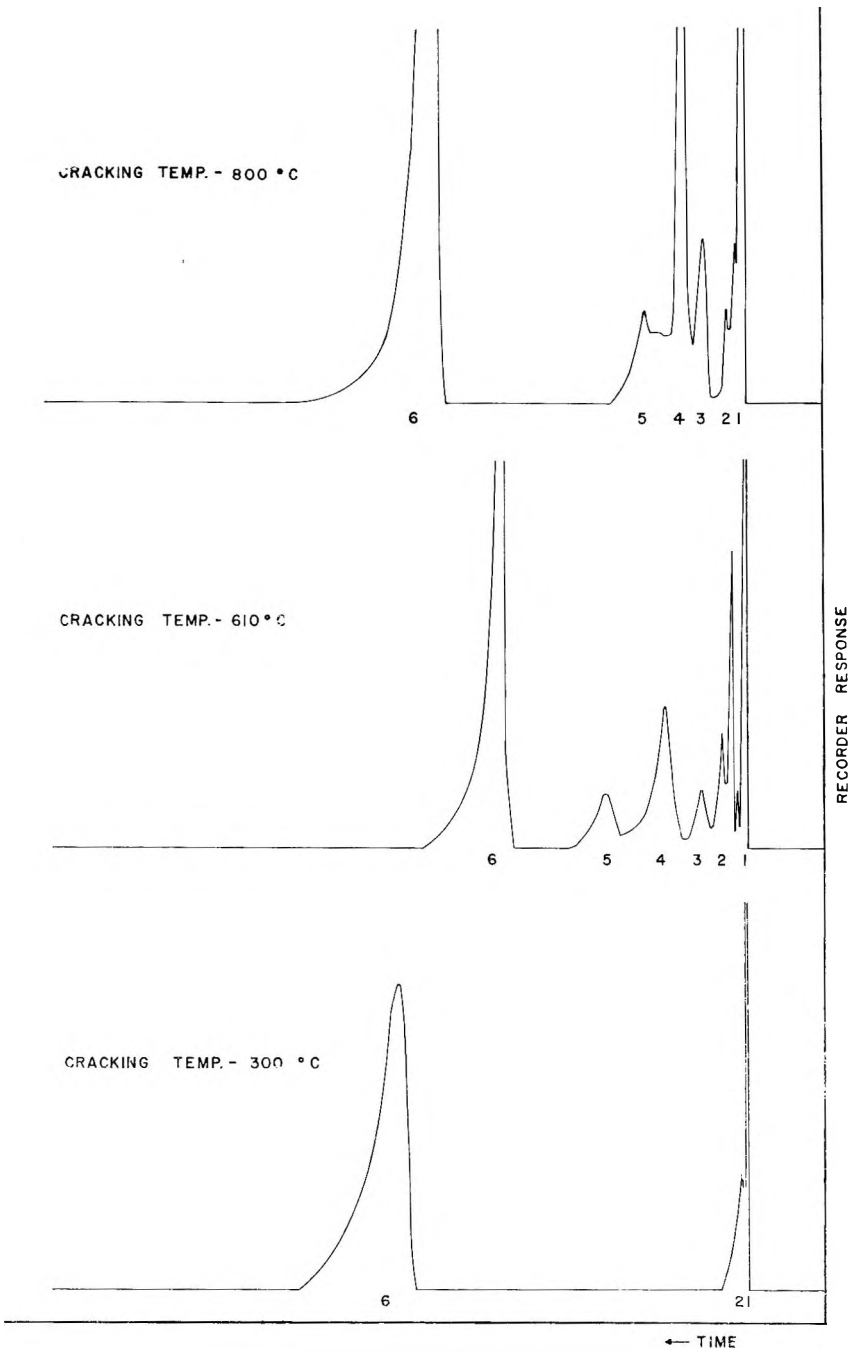

Fig. 1. Chromatograms showing the effect of cracking temperature on pyrolyzate from ethylene–vinyl acetate copolymer. Components: (1, 3, 4, 5) hydrocarbons; (2) vinyl acetate; (6) acetic acid.

The Role of Differential Thermal Analysis

As pointed out previously, the DTA technique is of primary value in analyzing the ethylene part of the copolymer. Essentially, DTA crystallinity of a copolymer system is merely a measure of the length of the carbon chain between comonomer interruptions. Actually any interruptions of the chain, whether due to methyl branching or comonomer branching, will lower the DTA crystallinity.[8,9] As most of the polymers discussed in this paper are copolymers made under the same conditions, it is fairly safe to assume that they contain the same methyl branching in the ethylene portion of the system, and therefore the DTA crystallinity is a measure of the interruptions in the carbon chain caused by comonomer units.

The causes of crystallinity in ethylene copolymers may be listed as follows: (*1*) the polymer is really a blend of two homopolymers; (*2*) the polymer is a block copolymer; (*3*) the polymer is a random copolymer, but the concentration of comonomer is below a critical value. While blending of two homopolymers may alter some of the physical characteristics of the system, the crystallinity associated with the ethylene portion of the system is not affected. Indeed DTA crystallinity has been detected in blends which contain only 5 wt.-% ethylene. DTA thermograms of block copolymers are identical to the curves obtained on polymer blends of the same composition. This point was checked by preparing a number of graft copolymers of methyl methacrylate and ethylene. The graft copolymers were prepared by adding methyl methacrylate and 0.3% benzoyl peroxide to polyethylene emulsion contained in benzene. After the solutions be-

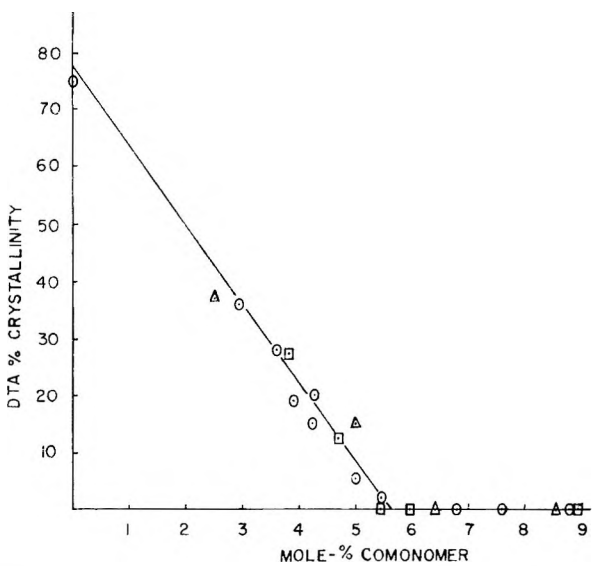

Fig. 2. Effect of comonomer concentration on DTA crystallinity of several ethylene copolymers: (⊙) methyl acrylate–ethylene; (⊡) methyl methacrylate–ethylene; (⊿) vinyl acetate–ethylene.

came viscous to stir, they were separated into two portions by their solubility in toluene at room temperature. Each mixture of polymer and copolymer was dissolved completely in hot toluene at 1–2% concentration. Each solution was allowed to cool very slowly to room temperature. The insoluble portion was assumed to be primarily graft copolymer. The insoluble graft copolymer was subsequently washed with methanol and dried. The methyl methacrylate contents of the graft copolymers were determined by infrared spectrometry. DTA curves obtained on these materials were identical to physical blends of the respective homopolymers.

A primary concern of the present paper is to discuss the crystallinity observed in random type copolymers. A number of these have been investigated, and above a certain critical composition no crystallinity is detected by DTA measurements. This point was discussed in the previous paper[1] where it was pointed out that a 20 wt.-% methyl acrylate copolymer of the random type possessed no crystallinity, whereas a block copolymer of the same composition possessed considerable crystallinity. At the 20% level the distinction between random and block methyl acrylate copolymers is quite dramatic; however, at lower comonomer levels even a random copolymer will show crystallinity. A random copolymer of low comonomer content will, however, always show a lower crystallinity than a corresponding block copolymer of similar composition.

It would be of interest to determine at what point the crystallinity of a random copolymer disappears. Therefore, a number of random copolymers containing varying amounts of methyl acrylate were prepared and DTA crystallinity measured on them. The results are given in Figure 2. As was pointed out previously, these samples were prepared under a given set of conditions and therefore the methyl branching is presumed to be more or less constant for the series. A more complete discussion of the effect of total branching (i.e., methyl plus comonomer) on the crystallinity of the system will be reported in a later paper.

Figure 2 indicates that under these conditions DTA crystallinity is a linear function of comonomer content. An intercept at about 5.5 mole-% is indicated, and above this "critical value" no crystallinity is observed. This means that 35–40 carbon atoms must be in a chain, if the polyethylene portion of the system is to crystallize. This is about half of the chain fold length of polyethylene crystals;[10,11] however, it is considerably greater than the minimum fold length of 5 carbon atoms calculated from Fisher-Hirschfelder atomic models.[11] It will be extremely interesting to see what the absolute number of carbon atoms in a chain is at the "critical value" when the total branching of the system is taken into account.

While the majority of the work has been done on methyl acrylate copolymers, some data on methyl methacrylate and vinyl acetate systems have been obtained. These results are also shown in Figure 2, and it is readily seen that on a mole basis all the comonomers affect the crystallinity in the same manner. This apparently means that crystallinity of the system is dependent only on the number of interruptions and not on their type.

This is in contrast to the chromatography results, where major pyrolyzate is primarily a function of the type and nature of the interruption of the carbon chain. It is for this reason that a combination of pyrolysis gas chromatography and DTA is extremely useful in analyzing copolymer systems.

References

1. Bombaugh, K. J., C. E. Cook, and B. H. Clampitt, *Anal. Chem.*, **35**, 1834 (1963).
2. Strassburger, J., M. T. Brauer, and A. F. Froziate, *Anal. Chem.*, **32**, 454 (1960).
3. Barrall, E. M., II, R. S. Porter, and J. F. Johnson, *Anal. Chem.*, **35**, 73 (1963).
4. Ettre, K., and F. Varadi, *Anal. Chem.*, **34**, 753 (1962).
5. Ettre, K., and P. F. Varadi, *Anal. Chem.*, **35**, 69 (1963).
6. Lehmann, F. A., and G. M. Brauer, *Anal. Chem.*, **33**, 673 (1961).
7. Clampitt, B. H., *Anal. Chem.*, **35**, 577 (1963).
8. Ke, B., *J. Polymer Sci.*, **61**, 47 (1962).
9. Wunderlich, B., and D. Poland, *J. Polymer Sci.*, **A1**, 357 (1963).
10. Lindenmeyer, P. H., *J. Polymer Sci.*, **C1**, 5 (1963).
11. Rånby, B. G., F. F. Morehead, and N. M. Walter, *J. Polymer Sci.*, **44**, 349 (1960).

Résumé

Ce travaile est une extension d'un travail antérieur dans lequel la chromatographie en phase gazeuse par pyrolyse thermique et l'analyse thermique différentielle avaient été combinées pour élucider la distribution des comonomères dans des copolymères éthylène–acrylate. Dans ce travail on considère les produits de dégradation thermique des copolymères éthylène–acrylate et éthylène–acetate de vinyle. L'influence de la température de cracking est considérée en fonction de l'utilité des résultats. Les mesures par analyse thermique différentielle concernant la cristallisation des chaînes d'éthylène entre les points de ramification. En effet on montre une relation linéaire entre la cristallinité obtenue par analyse thermique différentielle et la ramification.

Zusammenfassung

Die vorliegende Mitteilung ist die Weiterführung einer früheren Arbeit, in welcher Gaschromatographie bei thermischer Pyrolyse und Differentialthermoanalyse zur Aufklärung der Comonomerverteilung in Äthylen–Acrylatcopolymeren kombiniert wurden. In der vorliegenden Arbeit werden die thermischen Abbauprodukte von Äthylen–Acrylat- und Äthylen–Vinylacetatcopolymeren untersucht. Der Einfluss der Cracktemperatur wird in bezu gauf die Brauchbarkeit der Daten beurteilt. Die DTA-Messungen erfassen primär die Kristallisation der Äthylenketten zwischen den Verzweigungspunkten. Tatsächlich scheint eine lineare Beziehung zwischen DTA-Kristallinität und Verzweigung zu bestehen.

Received January 31, 1964
Revised May 11, 1964

JOURNAL OF POLYMER SCIENCE: PART A VOL. 3, PP. 813–825 (1965)

Field Strength Dependence of the Electric Birefringence of Potassium Polystyrenesulfonate Solutions

HARUO NAKAYAMA and KOSHIRO YOSHIOKA, *Department of Chemistry, College of General Education, University of Tokyo, Meguroku, Tokyo, Japan*

Synopsis

The electric birefringence of potassium polystyrenesulfonate (KPSS) in water and dioxane–water mixtures is proportional to the square of the field strength for limiting low fields. Saturation of the birefringence is observed at higher field strength. This effect is the more pronounced, the lower the polyelectrolyte concentration. The specific Kerr constant decreases with increasing polyelectrolyte concentration and with increasing dioxane content. On the other hand, the electric birefringence of KPSS in glycerol–water and ethylene glycol–water mixtures is related to the field strength E by the equation, $\Delta n/c = KE^n$, where c is the polyelectrolyte concentration, and K and n are constants. The exponent n changes from 1.05 to 1.70 in the range of the concentration studied (1.71×10^{-4}–1.01×10^{-3} g./cm.^{3}) in 50.9% glycerol–water. The deviation from the Kerr law is the more marked, the larger the fraction of glycerol. Alternatively, the two-term equation, $\Delta n/c = AE + BE^2$, reproduces the data fairly well. The coefficient A decreases with increasing polyelectrolyte concentration in 50.9% glycerol–water, whereas B initially increases, reaches a maximum, and then decreases. The appearance of the first-power term can not be explained by any existing theories of electric birefringence.

INTRODUCTION

The method of electric birefringence has proved to be extremely useful for studying the mechanism of orientation of macromolecules in an electric field.[1,2] For example, O'Konski and Haltner[3] concluded from electric birefringence studies that the electric orientation of tobacco mosaic virus in aqueous solution is due to the polarization of the ion atmosphere.

However, very few studies have been done on the electric birefringence of flexible polyelectrolytes in solution. O'Konski et al.[4] measured the electric birefringence of aqueous solutions of sodium polyethylenesulfonate (molecular weight 2.4×10^4). The specific Kerr constant of the solutions was exceptionally large at low polyelectrolyte concentrations, and saturation of the birefringence was observed at high field strength.

In this study, the authors have measured the electric birefringence of potassium polystyrenesulfonate in water, dioxane–water, glycerol–water and ethylene glycol–water mixtures as functions of the field strength and the polyelectrolyte concentration. In water and dioxane–water mixtures the Kerr law was found to hold for limiting low fields. On the other

hand, in glycerol–water and ethylene glycol–water mixtures anomalous behavior was observed. The electric birefringence was not proportional to the square of the field strength even for limiting low fields. Instead, it was expressed as the sum of the first-power term and the second-power term of the field strength. The appearance of the first-power term can not be explained by any existing theories.

EXPERIMENTAL

Materials

Potassium polystyrenesulfonate (KPSS) was prepared by polymerizing potassium *p*-styrenesulfonate. The monomer was synthesized following the procedure of Wiley and his co-workers:[5,6] β-bromoethylbenzene was chlorosulfonated, and subsequently the sulfonyl chloride obtained was hydrolyzed and dehydrohalogenated with potassium hydroxide in 95% ethanol.

The monomer was polymerized in 12% aqueous solution at 95°C. for 8 hr. in the presence of 0.05% $K_2S_2O_8$ under nitrogen atmosphere. The resulting viscous solution was added dropwise to a tenfold excess of vigorously stirred ethanol, and the precipitate obtained was filtered, washed with ethanol, and dried.

Fractionation was carried out by adding dioxane to a 4% aqueous solution of the polymer.[7] The fraction of the highest molecular weight was used throughout the present experiment. It was dried to constant weight in vacuo at 56°C. The molecular weight of this product was estimated to be 7.5×10^5 from its intrinsic viscosity of 128 cm.^{3}/g. in 0.2*N* KCl at 25°C.

The water used as solvent was twice-distilled and passed through a column of mixed-bed ion exchanger. The specific conductivity of this water was always less than 3×10^{-6} ohm^{-1} cm.$^{-1}$.

The solvents mixed with water were dioxane, glycerol and ethylene glycol. Dioxane was refluxed over potassium hydroxide for several hours and fractionally distilled over metallic sodium. Glycerol and ethylene glycol were of reagent grade and used without further purification.

Stock solutions were prepared by gravimetric method for each series of measurements and kept in polyethylene bottles. The solutions used in the actual experiments were obtained by dilution of the stock with solvent or adequate solutions.

Electric Birefringence Measurements

The electric birefringence apparatus was described before.[8] A collimated beam of light from a tungsten projection lamp is polarized by a polarizing Nicol prism set at 45° with respect to the electric field applied across a Kerr cell. The polarized light then traverses the cell containing the solution and passes through an analyzer on to a photomultiplier. The polarizer and the analyzer are crossed.

The Kerr cell used is a Beckman spectrophotometer cell and contains two platinum electrodes supported mechanically by Teflon at a distance 0.275 cm. apart. The cell is fitted into a thermostatted brass jacket.

Rectangular pulses adjustable in duration from 10 μsec. to 10 msec. and having amplitudes variable up to 1200 v. are applied to the electrodes. When the solution becomes birefringent, the light passing through the analyzer falls upon an RCA 1P28 photomultiplier whose output is displayed on the screen of a dual-beam oscilloscope, together with the attenuated pulse.

The optical retardation δ due to the electric field was calculated from the observed output signals following the procedure of O'Konski and Haltner.[9] Since the polarizer and the analyzer are crossed in the present experiment, we have:

$$\sin^2 (\delta/2) = \Delta I_\delta / I_0 \tag{1}$$

where ΔI_δ is the change in light intensity at the photomultiplier for an optical retardation δ and I_0 is the light intensity which would have reached the photomultiplier if the polarizer and the analyzer were parallel (excluding the stray light).

The electric birefringence Δn is related to δ by:

$$\Delta n = \lambda\delta/2\pi l \tag{2}$$

where l is the length of the path of light through the birefringent solution (l = 0.961 cm. in the present experiment) and λ is the wavelength of light in vacuum. Since white light was used in the present experiment, the observed δ will be a weighted mean over the region of spectral response of the optical system and only an effective value of λ may be estimated.[3] Therefore, experimental values were expressed in terms of $\Delta n/\lambda$ which is equal to δ divided by $2\pi l$, instead of Δn.

It was observed that the electric birefringence decreased when pulses were repeatedly applied to polyelectrolyte solutions. Therefore, the solution in the Kerr cell was replaced with a fresh one whenever a pulse was applied.

The pulse duration was adjusted so that it was long enough for the birefringence to reach the steady-state value. This was 50–100 μsec. for aqueous solutions, and 500–2000 μsec. for solutions in 50.9 wt.-% glycerol–water which is the most viscous solvent used in the present experiment. All the data of the birefringence in this paper are the steady-state values.

RESULTS

KPSS in Water and Dioxane Water Mixtures

The electric birefringence of KPSS was measured as a function of field strength over the range 8–23 e.s.u. in water and dioxane–water mixtures (28.31, 43.65, and 56.70 vol.-% dioxane) at 25°C. The range of polyelectrolyte concentration was 0.50×10^{-4} to 5.06×10^{-4} g./cm.^{3}. Figure 1

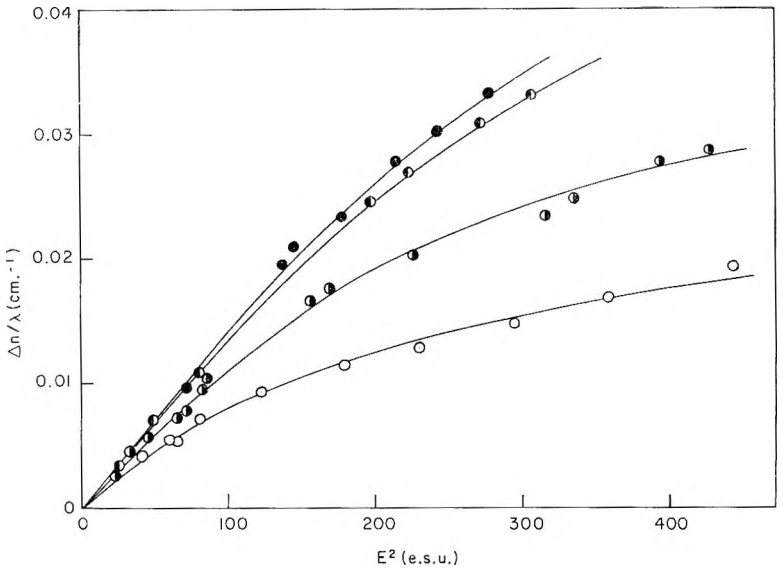

Fig. 1. Plots of $\Delta n/\lambda$ vs. E^2 for KPSS in water at various KPSS concentrations: (O) 0.50×10^{-4} g./cm.^{3}; (◑) 1.03×10^{-4} g./cm.^{3}; (◐) 3.05×10^{-4} g./cm.^{3}; (●) 4.07×10^{-4} g./cm.^{3}.

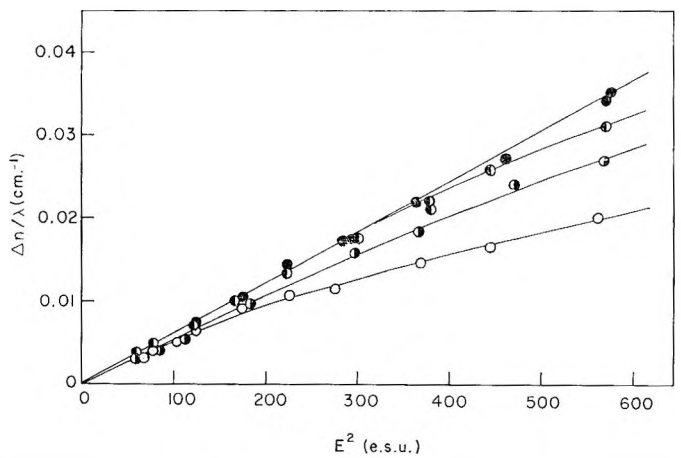

Fig. 2. Plots of $\Delta n/\lambda$ vs. E^2 for KPSS in 56.70 vol.-% dioxane–water at various KPSS concentrations: (O) 1.03×10^{-4} g./cm.^{3}; (◑) 2.02×10^{-4} g./cm.^{3}; (◐) 3.05×10^{-4} g./cm.^{3}; (●) 5.06×10^{-4} g./cm.^{3}.

presents plots of $\Delta n/\lambda$ versus E^2 for aqueous solutions, where E is the field strength. The birefringence is proportional to E^2 for limiting low fields; i.e., the Kerr law holds. Deviation from the Kerr law was observed at higher field strength. This effect is interpreted as saturation of the birefringence.[4] It is the more pronounced, the lower the polyelectrolyte concentration, as is evident from Figure 1.

Similar behavior was observed for KPSS in dioxane–water mixtures,

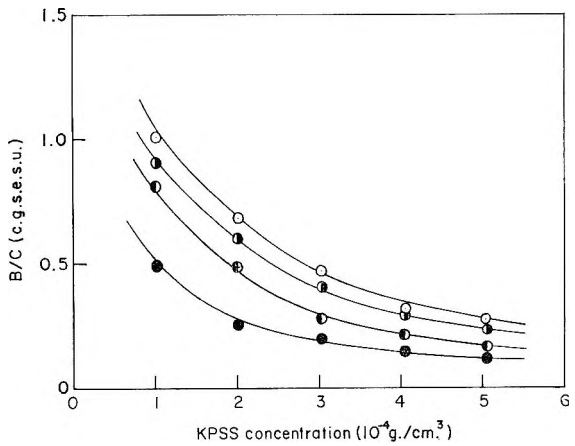

Fig. 3. Specific Kerr constant vs. concentration for KPSS in water and dioxane–water mixtures: (O) water; (◑) 28.31 vol.-% dioxane–water; (◐) 43.65 vol.-% dioxane–water; (●) 56.70 vol.-% dioxane–water.

although the saturation effect was less marked at higher dioxane content. The electric birefringence of KPSS in 56.70 vol.-% dioxane–water is shown in Figure 2, as an example.

The Kerr constant, $B = (\Delta n/\lambda E^2)_{E\to 0}$, was determined by extrapolation to zero field strength. The specific Kerr constant is defined here as B/c, where c is the concentration of solute expressed as grams/cubic centimeter. The unit of B/c is given by the c.g.s.-e.s.u. unit. Figure 3 shows the specific Kerr constant as functions of the solvent composition and the polyelectrolyte concentration. It is to be noted that the specific Kerr constant increases sharply with decreasing polyelectrolyte concentration like other properties of solutions of linear flexible polyelectrolytes, such as the reduced viscosity (η_{sp}/c)[10] and the reduced dielectric increment $(\Delta\epsilon/c)$.[11–13] These properties can not be extrapolated to zero concentration. At the same polyelectrolyte concentration, the specific Kerr constant decreases with increasing dioxane content of the solvent.

KPSS in Glycerol–Water and Ethylene Glycol–Water Mixtures

The electric birefringence of KPSS in glycerol–water mixtures exhibited anomalous behavior. In Figure 4 are shown plots of $\Delta n/\lambda c$ versus E for KPSS in 50.9 wt.-% glycerol–water at 27.5°C. When double logarithmic plots are employed as shown in Figure 5, nearly straight lines are obtained over the range of the field strength studied. The data can be correlated by the equation

$$\Delta n/\lambda c = KE^n \tag{3}$$

where K and n are constants. The exponent n for each polyelectrolyte concentration is given in Figure 5. It varies from 1.05 to 1.70 in the range of the polyelectrolyte concentration studied (1.71×10^{-5}–1.01×10^{-3}

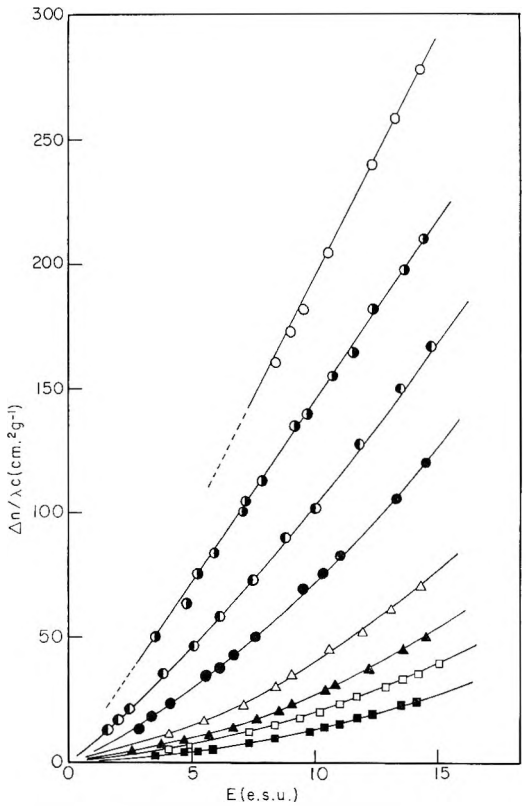

Fig. 4. Plots of $\Delta n/\lambda c$ vs. E for KPSS in 50.9 wt.-% glycerol–water at various KPSS concentrations: (○) 1.71×10^{-5} g./cm.^{3}; (◑) 4.36×10^{-5} g./cm.^{3}; (◐) 9.59×10^{-5} g./cm.^{3}; (●) 1.86×10^{-4} g./cm.^{3}; (△) 3.77×10^{-4} g./cm.^{3}; (▲) 5.33×10^{-4} g./cm.^{3}; (□) 7.01×10^{-4} g./cm.^{3}; (■) 1.01×10^{-3} g./cm.^{3}.

g./cm.^{3}). It is not certain whether the value of n approaches the Kerr law value 2 at much higher concentration.

Alternatively the two-term equation

$$\Delta n/\lambda c = AE + BE^2 \tag{4}$$

reproduces the data fairly well, where A and B are constants. Figure 6 presents plots of $\Delta n/\lambda cE$ versus E for the same systems as in Figure 4. Values of A, B, and A/B obtained from these plots are listed in Table I. As seen in the table, the coefficient A of the first-power term decreases with increasing polyelectrolyte concentration, whereas the coefficient B of the second-power term initially increases and after attaining a maximum decreases.

In Figure 7 is shown the field strength dependence of the electric birefringence for KPSS in water and 10, 30, and 50.9 wt.-% glycerol–water at a fixed polyelectrolyte concentration (9.59×10^{-5} g./cm.^{3}). In the case of the aqueous solution the log $(\Delta n/\lambda)$ vs. log E curve is not linear for higher field strengths because of the saturation effect, but the initial

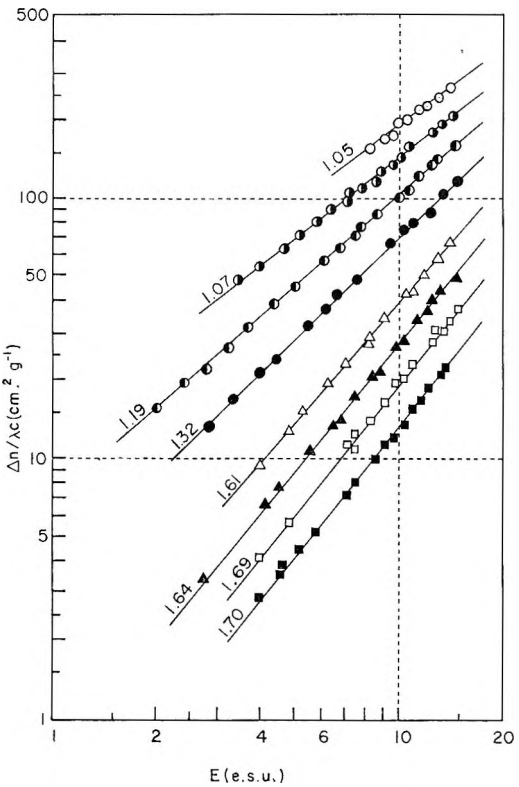

Fig. 5. Double logarithmic plots of $\Delta n/\lambda c$ vs. E for KPSS in 50.9 wt.-% glycerol–water. Symbols as in Fig. 4. Numbers indicate the slope of the straight lines.

slope is equal to 2 in accordance with the Kerr law. In the case of KPSS solutions in glycerol–water, on the other hand, the curves are almost linear over the range of the field strength studied. The slopes of the curves, equal to n in eq. (3) are 1.38, 1.33, and 1.19 for 10, 30, and 50.9 wt.-% glycerol–water, respectively. Thus the value of n decreases with increasing content of glycerol in the solvent.

TABLE I
Values of A, B, and A/B for KPSS in 50.9 wt.-% Glycerol–Water

KPSS concentration, g./cm.³	A	B	A/B
1.71×10^{-5}	19.3	0.033	590
4.36×10^{-5}	13.5	0.074	180
9.59×10^{-5}	8.2	0.22	37
1.86×10^{-4}	4.5	0.25	18
3.77×10^{-4}	1.5	0.27	5.6
5.33×10^{-4}	0.9	0.18	5.0
7.01×10^{-4}	0.6	0.13	4.6
1.01×10^{-3}	0.4	0.095	4.2

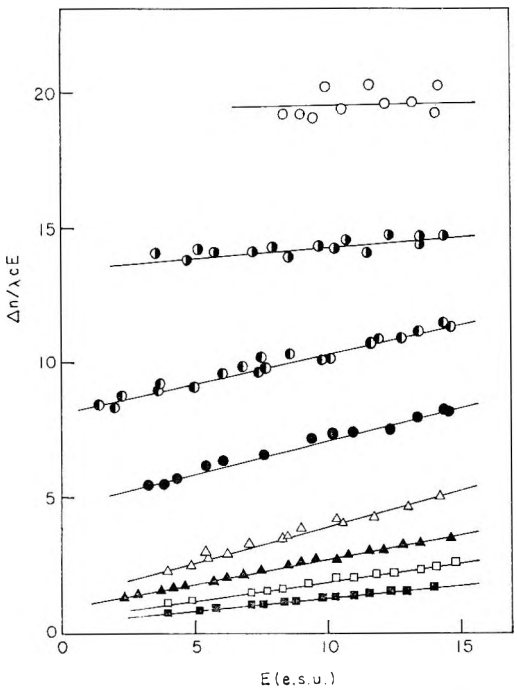

Fig. 6. Plots of $\Delta n/\lambda cE$ vs. E for KPSS in 50.9 wt.-% glycerol–water. Symbols as in Figure 4.

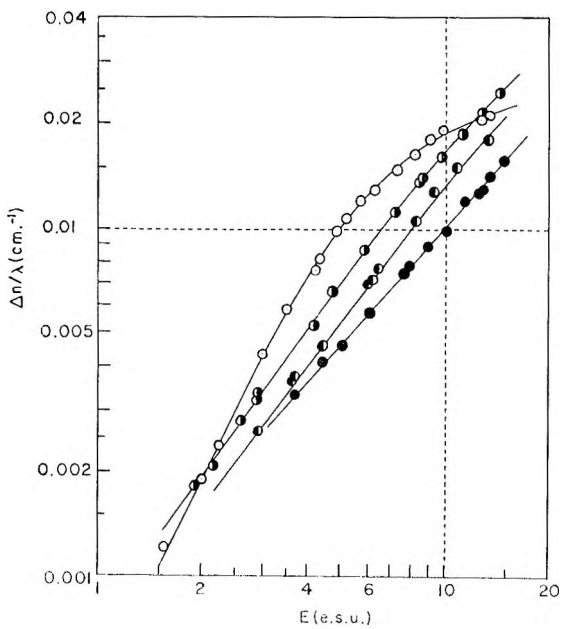

Fig. 7. Double logarithmic plots of $\Delta n/\lambda$ vs. E for KPSS in water and glycerol–water mixtures at a KPSS concentration of 9.59×10^{-5} g./cm.^{3}: (○) water; (◑) 10 wt.-% glycerol–water; (◐) 30 wt.-% glycerol–water; (●) 50.9 wt.-% glycerol–water.

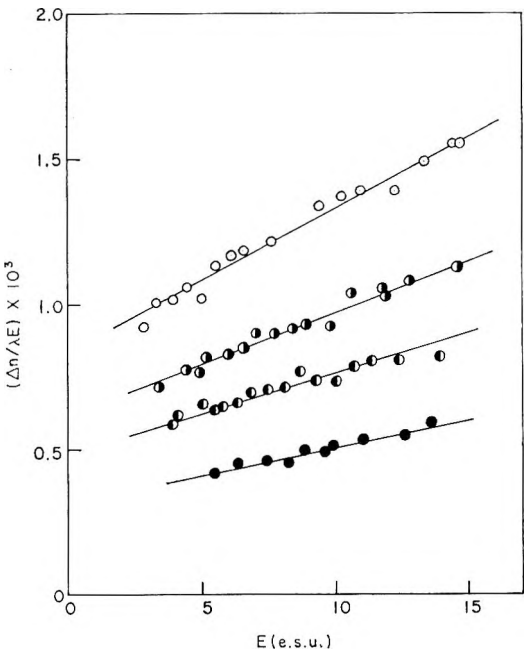

Fig. 8. Effect of KCl on the electric birefringence of KPSS in 50.9 wt.-% glycerol-water at a KPSS concentration of 8.38×10^{-4} equiv./l. (1.86×10^{-1} g./cm.^{3}) and various KCl concentration: (O) 0; (◑) 2.10×10^{-4} equiv./l.; (◐) 4.19×10^{-4} equiv./l.; (●) 8.38×10^{-4} equiv./l.

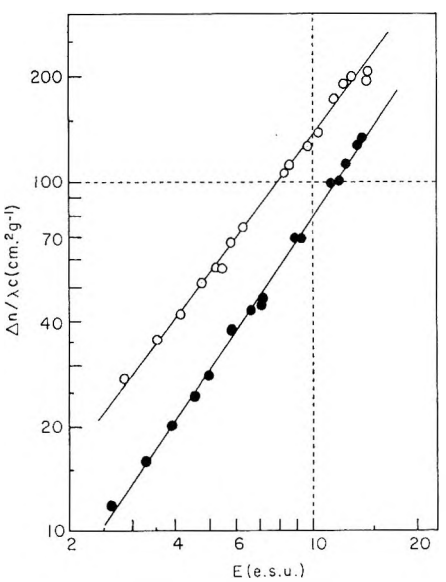

Fig. 9. Double logarithmic plots of $\Delta n/\lambda c$ vs. E for KPSS in 50 wt.-% ethyleneglycol-water at various KPSS concentrations: (O) 9.95×10^{-5} g./cm.^{3}; (●) 1.97×10^{-4} g./cm.^{3}

Next, the effect of potassium chloride on the electric birefringence of KPSS in 50.9 wt.-% glycerol–water was studied. The polyelectrolyte concentration was 1.86×10^{-4} g./cm.^{3}, i.e., 8.38×10^{-4} equiv./l. The equivalent concentration of potassium chloride added was varied from 2.10×10^{-4} to 8.38×10^{-4} equiv./l. The constants A and B in eq. (4) were obtained from plots of $\Delta n/\lambda E$ vs. E given in Figure 8. It is found that A and B decrease with the addition of potassium chloride, but the ratio A/B remains almost constant.

Similar measurements were carried out on KPSS–ethylene glycol–water systems. In Figure 9 are shown plots of $\log(\Delta n/\lambda c)$ versus $\log E$ for KPSS in 50 wt.-% ethylene glycol–water. The exponent n in eq. (3) is equal to 1.29 and 1.48 for KPSS concentration 9.95×10^{-5} and 1.97×10^{-4} g./cm.^{3}, respectively. The data can also be fitted by eq. (4).

DISCUSSION

The electric birefringence of KPSS in water may be caused by the polarization of the ion atmosphere. The polyion has approximately the shape of a rod at high dilution in a medium of high dielectric constant. The counterions more or less firmly bound to the polyion are polarized in the longitudinal direction by an external electric field; thus a large dipole moment is induced and the polyion is oriented.[3,14] This orientation gives rise to the anisotropy of the solution.

The orientation theory gives for the electric birefringence of a dilute solution of rigid axially symmetric macromolecules with no permanent dipole moment:[4]

$$\Delta n/\lambda = [2\pi (g_1 - g_2)/n\rho\lambda] \, c \, \Phi(\gamma) \tag{5}$$

with

$$\Phi(\gamma) = \frac{3}{4}\left[\frac{e^{\gamma}}{\sqrt{\gamma}\, E(\sqrt{\gamma})} - \frac{1}{\gamma}\right] - \frac{1}{2} \tag{6}$$

$$E(\sqrt{\gamma}) = \int_0^{\sqrt{\gamma}} \exp\{x^2\} dx \tag{7}$$

$$\gamma = [(\alpha_1 - \alpha_2)/2kT] \, E^2 \tag{8}$$

where α_1 and α_2 are the excess electrical polarizability in the direction of the symmetry axis and the transverse axis, respectively; $g_1 - g_2$ is the optical anisotropy factor, n is the refractive index of the solution and ρ is the density of the solute. For limiting low fields, eq. (5) reduces to the familiar expression for the specific Kerr constant:

$$\frac{B}{c} = \frac{1}{c}\left(\frac{\Delta n}{\lambda E^2}\right)_{E \to 0} = \frac{2\pi(g_1 - g_2)}{n\rho\lambda}\left(\frac{\alpha_1 - \alpha_2}{15kT}\right) \tag{9}$$

Figure 10 shows the comparison of experimental and theoretical values for an aqueous solution of KPSS ($c = 1.03 \times 10^{-4}$ g./cm.^{3}). The theoretical

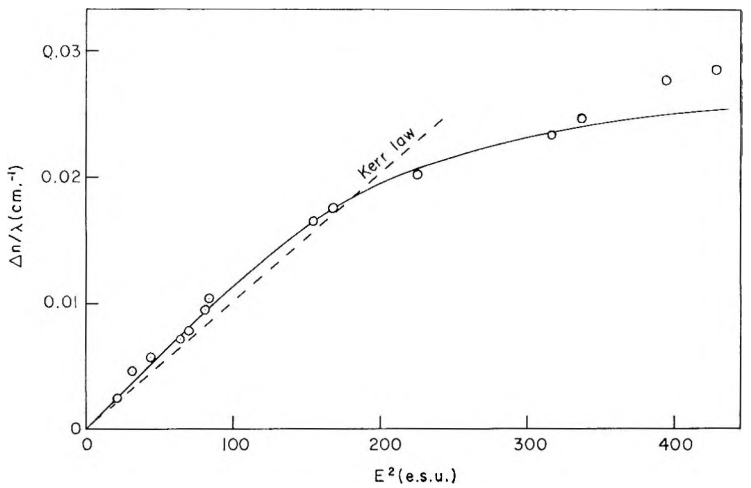

Fig. 10. Comparison of experimental and theoretical values of the electric birefringence for an aqueous solution of KPSS at 1.03×10^{-4} g./cm.^{3}: (O) experimental values; (——) theoretical curve for $\alpha_1 - \alpha_2 = 2.14 \times 10^{-15}$ cm.^{3} and $2\pi(g_1 - g_2)/n\rho\lambda = 2.9 \times 10^2$ cm.^{2}/g.

curve corresponds to values calculated from eq. (5) by using the parameters

$$\alpha_1 - \alpha_2 = 2.14 \times 10^{-15} \text{ cm.}^3,$$

$$2\pi(g_1 - g_2)/n\rho\lambda = 2.9 \times 10^2 \text{ cm.}^2/\text{g.}$$

These parameters were evaluated by curve fitting in the region of low field strength.

The agreement between theory and experiment is fairly good. However, experimental values are larger than theoretical values at higher field strength. This discrepancy may be partly due to the polydispersity of the sample. Another possible cause is that the counterions are stripped away by strong electric field (Wien effect, dissociation field effect) and, as a result, the polyion becomes more extended, thus leading to larger birefringence.

The magnitude of $\alpha_1 - \alpha_2$ cited above is of the right order, as expected from the ion atmosphere polarization for a rodlike polyion with a length of 10^3 A.* The increase of the specific Kerr constant with dilution will be ascribed to the increase of $\alpha_1 - \alpha_2$, mainly due to the extension of the polyion at lower ionic strength.

With increasing dioxane content in the solvent, the specific Kerr constant decreases and the saturation effect becomes less marked, as described in the foregoing section. This fact is explained by the diminution of $\alpha_1 - \alpha_2$ which is caused by the lowering of the dielectric constant of the medium and the coiling of the polyion.

* This value was estimated from the relaxation time of the birefringence decay.

On the other hand, the anomalous behavior observed in glycerol–water and ethylene glycol–water solutions can not be interpreted by any existing theories of electric birefringence. If the orientation of molecules is caused by the interaction of an electric field with permanent or induced dipole moment, the birefringence must be proportional to the square of the field strength for limiting low fields.

Two decades ago, Heller[15] called attention to the birefringence caused by the electrophoretic orientation, which would be due to the displacement of the particles relative to the medium. He suggested that, on this mechanism, the birefringence would be proportional to the first power of the field strength. However, his arguments have not yet been confirmed.[1–3]

Judging from our experimental results, it is probable that the anomalous effect is characteristic for polyelectrolytes in a medium of high viscosity and high dielectric constant. For reference, data for the viscosity and dielectric constant of some typical solvents used in the present experiment are listed in Table II.

TABLE II
Viscosity and Dielectric Constant of Solvents at 25°C.

Solvent	Viscosity, cpoise	Dielectric constant
Water	0.893	78.5
56.7 vol.-% Dioxane–water	1.91	30.3
50.0 wt.-% Glycerol–water	5.04	65.7
49.6 wt.-% Ethylene glycol–water	3.21	63.2

The elucidation of the nature of this new effect must await further investigations.

The authors wish to express their gratitude to Professor C. T. O'Konski of the University of California (Berkeley) for his valuable suggestions and comments on this work.

References

1. Benoit, H., *Ann. Phys.*, **6**, 561 (1951).
2. O'Konski, C. T., and B. H. Zimm, *Science*, **111**, 113 (1950).
3. O'Konski, C. T., and A. J. Haltner, *J. Am. Chem. Soc.*, **79**, 5634 (1957).
4. O'Konski, C. T., K. Yoshioka, and W. H. Orttung, *J. Phys. Chem.*, **63**, 1558 (1959).
5. Wiley, R. H., N. R. Smith, and C. C. Ketterer, *J. Am. Chem. Soc.*, **76**, 720 (1954).
6. Wiley, R. H., and S. F. Reed, *J. Am. Chem. Soc.*, **78**, 2171 (1956).
7. Cerney, L. C., *Bull. Soc. Chim. Belg.*, **66**, 93 (1957).
8. Watanabe, H., K. Yoshioka, and A. Wada, *Biopolymers*, **2**, 91 (1964).
9. O'Konski, C. T., and A. J. Haltner, *J. Am. Chem. Soc.*, **78**, 3604 (1956).
10. Fuoss, R. M., and U. P. Strauss, *J. Polymer Sci.*, **3**, 246, 602 (1948).
11. Dintzis, H. M., J. L. Oncley, and R. M. Fuoss, *Proc. Natl. Acad. Sci. U. S.*, **40**, 62 (1954).
12. Allgén, L.-G., *J. Polymer Sci.*, **14**, 281 (1954).
13. Allgén, L.-G., and S. Roswall, *J. Polymer Sci.*, **23**, 635 (1957).
14. Eigen, M., and G. Schwarz, *J. Colloid Sci.*, **12**, 181 (1957).
15. Heller, W., *Rev. Mod. Phys.*, **14**, 390 (1942).

Résumé

La biréfringence électrique deu polystyrène sulfonate de potassium (KPSS) en solution aqueuse et en solution dioxanne-eau est proportionnelle au carré du champ de force si on se limite aux champs faibles. On observe une saturation de la biréfringence dans le cas de champs élevés. Plus le concentration en polyélectrolyte est faible, plus l'effet est prononcé. La constante spécifique de Kern décroît quand la concentration en polyélectrolyte augmente et lorsque croît la teneur en dioxanne. D'autre part, la biréfringence électrique du KPSS dans un mélange glycérine—eau et éthylène glycol—eau est reliée au champs de forces E par l'équation $\Delta n/c = KE^n$ où c est la concentration en polyélectrolyte et où K et n sont des constantes. L'exposant n varie de 1.05 à 1.70 dans le domaine de concentrations étudié (1.71×10^{-5} à 1.01×10^{-3} g/cm^3) dans 50.9% de glycérine–eau. Plus la fraction en glycérol est grande, plus la déviation à la loi de Kerr est marquée. L'équation à deux termes, $\Delta n/c = AE + BE^2$, reproduit assez bien les résultats. Le coefficient A diminue avec l'accroissement de la concentration en polyélectrolyte dans 50.9% glycérol–eau, alors que B croît au début, passe par un maximum et décroît ensuite. L'apparition du terme à la première puissance ne peut pas être expliquée par une des théories existantes sur la biréfringence électrique

Zusammenfassung

Die elektrische Doppelbrechung von Kaliumpolystyrolsulfonat (KPSS) in Wasser und Dioxan-Wassermischungen ist in der Grenze kleiner Feldstärken dem Quadrat der Feldstärke proportional. Bei höherer Feldstärke wird eine Sättigung der Doppelbrechung beobachtet. Dieser Effekt tritt umso mehr hervor, je niedriger die Polyelektrolytkonzentration ist. Die spezifische Kerr-Konstante nimmt mit wachsender Polyelektrolytkonzentration und zunehmendem Dioxangehalt ab. Andrerseits ist die elektrische Doppelbrechung von KPSS in Glyzerin-Wasser- und Äthylenglycol-Wassermischungen mit der Feldstärke E durch folgende Gleichung verknüpft: $\Delta n/c = KE^n$, wo c die Polyelektrolytkonzentration und K und n Konstanten sind; der Exponent n wächst im untersuchten Konzentrationsbereich von 1,05 bis 1,70 ($1{,}71.10^{-5} - 1{,}01.10^{-3}$ g/cm^3) in 50,9% Glyzerin–Wasser. Die Abweichung vom Kerr-Gesetz ist umso ausgeprägter, je grösser der Bruchteil an Glyzerin ist. Eine alternativ ziemlich gute Darstellung der Daten ist durch die Zweitermgleichung $\Delta n/c = AE + BE^2$ möglich. Der Koeffizient A nimmt mit steigender Polyelektrolytkonzentration in 50,9% Glyzerin–Wasser ab; B steigt hingegen zunächst im Anfang an, erreicht ein Maximum und nimmt dann ab. Das Auftreten des Terms mit der Potenz eins kann durch keine bestehende Theorie der elektrischen Doppelbrechung erklärt werden.

Received March 16, 1964
Revised May 25, 1964

NOTES

*Poly-2-Methacryloxytropone. A Synthetic Biologically Active Polymer**

For two years, in our laboratories, we have been studying the effects of polymerization on the activity of selected biologically active monomers. There are three possible phenomena which might be observed if a polymer could be fashioned from an active monomer: (*a*) the biological activity of the polymer might be less than that of the monomer, (*b*) the biological activity might remain the same, or (*c*) the activity might be increased. Because of the probable insolubility of synthetic polymers in the physiological pH range and the probable resistance of such polymers to biological decomposition processes, it might be expected that possibility (*a*) would be the most likely. However, at present, our studies indicate that such may not be the case and that phenomena (*b*) and (*c*) occur more often than might be expected.

We should like to report on the synthesis, characterization, and biological activity of 2-methacryloxytropone (II) and the homopolymer (III) derived therefrom.

Reaction of tropolone (I) (.083 mole) under nitrogen for 1 hr. at 25° with methacrylyl chloride (.083 mole) in the presence of 0.1 g. of hydroquinone, 14 ml. of dry pyridine and 150 ml. of dry benzene followed by separation and washing of the organic phase with water, dilute hydrochloric acid, and water, gave, after drying, removal of solvent, and recrystallization from hexane, 12.4 g. (65%) of white needles (II), m.p. 78–79°.

ANAL. Calcd. for $C_{11}H_{10}O_3$: C, 69.49%; H, 5.29%. Found: C, 69.71%; H, 5.16%.

The infrared absorption data was as follows: 790w, 825w, 850w, 912w, 1000m, 1050m, 1080m, 1150s, 1250w, 1270m, 1350m, 1400w, 1480m, 1530m, 1600s, 1620s, 1650s, 1750s, 3020w, 3450w (w = weak absorption, m = medium absorption, s = strong absorption; units are cm.$^{-1}$).

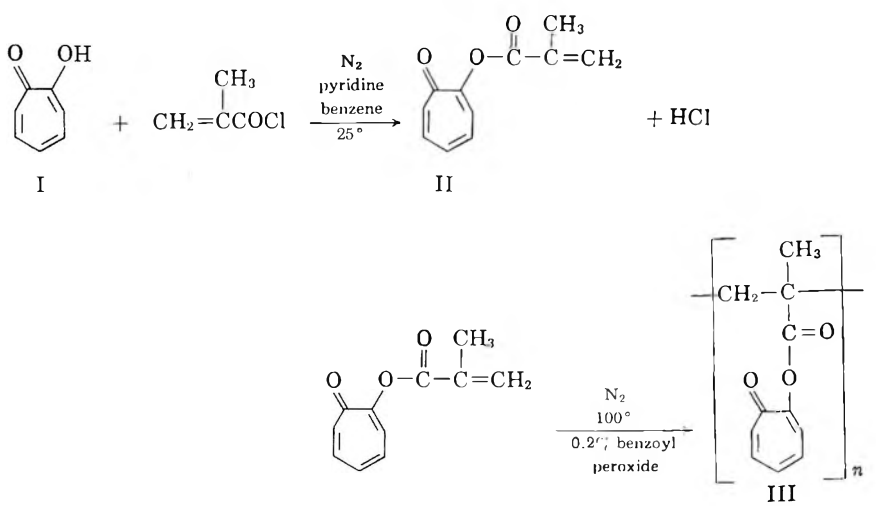

* From the thesis of Robert J. Cornell submitted in partial fulfillment of the requirements for the degree of Master of Science.

II was sparged with nitrogen in the melt at 100° for 15 min. followed by the addition of 0.2% benzoyl peroxide. After 10–15 min. further heating, a viscous melt formed. When movement of the nitrogen bubbles ceased, the polymer (III) was cooled, pulverized, and extracted with acetone to yield 90% of III. The product was slightly soluble in dimethylformamide. The polymer darkened and softened when heated above 200°.

ANAL. Calcd. for $C_{11}H_{10}O_3$: C, 69.49%; H, 5.20%; Found: C, 68.03%; H, 5.34%.

The infrared data was as follows: 800m, 850w, 885w, 965w, 1060s, 1090s, 1150s, 1230m 1270m, 1405m, 1485m, 1520m, 1600s, 1620s, 1650s, 1760s, 2990w, 3480w.

The monomer (II) and the polymer (III) were tested for anti-neoplastic activity in tissue culture screens.* In the first sequential screen, both the monomer and the polymer were active, but the polymer had a lower ED_{50}. (ED_{50} = the dose effective in 50% of the test specie). In the second sequential screen the polymer was active but the monomer was not.

The monomer and the polymer were also screened for activity against five different specie of bacteria.† These results are shown in Table I.

TABLE I
Activity of II and III Against Various Bacteria Specie

Bacteria Specie	Monomer activity[a]	Polymer activity
Staphyloccocus aureus no. 6538	15	12
Salmonella typhosa no. 6539	22	8
Salmonella choleraesuis no. 10708	17	8
Escherichia coli no. 11229	16	10
Streptococcus pyogenes no. 624	17	14

[a] Width of zone of growth inhibition in mm.

From Table I it can be seen that both II and III displayed a broad spectrum of antibacterial activity. However, in this case the monomer was more effective than the polymer.

From the anti-cancer and anti-bacterial screening data cited above it is indicated that polymerization may be useful as a technique for regulating the activity of drugs. Further studies concerning these observations are now underway with these and other monomers and polymers.

We are indebted to the Research Corporation for the financial support of this work.

ROBERT J. CORNELL
L. GUY DONARUMA

Department of Chemistry
Clarkson College of Technology
Potsdam, New York

Received September 18, 1964

* Anti-cancer screening was done by the Cancer Chemotherapy National Service Center, National Institutes of Health, Betheseda, Maryland.

† The agar plate technique was employed; U.S.D.A. Circular No. 198, 1931. Screening done at the Wisconsin Alumni Research Foundation, Madison, Wisconsin.

NMR Characteristics of o-, m-, *and* p-*Nitrostyrenes*

In the decarboxylation of *o*-formylcinnamic acid a cyclization takes place to give 1-indanone rather than *o*-formylstyrene.[1] Some of the properties of the product prepared by decarboxylation of *o*-nitrocinnamic acid suggest that it also has a cyclic or other isomeric structure rather than that of *o*-nitrostyrene.[2] To clarify this ambiguity the NMR spectra of the *o*-, *m*-, and *p*-isomers of nitrostyrene[2,3] have been examined.

The NMR data were obtained with a 60 mc, Varian HR 4320 spectrometer. Each sample was studied at three different concentrations in carbon tetrachloride and the τ-values, extrapolated to infinite dilution, are given in Table I. The absorption positions for the vinyl protons of the *para* and *meta* isomers are in good agreement with those reported for other substituted vinyl compounds[4] and for styrene as determined in carbon tetrachloride extrapolated to infinite dilution. The shift to low fields is attributed to the electron withdrawing nitro group. The differences in chemical shifts (σ) between the vinyl protons of styrene, 2,5-dichlorostyrene, and the nitro substituted styrenes are presented in Table I for comparison purposes.

TABLE I

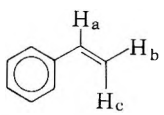

Compound	Chemical shifts[a]			Coupling constants[b]		
	H_a	H_b	H_c	J_{AB}	J_{AC}	J_{BC}
p-Nitrostyrene	3.22	4.54	4.13	10.7	17.4	0.8
	$\sigma = 0.11$[c]	$\sigma = 0.26$	$\sigma = 0.21$			
m-Nitrostyrene	3.24	4.60	4.16	11.4	18.8	0.8
	$\sigma = 0.09$	$\sigma = 0.20$	$\sigma = 0.18$			
o-Nitrostyrene	2.81	4.55	4.32	10.7	17.4	1.1
	$\sigma = 0.52$	$\sigma = 0.25$	$\sigma = 0.02$			
2,5-Dichloro-styrene	2.99	4.60	4.29	10.6	17.6	1.0
	$\sigma = 0.34$	$\sigma = 0.20$	$\sigma = 0.05$			
Styrene	3.33	4.80	4.34			

[a] Chemical shift values are reported in τ-values (ref. 8), extrapolated to infinite dilution.

[b] Coupling constants are expressed in cycle/sec.

[c] σ is the difference in chemical shift (ppm) between any proton and the analogous proton in unsubstituted styrene.

The NMR spectrum for the *ortho*-nitrostyrene is significantly different from that of the *para* and *meta* isomers presumably because the nitro group is near the vinyl group. There are two consequences which arise from this structural situation: (*1*) the magnetic anisotropy of the nitro group significantly influences the chemical shift of H_a; (*2*) there is a large steric overlap of the nitro group and H_c when the molecule assumes one of the planar configurations and a smaller but still real overlap of the nitro group and H_a when the phenyl ring is rotated 180° to assume the other planar arrangement. The most unhindered geometry places the benzene ring out of the plane of the vinyl group. This non-planar geometry locates H_c over the plane of the phenyl group in a shielding zone with a consequent increase in the τ-value of H_c in a situation similar to that observed previously.[5] The NMR data show both of these effects to be present in the *ortho* isomer.

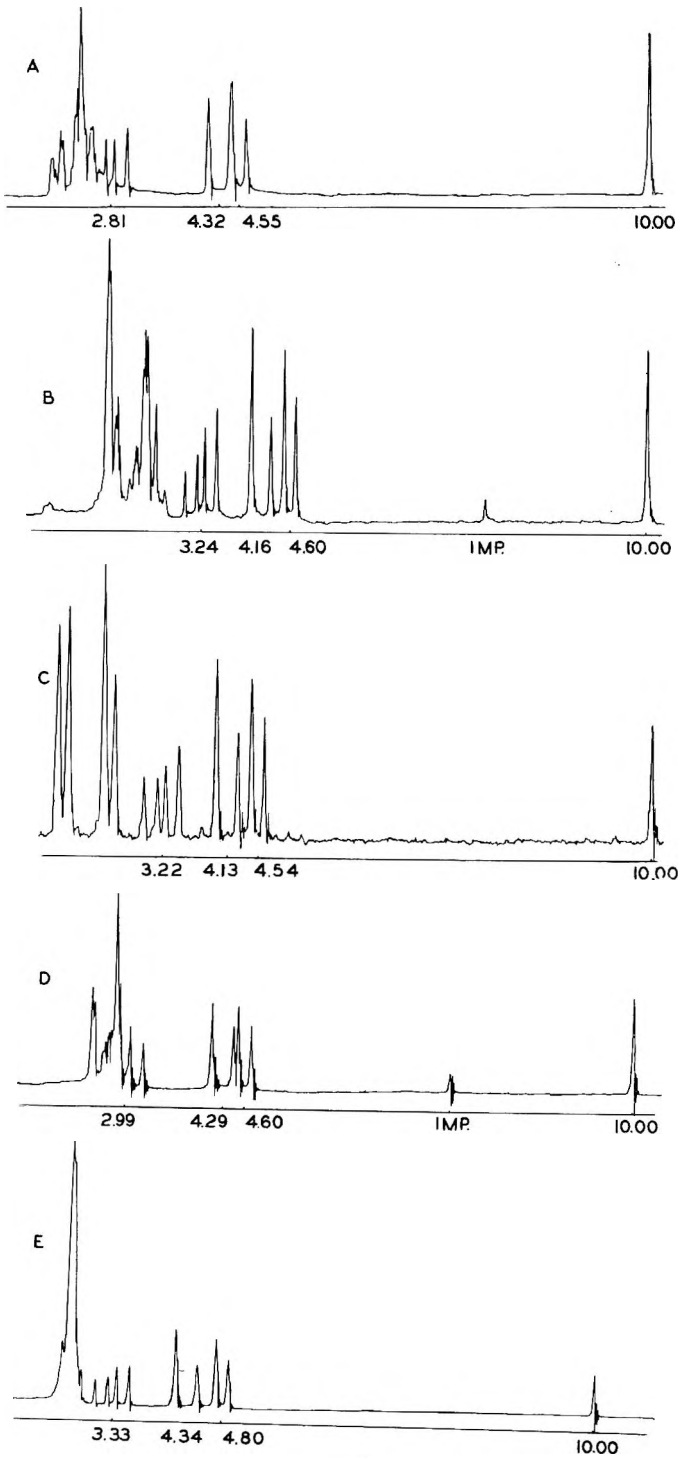

Fig. 1. Nuclear magnetic resonance (NMR) spectra: (*A*) *o*-nitrostyrene, (*B*) *m*-nitrostyrene, (*C*) *p*-nitrostyrene, (*D*) 2,5-dichlorostyrene, (*E*) styrene.

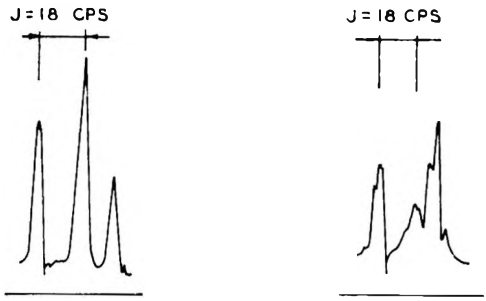

Fig. 2. Nuclear magnetic resonance (NMR) spectra: (*A*) H_b-H_c proton absorption, two doublets overlapping to form a triplet. (*B*) H_b-H_c proton absorption, H_c decoupled by irradiating H_a at 2.18τ. H_c appears as a doublet, still coupled to H_b.

The center of the quartet assigned to H_a of the *ortho* isomer is 0.52 ppm to lower field than that assigned to H_a in the *para* and *meta* isomers. This very large downfield shift is consistent with a deshielding mechanism analogous to that observed for carbonyl groups.[5,6]

The chemical shift in the absorbance at $\tau = 4.55$ attributable to H_b is apparently little influenced by the position of the nitro group on the ring. It appears within 0.06 ppm in the three isomers. The doublet assigned to H_c ($\tau = 4.32$) in the *ortho* isomer is observed at approximately 0.17 ppm higher field than that for H_c in the *para* and *meta* isomers. It is, however, only 0.02 ppm lower than that for H_c ($\tau = 4.34$) in unsubstituted styrene. Since the absorption for H_c of the *para* and *meta* isomers is 0.21 and 0.18 ppm lower than that for H_c of styrene, it appears that the shielding effect of the phenyl group in the *ortho* isomer is nearly equivalent to the deshielding due to the electron withdrawing effects of the nitro group.

A further complication in the splitting pattern of the spectrum of the *ortho* isomer arises as a consequence of the high field shift of the absorbance of H_c and the relative constancy of the absorbance of H_b which, however, further confirms the assignment. The doublet of H_b overlaps the doublet of H_c resulting in a triplet. The separation between the low field peak and the center of the triplet is 17.4 cycle/sec., while the separation of the center of the triplet from the high field peak is 10.7 cycle/sec. These values agree with the splitting values usually observed for *cis* and *trans* protons such as H_a coupled with H_b and H_c. The outermost peaks of the triplet are split into doublets while the center of the triplet itself appears as a triplet. The coupling is the same in all of these, approximately 1.1 cycle/sec., and is attributable to the spin coupling between H_b and H_c.

The double resonance technique[7] was used to spin decouple H_b from H_a, while observing the splitting of H_b. Figure 2 shows the change in the appearance of the triplet and the resultant formation of a doublet ($J = 18$ cps) and a singlet at high field, larger than either peak of the accompanying doublet.

The compound 2,5-dichlorostyrene was examined as a model compound to illustrate the effect of the phenyl group shielding H_c as a result of the non-planarity of the molecule. The two bulky chlorine atoms in the 2 and 5 positions preclude the possibility of a planar arrangement in this molecule. The electro-negative character of the chlorine atoms is demonstrated by the marked shift to low field (relative to styrene) for H_a ($\sigma = 0.34$ ppm) and H_b ($\sigma = 0.20$ ppm). This low field shift was not observed for H_c ($\sigma = 0.05$ ppm). The absence of this low field shift is analogous to the effect observed in the *ortho*-nitrostyrene molecule and supports the argument of a phenyl shielding effect and a non-planar molecule.

The authors acknowledge with gratitude support for this research through contracts and grants from the National Institute of Health, Atomic Energy Commission, Mead

Johnson Company, and Eli Lilly Company which made possible purchase of the instrument and accessories used. The manuscript was prepared during tenure of one of us (R. H. Wiley) as visiting professor in the Graduate Division of The City University of New York during 1963–64.

References

1. Wiley, R. H., and P. H. Hobson, *J. Am. Chem. Soc.*, **71**, 2429 (1949).
2. Wiley, R. H., and N. R. Smith, *ibid.*, **72**, 5198 (1950).
3. Wiley, R. H., and N. R. Smith, *ibid.*, **70**, 2295 (1948).
4. Bhacca, N. S., L. F. Johnson, and J. N. Shoolery, *NMR Spectra Catalog*, Varian Associates, 1962.
5. Wiley, R. H., T. H. Crawford, and C. E. Staples, *J. Org. Chem.*, **27**, 1535 (1962).
6. Jackman, L. M., and R. H. Wiley, *Proc. Chem. Soc.*, **1958**, 196.
7. Freeman, R., and M. Whiffen, *Mol. Phys.*, **4**, 321 (1961).
8. Tiers, G. V. D., *J. Phys. Chem.*, **62**, 1151 (1958).

Richard H. Wiley
T. H. Crawford

Department of Chemistry
University of Louisville
Louisville, Kentucky

Received September 21, 1964